Messenger RNA Studies in Alzheimer's Disease

Wendy Helen Wighton-Benn

Doctor of Medicine
University of Edinburgh
1999

Corrigenda

Table 4.2 Pearson's Correlation Coefficients for Total APP/Goα mRNA Data (Control, Age-Related Change, AD, AD + Parkinson's Disease and AD + Multi-Infarct Dementia Cases)					
	Total APP mRNA in Dentate Gyrus		**Total APP mRNA in CA4**		**Total APP mRNA in CA3**
Goα mRNA in Dentate Gyrus	0.825 (n = 25) **p < 0.001**	**Goα mRNA in CA4**	0.238 (n = 24) p = 0.263	**Goα mRNA in CA3**	0.463 (n = 16) p = 0.071

Pearson's Correlation Coefficients for Total APP/Goα mRNA Data (Control Cases Only)					
	Total APP mRNA in Dentate Gyrus		**Total APP mRNA in CA4**		**Total APP mRNA in CA3**
Goα mRNA in Dentate Gyrus	0.732 (n = 8) **p = 0.039**	**Goα mRNA in CA4**	-0.433 (n = 7) p = 0.332	**Goα mRNA in CA3**	-0.671 (n = 5) p = 0.215

Pearson's Correlation Coefficients for Total APP/Goα mRNA Data (AD Cases Only)					
	Total APP mRNA in Dentate Gyrus		**Total APP mRNA in CA4**		**Total APP mRNA in CA3**
Goα mRNA in Dentate Gyrus	0.892 (n = 12) **p < 0.001**	**Goα mRNA in CA4**	0.250 (n = 12) p = 0.433	**Goα mRNA in CA3**	0. 636 (n = 9) p = 0.065

Declaration

I declare that I am the author of this thesis, that the work contained in this thesis is my own, and that this thesis has not been accepted previously for a higher degree. Where I have received technical assistance this is indicated in the text.

Signature Date 1.8.1999.

Wendy Helen Wighton-Benn, M.B. Ch.B., M.R.C.Psych., M.Ed.

Abstract

Alzheimer's disease (AD) is the commonest cause of dementia. Its aetiology remains largely unknown and it is, as yet, untreatable. The prevalence of AD increases with age, afflicting 10.8% of 80 to 89 year olds (Rocca *et al.*, 1991). Moreover, a more than 100% increase in the U.K. population over 85 years is predicted to occur by the year 2022. AD represents a personal and societal tragedy the economic costs of which are enormous.

In this thesis, four independent studies of messenger RNA (mRNA), in tissue from normal and diseased post-mortem human brains, are presented. The following paragraphs summarise the findings in each of these four separate studies.

Gs and Go are members of the heterotrimeric G protein family whose members are crucial to cellular responsiveness. Gs stimulates the catalytic subunit of adenyl cyclase and a marked increase in the mRNA encoding the α subunit of Gs (Gsα) has been demonstrated in the hippocampus of AD sufferers in comparison to controls (Harrison *et al.*, 1991c). Four splice variants of Gsα mRNA are known to exist generated by the inclusion or exclusion of a span of 45 nucleotides encoded on exon 3 and by the use of a variable splice junction at the end of intron 3 (Kozasa *et al.*, 1988). However, it proved impossible to identify the splice variant(s) responsible for the increase identified in Gsα mRNA using the chosen technique of quantitative reverse transcription coupled with the polymerase chain reaction (RT-PCR).

Go is believed to regulate phospholipase C dependent phosphoinositide hydrolysis (Moriarty *et al.*, 1990) and to control neuronal calcium and potassium channels (Ewald *et al.*, 1988; Hescheler *et al.*, 1987; Kleuss *et al.*, 1991; VanDongen *et al.*, 1988). Nishimoto and colleagues (1993) postulate that Go is constitutively activated by amyloid precursor protein (APP) in AD. APP is a glycosylated transmembrane protein (Kang *et al.*, 1987) from which β–amyloid, the major protein constituent of the plaque and meningovascular amyloid deposits which characterise AD, is cleaved (Glenner and Wong, 1984; Masters *et al.*, 1985a). APP and Goα mRNA levels were found to be reduced in the dentate gyrus of AD sufferers in comparison to controls and were positively correlated in this region irrespective of diagnosis.

The APP gene is encoded on chromosome 21 and APP mRNA levels are increased in Down's syndrome in keeping with the 50% increase in gene dosage associated with trisomy 21 (Tanzi *et al.*, 1987). Increased APP mRNA levels are postulated to be responsible for the early appearance of the pathological stigmata of AD in individuals with this condition. However, a comprehensive analysis of APP mRNA levels in the hippocampus and visual cortex of diseased and control brains concluded that increased APP mRNA levels are not a feature of AD. An increase in the ratio of potentially amyloidogenic KPI-encoding, relative to KPI-lacking, APP mRNA transcripts was documented with age in the visual cortex of diseased and control brains. Further, the major determinant of this ratio differed between the visual cortex and the hippocampus.

Ubiquitin is a highly conserved member of the heat shock protein family essential to ATP-dependent non-lysosomal proteolysis. Ubiquitin mRNA, when expressed as a proportion of polyadenylated mRNA, was increased in the visual cortex of individuals diagnosed as suffering from borderline AD in comparison to the other diagnostic groups studied.

In conclusion, the challenges inherent in the application of biomedical research techniques to the study of a uniquely human disease like AD, using human post-mortem brain tissue, are briefly discussed.

Messenger RNA Studies in Alzheimer's Disease

Contents

Chapter 2

Materials and Methods

Chapter 5

The Messenger RNA Encoding Amyloid Precursor Protein

List of Figures

List of Tables

Chapter 3

Chapter 4

Chapter 5

Abbreviations

A	adenine
AD	Alzheimer's disease
ADP	adenosine diphosphate
ANOVA	analysis of variance
AOD	approximate optical density
APLP1 and APLP2	amyloid precursor-like protein 1 and 2
APP	amyloid precursor protein
APP-695_S and APP-751_S	α secretase cleaved 695 and 751 amino acid isoforms of the APP peptide
ATP	adenosine triphosphate
BAD	borderline Alzheimer's disease
C	cytosine
CA	cornu Ammonis
CAMDEX	Cambridge diagnostic examination
cAMP	cyclic adenosine monophosphate
cDNA	complementary DNA
CDS	Cornell depression scale
CERAD	Consortium to Establish a Registry for Alzheimer's Disease
CREB	cAMP response element binding protein
CSF	cerebrospinal fluid
CT Scan	computerised tomography scan
DEPC	diethylpyrocarbonate

dNTP	deoxynucleotide triphosphate
DSM-IIIR	Diagnostic and Statistical Manual of Disease, 3rd Edition Revised
DTT	dithiothreitol
dUTP	deoxyuridine triphosphate
EDTA	disodium ethylene diamine tetraacetate
ETR	estimated tissue radioactivity
FAD	AD inherited in an autosomal dominant fashion with apparently complete penetrance
G	guanine
GABA	gamma amino butyric acid
GAD	glutamic acid decarboxylase
GAP-43	growth associated protein-43
GDP	guanosine diphosphate
Gi-2α and Gi-3α	isoforms of the α subunit of the inhibitory heterotrimeric G protein, Gi
Goα	α subunit of the heterotrimeric G protein, Go
Gsα	α subunit of the heterotrimeric G protein, Gs
GTP	guanosine triphosphate
5-HT	5-hydroxytryptamine
HC	hippocampus
HPLC	high-performance liquid chromatography
HSF	heat shock transcription factor

hsp70	70 kDa members of the heat shock protein family
hsx70	specific 70 kDa member of the heat shock protein family
ISHH	*in situ* hybridisation histochemistry
KPI	Kunitz-type serine protease inhibitor
L-APP	leucocyte-derived APP
LDL	low density lipoprotein
MAC	membrane attack complex of complement
MAP-2	microtubule associated protein 2
MHC	major histocompatibility complex
MRNA	messenger RNA
NFT	neurofibrillary tangle
NINCDS-ADRDA	National Institute of Neurological and Communicative Disorders and Stroke-Alzheimer's Disease and Related Disorders Association
OAG	1-oleoly-2-acetylglycerol
OPTIMA	Oxford Project to Investigate Memory in Ageing
^{32}P	^{32}phosphorus
PBS	phosphate buffered saline
PET	positron emission tomography
PCR	polymerase chain reaction
PFA	paraformaldehyde
PKC	protein kinase

PHF	paired helical filament
PMI	post-mortem interval
poly(A)$^+$ mRNA	polyadenylated mRNA
RDC	Research Diagnostic Criteria
RT	reverse transcription
^{35}S	^{35}sulphur
SDS	sodium dodecylsulphate
SNuPE	single nucleotide primer extension
SPECT	single photon emission tomography
SSC	standard citrate saline
STE	sodium chloride/tris/EDTA
T	thymine
TEA	triethanolamine hydrochloride
Taq DNA polymerase	*thermus thermophilus* DNA polymerase
Tm	melt temperature
TBE	trisodium citrate borate EDTA buffer
TEMED	N,N,N',N'-tetramethyl-ethylenediamine
THA	1,2,3,4-tetrahydro-9-aminoacridine or tacrine
TPA	12-o-tetradecanoylphorbol 13-acetate
TRH	thyrotropin releasing hormone
tris	tris (hydroxymethyl) aminomethane
TSH	thyroid stimulating hormone

TUNEL	terminal deoxynucleotide transferase mediated deoxyuridine triphosphate nick end labelling
U	uracil
V642I/G/F	valine at position 642 of APP converted to isoleucine, glycine or phenylalanine
VIP	vasoactive intestinal peptide

Acknowledgements

I was fortunate to have the opportunity to work with Dr. M.F. Weiner, Professor and Vice-Chairman of the Department of Psychiatry at the University of Texas Southwestern Medical Center at Dallas at the Alzheimer's and Related Diseases Research Center. Dr. Weiner's holistic and committed approach to the care of those afflicted with Alzheimer's disease and his energy and enthusiasm for research into this disease inspired me to pursue a research career in this field.

My supervisor, Professor R.C.A. Pearson, has laboured to imbue me with a perspicacious understanding of the principles of neuroscientific research. My neuroscience training has been the richer for his piercing intellect and coruscating wit. Without Dr. P.J. Harrison's help I would not have had access to tissue from the Oxford Project to Investigate Memory in Ageing and for this I am grateful. I have profited enormously from discussions with both.

This thesis would not have been completed without the help of chief technician, Mr. M.W. Sanders, whose technical expertise and industry made it possible. Always good humoured and fair, Maurice was a joy to work with. Miss J.M. Heffernan, now a research assistant at the University of Oxford, contributed substantially to all stages of this project. She has been an unfailing source of support. She has been sorely missed since leaving Sheffield. I am indebted to Doctors P.R. Heath, P.J. Harrison and A.J.L. Barton for validating the oligodeoxynucleotide probes used in this thesis and for the many discussions on research theory and practice. I am grateful to Dr. A.J.L. Barton and Dr. M.H. Griffiths for the opportunity to analyse data they generated. Miss J.M. Russell was infinitely patient in providing me with exhaustive statistical support and to her I owe special thanks. The photographs included in this thesis are the exemplary, and apparently effortless, work of the genial and accommodating Mr. M. Turton.

I am grateful to the Medical Research Council, Trent Regional Health Authority, the Mason Medical Research Foundation, the Nuffield Foundation and the University of Sheffield from whom I have received generous financial support.

Finally, my thanks go to my husband, Mike Benn, who bore with fortitude my preoccupation with Alzheimer's disease and to my baby son, Kieran Andrew Wighton Benn, who provided me with the impetus to complete this thesis before his first birthday.

Chapter 1

Introduction

1.1 The Clinical Diagnosis of Alzheimer's Disease

Alzheimer's disease (AD) is the commonest cause of dementia. Its aetiology remains largely unknown and it is, as yet, untreatable. In 1906 Alois Alzheimer (1864-1915), the Bavarian psychiatrist and neuropathologist (Thomas and Isaac, 1987), presented the case of a 51 year old woman whose illness he believed merited the status of a new syndrome. Using the silver stain developed by Bielschowsky in 1902, Alzheimer demonstrated the senile plaques and neurofibrillary tangles now regarded as the pathological stigmata of AD. Alzheimer published his preliminary findings the same year, followed in 1907 by his paper *Über eine eigenartige Erkrankung der Hirnrinde*, (About a peculiar disease of the cerebral cortex) in the *Allgemeine Zeitschrift für Psychiatrie und Psychisch-Gerichtliche Medizin.*

Dementia is a global impairment of cognitive function, accompanied by a deterioration in personality and behaviour, which occurs in clear consciousness (World Health Organisation, 1992). Dementing illnesses are aetiologically, clinically and neuropathologically heterogeneous and primarily afflict the elderly, but may occur in individuals as young as 18 years (Will *et al.*, 1996). Particularly at risk are those individuals who suffer from Down's syndrome (trisomy 21), who invariably develop symptoms of dementia characterised neuropathologically as AD, if they survive beyond the age of 40 years (Mann, 1988). Examination of the brains of Down's syndrome individuals allows the earliest manifestations of AD to be studied in a population destined ultimately to develop the disease. Thus, the

developmental sequence of the neuropathology of AD may be discerned (Mann *et al.*, 1989).

Jorm (1987), in his meta-analysis of prevalence studies for dementia published world-wide between 1945 and 1985, found the rate doubled every 5.1 years up to the age of 95 years. Prevalence rates for the over 65 years age group vary from 3.6 to 10.5%, while for populations over 85 years, prevalence rates reach 23.9 to 29.8% (Ebly *et al.*, 1994). Approximately 1-2% of the population aged 65 years and over develop dementia each year (Brayne, 1993).

There are at least 60 disorders which can give rise to dementia (Tien *et al.*, 1993) and since there is no definitive, non-invasive test for AD it is a diagnosis of exclusion. Prevalence rates for AD are, therefore, affected by how assiduously other causes of dementia are excluded. In North America and Europe, AD accounts for approximately 50% of all cases of dementia (Breitner and Folstein, 1984). The proportion of dementia cases attributable to AD increases with age up to the age of 85 years. A Canadian study of the very old attributed 75.3% of cases of dementia in the 85 years and over group to AD (Ebly *et al.*, 1994). Rocca and colleagues (1991), in an analysis of 1980 to 1990 European prevalence studies of AD, arrived at an overall European prevalence rate of 0.3% population for the age group 60 to 69 years and 10.8% population for the age group 80 to 89 years. Though there is no sex difference in the prevalence of dementia overall, prevalence rates for AD in women are significantly higher than those for men of the same age (Jorm *et al.*, 1987; Rocca *et al.*, 1991). In contrast to the presumed significant international differences in risk factors for AD, incidence and prevalence rates for the disease show little geographical variability (Rocca *et al.*, 1991).

A substantial surge is predicted in the number of people living to be very old due to the increased life expectancy of those born in the decade following the second world war, the so called 'baby boomers'. Over the next 23 years the number of people in the UK over the age of 65 years is predicted to increase from 9 to 14.5 million. The UK population over the age of 85 years, meanwhile, is set to increase from 1 to 2.2 million by the year 2022; a more than 100% increase (Department of Health, 1997). Since age is a major risk factor for AD, the prevalence of AD is set to increase accordingly. AD represents an enormous personal, social (Selkoe, 1991) and financial cost. Minimum losses to the US economy for the year 1991, as a result of AD, have been estimated at 536 billion (annual direct) and 1.75 trillion (total cost) dollars (Ernst and Hay, 1994). Gray and Fenn (1993), in a more cautious analysis which excluded the costs of informal care, estimated the total annual cost of providing health and social services, to individuals over the age of 65 years suffering from AD in England, to be £1,039 million at 1990/1991 prices.

The clinical manifestations of AD present themselves insidiously. Memory impairment is the most prominent and usually the first symptom (Weiner *et al.*, 1991a) and at presentation is universal (Price *et al.*, 1993). Over a two to three year period, abnormalities in other cognitive domains follow, though the pattern of cognitive deficits is highly variable (Kurz *et al.*, 1992) and no orderly progression of cognitive involvement in AD can be discerned (Ritchie and Touchon, 1992). Nevertheless, focal abnormalities or prominent behavioural difficulties at presentation are rare in AD that develops in middle to late adulthood (Price *et al.*, 1993). Deterioration is steady and relentless: neither fluctuations nor remissions are characteristic of the disease (Lishman, 1987). AD sufferers lose the ability to deal with abstract concepts and complete complex tasks, and their grasp of language dwindles. The language deficit in AD is almost always that of a fluent aphasia (Price

et al., 1993). Sufferers become disorientated and display impaired social judgement. They develop apraxias and agnosias.

Depressive symptoms, such as feelings of sadness or despair, are a common accompaniment to AD (Burns *et al.*, 1990a; Weiner *et al.*, 1991b), but the incidence and prevalence of major depression is low (Burns *et al.*, 1990a; Weiner *et al.*, 1994). Ballard and colleagues (1997) have demonstrated that depressive illnesses identified in dementia sufferers are of similar severity and duration regardless of whether the Diagnostic and Statistical Manual of Disease, 3rd Edition Revised (DSM-III-R), the Research Diagnostic Criteria (RDC) or the Cornell Depression Scale (CDS), a scale developed specifically for the assessment of depression occurring in the setting of dementia, is employed. Weiner and colleagues (1991b) conclude that depression is relatively mild or absent in those with organic brain disease and that it is a rare cause of excess morbidity in AD.

Half or more of individuals with dementing illnesses suffer agitation or psychotic symptoms, or both, during the course of their illness (Tariot, 1996). A significant proportion of AD sufferers exhibit behavioural disturbances such as aggression, wandering and incontinence (Burns *et al.*, 1990b) and it is often these behaviours which precipitate admission to institutional care (Hope and Keene, 1996). Behavioural disturbances become more common as dementia severity increases (Burns *et al.*, 1990b).

In the final stage of AD, bladder and bowel control is lost and bodily wasting is prominent. In advanced disease, primitive reflexes, myoclonus and dyskinesias appear (Benesch *et al.*, 1993) and the gait becomes stooped and shuffling. Save for these neurological signs, there are no clinically observable physical stigmata of the

disease (Weiner *et al.*, 1991a). Death supervenes approximately 4 to 10 years from diagnosis, usually as a result of sepsis to which the enfeebled, bed-ridden elderly are particularly susceptible (Weiner *et al.*, 1991a).

The clinical diagnosis of AD necessitates a detailed history from the patient, and an informant, and a thorough physical examination. The clinical guidelines of McKhann and colleagues (1984), developed by a National Institute of Neurological and Communicative Disorders and Stroke-Alzheimer's Disease and Related Disorders Association (NINCDS-ADRDA) work group, under the auspices of the Department of Health and Human Services Task Force on Alzheimer's Disease in the USA, remain the gold standard for the clinical diagnosis of AD.

No specific laboratory test exists to support the diagnosis of AD, though ancillary investigations may help exclude other diagnoses. Computerised tomography has proved useful as an adjunct to clinical examination, particularly for the exclusion of intracranial mass lesions, though it has, thus far, proved disappointing as a means of distinguishing the normal aged elderly from those suffering from AD (Burns, 1990). Functional neuroimageing techniques, such as positron emission tomography (PET) and single photon emission tomography (SPECT), yield characteristic abnormalities in AD and have been reported to be of great use in the diagnosis of the disease (Tien *et al.*, 1993). SPECT studies have demonstrated bilaterally decreased cerebral blood flow in the parietal and temporal lobes, with involvement of the frontal lobes in advanced disease (Geaney and Abou-Saleh, 1990), and are consistent with the regional decreases in metabolism and cerebral blood flow identified by PET (Foster *et al.*, 1984). Perfusion abnormalities on SPECT imageing with ^{99m}Tc-bicisate have been shown to correlate significantly with severity of cognitive impairment (Waldemar *et al.*, 1994). However, Powers and co-workers (1992) found the

sensitivity of PET to be too low to be of routine clinical use. Similarly, Van Gool and colleagues (1995) concluded from a study of ^{99m}Tc-HMPAO SPECT that routine scans performed in the mildly demented elderly did not substantially contribute to diagnostic accuracy.

A definitive diagnosis of AD is only possible on histological examination of brain tissue obtained either at biopsy or autopsy (Powers *et al.*, 1992). The neuropathological criteria for AD, established at a National Institute of Mental Health and American Association of Retired Persons workshop on AD (Khachaturian, 1985), are widely, though not universally (Mirra *et al.*, 1991), applied to the neuropathological diagnosis of AD. These criteria, however, were developed as guidelines to aid in uniform assessment of neuropathological specimens, rather than as quantitative thresholds, and have not yet been empirically validated (Silverman and Wisniewski, 1993).

Martin and co-workers (1987) assessed the accuracy of a clinical diagnosis of 'probable AD' made according to the NINCDS-ADRDA criteria of McKhann and colleagues (1984). The diagnosis of AD in this small (n=11), highly selected group with clinically typical AD was 100% accurate. The utility of these criteria was affirmed in another study (Galasko *et al.*, 1994), which reported a 90% accuracy of the diagnoses of 'probable' or 'possible' AD according to NINCDS-ADRDA criteria. Unsurprisingly, the diagnosis of 'possible' AD and non-AD dementias is less accurate than that of 'probable' AD resulting in calls for more specific clinical guidelines for the diagnosis of non-AD dementias and the sub-division of the 'possible' AD group to improve accuracy (Galasko *et al.*, 1994). Joachim and colleagues (1988a) studied the histological findings in an unselected group of 150 patients who came to autopsy from multiple sources in several different US states, with a clinical diagnosis of AD

made by many different physicians. In their study, 87% of those diagnosed clinically as suffering from AD were found to have a pathological diagnosis of AD with or without additional pathology. In two of their clinically demented subjects no histological correlate for dementia could be found. They concluded that the wide range of physicians involved in their study were highly accurate in their diagnosis of clinical AD.

1.2 The Neuropathology of Alzheimer's Disease

1.2.1 Introduction

The first description of the clinicopathological condition that Alzheimer was to establish as a distinct syndrome, appeared in 1865 in Wilhelm Griesinger's textbook entitled *Die Pathologie und Therapie der Psychischen Krankheiten* (Thomas and Isaac, 1987). He described a presenile dementing process, distinct from that due to neurosyphilis or arterial disease, in which brain atrophy was a constant feature. The gross atrophy, particularly of the temporal and frontal lobes which characterises AD, is the result of extensive neuronal degeneration (Lishman, 1987). Mann (1996) concludes, that the neocortical neurons lost in AD are primarily large pyramidal cells; the same cells most affected by neurofibrillary tangle formation. Younger AD afflicted subjects exhibit a more profound loss of these large pyramidal cells than those individuals who develop the disease in old age. However, loss of large nerve cells is a feature of normal ageing, thus total cell loss is the same in both groups of patients (Mann, 1996). Astrocytosis is a feature of normal ageing, but the proliferation of astrocytes is accentuated in degenerative diseases of the central nervous system, including AD (Frederickson, 1992). In addition, subtle, but definite, abnormalities in the blood brain barrier have been identified in AD (Stewart *et al.*, 1992).

The neuropathological stigmata of AD are found throughout the cerebral cortex, though there is relative sparing of the primary sensory and motor areas (Terry, 1993). The most extensive neuropathological change within the cortex is seen in the medial temporal lobe, including the parahippocampal gyrus, the entorhinal cortex, the amygdala and the hippocampus, particularly CA1 (Pearson and Powell, 1989). AD neuropathological change has been demonstrated to progress in a predictable fashion (Pearson and Powell, 1989) from the most severely affected medial temporal lobe to areas of association cortex in the parietotemporal and frontal lobes. Degeneration is also seen in the projection neurons of the nucleus basalis of Meynert, locus ceruleus, dorsal raphe and ventral tegmental area. The lower brainstem and spinal cord, in contrast, are unaffected by the disease process and the cerebellum shows only minimal involvement (Terry, 1993).

Microscopically, the major hallmarks of AD are the senile plaques and neurofibrillary tangles first described by Alzheimer (1907). Both structures contain amyloid, a generic term for a family of pathological, extracellular filaments, derived from a variety of proteins, which share certain physical and optical properties (Wisniewski, 1993). All amyloids are associated with two extracellular matrix components, heparan sulfate proteoglycan and amyloid P component (Perlmutter *et al.*, 1994). In addition to these features, degeneration with Hirano body formation and granulovacuolar degeneration, especially of the hippocampal pyramidal cells, are also seen in AD (Wisniewski and Wegiel, 1992).

1.2.2 Plaques in Alzheimer's Disease

Plaques are active structures and exist in a number of forms thought to represent stages in the development of the plaque from nascence to maturity (Mann *et al.*, 1989). The major proteinaceous component of AD plaques is β-amyloid, a 40 to 43

amino acid cleavage product of amyloid precursor protein (APP) (Masters *et al.*, 1985a). Abundant cortical β-amyloid containing plaques are a feature not only of Alzheimer's disease (McKee *et al.*, 1991), but also of normal ageing (McKee *et al.*, 1991), Down's syndrome (Mann *et al.*, 1986) and dementia pugilistica (Gentleman *et al.*, 1993).

Plaques are classified as diffuse or neuritic. Neuritic plaques may be either primitive or mature: mature neuritic plaques are also referred to as senile plaques. Diffuse plaques are amorphous collections of non-aggregated β-amyloid identifiable in normal aged, AD and Down's syndrome brains (Frucht *et al.*, 1992) and in the brains of individuals with dementia pugilistica (Gentleman *et al.*, 1993). They are thought to represent an early stage in plaque formation (Giaccone *et al.*, 1989). Diffuse plaques do not stain with classical silver staining techniques, nor do they exhibit green birefringence on exposure to polarised light when stained with Congo red (Yamaguchi *et al.*, 1988). They fail to generate a neuritic reaction in the surrounding neuropil and are not surrounded by reactive astrocytes or activated microglia. Diffuse plaques are identifiable using antiserum to synthetic β-amyloid peptide (Yamaguchi *et al.*, 1988) or by the application of modified silver staining methods, such as the Campbell-Switzer modification of the Hicks silver method (Campbell *et al.*, 1987) or Hedreen and colleagues (1994) modification of Bielschowsky-type silver staining.

Primitive neuritic plaques are thought to represent an intermediate stage of plaque development. Such plaques are surrounded by neuritic pathology and contain irregularly aggregated fibrillary β-amyloid, but lack a central compacted core (Wisniewski, 1993). Senile, or mature neuritic plaques, consist of a compacted, spherical core of β-amyloid surrounded by a halo of activated microglia, reactive

astrocytes and distended, dystrophic axons, dendrites and synaptic processes (Wegiel and Wisniewski, 1990). The activated microglia cover 80% or more of the surface area of the amyloid core (Wegiel and Wisniewski, 1990). The core consists of aggregated 7 to 10 ηm fibrils of β-amyloid (Wisniewski and Wegiel, 1992). Such plaques are argyrophilic with classical silver stains and exhibit green birefringence on exposure to polarised light following staining with Congo red, suggesting that the β-amyloid has adopted a β-pleated sheet conformation (Wisniewski and Wegiel, 1992). Other components of senile plaque cores include aluminosilicates (Candy *et al.*, 1986), heparin sulfate proteoglycans, amyloid P component, nucleoside diphosphatase, α-1-antichymotrypsin and cathepsins D and B (Frank and Greenberg, 1994).

1.2.3 Neurofibrillary Tangles and Dystrophic Neurites

Neurofibrillary tangles (NFT) are intracellular bundles of fragmented and twisted fibres that occupy the perikarya of cells in a number of neurodegenerative diseases, including AD. These fibre bundles are composed of paired helical filaments (PHF), straight 10 ηm filaments and combinations of both paired and straight filaments (Markesbery *et al.*, 1993). PHF consist of pairs of fibrils of 10-13 ηm in diameter wound around each other to form either a right handed or left handed helix.

Dystrophic neurites, also known as curly fibers or neuropil threads, are ultrastructurally similar to NFT, but are located in dendritic and axonal processes (Kowall and McKee, 1993). It is hypothesised that the disruption of fine neuronal processes, consequent upon the formation of dystrophic neurites, results in NFT formation and ultimately in cell death. While dystrophic neurites are associated with senile plaques in AD (Iqbal *et al.*, 1987), the majority are found in the neuropil independent of senile plaques (Markesbery *et al.*, 1993).

In 1985, Masters and colleagues concluded that the NFT was composed of the same 4 kDa peptide from which AD amyloid plaque cores and the cerebrovascular deposits of amyloid in AD were formed (Masters *et al.*, 1985b). Perry and colleagues (1992) extended these observations, demonstrating that β-amyloid immunoreactivity could be enhanced by pre-treatment with formic acid such that previously unreactive extracellular NFT became immunoreactive. However, Joachim and co-workers (1988b), in their protein chemical and immunochemical study of cerebrovascular amyloid, provided data suggesting that NFT were not composed of β-amyloid. In 1994 Zelman and colleagues attempted to clarify these conflicting results by electrophoretically purifying PHF. They found PHF to be largely composed of a 66 kDa peptide that was immunoreactive to antibodies raised against the β-amyloid region of the carboxyl terminus of APP. Their data prompted them to reject the hypotheses that PHF was contaminated by β-amyloid, or that the two peptides shared homologous sequences, and conclude that conformational homologies between β-amyloid and PHF were responsible for the cross-reactivity observed between PHF and β-amyloid detecting antibodies.

The main protein constituent of PHF is believed to be abnormally hyperphosphorylated *tau*, a major microtubule associated protein (Khatoon *et al.*, 1994) which forms part of the neuronal cytoskeleton. It is unclear whether differences in amino acid sequence identified between PHF and *tau* are due to contamination, alternative post-translational modification, or differing amino acid composition, or indeed whether PHF contain other substances in addition to *tau* (Iqbal *et al.*, 1987). Soluble, abnormally hyperphosphorylated *tau* is also found in the cytosol in AD. The phosphorylation state of *tau in vitro* has been demonstrated to influence the speed and extent of microtubule assembly (Lindwall and Cole, 1984), and immunochemical studies in AD suggest that microtubule stability is lost

in AD (Kowall and McKee, 1993). Like primitive and mature neuritic plaques, NFTs are argyrophilic and congophilic due to their β-pleated sheet conformation. Ultimately, the cell membrane may disintegrate releasing the NFT. Such 'ghost' or 'tombstone' NFTs are usually found in the entorhinal cortex and are unusual in neocortex (Terry, 1993).

NFTs are not restricted to AD. They are also found in Guam Parkinsonism dementia complex, dementia pugilistica, post-encephalitic Parkinsonism and Down's syndrome (Iqbal *et al.*, 1987). Thus, they can be found in neurodegenerative disorders of traumatic, viral, toxic and metabolic origin. However, NFTs and dystrophic neurites in the neocortex are constant neuropathological features in those individuals with AD whose cognitive impairment is functionally significant (McKee *et al.*, 1991). The projection cells of the pre-α layer of the transentorhinal/entorhinal cortex are among the first neurons in the brain to exhibit neurofibrillary change (Braak *et al.*, 1994). Further, Braak and colleagues (1994) have demonstrated that the formation of dystrophic neurites and NFTs in this region is preceded by the appearance of immunochemically detectable, abnormally hyperphosphorylated *tau* throughout the entire nerve cell.

1.2.4 Meningovascular Amyloid

Cerebrovascular amyloidosis, the deposition of β-amyloid in the meningeal and/or cortical vessels, is a virtually invariable accompaniment to AD, though its severity varies widely (Joachim *et al.*, 1988a). Initially, β-amyloid is found deposited between the smooth muscle cells of the tunica media or in the cytoplasm of these cells, but later is found in all layers of the walls of affected vessels (Frackowiak *et al.*, 1994). Mandybur (1975) found cerebrovascular amyloid to be variously absent, minimal or severe in AD, and was unable to establish a clear relationship between

the presence or degree of cerebrovascular amyloid and the age of the patient, duration of their illness or the degree of cortical atrophy present. Glenner and Wong first isolated, purified and sequenced cerebrovascular β-amyloid in 1984. The following year Masters and colleagues purified and characterised the amyloid of plaque cores in AD establishing the common origin of these proteins (Masters *et al.*, 1985a). The β-amyloid deposited in the cerebrovasculature in AD, however, is subtly different from the β-amyloid found in AD plaques. The amino termini of plaque β-amyloid are variable, possibly because they undergo processing *in situ* (Masters *et al.*, 1985a), whereas minimal heterogeneity is encountered in the amino termini of vascular β-amyloid. Further, meningovascular β-amyloid has three residues missing from the carboxyl end of the peptide such that it is generally 39 amino acids in length. In β-amyloid derived from AD and Down's syndrome plaque cores, and from Down's syndrome meningovasculature, a glutamic acid residue is found at position 11 (Masters *et al.*, 1985a). In contrast, in β-amyloid derived from AD meningovasculature the glutamic acid residue is replaced by glutamate. These findings were confirmed by Prelli and colleagues (1988) who hypothesised that β -amyloid is processed in a tissue specific manner.

1.2.5 The Relationship between Senile Plaques and Neurofibrillary Tangles in Alzheimer's Disease

In a study of mentally retarded adults without a history of Down's syndrome, hydrocephalus or metabolic disorders, Silverman and co-workers (1993) found no regional association between senile plaques and NFTs. They concluded that the production of senile plaques and NFTs proceeds independently. In AD, the relationship between senile plaques and NFTs remains elusive (Kowall and McKee, 1993) and controversial. However, since neuropathologically cases with numerous senile plaques in the presence of minimal numbers of NFTs are seen and vice versa,

the two lesions would appear to be independent of one another in the disease (Iqbal *et al.*, 1987).

Beta-amyloid load increases with age, but is not an invariable feature of aged brain (McKee *et al.*, 1991) and widespread and numerous senile plaques are found in cognitively well-preserved elderly persons (Tomlinson 1970, 1968; McKee *et al.*, 1991). Kowall and McKee (1993) believe that β-amyloid deposition precedes neurofibrillary pathology. In a study of brain tissue from Down's syndrome patients of varying ages, whose morphological features are presumed to reveal an age-related sequence of events in the development of the neuropathology of AD, Mann and colleagues (1989) established that β-amyloid deposition occurred prior to the development of dystrophic neurites or NFTs. Conversely, Braak and Braak (1991) demonstrated that cortical neurofibrillary change occurred in a number of the AD cases they examined histologically that had no evidence of β-amyloid deposition and concluded that β-amyloid deposition is not a necessary prerequisite for neurofibrillary change. Braak and Braak (1991) introduced the concept of neuropathological stageing in AD, based on qualitative evaluation of the distribution patterns of NFTs and dystrophic neurites. They point out that the development of neuropathological change in AD is a seamless process, such that the differentiation of AD from non-AD dementia is artificial (Braak and Braak, 1991).

1.3 Neurotransmitter Abnormalities in Alzheimer's Disease

The identification, in post-mortem human brain, of AD-specific neurotransmitter dysfunction is complicated by the effects of agonal state, the instability of proteins post-mortem and the variable length of post-mortem delay, and the fact that most tissue examined post-mortem represents the end-stage of the disease. Numerous abnormalities have been identified in neurotransmitter and neuromodulator levels in

AD, in the concentrations of the enzymes that synthesise them and in the morphology of the neurotransmitter and neuromodulator producing neurons themselves (Selkoe, 1991). Projection neurons synthesising acetylcholine, noradrenaline, serotonin and dopamine and cortical neurons producing gamma butyric acid (GABA), glutamate, somatostatin, neuropeptide Y, cortocotrophin releasing factor, substance P and other neuromodulators have been shown to be affected in AD (Selkoe, 1991).

The cholinergic system was the first neurotransmitter system to be identified as abnormal in AD and led to the cholinergic hypothesis of the disease. In 1976, Bowen and colleagues demonstrated a reduction in choline acetyltransferase activity in post-mortem AD brain; a finding replicated in numerous subsequent studies (Palmer, 1996). Ante-mortem studies of biopsy tissue from AD sufferers has confirmed that there is presynaptic cholinergic dysfunction in the disease and that this is an early event in the pathogenesis of the disease (Palmer, 1996). Empirical support for the cholinergic hypothesis comes from the demonstration of cognitive deficits similar to those seen in individuals suffering from mild, but not moderate or severe, AD in young and elderly persons treated with the cholinergic blocking drug scopolamine (Christensen *et al.*, 1992).

The reactive astrocytes found in association with senile plaques in AD have been demonstrated *in vitro* to bear muscarinic acetylcholine receptors, suggesting that astrocytes in this location may be responsive to acetylcholine and, therefore, potentially to cholinergic drugs (Messamore *et al.*, 1994). Further, Nitsch and colleagues (1992) have demonstrated that the release of soluble APP derivatives from a human embryonal kidney cell line transfected with the genes for human brain muscarinic acetylcholine receptors, could be increased by stimulation of the m1 and

m3 muscarinic acetylcholine receptor subtypes. Thus, APP processing appears to be under neurotransmitter control (Nitsch, 1996).

Palmer and colleagues (1987) demonstrated a presynaptic deficit in noradrenergic transmission in a study of tissue from AD temporal cortex obtained ante-mortem. Similar findings were obtained on examination of patients who had been symptomatic for less than two years, suggesting that noradrenergic disturbance is an early feature of AD. Post-mortem data suggestive of serotonergic dysfunction in AD has been confirmed by ante-mortem work that has established serotonergic denervation as an early feature of the disease (Palmer *et al.*, 1987; Palmer, 1996).

Cortical dopaminergic function is preserved in AD (Palmer *et al.*, 1987), though neostriatal dopaminergic function may not be (Palmer, 1996). Abnormalities observed in the GABA and somatostatin neurotransmitter systems in post-mortem AD brain have not been confirmed in ante-mortem studies and likely represent either the end-stage of the disease process or a post-mortem artefact (Palmer, 1996; Yates *et al.*, 1990).

1.4 Clinicopathological Correlations

Elucidation of the pathological correlates of cognitive decline in AD has been fraught with difficulties. Initial studies suggested that the severity of dementia in AD was related to the numbers of senile plaques, but later work has undermined this conclusion (See Kowall and McKee, 1993 for review). McKee and co-workers (1991) found that the number of NFTs and dystrophic neurites were correlated with the clinical severity of dementia. Further, in their study, the presence of dystrophic neurites in the neocortical neuropil successfully differentiated the AD subjects from the control subjects. However, the authors specifically excluded those individuals

with early or atypical features of AD and acknowledge that the presence of dystrophic neurites might be a feature of individuals with AD who exhibit functionally significant cognitive impairment rather than a marker of those with AD *per se*. Other workers have found inverse correlations between the clinical severity of dementia and the degree of cholinergic dysfunction (Perry *et al*, 1978; Palmer *et al*, 1987; Palmer, 1996), loss of neurons (Neary *et al*, 1986; Procter, 1996; Mann, 1996; Palmer, 1996) and loss of synapses (Sambrook *et al.*, 1989). Mann (1996) points out that the strong correlations found between the degree of cognitive impairment and the numbers of surviving pyramidal cells or synapses is not unexpected, given that the latter two represent both damage accumulated over the whole time course of the disease and the integrative capacity of the neocortex.

1.5 Factors Predisposing to the Development of Alzheimer's Disease

1.5.1 The Genetics of Alzheimer's Disease

1.5.1.1 Introduction

Dissection of the heterogeneous and complex genetic underpinnings of AD (St George-Hyslop *et al.*, 1990) has proved both attractive to investigators and fruitful (Schellenberg, 1995). The painstaking collection of family pedigrees and the rigorous attention to accurate diagnosis of AD can proceed successfully even when, as now, the aetiology and pathogenesis of AD remains largely obscure. Schellenberg (1995) has likened the biochemical analysis of post-mortem human AD brain tissue to molecular archaeology, yet genetic analysis is not without its difficulties. The accurate diagnosis of AD, especially in older age groups where the diagnosis is complicated by inter-current physical and psychological diseases and when other causes of dementia, some of them superficially similar to AD, are common, is fraught with difficulties. Further, AD is a common disorder, particularly among the

old, so that family clustering need not necessarily indicate a common genetic basis for the disease; it may represent, for example, a chance occurrence, or the presence of more than one aetiologically distinct form of AD (Schellenberg, 1995). Finally, the collection of large family pedigrees in which to examine the inheritance of AD is problematic in a disease the prevalence of which increases with age, since some individuals may succumb to other diseases before they could be expected to develop the stigmata of AD (Schellenberg, 1995).

Approximately 15 to 20% of all cases of AD arise before the age of 65 years: a subgroup referred to as suffering from early onset AD or pre-senile dementia. Of all cases of AD developing before the age of 60 years, between 10 and 50% exhibit a pattern of autosomal dominant inheritance with apparently complete penetrance, and these family pedigrees are often referred to as suffering from Familial AD (FAD) (Sandbrink *et al.*, 1996). In this discussion, the abbreviation 'FAD' will be used solely to denote those cases of AD that exhibit this pattern of autosomal dominant inheritance with apparently complete penetrance: cases which generally also present at an early age. The unabbreviated term 'familial' will be retained to describe those cases of AD for whom at least one first degree relative can be identified who also suffers from the disease. Sporadic AD refers to those cases for whom no other family members can be identified as suffering from the disease, though this by no means implies that the disease is non-genetic in origin (Schellenberg, 1995). Significantly, no consistent, recognisable clinical pattern can be discerned that would allow differentiation of sporadic AD from FAD cases (Sandbrink *et al.*, 1996).

1.5.1.2 Amyloid Precursor Protein

The majority, if not all, of the FAD forms of AD have now been identified (Sandbrink *et al.*, 1996). Though they represent a minority of all cases of AD,

elucidation of their genetic basis and exploration of the mechanism by which these genetic abnormalities result in disease may point to fruitful avenues of research into the more common sporadic form of AD. The association between Down's syndrome and AD, and the localisation to the APP gene to chromosome 21, made the APP gene an obvious target for study (Schellenberg, 1995). The first mutation in the APP gene to be associated with neurological disease was a point mutation in codon 693 of exon 17 that results in the substitution of glutamic acid with glutamine. This mutation is associated with Hereditary Cerebral Haemorrhage with amyloidosis of Dutch type, a rare disorder with an autosomal dominant inheritance that results in extensive amyloid deposition in the meningeal and cerebral microvessels. The disease is characterised by recurrent cerebral haemorrhages from the age of 25 years with death occurring prematurely in the sixth decade (Levy *et al.*, 1990). The identification of other mutations in the APP gene associated with FAD followed. John Hardy's group at St. Mary's Hospital Medical School (Goate *et al.*, 1991) identified a point mutation in codon 717 of exon 17 which results in an amino acid substitution. In these families, the amino acid three residues beyond amino acid 43 of β-amyloid, is converted from valine to isoleucine. Two other point mutations in codon 717 of exon 17 were identified in two other FAD kindreds which result in the substitution of valine with glycine (Chartier-Harlin *et al.*, 1991) and valine with phenylalanine (Murrell *et al.*, 1991). In 1992 a double mutation in exon 16 of the APP gene was identified that co-segregated with the AD phenotype in two Swedish families with early onset disease (Mullan *et al.*, 1992). These two base pair changes result in the substitution of two amino acids immediately preceding the β-amyloid sequence. The Swedish double mutation results in the conversion of codon 670 from lysine to asparagine and the conversion of codon 671 from methionine to leucine. A further mutation has been identified within the β-amyloid sequence of APP that co-segregates with a clinical presentation of cerebral haemorrhage and early onset

dementia in a family of Dutch origin. This mutation at codon 692 results in the replacement of alanine with glycine (Hendriks *et al.*, 1992).

1.5.1.3 Apolipoprotein E and Alzheimer's Disease

The apolipoprotein E gene appears to act as a susceptibility gene for the development of late onset sporadic AD (Saunder *et al.*, 1993), sporadic AD (Rebeck *et al.*, 1993) and late onset AD in families in which at least one other member can be identified who has the disease (Strittmatter *et al.*, 1993). Apolipoprotein E is a protein constituent of plasma lipoproteins that exhibits high affinity binding to the low density lipoprotein (LDL) receptor, leading to cellular uptake and degradation of cholesterol and other lipids. Two other receptors bind apolipoprotein E containing complexes: the LDL receptor-related protein (LRP), also known as the α_2-macroglobulin receptor (Rebeck *et al.*, 1993), and a postulated hepatic receptor known as the 'chylomicron remnant receptor' (Mahley, 1988). While plasma lipoproteins are crucial to lipid transport and cholesterol homeostasis (Pitas *et al.*, 1987), the precise function of brain apolipoprotein E is unknown, though it is postulated to play a role in lipid transport, tissue repair, immunoregulation and the modulation of cell growth and differentiation (Mahley, 1988). Since, unlike plasma, there is no apolipoprotein B in cerebrospinal fluid (CSF), apolipoprotein E is a major lipoprotein in the CSF.

Apolipoprotein E is secreted by astrocytes, including specialised astrocytic cells, but not by neurons or other glia (Boyles *et al.*, 1985). The CNS is second only to liver as a source of apolipoprotein E. Rat astrocytes in primary culture possess LDL receptors capable of binding and internalising apolipoprotein E containing lipoproteins (Pitas *et al.*, 1987). Furthermore, Pitas and co-workers (1987) have demonstrated that LDL receptors are down-regulated by the internalisation of

lipoprotein cholesterol. Thus, appropriate lipid metabolism in brain requires co-ordination of both apolipoprotein synthesis and LDL receptor expression.

Three major apolipoprotein E alleles, ε2, ε3 and ε4, exist at a single gene locus on chromosome 19 (Das *et al.*, 1985). The apolipoprotein E isoform ε3 is regarded as the parent form of the protein, with the ε2 and ε4 forms existing as variants (Mahley, 1988). Apolipoprotein E ε2 differs from the parent form by a single amino acid: the arginine at position 158 is replaced by a cysteine residue. Apolipoprotein E ε4 differs from apolipoprotein E ε3 at amino acid position 112 by substitution of the cysteine for an arginine. Post-translational glycosylation results in a secondary form of polymorphism of apolipoprotein E.

The different apolipoprotein E alleles appear to affect the rate of expression of AD (Corder *et al.*, 1993). Corder and co-workers (1993) studied individuals aged 60 years and above, both affected and unaffected by AD, who had a family history of late onset AD. They observed that the proportion of AD afflicted individuals increased with the number of ε4 apolipoprotein E alleles, such that the rate of development of AD was 20% of individuals bearing the genotype ε2/ε3 or ε3/ε3, 47% of individuals with the genotype ε2/ε4 or ε3/ε4 and 91% of subjects bearing the ε4/ε4 genotype. The age of onset of the disease was also decreased in proportion to the number of ε4 alleles. The authors concluded that a double dose of the ε4 allele was virtually sufficient to cause AD by the age of 80 years. The apolipoprotein ε4 allele is not, however, either necessary nor sufficient to cause AD, since between 50 and 60% of all AD patients do not possess such an allele (Schellenberg, 1995), and not all ε4/ε4 individuals develop the disease (Sandbrink *et al.*, 1996).

Zubenko and co-workers (1994), in a series of autopsy-confirmed cases, confirmed the association between apolipoprotein E ε4 genotype and AD, though not the association between the dosage of the ε4 allele and the age of onset of the disease. Kawamata and colleagues (1994), in their study of Japanese patients, found a significantly increased frequency of the ε4 apolipoprotein E allele in patients with late onset sporadic AD, but not in those with early onset sporadic AD or in vascular dementia compared with controls. However, Frisoni and co-workers (1994) found an association between the apolipoprotein E ε4 allele and not only AD, but vascular dementia and dementia of the frontal type, in a Caucasian population.

The contention, that the association between apolipoprotein E ε4 genotype and AD is the result of a genetic linkage disequilibrium, is rejected by Tsuda and colleagues (1994) who studied the allelic frequency of polymorphisms in the apolipoprotein E and apolipoprotein CII genes in late onset AD and control subjects of Ashkenazi Jewish origin. The authors found that the apolipoprotein E ε4 genotype was associated with late onset AD, but that apolipoprotein CII, which lies within 50 kb of apolipoprotein E gene, was not. Thus, the authors demonstrated in this single ethnic group that the two genes do not necessarily co-segregate. While they point out that this does not exclude a genetic linkage disequilibrium, it makes it less likely. Further, the association of apolipoprotein E genotype with late onset AD in diverse ethnic groups argues against a spurious association between the two.

In vitro studies regarding the binding of apolipoprotein E isoforms to β-amyloid have yielded conflicting results. Strittmatter and colleagues (1993) observed that the β-amyloid peptide bound more avidly to the ε4 than to the ε3 form of apolipoprotein E while, in contrast, LaDu and co-workers (1994) found a higher degree of binding of β-amyloid to the ε3 than to the ε4 isoform. In addition, the

microtubule-associated protein *tau* has been demonstrated to bind avidly, *in vitro*, to the apolipoprotein E ε3 isoform, but not to the ε4 isoform (Strittmatter *et al.*, 1994). Strittmatter and colleagues (1994) demonstrated that it is the LDL receptor-binding domain of apolipoprotein E ε3 that interacts with *tau*. *Tau* adheres to apolipoprotein E ε3 through its microtubule-binding domain, the region believed to cause the self-assembly of *tau* into paired helical filaments. The authors suggest that interactions between *tau* and specific isoforms of apolipoprotein E may regulate the metabolism of *tau* and influence the rate of formation of paired helical filaments and NFTs. Wisniewski and his colleagues (1993) suggest, from their work on the binding of apolipoprotein E to synthetic β-amyloid bound to affinity membranes, that apolipoprotein E is capable of binding to soluble β-amyloid, a normally occurring peptide in the CSF and other biological fluids.

In AD, apolipoprotein E immunoreactivity is present on NFTs and neuropil threads, and on the amyloid of senile plaques and the congophilic angiopathy of cerebral vessels (Namba *et al.*, 1991). Wisniewski and Frangione (1992) suggest that apolipoprotein E acts as a pathological chaperone that reduces the solubility, and promotes the aggregation, of β-amyloid and other amyloidogenic proteins. Han and colleagues (1994a), predictably, found immunochemical evidence of apolipoprotein E in non-neuronal cells and tangle bearing neurons in AD. However, they also identified apolipoprotein E in neurons free of neurofibrillary pathology in AD and in the hippocampal neurons of aged, non-demented controls. They concluded that apolipoprotein E is a feature of apparently normal hippocampal neurons in AD, Parkinson's diseased and normal aged brain. Thus, since apolipoprotein E is intraneuronal, it may be capable of influencing the development of neuronal pathology in AD from its earliest stage (Han *et al.*, 1994)

1.5.1.4 Presenilin 1 and Presenilin 2

It became clear that mutations in APP could not be responsible for most of the cases of either FAD or late onset AD, since no linkage to chromosome 21 could be found in studies involving large numbers of such families, and recombinants between the APP gene and the FAD gene were found in a large numbers of FAD kindreds (Schellenberg, 1995). Evidence of linkage of FAD to a locus on chromosome 14 was first made by Schellenberg and colleagues in 1992. In 1995, Sherrington and co-workers identified five different missense mutations in a novel gene on chromosome 14 referred to as S182 and later renamed presenilin 1. In total thirty-one FAD associated mutations have now been identified in this gene (Sandbrink and Beyreuther, 1996), which is believed to encode an integral membrane protein that spans the membrane between six and nine times (Sandbrink *et al.*, 1996). Sherrington and colleagues (1995) hypothesise that it functions as a receptor, channel protein or structural membrane protein. Mutations in presenilin 1 are believed to account for approximately 70% of all cases of FAD (Sandbrink *et al.*, 1996).

However, genetic linkage to chromosomes 21, 19 or 14 could not be established for a smaller group of FAD families referred to as the 'Volga Germans', implicating a further gene responsible for FAD. The Volga Germans emigrated from the Hesse region of Germany to the Volga valley in Russia in the 1760's where they remained culturally distinct from the local population. At the end of the nineteenth century a further migration of this kinship to the USA occurred. Missense mutations amongst these subjects have been identified by two research groups. Levy-Lahad and co-workers (1995) discovered a point mutation in a gene on chromosome 1, later to be denoted presenilin 2, that was highly homologous to the presenilin 1 gene on chromosome 14 already discovered. The base substitution they uncovered in

codon 141 resulted in the conversion of asparagine to isoleucine. The same substitution was identified simultaneously by another group (Rogaev *et al.*, 1995), who documented a further point mutation at codon 239 resulting in the replacement of methionine with valine in a family of Italian origin with pathologically confirmed FAD.

Significantly, all of the FAD mutations examined thus far are associated with an increase in the levels of extracellular β-amyloid(1-42), with or without increased levels of extracellular β-amyloid(1-40) (Sandbrink and Beyreuther, 1996). However, as Sandbrink and Beyreuther (1996) observe, only 10% of sporadic AD subjects exhibit increased plasma β-amyloid(1-42) levels. Nevertheless, such a marker may be of diagnostic importance in the future if it allows targeting of effective preventive strategies if, and when, these become available.

1.5.2 Head Injury and Alzheimer's Disease

Severe head injury resulting in concussion is the environmental factor most consistently associated with AD (Gentleman *et al.*, 1993). Rarely, classical AD has been documented to occur after a single severe head injury (Rudelli et al. 1982).

Dementia pugilistica afflicts approximately 17% of professional boxers as a result of repeated head trauma (Roberts *et al.*, 1990a) and the condition has also been documented in a victim of repeated domestic violence (Roberts *et al.*, 1990b). These individuals exhibit cortical NFTs that are immunochemically and morphologically indistinguishable from the NFTs of AD, and β-amyloid deposition in the form of diffuse plaques. In addition, abnormalities of the septum pellucidum, cerebellar scarring and loss of pigmented neurons in the substantia nigra (Roberts et al. 1990)

are also seen. The link between trauma and AD is unclear, but Gentleman and co-workers (1993) hypothesise that head trauma precipitates the deposition of β-amyloid in the brains of vulnerable individuals and that, further, the induction of APP expression in brain is a neuronal response to stress.

1.5.3 Other Factors Relating to the Development of Alzheimer's Disease

1.5.3.1 Inflammation and Immune System Dysfunction

Several lines of evidence point to the involvement of immune and inflammatory mechanisms in the pathophysiology of AD. The central amyloid cores of senile plaques in AD are surrounded by a halo of activated microglia for which β-amyloid may be the chemotactic stimulus (Davis *et al.*, 1992). Glial-derived proteins, such as α1-antichymotrypsin, heparan sulphate proteoglycan, apolipoproteins E and J, interleukin-1, interleukin-6 and other acute-phase proteins, are found in abundance in AD plaque amyloid (Saitoh *et al.*, 1997). Microglia, when activated, proliferate and undergo phenotypic and morphological changes (McRae *et al.*, 1997). They are known to possess antigens of the major histocompatibility complex (MHC) whose expression alters with the state of activation of the microglial cell (McRae *et al.*, 1997). Reactive microglia strongly expressing MHC surface glycoproteins are found in the plaques and NFTs of AD (Palmer, 1996). Cytokines, particularly interleukin-1, interleukin-6 and tumour necrosis factor, are the primary mediators of the acute phase response (Aisen and Davis, 1994). Microglia are the primary source of interleukin-1 in brain (Rothwell and Relton, 1993) and are likely to be pivotal to the acute phase response in brain (Aisen and Davis, 1994). Resting microglia are immunoreactive for β-2 integrins, some of which are receptors for complement proteins, and these molecules are up-regulated in reactive microglia (Akiyama and McGreer, 1990). It is thus conceivable, that the co-localisation of senile plaques and reactive microglia in AD is complement-mediated (Lue and Rogers, 1992).

Senile plaque amyloid and extracellular ghost tangles in AD are heavily decorated by complement proteins of the classical complement cascade (Itagaki *et al.*, 1994). The classical cascade, however, is usually activated by immune complexes. Though immunoglobulin deposition has been demonstrated immunochemically in AD brain, such immunoreactivity does not co-localise with senile plaques (Eikelenboom and Stam, 1982) and, indeed, may be artefactual, since extravascular leakage and uptake of serum proteins into neurons, especially damaged neurons, has been demonstrated in aged control and AD brains (Mori *et al.*, 1991). β-amyloid has been demonstrated, *in vitro*, to bind and activate C1q of the complement cytolytic pathway, which leads to activation of the classical complement cascade, in the absence of immunoglobulin (Rogers et al, 1992). Thus, β-amyloid may exert neurotoxic effects through complement activation in an antibody independent fashion (Aisen and Davis, 1994). Activation of the classical cascade of complement leads to the formation of a macromolecule known as C5b-9 or the 'membrane attack complex of complement' (MAC). This complex inserts itself into the lipid bilayer of cell membranes forming transmembrane channels that are implicated in cell lysis (Itagaki *et al.*, 1994). Using immunochemical techniques, Itagaki and colleagues (1994) demonstrated the presence of MAC-like deposits in association with dystrophic neurites and tangle bearing neurons in AD, suggesting that these structures are the targets of complement-mediated injury in the disease. The authors postulate that complement activation occurs at sites of amyloid deposition and that the resulting MAC inserts into neuronal membranes nearby. In a study of cerebellar plaques, MAC immunoreactivity could only be identified in senile and not diffuse plaques (Lue and Rogers, 1992). APP has itself been considered an acute phase reactant since interleukin-1 and interleukin-6 dramatically influence its expression (Aisen and Davis, 1994).

Individuals taking anti-inflammatory drugs long term, such as those suffering from rheumatoid arthritis, are believed to be less likely to develop AD (Palmer, 1996; Wilcock, 1996), and Breitner and colleagues (1995) report that sustained use of non-steroidal anti-inflammatory drugs is associated with a reduced risk, and delayed onset, of AD in sibships with a high risk of the disease. Rogers and colleagues (1993) in a small, double-blind, placebo-controlled trial, found that 100 to 150 mg per day of the non-steroidal anti-inflammatory drug indomethacin had a significant protective effect in mild to moderate AD.

However, the usually encountered stigmata of inflammatory disease are not apparent on physical examination of the AD patient (Aisen and Davis, 1994), and plasma concentrations of acute phase reactants in AD sufferers are similar to those of age-matched normal aged controls (Kalaria *et al.*, 1996a), suggesting that any inflammatory response is confined to the brain. Further, there is no direct evidence that inflammatory or immune mechanisms result in the stigmata of AD, and the slow progression of the disease is not in keeping with a disorder of inflammatory aetiology (Aisen and Davis, 1994).

Nevertheless, in 1994 Aisen and Davis concluded that sufficient evidence had accrued to warrant clinical trials of anti-inflammatory and immunosuppressive drugs in AD and results of the drug studies performed to date, suggest that these drugs are of some benefit in the disease (Wilcock, 1996; Kalaria *et al,* 1996a).

1.5.3.2 Educational Status

The prevalence of dementia, particularly AD, has been found to be inversely related to educational status (Ott *et al.*, 1995). This finding is reviewed by Katzman (1993), who proposes that education mediates its protective effect by stimulating an increase

in synaptic density in neocortical association areas. The consequent delay in the emergence of the symptoms of AD results in a reduction in the prevalence of dementia.

1.5.3.3 Gender and Oestrogen Deficiency

Age-specific prevalence rates of AD are higher for women than for men, and some studies suggest that the incidence rate of AD in women is higher also (Rocca *et al,* 1991). Some authors have proposed that oestrogen loss, associated with the menopause, might contribute to the increased risk of AD for women (Paganini-Hill and Henderson, 1994; Brenner *et al.*, 1994). Henderson and colleagues (1994), in a case-control retrospective analysis of oestrogen replacement therapy, found a significantly lower rate of oral oestrogen use among AD subjects compared with non-demented control subjects. AD subjects using oestrogen preparations at the time of the study did not differ from non-oestrogen users suffering from AD in terms of age, education or symptom duration, yet their mini-mental state examination scores were significantly better. The authors concluded that post-menopausal oestrogen replacement therapy may decrease the risk of AD and improve the cognitive performance of women with the disease. In contrast, Brenner and colleagues (1994), in a case-control study in which exposure to oestrogen was ascertained from computerised pharmacy records, found no evidence that oestrogen exposure had any impact on the risk of developing AD among women. In the light of the above studies, Tang and co-workers (1996) interviewed 1124 elderly women, initially free of AD, Parkinson's disease or stroke, about their use of oestrogen, and found that a history of oestrogen use during the post-menopausal period significantly delayed the onset, and lowered the risk, of AD.

1.6 Clinical Management of Alzheimer's Disease

Old age psychiatrists specialise in the care of people over the age of 65 years suffering from mental illnesses including dementia. They clinically examine, investigate and diagnose cases of dementia, and manage co-existing psychological and behavioural disturbances. They also support carers, place elderly people in appropriate care, gate-keep expensive investigations, advise on legal matters, such as power of attorney, act as advocates for their patients and occasionally act as the moral guardians of the elderly people in their care. They co-ordinate nursing, home-help and social services, advise and support general practitioners and other physicians, and liaise with voluntary bodies serving the elderly.

There are no drugs available, as yet, that are proven to be capable of preventing AD or delaying its onset (Schneider, 1996). Amongst the most promising agents are the cholinesterase inhibitors. Tacrine or 1,2,3,4-tetrahydro-9-aminoacridine (THA) was the first agent to be approved in the United States by the Food and Drug Administration for the treatment of AD and is a reversible, non-selective inhibitor of both acetylcholinesterase and butyrlcholinesterase. A statistically significant, though clinically modest, improvement in cognitive function has been demonstrated with THA (Rabins, 1996), though its use is complicated by an elevation in hepatic transaminase in a substantial number of patients taking the drug (Schneider, 1996). Donepezil hydrochloride (E2020) is a second generation acetylcholinesterase inhibitor that was cleared for marketing for the treatment of AD by the Food and Drug Administration in the USA in November 1996 and became the first UK licensed treatment for AD, amid a blaze of publicity (McIntosh, 1997), in April 1997. Donepezil hydrochloride, trade name Aricept, is a reversible selective inhibitor of acetylcholinesterase that has little effect on peripheral butyrylcholinesterase (Rogers *et al.*, 1991). Improvements in quality of life and

cognitive function have been demonstrated for donepezil hydrochloride in sufferers of mild to moderate AD (Rogers *et al.*, 1996). A month's supply of the 5 mg per day starting dose of the new drug costs £68 while a month's supply of the 10 mg per day dose costs £95. The approximate cost of donepezil hydrochloride per patient, per year, is one thousand pounds, yet since this amount is only sufficient to pay for three to four weeks of nursing home care, even slight clinical improvements as a result of the drug may make it a financially defensible option (McKeith, 1997).

The availability of a drug in the UK licensed specifically for the treatment of AD has profound implications for existing psychiatric and geriatric services. It is likely that, aside from the expense of the drug itself, demands on resources will rise as referrals for accurate diagnosis of dementia increase and existing services are forced to monitor systematically the physical, cognitive, psychological and behavioural effects of the drug on those individuals for whom it is prescribed. No doubt considerable energy will also be expended counselling those for whom the drug is deemed to be unsuitable. Further, autopsy confirmation of AD may become more attractive given the hope of treatment in promptly recognised AD in surviving family members.

The interpretation of a double-blind, placebo-controlled, multi-centre trial of selegiline and alpha-tocopherol in the treatment of moderately severe AD is complicated by differences in mini-mental state scores at base-line between the placebo and treatment groups (Sano *et al.*, 1997). When the authors adjusted for these differences in their analysis, both agents could be shown to significantly delay functional deterioration in those with the disease. No effect on cognitive function was observed. As Sano and colleagues (1997) point out, this finding requires replication and extension to groups of patients with less advanced disease. Other therapeutic approaches in AD include the use of muscarinic and nicotinic agonists,

modifiers of acetylcholine release, monoamine oxidase inhibitors and growth factors (See Schneider, 1996 for review).

1.7 Experimental Considerations

1.7.1 The Rationale for Using Human Post-mortem Tissue

The lack of a completely satisfactory animal model of AD is regarded by some as a major obstacle to AD research (Games *et al.*, 1995). Animal studies allow the living conditions, food and opportunities for socialisation of the animals, for example, to be controlled. The animals can be killed, not only swiftly, but in a uniform manner and dissection and freezing of the brain tissue can be rapid. The most promising animal model of AD is a transgenic mouse expressing all three major isoforms of a mutant human APP. These mice exhibit Alzheimer-like pathology in the form of numerous extracellular fibrillar deposits of β-amyloid, neuritic plaques, synaptic loss, astrocytosis and microgliosis. They do not, however, display NFTs: a major neuropathological hallmark of AD (Games *et al.*, 1995).

The use of human tissue for molecular biological research certainly poses a number of problems not encountered in animal work, yet these are not insurmountable, and certain benefits accrue from the use of such tissue. Wisniewski (1993) has described the brain as a 'multi-organ organ' with respect to the number of distinct, but inter-related, functional groups of cells within it and, indeed, no less than a third of the genome is committed to brain mRNA (Harrison and Pearson, 1989). No doubt there are important species-specific aspects of brain function, such that no model of a uniquely human neuropsychiatric disease like AD can be complete in all its respects. Identifying and grappling with the difficulties posed by the use of human tissue in experimental work allows us to work with the real disease: a crucial

complement to animal and tissue culture work in arriving at a balanced understanding of AD.

Consent for the use of tissue for research purposes can be faced squarely with human subjects, though requesting permission for autopsy is not without its difficulties (Turner and Raphael, 1997). Further, the confirmation of AD already requires removal of tissue at autopsy or biopsy for neuropathological examination (Powers *et al.*, 1992). It is also conceivable that identifying the problems inherent in the use of human tissue for research, and adapting to accommodate them, may expand the number of applications for which human tissue is suitable. It is likely that demand for accurate post-mortem diagnosis of AD will increase in the future, in order to refine diagnosis of the disease during life now that drugs specifically aimed at AD are available. It is conceivable that the availability of tissue for research purposes will increase also.

Tissue from brain biopsy is rarely available in the UK, most tissue being obtained at post-mortem. The processing of post-mortem brain can be time-consuming. The brain must be manipulated from the cranium, weighed, examined for evidence of gross pathology and dissected, before tissue can be taken for freezing. Scrutiny of all aspects of the handling of post-mortem human tissue is necessary if it is to be optimally preserved.

It is possible to extract approximately 600 μg/g of total RNA from post-mortem human tissue, and no significant differences in yield of either total RNA or mRNA per gram of tissue have been demonstrated between normal and diseased human post-mortem brains (Leonard *et al.*, 1993). However, the yield, intactness and activity of RNA may vary several fold between individual human brains (Barton *et*

al., 1993; Harrison *et al.*, 1995). Ross and colleagues (1992) found that the difference in mRNA levels between sample groups was dwarfed by inter-individual differences in mRNA. This study is instructive since, though differences in the interval between post-mortem and freezing of the tissue between the sample groups was addressed, pre-mortem factors such as pyrexia, drug use, hypoxia and mode of death, were not. Such heterogeneity in routine clinical samples may necessitate the use of large numbers of subjects to ensure statistically meaningful results (Leonard *et al.*, 1993) and render minor differences in RNA between sample groups invisible (Barton *et al.*, 1993). Similarly, AD subjects must be appropriately and carefully matched to a control group of subjects free of neurological disease. In addition, positive controls, such as individuals suffering from non-AD neurodegenerative conditions like Picks disease, multi-infarct dementia and Parkinson's disease, are useful in controlling for non-specific factors associated with chronic neurodegenerative brain disease (Harrison *et al.*, 1991a). Three other factors are of importance in the use of post-mortem human tissue for the study of mRNA: the interval between death and freezing of the tissue, known as the post-mortem interval or PMI, the pre-mortem course of the patient's illness, also known as the agonal state, and storage of the tissue prior to use.

1.7.2 The Effect of Agonal State on RNA levels in Post-mortem Human Brain

No effect of agonal state has been demonstrated on overall levels or activity of RNA in post-mortem human brain (Barton *et al.*, 1993). However, there is evidence that some mRNAs are vulnerable to the effects of agonal state (Barton *et al.*, 1993), while others are not (Harrison *et al.*, 1993). Harrison and colleagues (1991a), in a study of temporal cortex from individuals with AD and other neurodegenerative conditions, found no association between total polyadenylated mRNA levels and

duration of coma. However, glutamate decarboxylase (GAD) activity and M1 muscarinic receptor mRNA levels both significantly declined in association with increasing duration of coma. Other mRNA species, such as hsx70 a member of the 70 kDa heat shock protein family, appear to be uninfluenced by agonal state factors such as pyrexia and coma (Harrison *et al.*, 1993). The basis of this selective vulnerability of mRNA species to the effects of agonal state is unknown (Barton *et al.*, 1993).

In 1976, Bowen and colleagues demonstrated that GAD activity in post-mortem human brain was affected by agonal state and hypothesised that terminal cerebral hypoxia was responsible for its depletion. Tissue pH is also related to the severity of agonal state (Harrison *et al.*, 1995; Yates *et al.*, 1990) and has been found to be a useful measure of pre-mortem acidosis and hypoxia (Barton *et al.*, 1993). Yates and co-workers (1990) found GAD activity to be correlated with tissue pH and lactate in human post-mortem brain and concluded that acidosis, consequent upon terminal hypoxia, has a detrimental effect on GAD activity. Harrison and colleagues (1995) concluded that the pH of homogenised brain tissue was superior to clinical assessment of pre-mortem course in predicting the preservation of mRNA. A linear relationship exists between brain and CSF pH and, moreover, brain pH is stable after death and during freezer storage (Harrison *et al.*, 1995). Harrison and co-workers (1991b) found no relationship between pH and poly(A^+) mRNA levels in human post-mortem brain, and though they demonstrated that some mRNA species were vulnerable to pH, others were not. The study of enzyme activity in post-mortem human brain has similarly revealed that the activity of some enzymes is influenced by pH while others are resistant to the effects of acidosis (Yates *et al.*, 1990).

Kingsbury and co-workers (1995) studied a large series of normal and neurologically diseased subjects and found that tissue pH was strongly correlated with the preservation of four specific mRNA species: aldolase C, an enzyme, β-tubulin, a structural protein, and preproenkephalin and preprotachykinin, both neurotransmitter peptides. Acidotic samples were associated with low or absent ISHH signal over all three brain regions studied, and electrophoresis and Northern blotting of these samples demonstrated little intact ribosomal RNA. Age of the subjects at death did not appear to influence the vulnerability of mRNA to degradation. Most of the diseased brains employed in this study were obtained from individuals who had suffered from Parkinson's disease and no association was identified between brain disease and brain tissue pH. Further, mRNA preservation was similar in control and diseased brains of similar pH. While Kingsbury and colleagues (1995) found no difference in the relationship of pH to mRNA across the three brain areas studied, Harrison and colleagues (1995) suspect that there may be regional differences in the response of mRNA to pH.

1.7.3 The Effect of Post-mortem Interval on RNA Levels in Post-mortem Human Tissue

The effect of PMI has been extensively studied in relation to post-mortem human tissue (See Barton *et al.*, 1993 for review). Ross and co-workers (1992) found RNA degradation correlated poorly with PMI, and Leonard and colleagues (1993), in their examination of the suitability of brain bank tissue for RNA work, concluded that PMI was unlikely to be a significant factor in the degradation of RNA. Robinson and co-workers (1994) found no relationship between RNA degradation and a PMI of up to 24 hours. Barton and colleagues (1993), in a review of the subject, concluded that abundant and biologically active RNA exists in human tissue frozen 36 or more hours after death, and that as such routine autopsy tissue is suitable for

RNA studies. Harrison and co-workers (1995) have confirmed, in the rat, the robustness of RNA to the effects of increasing PMI, demonstrating no effect of a PMI of up to 48 hours. Data from rat studies also confirm that no changes in mRNA occur in the first few hours after death, a time period inaccessible to investigators using post-mortem human tissue (Harrison *et al.*, 1995), and this concurs with the findings in biopsied human tissue (Barton *et al.*, 1993). Kingsbury and colleagues (1995) found no correlation between PMI and mRNA preservation among either their control or neuropathologically diseased subjects, suggesting that the presence of disease does not make mRNA degradation with increasing duration of PMI more likely.

Unsurprisingly, no correlation has been demonstrated between poly(A^+) mRNA levels and PMI (Barton *et al.*, 1993). The conclusion, however, that all mRNA species are equally impervious to PMI may be erroneous (Leonard *et al.*, 1993; Barton *et al.*, 1993), since as Barton and co-workers (1993) caution, the effect of PMI on peptides is selective and, while disease state, age and region of brain (Ross *et al.*, 1992) have not been demonstrated to influence the sensitivity of mRNA to PMI, it cannot be concluded that this is invariably the case (Barton *et al.*, 1993). Robinson and colleagues (1994), in a study of post-mortem human neocortex, found that sensitivity to degradation differed between mRNA transcripts, and Burke and co-workers (1991) found the three major isoforms of APP mRNA to be differentially affected by pre-mortem and post-mortem variables.

Johnston and co-workers (1996a) employed solution hybridisation-RNase protection assay to examine the effects of PMI on APP mRNA levels in AD brain and in the brains of non-demented controls and those with other neurological diseases. This technique can be performed on fragmented mRNA and is sensitive; it can detect 1 ρg

of target mRNA and so does not require target amplification using the polymerase chain reaction. Johnston and colleagues (1996a) found a significant correlation between increased duration of PMI and reduced APP, APLP2 and KPI-containing isoforms of APP mRNA in the superior frontal, but not mid-temporal cortex, in AD. No correlation between PMI and mRNA reduction was observed for the control groups, even though the longest PMI in the AD group was only 280 minutes while the PMI in the control groups were generally longer than this. Johnston and colleagues (1996a) speculate that a region-specific loss of APP and APLP2 mRNA may be occurring in AD tissue in the hours immediately following death that are masked by using longer PMI. In contrast, Harrison and colleagues (1994) found no effect of PMI on APP mRNA levels in the frontal cortex in AD in a series of rapid autopsy brains using ISHH. The longest PMI of the brains used was 210 minutes. It is conceivable that solution hybridisation-RNase protection assay is more sensitive to the amounts of specific mRNA species than ISHH. In conclusion, while it appears that PMI is not a barrier to the use of human post-mortem tissue for RNA research, specific mRNA species in specific brain areas may be adversely affected by PMI. Therefore, scrupulous attention to matching pre-mortem and post-mortem variables between diseased and control subjects is advised (Burke *et al.*, 1991).

1.7.4 Freezer Storage of Post-mortem Human Tissue

Leonard and co-workers (1993) concluded that less than five years freezer storage of post-mortem human tissue does not significantly diminish the yield of mRNA, but that storage of tissue for more than five years might be detrimental to specific mRNA species. Harrison and co-workers (1995) found no loss of any of the eight species of mRNA they studied in post-mortem human brain with freezer storage of up to 33 months at -70°C. There is widespread agreement, however, that repeated thaw-freeze cycles are deleterious to mRNA (Ross *et al.*, 1992; Harrison *et al.*,

1995). The true limit of freezer storage of post-mortem human tissue is unknown (Harrison *et al.*, 1995).

1.8 Aims and Objectives

Gene expression encompasses all of the events from the transcription of deoxyribonucleic acid (DNA), the genetic basis for heredity, into messenger ribonucleic acid (mRNA), to the delivery of a functionally competent protein to the correct location. Messenger RNA is, thus, a key intermediary in gene expression (Harrison *et al.*, 1991) and accounts for between 3% and 5% of total cellular RNA. Messenger RNA levels are dynamic and accessible to study using techniques such as RNA extraction, purification of mRNA from total RNA, Northern blotting, reverse transcription, the polymerase chain reaction, *in vitro* translation and *in situ* hybridisation histochemistry. The presence of a specific mRNA indicates that the region or cells examined are actively transcribing the corresponding genes and are synthesising the encoded protein. Further, in general, the abundance of a given mRNA reflects the rate of synthesis of the encoded protein (Harrison *et al.*, 1991b). As is usual in RNA research (Barton *et al.*, 1993), this study concentrated on the examination of a number of specific species of mRNA, although in some cerebral regions measurements of total mRNA were also made. The techniques of RNA extraction, Northern blotting, reverse transcription, amplification of reverse transcribed mRNA by the polymerase chain reaction and *in situ* hybridisation histochemistry were employed in this study to explore mRNA levels in an attempt to elucidate further the molecular underpinnings of AD.

The brain in AD is characterised by abnormal peptide aggregations in the form of β-amyloid containing plaques and NFTs, and by the persistence of usually short-lived peptides such as ubiquitin, a member of the evolutionarily conserved heat

shock protein family. It is unclear whether increased gene expression, unusual stability of the peptide produced, failure of the degradative pathways or a combination of these factors, results in the abnormal accumulation of these peptide forms.

The expression, in AD, of two specific mRNA species, Goα, a member of the heterotrimeric G protein family involved in signal transduction, and ubiquitin, a peptide that tags abnormal and short-lived proteins in an energy dependent process in preparation for their proteolysis, was addressed in this thesis. The rationale for the selection of these particular species of mRNA in relation to AD is discussed fully in the appropriate chapters. However, the main body of work contained in this thesis addresses the expression of APP mRNA in AD. The deposition of β-amyloid appears to play a fundamental role in the pathophysiology of AD (Wilcock, 1996) and simple overexpression of APP, as is proposed to be the case in Down's syndrome, might be one mechanism by which the aggregation of β-amyloid is triggered (Harrison *et al*, 1996). However, although the question as to whether APP mRNA expression in the brain is indeed altered in AD is a pivotal one, it has been exceedingly difficult to answer unequivocally (Harrison *et al*, 1996). The basis upon which an attempt was made to answer this question definitively was as follows. Brain tissue was carefully selected from a large number of human post-mortems. In some cases this tissue was characterised by the availability of pre-mortem and post-mortem information unparalleled in its detail. Control and diseased brains were assiduously matched for known confounding variables and accepted methods of handling the raw data generated were critically appraised. Following the exacting prosecution of this work, the advice of a biomedical statistician was sought to ensure that the complex statistics performed on the raw data were exemplary and the conclusions drawn beyond reasonable doubt.

Chapter 2

Materials and Methods

2.1 Introduction

In situ hybridisation histochemistry (ISHH), the main technique employed in this thesis, has been described as an elegant synthesis of molecular biology and histology (Palmert *et al*, 1988). This method is particularly apposite to the study of complex heterogeneous populations of cells such as exists in the central nervous system, since in allows scrutiny of gene expression within both discrete anatomical regions and single cells.

ISHH allows the detection, localisation and relative quantitation of mRNA species by the use of specifically designed and tagged probes. The tendency for the basic side chains of single stranded nucleic acids to form stable bonds in a highly specific way is the principle upon which ISHH is based. The nucleic acids DNA and RNA are linear polymers composed of nucleotides. Each nucleotide is composed of a pentose, a phosphate group and a basic side-chain. The basic side-chains, the purines guanine (G) and adenine (A), and the pyrimidines, cytosine (C), thymine (T) and uracil (U), form base pairs according to the following rules: G forms three bonds with C, and A forms two bonds with T, in DNA, or U, in RNA. Where the nucleotide sequence of a target mRNA is known, a strand complementary to it, and in the reverse orientation, can be synthesised. Under predetermined conditions this 'probe' is allowed to hybridise to the mRNA of the tissue specimen under investigation. Appropriate tagging of the probe allows the hybrids to be detected by either autoradiographic or histochemical means. Accompanying controls are designed to minimise the risk of the probe hybridising to a similar, but unrelated,

mRNA and to quantify the extent of non-specific binding of the probe to the tissue or glass slide.

Messenger RNA is transcribed from nuclear DNA by RNA polymerase II. Within the nucleus, the introns of the primary transcript are spliced out and a cap of 7-methylguanosine attached to the 5' end. A sequence of adenylate residues attached to the 3' end of the mRNA, the poly(A)$^+$ tail, is also added to most mRNAs before they are transported, fully matured, to the cytoplasm. The presence of a particular mRNA in the cytoplasm of a cell is suggestive that the cell is actively synthesising the encoded peptide, and in an amount proportional to the abundance of the mRNA. Of course, ISHH cannot guarantee the integrity of the detected mRNA or establish that it is being translated normally, nor can it provide assurance that any protein produced will reach its correct destination and be functionally active on its arrival.

ISHH in this study was performed on cryostat cut frozen tissue sections mounted on glass slides. It therefore allowed the examination of specific mRNAs without disruption of the surrounding tissue, permitting not only regional, but cellular, localisation of the mRNA under study. Clearly, ISHH, which can allow examination of a specific region or cellular type, has important advantages over techniques that involve the homogenisation of a mixed population of cells.

The probes employed in this thesis were 30 to 45 base oligodeoxynucleotide probes, commercially synthesised to order, and 3' end labelled with radioactive [^{35}S]dATP. Radioactive labels have the advantage of superior sensitivity over non-radioactive methods and the β particles emitted by this isotope are of relatively low energy (167 keV) permitting single cell resolution of ISHH signal. While excellent accuracy is also achievable with the low energy β particles (18.5 keV) emitted by [^{3}H], the

12.35 year half life, and therefore long exposure times required by this isotope, preclude its convenient use. In this respect [^{35}S] with its 87.5 day half life and thus relatively short exposure times compares favourably. While the half life of [^{32}P] is only 14.2 days, the high energy β particles emitted by this isotope (1.6 MeV) result in relatively poor spatial resolution of ISHH signal and necessitate the use of appreciable protective shielding.

2.2 Preparation for ISHH

Endogenous and exogenous ribonucleases, capable of degrading the desired target mRNA, are ubiquitous. Precautions were taken to eliminate, as far as possible, contamination by ribonucleases. Deionised purified water, incubated with diethylpyrocarbonate (DEPC) and subsequently autoclaved, was used for all solutions. Prepared solutions, glassware and plasticware were autoclaved before use. Disposable, sterile gloves were used throughout the procedure.

2.3 Collection of Post-mortem Human Brain Tissue

Four series of brains were used in the course of this work, the details of which are presented in appendix II. Series I and II comprised brains collected mainly from Oxford (courtesy of Drs. B. McDonald and M. Esiri, Radcliffe Infirmary) but also from the North Middlesex Hospital, London (courtesy of Dr. W.J. Harrison). Donated control brains, in these series, were accepted from individuals clinically free of neuropsychiatric disease. Series III was obtained from the Oxford Study to Investigate Memory in Ageing (OPTIMA) project (courtesy of Drs. P.J. Harrison, Z. Nagy, B. McDonald, M. Esiri, C. Joachim, J. Morris, L. Barnetson and A.D. Smith). The use of brains from Series III afforded the opportunity to study tissue obtained from individuals, both dementia sufferers and age matched controls, who were extensively investigated during life. Series IV comprised selected cases from Series

II and Series III, supplemented by cases studied by two other independent investigators working in Professor Pearson's laboratory, Dr. A.J. Barton and Dr. M. Griffith.

The brains were dissected by Drs. P.J. Harrison, B. McDonald and Prof. M. Esiri (Department of Neuropathology, University of Oxford) or Prof. P. Lantos (Medical Research Council Brain Bank, Department of Neuropathology, Institute of Psychiatry, London). All AD cases were diagnosed clinically and satisfied standard histopathological criteria for the disease (Khachaturian, 1985).

At post-mortem, tissue blocks of approximately 1 cm^3 were taken from visual cortex (Brodmann area 17), middle temporal gyrus (Brodmann area 21) and mid-hippocampus. Tissue blocks from Series I and II were embedded in OCT embedding compound on a dry ice and alcohol slurry and stored at -70°C in individual plastic bags. Series III tissue blocks were mounted on cork discs with OCT embedding compound and stored at -70°C in individual plastic bags. Ten μm (Series I and II) or eighteen μm (Series III), fresh frozen sections were cut on a Bright cryostat at -20°C with the assistance of Mr M.W. Sanders and Miss J.M. Heffernan, and thaw mounted on subbed slides (see appendix I). Thereafter, the sections were stored at -20°C for less than two weeks until pre-treated. The sections were labelled with individual codes that gave no indication as to diagnosis; thus sections were processed blind to case details.

2.4 Pre-treatment of Cryostat Cut Frozen Tissue

Pre-treatment of the mounted, cryostat cut, frozen sections prior to ISHH had three objectives: to preserve tissue RNA, protect the cytoarchitecture of the tissue and minimise non-specific binding of the radio-labelled oligodeoxynucleotide probes

(Heath *et al*, 1996). In addition, the fixative chosen had to permit adequate penetration of the probe.

The sections were allowed to thaw at room temperature and then transferred to autoclaved racks. Where possible, solutions and equipment were autoclaved before use. All solutions used were at room temperature and the procedure was carried out in a fume hood. The following solutions were used:

4% paraformaldehyde/phosphate buffered saline	5 minutes
Phosphate buffered saline	Brief rinse
Triethanolamine hydrochloride/acetic anhydride	10 minutes
Phosphate buffered saline	Brief rinse
70% ethanol	2 minutes
80% ethanol	2 minutes
95% ethanol	2 minutes
100% ethanol	2 minutes
Chloroform	10 minutes
100% ethanol	1 minute
95% ethanol	1 minute

Paraformaldehyde (PFA) was freshly prepared before use, because of its tendency to polymerise on standing, and particular care was taken to time this step accurately. PFA, an aldehyde fixative, acts by promoting cross-linking of tissue proteins and combines superior mRNA retention and good tissue morphology with adequate probe penetration. An approximate physiological solution with buffering capacity, phosphate buffered saline, was used to rinse the tissue.

The acetic anhydride acetylates basic proteins and neutralises negative charges on the glass slides, preventing electrostatic binding of the radio-labelled oligodeoxynucleotide probe to the specimen and surrounding slide. It cannot be autoclaved and was added to the triethanolamine immediately prior to use. Following dehydration of the tissue by immersion in increasing concentrations of alcohol, delipidation of the sections was achieved by a ten minute incubation in chloroform. Lipids are present in high concentration in nervous tissue and promote troublesome non-specific binding of oligodeoxynucleotide probes. The sections were air dried, returned to their boxes and stored at -20°C until needed. Pre-treatment solutions were discarded after treatment of approximately 200 sections. For details of all solutions see appendix I.

2.5 Oligodeoxynucleotide Probe Selection

DNA probes are inherently more robust than RNA probes. The shorter the nucleotide sequence chosen as the probe, the higher the chance of this same sequence existing in another unrelated mRNA. In practice probe sequences of 30 to 45 bases can be highly target specific. Full length probes show poorer tissue penetration than oligodeoxynucleotide probes, require higher hybridisation temperatures, with the risk of tissue damage, and are obviously unsuitable for investigation of alternatively spliced variants of a single gene. The incorporation of radioactively labelled bases into full length probes can improve sensitivity of signal when investigating a very low copy gene or when using less suitable tissue. In this study, however, 3' end labelling, in which approximately 10 labelled bases are added to each oligodeoxynucleotide probe, provided perfectly satisfactory sensitivity in relation to the mRNA species examined.

HPLC purified oligodeoxynucleotide probes were purchased from Oswel DNA Services (Edinburgh) and later obtained from the UK Human Genome Mapping Project Resource Centre free of charge. Oligodeoxynucleotide probes of 30 and 45 bases, that were complementary, and in the reverse orientation, to the region of the target mRNA selected, were designed and synthesised to order. The published cDNA sequence of the mRNA under investigation was scanned for an area of 30 or 45 nucleotides of which approximately 50% had guanine or cytosine bases. A higher GC content increases the stability of the probe-mRNA hybrids and so increases the required hybridisation and wash temperatures. Areas of the mRNA likely to encode amino acid sequences shared with other functionally related proteins were avoided. Sense oligodeoxynucleotide probes with an identical sequence of bases in the same orientation as the target region of the mRNA species to be examined, were synthesised to allow for correction of non-specific binding.

The proposed sense and antisense sequences were checked against the European Molecular Biology Laboratory gene database to establish whether the same nucleotide sequence, with up to 4 mismatches, existed in another published sequence. Such a precaution does not, of course, exclude the possibility that another, as yet unidentified mRNA exists with a similar nucleotide sequence to which the probe might bind. If no homologies were found the oligodeoxynucleotide probe was ordered. Where other considerations were pertinent to probe selection they are discussed in the individual chapters.

The oligodeoxynucleotide probes were stored at a concentration of 2 pmoles/μl in 50 μl aliquots at -70°C until needed.

2.6 Calculation of Melt Temperature

The stability of the oligodeoxynucleotide probe-mRNA hybrids depends on a number of factors such as the number of GC as opposed to AT bonds maintaining the hybrid, the degree of mismatch between the probe and the mRNA, the concentration of sodium ions and the presence of destabilising agents, such as formamide, in the hybridisation buffer, the length of the probe and the temperature at which hybridisation and washing take place. The temperature at which 50% of the hybrids spontaneously dissociate the 'melt temperature' (Tm) is calculated according to the following formula (Davis *et al*, 1986):

$$Tm\ (°C) = 16.6 \log[M] + 0.41[Pgc] + 81.5 - Pm - B/L - 0.65[Pf]$$

Where:

M is the molar concentration of sodium ions to a maximum of 0.5. (0.5 for the concentration of sodium ions during hybridisation and 0.195 for the concentration of sodium ions during washing).

Pgc is the percentage of G and C nucleotides in the oligodeoxynucleotide probe sequence.

Pm is the percentage of mismatches between the oligodeoxynucleotide probe and the target mRNA.

Pf is the percentage of formamide in the buffer.

B is 675 for synthetic oligodeoxynucleotide probes of up to 100 bases.

L is the length of the oligodeoxynucleotide probe.

Temperatures of 15°C below the calculated hybridisation and wash temperatures were found to give adequate specificity without loss of sensitivity.

2.7 Preparation of ^{35}S Labelled Oligodeoxynucleotide Probes

The antisense and sense oligodeoxynucleotide probes employed in this study were 3' end labelled with [^{35}S]dATP. Approximately 10 radioactively labelled deoxyadenylate nucleotides, not themselves specific for the target sequence, were added to each oligodeoxynucleotide probe. The oligodeoxynucleotide probes used were prepared and purified using a commercially available kit (NEN/DuPont oligonucleotide 3' end labelling system). Sterile gloves were worn throughout the procedure and all plasticware used was autoclaved before use. 3' end labelling of the probes with [^{35}S]dATP (NEN/DuPont) was carried out as detailed below.

The following reagents were added, in order, to a 1 ml sterile centrifuge tube:

7.5 µl	pure water
5 µl	oligodeoxynucleotide probe (2 ρmol/µl)
2.5 µl	cobalt chloride
12.5 µl	terminal transferase reaction buffer

The tube was tapped to mix the reagents and then centrifuged for a few seconds. Vortexing was avoided to prevent shearing of the oligodeoxynucleotide probe. 5 µl of [^{35}S]dATP (NEN/DuPont) was then added and the mixture tapped and centrifuged as before. Finally, 2.5 µl of terminal deoxynucleotide transferase, stored in a bench top freezer box, was added to the centrifuge tube. After mixing and centrifugation the tube was placed in a water bath at 37°C for 1 hour. At the end of the incubation period the reaction was stopped by the addition of 400 µl of Reagent A (NEN/DuPont) and the tube was cooled on ice.

After labelling, the [^{35}S]dATP labelled oligodeoxynucleotide probe was chromatographically purified from any unincorporated nucleotides, excess salt and low molecular weight materials using a commercially available nucleic acid

purification cartridge (NENSORB: NEN/DuPont). Gentle tapping concentrated the sorbant in the bottom of the cartridge which was then clamped vertically. The cartridge lid was replaced with an adapter that allowed an air-filled syringe to be fitted to the top of the cartridge. The sorbant was then activated by the application of 2 ml of 100% methanol to the top of the sorbant. Gentle, constant pressure applied to the air-filled syringe pushed the alcohol through the sorbant. Once the meniscus reached the top of the sorbant, 2 ml of Reagent A (NEN/DuPont) was applied to the top of the sorbant and likewise pushed through the cartridge. Care was taken to ensure that the sorbant did not dry out at any stage in the procedure. The sample containing the labelled probe was then applied to the top of the cartridge and pushed through the sorbant. The effluent, containing any unincorporated nucleotides, was collected in centrifuge tube number 1. Any excess salt, low molecular weight materials and remaining unincorporated nucleotides were washed from the cartridge by pushing through a further 2 ml of Reagent A (NEN/DuPont), which was collected in centrifuge tubes 2 and 3. The radio-labelled probe was then eluted from the sorbant with 1 ml of 50% ethanol. Three drops of the resulting effluent were collected in tube 4, 14 drops in tube 5, 5 drops in tube 6 and the remainder was collected in tube 7. Less than 30% of the radioactivity was expected to be in tubes 1 to 3 with most of the radioactivity being in tube 5.

The efficiency of the labelling was measured by mixing a 5 µl aliquot from each tube with 1 ml of scintillant and measuring on a scintillation counter. The radioactivity, in counts per minute, was calculated for tube 5 and used to determine what volume of the purified, radio-labelled probe was required to give 10^6 counts per minute. The probe was stored at 4°C until use, which was always within 24 hours of purification. Where several labelling reactions were required to produce sufficient labelled probe,

the probes were pooled, mixed and re-measured to eliminate any differences between the batches.

2.8 *In situ* Hybridisation Histochemistry with [^{35}S]dATP Oligodeoxynucleotide Probes

A stock solution of 20 × standard citrate solution (SSC) was prepared and autoclaved before use. Deionised, purified water was incubated overnight with 1 ml of diethylpyrocarbonate per litre before being autoclaved. Sections from each brain were hybridised in triplicate with antisense probe. The selected tissue sections were placed in lidded bioassay dishes (Nunc) lined with two layers of absorbent paper (Whatman number 3MM) soaked in 4 × SSC. All sections were marked with the name of the probe and appropriately labelled as sense or antisense for later identification.

Hybridisation buffer was prepared in advance and stored at -20°C until required. Before use, the hybridisation buffer was thawed, boiled for 10 minutes and then quenched on ice. The final hybridisation solution per section consisted of the volume of radio-labelled probe required to give 10^6 counts per minute, 1 µl 1 molar dithiothreitol (DTT) and sufficient hybridisation buffer to achieve a final volume of 100 µl. 100 µl of hybridisation solution was applied to each section and evenly spread. Sections were then covered with a piece of laboratory film (Nescofilm) and hybridised in an incubator for approximately 18 hours at the appropriate temperature. A bioassay dish of 4 × SSC was placed in the base of the incubator to ensure that the atmosphere was kept moist.

2.9 Experimental Controls for ISHH

The controls employed were designed to verify that any ISHH signal detected was as a result of specific hybridisation of the chosen oligodeoxynucleotide probe to the particular mRNA under investigation, and not from non-specific binding of the oligodeoxynucleotide probe to other macromolecules, or its specific hybridisation to another mRNA species.

The specificity of hybridisation in human brain for each of the oligodeoxynucleotide probes employed in this thesis was determined by Northern blotting. The probes were labelled with [^{32}P]dATP and hybridised to 25 μg total RNA extracted from the frontal cortex of a control subject. The number, size and abundance of the mRNAs to which the labelled oligodeoxynucleotide probe hybridised was estimated by the position and intensity of the band(s) on gel electrophoresis and compared with published data. Northern blotting was performed by Drs. A.J. Barton, P.J. Harrison and P.R. Heath solely to verify the specificity of the oligodeoxynucleotide probes.

In each ISHH experiment, concurrent hybridisation of a [^{35}S]dATP labelled sense oligodeoxynucleotide probe, identical in nucleotide sequence to the mRNA under study, was used to assess the extent of non-specific hybridisation. The labelled sense probe was applied to a sub-sample of the tissue sections to be examined. These sense sections were then hybridised under identical conditions to the antisense sections.

Abolition of ISHH signal was demonstrated by diluting labelled antisense probe 100-fold with unlabelled antisense probe. Where an antisense probe binds specifically to a selected mRNA species, the number of binding sites is finite and an

excess of cold, unlabelled antisense probe can monopolise available sites and displace the radioactively labelled antisense probe.

The volume of purified, radio-labelled, antisense probe required to give 10^6 counts per minute per section was calculated and aliquotted into a separate centrifuge tube. This volume was increased 100-fold by the addition of unlabelled antisense probe. This diluted probe was then substituted for the normally radio-labelled probe in the hybridisation solution which was prepared in the normal way. Hybridisation, washing and detection of ISHH signal was performed as described. Concurrent sections hybridised with normally prepared [^{35}S]dATP labelled antisense probe served as positive controls.

Finally, loss of ISHH signal was demonstrated on pre-treatment of a sub-sample of tissue sections with a solution containing the ribonuclease, RNase A (Sigma). The sections were incubated in the solution for 60 minutes at 37°C prior to the other pre-treatment steps. (For preparation of ribonuclease pre-treatment solution see appendix I.)

2.10 Post-Hybridisation Washing

After overnight incubation, the laboratory film (Nescofilm) covers were removed from the sections, along with any unhybridised probe, by washing in a large volume of 1 × SSC at room temperature. The slides were racked and stored in 1 × SSC at room temperature in preparation for the high stringency washes. A wash temperature 15°C lower than the calculated melt temperature was used. This temperature, and the salt concentration of 1 × SSC, is believed to provide a reasonable level of stringency. Care was taken to ensure that the sections did not dry

out at any stage of the washing procedure as this can result in a significant increase in background labelling.

The sections were washed in 1 × SSC at the calculated wash temperature for 15 minutes. This wash was repeated three further times. Two separate hour long washes in 1 × SSC at room temperature followed. Finally, the sections were rinsed briefly in distilled water to remove any salt residue and allowed to air dry.

2.11 Direct Autoradiography

Once dry, the slides were mounted on cardboard in lightsafe cassettes and opposed against autoradiographic X-ray film (Hyperfilm-βmax, Amersham) at room temperature for an appropriate amount of time to generate autoradiograms.

Hyperfilm-βmax (Amersham) is an X-ray film composed of a flexible plastic base coated on one side with a photographic emulsion of high sensitivity protected by an anti-scratch layer. This film type is designed for use in direct autoradiography in which film and sample are in intimate contact, and it is relatively insensitive to the blue and ultraviolet light produced in indirect autoradiography by the use of fluor-impregnated substrates and intensifying screens (Amersham, 1992). Direct autoradiography is suitable for the detection of ^{35}S, since the layer of photographic emulsion overlying the sample absorbs most of the weak β particles emitted by this radioisotope.

A photographic emulsion consists of numerous photosensitive silver halide, usually silver bromide, crystals suspended in a clear solution composed mainly of gelatin. Beta particles have the same mass and single negative charge as electrons, and are ejected from radioactive nuclei in order to achieve stability (Rogers, 1979). Beta

particles striking the silver halide crystals in the emulsion cause reduction of some of the silver ions to atoms of metallic silver. This change produces what is known as a latent image. On development of the film, these silver atoms catalyse the reduction of the entire silver halide crystal in which they are located to a tiny particle or grain of metallic silver. Since a single hit by a β particle is sufficient to convert an entire silver halide crystal to a grain of silver on development of the film, the blackening of an autoradiographic film is directly proportional to the amount of radioactivity reaching it (Laskey, 1993). Silver halide crystals which remain unchanged are washed away during the development process leaving the film transparent.

2.12 Development of Autoradiograms

One litre each of developer, stop solution and fixative, diluted to the appropriate concentration with purified, deionised water, was required to develop two autoradiographic films. The cassettes were opened in a dark room illuminated under safe light conditions. The films were gently agitated in a solution of Ilford PQ Universal Developer at a concentration of 1 part developer to 9 parts water for 5 minutes. The developer reduces silver ions to metallic silver in a self catalytic process which is far faster in crystals already containing atomic silver (Rogers, 1979). The reaction was stopped by immersing the films in a 2% acetic acid solution for 30 seconds and the films were then fixed by gently agitating them in a solution of 1 part Ilford Hypam Fixer in 4 parts water for 5 minutes. The lowered pH of the 2% acetic acid solution stops the development of the film and slightly hardens the gelatin. The fixative solution is designed to wash away any unchanged silver halide crystals remaining in the emulsion. The films were then immersed in running tap water for approximately 30 minutes before being hung up to air dry. Once dry, the autoradiograms were labelled with a permanent marker and the films stored ready for regional quantification of ISHH signal.

2.13 Dipping of Slides for Autoradiography

For cellular localisation of hybridisation signal, the sections were removed from the cardboard inserts lining the lightsafe cassettes under safe light conditions and assembled in racks. An appropriate volume of Ilford K5 Photographic Emulsion was melted in a water bath at 45°C and then mixed with an equal volume of distilled water to which a drop of glycerol had been added. The solution was stirred gently to mix and poured into a slide container set in a beaker of water in the water bath. A number of blank slides were dipped in the emulsion to ensure that it was free of bubbles and coated the slides evenly before the experimental slides were dipped. Each slide was lowered into the emulsion for 5 seconds and then slowly and steadily withdrawn. The emulsion was wiped from the back of each slide which was then placed on a cold plate for 15 minutes to allow the photographic emulsion to gel. Once set, the slides were laid out to dry at room temperature for approximately 3 hours. The dry slides were racked and placed in black plastic boxes sealed with adhesive tape and wrapped in two layers of silver foil. A package of silica gel was placed in each box as a drying agent. The boxes were sealed in black plastic bags and stored in a refrigerator for the appropriate exposure time for the individual probe; approximately two to three times the length of time required to generate autoradiograms.

2.14 Development of Dipped Autoradiographic Sections

Under safe light conditions the dipped autoradiographic sections were allowed to warm to room temperature. The adhesive tape sealing the black boxes was stripped from all of them before any were opened, to prevent artefactual exposure of the sections to sparks of light. The developer, stop solution and fixative used were diluted with purified, deionised water. The slides were gently agitated in Ilford Phenisol Developer, 1 part to 4 parts water, for 2 minutes and then transferred to a

2% acetic acid solution for 30 seconds. The lowered pH of the acetic acid solution halts the process of development while slightly hardening the gelatine in which the silver bromide crystals of the emulsion are suspended. The slides were then immersed in a fixative solution of 30% sodium thiosulphate for 5 minutes to dissolve any silver bromide crystals remaining in the emulsion. Some of the silver thiosulphate complexes produced during this process are light sensitive, thus safe light conditions were maintained until the 30 minute wash in gently running tap water, designed to wash the fixative out of the emulsion, was completed. The slides were then briefly rinsed in purified, deionised water and allowed to dry.

The developed sections were counter-stained by immersion in a 0.1% cresyl violet solution for 1-2 minutes and then dehydrated by passage through a series of alcohols of increasing concentration. Once dehydrated, the sections were immersed in xylene until coverslipped using DePeX (BDH Laboratory Supplies) as a mountant.

2.15 The Calculation of Optical Density

Since the energy from a single β particle is sufficient to reduce an entire silver halide crystal to a grain of metallic silver on subsequent development of the photographic film, the local blackening of the film is directly proportional to the amount of radioactivity reaching it (Laskey, 1993). Thus, the response of autoradiographic X-ray film to exposure to ionising radiation is conventionally measured by estimating the optical density of the developed film. Optical density is a measure of the extent to which an object prevents light from passing through it and has been confirmed by several workers as being proportional to the mass of silver per unit area (See Mees, 1942 for review). Essentially, optical density is the ratio of the transmitted to the incident light expressed as a logarithm to the base 10. Thus:

$$\text{Optical density} = \log 10\left(\frac{\text{transmitted light}}{\text{incident light}}\right)$$

Since the transmitted light must always be less than, or equal to, the incident light and the logarithm to the base 10 of a number between zero and 1 is always negative, this logarithm is always either a negative number or zero. By convention, in reporting optical densities, this negative sign is omitted since it conveys no useful information.

Where A = transmitted light and B = incident light, then:

$$\text{Optical density} = \log 10\left(\frac{A}{B}\right)$$

or

$$\text{Optical density} = \log 10 A - \log 10 B$$

and

$$-\text{Optical density} = -\log 10 A + \log 10 B$$

therefore

$$-\text{Optical density} = \log 10\left(\frac{B}{A}\right)$$

or

$$-\text{Optical density} = \log 10\left(\frac{\text{incident light}}{\text{transmitted light}}\right)$$

The intensity of light transmitted through the autoradiographic films was measured using one of two image analysis systems. Both systems, like most video based systems, were calibrated to assign the amount of light transmitted through an object of optical black to zero. Pure white light was registered by both systems as having a value of 255 and shades of grey were linearly assigned to the numbers between zero and 255. Incident light, presumed to be pure white light, is therefore a constant and the calculation of negative optical density yields the positive number required by convention. The final version of the equation is thus:

$$-\text{Optical density} = \log 10\left(\frac{255}{\text{transmitted light}}\right)$$

2.16 The Relationship Between Optical Density and Radioactive Exposure

The optical density of a developed direct autoradiogram is linearly related, within certain limits, to the exposure to radioactivity of the film (Laskey, 1993). A direct plot of exposure against optical density with respect to ionising radiations yields a straight line at low densities (Goldstein and Williams, 1971). This is in contrast to the classical sigmoid Hurter-Driffield curve which is more suited to the study of multi-hit processes such as characterises the response of photographic film to visible light (Goldstein and Williams, 1979; Rogers, 1979). With intensive or prolonged exposure to ionising radiation all of the available silver halide crystals in the photographic emulsion are reduced to metallic silver and optical density reaches a plateau. Accurate quantitation, therefore, requires exposure levels which do not saturate the absorbance of the film (Laskey, 1993). Similarly, at low levels of radioactivity the errors inherent to the system becomes so great in relation to the response to be measured as to render optical density measurements inaccurate.

2.17 Problems Associated with the Measurement of Optical Density

In practice the measurement of optical density is problematic. Each system employed to measure optical density must be individually calibrated to ensure that it does so accurately. The measurement of optical density, using the image analysis systems employed in this study, required that the sample be illuminated using monochromatic light and that those parts of the stabilised light source not directly below the video camera were masked. Further, it was determined that optical black was not precisely registered by either system as having an optical density of zero, and it is known that such offsets in optical density may vary with time and temperature (Aldridge, 1993). In view of these limitations the term 'approximate optical density'

(AOD) is used throughout this study in acknowledgement of the inaccuracies inherent in the system.

2.18 The Application of Radioactive Standards

The relationship between radioactive exposure and approximate optical density was studied in my system using ^{14}Carbon (^{14}C) standards. Miller (1991) studied the response of Hyperfilm (Amersham), a single coated autoradiographic film, to both ^{14}C labelled standards and ^{35}S labelled brain paste, and demonstrated a simple linear relationship between the two. Further, the optical density obtained by exposing autoradiographic film to ^{35}S at various concentrations and for various exposure times, covaried with the response of the film to the ^{14}C labelled standards, suggesting that the film responded similarly to the two isotopes. Miller concluded that ^{14}C labelled standards provide a reliable means of calibrating the response of autoradiographic film to ^{35}S.

^{14}C microscales (Codes RPA 504 and RPA 511, Amersham) were opposed to autoradiographic film alongside specimen sections and analysed at the same time as the related experiment and in the same way. These microscales are composed of eight (RPA 504) or ten (RPA 511) individual sheets of ^{14}C polymer sandwiched between alternate layers of coloured, inactive, methacrylate polymer. An average approximate optical density reading was obtained for each radioactive layer of the polymer. This value was plotted against the tissue equivalent radioactivity of that layer in ηCi/g as supplied by the manufacturer. As predicted, a linear relationship was demonstrated between the two at low optical density readings. Details of the calibration of individual experiments is presented in the appropriate chapter.

2.19 Quantification of Autoradiographic Film

Two similar image analysis systems were employed in the analysis of the autoradiographic films produced during this study: Image Manager PC, Sight Systems, Newbury and Seescan Plc, Cambridge. Image analysis systems allow rapid, accurate and consistent estimation of greyness of autoradiographic films. Certain precautions, however, are necessary to ensure the accuracy and reproducibility of data.

The film was transilluminated on a stabilised light box and a charge coupled device (CCD) camera employed to produce a computerised image of the specimen on a video monitor. The camera aperture and magnification that afforded the clearest representation on the video screen of the tissue section to be measured was determined at the outset of analysis. These settings were then maintained without change until the analysis of an individual experiment was complete.

The video signal provided by the camera is achieved by scanning the image horizontally from top left to bottom right, dividing the screen into an array of 512 separate points or 'pixels' horizontally and 512 pixels vertically. The image at each pixel is digitised and stored.

Before capturing on the video screen the image to be measured, a blank portion of the same autoradiogram was analysed, to allow estimation of the extent to which the film itself inhibited the passage of incident light. Since this varies slightly from film to film, a blank portion of each new film was measured before analysis began. During so called 'shade correction' the recorded intensity of light transmitted through the image is adjusted pixel by pixel to take into account the effect of the barrier presented by the film itself. In order for this adjustment to be valid, the incident light

and the configuration of the image capturing optics must remain constant between measurement of the blank film and measurement of the image. For this reason the use of a stabilised light box, which provides a constant, diffuse and even light, constant ambient lighting and the avoidance of overhead glare are crucial. At the start of each experiment an antisense specimen was chosen as a control and was measured at the beginning of each session of image analysis and at frequent intervals during sessions to ensure the reproducibility of the results. It became clear that the apparatus required a minimum period to 'warm up' after which the grey levels obtained were gratifyingly reliable.

2.20 Correction for Non-Specific Binding

Sense oligodeoxynucleotide probes, identical in nucleotide sequence to the mRNA under study, were employed to assess the extent of non-specific binding. Initially, sections from a subset of cases were hybridised with the sense probe and a mean sense AOD reading obtained for each diagnostic category examined. However, the diagnosis specific mean AOD for the sense sections were often identical, since sense strand hybridisation tends to be uniform and virtually negligible, resulting in the same value being subtracted from each antisense AOD. In some experiments a suitable sense oligodeoxynucleotide probe was not available and the antisense readings were therefore not corrected for non-specific binding. Ideally, an AOD reading for the appropriate sense probe would be available for each case employed, allowing the antisense readings for each individual case to be corrected for non-specific binding. This was attempted with Series III (the OPTIMA series) where an additional section was selected from each case and hybridised with the appropriate sense probe. Subsequent careful scrutiny of the calibration curves generated for these probes suggested that the very low sense AOD readings obtained were often beyond the linear extent of the relationship between AOD and estimated

tissue radioactivity. It was, therefore, decided that it was not meaningful to subtract such sense AOD readings from the AOD readings obtained for the corresponding antisense probe.

The problems inherent in correcting for non-specific binding and the methods chosen to resolve them are discussed in the individual chapters.

2.21 Quantification of Autoradiographic Slides

Intensity of ISHH signal on dipped slides was estimated by counting the average number of silver grains per unit area over specific cells using the semi-automated image analysis systems described above. In addition to the principles discussed above in relation to the quantification of autoradiograms, a number of other considerations are important in quantifying ISHH signal over cells.

Quantification can only be carried out at a cellular level if the cells are sufficiently dispersed to allow the signal derived from one cell to be clearly identifiable. The system was first calibrated using a graticule and then optimised for the clear visualisation of silver grains without the loss of cellular outlines. The threshold of the image analysis system was optimised empirically to ensure that all of the silver grains visible by eye were identified, and measured, by the system. The average area of a silver grain was estimated by measurement of the total area of numerous clumps of silver grains followed by counting by eye the number of silver grains in each clump. The average area of a silver grain was then entered into the image analysis equipment. Three sections labelled with antisense probe were available from each case. Approximately 17 cells were selected from each of three fields of each section. A final measure of silver grain counts per unit area of cell was obtained. The average silver grain count over the sense sections was subtracted from the antisense

readings to eliminate the effect of background labelling. Since an approximately linear relationship exists between number of silver grains and radiation dose (Goldstein and Williams, 1971), it is not necessary to transform logarithmically the readings obtained.

2.22 Statistical Analysis

All statistical analysis was performed using the statistical package SPSS for Windows version 6.0.

Chapter 3

The Application of the Quantitative Polymerase Chain Reaction to Analysis of Reverse Transcribed Gsα mRNA

3.1 Introduction

3.1.1 The Heterotrimeric G-Proteins

The heterotrimeric G-proteins represent a family of highly homologous proteins attached to the cytoplasmic leaflet of the plasma membrane that are involved in signal transduction. Approximately eight out of ten neurotransmitters and hormones, as well as many autocrine and paracrine factors, rely on the heterotrimeric G-proteins to communicate with the interior of the cell (Birnbaumer *et al.*, 1990). Heterotrimeric G-proteins are composed of subunits of decreasing molecular weight named α, β and γ and bind guanosine phosphate moieties, hence their name. The α subunit confers specificity of action on the G-protein, is hydrophilic (Graziano *et al.*, 1987) and possesses weak, inherent guanosine triphosphatase (GTPase) activity (Northup *et al.*, 1980). The β and γ subunits exist as dimers that are believed to anchor the α subunit to the plasma wall (Sternweis, 1986; Graziano *et al.*, 1987).

At rest, the heterotrimeric G-proteins exist predominantly as trimers with guanosine diphosphate (GDP) attached to the α subunit (See Birnbaumer *et al.*, 1990 and Gilman, 1987 for review). Ligand occupancy of a G-protein linked receptor, results in a conformational change in the receptor that allows it to attach to an appropriate G-protein. Association of a ligand-bound receptor with a G-protein results in the release of GDP from the α subunit and the binding of guanosine triphosphate (GTP). The binding of GTP to the α subunit reduces the affinity of the ligand for the receptor leading to an alteration in the equilibrium of bound to unbound first

messenger. The βγ dimer dissociates from the activated α subunit that now has the capacity to modify the activity of the downstream effector systems for which it is specific. Within seconds, the inherent GTPase activity of the α subunit results in the hydrolysis of GTP to GDP whereupon the G-protein is inactivated and the trimer reassembles.

Two characteristic features of heterotrimeric G-protein-mediated signal transduction are worthy of note. Firstly, it allows amplification of the first messenger borne signal. Both the G-protein-coupled receptor and the G-protein itself can move freely in the plasma membrane such that a ligand-bound receptor can activate numerous G-proteins before the release of its bound ligand. Moreover, each activated G-protein is capable of activating numerous downstream effectors before its bound GTP is hydrolysed to GDP and it is returned to its inactive state. Secondly, since the active conformation of a G-protein is intrinsically short-lived and persistent activation is only possible in the continued presence of first messenger, the system is supremely sensitive to alterations in the hormonal milieu.

Four groups of G-protein α subunits have been identified (Lyons, 1994). The first group includes Gsα and the olfactory α subunits that are capable of activating adenyl cyclase. The second group includes the inhibitory α subunits Gi1, Gi2, Gi3, Go and transducin. These inhibitory G-proteins are vulnerable to ADP-ribosylation by the ATP dependent ADP-ribosyltransferase present in the neurotoxin released by the bacteria Bordetella pertussis. The Gq group of α subunits activate phospholipase C and are pertussis toxin insensitive. The fourth group includes G12 and G13; α subunits that have been demonstrated by sequencing to be distinct from the other three groups. The β and γ subunits are tightly associated under non-denaturing

conditions (Watson and Arkinstall, 1994). Five different β and seven different γ chains are known to exist (Watson and Arkinstall, 1994).

3.1.2 The α Subunit of Gs

Gs was first isolated by scientists working in Alfred G. Gilman's laboratory in 1980 (Northup *et al.*, 1980). Three subunits of Gs, of molecular weights 52 000, 45 000 and 35 000, were identified on sodium dodecyl sulphate-polyacrylamide gel electrophoresis. Subsequent purification and characterisation of Gs (Sternweis *et al.*, 1981; Codina *et al.*, 1984) established that the 52 000 and 45 000 molecular weight subunits of Gs were two forms of the Gsα protein. The large and small molecular weight isoforms of Gsα protein, and the mRNAs on which they are encoded, are designated Gsα-L and Gsα-S respectively. It has been established unequivocally that Gs stimulates the catalytic subunit of adenyl cyclase (May *et al.*, 1985), a membrane-bound enzyme which displays strict Gs selectivity (Cooper *et al.*, 1990). Adenyl cyclase catalyses conversion of its physiological substrate magnesium-ATP, into cAMP, and is inactive in the absence of Gs. Gs has also been implicated in the regulation of magnesium ion transport across the plasma membrane (Maguire *et al.*, 1980) and in the inhibition of the calcium pump responsible for the extrusion of ionic calcium in rat liver (Jouneaux *et al.*, 1994). Yatani and co-workers (1987) used excised membrane patches from guinea pig cardiac myocytes and bovine cardiac sarcolemmal vesicles to demonstrate that Gs could activate voltage-gated calcium channels directly. Three of the four isoforms of Gs were subsequently shown to activate both adenyl cyclase and voltage-gated calcium channels (Mattera *et al.*, 1989). It is of interest that constitutive activation of the G-protein linked adenosine A2 receptor in transgenic mice has been linked with chronic over-stimulation of the cAMP cascade and ultimately oncogenesis.

Sternweis and colleagues (1981) proposed that the 52 000 molecular weight species of Gsα, Gsα-L, was more rapidly activated by GTP analogues, and was the more efficient hormone-stimulated activator of adenyl cyclase, than the 42 000 polypeptide, Gsα-S. Initially, Graziano and his colleagues (1987) inserted complementary DNAs encoding both forms into plasmid vectors in *Escherichia coli* and found them to be equally active. However, in subsequent experiments Gilman's team (Graziano *et al.*, 1989) demonstrated that though the rate of GTP hydrolysis is similar for both species, the rate of dissociation of GDP from Gsα-L is 2 to 3 fold faster than the rate of GDP dissociation from Gsα-S.

Gsα undergoes dynamic palmitoylation which helps determine its subcellular location (Mumby *et al.*, 1994). The covalent attachment of the fatty acid palmitate to the amino terminal cysteine residue of Gsα, through a labile thioester bond, promotes stable association of Gsα with the plasma membrane (Wedegaertner and Bourne, 1994). Activation of Gs is associated with the rapid depalmitoylation of its α subunit and its translocation to the cytoplasm (Wedegaertner and Bourne, 1994). Gsα is also a substrate for the ADP-ribosyltransferase contained in the toxin produced by the bacteria *Vibrio cholerae*. ADP ribosylation of arginine 201 of Gsα results in constitutive activation of the G-protein due to a marked reduction in its GTPase activity (Weinstein and Shenker, 1993).

3.1.3 The Structure of the Human Gsα Gene

The Gsα gene has been analysed in rat (Itoh *et al.*, 1986), cattle (Graziano *et al.*, 1987; Robinshaw *et al.*, 1986a; Robinshaw *et al.*, 1986b), rabbit (Graziano *et al.*, 1989) and man (Harris, 1988; Bray *et al.*, 1986). Study of complementary DNAs and human genomic DNA (Kozasa *et al.*, 1988), indicates that four splice variants of Gsα exist in humans generated by alternative splicing of a single gene located on

chromosome 12. The Gsα gene is a split gene that spans approximately 20 kilobases and is composed of 13 exons and 12 introns (Kozasa *et al.*, 1988). It is probably the most remote of the G-protein α subunits since it includes two large sequences not seen in other G-proteins (Itoh *et al.*, 1986). The four splice variants of Gsα mRNA are generated by the inclusion or exclusion of a span of 45 nucleotides encoded on exon 3, and by the use of a variable splice junction at the end of intron 3 (Kozasa *et al.*, 1988). The cDNA encoding Gsα-1 contains exon 3 alone while Gsα-2 contains both exon 3 and 3 additional nucleotides, deoxycytidylate, deoxyadenylate and deoxyguanylate (CAG) that are split between two codons and result in an additional serine residue at position 87 (Bray *et al.*, 1986). Gsα-3 contains neither exon 3 nor the additional 3 nucleotides and Gsα-4 contains the 3 nucleotides only, and thus contains an extra serine residue at position 72. The four isoforms of Gsα are illustrated in figure 3.1. This splicing model implies the use of an unusual 3' splice junction, TG-AG, instead of the usually strictly conserved sequence of GT-AG. The variable splice junction at the end of intron 3 results in the three additional nucleotides, CAG, being present in two of the four isoforms of Gsα. This serine residue is a potential site of phosphorylation by protein kinase C (Kishimoto *et al.*, 1985), but not by cAMP-dependent protein kinase A (Bray *et al.*, 1986). Exon 3 is unique to Gsα and encodes a hydrophilic amino acid sequence located on the surface of Gsα which is hypothesised to have a functional role in the regulation of adenyl cyclase (Kozasa *et al.*, 1988).

3.1.4 Studies of Gsα Messenger RNA

In screening a human brain cDNA library, Bray and colleagues (1986) detected four types of Gsα cDNA that differed in nucleotide sequence in the region corresponding to amino acid residues 71 to 88. The authors hypothesised that four types of Gsα mRNA existed and using an S1 nuclease protection assay demonstrated the existence

The Variably Spliced Exon 3 Region of the Gsα Gene

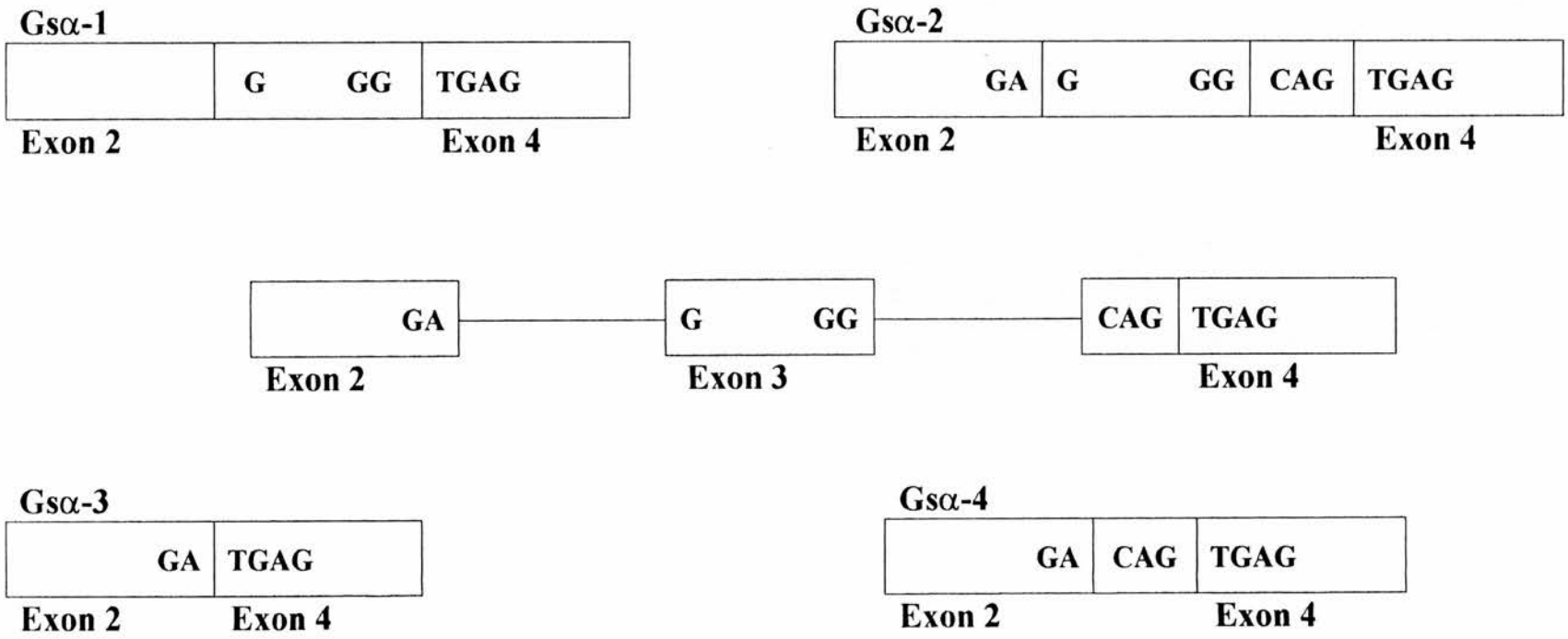

Kozasa *et al.*, 1988

Figure 3.1

of two splice variants of Gsα mRNA. Since the two long and two short forms of Gsα mRNA differ by only 3 nucleotide residues, the authors suggest that these three unpaired bases were not appreciably cleaved by S1 nuclease and hence could not be demonstrated using this assay. Granneman and colleagues (1991) studied the pattern of mRNA splicing of Gsα in human adult brain using a method based on the polymerase chain reaction (PCR). Products of 285 and 325 base pairs were generated and separated on gel electrophoresis on a 2 to 3% agarose gel containing ethidium bromide. Gsα-L was found to account for 84% of total Gsα mRNA in the hippocampus and cortex, but only 66% of total Gsα mRNA in the striatum. Since the serine-encoding form of Gsα-S mRNA contains a BsmA1 restriction site, it was possible to determine the contribution of this form of Gsα-S to the total amount of Gsα-S mRNA. Approximately 40% of Gsα-S mRNA is serine-encoding and no regional variations were found in the amount of this splice variant. This method relies heavily, however, on the complete digestion of Gsα-2. No such restriction site could be identified in the exon 3-containing splice variants of Gsα which would allow differentiation of the serine-encoding forms of Gsα-L from those containing exon 3 alone. Therefore, attempts to quantify the relative contribution of these two splice variants were unsuccessful.

Thyroid stimulating hormone (TSH) and forskolin have been shown to produce a significant increase in Gsα mRNA, as measured by Northern blotting, and in Gsα protein, in cultured pig thyroid cells (Dib *et al.*, 1994). The up-regulation of Gsα mRNA in response to TSH or forskolin could be prevented by long term exposure of the cells to 12-o-tetradecanoylphorbol 13-acetate (TPA), an activator of protein kinase C, suggesting that protein kinase C activation prevents the cAMP-dependent up-regulation of Gsα mRNA and Gsα protein.

Harrison and colleagues (1991c) have demonstrated a marked increase in the mRNA encoding the α subunit of Gsα in the hippocampus of AD sufferers in comparison to neurologically normal controls. This increase was not the result of a generalised increase in mRNA expression, as the increase in Gsα mRNA remained even when expressed as a proportion of total poly(A)$^+$ mRNA levels in the same cell populations. The magnitude of the increase in Gsα mRNA identified, implied that, should rates of transcription and translation be unchanged, Gsα protein synthesis would be enhanced.

3.1.5 Gsα Protein Levels

Gsα isoform levels appear to be developmentally regulated in the rat (Babila *et al.*, 1992). Pineal levels of Gsα-L protein remain constant throughout life. Gsα-S protein, however, is virtually absent from the rat pineal at birth, but increases markedly in abundance thereafter. Moreover, the ratio between the long and short forms of Gsα protein decreases from 11 in the newborn rat to approximately 2 in the adult. The appearance of Gsα-S protein coincides with the development of the cGMP response to adrenergic stimuli and to hydroxyindole-o-methyltransferase activity, though is not necessarily functionally related to either (Babila *et al.*, 1992).

In contrast to Granneman and Bannon (1991) findings regarding Gsα mRNA, Cooper and co-workers (1990) found Gsα-S protein to be the predominant form of Gsα protein in the striatum, while in the cerebellum Gsα-L was the most abundant form of Gsα protein. The authors comment that at least two forms of adenyl cyclase exist in the brain that differ in their sensitivity to ionic calcium/calmodulin. The cerebellum is far richer in the calcium/calmodulin sensitive form of adenyl cyclase than is the striatum. On the basis of the co-localisation of Gsα-S and the calcium/calmodulin independent form of adenyl cyclase, the authors hypothesise that

Gsα-S selectively associates with this form of adenyl cyclase, and that thus the balance between Gsα-L and Gsα-S may be functionally important.

Protein studies in AD hippocampi have failed to identify any increase in Gsα subunits in comparison with control tissue as would have been predicted from the findings of Harrison and colleagues (1991c) regarding Gsα mRNA. Using immunoblotting, McLaughlin and co-workers (1991) found no statistically significant differences in the abundance of Gsα-L and Gsα-S protein, or in the levels of the α subunits of Gi1, Gi2 and Go between AD and control hippocampus, cerebellum and frontal cortex. The tissue used was age-matched, but the PMI for the control group was significantly longer than that for the AD group and agonal state information was not provided. Similarly, O'Neill and colleagues (1994) examined Gsα protein levels in crude synaptic membrane fractions from temporal cortex, angular gyrus and hippocampus of control and AD brains matched for age, tissue pH and gender. They found no statistically significant difference in the amounts of Gsα-L or Gsα-S between control and AD tissue. However, the ratio of Gsα-L to Gsα-S was found to be significantly increased in the hippocampi and angular gyri of the AD cases when compared with the controls. Unfortunately, the PMI of the control group, as in McLaughlin and co-workers (1991) study, was significantly longer than the PMI of the AD group. O'Neill and colleagues (1994) found Gsα stimulated adenyl cyclase activity to be impaired in AD hippocampus, although no change was detected in G-protein mediated inhibition, or forskolin stimulated, adenyl cyclase activity.

Li and colleagues (1996) examined Gsα protein levels in human pre-frontal cortex, superior temporal gyrus and occipital cortex and found them to be equal to those in age and PMI matched controls. Li and co-workers found Gsα protein levels to be

remarkably stable over post-mortem intervals of between 5 and 21 hours though, as the authors point out, these findings cannot necessarily be generated to other brain regions. No assessment of agonal state was made in this study.

Cowburn and workers (1992) have identified a decrease in Gs stimulated adenyl cyclase activity in the neocortex and cerebellum in AD in comparison to non-demented controls in the presence of preserved basal and forskolin stimulated adenyl cyclase activity. The authors postulate that the altered Gsα expression documented by Harrison and colleagues (1991c) reflects a compensatory up-regulation in Gsα expression in response to the functional impairment in adenyl cyclase activation.

Paulssen and colleagues (1992) have investigated the effects of phospholipase C on Gsα protein levels in cultured prolactin producing rat pituitary adenoma cells. Pre-treatment of the cells with of 1-oleoly-2-acetylglycerol (OAG), an activator of protein kinase C, resulted in a decrease in Gsα protein levels and a slight decrease in the responsiveness of adenyl cyclase to vasoactive intestinal peptide (VIP) and the virtual abolition of responsiveness of adenyl cyclase to thyrotropin releasing hormone (TRH). Ionomycin mobilises calcium from intracellular stores resulted in a transient decrease in Gsα protein paralleled by a decrease in the responsiveness of adenyl cyclase to both TRH and VIP. Thus, it would appear, that there is interplay between G protein coupled second messenger systems and the phosphatidylinositol 4,5-biphosphate pathway and that first messengers can influence the abundance of G protein subunits.

3.1.6 The Polymerase Chain Reaction

The polymerase chain reaction (PCR), invented by Kary B. Mullis in 1985 (K.B. Mullis, U.S. patent 4,683,195, July 1987; U.S. patent 4,683,202, July 1987; See Mullis, 1994), is an ingenious and powerful means of amplifying DNA. James D. Watson, in his foreword to *The Polymerase Chain Reaction* (1994), described this rapid, exquisitely sensitive and specific molecular biology technique as indispensable.

Primers are chosen whose base sequences are complementary, and in the reverse orientation, to the base sequences flanking the area of DNA of interest. After denaturation of the DNA template by heating, the primers are allowed to anneal to the DNA under carefully optimised PCR conditions. Chain elongation is effected by the heat stable *Taq* DNA polymerase and the newly formed duplexes are then denatured by heating in preparation for another cycle of the PCR.

As few as 10 specific nucleic acid molecules in a background of hundreds of millions can be reliably reproduced (Ferré *et al.*, 1994) and PCR can even be started from a single molecule of DNA (Hayashi, 1994). The PCR results in an exponential increase in the products of the reaction as the amplicons produced with each cycle of the chain reaction become the substrates for the next round of amplification (Siebert, 1993). In theory, the amount of product doubles with each PCR cycle according to the equation $A_n=A_0 2^n$ where A_0 represents the amount of starting material, n equals the number of PCR cycles and A_n represents the amount of product after n cycles of the PCR. Of course, this equation assumes that the PCR proceeds with 100% efficiency whereas in reality an efficiency, R, of between 0.5 and 0.8 is more usual (Salomon, 1995a). Logging the parameters of the equation, $A_n=A_0(1+R)^n$, converts it to a linear equation allowing the ideal PCR reaction to be represented graphically

by a straight line. In reality, the exponential increase in the products of the PCR begins to plateau after approximately 20 cycles (Salomon, 1995a) as a result of diminishing amounts of reagents, enzyme and primers and competition for binding sites with the increasing amounts of template. Thus, the amplification efficiency of the reaction is constant only during the linear phase of product accumulation.

Unfortunately, however, the PCR is subject to unpredictable and perplexing variations in yield (Salomon, 1995a). Significant tube-to-tube variation in the products of a reaction has been documented even with precise control of PCR conditions, such as when a reaction has been assembled as a master mix, divided into individual tubes and amplified during the same run (Gilliland *et al.*, 1990).

3.1.7 Coupling of Reverse Transcription to the Polymerase Chain Reaction

The adaptation of PCR, which allowed conversion of mRNA to complementary DNA (cDNA) by the intermediate step of reverse transcription, (RT-PCR), revolutionised the detection and quantitation of RNA. Prior to the application of RT-PCR, ISHH was the most sensitive method for detecting mRNA, being capable of detecting 10 to 100 molecules of mRNA in a single cell (Kawasaki, 1990). However, ISHH is widely regarded as technically difficult and the technique is not well suited to the processing of large numbers of samples. Other methods for detecting RNA such as Northern blots, S-1 nuclease protection assays and RNase A protection studies require considerably higher concentrations of RNA at approximately 10^5 to 10^6 target molecules (Kawasaki, 1990). RT-PCR, in contrast, allows the detection of rare mRNAs and mRNAs from small numbers of cells or in small quantities of tissue (Siebert, 1993). The reproducibility of the reverse transcription reaction is, however, notoriously poor with reported efficiency rates for cDNA synthesis of between 5 and 90% (Ferré *et al.*, 1994) though some authors have

argued that the major source of error in quantitation of RT-PCR is, in fact, the difficulties inherent in the accurate measurement of the starting RNA and its variable integrity (See Ferré *et al.*, 1994 for discussion).

The double-stranded starting point required by the enzyme reverse transcriptase can be achieved in three ways (Salomon, 1995b). Oligo dT primers consist of a string of deoxythymidylates capable of annealing to the poly (A) tail present on most mRNAs. Where the RNA sample is degraded or the RNA sequence of interest is distant from the poly (A) tail, however, the cDNA yield from oligo dT may be disappointing. Like oligo dT, random oligodeoxynucleotide primers are capable of annealing to potentially all mRNA species in the total RNA sample, but are less dependent on the integrity of the mRNAs (Salomon, 1995b). Where oligodeoxynucleotide primers specific for the mRNA species of interest are chosen, the cDNA generated cannot be used to amplify any other target, though where a sample is likely to be significantly degraded they are more useful than the other two primers.

3.1.8 Quantitative RT-PCR

Salomon (1995a) and Vandevyver and Raus (1995) warn that quantitative RT-PCR is not a trivial undertaking. Though two successive enzymatic reactions immediately present difficulties of quantitation, it is the unwieldy increase in the desired products which is characteristic of PCR that presents the greatest challenge to the quantitative assessment of PCR amplified RNA (Siebert, 1993). During the initial cycles of PCR, the products of the reaction accumulate at an exponential rate and the efficiency of the amplification reaction remains constant. During this period the amount of product is directly related to the abundance of the cDNA of interest in the sample. Where two different products are known to amplify with the same efficiency, the relative abundance of the two amplicons can be compared. Of course, with

increasing cycle number the amplification efficiency declines and the accumulated product can no longer be directly related to the amount of starting material.

The efficiency of a PCR depends on factors such as the starting amount of DNA, the presence of contaminants, the length and complexity of the sequence to be amplified and the degree which optimisation of reagents has been achieved (Vandevyver and Raus, 1995). It is obvious that when more than one product is to be amplified, they might amplify with different efficiencies. Two primer pairs may exhibit marked differences in amplification efficiency, such that the ratio between the products of the RT-PCR of total RNA does not reflect the ratio between the two native species in the original sample (Salomon, 1995a). Moreover, given the nature of PCR a minute alteration in the starting number of template DNA molecules or a slight difference in the amplification efficiency of the reaction can, over a number of PCR cycles, result in dramatic differences in the amount of reaction product (Scheuermann and Bauer, 1993).

The quantitation of RT-PCR can be relative or absolute (Ferré *et al.*, 1994). The relative quantitation of RT-PCR involves comparison of the relative amounts of a particular mRNA species between samples. Since modest differences between samples can result in dramatic differences in product generated, the relative quantitation of mRNA is problematic without the inclusion of internal or external standards. RNA standards are generally preferred given that they can control for the relatively inefficient and highly variable RT step (Ferré *et al.*, 1994). The co-amplified RNA is either an endogenous species, the abundance of which is not believed to vary with cell cycle, or an exogenous mRNA. Co-amplification of an endogenous RNA control provides data on the success of the extraction process. Alternatively, the co-amplification of an external mRNA allows the amount of

external standard added to be adjusted such that it is keeping with the concentration of the target mRNA, given that quantitative RT-PCR is best performed with two equally abundant templates. Further, if the exact amount of the external standard is known, and the amplification efficiency of the two reactions is equal, the number of starting molecules of the mRNA of interest can be estimated and absolute quantitation attempted. Unhappily, the competing amplification of the standard may interfere with the amplification of the desired template (Ferré *et al.*, 1994). In any event, it is acknowledged that the absolute quantitation of RT-PCR is extremely difficult (Ferré *et al.*, 1994).

3.1.9 Aims of the RT-PCR Study of Gsα mRNA

The Gsα gene is a member of the expansive heterotrimeric G protein gene family crucial to cellular responsiveness (O'Neill *et al.*, 1994) that appears to have diverged from the others early in evolution (Kozasa *et al.*, 1988). Gsα is believed to be the most remote of the G proteins (Itoh *et al.*, 1986) and one of the two large sequences in Gsα not seen in other G-proteins (Itoh *et al.*, 1986) is encoded on exon 3 (Bray *et al.*, 1986). The 15 amino acids encoded by exon 3 constitute a relatively hydrophilic, negatively charged region present in two of the four known isoforms of Gsα protein (Bray *et al.*, 1986) and may have a role in the control of adenyl cyclase (Kozasa *et al.*, 1988). An additional serine residue, that is a potential phosphorylation site, is also present in this region in Gsα isoforms Gsα-2 and Gsα-4 (Bray *et al.*, 1986). Though most tissues contain both Gsα-S and Gsα-L, the functional importance of the different isoforms is unknown (Robinshaw *et al.*, 1986b).

Using an S1 nuclease protection assay, Bray and colleagues (1986) identified Gsα-S and Gsα-L but were unable to differentiate between the serine encoding and serine

lacking isoforms of Gsα mRNA. Granneman and Bannon (1991), using a PCR based technique, were able to explore the relative contribution of Gsα-3 mRNA and Gsα-4 mRNA to Gsα-S mRNA by virtue of a *Bsm*A1 restriction site in Gsα-4 mRNA, but the of relative abundance of the two splice variants of Gsα-L mRNA remains elusive.

Harrison and colleagues (1991c) have established that Gsα mRNA is increased in the hippocampus in AD, while studies of Gsα protein suggest that it is unchanged (O'Neill *et al.*, 1994; McLaughlin *et al.*, 1991; Li *et al.*, 1996). The AD and control cases used by Li and colleagues (1996) in their examination of Gsα protein levels were matched for PMI. However, unlike O'Neill and co-workers (1994), Li and colleagues did not control for agonal state factors, and the variable effect of tissue acidosis on protein is well documented (Yates *et al.*, 1990), and they did not examine hippocampus. In contrast, both O'Neill and co-workers (1994) and McLaughlin and colleagues (1991), in their examination of Gsα protein levels in AD hippocampus, employed control tissue with significantly longer PMIs than those of their AD cases. However, the G proteins appear to be relatively resistant to post-mortem delay (Li *et al.*, 1996), further, there is no real possibility that extended PMIs in the control cases would result in an increase in Gsα protein. Thus, the discrepancy in length of PMI between the AD and control cases would be predicted to enhance, rather than diminish, the probability of identifying an increase in Gsα protein in the AD cases. Therefore, while there is no conclusive evidence that Gsα protein levels in AD hippocampus are equal to that in controls, the hypothesis that they are, and that it is the impairment in adenyl cyclase stimulation that results in up-regulation of Gsα expression, is intriguing (Cowburn *et al.*, 1992).

It was hoped that by using quantitative RT-PCR, it would be possible to generate products of sufficiently small size that the predicted 3 residue difference between Gsα-1 and Gsα-2 mRNA, and between Gsα-3 and Gsα-4 mRNA, would be sufficient to allow their differentiation on subsequent electrophoresis. The technique could be performed on minute quantities of tissue and would be rapid, allowing characterisation of a large number of control samples before comparing the relative abundance of the four isoforms in AD. A large and well characterised series of brain tissue from AD sufferers and controls were available for this work.

3.2 Materials and Methods

3.2.1 Prevention of Contamination

Initial RT-PCR experiments were beleaguered by contamination. Gel electrophoresis repeatedly demonstrated bands in template-free controls suggestive of contamination with amplified DNA (Figure 3.2).

Careful consideration was given as to the likely source(s) of the contamination. Vortexing, opening microcentrifuge tubes, pipetting and tip ejection can all generate aerosol particles which may be as large as 20 μm in diameter or 4×10^{-6} μl in volume. Since 24 000 copies of an amplified product may exist in such a volume (Orrego, 1990), the prevention of aerosols was deemed crucial. A safety cabinet, in an area of the laboratory geographically distant from where post amplification procedures were carried out, was washed out with a 1% Virkon solution (Antec International) before use and was reserved for all procedures up to, and including, the setting up of PCR reactions. A set of conventional air-displacement micropipettes, fitted with sterile aerosol resistant tips, were reserved for PCR set-up and the procedures preceding it. All reagents were divided into single use volumes in the PCR set-up area and stored in disposable, autoclaved plastic ware at -20°C.

Reagent and sample tubes were spun briefly in a microcentrifuge before opening and all non-sample PCR components were added to the reaction tube before the addition of sample DNA. All plastic ware was autoclaved before use and all metal instruments soaked in a 1% Virkon solution. Disposable gloves were worn for all procedures and changed frequently.

3.2.2 Extraction of Total RNA from Frozen Human Brain Tissue

Total RNA was extracted from cryostat cut frozen brain tissue using TRIzol Reagent (Gibco BRL). TRIzol isolation of RNA represents a modification of the one step RNA isolation method developed by Chomczynski and Sacchi (1987). Successful isolation of intact RNA requires that the tissue used is efficiently disrupted, that the endogenous nucleases released from membrane bound organelles during this process are immediately inactivated, that the nucleoprotein complexes are denatured and that the isolated RNA is free of DNA and protein.

RNA isolation was performed at room temperature in the safety cabinet within the laboratory area reserved for PCR preparation. Twelve 18 μm cryostat cut sections were lowered into 40 μl of TRIzol in a sterile 1 ml microcentrifuge tube on ice, with a pair of ice-cold plastic tweezers. The tissue was homogenised to smoothness with a hand-held homogeniser and a further 360 μl of TRIzol mixed in. The reaction was incubated at room temperature for 5 minutes to allow complete dissociation of the nucleoprotein complexes. Eighty μl of chloroform was added, the microcentrifuge tube firmly capped and the mixture shaken by hand for 15 seconds. The tube was incubated at room temperature for 3 minutes and then spun at 12 000 × g for 15 minutes at 4°C. The colourless, aqueous, upper phase containing the RNA was removed into a fresh, sterile, microcentrifuge tube taking care not to disturb the interface with the lower organic phase. The RNA was precipitated from the aqueous

phase by incubating the sample at room temperature for 10 minutes with 200 ml of isopropanol and 1 µl of glycogen and spinning at 12 000 × g for 10 minutes at 4°C. The pellet so formed was washed by vortexing with 75% ethanol in DEPC treated water and spun at 7 500 × g for 5 minutes at 4°C. The pellet was then air-dried at room temperature for 10 minutes and re-suspended in DEPC treated water by passing the solution through a pipette tip several times and incubating for 10 minutes at 55°C. Samples were stored under DEPC treated water at -70°C until required.

3.2.3 Measurement of Extracted RNA

The concentration and purity of the extracted RNA was assessed using a GeneQuant spectrophotometer (Pharmacia Biotech). A dilution of 1 part sample to 19 parts DEPC treated water in a total volume of 70 µl was placed in a cuvette. The ratio of the absorbance reading at 260 ηm (A_{260}) to the absorbance reading at 280 ηm (A_{280}) of pure RNA is 2.0 but A_{260}/A_{280} ratios of between 1.7 and 2.0 were accepted.

3.2.4 Reverse Transcription of Total RNA

Reverse transcription (RT) was performed by dissolving the required quantity of total RNA (0.04 to 2.5 µg) in 11 µl of water and adding 1 µl of oligo d(T). The reaction was incubated at 70°C for ten minutes, chilled on ice and pulsed briefly in a microcentrifuge. The following reagents were added:

5 × first strand buffer	4 µl
purified, deionised water	0.75 µl
0.1 M DTT	2 µl
mixed dNTP stock 10 mmolar for each dNTP	0.25 µl
SuperScript RNase H^- Reverse Transcriptase (200 units/µl)	1 µl

The reaction was incubated at 42°C for one hour and then heated to 99°C for 5 minutes to denature the cDNA-RNA hybrids and inactivate the reverse transcriptase enzyme. All RT reactions were performed in a Progene Thermal Cycler, (Techne). Two control tubes accompanied each RT reaction. Reverse transcriptase enzyme was omitted from one of the controls and in the other purified, deionised water replaced the RNA template. On completion, the RT samples were stored at -20°C until required. Two microlitres of the RT reaction volume was used in all PCR experiments.

While the above protocol proved satisfactory for reverse transcription of control human tissue (0.38-2.38 μg/μl), the yield obtained from AD tissue (0.22-0.58 μg/μl) proved disappointing.

3.2.5 Primer Design

Two 16 base primers were designed by scanning exons 2 and 4 of the human Gsα gene (Kozasa *et al.*, 1988) for regions, as close to the variably spliced region as possible, that had a GC content of 50%. Complementarity at the 3' ends of the primers was avoided as far as possible. RT-PCR was predicted to generate four products of 98 bases (Gsα-1), 95 bases (Gsα-2), 53 bases (Gsα-4) and 50 bases (Gsα-3) in length. It was hoped that since the primers were designed to anneal to different exons, the amplification of contaminating genomic DNA would be inhibited (Kawasaki, 1990).

The selected primers were entered into the European Molecular Biology Laboratory gene database to ascertain what known cDNA sequences, with a mismatch of 4 bases, were likely hybridise with the chosen primer sequences. When a primer pair was identified that were not homologous to any known cDNA sequence, the primers

were ordered from the Human Genome Mapping Resource Centre. The chosen sequences were as follows:

Exon 2 Primer	5'	C CTG CAT GTT AAT GGG	3'
Exon 4 Primer	5'	C CTG CAC TTT GGT TGC	3'

The exon 2 stock primer was obtained at a concentration of 4.2 mg/ml and the exon 4 stock primer at a concentration of 0.7 mg/ml. Diluted aliquots of the primers and the stock primers were stored at -70°C in separate freezers until use.

3.2.6 Calculation of the Annealing Temperature

The annealing temperatures of the primers were calculated as follows:

$$\text{Annealing Temperature} = [(\text{number of A+T}) \times 2°C + (\text{number of G+C}) \times 4°C]$$

Using this formula, the annealing temperature of the exon 2 primer was calculated to be 48°C and the annealing temperature of the exon 4 primer to be 50°C. Though *Taq* DNA polymerase is active over a wide range of temperatures, optimal annealing temperatures for the enzyme are between 55 and 72°C.

3.2.7 The PCR Protocol

A PCR programme was designed from first principles and optimised empirically thereafter. A range of annealing temperatures of between 40°C and 50°C were employed in an effort to maximise the efficiency of amplification of the desired products while minimising the generation of non-specific products. A permissive annealing temperature of 40°C was chosen initially and gradually increased since

low annealing temperatures facilitate incorrect annealing of primers and misextension of incorrect nucleotides at their 3' ends.

The final PCR programme was as follows:

Initial denaturation	96 °C	5 minutes

35 cycles of PCR were performed according to the following temperature profile:

Denature	94 °C	1 minute
Anneal	49.5°C	30 seconds
Extend	72 °C	1 minute
Final Extension	72 °C	3 minutes

Latterly, it was concluded that the initial denaturation step was too long and potentially damageing to the *Taq* DNA polymerase, therefore, it was reduced to 2 minutes without any detectable change in the products of the reaction.

A range of primer concentrations from 5 ηg/50 μl reaction mix to 500 ηg/50 μl reaction mix were employed in an effort to maximise the intensity of the desired bands on gel electrophoresis while minimising primer-dimer formation and the generation of non-specific products. Primer-dimer complexes are duplex PCR products in which the extension added to one primer is the antiparallel complement of the other primer (Innis and Gelfand, 1990). As such, primer-dimers represent a template-independent artefact, which, like non-specific background products, can themselves act as substrates in subsequent PCR cycles. Low annealing temperatures, high enzyme and primer concentrations and complementarity between the 3' ends of

primers enhance primer-dimer formation (Gelfand and White, 1990). Once present such products are prone to amplify efficiently and therefore compete for reagents.

A primer concentration of between 30 and 50 ηg/50 μl of reaction mix proved the most satisfactory. For ease of use, a primer concentration of 50 ηg/50 μl (10.1 ρmoles/50 μl) of reaction mix was used in all subsequent experiments. This resulted in a final molarity of primer of 0.2 μM: a figure within the range of 0.1 to 0.5 μM generally recommended (Innis and Gelfand, 1990).

Magnesium was added to the PCR as a 25 mM solution of magnesium chloride and a range of magnesium concentrations was studied. The magnesium concentration in the PCR mixture is crucial to the specificity, fidelity and yield of the reaction. Magnesium levels affect enzyme fidelity and activity, primer annealing, the temperature at which strand dissociation of both template and PCR products occurs, the specificity of the reaction and the formation of primer-dimer complexes (Innis and Gelfand, 1990). The addition of 4.5 μl of 25 mM magnesium chloride solution to each 50 μl of reaction mixture resulted in the greatest intensity of the desired bands on gel electrophoresis with a minimum of additional unwanted bands.

Care was taken to ensure that equal concentrations of the four dNTPs were added to the reaction volume to minimise the risk of incorporation errors.

The final PCR reaction mix consisted of the following reagents:

Thermo DNA Polymerase 10 times × reaction buffer	5 μl
mixed dNTP stock 10 mmolar for each dNTP	1 μl
25 mM $MgCl_2$ solution	4.5 μl
Taq DNA Polymerase in Storage Buffer A (5 000 units/ml)	0.25 μl
H_2O	32.25 μl
Exon 2 Primer 50 ηg/μl	1 μl
Exon 4 Primer 50 ηg/μl	1 μl
Reverse Transcription mix	2 μl

The reaction volume was overlaid with 25 μl mineral oil. All PCR reactions were carried out in the same Hybaid OmniGene PCR machine. The wells in the block were used randomly.

3.2.8 Polyacrylamide Gel Electrophoresis

In view of the small size of 98, 95, 53 and 50 bases of the expected products, 20% non-denaturing polyacrylamide gels, capable of resolving products of 6 to 100 bases, were employed initially to crudely separate the products of the PCR on electrophoresis.

Gels, 1 mm in thickness, were cast between glass plates of 100 × 82 and 100 ×72 mm on a vertical gel casting and electrophoresis apparatus (Bio-Rad Mini Trans Blot). The wells were created with a comb of 10 × 5 mm teeth. The glass plates, spacer and comb were washed after each use in a solution of detergent in warm water and rinsed in first tap water, and then distilled water, to remove any spots of grease which might impair the performance of the gel. Immediately prior to use, the

glass plates, spacer and comb were wiped over with absolute alcohol and allowed to dry before assembly.

A stock solution of 30% acrylamide was prepared as follows in a fume hood and stored in a dark bottle at room temperature until use. Twenty-nine grams of acrylamide and 1 g of N,N'-methylenebisacrylamide were measured into a flask and 60 ml of water added. The chemicals were dissolved by heating at 37°C in the fume hood and the solution was adjusted to a final volume of 100 ml and pH of 7.0.

Twenty % polyacrylamide gels were prepared from the 30% acrylamide stock as follows: 8.7 ml of 30% acrylamide stock was combined with 1.7 ml of purified, deionised water and 2.6 ml of 5 × tris borate EDTA buffer (TBE-see appendix I). Polymerisation was achieved by the addition of 7 µl of N,N,N',N'-tetramethyl-ethylenediamine (TEMED) and 70 µl of 25% ammonium persulphate (0.25g/ml). The solution was swirled gently to mix and immediately drawn into a disposable plastic pipette. The nozzle of the pipette was introduced into the space between the glass plates and the acrylamide solution gently expelled. The comb was gently lowered into the gel. Once set, the gel was removed from the casting apparatus and fitted into the gel tank. The tank was filled with 1 × TBE and the comb removed. The wells were immediately rinsed with 1 × TBE from the gel tank to remove any unpolymerised acrylamide solution. Acrylamide gels were cast in duplicate and after rinsing of the wells with 1 × TBE were stored at 4 °C under 1 × TBE until use. No impairment in the quality of the gels was apparent with storage of up to one week.

Five microlitres of loading gel buffer (see appendix I) was added to each 50 µl PCR reaction volume and, after mixing, 10 µl of each sample was loaded onto the gel.

Gels were run at 120 volts until the dye front was three-quarters of the way down the gel. Gels were stained in 5 μl of ethidium bromide in 200 ml of 1 × TBE for 20 minutes. Once stained, the gel was viewed by transillumination on an ultraviolet light box and photographed with a 5" Polaroid camera.

3.2.9 Size Determination of the Reaction Products on Non-Denaturing Polyacrylamide Gel Electrophoresis

A θX174 DNA/*Hinf* I marker, prepared by digestion of θX174 DNA to completion with *Hinf* I, was used to aid in identification of the products of the PCR. θX174 DNA/*Hinf* I markers are composed of 20 DNA fragments varying in length from 726 to 24 base pairs. One μl of θX174 DNA/*Hinf* I marker stock was added to 19 μl of water and 2 μl of loading gel buffer. Initially, a 100 base ladder was loaded onto each gel in addition to aid in identification of the products of the reaction.

Two bands of approximately 50 and 100 bases were clearly visible on non-denaturing polyacrylamide gel electrophoresis, corresponding to the long and short isoforms of Gsα, as well as a number of unexpected reaction products (Figure 3.2).

3.2.10 The Preparation and Purification of γ^{32}PATP Labelled Primer

Despite assiduous attempts at optimisation of the RT-PCR of the variable exon 2 to exon 4 region of Gsα mRNA, it was not possible to eliminate a number of unwanted, apparently non-specific, PCR products. Reducing the concentration of the primers or, indeed, increasing the annealing temperature used, resulted in loss of both the unwanted and the desired bands. These bands may result from cross reaction of the primers with RNA species derived from other genes, conceivably as yet undiscovered members of the G protein family that are highly homologous with Gsα,

Figure 3.2 RT-PCR of Gsα from total RNA using [^{32}P]ATP labelled exon 2 primer run on a 20% non-denaturing polyacrylamide gel at 200 volts. Two bands of approximately 50 and 100 kilobases, corresponding to the short and long splice variants of Gsα mRNA, are clearly visible as well as a number of unexpected reaction products. Gel electrophoresis, such as this, repeatedly demonstrated bands in template free controls suggestive of contamination with amplified DNA.

In the extreme left hand lane of each gel is a θX174 DNA/*Hinf* I marker (base pairs).

Gel A

Lane 1	Positive control.
Lane 2	Newly reverse transcribed RNA.
Lane 3	Newly reverse transcribed RNA.
Lane 4	No RNA.
Lane 5	No reverse transcriptase enzyme.
Lane 6	No RNA.
Lane 7	No reverse transcriptase enzyme.
Lane 8	Empty lane.

Gel B

Lane 1	Starting total RNA of approximately 2.50 μg.
Lane 2	Starting total RNA of approximately 1.25 μg.
Lane 3	Starting total RNA of approximately 0.63 μg.
Lane 4	Starting total RNA of approximately 0.31 μg.
Lane 5	Starting total RNA of approximately 0.16 μg.
Lane 6	Starting total RNA of approximately 0.08 μg.
Lane 7	Starting total RNA of approximately 0.04 μg.
Lane 8	Starting total RNA of approximately 0.02 μg.

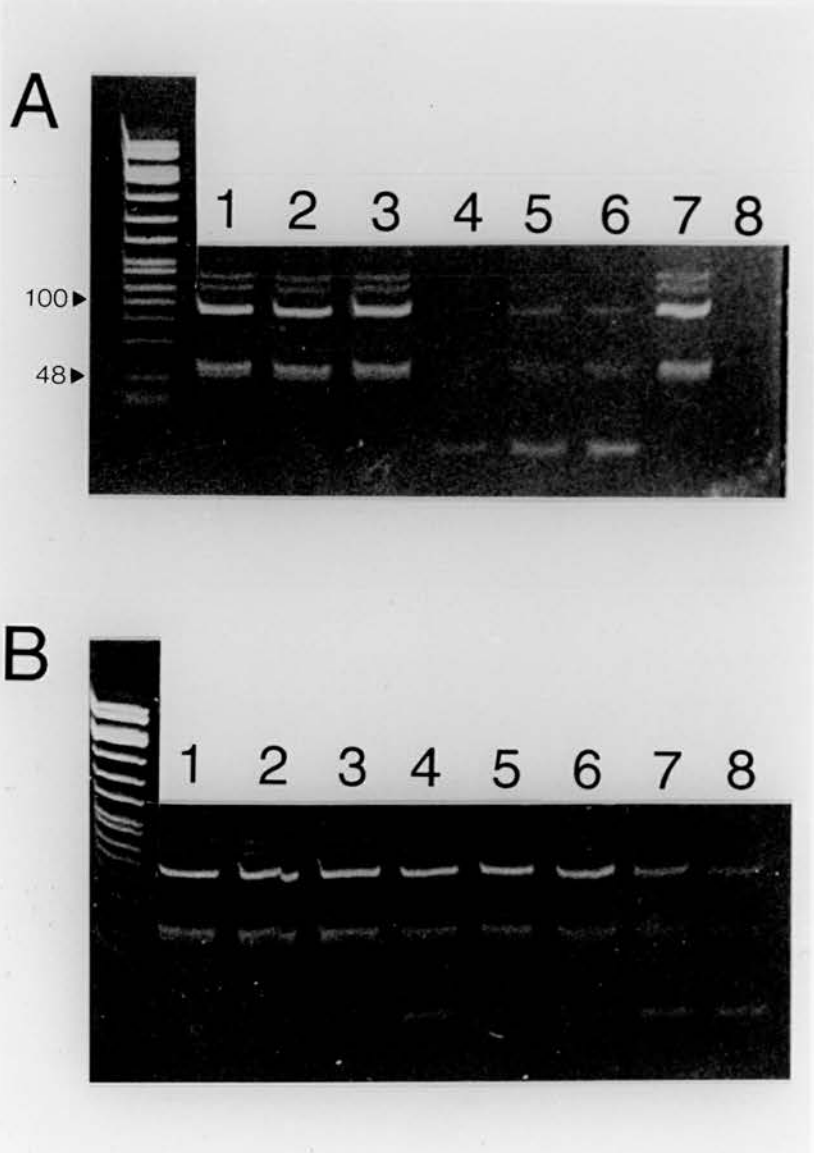
A
1 2 3 4 5 6 7 8
100▶
48▶
B
1 2 3 4 5 6 7 8

or previously unrecognised alternative splice products of Gsα. The bands were too small to be contaminating genomic DNA. Despite the presence of these additional, unwanted bands it was decided to pursue RT-PCR of Gsα mRNA using the primers already described.

To allow quantitation of the PCR products generated, the exon 2 Gsα primer was labelled with γ^{32}phosphorus ATP (γ^{32}PATP). This radioisotope has a half-life of 14.2 days and is a high energy (1.6 MeV) β emitter, therefore, all experiments involving γ^{32}PATP were conducted behind a 10 mm Perspex screen or within a Perspex β station. Microcentrifuge tubes in use were racked within a lidded-Perspex box, opened with a tube opener and closed with the aid of stainless steel forceps and tweezers. Tips and eppendorfs were discarded into a 10 mm lidded Perspex box. A solution of decontaminating fluid (Decon 90, BDH/Merck) was available throughout the experiments and the area was regularly monitored with a Geiger counter. A dosimeter badge and finger rings were worn throughout.

Five hundred pmoles (sufficient for approximately 49 reactions of 50 μl each) of the exon 2 primer were labelled with γ^{32}PATP. The following were assembled in a sterile 1 ml eppendorf:

500 pmoles exon 2 primer	24.8 μl of 100 ηg/μl concentration
DEPC treated water	to final volume of 50 μl
5 × kinase buffer	10 μl
γ^{32}PATP	5 μl
T4 polynucleotide kinase	1 μl

The reaction was heated to 37°C for 10 minutes before the addition of 1 µl of rATP (ribonucleoside ATP). A further 10 minute incubation at 37°C followed. ProbeQuant G-50 Micro Columns (Pharmacia Biotech) were used to separate the labelled probe from any unincorporated nucleotides. The Sephadex G-50 DNA Grade F resin in the columns was re-suspended by vortexing. The cap was loosened by a quarter of a turn and the bottom closure on the column was snapped off. The column was supported in a 1 ml microcentrifuge tube and spun at 735 × g for 1 minute. The column was removed to a fresh supporting 1 ml microcentrifuge tube and the 50 µl reaction volume was slowly applied to the top centre of the resin. The column was spun at 735 × g for a further 2 minutes. A Geiger counter was held at a standard distance from the tube and the intensity of radioactivity estimated. The volume of the purified probe was measured and the tube capped. γ^{32}PATP labelled probes were stored in lead containers at -20°C until use, which was always within 10 days. A positive and three negative control reactions were performed to ensure that the efficiency of the labelling was adequate for subsequent experiments and to demonstrate that the labelled primer was free from DNA contamination.

3.2.11 The Preparation of γ^{32}PATP Labelled θX174 DNA/*Hin*f I Ladder

The θX174 DNA/*Hin*f I ladder was dephosphorylated prior to γ^{32}PATP labelling since the addition of γ^{32}PATP groups to a dephosphorylated substrate proceeds more efficiently than an exchange reaction. The 5' phosphate groups were removed by incubating 10 µl of the θX174 DNA/*Hin*f I ladder stock with 2 µl of calf intestinal alkaline phosphatase at 37°C for 10 minutes. The enzyme was subsequently denatured by heating at 85°C for 15 minutes.

2.5 µl of the dephosphorylated ladder was then labelled as follows:

2.5 µl	dephosphorylated θX174 DNA/*Hinf* I ladder
10.5 µl	water
4 µl	5 × kinase buffer
2 µl	γ^{32}PATP
1 µl	T4 polynucleotide kinase

The reaction was incubated at 37 °C for 10 minutes before the addition of 5 µl of rATP followed by a further 10 minute incubation at 37°C. A final reaction volume of 50 µl was achieved by the addition of 30 µl of autoclaved STE buffer (see appendix I). The labelled ladder was purified using the ProbeQuant G-50 Micro Columns (Pharmacia Biotech) described above. The volume of labelled ladder and the intensity of the labelling were estimated as for the labelled primer. 1 µl of the radioactively labelled ladder was combined with 1 µl of loading gel buffer and 8 µl of water in preparation for loading on the 20% polyacrylamide gels.

3.2.12 Quantitative RT-PCR of Gsα Using γ^{32}PATP Labelled Exon 2 Primer

In order to establish the optimum cycle number for subsequent RT-PCR amplifications, 40 µl of RT mixture from a single RT experiment with a starting RNA of 1 µg/12 µl RT reaction mixture, was amplified over a range of between 22 and 33 reaction cycles. It is crucial that the PCR is stopped while the products are continuing to accumulate exponentially and the starting amount of RNA can be linearly related to the amount of product. Product accumulation such that the strands reanneal or fail to denature at high temperature, diminution of required reagents, inhibition by end products and competition for the reagents from unwanted

non-specific products or primer-dimer, all impair the efficiency of the reaction (Innis and Gelfand, 1990) and ultimately the amount of product reaches a plateau.

The approximate volume of γ^{32}PATP labelled exon 2 primer containing 10.1 pmoles of primer was calculated. A master mix sufficient for 20 reaction volumes of 50 µl each containing all of the reagents required for the RT-PCR, with the exception of the RT mixture, was assembled and mixed thoroughly. Three aliquots of master mix were removed for the control reactions and an appropriate amount of cDNA was added to the master tube and mixed. The solution was aliquotted, overlaid with 25 µl of mineral oil and placed randomly in the wells of the Hybaid OmniGene thermal cycler.

Once the reaction reached completion the samples were prepared and loaded on a 20% non-denaturing polyacrylamide gel as described above. The gel was not stained in order to avoid introducing an unnecessary step, but was immediately fixed by immersion in a combination of 10% methanol and 10% acetic acid in deionised water for 20 minutes. The gel was then mounted on a piece of card, covered with clingfilm and dried at 80°C for 1 hour on a gel dryer. Once dry the gel was taped to a phosphoimageing cassette, covered with a sheet of screen guard and opposed against the phosphoimageing screen for 1 hour. The screen was then loaded into a scanner and the image analysed using the software package Molecular Analyst for Windows on a dedicated personal computer. The bands of interest were outlined and their volume, adjusted for background, was measured. This technique is far less labour intensive than cutting out the radioactive bands and subjecting them to scintillation counting.

In only three lanes of the gel were product bands visible. Two product bands of the appropriate size were seen in the lanes of the gel corresponding to 25, 28 and 32 cycles of the PCR. The experiment was reviewed and the possible sources of error considered. On meticulous repetition of the experiment, the same pattern of products was obtained. In some lanes two bands of clearly visible radioactivity, corresponding to the RT-PCR of the long and short forms of Gsα mRNA, were obtained. In other lanes a broad band of radioactivity, level with the end of the gel, but no distinguishable product bands, was seen (Figure 3.3).

On review of the experiment it was clear that sufficient accumulation of product occurred after 26 cycles of PCR for bands to be visible on non-denaturing polyacrylamide gel electrophoresis. It was highly unlikely that the reaction had reached a plateau by this stage and so the thermal cycler was programmed for 26 cycles of PCR only.

Having gauged the optimal number of PCR cycles, the starting quantity of extracted total RNA at which the reaction was likely to progress most efficiently was investigated. It was also necessary to demonstrate that the relationship between the long and short forms of Gsα was resistant to variations in the amount of total RNA added to the RT-PCR.

A dilution series was prepared from 5 μg of total RNA extracted from control frontal cortex dissolved in 20 μl autoclaved, deionised water. Ten μl containing 2.5 μg total RNA was removed to a fresh eppendorf and the remaining aliquot was diluted with a further 10 μl of autoclaved, deoinised water. This procedure was repeated until the final eppendorf contained 10 μl containing 1/64 of the initial 2.5 μg of total RNA. Each tube was reverse transcribed as described above. A master mix, containing all

Figure 3.3 RT-PCR of Gsα from total RNA using [^{32}P]ATP labelled exon 2 primer run on a 20% non-denaturing polyacrylamide gel at 200 volts. Two product bands of the appropriate size are seen in lanes representing 25, 28 and 32 cycles of the PCR. No distinguishable product bands are visible in the other lanes.

Lane 15	No RNA.
Lane 14	No reverse transcriptase enzyme.
Lane 13	33 PCR cycles.
Lane 12	32 PCR cycles.
Lane 11	31 PCR cycles.
Lane 10	30 PCR cycles.
Lane 9	29 PCR cycles.
Lane 8	28 PCR cycles.
Lane 7	27 PCR cycles.
Lane 6	26 PCR cycles.
Lane 5	25 PCR cycles.
Lane 4	24 PCR cycles.
Lane 3	23 PCR cycles.
Lane 2	22 PCR cycles.
Lane 1	θX174 DNA/*Hin*f I marker.

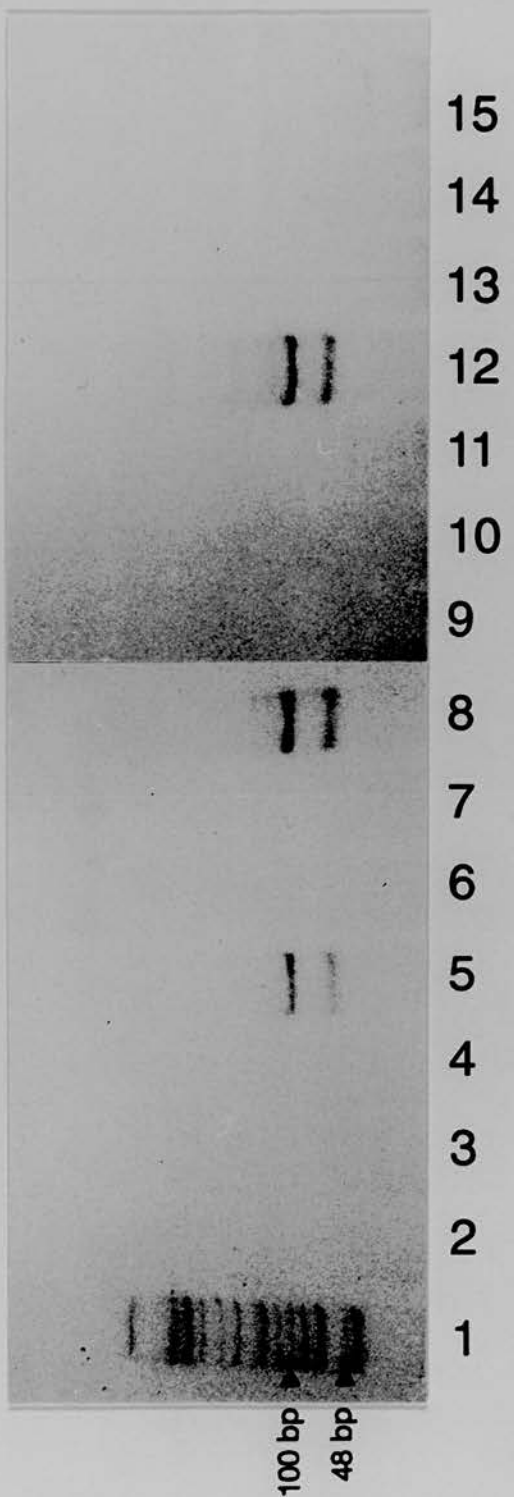
15
14
13
12
11
10
9
8
7
6
5
4
3
2
1
100 bp
48 bp

of the reagents required for PCR, including the γ^{32}PATP labelled exon 2 primer, was assembled and aliquotted into a series of eppendorfs containing 2 μl of each of the RT reactions prepared from the RNA dilution series. The tubes were placed randomly in the thermal cycler and following 26 cycles of PCR the reaction mixture was prepared for loading on a 20% non-denaturing polyacrylamide gel. The gel revealed poor amplification both at high (2.5 μg) and low (1/64 of 2.5 μg) starting concentrations of RNA. The experiment was repeated with a fresh total RNA dilution series employing a narrower range of starting total RNA from 1.25 μg/10 μl to 0.4 μg/10 μl total RNA. Amplification was observed to proceed most efficiently with an intermediate concentration of starting total RNA of approximately 0.6 μg/10 μl. Higher and lower concentrations of total RNA resulted in less efficient amplification (Figure 3.4).

Since the variable efficiency of the RT-PCR might reasonably have been predicted to affect both products equally, the ratio between the volumes, adjusted for background radioactivity, of the two bands corresponding to Gsα-S and Gsα-L was calculated. An approximately two-fold variation in this ratio was observed over a range of starting total RNA of 0.04 μg to 1.25 μg (Table 3.1). When a narrower range of starting total RNA from 0.4 μg to 1.25 μg was employed, there was no appreciable improvement in this ratio.

3.3 Discussion

3.3.1 Overview of the Study

In retrospect, this study was extremely ambitious given the universally acknowledged technical difficulty of the work (Salomon, 1995a; Vandevyver and Raus, 1995), my lack of experience with RT-PCR and, perhaps, the failure of other groups to answer this research question (Bray *et al.*, 1986; Granneman and Bannon,

Figure 3.4 RT-PCR of Gsα from total RNA using [^{32}P]ATP labelled exon 2 primer run on a 20% non-denaturing polyacrylamide gel at 200 volts.

A dilution series of total RNA was prepared ranging from approximately 1.25 to 0.4 μg of total RNA/10 μl. Amplification was observed to proceed most efficiently with an intermediate amount of starting total RNA of approximately 0.6 μg/10 μl.

Lane 1	θX174 DNA/*Hinf* I marker.
Lane 2	1.25 μg starting total RNA/10 μl.
Lane 3	1.0 μg starting total RNA/10 μl.
Lane 4	0.8 μg starting total RNA/10 μl.
Lane 5	0.6 μg starting total RNA/10 μl.
Lane 6	0.4 μg starting total RNA/10 μl.
Lane 7	No reverse transcriptase enzyme.
Lane 8	No RNA.


1 2 3 4 5 6 7 8
100 bp
48 bp

Phosphoimaging Results of Quantitative RT-PCR of Gsα Using ^{32}PATP Labelled Exon 2 Primer

Concentration of Starting RNA (μg)	Volume, Adjusted for Background, of Electrophoretic Band Corresponding to Gsα-L mRNA	Volume, Adjusted for Background, of Electrophoretic Band Corresponding to Gsα-S mRNA	Ratio of Volume of Gsα-L to Volume of Gsα-S
1.25	10506	5343	1.966
0.62	3169	2273	1.394
0.31	22083	10754	2.053
0.16	54811	38252	1.433
0.08	34528	22922	1.506
0.04	8194	3937	2.081

Table 3.1

1991). However, it was possible to co-amplify two products corresponding in size to Gsα-S and Gsα-L using the technique and to explore systematically, identify and eradicate the persistent contamination which hampered early optimisation experiments. Radioactive labelling of the exon 2 primer with γ^{32}PATP was successful and the resulting images could be transformed and analysed satisfactorily with the phosphoimageing equipment. Nonetheless, it proved impossible to answer the three main scientific questions that the study was designed to address namely: What is the relationship between all four known isoforms of Gsα in the hippocampus of neurologically normal controls? Is overall Gsα expression altered in homogenised hippocampus in AD and if so, changes in which isoform(s) of Gsα is/are responsible for this overall effect? Latterly, a judgement had to be made as to whether continuing to persevere with this study was a measure of my tenacity and perseverance or, alternatively, simply obsessional and imprudent.

3.3.2 Technical Problems Inherent to the Design of the Study

The study's basic design generated a number of technical problems. Firstly, the exon 2 and exon 4 primers were deliberately abbreviated in an attempt to ensure that the size difference between the various isoforms of Gsα was as great a proportion of the total length of the synthesised products as possible. However, primers of 18 to 22 bases in length (Kawasaki, 1990) are generally recommended for PCR and a 16 base primer with a 50% GC content necessitates an annealing temperature of 49.5°C, when a temperature of greater than 55°C is advised (Innis and Gelfand, 1990). Secondly, γ^{32}PATP labelled primers were chosen because of the speed and sensitivity with which radioactively labelled bands can be detected on subsequent gel electrophoresis of reaction products. The optimisation of cycle number and RNA concentration, however, required significant quantities of radioactively labelled primer and the short half-life of 14.2 days of γ^{32} necessitated that fresh primer be

prepared frequently. Aside from the hazards posed by intensive exposure to γ^{32}, the shielding required is cumbersome, especially where large numbers of samples are being prepared and clearing up following radioactive work is laborious and necessarily meticulous. A non-radioactive detection method would have been more agreeable and might ultimately have proved less time consuming. Finally, the use of only one set of primers to generate all four desired products eliminated differences in amplification efficiency between primer sets (Singer-Sam and Riggs, 1993). However, had primer sets been chosen which allowed me to examine the RT-PCR of Gsα-L and Gsα-S separately it would have been possible to optimise the two reactions independently and determine whether their co-amplification was theoretically probable. Differences in the lengths of the template cDNA sequences to be amplified can affect primer/template hybridisation (Singer-Sam and Riggs, 1993). Further, variations in the secondary structure or sequence of target species between their identical priming sites can cause differences in amplification efficiency even with the same primer set (Scheuermann and Bauer, 1993).

3.3.3 Aspects of the Study Which Could Have Been Improved

A number of other aspects of the study could have been improved. The initially intractable problem of contamination, eventually eradicated, made for an exhausting and vexing start to the study. Further attention should have been paid to the dNTP concentration since it is conceivable that it was too high. Plentiful dNTPs make mispriming at non-target sites and the extension of misincorporated nucleotides more likely and an attempt should have been made to ensure that the dNTP concentration in the reaction mixture was thoroughly optimised. Further, the rate of errors produced by *Taq* DNA polymerase is increased at high dNTP concentrations (Hayashi, 1994). The final yield of amplified product might have been improved had random hexamers been used for first strand synthesis, since they are believed to

afford the most efficient and consistent results and the greatest final yield of amplified product (Kawasaki, 1990). Their use minimises the effects of mRNA secondary structure and sequence complexity. They are particularly useful when the mRNA sequence of interest is at a distance from the poly(A)$^+$ tail and especially when samples are likely to contain partially degraded mRNAs (Noonan and Roninson, 1988). Since this study hoped to employ total RNA from diseased human tissue, exploration of this method of first strand synthesis might have been worthwhile. Finally, Ferré and colleagues (1994) warn that variations in the purity of RNA obtained from the one step RNA extraction method employed in this study may prevent the precise quantitation of mRNA by impairing the efficiency of RT-PCR (Ferré *et al.*, 1994).

3.3.4 Analysis of the Outcome of This Study

The results, generated using the phosphoimageing software, of the RT-PCR of Gsα over a variable number of cycles of PCR, appeared at first to be inexplicable. The reagents were assembled as a master mix and clearly some of the tubes had amplified successfully effectively ruling out the possibility of reagent or template omission or their failure. That the RNA used was of poor quality was rejected on subsequent RT-PCR of the same aliquot of RNA. The possibility remained that the RT mixture had been inadequately mixed into the master mix thus the experiment was repeated with assiduous attention to detail resulting in a similar pattern of intermittent amplification with successive cycle numbers of PCR. This particular experiment was unusual in that it required a large number of sample tubes, which were placed randomly in the wells of the Hybaid GeneQuant thermal cycler, to be processed simultaneously. Thus, wells of the heating block not required in earlier optimisation experiments were pressed into service and it is conceivable that some of these were faulty. There is support for this view in the literature, since Orrego

(1990) studied two commonly employed thermal cyclers and concluded that temperature gradients across heating blocks were frequent when short step times are used. He specifically advises using the central wells in PCR heating blocks. Hoof and co-workers (1991) regard the thermocycler as an important source of variability in PCR and indeed Salomon (1995a) attributes the large increase in researchers successfully engaged in quantitative PCR, in part, to the development of thermocyclers that exhibit minimal well-to-well variability in cycle parameters. Alternatively, it is possible that the contact between the microcentifuge tubes employed and the wells of the PCR machine was poor, since, for reasons of economy, they were not those specified for use in the Hybaid GeneQuant Thermal Cycler. Hybaid do manufacture a range of thin walled PCR tubes which precisely fit their thermal cyclers and ensure maximal surface contact between the tubes and the block for optimal thermal transfer and in retrospect it would have been a wise investment to purchase these. The optimisation of vessel/heating block contact during design and manufacture makes for good tube fit which is critical for efficient thermal transfer (Newton, 1997). Ultimately, this economy may have proved costly.

The experimental design of the RT-PCR of Gsα obviated the need for an internal standard. Rather than attempt to measure the absolute amount of Gsα mRNA, it was the relationship between the four isoforms of Gsα in normal hippocampus, and the amount of Gsα generated from a fixed quantity of total RNA from AD versus control tissue, that was to be studied. The true relationship between the four isoforms of Gsα can only be discerned, however, if all four forms amplify with equal efficiency under the RT-PCR conditions employed. Further, alterations in the reaction conditions, such as might realistically occur experimentally, should influence the efficiency of the RT-PCR of all four isoforms equally. In reality, Gsα-S and Gsα-L

appeared to be differentially affected by changes in the reaction conditions and this was especially true for the starting amount of total RNA.

It is recognised that the amplification of individual species of cDNA can be differentially affected by reaction conditions such as RNA concentration or quality or the presence of contaminants. Reagents left over from RNA preparation or one or more components of the cDNA reaction mixture can inhibit amplification of cDNA species in a non-uniform way by, for example, impairing the activity of *Taq* DNA polymerase, competing for binding sites or altering the conformation of the template DNA (Siebert, 1993). It proved impossible to eliminate a number of unwanted bands visible on non-denaturing polyacrylamide gel electrophoresis and it is conceivable that they too might differentially affect accumulation of the different isoforms of Gsα and interfere with the dynamics of the reaction. Scheuermann and Bauer (1993) have demonstrated that an alteration in the reaction conditions of an experiment can result in the same RNA molecules amplifying with a different efficiency. Crucially, in quantitative RT-PCR any differences in the amplification efficiencies of the reaction products can, with repeated cycles of PCR, result in dramatic differences in the final results (Scheuermann and Bauer, 1993).

The efficiency of the reaction peaked at a starting concentration of RNA of 0.6 μg of total RNA per 12 μl of RT reaction, but at lower and higher concentrations fell away steeply. It appeared that the reaction was not robust and that relatively minor variations in the reaction conditions further impaired template amplification. Minor pipetting errors are to be expected in RT-PCR, even when pipettes are regularly serviced and calibrated and used with care. It was clear that variations in the amount of starting RNA could lead to pronounced loss of product. It was possible, however, that though the RT-PCR was less efficient, that all four isoforms of Gsα were

equally disadvantaged and that the relationship between them in native tissue would be maintained. Therefore, the ratio between Gsα-L and Gsα-S was calculated for the range of RNA concentrations studied. It became clear that the amplification of Gsα-S and Gsα-L were differentially affected by alterations in the starting concentration of RNA, since modest, and experimentally probable, alterations in the concentration of RNA extracted from a single control brain resulted in a two-fold change in the ratio between Gsα-L and Gsα-S. It was concluded that the relationship between Gsα-L and Gsα-S could not be meaningfully examined by their co-amplification by RT-PCR under the experimental conditions chosen.

3.3.5 Implications

By using ISHH, Harrison and co-workers (1991c) were able to examine Gsα mRNA levels in a neuronally rich sub-population of hippocampal cells demonstrating a marked increase in Gsα mRNA in AD tissue compared to controls. In contrast, both McLaughlin and colleagues (1991) and O'Neill and co-workers (1994) examined Gsα protein levels in homogenised hippocampal tissue. Studies of a mixed population of cells do not, of course, exclude the possibility of a neuronally specific increase in Gsα protein in hippocampus in keeping with Harrison and co-workers (1991c) mRNA findings. Indeed, should an exclusively neuronal increase in Gsα protein levels occur in AD, this increase is likely to be obscured by the large numbers of other cell types present in a tissue homogenate. This would be especially true of tissue from AD sufferers given the prominence of gliosis in the pathophysiology of the disease. It would be interesting to compare Harrison and colleagues (1991c) results with the analysis of a multi-cellular pre-selected area of hippocampus that had been subjected to ISHH with the same Gsα probe employed by Harrison and co-workers (1991c). This would provide an estimate of Gsα mRNA

in a mixed population of hippocampal cells that could be more meaningfully compared with the Gsα protein studies discussed above.

3.3.6 Future Work

Further study of the mRNAs encoding the various isoforms of Gsα in AD is a crucial follow up to the work of Harrison and colleagues (1991c). It would be experimentally feasible, using ISHH, to quantify separately the mRNA levels of Gsα-S and Gsα-L in the hippocampus of AD and control tissue. ISHH, performed with a ^{35}S labelled oligodeoxynucleotide probe specific for exon 3 of Gsα mRNA, would allow selective analysis of Gsα-L. A second oligodeoxynucleotide probe, designed to hybridise to those bases found at either end of exon 3, would allow the detection of isoforms of GSα in which these bases were continuous, and therefore only to Gsα-S. Thus, the contribution of these two forms of Gsα mRNA to the increase in total Gsα mRNA identified in AD hippocampus in comparison to control hippocampus could be discerned.

Exon 3 encodes a 45 nucleotide insert which is present in the large isoforms of Gsα mRNA. The region of the large isoforms of Gsα protein encoded by exon 3, is a hydrophilic section hypothesised to interact with adenyl cyclase. A Gsα-mediated increase in the activity of adenyl cyclase resulting in higher levels of cAMP, increased protein kinase activity and ultimately increased phosphorylation, would be of enormous interest in AD.

Both an S1 nuclease protection assay and a PCR based technique have failed to disentangle the contribution of the four known isoforms of Gsα mRNA to the overall increase in Gsα mRNA identified in AD hippocampus. Had it been possible to establish the robust amplification of two RNA species corresponding in molecular

weight to Gsα-L and Gsα-S, an alternative way of quantifying the relative contribution of each of the four isoforms of Gsα to overall levels of Gsα mRNA might have been feasible. Single nucleotide primer extension (SNuPE) (Singer-Sam and Riggs, 1993) has been used to quantify the relative abundance of two mRNA species that differ by only a single base. This technique could be applied to the study of Gsα mRNA levels as follows. Non-radioactive RT-PCR of the variably spliced exon 3 region of Gsα mRNA could be performed, the products gel purified and the two bands, corresponding to Gsα-L and Gsα-S, excised. The band containing Gsα-L could then be incubated with *Taq* polymerase for one round of extension with a primer, the SNuPE primer, whose 3' end is just 5' to the adenine residue of the variably included 'CAG' nucleotide sequence. The sample could then be incubated in separate tubes with either γ^{32} dCTP or γ^{32} dTTP and the products of the two reactions subject to denaturing polyacrylamide gel electrophoresis. The amount of radioactivity in the appropriately sized bands could be measured and the ratio between Gs-α-1 and Gsα-2 mRNA calculated. A similar procedure could be performed on the excised band containing Gsα-S to examine the relative contribution of Gsα-3 and Gsα-4 mRNA to Gsα-S mRNA.

The central role of Gsα in cellular responsiveness merits the application of such techniques and renders its further investigation essential.

Chapter 4

Goα mRNA Levels are Decreased in the Dentate Gyrus in Alzheimer's Disease and are Correlated with Total Amyloid Precursor Protein mRNA Levels in this Region

4.1 Introduction

APP is a glycosylated transmembrane protein (Kang *et al.*, 1987) from which β–amyloid, the major protein constituent of the plaque and meningovascular amyloid deposits which characterise AD, is cleaved (Glenner and Wong, 1984; Masters *et al.*, 1985a). APP has characteristics reminiscent of a cell surface receptor (Kang *et al.*, 1987). It is located in cellular membranes, including at the cell surface, possesses a single membrane spanning domain and bears a consensus sequence on its cytoplasmic tail that is thought to be necessary for ligand dependent internalisation in a clathrin coated pit (Chen *et al.*, 1990). No receptor function has yet been ascribed to APP, but Nishimoto and colleagues (1993) hypothesise that APP is a receptor linked to Go, a member of the signal-transducing, heterotrimeric G protein family, believed to regulate phospholipase C dependent phosphoinositide hydrolysis (Moriarty *et al.*, 1990) and control neuronal calcium and potassium channels (Ewald *et al.*, 1988; Hescheler *et al.*, 1987; Kleuss *et al.*, 1991; VanDongen *et al.*, 1988). Nishimoto and co-workers (1993) have demonstrated that Go forms a complex with APP, and that the His^{657}-Lys^{676} domain in the cytoplasmic sequence of APP is necessary for formation of this complex and activation of Go (Nishimoto *et al.*, 1993). The authors propose that, in AD, Go is constitutively activated by APP.

Go interaction with dopamine D2 (Lledo *et al.*, 1992), muscarinic m2 and m4 (Matesic *et al.*, 1991), somatostatin (Law *et al.*, 1993) and opioid μ and δ receptors

(Roerig *et al.*, 1992; Laugwitz *et al.*, 1993) has been demonstrated in native membranes. As well as its hypothesised role in APP signal transduction, Go is postulated to activate effector systems in response to other novel factors such as the intracellular growth associated protein GAP-43 (Strittmatter *et al.*, 1990, 1991). Go has been demonstrated to inhibit adenyl cyclase in JEG-3 cells on muscarinic receptor activation and on constitutive activation of Goα (Migeon *et al.*, 1994); the apoptosis and negative transactivation of cAMP response element, documented to occur in response to mutated forms of APP in COS-NK1 cells, is also hypothesised to be mediated through Go (Yamatsuji *et al.*, 1996a; Ikezu *et al.*, 1996).

Go, or the 'other' GTP-binding protein as it was labelled by Sternweis and Robinshaw in 1984, is a member of the G protein family that is preferentially expressed in the central nervous system (Price *et al.*, 1989). Go accounts for approximately 0.5 to 1% of membrane protein in the brain (Bertrand *et al.*, 1990). It is generally highly concentrated in synaptic-rich neuropil and absent from neuronal cell bodies (Worley *et al.*, 1986). At least three mRNAs, of 5.7, 4.2 and 3.2 kilobases, code for Goα in brain. All three mRNAs encoding Goα are spliced from a single gene (Bertrand *et al.*, 1990) that exhibits 45% gene homology with Gsα (Itoh *et al.*, 1986). Two 354 amino acid isoforms of Goα exist in brain, labelled Goα1 and Goα2, which differ in 26 of their 106 carboxyl terminal amino acids (Hsu *et al.*, 1990). Spicher and co-workers (1992) have investigated the existence of a third form of Goα in mammalian brain which is electrophoretically distinct from the other two, but it is unclear whether the protein identified is indeed a hitherto undiscovered product of the Goα gene, or merely the result of alternative co- or post-translational processing of one of the already identified forms. Goα is both myristoylated and palmitoylated and both acylations contribute to the association of Goα with the membrane (Mumby *et al.*, 1994).

Gs, as was discussed in chapter three, is a specific G protein known to stimulate the catalytic subunit of adenyl cyclase (May *et al.*, 1985) and to activate voltage-gated calcium channels in cardiac and skeletal muscle (Yatani *et al.*, 1987; Mattera *et al.*, 1989). The mRNA encoding Gsα has been shown to be significantly increased in hippocampal fields CA1, CA3 and CA4 and in the dentate gyrus in AD brain in comparison to neurologically normal controls (Harrison *et al.*, 1991c). This increase was not the result of a generalised increase in mRNA expression, as the increase in Gsα mRNA remained even when expressed as a proportion of total poly(A)$^+$ mRNA levels in the same cell populations. McLaughlin and colleagues (1991) and O'Neill and co-workers (1994) failed to demonstrate a concomitant increase in Gsα protein in hippocampus in AD in using immunoblotting, though O'Neill and colleagues found that the ratio of large to small molecular weight isoforms of Gsα was significantly increased in the hippocampus and angular gyrus of AD brains in comparison to controls.

Thus, Go represents an incompletely investigated member of a family of proteins common to many of the neurotransmitter systems known to be abnormal in AD. Elucidation of the extent of G protein α subunit mRNA abnormalities in AD is crucial to the interpretation of functional neurotransmitter deficits in the disease. Further, the success of therapeutic strategies involving provision of neurotransmitter precursors, direct agonists or inhibitors of neurotransmitter metabolism depend on the functional integrity of associated signal transduction mechanisms. To assume that these are intact may be erroneous, since abnormalities in signal transduction in AD have been documented at numerous stages of the signal transduction cascade (See Fowler *et al.*, 1992 for review).

Goα mRNA expression was investigated in the hippocampi of a series of AD brains

and age matched neurologically normal controls. The aims of the study were twofold. Firstly, to explore whether the documented increase in Gsα mRNA in AD is a gene specific abnormality, or whether other members of the G protein family also exhibit increased mRNA levels. Secondly, given the functional association postulated to exist between Go and APP by Nishimoto and colleagues (1993), to determine whether any correlation exists between hippocampal Goα and APP gene expression in the same series of brains.

4.2 Materials and Methods

4.2.1 Introduction

This experiment was performed with the assistance of Dr. A.J.L. Barton on brains from series I. The clinical and demographic details of these cases, along with information relating to agonal state scores, PMI, storage time as a block and storage time as cryostat cut sections, is presented in appendix II. Summarised information relating to the cases included in series I is presented in table 4.1. The brains were prepared and hybridised as described in chapter 2.

4.2.2 Oligodeoxynucleotide Probe Selection

The Goα antisense probe consisted of a 45 base oligodeoxynucleotide (Oswell DNA Services) directed against bases 1-45 of the coding region of the human genomic clone (Lavu *et al.*, 1988). Total APP mRNA was detected by combining two 30 base probes, the APP-insert oligodeoxynucleotide probe and the APP-junction oligodeoxynucleotide probe, and applying them to the sections. The APP-insert antisense oligodeoxynucleotide probe is directed at bases 1047 to 1076 of the APP-751 cDNA sequence published by Ponte and co-workers (1988) and theoretically detects APP mRNA isoforms APP-751, APP-770, APP-563 and APP-365. The APP-junction antisense oligodeoxynucleotide probe is directed

Diagnosis, Demographic, Agonal State Score and Storage Details of Series I Cases

Diagnosis	Number of Cases	Sex	Age in Years (mean ± SD)	Post Mortem Delay in Hours (mean ± SD)	Agonal State Score (mean ± SD)	Block Storage Time in Days (mean ± SD)	Section Storage Time in Days (mean ± SD)	Total Storage Time in Days (mean ± SD)
Control Group of Cases	15	Female = 6 Male = 9	77.3 ± 10.7 (n = 15)	36.8 ± 17.3 (n = 10)	2.2 ± 1.3 (n = 8)	218.7 ± 181.3 (n = 15)	551.6 ± 378.7 (n = 15)	770.3 ± 274.2 (n = 15)
AD Group of Cases	30	Female = 17 Male = 13	81.2 ± 10.8 (n = 30)	35.2 ± 17.2 (n = 28)	2.8 ± 1.1 (n = 20)	307.3 ± 227.6 (n = 30)	517.2 ± 360.0 (n = 30)	824.5 ± 302.4 (n = 30)
Total	45	Female = 23 Male = 22	79.9 ± 10.8 (n = 45)	35.6 ± 17.0 (n = 38)	2.6 ± 1.1 (n = 28)	277.8 ± 215.4 (n = 45)	528.6 ± 362.4 (n = 45)	806.4 ± 291.3 (n = 45)

Control group of cases = Neurologically normal controls and Age-related change cases
AD group of cases = Alzheimer's disease, Borderline Alzheimer's disease and Mixed diagnostic categories

Table 4.1

against bases 975 to 989 and 1158 to 1172 of the APP-751 cDNA sequence published by Ponte and colleagues (1988) and therefore only hybridises to APP isoforms in which the flanking regions of the KPI domain are contiguous, as in APP-695 alone (see Harrison *et al*, 1994). Goα and APP-junction sense oligodeoxynucleotide probes were employed to control for the effects of non-specific binding.

4.2.3 Experimental Controls

Dr. A.J. Barton demonstrated the specificity of the Goα oligodeoxynucleotide probe using Northern blotting with a [^{32}P]-dATP-labelled probe hybridised to 20 µg total RNA extracted from the frontal cortex of a control subject (Figure 4.1). The specificity of the APP-insert and APP-junction oligodeoxynucleotide probes has been demonstrated in our laboratory by Dr. P.J. Harrison by Northern blotting of RNA extracted from frontal cortex. The APP-insert probe detects a single band of 3.4 kb and the APP-junction probe detects a single band of 3.3 kb (Harrison *et al.*, 1994). Concurrent hybridisation of adjacent sections under identical conditions with the complementary sense strand oligodeoxynucleotide probe was also performed.

4.2.4 In Situ Hybridisation Histochemistry

The total APP probe was prepared by combining the APP-junction probe with the APP-insert probe such that 0.57 million counts per minute of each probe in a total volume of 100 µl was applied to the sections. The hybridised sections were incubated for approximately 18 hours, at 40°C for the Goα probe, and at 27°C for the total APP probe. The slides were then washed in 1 × SSC (4 × 15 minute washes) at 60°C for the Goα probe, and at 52.5°C for the total APP probe. These washes were then followed by 2 × 60 minute washes at room temperature. Once dry, the hybridised sections were placed against film (Hyperfilm-βmax, Amersham) at room

Figure 4.1 Northern blot provided by Dr. A.J.L. Barton demonstrating the specificity of the Goα oligodeoxynucleotide probe. The oligodeoxynucleotide probe was labelled with [^{32}P]-dATP and hybridised to 20 μg of total RNA extracted from the frontal cortex of a neurologically normal control. A major band of Goα mRNA of 3.4 kilobases is seen.

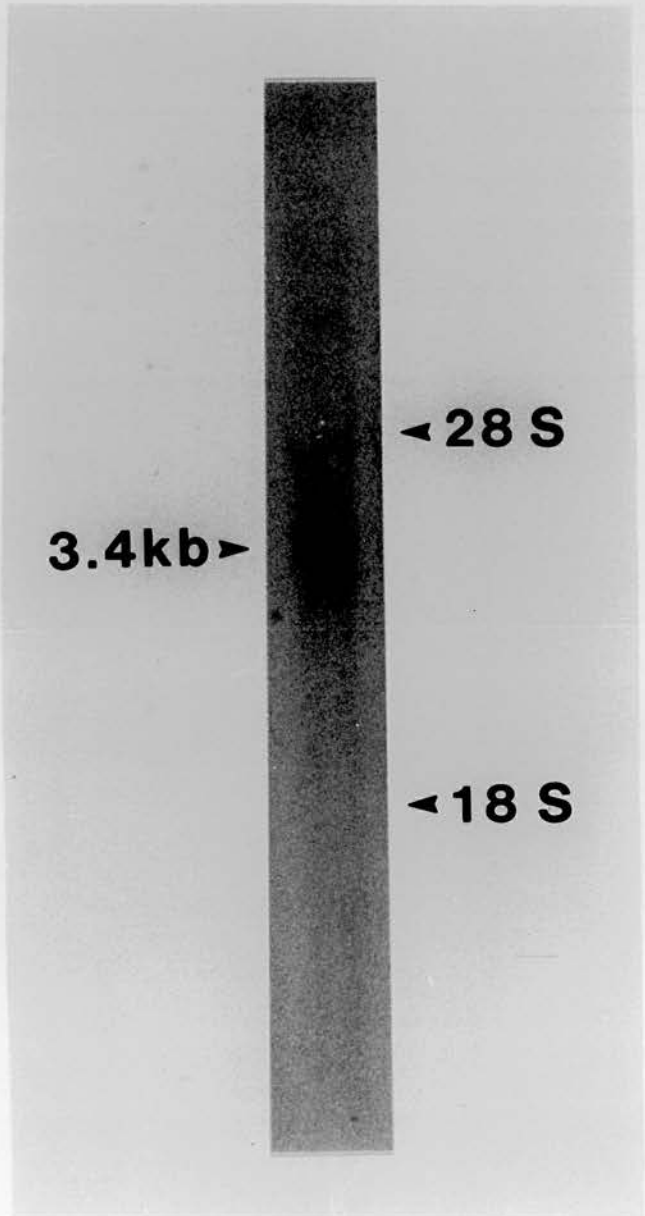
28 S
3.4kb
18 S

temperature for 46 days to generate autoradiograms (Figure 4.2).

4.2.5 Detection of Polyadenylated Messenger RNA

Where available, additional hippocampal sections from each case were hybridised with a sense and antisense probe directed against the poly(A)$^+$ tail of polyadenylated mRNAs in order to correct, at least partially, for the differences in overall mRNA content between individual brains and diagnostic groups (Harrison *et al.*, 1991b, 1993). The antisense probe comprised a strand 30 thymine deoxynucleotides, while the sense probe consisted of a strand of 30 adenine deoxynucleotides. The specificity of the poly(dT) oligodeoxynucleotide probe was demonstrated by incubation of a subset of hippocampal sections with an excess of unlabelled poly(dT) probe resulting in the abolition of signal. Similarly, pre-treatment of a subset of hippocampal sections with ribonuclease abolished hybridisation of the labelled oligodeoxynucleotide probe. The autoradiograms generated by the above cold displacement and ribonuclease pre-treatment were completely blank. The standard ISHH protocol, as detailed in the Materials and Methods chapter, was modified for this experiment. Briefly, the hybridisation buffer was prepared with 2 × SSC, rather than 20 × SSC, and 20%, rather than 50%, of formamide was added to the solution. The sections hybridised with the poly(A)$^+$ antisense and sense probes were incubated for approximately 18 hours at 25°C and washed at 35°C. The hybridised sections were exposed to autoradiographic film for 40 minutes to generate autoradiograms (Figure 4.3). The strength of ISHH signal was analysed over dentate gyrus only for each case.

Figure 4.2 *In situ* hybridisation histochemistry using [^{35}S]dATP labelled oligodeoxynucleotide probes performed on hippocampal sections from the same control case from series I. The images presented are direct photographs of transilluminated autoradiograms generated from this single case and hybridised with the following oligodeoxynucleotide probes. The blacker the image of the autoradiogram the greater was the exposure of the autoradiographic film to radioactivity and the more intensely labelled was the section.

A Goα antisense oligodeoxynucleotide probe.

B Goα sense oligodeoxynucleotide probe.

C Total APP antisense oligodeoxynucleotide probe.

D Total APP sense oligodeoxynucleotide probe.

DG dentate gyrus
CA1 cornu Ammonis subfield 1
CA3 cornu Ammonis subfield 3
* cornu Ammonis subfield 4

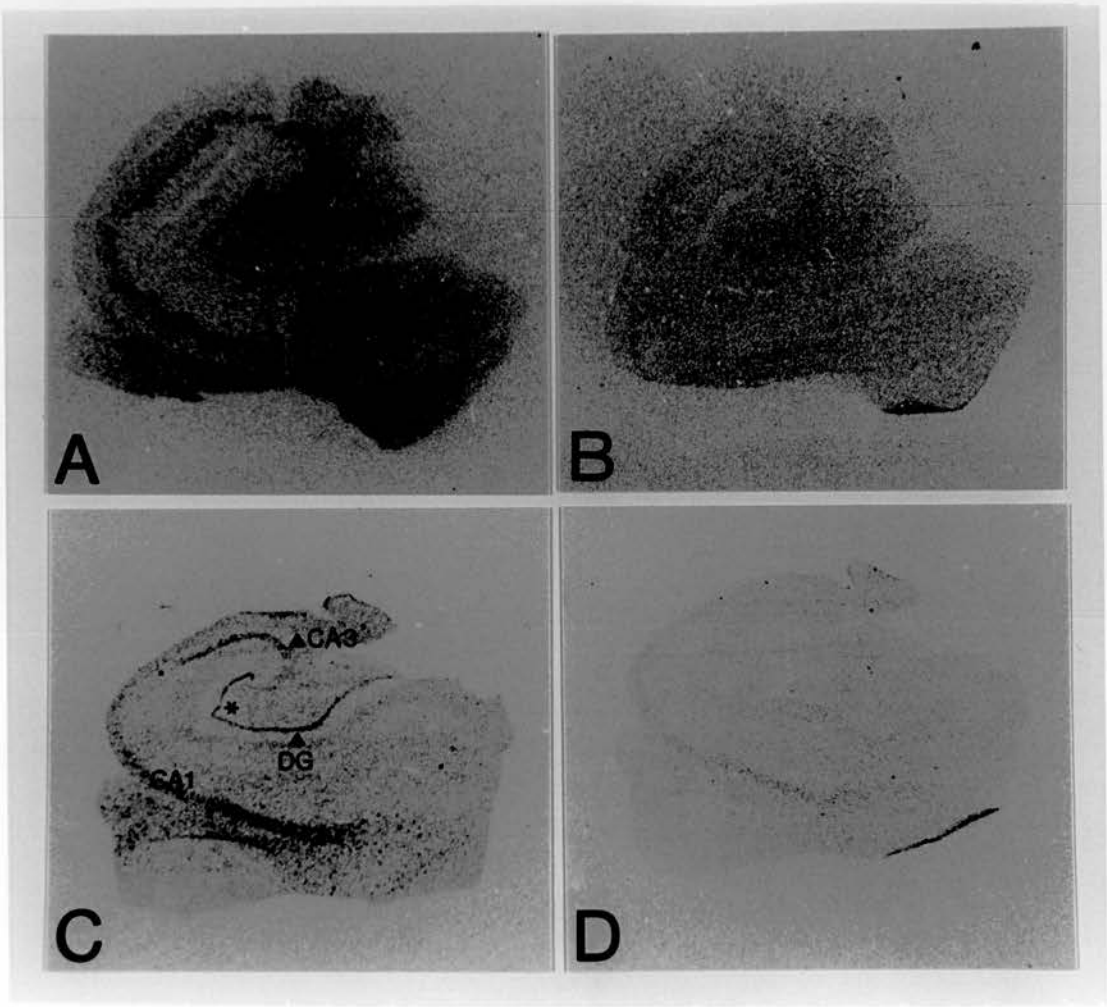
A
B
CA3
DG
CA1
C
D

Figure 4.3 Autoradiogram of a hippocampal section from an AD case from series I hybridised with the [^{35}S]dTTP labelled poly(dT) oligodeoxynucleotide probe. The autoradiogram of the corresponding sense section was completely blank.

This image was obtained by direct photography of the transilluminated autoradiogram. Thus, the blacker the image of the autoradiogram the greater was the exposure of the autoradiographic film to radioactivity and the more intensely labelled was the section.

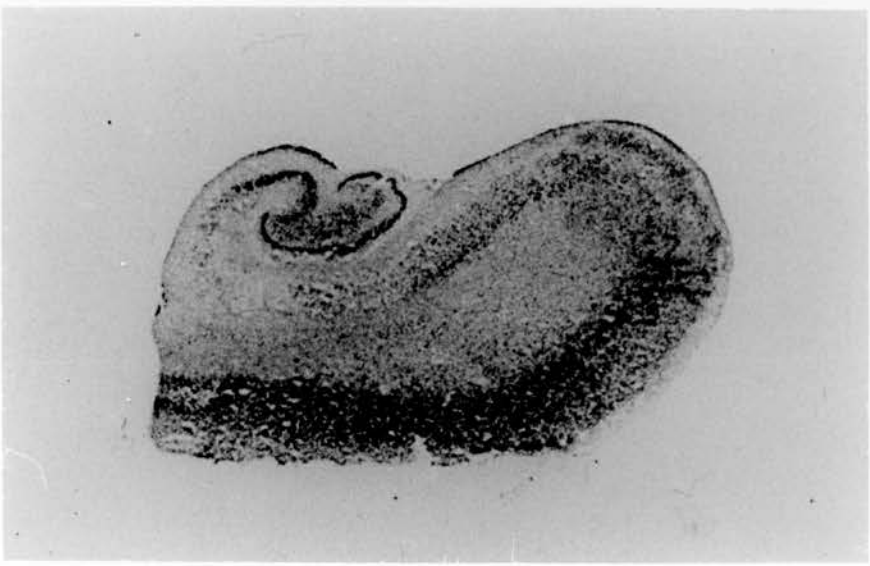

4.2.6 Quantification of ISHH Signal

Quantitative assessment of ISHH signal, reflecting relative abundance of Goα and total APP mRNAs, was made on the autoradiograms using an image analysis system (Image Manager PC, Sight Systems, Newbury). Grain counting over individual neurons was not possible in this series given the histological quality of the tissue. Mean grey density was calculated, blind to case details, over the stratum granulosum of the dentate gyrus and over the stratum pyramidale of hippocampal fields CA3 and CA4. The mean value from each set of triplicates was used for subsequent calculations. AOD readings, obtained by dividing 255 by the mean grey density, adjusted for background, and logging the result, were used in all statistical analyses. Mean grey density over hippocampus was calculated for the Goα and APP-junction sense oligodeoxynucleotide probes. The AOD of each of the sense probes, representing non-specific binding, was calculated as above. The AOD of the Goα sense probe in both the AD and control groups was 0.020, while the AOD of the APP-junction sense probe was 0.023 in both groups. These AOD readings were subtracted from the AOD readings calculated for the appropriate antisense probe prior to statistical analysis.

4.2.7 The Relationship between Radioactivity and Approximate Optical Density

^{14}C microscales (Codes RPA 504 and RPA 511, Amersham) were opposed to the autoradiographic film alongside the specimen sections and analysed with them and in the same way. An average AOD reading was obtained for each radioactive layer of the polymer. This value was plotted against the tissue equivalent radioactivity of that layer in nCi/g as supplied by the manufacturer (Figure 4.4). A linear relationship was demonstrated between the AOD and tissue equivalent radioactivity at AOD readings of less than 1.33. Since no AOD readings pertaining to this experiment

Figure 4.4 Tissue Equivalent Radioactivity in nCi/g Against Approximate Optical Density for ^{14}C Microscales Accompanying Goalpha Experiment

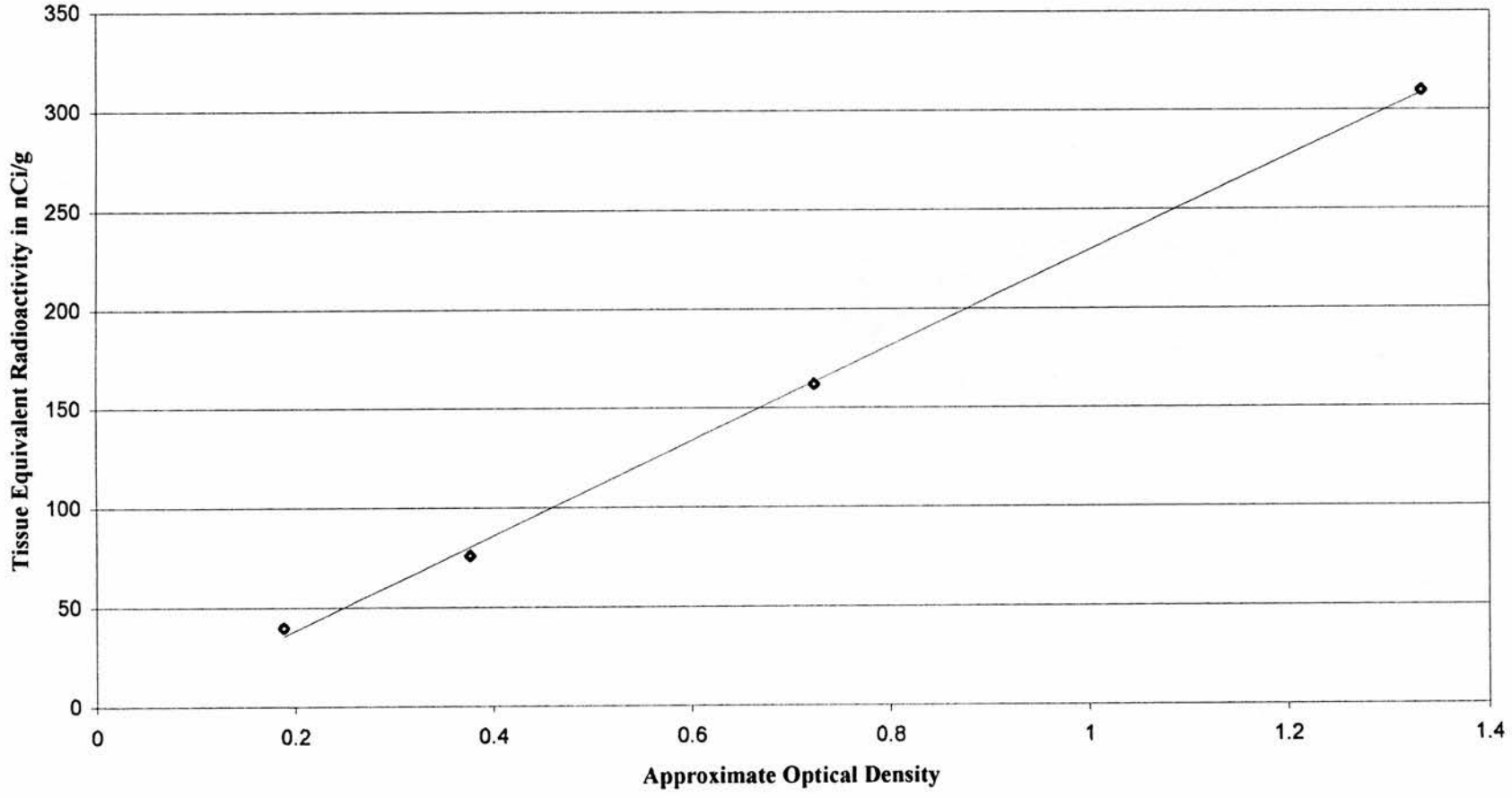

were obtained which were in excess of this level, all readings fell within the linear portion of the graph.

The equation of the line of best fit for the plot of AOD against tissue equivalent radioactivity for the ^{14}C microscales was calculated to be:

$$y = 239x - 9.29$$

Computation of the F statistic for this line revealed a figure of 2018 suggesting that the probability that the straight line fit of this data occurred by chance was $p < 0.001$. Thus, the straight line fit of this data is highly significant.

4.2.8 Statistical Analysis

All statistical analysis was performed using SPSS for Windows version 6.0. A two-tailed Student's *t* test was used to compare the control and AD group of cases. Where Levene's test for homogeneity of variance was not significant, it was assumed that the requirements of the Student's *t* test had been met. Where Levene's test was significant, it was assumed that the requirements for the parametric test had been violated and the data was examined using the non-parametric Mann-Whitney U.

Correlation matrices were constructed using both Pearson's correlation coefficient and Spearman's rank correlation coefficient. When the two tests were in agreement, the result was accepted, when a discrepancy was observed, the data was analysed further, as detailed in the text.

4.3 Results

The Goα antisense probe has been demonstrated to hybridise to a major band of 3.4 kb on a Northern blot performed on RNA extracted from frontal cortex from a neurologically normal control (Figure 4.1). The specificity of the APP-insert and

APP-junction antisense probes has been demonstrated by Northern blotting of RNA extracted from frontal cortex; the oligodeoxynucleotide probes detect single bands of 3.4 and 3.3 kb respectively, and do not cross-hybridise to each other's target APP mRNA isoforms (Harrison *et al.*, 1991d, 1994).

No statistically significant differences were found between the control and AD group of cases in terms of age, agonal state score, PMI or storage duration of the tissue, as a block or as cryostat cut sections, using a two-tailed Student's *t* test. No significant difference was observed in poly(A)$^+$ mRNA levels between the control and AD group of cases using a two-tailed Student's *t* test (Figure 4.5).

Comparison of Goα mRNA ISHH signal between the control group of cases (control and age-related change cases) and the AD group of cases (AD, borderline AD, mixed AD and Parkinson's disease and mixed AD and multi-infarct dementia cases), revealed that Goα mRNA signal was reduced in the dentate gyrus of the AD group in comparison to the control group (two-tailed Student's *t* test $p = 0.001$). No statistically significant difference in Goα mRNA levels was found, however, between the two groups in fields CA3 or CA4 of the hippocampus (Figure 4.6).

Total APP mRNA levels were also found to be statistically significantly lower in the AD group of cases when compared with the control group of cases in the dentate gyrus (Mann-Whitney U two tailed corrected for ties $p < 0.001$). No statistically significant difference between the groups in total APP mRNA level was apparent over hippocampal fields CA3 or CA4 using a two-tailed Student's *t* test (Figure 4.7).

Nishimoto and colleagues (1993) have shown that APP forms a complex with Go and have identified a cytoplasmic sequence, the His^{657}-Lys^{676} domain, in APP which

Figure 4.5 Poly(A^+) mRNA Expression in the Dentate Gyrus of Series I Alzheimer's Diseased and Control Brains

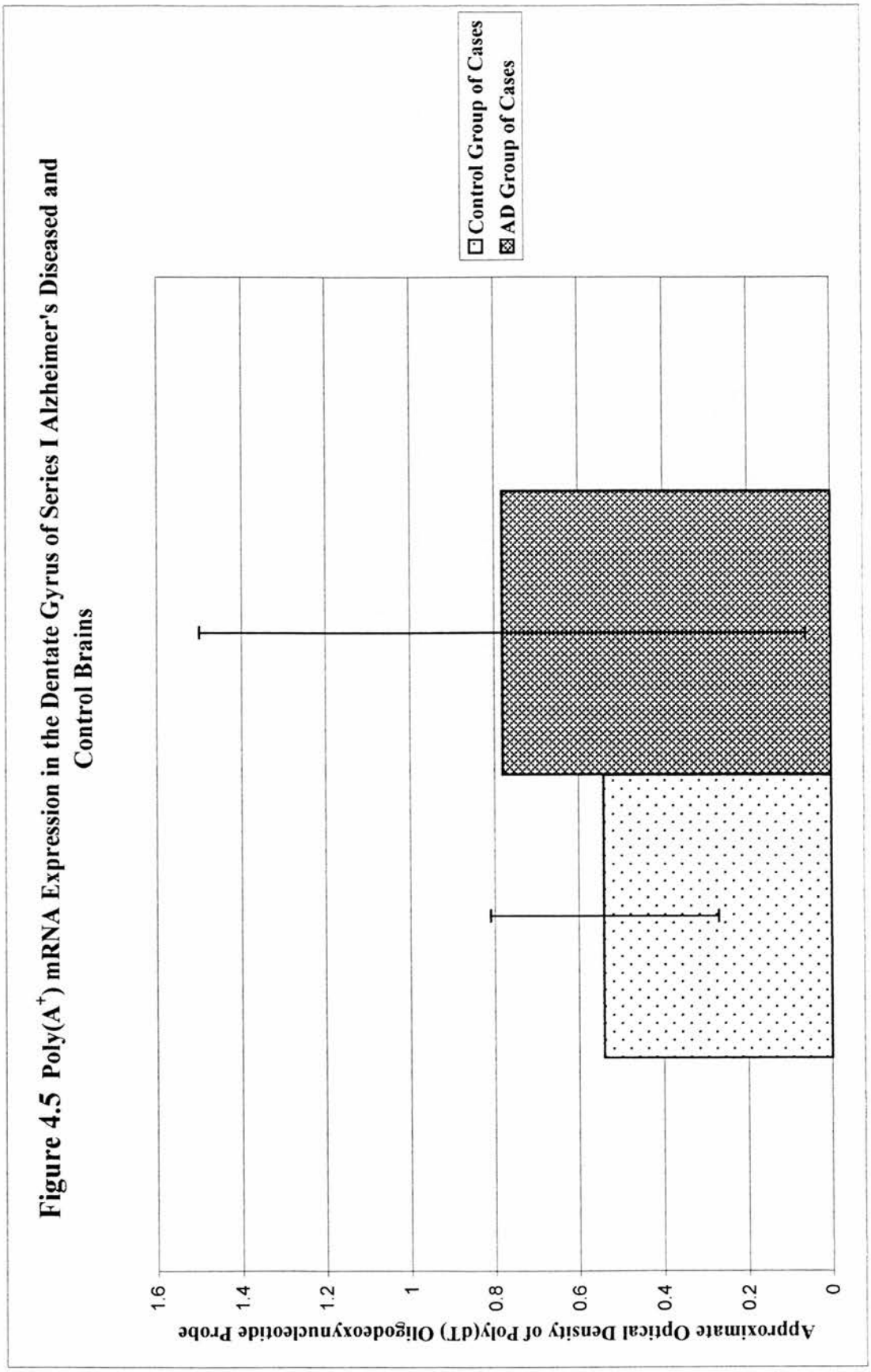

Figure 4.6 Goalpha mRNA Expression in the Hippocampus in Alzheimer's Diseased Versus Control Brains

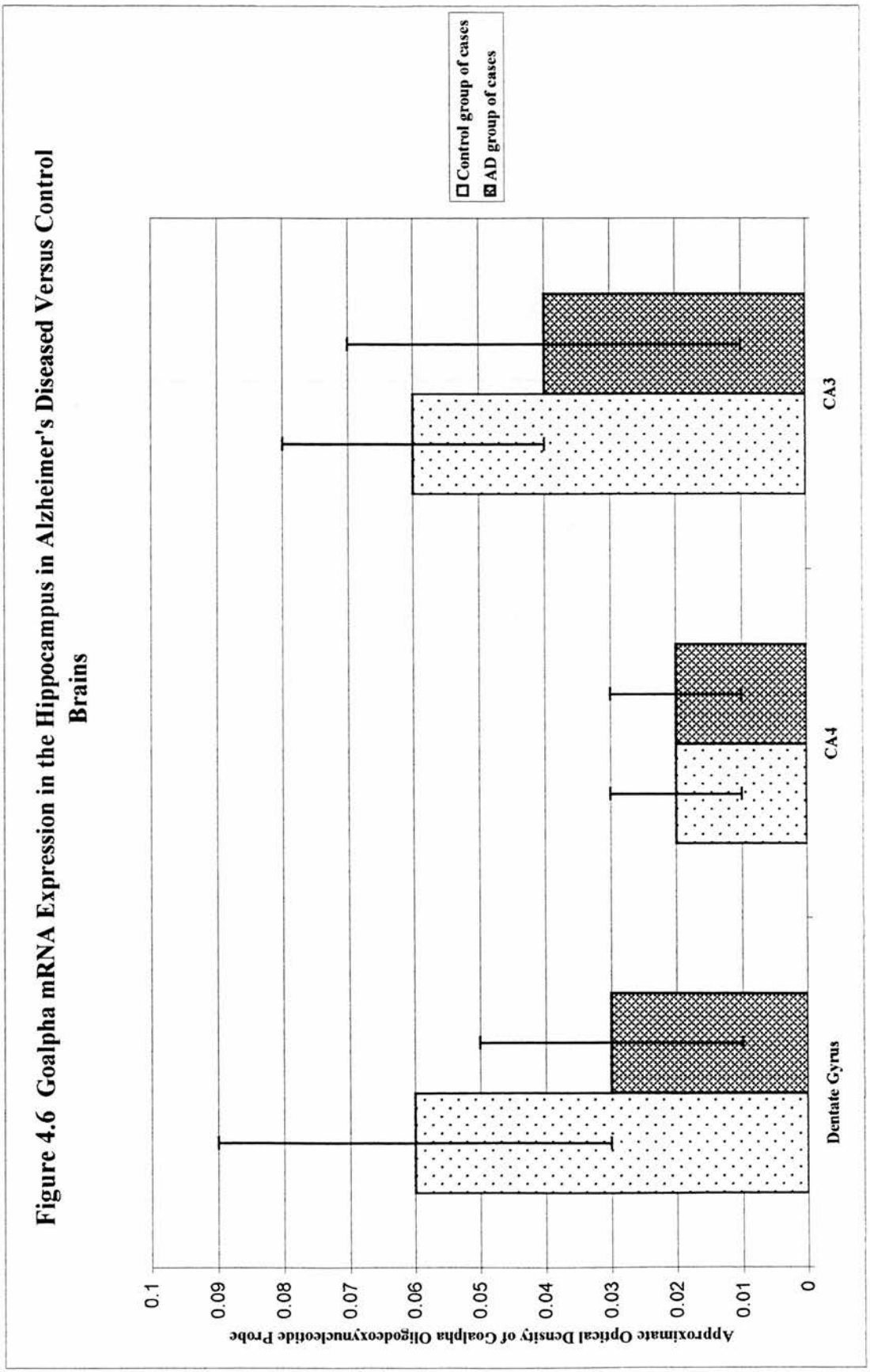

Figure 4.7 Total APP mRNA Expression in the Hippocampus in Alzheimer's Diseased Versus Control Brains

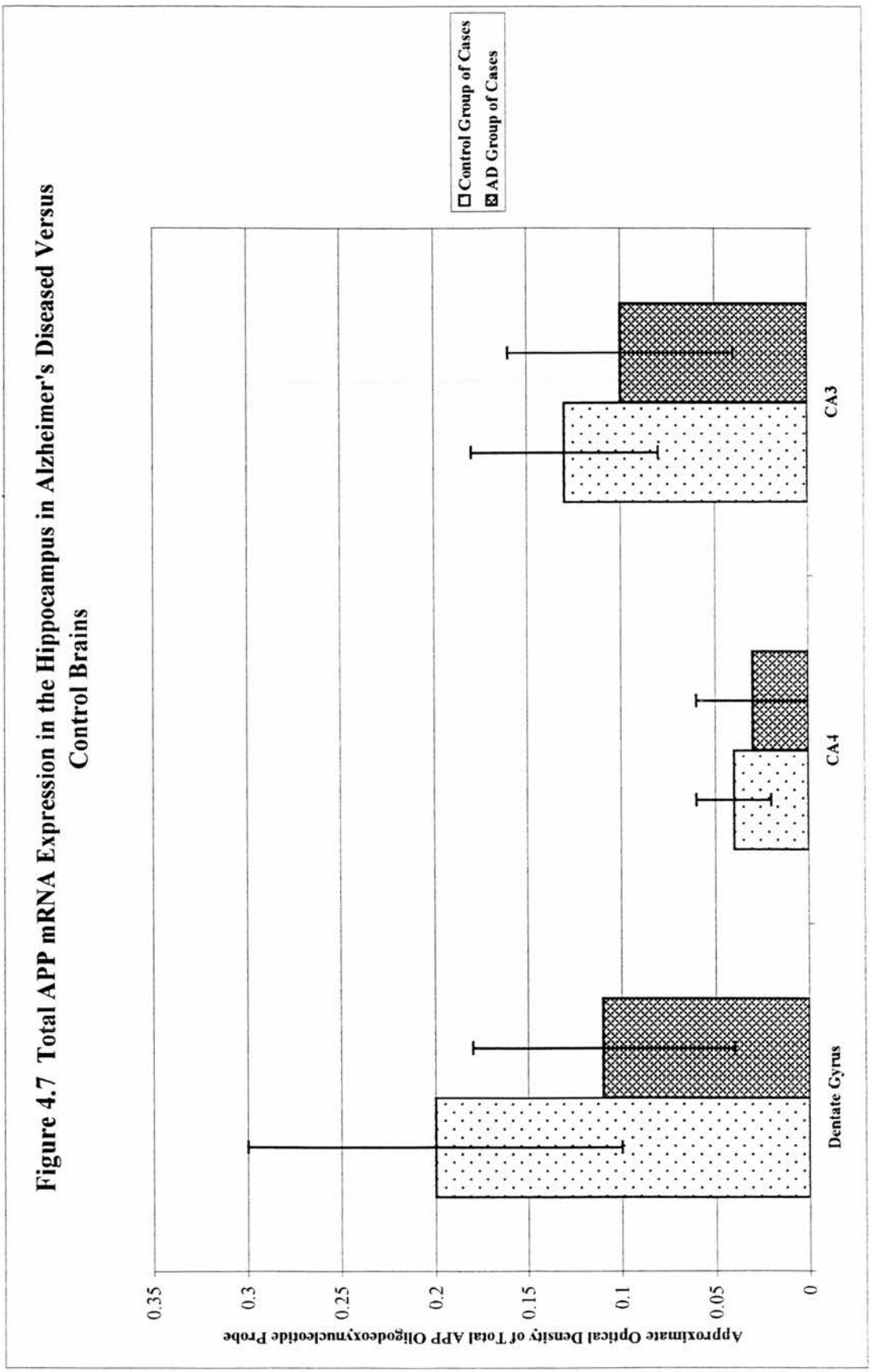

is necessary for complex formation. Thus, we were curious as to whether APP and Go mRNA levels might be correlated if studied in the same series of brains (Table 4.2). Pearson's correlation coefficient relating Goα and APP mRNAs in the dentate gyrus of all cases yielded a correlation coefficient of 0.825 ($p < 0.001$). The mRNA levels of Goα and total APP were not statistically significantly correlated in either CA3 or CA4 of the hippocampus. No statistically significant correlation was found between Goα mRNA and poly(A)$^+$ mRNA levels or between total APP mRNA and poly(A)$^+$ mRNA levels in dentate gyrus using Pearson's correlation coefficient (Table 4.2).

Total APP mRNA levels in CA4 were found to be negatively correlated with agonal state with a Pearson's correlation coefficient of –0.466 ($p = 0.022$). Agonal state was not correlated with total APP mRNA levels in CA3 or CA4 and did not correlate with poly(A)$^+$ or Goα mRNA levels in any of the regions measured (Table 4.2).

No correlations were found between total APP or poly(A)$^+$ mRNA levels and age, PMI or storage duration of the tissue, as a block or as cryostat cut sections. Goα mRNA levels were not correlated with age, PMI or storage duration of the tissue as cryostat cut sections. However, Goα mRNA levels were negatively correlated with the duration of storage of the tissue as a block in CA3 with a Pearson's correlation coefficient of -0.415 ($p = 0.049$). Spearman's rank correlation coefficient was not significant (-0.355; $p = 0.096$), but the p value was sufficiently low to suggest that the non-parametric test merely lacked the statistical power to demonstrate the relationship between the two parameters (Table 4.2).

4.4 Discussion

A statistically significant reduction in Goα and total APP mRNA levels in the

Table 4.2 Pearson's Correlation Coefficients for Total APP/Goα mRNA Data						
	Total APP mRNA in Dentate Gyrus	**Total APP mRNA in CA4**	**Total APP mRNA in CA3**	**Goα mRNA in Dentate Gyrus**	**Goα mRNA in CA4**	**Goα mRNA in CA3**
Age	-0.016 (n = 37) p = 0.926	0.003 (n = 36) p = 0.987	0.003 (n = 27) p = 0.986	-0.036 (n = 32) p = 0.843	-0.198 (n =30) p = 0.295	0.008 (n = 23) p = 0.973
Agonal State Score	-0.347 (n = 24) p = 0.096	-0.466 (n = 24) **p = 0.022**	-0.374 (n = 20) p = 0.104	-0.336 (n = 22) p = 0.127	-0.126 (n = 21) p = 0.588	-0.119 (n = 16) p = 0.660
Post-Mortem Delay	-0.001 (n = 32) p = 0.995	0.155 (n = 32) p = 0.396	0.060 (n = 25) p = 0.777	0.121 (n = 26) p = 0.556	0.172 (n = 25) p = 0.411	0.048 (n = 19) p = 0.845
Poly(dT) Probe	0.209 (n = 22) p = 0.350	0.306 (n = 21) p = 0.177	0.254 (n = 17) p = 0.324	0.080 (n = 19) p = 0.743	0.206 (n = 18) p = 0.413	0.398 (n = 13) p = 0.178
Block Storage Time	-0.091 (n = 37) p = 0.593	0.054 (n = 36) p = 0.756	0.143 (n = 27) p = 0.476	-0.054 (n = 32) p = 0.770	-0.006 (n = 30) p = 0.977	-0.415 (n = 23) **p = 0.049**
Section Storage Time	-0.148 (n = 37) p = 0.383	-0.282 (n = 36) p = 0.095	-0.304 (n = 27) p = 0.123	-0.135 (n = 32) p = 0.461	-0.044 (n = 30) p = 0.817	-0.034 (n = 23) p = 0.877

Pearson's Correlation Coefficients for Total APP/Goα mRNA Data					
	Total APP mRNA in Dentate Gyrus		**Total APP mRNA in CA4**		**Total APP mRNA in CA3**
Goα mRNA in Dentate Gyrus	0.825 (n = 25) **p < 0.001**	**Goα mRNA in CA4**	0.238 (n = 24) p = 0.263	**Goα mRNA in CA3**	0.463 (n = 16) p = 0.071

dentate gyri of the AD group of cases compared to the control group of cases was demonstrated in this study. Further, Goα and total APP mRNA levels were correlated in the dentate gyri of this series of brains irrespective of diagnosis.

Since both Goα and total APP mRNA levels were found to be statistically significantly decreased in the dentate gyri of the AD group of cases in comparison with the control group of cases, it was possible that the positive linear correlation found between Go and total APP mRNA levels in the dentate gyrus was spurious. Indiscriminate destruction of all mRNAs in the dentate gyri of the diseased tissue might result in an artefactual correlation between the two mRNA species when all of the cases were considered together. However, this correlation remained in dentate gyrus on analysis of the control group of cases alone and a scatter plot of all cases revealed that the subjects of both groups were evenly scattered about the line of best fit (Figure 4.8), suggesting that the correlation found between these two mRNA species is genuine. Further, this particular series of brains has been extensively studied in Professor Pearson's laboratory and is well characterised. In 1991, Makridimitri and colleagues found no significant difference in synaptophysin mRNA in the dentate gyrus or CA1, CA3 and CA4 hippocampal fields of Alzheimer's diseased brains in comparison to neurologically normal controls. Importantly, this series included nineteen of the cases used in the present study suggesting that there is preservation of selected mRNAs in the hippocampi of this series of brains. However, the most compelling evidence in support of a real correlation between Goα and total APP mRNA levels in the dentate gyri of this series of brains is the fact that the mRNA levels of both species appear insensitive to the level of poly(A)$^{+}$ mRNA in this region, suggesting that both are uninfluenced by total mRNA levels.

Gs and Go are members of a multi-gene family, the heterotrimeric G proteins, whose

Figure 4.8 Goalpha mRNA Expression Against Total APP mRNA Expression in the Dentate Gyrus of Alzheimer's Diseased and Control Brains

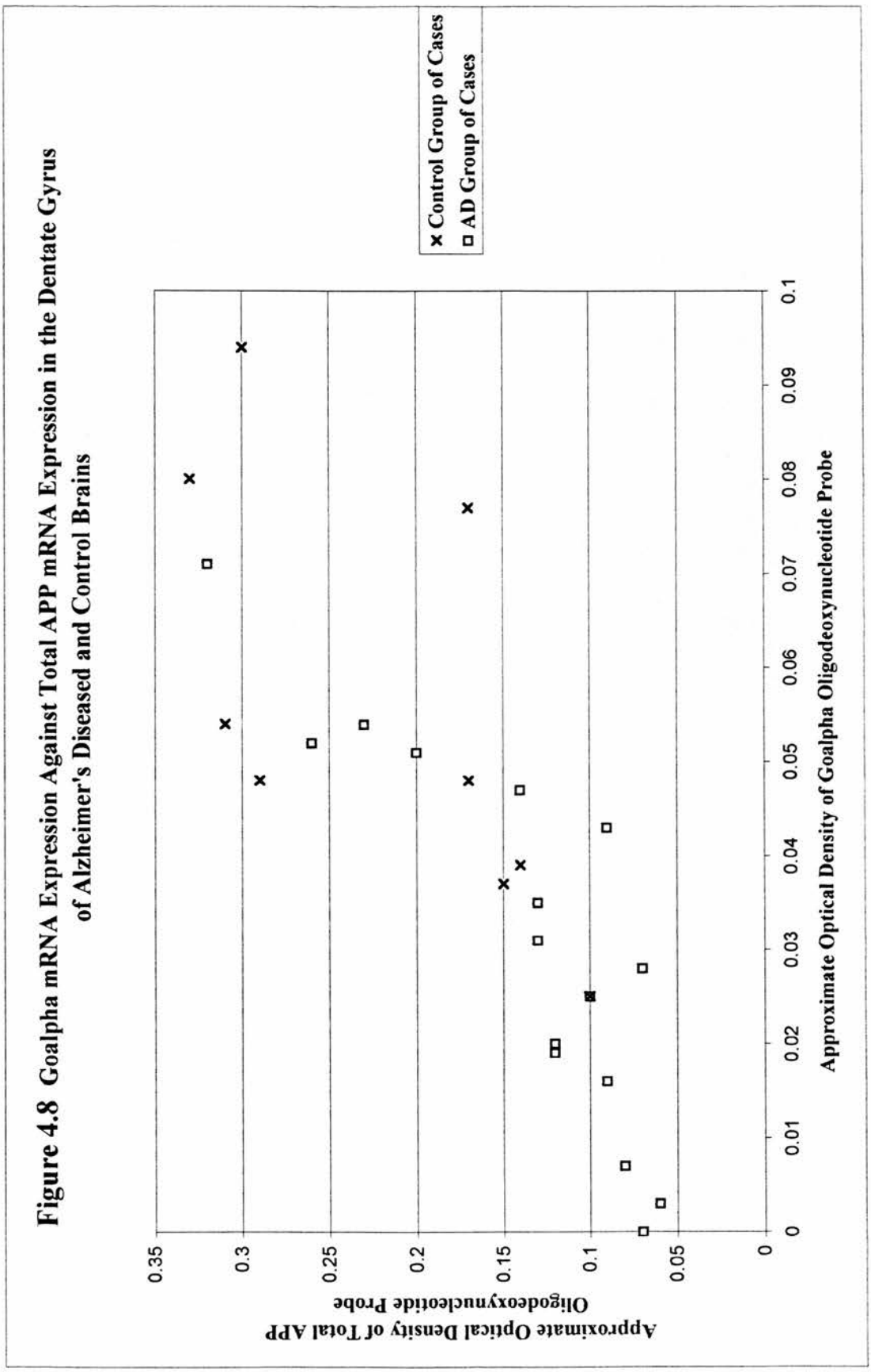

subunits exhibit approximately 45% gene homology. In contrast to previous ISHH work examining Gsα mRNA (Harrison *et al.*, 1991c), this study demonstrates a significant decrease in Goα mRNA in dentate gyrus, and unchanged levels of Goα mRNA in the other hippocampal fields examined, in AD cases in comparison to neurologically normal controls. Despite the decline in total mRNA documented in the hippocampal CA3 field in AD (Harrison *et al.*, 1991b), and the involvement of the hippocampus at an early stage in the pathophysiology of the disease (Braak and Braak, 1991), perusal of studies of specific hippocampal mRNA species in AD reveals mixed results. The APP-insert probe, which hybridises to APP mRNA isoforms 751 and 770, is increased in CA3, but unchanged elsewhere in the hippocampus (Pearson *et al.*, 1992). The APP-junction probe, which hybridises to APP isoform 695, is increased in the CA3 field and dentate gyrus when expressed as a proportion of total polyadenylated mRNA, but unchanged elsewhere (Pearson *et al.*, 1992). Palmert and co-workers (1988), using ISHH, found no change in total APP gene expression or in expression of APP-insert containing isoforms of APP in subicular hippocampal neurons in AD. Johnson and colleagues (1989), in a Northern blotting study, found APP-695 mRNA to be greatly decreased in the hippocampus in AD: a decrease which the authors believe cannot be solely accounted for by the extensive neuronal loss expected in the subiculum and CA1 fields in AD.

Li and colleagues (1996) examined Goα protein levels in human prefrontal cortex and demonstrated a statistically significant decline in Goα protein with increased PMI, and a loss of this protein of approximately 4% per ten years of ageing in this region. However, the authors found no statistically significant alteration in Goα protein in the prefrontal cortex, superior temporal gyrus or occipital cortex of AD brains in comparison with age and PMI matched controls. The mRNA findings in fields CA3 and CA4 of the hippocampi in this series are in keeping with studies

showing no difference in Goα protein levels, as measured by Western blotting, between the hippocampi of AD and control brains (O'Neill *et al.*, 1994; McLaughlin *et al.*, 1991). O'Neill and colleagues (1994), however, used crude synaptic membrane fractions prepared from mid hippocampal tissue, including CA1, dentate gyrus and a small piece of entorhinal cortex, while McLaughlin and co-workers (1991), performed their immunoblot analysis of G-protein levels in the hippocampus on tissue homogenates. It is conceivable, that a decrease in Goα subunits in dentate gyrus, corresponding to the decreased Goα mRNA levels identified in dentate gyrus in our study, is masked when Goα protein levels are examined in the hippocampus as a whole.

Evidence suggests that the genes for all of the G-protein α subunits have evolved from a common ancestral gene (Matsuoka *et al.*, 1990). However, despite the considerable sequence conservation in the coding regions of the G protein α subunit genes, there is little sequence homology in the promoter regions and untranslated 5' regions of different classes of these genes (Raport *et al.*, 1989), and different transcription factors appear to regulate the various G protein α subunits (Valerio *et al.*, 1993). It is likely that controls at the level of transcription are important in determining levels of at least some of the G-proteins (Müller *et al.*, 1993). There is evidence, for example, that upregulation of the Gi-2α gene depends on the integrity of cAMP dependent protein kinase A^{26}, and that the Gi-2α gene contains consensus sequences suggestive of a cAMP response element which the Gsα gene does not have (Müller *et al.*, 1993). Further evidence for the differential control of different G-proteins comes from an ISHH study of chronically morphine-treated rats, who exhibited significant increases in both Gsα and Goα mRNA in brain when compared with control rats, in contrast to brain Gi-2α mRNA levels which were unchanged (Parolaro *et al.*, 1993). Gsα mRNA levels, however, were significantly increased

only in the hypothalamic paraventricular nucleus of the morphine-tolerant rats, while Goα mRNA was significantly increased only in the claustrum and endopiriform nucleus of such animals (Parolaro *et al.*, 1993). Differential effects of isoprenaline on G protein α subunit transcription have also been demonstrated in rat heart, with a 40% increase in the transcriptional activity of the Gi-2α gene in response to the drug, in contrast to the activity of the Gsα gene, which was unchanged (Müller *et al.*, 1993). Studies of G protein expression in failing human hearts have demonstrated a significant increase in steady state levels of Gsα and Gi-3α mRNA, but no significant alteration in Goα mRNA levels, when compared with non-failing human hearts (Feldman *et al.*, 1989). While it is conceivable that pre-mortem factors might increase expression of Gsα mRNA in AD selectively, this seems unlikely as Harrison and co-workers (1991c), in examining the expression of Gsα in human brain, found no correlation between Gsα mRNA levels and agonal state.

Worley and colleagues (1986) have demonstrated that Go is widely but unevenly distributed in brain. They found a selective enrichment of Go in the synaptic zones of rat brain using a selective polyclonal antiserum to the α_{39} subunit of Go, and Strittmatter and co-workers (1990) found Go to be one of the main components of the growth cone membrane. It is clear, therefore, that Go is not uniformly distributed in brain either at a regional or an intracellular level. In this study Goα mRNA was measured in the dentate gyrus and CA3 and CA4 fields of the hippocampus in human brain. It is conceivable that regional quantification has masked differential alterations in Goα expression in subgroups of hippocampal neurons. The Goα mRNA levels observed might be composed of an increase in expression of this particular mRNA at the growth cone of surviving neurons undergoing aberrant sprouting, but decreased expression elsewhere. Of course, levels of Goα mRNA comparable to those found in neurologically normal brains does not guarantee that

the mRNA is normally transcribed, or that the encoded protein is functionally active and correctly coupled to effector systems.

Goα and total APP mRNA levels were found to be positively correlated in the dentate gyri of this series of brains. If, as Nishimoto and colleagues (1993) predict, APP is abnormally cleaved in AD such that it binds tonically to Go and constitutively activates it, one would expect levels of Goα mRNA to fluctuate in accordance with the requirement for Goα subunits. It is recognised that chronic exposure of cells to agonists which rely on G-proteins for signal transduction can lead to alterations in their G-protein levels (Mullaney *et al.*, 1993). Of course, it is conceivable that Goα might only bind to specific isoforms of APP and, thus, that any correlation between Goα and APP mRNAs might be weakened by looking at estimates of total APP mRNA levels.

Migeon and colleagues (1994), investigated the properties of Goα using a luciferase reporter gene under the transcriptional control of a cAMP response element in JEG-3 cells. This system is sensitive to small, physiologically relevant, increases in the intracellular second messenger cAMP, the abundance of which is determined by receptor mediated activation or inhibition of adenyl cyclase. JEG-3 cells express Gi1α and Gi3α, but not Gi2α or Goα. The authors demonstrated that wild type Goα can couple the m4 muscarinic receptor to inhibition of adenyl cyclase in JEG-3 cells and that mutated, constitutively activated Goα can inhibit forskolin-stimulated luciferase activity in these cells.

Cyclic AMP is centrally involved in learning and memory (Yin *et al.*, 1994). Intracellular cAMP exerts its effects primarily through activation of the regulatory subunit of protein kinase A, which allows translocation of the catalytic subunit of

protein kinase A to the nucleus (Bonkale, 1996). Protein kinase A is capable of transferring the terminal phosphate group of ATP to the serine, threonine or tyrosine residues of substrate proteins. The transcription factor cAMP response element binding protein (CREB) (Montminy *et al.*, 1987) is regulated by translocated cAMP dependent protein kinase A induced phosphorylation at serine 133 (Gonzalez and Montminy, 1989). CREB, and its role in memory, has been highly conserved through evolution (Frank and Greenberg, 1994). Activated CREB binds to the cAMP response element found in the upstream control region of many cAMP responsive genes. Long term memory, in contrast to short term memory, relies on the synthesis of new RNA and protein (Huang *et al.*, 1994). Long term potentiation refers to the activity dependent increase in synaptic strength in neurons of the hippocampus that occurs in response to brief, high frequency bursts of action potentials (Huang *et al.*, 1994), and hippocampal long term potentiation is believed to contribute to memory storage. The late phase of long term potentiation is stimulated by cAMP in all three of the major hippocampal synaptic relays identified, namely the perforant, mossy fibre and Schaffer collateral pathways (Huang *et al.*, 1994). Induction of expression of a dominant negative member of the fly CREB family in Drosophila results in a loss of long term memory in the presence of preserved short term memory and learning (Yin *et al.*, 1994). This observation was extended to mammals with the discovery that mice with targeted disruptions of the α and δ isoforms of CREB were profoundly deficient in long term memory (Bourtchuladze *et al.*, 1994). Go mediated regulation of the cAMP response element has been studied in NK1 cells; naturally occurring transformants of COS cells which express endogenous Goα. COS-NK1 cells transfected with mutated forms of APP-695, in which the valine at position 642 had been converted to glycine, isoleucine or phenylalanine (V642I/G/F), induced negative regulation of the cAMP response element while wild-type APP-695 did not (Ikezu *et al.*, 1996). Such

V642I/G/F mutations are highly correlated with AD phenotype in humans. The possibility that disrupted cAMP dependent phosphorylation of CREB, as a consequence of constitutively activated Go, might underlie the memory loss which is one of the earliest manifestations of AD (Ikezu *et al.*, 1996), is intriguing.

Transfection with APP-695 mutants associated with familial AD have also been reported to induce neuronal DNA fragmentation in F11 cells; hybrids of a primary rat dorsal root ganglion neuron and a mouse neuroblastoma cell line that exhibits neuronal traits (Yamatsuji *et al.*, 1996b). This effect is critically dependent on the His^{657}-Lys^{676} domain of APP-695, and is believed to be Go mediated. Yamatsuji and co-workers (1996a) have demonstrated that COS-NK1 cells transfected with V642I/G/F mutations of APP-695, undergo typical bcl-2 sensitive apoptosis, and that the His^{657}-Lys^{676} domain of APP-695 is necessary for this effect. A single point mutation within codon 642 of APP-695 can result in conversion of valine to one of six other amino acids. Only substitutions of valine with glycine, isoleucine or phenylalanine have been associated with the familial AD phenotype, while point mutations which result in conversion of amino acid 642 to leucine, alanine or aspartic acid have not. Similarly, *in vitro* mutations of APP-695 incorporating leucine, alanine or aspartic acid in place of valine at codon 642, do not result in a significant increase in apoptosis in the COS-NK1 model system. The congruence between *in vivo* and *in vitro* studies suggests that V642I/G/F induced, Go mediated apoptosis may be fundamental to the pathology of this form of FAD (Yamatsuji *et al.*, 1996a). While it is likely that the cytotoxic effects of mutated APP-695 are induced via direct activation of Go (Yamatsuji *et al.*, 1996a), it should be noted that cells transfected with V642I/G/F mutations secrete more β-amyloid(1-42) and less β-amyloid(1-40) than cells transfected with wild type APP-695 (Suzuki *et al.*, 1994). Importantly, β-amyloid(1-42) has been identified to adopt a toxic, aggregated state

following an incubation of several days while the 1-40 amino acid form of β-amyloid does not (Pike *et al.*, 1991a). Furthermore, immunochemical studies of brain tissue from sufferers of sporadic AD suggests that the initial β-amyloid species deposited in plaques is β-amyloid(1-42) and not β-amyloid(1-40) (Iwatsubo *et al.*, 1994). However, Yamatsuji and co-workers (1996b) demonstrated that neuronal DNA fragmentation was not induced by incubating the F11 cells in 50 M synthetic β-amyloid(1-42), or in conditioned media from transfected cells themselves undergoing DNA fragmentation, or following incubation in conditioned media from cells undergoing DNA fragmentation combined with 50 M synthetic β-amyloid(1-42). Nor could any significant apoptosis be induced in COS-NK1 cells in response to incubation with 50 M synthetic β-amyloid(1-42), or with conditioned media from transfected cells supplemented with 50 M synthetic β-amyloid(1-42) (Yamatsuji *et al.*, 1996a). Significantly, both of these studies imply that the cytotoxic effects examined are mediated by V642I/G/F APP-695 mutations in a manner independent of β-amyloid.

Lassmann and colleagues (1995), using terminal deoxynucleotide transferase mediated deoxyuridine triphosphate nick end labelling (TUNEL), in which the 3'-OH termini of DNA strand breaks generated during DNA fragmentation are labelled with a digoxigenin or biotin tagged dUTP, estimated that the number of cells undergoing DNA fragmentation in AD brains was approximately thirty times that of control brains. Cotman and Anderson (1995) employing the same technique observed several features they believe to be suggestive of apoptosis in AD brain.

Profound cellular consequences of a point mutation in the transmembrane domain of a cell surface molecule has previously been described for the receptor like protein, p185, a product of the rat Neu gene (Bargmann and Weinberg, 1988). Conversion of

the 664 valine of this protein to a glutamine or glutamic acid residue results in its unregulated activation. The similarities between the transforming effect of a point mutation in the Neu gene and the apoptotic effect of such a mutation in the APP gene are obvious.

Previously, the distinct α subunits were thought to bind to a common pool of βγ dimers but recent work has demonstrated that the activity of the α subunit, and its susceptibility to adenosine triphosphate (ADP) ribosylation by pertussis toxin, is modulated by the subtype of γ subunit to which the α subunit is bound (Sohma *et al.*, 1993). Further, Kleuss and co-workers (Kleuss *et al.*, 1993) have shown that the γ subtype, γ3, is required for mediation of somatostatin stimulated inhibition of voltage-sensitive calcium channels through Go, whereas γ4 is required for coupling of m4 muscarinic receptors through Go to the same effector. Dissociated βγ dimers are thought to inhibit the action of the α subunits by binding to them as a result of a mass action effect (Katada *et al.*, 1984), and may also interact with effectors directly (Enomoto and Asakawa, 1986). Katada and colleagues (1984) hypothesise that the Gi mediated inhibition of the catalytic subunit of adenyl cyclase results from the mass action effect of the βγ dimers liberated by the dissociation of Gi, binding to Gsα and restoring it to its heterotrimeric and inactive conformation (Katada *et al.*, 1984). Since the βγ dimers constitute a common pool and appear to be important in specifying the receptor-effector specificity of the α subunits, it is tempting to speculate on the impact of increased Gsα on the availability of βγ dimers to associate with α subunits of the other G proteins.

The present data suggests that one aspect of the G protein system, expression of Goα mRNA, is selectively down-regulated in the dentate gyrus in AD. This is in contrast to the increase in Gsα mRNA in hippocampus documented to occur in the disease.

Elucidation of the mRNA levels of other α subunits of the G protein family are needed in order to establish whether the alterations identified are shared by other α subunits of the G protein family which are more highly homologous than Goα and Gsα or whether these effects are in fact gene specific. The possible relationship of Goα with APP, indicated by the correlation of Goα and APP mRNA abundance, gives further reason to propose that the alteration in Goα mRNA may be of pathophysiological significance.

Chapter 5

The Messenger RNA Encoding Amyloid Precursor Protein

5.1 Introduction

5.1.1 Amyloid Precursor Protein

The major proteinaceous component of the plaque and meningovascular amyloid deposits which characterise AD is β-amyloid, a 39 to 43 amino acid peptide (Glenner and Wong, 1984; Masters *et al.*, 1985a) identified as being the cleavage product of a larger precursor protein known as APP (Kang *et al.*, 1987; Tanzi *et al.*, 1987). In 1987, Kang and colleagues identified the first APP cDNA clone and predicted APP to be a 695 amino acid protein with characteristics reminiscent of a glycosylated cell-surface receptor. Now at least six isoforms of APP of 365, 563, 695, 714, 751 and 770 amino acids are known to exist in humans.

APP (Figure 5.1) is composed of a short cytoplasmic domain, a single membrane spanning region and a long extracellular domain. The β-amyloid sequence lies at the junction of the extracellular and transmembrane domains of APP, extending 28 amino acids into the extracellular region and between 11 and 15 amino acids into the transmembranous portion. The forty-three-residue form of β-amyloid terminates at, and the forty-two-residue form terminates just before, the first of the two threonine residues found in the membrane spanning domain (Kang *et al.*, 1987).

Figure 5.1 The 770 Amino Acid Isoform of Amyloid Precursor Protein

(Drawn to scale 1 cm = 35 amino acid residues)

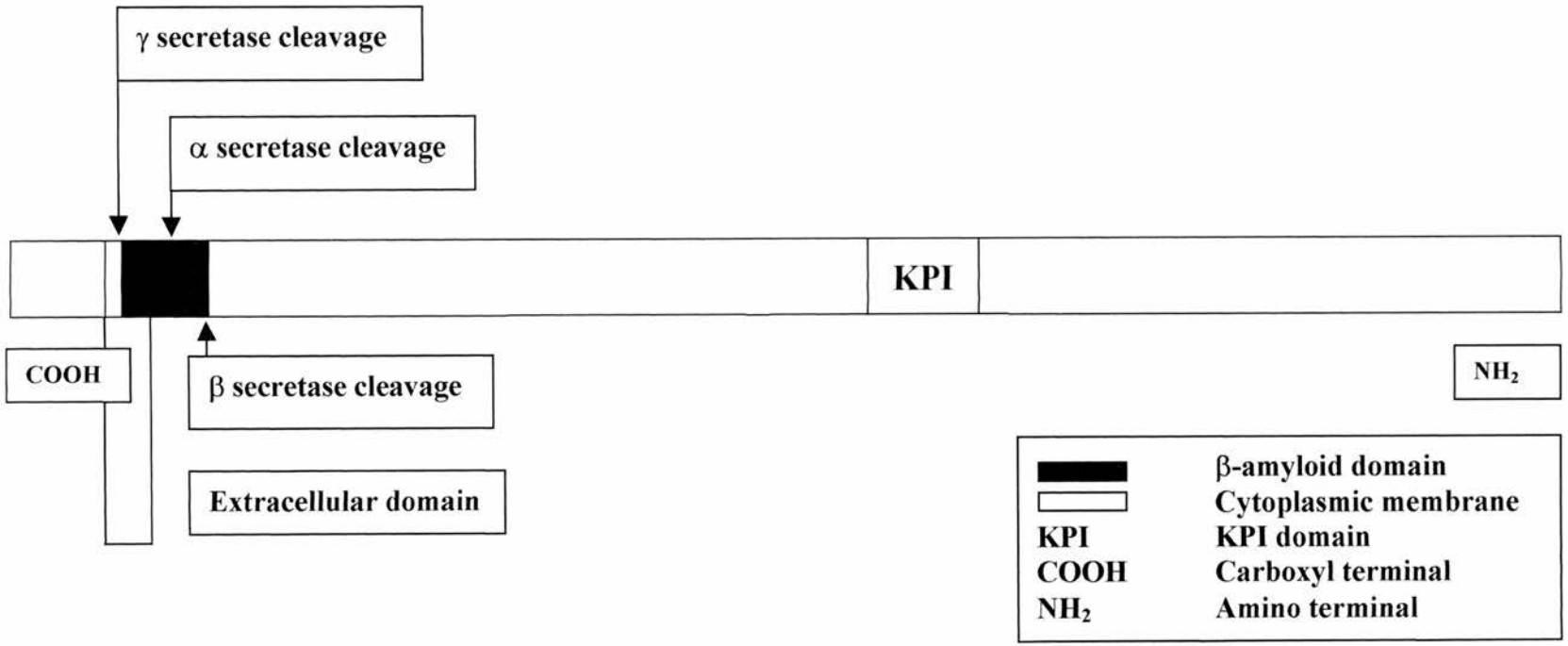

APP mRNAs are spliced from a single gene on chromosome 21 (Tanzi *et al.*, 1987) that is composed of 19 exons (König *et al.*, 1992). Northern blotting of total RNA from normal, adult, human cortex reveals APP mRNA transcripts of 3.4 and 3.2 kilobases (Kang *et al.*, 1987) and APP mRNA has been detected in a wide variety of human tissues including brain, liver, spleen, skeletal muscle, pancreas, kidney, adrenal gland and small intestine (Tanzi *et al.*, 1987). The confinement of β-amyloid deposition to brain, despite the virtually ubiquitous distribution of its precursor, is unexplained (Weidemann *et al.*, 1989). An increase in APP mRNA has been identified in brain tissue from Down's syndrome foetuses aborted at nineteen weeks gestation when compared with brain tissue from normal foetuses aborted at this time (Tanzi *et al.*, 1987), in keeping with the 50% increase in APP gene dosage associated with trisomy 21.

APP is synthesised as an immature N-glycosylated protein (Oltersdorf *et al.*, 1990), that undergoes extensive post-translational modification, to become a tyrosine-sulfated and N- and O-gylcosylated membrane glycoprotein (Weidemann *et al.*, 1989; Oltersdorf *et al.*, 1990; Moya *et al.*, 1994). In keeping with the proposed function of APP as a cell-surface receptor, a consensus sequence required for coated pit-mediated internalisation, the NPXY domain, has been found in the cytoplasmic domain of APP (Chen *et al.*, 1990). In addition, APP has been demonstrated to bind and activate the heterotrimeric GTP binding protein, Go, in a ligand-dependent and ligand-specific manner (Okamoto *et al.*, 1995), via a cytoplasmic binding domain.

The β-amyloid sequence is encoded by nucleotides from exons 16 and 17. The multiple splice variants of APP identified arise from alternative splicing of exons 7, 8 and 15. Exon 7 consists of 168 nucleotides that encode a 56 amino acid domain, the KPI domain, that is highly homologous with a Kunitz-type serine protease inhibitor (Tanzi *et al.*, 1988; Kitaguchi *et al.*, 1988; Ponte *et al.*, 1988). Such inhibitors exhibit specificity for serine proteases such as trypsin, chymotrypsin, elastase, plasmin and cathepsin G. In 1989, Oltersdorf and colleagues established that the sequence of a secreted, KPI domain-containing derivative of APP was identical to that of a cell-secreted protease inhibitor known as protease nexin II. Protease nexin II forms inhibitory complexes with trypsin and is capable of inhibiting factors IXa and XIa of the coagulation cascade.

Exon 8 encodes a 19 amino acid domain that exhibits 47% homology with the MRC OX-2 antigen, a cell surface glycoprotein with an overall structure similar to an immunoglobulin light chain or the T cell receptor β chain (Clark *et al.*, 1985). Exon 15 is composed of 54 nucleotides and encodes 18 amino acids that precede the amino terminus of the β-amyloid sequence by 16 amino acids.

The three major isoforms of APP in neuronal and non-neuronal cells, designated according to their length in amino acids, are APP-695, APP-751 and APP-770 (Weidemann *et al.*, 1989). APP-695 mRNA lacks both exon 7 and exon 8, APP-751 mRNA lacks exon 8 and APP-770 mRNA contains all 18 exons. The APP-714 mRNA isoform lacks exon 7 and represents a small proportion of total APP mRNA

in brain (Harrison *et al.*, 1996). Indeed, Jacobsen and colleagues (1991) found that APP-714 consistently represented less than 1% of total APP mRNA in human post-mortem brain samples from both AD and control donors. APP-563 mRNA (de Sauvage and Octave, 1989) lacks exons 16, 17 and 18 and APP-365 mRNA (Jacobsen *et al.*, 1991) lacks exons 8 to 18. These two isoforms of APP are carboxyl terminal-truncated forms that lack the cell-anchoring transmembrane domain and thus do not contain the β-amyloid sequence. APP-563 contains the KPI domain and is believed to be a secreted form of APP-751 in which the terminal 208 amino acids of the peptide are replaced with 20 amino acids with homology to the consensus repeat recognition sequence for the restriction enzyme AluI (de Sauvage and Octave, 1989).

APP mRNA transcripts which lack exon 15 were first discovered in peripheral leucocytes and immunocompetent cells of the brain and are thus known as leucocyte-derived APP (L-APP) mRNAs (König *et al.*, 1992). Cleavage of exon 15 and fusion of exons 14 and 16 creates the sequence Glu-Xaa-Ser-Gly, a consensus sequence for xylosyltransferase mediated attachment of a chondroitin sulfate side chain (Pangalos *et al.*, 1996). The side chain is attached to serine 619 of L-APP, 16 amino acids upstream from the β-amyloid sequence, and the resulting proteoglycan is known as appican (Pangalos *et al.*, 1996). Proteoglycan molecules are highly ionic and the chondroitin sulfate proteoglycan form of L-APP is proposed by Pangalos and co-workers (1996) to be a strong cell adhesion molecule. L-APP transcripts are not expressed in neurons (Sandbrink *et al.*, 1994a; Sandbrink *et al.*, 1997), but are

otherwise ubiquitous (Sandbrink *et al.*, 1994a) and all four possible exon 15 lacking transcripts of APP, L-APP-752, L-APP-733, L-APP-696 and L-APP-677, are known to exist.

5.1.2 Human Homologues of Amyloid Precursor Protein

APP is a member of an evolutionarily conserved multigene family that includes amyloid precursor-like protein 1 (APLP1) and amyloid precursor-like protein 2 (APLP2). The overall structures of APLP1 and APLP2 are strikingly similar to that of APP, since all consist of a short cytoplasmic domain, a single membrane spanning region and a large extracellular domain. However, APLP1 and APLP2 both lack the β-amyloid sequence. APLP1 was first identified in the mouse (Wasco *et al.*, 1992), followed swiftly by the identification of its human homologue (Wasco *et al.*, 1993). APLP1 is a 653 amino acid protein that is 42% identical, and 64% similar, to APP-695. It has been mapped by Wasco and colleagues to chromosome 19 (1992b).

Human APLP2 was isolated and characterised by Wasco and colleagues in 1993, who demonstrated that the expression of APLP2 in the brain and periphery was strikingly similar to that of APP. APLP2 maps to chromosome 11 and is a 752 amino acid protein predicted to be 52% identical, and 71% similar, to APP-751 (Wasco *et al.*, 1993). It is expressed in a wide variety of human tissues including brain, placenta, heart, lung, liver and kidney (Sprecher *et al.*, 1993). Two alternatively spliced inserts have been identified in APLP2: a KPI encoding region highly homologous to exon 7 of the APP gene and a 12 amino acid sequence

embedded in the region of APLP2 that exhibits the greatest divergence in sequence from APP (Sandbrink *et al.*, 1994b). Interestingly, splicing out of the 12 amino acid encoding exon creates the same xylosyltransferase signal motif as exists in exon 15-lacking L-APP isoforms. In the rat, the 12 amino acid domain is present in the majority of intraneuronal transcripts of APLP2, but is present in only a minority of peripheral forms of APLP2 (Sandbrink *et al.*, 1997). Thus, it appears that regulation of L-APP and APLP2 glycosylation occurs partly at the level of mRNA splicing (Sandbrink *et al.*, 1997). APLP2 matures, like APP, through a secretory pathway, and secreted, soluble, carboxyl terminal-truncated derivatives of APLP2 have been identified in the conditioned media of Chinese hamster ovary cells transfected with a cDNA encoding mouse APLP2 (Slunt *et al.*, 1994). Webster and colleagues (1995) identified soluble, secreted, truncated forms of APLP2 in human CSF, suggesting that this pathway also exists *in vivo*. Like APP, APLP2 harbours a consensus sequence in its cytoplasmic domain predicted to bind to the heterotrimeric GTP-binding protein Go (Wasco *et al.*, 1993).

5.1.3 Control of Amyloid Precursor Protein Expression

The promoter of the APP gene was cloned and characterised by Salbaum and colleagues in 1988 and strongly resembles that of a housekeeping gene consistent with the virtually universal expression of APP mRNA (Tanzi *et al.*, 1987). At least five mechanisms exist by which APP expression might be controlled at the level of transcription. The APP gene promoter contains four potential regulatory elements: a stress-inducible heat shock control element, a sequence resembling the consensus

binding site for the transcription factor AP-1 and the oncogene products v-*jun* and c-*fos*, a region with a high frequency of CpG dinucleotides capable of DNA methylation, a known mechanism of gene expression control, and, lastly, a potential binding site at a GC-rich element between positions -200 and -100 (Salbaum *et al.*, 1988). Gegelashvili and co-workers (1996) draw a further parallel between APP transcription and the transcription of heat shock protein genes, in demonstrating that upregulation of APP mRNA in a glioma cell line occurs in response to cAMP.

APP mRNA's contain multiple UTR AUUUA motifs encoded in the untranslated 3'-region of the gene that are hypothesised to destabilise the mRNA and prevent its accumulation. Such recognition sites are frequently identified in mRNA species subject to rapid cytoplasmic decay (Shaw and Kamen, 1986). The stability of APP mRNA, as studied in neuronal tumour cell lines and peripheral blood mononuclear cells, is regulated by a 29 base element in the 3'-untranslated region of APP mRNA approximately 200 bases from the stop codon (Zaidi *et al.*, 1994). In resting, normal cells this 29 base region appears to function in *cis* to destabilise APP mRNA. On cellular activation APP mRNA-binding proteins are induced which attach to this 29 base region and stabilise APP mRNA (Zaidi and Malter, 1994).

The abundance of another glycoprotein, the major myelin glycoprotein, has been demonstrated in Schwann cells to be partly controlled by post-translational catabolism of the nascent protein (Brunden *et al.*, 1990). The protein is processed at least as far as the medial Golgi before its efficient transfer to lysosomes where it is

rapidly degraded. APP has been localised to secondary lysosomes in cultured, human, neuronal cell lines (Cole *et al.*, 1989) and to neuronal secondary lysosomes in both normal and AD diseased brains (Benowitz *et al.*, 1989). Steady state levels of APP in cultured cells have been observed to rise in the presence of lysosomal inhibitors (Cole *et al.*, 1989). C6 glioma cell lines, transfected with secreted placental alkaline phosphatase-tagged fusion recombinant APP proteins, exhibit intracytoplasmic accumulation of APP on heat shock (Pappolla *et al.*, 1995). The promoter employed was not heat shock inducible and the intracytoplasmic accumulation of APP, demonstrated on cytochemistry, was Golgi-like. Thus, it is conceivable that APP expression might be controlled by post-translational catabolism (Pappolla *et al.*, 1995).

5.1.4 Processing of Amyloid Precursor Protein

5.1.4.1 Introduction

A number of physiological functions have been ascribed to APP, though its definitive role in human brain remains unknown (Adams, 1997). APP is hypothesised to be processed in at least two major ways: a secretory pathway, in which APP is cleaved intracellularly, or at the cell membrane, in preparation for its secretion from the cell, and an endosomal-lysosomal route which involves targeting of APP, either from the Golgi or the cell membrane, to endosomes-lysosomes. Early attempts to delineate the processing of APP envisioned a simple scheme whereby β-amyloid was the pathological product of the endososomal-lysosomal processing of APP (Haass *et al.*, 1992a). Secretory processing was assumed to cleave APP at one location within the

β-amyloid domain and thus to be non-amyloidogenic (Sisodia *et al.*, 1990). The complexity of APP processing has since become obvious. It would seem unwise to assume that current opinions about APP metabolism are wholly accurate and entirely applicable *in vivo*.

5.1.4.2 Processing of Amyloid Precursor Protein by the Secretory Pathway

In 1988, Selkoe and colleagues, using two antibodies to the carboxyl terminus of APP, identified APP immunochemically in various membrane-rich, sub-cellular fractions of brain and non-neural human tissues. The APP forms identified were heterogeneous, ranging from 110 to 135 kDa, and the authors postulated that variations in the glycosylated side-chains attached to the extracellular domain of APP, or proteolytic cleavage of the full length form, might be responsible for the variability observed. Sisodia (1992) demonstrated cleavage of mature, membrane-bound APP within the β-amyloid domain in cultured cells by a membrane-bound endoprotease dubbed α secretase. Cleavage by this enzyme is predicted to take place at the Lys16-Leu17 bond of the β-amyloid sequence and therefore precludes the formation of β-amyloid (Sisodia, 1992). Alpha secretase exhibits a relaxed sequence specificity: the primary determinants of cleavage are the presence of an α helical conformation and a distance of 12 to 13 amino acids of the hydrolysed bond from the plasma membrane (Sisodia, 1992). Cleavage at this site releases a soluble, amino terminal fragment of APP into the extracellular space, leaving a truncated, carboxyl terminal derivative of APP, known as p10, embedded in the membrane. It now appears likely that α secretase cleavage can occur both at

the cell membrane, with fully matured APP as a substrate, and intracellularly, probably in secretory vesicles or in the *trans*-Golgi network or late *trans*-Golgi compartment (See Checler, 1995 for review). The secretory and membrane-bound forms of the protein are likely to follow the same route, being separated after N-glycosylation in the endoplasmic reticulum at the earliest (Weidemann *et al*, 1989). Weidemann and co-workers (1989) have identified carboxyl terminal and transmembrane domain-lacking secretory products of APP-695, APP-751 and APP-770 in the CSF of both AD sufferers and normal controls.

Golde and colleagues (1992) analysed the amino terminal derivatives of APP secreted into the conditioned media of human embryonic kidney cells. They concluded that such derivatives arose as the result of cleavage at a single α secretase site generating one secreted derivative and one carboxyl terminal fragment. However, in 1993 Seubert and co-workers identified another, far rarer, soluble amino terminal derivative of APP in the conditioned media of human mixed brain cultures, suggesting that a further APP processing route existed. This derivative arose from cleavage of APP between Met 596 and Asp 597, the bond precisely at the amino terminus of the β-amyloid sequence. Seubert and colleagues (1993) proposed that the membrane-bound secreting system responsible for cleavage at this site be referred to as β secretase. Beta secretase cleavage occurs at a privileged peptide bond corresponding to the bond between Met671 and Asp672 of the APP-770 sequence and may be the rate limiting step in the release of soluble β-amyloid (Maruyama *et al.*, 1994). Cleavage at the β secretase site yields a soluble, amino

terminal derivative of APP and a membrane-bound derivative that contains the whole of the β-amyloid sequence at, or near to, its amino terminus. The discovery of β secretase cleaved APP derivatives in CSF (Seubert *et al.*, 1993) confirmed the existence of this pathway *in vivo*. The identification, by Estus and colleagues (1992), of a complex set of carboxyl terminal APP fragments in human brain, some of them large enough to contain the entire β-amyloid sequence, confirmed that this pathway was potentially amyloidogenic *in vivo*.

A further, alternative, cleavage site was documented by Kametani and colleagues (1994) in Down's syndrome brain, whereby soluble β-amyloid is generated by secretory processing of carboxyl terminal fragments by cleavage at Glu-7-Ile-6 and Glu-4-Val-3.

To generate β-amyloid APP must also be cleaved at the carboxyl terminal of β-amyloid: a site that lies within the transmembrane domain of APP. An enzyme, dubbed γ secretase, is postulated to effect this cleavage, though how it might occur remains obscure (Checler, 1995). A soluble, amino terminal derivative of APP, that reacts with a polyclonal antiserum directed against residues Ala21 to Lys28 of the β-amyloid sequence, has been identified in the culture medium of human kidney 293 cells (Anderson *et al.*, 1992), suggesting that γ secretase cleavage can indeed occur *in vivo*. The exact site of γ secretase cleavage is clearly variable, since the β-amyloid peptide exhibits a range of lengths from 39 to 43 amino acids, (Checler, 1995). Cleavage of p10 at the γ secretase site yields a membrane-bound fragment,

p7 and the carboxyl terminal fragment of β-amyloid, p3. It is noteworthy, that the α, β and γ proteases responsible for the cleavage of APP have not, as yet, been isolated or cloned (Reaume *et al.*, 1996).

Interference with both α and β secretase activity by the KPI domain of APP has been proposed. Ho and co-workers (1996) have documented impaired α secretase cleavage of APP in cells transfected with human APP-751 in comparison to those transfected with human APP-695. While Ho and colleagues (1996) data are consistent with direct inhibition of α secretase by the KPI domain, it is also possible that the protein conformation of KPI containing isoforms of APP render them less vulnerable to α secretase cleavage or, alternatively, that intracellular trafficking of such forms removes them from the site of action of this protease (Ho *et al.*, 1996).

Lymphoblasts derived from individuals with early onset familial AD exhibit slow processing and cytosolic accumulation of β-amyloid (Matsumoto and Matsumoto, 1994). They also express large amounts of a calcium dependent, 68 kDa, serine protease of the chymotrypsin type hypothesised to cleave APP at the amino terminus of β-amyloid (Matsumoto, 1994). This serine protease has been demonstrated to form SDS-stable, heat-labile, complexes with the KPI domain of APP (Matsumoto, 1994). Matsumoto (1994) proposes that KPI containing isoforms of APP may be able to trap and inactivate potentially proteolytic peptides and thus alter the spectrum of proteases available to cleave APP.

Reaume and colleagues (1996) studied gene-targeted mice bearing the Swedish mutation K670N/M671L and a humanised β-amyloid sequence. The authors demonstrated enhanced, accurate β secretase cleavage, and depressed non-amyloidogenic cleavage, of the mutated APP. Importantly, this model demonstrates that amyloidogenic and non-amyloidogenic pathways of APP metabolism are linked *in vivo* and that the production of β-amyloid can be enhanced without an increase in APP synthesis.

5.1.4.3 Processing of Amyloid Precursor Protein by the Endosomal-Lysosomal Pathway

The non-amyloidogenic nature of the α secretase pathway, and the inaccessible membranous location of the γ secretase cleavage site, prompted researchers to search for another mechanism by which β-amyloid could be generated from APP. In 1989, Cole and colleagues observed a rapid and dramatic increase in steady state levels of immunochemically detectable APP in a neuronal cell line in response to inhibitors of lysosomal proteolysis and proposed that APP is normally degraded in lysosomes. Examination of the swollen, dystrophic neurites of senile plaques, has shown them to be filled with acid phosphatase-positive dense bodies thought to be of lysosomal origin (Suzuki and Terry, 1967) and APP in neurons (Cole *et al.*, 1989), and in the dystrophic neurites of senile plaques (Cole *et al.*, 1989; Shoji *et al.*, 1990), has been localised immunochemically to membrane bound organelles believed to be secondary lysosomes. In 1989, Neve's laboratory (Benowitz *et al.*, 1989) demonstrated punctate concentrations of immunochemically labelled APP in

neocortical pyramidal cells, especially in associative regions, in normal brain. Intense immunochemical staining for APP was also found in the pyramidal cells of hippocampal subfield CA1 in normal brain. In AD, abnormally dense concentrations of APP were observed in hippocampal subfield CA1, along with severe atrophy of the pyramidal cells in this region. Benowitz and co-workers (1989) hypothesise that APP accumulates in secondary lysosomes in AD, leading to proteolytic events that form β-amyloid. The presence of the consensus sequence, NPXY, on the cytoplasmic tail of APP (Chen *et al.*, 1990) suggests that it is internalised in clathrin-coated pits, and, further, the internalisation of full length APP and its targeting to endosomes-lysosomes has been demonstrated (Haass *et al.*, 1992a).

Golde and colleagues (1992) analysed the products of endosomal-lysosomal processing of APP in human embryonic kidney 293 cells transfected with cDNA encoding APP-695. They identified a complex set of carboxyl terminal APP derivatives of between 8 and 12 kDa in size, some of which were long enough to contain the entire β-amyloid sequence at their amino termini Both leupeptin, an inhibitor of serine and cysteine proteases, and ammonium chloride, a weak base amine that is concentrated in acidic compartments and inhibits lysosomes by increasing their pH, inhibited the production of these carboxyl derivatives of APP.

Haass and co-workers (1992a) incubated living human endothelial cells with antibody to the extramembranous portion of APP and demonstrated the uptake of APP-antibody complexes into lysosomes. Subsequent purification of the lysosomes

revealed full length APP and an extensive array of β-amyloid containing proteolytic products. In addition, lysosomes extracted from leupeptin treated cells were enriched with full length APP and carboxyl terminal derivatives of APP of 10 kDa and longer, indicating that carboxyl terminal derivatives of APP, like APP itself, are stabilised by inhibitors of lysosomal proteolysis. This work confirmed that re-internalisation of fully matured, membrane-associated APP occurs and established that β-amyloid bearing substrates are available to lysosomal proteases. Haass and colleagues (1992a) noted, however, that their findings did not preclude the targeting of APP directly from the late *trans*-Golgi network to lysosomes.

Hayashi and colleagues (1992) transfected human APP cDNAs into a glioma cell line and examined the effect of lysosomal inhibitors on the metabolism of APP. The protease inhibitors, leupeptin and E-64, led to the accumulation of aberrant, potentially amyloidogenic fragments of APP in lysosome-like organelles in the transfected cells. Whereas chloroquine caused little degenerative change in the untransfected control cells, the transfected cells exhibited cellular degeneration in response to chloroquine. The cytotoxic effects of chloroquine were potentiated by pre-treatment of the transfected cells with the protease inhibitors, leupeptin and E-64, suggesting that lysosomal inhibition results in the accumulation of cytotoxic fragments of APP.

Fraser and colleagues (1996) have demonstrated that carboxyl terminal β-amyloid containing derivatives of APP are extremely potent inducers of non-selective ion

currents in *Xenopus* oocytes, a model system widely used to investigate electrophysiological aspects of signalling. The induction of such currents implies that carboxyl terminal β-amyloid containing derivatives of APP may be involved in the neural toxicity characteristic of AD.

5.1.4.4 Soluble β-amyloid is a Product of Normal Cellular Metabolism

The belief that β-amyloid is the product of aberrant cellular metabolism was challenged by Haass and colleagues (1992b), who identified soluble β-amyloid in the media of cultured human kidney 293 cells stably transfected with cDNA encoding APP-695 and grown under normal conditions. Shoji and co-workers (1992) independently identified soluble β-amyloid in the culture medium of human mononuclear leukemic cells stably transfected with a carboxyl terminal β-amyloid bearing APP-derived construct, confirming that soluble β-amyloid was the product of normal cellular metabolism in these cells. Further, the same authors (Shoji *et al.*, 1992) demonstrated that the production of soluble β-amyloid could be reduced by the addition to the culture medium of lysosomotropic agents capable of increasing the pH of acidic intracellular compartments. Thus, it appears that soluble β-amyloid is produced, at least in part, in lysosomes.

Soluble β-amyloid has since been identified in human plasma, CSF obtained at autopsy (Seubert *et al.*, 1992) and CSF obtained during life (Shoji *et al.*, 1992), confirming the existence of this pathway *in vivo* (Seubert *et al.*, 1992). Considerable overlap has been found between AD and control groups in the abundance of this

peptide (Tabaton *et al.*, 1994). Van Gool and co-workers (1994) observed a significant, positive correlation between soluble β-amyloid levels detected in CSF and age in subjects free of neurodegenerative disease. Kalaria and colleagues (1996b) have demonstrated that soluble β-amyloid is constitutively produced by meningeal vessels, large and small cerebral microvessels and the choroid plexus in human brain. Soluble β-amyloid can be identified intracellularly, in a membrane-associated form, or free in the extracellular space. Further, the authors found soluble β-amyloid levels to be increased in vascular tissue from AD subjects in comparison to that from age-matched controls

5.1.4.5 Regulation of Amyloid Precursor Protein Processing

The control of APP processing *in vivo* is currently the focus of intense research activity. Cell culture studies suggest that amyloidogenic and non-amyloidogenic pathways of APP metabolism are stoichiometrically coupled (Nitsch, 1996), probably through competition for substrate (Gandy and Greengard, 1994), and evidence regarding control of the metabolic fate of APP is emerging. Stimulation of m1 and m3 muscarinic acetylcholine receptors in human embryonic kidney cell lines transfected with human brain muscarinic acetylcholine receptors results in the rapid release of soluble amino terminal derivatives of APP (Nitsch *et al.*, 1992). The time course of the appearance of these cleavage products suggests that cell surface receptor stimulation enhances the secretory cleavage of pre-existing APP. Buxbaum and colleagues (1992) independently demonstrated muscarinic acetylcholine receptor regulated APP processing in human glioma and neuroblastoma cells, and, in

addition, showed that interleukin-1 stimulates secretory processing of APP in human endothelial and glioma cells. Metabotropic glutamate (Lee *et al.*, 1995), 5-HT2a and 5-HT2c receptors (Nitsch *et al.*, 1996) have also been shown *in vitro* to enhance α secretase cleavage of APP and inhibit the production of β-amyloid. The neuropeptides, vasopressin and bradykinin, have been demonstrated to increase secretion of amino terminal derivatives (Nitsch, 1996), as has electrical stimulation of rat brain hippocampal slices (Nitsch *et al.*, 1997). Neurotransmitter receptor-mediated cleavage and release of soluble amino terminal derivatives of APP is insensitive to colchicine, suggesting that the cleaved substrate is either at the plasma membrane or is transported to the membrane in colchicine-insensitive secretory vesicles (Nitsch *et al.*, 1997).

It is of note, that muscarinic m1 and m3 receptors, like the bradykinin receptor, are linked through two homologous heterotrimer G proteins, Gq and G11, to activation of phospholipase C. Phospholipase C is responsible for the cleavage of phosphatidylinositol 4,5-biphosphate to inositol 1,4,5-triphosphate and 1,2-diacylglycerol. Along with intracellular ionic calcium, 1,2-diacylglycerol helps activate protein kinase C (PKC), while inositol 1,4,5-triphosphate regulates the release of calcium from intracellular stores.

Nitsch and colleagues (1992) hypothesise that the neural control of APP processing is mediated by protein kinases, possibly PKC (Nitsch *et al.*, 1997; Nitsch *et al.*, 1992), since staurosporine, an inhibitor of protein kinase, blocks the effect of m1 and

m3 acetylcholine receptor stimulated release of soluble APP derivatives. Intracellular ionic calcium enhances m1 and m3 acetylcholine receptor-mediated release of soluble APP derivatives (Nitsch *et al.*, 1997), though it is not necessary for this effect. Calcium alone is unable to mediate the release of soluble APP derivatives (Nitsch *et al.*, 1997).

Buxbaum and colleagues (1994) have identified another phospholipase C-dependent mechanism by which the secretion of soluble APP derivatives is enhanced, and the production of β-amyloid usually decreased, which relies on increased intracellular calcium, but which is independent of PKC.

Further evidence implicating PKC, which is proposed to have a general role in membrane trafficking (Luini and De Matteis, 1993), in the regulation of APP processing, comes from study of the effects of phorbol esters on the secretion of soluble amino terminal derivatives of APP. Phorbol esters usually alter the intracellular distribution and trafficking of proteins by phosphorylation, either of the protein itself or an ancillary protein, through stimulation of PKC (Efthimiopoulos *et al.*, 1994). Phorbol ester treatment of a rat C6 glioma cell line resulted in an increase in the production and secretion of the 110 to 125 kDa soluble ectodomain of APP and a decrease in the production of β-amyloid (Efthimiopoulos *et al.*, 1994), suggesting the β-amyloid levels can be manipulated pharmacologically. While the membrane-anchoring domain and site of α secretase cleavage were necessary for the effect, the ectodomain was not (Efthimiopoulos *et al.*, 1994). Further, while the

cytoplasmic domain was not required for phorbol induced modulation of APP processing, the cytoplasmic sequence 707 to 719 did affect the magnitude of the response. The authors hypothesise that removal of this cytoplasmic sequence enhanced the effect of phorbol esters either because its absence precluded entry into pathways other than the α secretase one or because this mutant proved a better substrate for the α secretase enzyme. Thus, it appears that the cytoplasmic tail plays little, if any, role in the regulation of α secretase cleavage of APP (Gandy and Greengard, 1994).

The effect of phorbol esters in the above system appears to be modulated by a cholera toxin sensitive heterotrimeric G protein (Efthimiopoulos *et al.*, 1994) and is independent of substrate phosphorylation (Jacobsen *et al.*, 1994). Okadaic acid, which inhibits protein phosphatases 1 and 2A, and tyrosine phosphorylation can also accelerate processing and secretion of α cleaved APP in a receptor-mediated fashion (Kingsbury *et al.*, 1995).

Significantly, the m1 muscarinic acetylcholine receptor is largely expressed in the CNS, unlike m2, m3 or m4 receptors that are widely distributed in peripheral tissues. Further, preliminary studies suggest that m1 agonists are safe and relatively free of troublesome side effects and that they slow the rate of progression of AD (Nitsch, 1996).

5.1.5 The Proposed Functions of Amyloid Precursor Protein

The physiological function of APP remains unknown (Adams, 1997), though a wide variety of potential roles for APP, its soluble, amino terminal truncated derivatives and residual carboxyl terminal fragments and β-amyloid are currently being explored.

After its synthesis in neurons, APP is transported by fast, anterograde, axonal transport. Indeed, APP can be seen to accumulate within three hours of neuronal injury as a consequence of cytoskeletal breakdown (Sherriff *et al.*, 1994). The various isoforms of APP are differentially expressed and their expression appears to be tightly regulated, suggesting they may have different actions (Moya *et al.*, 1994). Furthermore, their cellular effects may depend on the developmental stage of the cells exposed to them (Shea, 1994). APP is hypothesised to be a cell surface receptor linked to the heterotrimeric G protein, Go, and has been shown to bind to and activate Go in a ligand specific and ligand dependent manner (Okamoto *et al.*, 1995). It is probable that a naturally occurring ligand exists for this putative APP receptor, though none, as yet, has been identified (Okamoto *et al.*, 1995).

Small quantities of full-length, soluble forms of APP have been identified in the soluble fraction of PC12 cell extracts and in the conditioned media of these cells (Ripellino *et al*, 1994). Incubation of the membrane fraction of these cells at 37°C results in solubilisation of a full-length, mature form of APP. Though representative of a small fraction of the total APP in PC12 cells, the authors comment that this form

of APP is free of the plasma membrane and, therefore, accessible to proteolytic enzymes. In this model, release of soluble APP from the cell membrane was blocked by certain serine protease inhibitors and was inhibited by the presence of specific metal cations. It was also temperature and pH sensitive, all of which suggests the involvement of a serine protease in the process.

Severe degeneration has been described in post-mitotic neurons over-expressing APP (Yoshikawa *et al.*, 1992). Murine embryonal carcinoma P19 cells that differentiate into neurons and astrocytes on exposure to retinoic acid were transfected with cDNA for full-length human APP. Severe degenerative changes were identified in the neurons, which contain large amounts of carboxyl terminal β-amyloid containing peptides.

By analogy with the secreted, soluble derivatives of other proteins, the soluble, carboxyl truncated forms of APP are likely to be functionally important (Palmert *et al.*, 1989). Soluble, α secretase cleaved, APP-695 (APP-695_S) is believed to be neuroprotective *in vitro*, since conditioned medium from cells overproducing APP-695 has been shown to promote neurite extension in a clonal CNS neuronal cell line, B103 (Jin *et al.*, 1994). A 17 amino acid region of APP-695_S, from Ala319 to Met335, a domain known as the Kang sequence, has been identified as being responsible for this effect. The Kang sequence binds to specific and saturable cell surface binding sites and neither the KPI domain and nor the β-amyloid sequence is necessary for it to exert its effects. A shorter, five amino acid sequence known as the

RERMS sequence that spans amino acids 328 to 332 of APP-695_S, was identified as the active site crucial for such binding, though its effects were less potent than those of the Kang sequence. A role for APP-695_S in synaptic integrity has, therefore, been proposed (Jin *et al.*, 1994). The Kang sequence is also capable of inducing the accumulation of inositol polyphosphates, suggesting that this sequence is involved in the activation of inositol phospholipid signal transduction systems (Jin *et al.*, 1994). Evidence of a specific cell surface receptor for the soluble, carboxyl terminal truncated forms of APP comes from Johnson-Wood and colleagues (1994). They have identified a specific binding site for APP-751_S, the α secretase cleaved APP-751 isoform of APP that is identical to protease nexin II (Oltersdorf *et al.*, 1989), in cultured fibroblasts. The identified binding sites constituted a single class of high affinity sites that were saturable and to which binding was reversible. The identity of these binding sites remains unknown, but it is postulated to be either a cell surface receptor or a cell adhesion molecule. It is conceivable that such binding is the basis for the biological activities ascribed to APP-751_S (Johnson-Wood *et al.*, 1994).

A role as a cell adhesion molecule in the CNS has been postulated for APP as a result of both *in vitro* (Ho *et al.*, 1994) and *in vivo* (Moya *et al.*, 1994) evidence. Ho and colleagues (1994) have demonstrated that purified APP-770 is a substrate for tissue transglutaminase, an enzyme responsible for the calcium dependent intermolecular cross-linking of proteins via glutamine and lysine residues. Ho and co-workers conclude from their work and that of others that the secreted form of

APP-770 is an essential component of the extracellular matrix and that it contributes to the supporting infrastructure of the cell.

The neuroprotective effects of APP-695_S and APP-751_S *in vivo* have been studied by Smith-Swintosky and colleagues (1994), who administered these proteins intracerebroventricularly to rats within ten minutes of a period of cerebral ischaemia. The survival of neurons in the CA1 field of rat hippocampus was increased in rats that had been injected with APP-695_S and APP-751_S. The surviving neurons were both structurally and functionally intact and, in addition, APP-751_S partially prevented the decrease in microtubule-associated protein 2 (MAP-2) immunoreactivity that usually accompanies cerebral ischaemia, suggesting dendritic preservation. Bowes and colleagues (1994) employed a rabbit model of focal cerebral ischaemia to examine the effects of the 17 amino acid Kang sequence when administered intrathecally. They demonstrated a significant increase in the duration of the period of ischaemia required to produce permanent neurological damage when the Kang sequence was administered prior to, and for three days following, the period of ischaemia. Since the effect of this peptide was evident 4 days, but not 18 hours, post-ischaemia, Bowes and co-workers suggest that its function is restorative rather than protective. Thus, it would appear that the Kang sequence has a role in cellular stress management.

In an unusual study, Wagner and colleagues (1994) examined soluble amino terminal derivatives of APP, mostly the result of α secretase cleavage, in the CSF of three

pairs of monozygous twins. Lower levels of soluble, amino terminal derivatives of APP were found in the CSF of the AD subjects in comparison with the level found in the CSF of their normal or less affected twin.

5.1.6 The Neurotrophic and Neurotoxic Actions of β-amyloid

Yanker and colleagues (1990) exposed cultures of embryonic, rat, hippocampal neurons to β-amyloid and observed that low concentrations of this peptide had a neurotrophic effect on undifferentiated neurons. In contrast, higher concentrations of β-amyloid were neurotoxic to mature neurons. Substance P proved the most potent mammalian inhibitor of both the neurotoxic and neurotrophic actions of β-amyloid, implying that a substance P receptor might be involved in these phenomena. Yankner's team (Kowall *et al.*, 1991) went on to demonstrate that the forty-residue form of β-amyloid (β-amyloid(1-40)) was toxic *in vivo* by injecting rats intracerebrally with this form of the peptide.

In 1991, Pike and co-workers (Pike *et al.*, 1991a; 1991b) demonstrated that the forty-two-residue form of β-amyloid (β-amyloid(1-42)) adopts an aggregated conformation following several days incubation and is toxic to cultured, rat, hippocampal neurons. A twenty-eight-residue form of β-amyloid (β-amyloid(1-28)), however, did not aggregate under similar conditions and was not toxic to such neurons. Exposure of rat, hippocampal cultures to aggregated deposits of β-amyloid resulted in dystrophic neuronal processes (Pike *et al.*, 1992), yet, once in contact with deposits of aggregated β-amyloid the neuronal processes grew extensively over

them and rarely extended beyond them. Scanning electron microscopy confirmed that neurites in contact with aggregated β-amyloid deposits degenerated, that they appeared orientated towards the deposits and that they tended not to leave the deposits once they had established contact with them. Processes not in physical contact with the deposits remained normal, even when other processes from the same neuron were in contact with aggregated β-amyloid deposits and were degenerating.

Cotman and colleagues (1993), studied the neurotrophic effects of β-amyloid using vulnerable, low density, neuronal cultures of 7 000 cells/cm^2. These cultures degenerate unless supplied with trophic factors and, thus, are sensitive to the effects of trophic stimuli. Soluble β-amyloid(1-40) and soluble β-amyloid(1-42) were shown to increase the survival of these cultured, rat, hippocampal neurons. Further, when supplied with newly solublised and non-aggregated β-amyloid(1-42) they exhibited significant axonal elongation and dendritic arborisation.

β-amyloid is a self-aggregating peptide (Pike *et al.*, 1992). When a concentrated solution of β-amyloid(1-42) is incubated at a slightly acidic pH it forms sheet-like aggregates in solution visible on light microscopy (Cotman *et al.*, 1993). Further, reducing gel electrophoresis of incubated β-amyloid(1-42), reveals not only a band at the predicted monomeric molecular weight, but other higher order bands suggestive of aggregation. Such aggregates exhibit the tinctorial and optical properties that characterise the β-amyloid of senile plaque cores (Cotman *et al.*, 1993). Barrow and Zagorski (1991) established that the hydrophobic, carboxyl domains of β-amyloid,

represented by residues 29-42, exist in solution solely in an oligomeric β pleated sheet conformation, irrespective of the pH and temperature of the solution or the solvent used. The authors suggest that it is this highly aggregable domain that directs folding of the β-amyloid(1-42) peptide. The toxic effects of aggregated β-amyloid(1-40) on cultured rat pheochromocytoma PC12 cells can be significantly reduced by ageing the peptide in the presence of the rifampicin (Tomiyama *et al.*, 1994), an antibiotic that has been shown *in vitro* to inhibit the aggregation of β-amyloid(1-40) in a dose-dependent manner. The aggregation of β-amyloid(1-42) is known to occur under physiological conditions (Pike *et al.*, 1991a). Cotman and co-workers (1993) conclude that aged, aggregated β-amyloid(1-42) is toxic and that β-amyloid(1-28), which lacks a hydrophobic domain and does not aggregate on incubation, is not.

However, it has been postulated that soluble β-amyloid does have toxic effects. A type of potassium channel dysfunction documented to occur in AD fibroblasts has been ascribed to soluble β-amyloid (Etcheberrigaray *et al.*, 1994) and soluble β-amyloid(1-42), while not toxic to mature, healthy, neuronal cultures, appears to render the cells exposed to it more vulnerable to other insults (Cotman *et al.*, 1992). Glucose deprivation, glutamate excitotoxicity and exposure to nerve growth factor are among such insults (Cotman *et al.*, 1993). Binding of nerve growth factor to low affinity receptors inhibits β-amyloid toxicity, while binding to high affinity nerve growth factor receptors potentates β-amyloid induced neurotoxicity (Rabizadeh *et al.*, 1994). Protease nexin II, the secreted form of KPI-containing APP, has been

shown to form complexes with the gamma subunit of nerve growth factor (Oltersdorf *et al.*, 1989), though whether this might enhance or diminish the toxicity of nerve growth factor is unclear.

The spontaneous polymerisation of β-amyloid displays nucleation-dependent kinetics (Jarrett *et al.*, 1993). The formation of a nidus or seed is thermodynamically unfavourable and slow, but once formed, further, ordered protein polymerisation of a supersaturated solution is thermodynamically favourable and rapid. Thus, it is conceivable that a small amount of highly aggregable, hydrophobic β-amyloid(1-42) or the forty-three-residue form of β-amyloid (β-amyloid(1-43)) could serve as the seed around which β-amyloid(1-40) could readily aggregate. Growth of this nucleus could be sustained by β-amyloid(1-40), which Maness and colleagues (1994) attest could come from the periphery, since β-amyloid(1-40) administered intravenously to mice crossed the blood-brain barrier and accumulated intact in brain by a non-saturable mechanism. It would appear that it is the carboxyl terminal of β-amyloid which is critical and the relative concentration of β-amyloid(1-42) that is important, rather than the total concentration of β-amyloid (Jarrett *et al.*, 1993). Furthermore, Wisniewski and co-workers (1994) have shown that the ε4 allele of apolipoprotein E accelerates β-amyloid fibril formation in the presence of a high concentration of β-amyloid.

Citron and colleagues (1992) studied β-amyloid production in cultured human kidney 293 cells transfected with APP bearing the double mutation found in a

Swedish family with FAD (Mullan *et al*, 1992). They demonstrated a six to eight fold increase in β-amyloid production in cells transfected with the mutated APP compared with cells transfected with wild type APP, implying that increased β-amyloid production is fundamental to the disease. Suzuki and co-workers (1994) provided further evidence for the crucial role of the long forms of β-amyloid in β-amyloid-induced neurotoxicity. They transfected human neuroblastoma cells with wild-type human APP or APP mutated at the 717 position from valine to isoleucine, glycine or phenylalanine. The wild-type transfectants expressed primarily, though not exclusively, β-amyloid(1-40), while the APP717 mutants exhibited a 1.5 to 1.9 fold increase in the percentage of highly amyloidogenic β-amyloid(1-42) and β-amyloid(1-43) forms expressed.

5.1.7 The Deposition of β-amyloid *In Vivo*

Yang and colleagues (1994) found abundant β-amyloid(1-42) in all of the diffuse plaques, senile plaque cores and vascular amyloid deposits they identified in AD frontal cortex, while only a subset were positive for β-amyloid(1-40). The same workers concluded that β-amyloid(1-42) is the earliest form of β-amyloid deposited in the AD brain and hypothesised that region specific metabolism of β-amyloid might account for the characteristic distribution of pathology in AD (Mak *et al.*, 1994). In support of this, the authors demonstrated only weak, or non-specific staining, of diffuse plaques in response to antibodies directed against β-amyloid(1-40) or β-amyloid(1-42) in the striatum in AD brain, an area relatively spared in the disease.

On immunochemical analysis, Iwatsubo and co-workers (1994) found all senile plaques identified in AD cortex to be positive for β-amyloid(1-42) or β-amyloid(1-43), but found that only a third were positive for β-amyloid(1-40). Moreover, diffuse plaques were labelled exclusively with β-amyloid(1-42) or β-amyloid(1-43) and were negative for β-amyloid(1-40). A strong correlation was found between mature plaques and β-amyloid(1-40) positivity. The cases of FAD examined were distinctive in that β-amyloid(1-42) and β-amyloid(1-43) positive and β-amyloid(1-40) negative plaques predominated. Thus, in keeping with *in vitro* evidence, plaque formation *in vivo* appears to begin with the deposition of highly amyloidogenic forms of β-amyloid. LaFerla and co-workers (1995) examined the effects of the selective overexpression of the β-amyloid peptide in mice by introducing a strong, neuron-specific promoter to drive the intracellular expression of the murine homologue of human β-amyloid. The overexpression of β-amyloid in the brains of these transgenic mice was not uniform, being extensive throughout the cortex and hippocampus, regions that are significantly affected in AD. Extensive neuronal degeneration and evidence of apoptotic cell death was apparent in the brains of the transgenic mice. Thus, in conclusion, it appears that neurons are vulnerable to overexpression of β-amyloid containing APP fragments, β-amyloid itself, and impaired degradation of APP.

5.1.8 Potential Mechanisms of β-amyloid Toxicity

While there is consensus that aggregated β-amyloid is neurotoxic, there is no one, unifying theory as to how this toxicity might occur and, as yet, no formally proven mechanism (Rogers *et al.*, 1992).

It is conceivable, that the toxic effects of β-amyloid are mediated by changes in protein tyrosine phosphorylation (Zhang *et al.*, 1994), since aggregated β-amyloid is associated with a significant increase in the level of tyrosine phosphorylation of focal adhesion kinase in cells of neuronal lineage. Signal transduction via tyrosine phosphorylation participates in functions such as cell adhesion, axonogenesis, cytoskeletal organisation, gene expression, mitosis and apoptosis (Zhang *et al.*, 1994), some of which have been ascribed to β-amyloid.

Two broad mechanisms of cell death exist: necrosis and apoptosis. Necrosis is accompanied by inflammation, damage to surrounding cells and the random degradation of cellular DNA visible as a smear on gel electrophoresis. In contrast, apoptosis, a form of programmed cell death in which the cell itself participates in its own demise, induces a minimal amount of inflammation and is associated with activation of nuclear endonucleases which cleave DNA into 180 base pair fragments visible as a ladder on gel electrophoresis (Lassmann *et al.*, 1995). Aggregated β-amyloid has been shown to induce apoptotic cell death in cultured neurons (Cotman and Anderson, 1995).

The immediate early genes, some of which have transcriptional capabilities, have been implicated in the control of apoptosis (Cotman and Anderson, 1995). Such an arrangement would seem logical given the involvement of the immediate early genes in manageing cellular stress and the need to remove irretrievable damaged cells with the minimum of disruption to surrounding tissues. Cotman and Anderson (1995) report increased immunochemically detectable Jun-related proteins in cultures of young and mature primary hippocampal neurons exposed to β-amyloid. Interestingly, GABA neurons, which are resistant to apoptosis in both culture and *in vivo* in AD, show no evidence of induction of Jun proteins in response to β-amyloid (Cotman and Anderson, 1995).

Another potential molecular mechanism by which β-amyloid might be neurotoxic is in the generation of reactive oxygen species (Davis, 1996). The inhibition of hydrogen peroxide accumulation and prevention of cell death, in response to antioxidants and inhibitors of the enzymes superoxide dismutase and superoxide, are compelling evidence for the role of reactive oxygen species in β-amyloid induced toxicity. Further, oxidative injury has been shown to induce apoptotic cell death *in vitro* (Cotman and Anderson, 1995).

The β-amyloid peptide is known to bind and activate the C1q component of C1 of the classical complement cascade that results ultimately in the formation of the membrane attack complex (MAC). MAC exerts its cytotoxic effects by inserting a lytic plug in nearby cell membranes. The conventional mechanism by which the

classical complement cascade is activated is through C1q binding to the Fc region of immunoglobulins. While immunoglobulins do not co-localise with senile plaques in AD, antibody-independent activation of complement activation is a recognised phenomenon (Rogers *et al.*, 1992). When C1q is inappropriately bound to a non-immunoglobulin substrate mechanisms exist whereby it can be disarmed. Rogers and colleagues postulate, however, that since β-amyloid is insoluble in the fluid phase, it is able to evade both cellular defence mechanisms and fluid phase inhibitors and stimulate inappropriate activation of the complement cascade.

5.1.9 Amyloid Precursor Protein mRNA Expression

Koo and colleagues (1990) conclude, from their work in human and primate brains, that APP mRNA levels are developmentally regulated. They found APP-695 mRNA is three times more abundant than KPI-containing transcripts of APP mRNA in human foetal brain, while in young adults the expression of APP-695 mRNA and KPI-containing transcripts of APP mRNA was approximately equal. In aged controls and AD sufferers, however, KPI-containing transcripts of APP mRNA predominated over APP-695 mRNA, though the change in the ratio between KPI-containing APP mRNA transcripts and APP-695 mRNA was similar in both groups (Koo *et al.*, 1990).

Levels of APP-695 mRNA in hippocampal neurons have been shown to decline with age in female, but not male, rats and hippocampal APP-695 mRNA expression is enhanced in young, ovarectomised, female rats on exposure to oestrogen and

progesterone (Chao *et al.*, 1994). Chao and colleagues (1994) proposed that a decrease in APP-695 mRNA expression in the hippocampus, particularly the CA1 field, as a consequence of a decline in sex steroid levels with age, may contribute to the neuronal degeneration seen in elderly, female rats.

Weidemann and colleagues (1989) established the presence of the three major protein isoforms of APP, APP-695, APP-751 and APP-770, in neuronal and non-neuronal cells. Extracts of RNA from pure cultures of rat neurons suggest that APP-695 mRNA is the predominant form of APP mRNA in neurons, representing 95% or more of APP mRNA transcripts (Sandbrink *et al.*, 1997). However, Moya and colleagues (1994) have demonstrated intraneuronal synthesis of KPI-containing isoforms of APP *in vivo*. Rat neuronal cells are virtually devoid of L-APP transcripts, though such transcripts represent almost half of the APP transcripts in rat astrocytes and microglia (Sandbrink *et al.*, 1997). Only subtle regional variations in the pattern of APP mRNA isoform expression have been identified in rat on analysis of cultured neurons extracted from the hippocampus, cortex and striatum (Sandbrink *et al.*, 1997). Sandbrink and colleagues (1997) used RT-PCR and DNA extracted from the parietal cortex of a single, aged, human control to study L-APP mRNA expression in humans. The results obtained from examination of this subject were representative of a larger number of brains studied. The authors found that L-APP transcripts represented a significantly lower proportion of total APP mRNA transcripts, while L-APLP2 transcripts represented a greater proportion of total APLP2 mRNA transcripts than in rat cerebral cortex.

Ebstein and co-workers (1996) have examined the effects of age and disease on APP-751 and APP-770 mRNA levels in lymphocytes in the belief that they may reflect changes in brain APP mRNA expression pertinent to AD. Using quantitative RT-PCR, the authors demonstrated that APP-751 mRNA expression was positively correlated with age in 64 cognitively intact individuals ranging from 20 to 91 years of age. The nineteen AD subjects studied exhibited APP-751 mRNA levels equivalent to that found in the age-matched control group. The ratio of APP-751 to APP-770 mRNA transcripts, however, was lower in the AD group than in the group of age-matched control subjects over 55 years. The authors attribute this finding to the average 31% increase in APP-770 mRNA transcripts in lymphocytes from AD subjects compared with an average 12% increase in this isoform in the lymphocytes of control subjects over the age of 55 years.

Johnston and colleagues (1996b) have developed a sensitive, reproducible assay for specific mRNA species based on solution hybridisation with an RNA antisense probe, followed by degradation of non-hybridised RNA with a ribonuclease enzyme. The assay is capable of detecting subtle, physiologically relevant, alterations in mRNA expression, can detect as little as 1 ρg of RNA and has low inter and intra assay variability. A standard curve can be constructed for a particular mRNA species if the solution hybridisation experiment is carried out using known quantities of *in vitro* transcribed sense RNA. Absolute quantification of the mRNA species under investigation can then be achieved by reference to the standard curve. Like

PCR, this assay does not require that the mRNA species to be examined is intact and it can be performed on small fragments of RNA.

Johnston and co-workers (1996b) examined cortical and cerebellar levels of APP and APLP2 mRNA in homogenised, post-mortem, human brain tissue from 3 control subjects matched for age and PMI, but not for agonal state. The expression of both APP and APLP2 mRNA was highest in the temporal cortex, lowest in cerebellum and intermediate in the frontal and occipital cortices. The ratio of APP:APLP2 was 1:0.3 in neocortex and 1:0.8 in cerebellum. Levels of KPI-containing APP mRNA transcripts were highest in the frontal and temporal cortices, lowest in cerebellum and intermediate in the occipital cortex. Johnston and co-workers (1996b) data suggests that regional differences in the levels of APP and APLP2 mRNA, and in APP splicing, do exist in control, post-mortem, human brain. Further, APP and APLP2 mRNA expression and levels of KPI-containing transcripts of APP reflect the pattern of pathological involvement in AD being highest in the temporal cortex, intermediate in the occipital cortex and low in the relatively spared cerebellum.

Astrocytes do not normally contain either APP or APP mRNA, but rat astrocytes accumulate large amounts of immunochemically detectable APP following neuronal damage (Siman *et al.*, 1989). Damage to rat hippocampal neurons results in the accumulation of APP in glial fibrillary acidic protein-positive astrocytes immediately adjacent to the injury (Siman *et al.*, 1989). Glial fibrillary acidic protein mRNA is also increased in AD (Robinson *et al.*, 1994). The mechanism responsible for this

increase, and the specific isoforms of APP present in the reactive astrocytes, is unknown.

In 1989, in a study of 17 individuals suffering from Down's syndrome, Rumble and colleagues established that the serum concentrations of APP in these subjects were 1.5 fold higher than those found in control subjects. Patients with AD had similar serum APP levels to the controls. Triplication of the APP gene on chromosome 21 was hypothesised to result in overexpression of APP and subsequently amyloid deposition in individuals with trisomy 21 (Rumble *et al.*, 1989). Examination of APP mRNA extracted from the brain tissue of aborted Down's syndrome foetuses, suggests that APP mRNA is increased in the brains of these foetuses in comparison to levels found in control foetal brains (Tanzi *et al.*, 1987). Querfurth and colleagues (1995) identified a 1.8 fold increase in APP mRNA levels in fibroblast cell lines from individuals with Down's syndrome relative to age-matched normal controls. This increase was not significant, but when the cells were grown under conditions of stress in 0.5% serum, a significant, 2 fold increase in APP mRNA levels was observed in the fibroblast cell lines obtained from Down's syndrome individuals.

Querfurth and co-workers (1995) have also demonstrated an apparent increase in transcription of APP in fibroblast cell lines from a Canadian pedigree with FAD that shows strong linkage to chromosome 14. A 1.6 fold increase in APP mRNA was identified in fibroblast cell lines from affected members of the Canadian FAD pedigree in comparison with fibroblast cell lines from unaffected members of the

pedigree. This rose to a 1.9 fold increase in APP mRNA in fibroblasts from affected probands stressed by serum free conditions of growth and was accompanied by a 2 fold increase in levels of the APP protein and a 2.5 fold increase in the β-amyloid peptide in these fibroblasts. Transient transfection of fibroblast cell lines from affected members of the Canadian FAD pedigree with a reporter gene driven by the APP promoter, revealed a four-fold increase in APP promoter activity in these cell lines, suggesting that the increase in APP mRNA is not attributable to an increase in mRNA stability. Querfurth and co-workers (1995) conclude that their results are most consistent with an alteration in the amount or function of a nuclear, regulatory transcription factor for the APP gene in the Canadian FAD pedigree. Fibroblast cell lines from another FAD pedigree of Italian origin with linkage to chromosome 14 did not exhibit any increase in APP expression (Querfurth *et al.*, 1995).

Harrison and colleagues (1991d) examined brain APP mRNA levels in FAD using ISHH. Four brain regions were examined in three FAD and three control cases. The authors found no difference in the distribution or quantity of either KPI-containing or non-KPI splice variants of APP in the FAD cases compared to the controls.

However, further evidence that increased APP mRNA levels may be important in the pathophysiology of AD in some subjects comes from Rockenstein and co-workers (1995). Rockenstein and colleagues observed AD-type pathology in a transgenic mouse model in which neuronal expression of an alternatively spliced minigene encoding human APP was driven by a platelet-derived growth factor promoter. A

substantial increase in total, and transfected human, APP mRNA levels were observed in the transgenic mice. Elevated APP mRNA levels were not found in other transgenic mouse lines that did not exhibit AD-like pathology. Thus, high levels of APP mRNA expression appear to be necessary for the production of robust AD-like pathology in these transgenic mouse lines (Rockenstein *et al.*, 1995). The same workers (Rockenstein *et al.*, 1995), examined APP mRNA levels in human frontal cortex and identified a subtle increase in the relative amounts of APP-751 and APP-563 mRNA transcripts, but no increase in total APP mRNA levels, in AD compared to control brain. PMI was less than eight hours for all samples, but pre-mortem factors were not analysed in this study and only four AD cases and five control cases, selected for their relatively good preservation of RNA, were examined.

Cohen and co-workers (1988) examined APP mRNA transcripts containing the β-amyloid sequence in the cerebral cortex and nucleus basalis of five AD and five control brains using ISHH. The brains were matched for age and PMI, but pre-mortem factors were not assessed. The authors demonstrated an increase in APP mRNA expression in the nucleus basalis in AD, but APP mRNA expression in the cerebral cortex was unchanged. No ISHH labelling was observed over glia or endothelial cells.

Palmert and co-workers (1988) examined total and KPI-containing APP mRNA transcripts in eleven AD and seven control subjects using ISHH. The subjects were matched for age and PMI, but no information on pre-mortem course was presented.

No differences between the AD and control brains were observed in the basis pontis, occipital cortex or hippocampal subicular neurons. However, total APP mRNA levels were increased two fold in the nucleus basalis of Meynert and the locus ceruleus of the AD brains in comparison to the control brains. The level of KPI-containing APP mRNA transcripts remained unchanged in these areas. The authors propose that the increase observed in total APP is exclusively accounted for by an increase in non-KPI containing transcripts: presumably APP-695, though conceivably APP-714. No labelling of glial or endothelial cells was seen with either probe. Since fewer specific grains were detected over tangle-bearing neurons than over tangle-free neurons, the authors suggest that increased APP mRNA expression is a compensatory response in surviving neurons.

Goedert (1987) found little variation in APP RNA levels in different cortical areas of normal control brains by Northern blotting. In particular, no difference was evident between areas severely involved in AD, such as the temporal and frontal cortex, and areas typically spared, such as the thalamus and the striatum. Northern blotting of four AD cases and four control cases demonstrated a decrease in APP mRNA in the frontal cortex in AD. Goedert (1987) complemented his Northern blotting work with an ISHH study of AD and control brains. Four AD and three control cases, all aged more than 65 years and with PMI of less than 4 hours, were examined. No information was presented on the pre-mortem course of any of the patients whose brains were examined. Specific labelling was detected over cortical pyramidal cells and over pyramidal and granule cells in the hippocampus. No specific labelling of

glial or endothelial cells was observed. No disease specific differences in APP mRNA expression were identified using ISHH in this study.

Johnson and colleagues (1989) applied a complementary methodology, RNA gel blot analysis using single-stranded cRNA probes, to the study of APP mRNA transcripts in nine AD and ten control subjects. The cases were matched for age and PMI, but not for pre-mortem factors. The results of this study are not comparable with those of the ISHH studies, since the cells examined are heterogeneous in type. Using powdered, frozen tissue from neocortex, hippocampus and cerebellum, Johnson and co-workers examined APP-751 and APP-695 mRNA levels. They found APP-751 mRNA to be essentially unchanged in all of the regions they examined in AD in comparison to control tissue, but APP-695 mRNA was reduced in the hippocampus and neocortex in AD. The ratio between APP-751 and APP-695 mRNA levels, however, was increased two fold in AD hippocampus in comparison to control hippocampus. The APP-751/APP-695 ratio was found to be six fold lower in cerebellum than in hippocampus or neocortex and to be unaltered in AD. Johnson and colleagues (1990) went on to confirm that the APP-751/APP-695 ratio was increased in hippocampal neurons in AD in comparison with non-AD hippocampal neurons, using ISHH. The group compared tissue from seven cases of neuropathologically confirmed AD with four non-AD cases. One of these cases was a normal control subject, one had suffered from mixed multi-infarct dementia and Parkinson's disease during life and two had suffered from Parkinson's disease alone. Though the subjects in the two groups were matched for age, no information was

presented on PMI or the pre-mortem course of the patients' illnesses. The study found the pyramidal cell APP-751/APP-695 mRNA ratio to be positively correlated with hippocampal and entorhinal plaque density. Crucially, however, this study demonstrated an increase in APP-751 mRNA in the hippocampus and the authors attributed the increased APP-751/APP-695 mRNA ratio to this, rather than to a decrease in APP-695 mRNA as they had previously reported.

Koo and co-workers (1990) were unable to identify any disease-specific alterations in the ratio between APP695 and KPI-containing transcripts of APP mRNA in a study of seven AD and seven control cases unmatched for age, PMI or pre-mortem course.

Neve and colleagues (1990) probed RNA extracted from six brain areas from AD and control subjects with probes specific for APP-563, APP-695, APP-751 and APP-770, using RNA slot blots. The RNA extracted from all five control and five AD cases was intact, as assessed by Northern blotting, and the cases were matched for age. No information was presented, however, regarding pre-mortem factors or PMI. No changes were observed in the splice variants examined in the primary visual cortex, basal ganglia or hippocampal formation in AD. However, a significant and specific increase in APP-563 RNA was detected in the nucleus basalis, occipitotemporal cortex and parahippocampal gyrus in AD. In the nucleus basalis alone, the authors used ISHH and PCR to confirm that APP-563 mRNA was increased. Increased expression of APP-563 mRNA in AD was evident in the

magnocellular neurons of the nucleus basalis, but also in smaller cells in this region, possibly glia, which appeared to be a new population of cells recruited in AD. All other APP mRNA transcripts were unchanged in the nucleus basalis in AD, implying that the change detected in APP-563 was not a simply a reflection of altered mRNA expression in general. In AD, APP-695 mRNA was decreased in the parahippocampal gyrus and APP-751 mRNA was slightly increased in the occipotemporal cortex. Neve and co-workers ascribe the latter finding to cross-hybridisation of the APP-751 oligonucleotide probe with APP563 mRNA.

In 1993, Tanzi and colleagues investigated the cellular localisation of APP-695 and APP-751 mRNA in eleven AD and nine control hippocampi. The cases were matched for age and PMI, but no information on pre-mortem factors was presented. The authors concluded that APP-695 and APP-751 mRNA were both expressed in neurons, that their cellular specificity, and regional distribution, was similar and that both were unaltered in AD brain in comparison to control brain. In contrast, glial cells exhibited little or no APP-695 or APP-751 mRNA, even in AD brains displaying marked gliosis.

Jacobsen and colleagues (1991) used an S1 nuclease protection assay to examine mRNA levels of the individual APP transcripts: APP-365, APP-695, APP-751 and APP-770 in the frontal, temporal, occipital and parietal cortices of sixteen AD and nine control brains. The authors concluded, by comparing young and old sub-populations of their normal control group and age-matched AD and control sub-populations, that age has no effect on APP mRNA levels. Since PMI and

pre-mortem factors were not taken into account in the analysis, the decision not to age-match the AD and control groups appears presumptuous. Nevertheless, Jacobsen and co-workers (1991) treatment of the data is interesting. Significant increases were observed in APP-695 and APP-770 mRNA levels when expressed relative to cyclophilin mRNA in AD subjects in comparison to controls. However, total APP mRNA levels when expressed relative to cyclophilin mRNA levels were unchanged in the frontal, temporal, parietal or occipital cortex in the AD subjects in comparison to the controls. When total APP mRNA levels were expressed relative to the mRNA levels of microtubule associated protein 2 (MAP-2), a largely neuron specific mRNA, total APP mRNA levels were found to be increased in the AD subjects in comparison to the controls in all of the cortical regions examined. Moreover, the total APP/MAP-2 ratios in AD were greater in the temporal and frontal cortices than in the parietal and occipital cortices. In normal subjects MAP-2 mRNA levels were 2.4 fold that of cyclophilin mRNA levels, while in the AD subjects MAP-2 mRNA levels were half that of cyclophilin mRNA levels. The authors surmise that in AD MAP-2 mRNA is decreased, cyclophilin mRNA is increased, or alterations occur in both mRNA species. The authors preferred explanation of their findings is that MAP-2 mRNA levels are decreased in AD. Assuming that this is so, and that cyclophilin mRNA levels are unchanged in AD, Jacobsen and co-workers (1991) findings regarding overall levels of APP mRNA can be interpreted in several ways. APP mRNA levels in AD might be truly unchanged; alternatively, increased amounts of APP mRNA might be produced by less cells, or less produced by more cells. Further, selected transcripts of APP mRNA might be

increased while others were decreased and this balanced change need not occur within individual cells.

The authors state explicitly that there is no significant increase in total APP mRNA, when expressed relative to cyclophilin mRNA, in AD cases in comparison to controls. However, mRNA levels of the individual transcripts of APP, when expressed relative to cyclophilin mRNA levels, are altered in AD, though show no discernible link with amyloid pathology in the disease. When individual APP isoform mRNA levels are expressed as a fraction of total APP mRNA, however, these can be related to AD pathology. In the frontal and temporal cortices in AD, the cortical regions most heavily involved in the disease process, the fraction of total APP mRNA attributable to APP-695 mRNA was increased and that attributable to APP-751 and APP-365 mRNA decreased. In addition, a small, but significant, increase in the APP-770 mRNA fraction of total APP mRNA was observed in all of the cortical areas measured in AD. The individual transcripts of APP mRNA when expressed as a proportion of total APP mRNA are related to pathology, yet no such association is apparent when the individual APP mRNA transcripts are related to cyclophilin mRNA levels. The significance of this finding is not discussed.

Robinson and co-workers (1994) demonstrated a marked decrease in APP-695, and a moderate decrease in KPI-containing transcripts of APP mRNA, in AD tissue from the superior and middle pre-frontal cortex in comparison to age-matched control tissue, using Northern blotting. Forty-two AD cases and thirteen control cases were

selected for their fair or excellent RNA content on agarose formaldehyde gel electrophoresis. The cases were not matched for agonal state or PMI. The ratio between KPI-containing transcripts of APP mRNA and APP-695 mRNA was 1.12 for the AD cases and 0.73 for the control cases: a difference that is statistically significant.

In an important paper in 1994, Harrison and colleagues investigated the effects of AD, other dementing illnesses and pre-mortem course on APP mRNA, using ISHH performed on frontal cortex obtained at rapid autopsy. Eleven AD cases, four controls and six cases of non-AD dementia, on whom data was available regarding age, PMI and pre-mortem course, were examined. APP mRNA abundance was found to correlate strongly with GAD activity and was reduced in association with terminal pyrexia. Both KPI-containing and non-KPI transcripts of APP mRNA, normalised to levels of polyadenylated mRNA, were reduced in the AD cases in comparison to the control or non-AD dementia cases. This study demonstrated that APP mRNA levels are susceptible to pre-mortem influences such as coma and pyrexia and established that potentially confounding agonal state factors should be taken into account when interpreting changes in APP mRNA levels in human brain.

In a review of the published literature, Harrison and co-workers (1996) concluded that no unequivocal, specific abnormality in APP mRNA expression has been documented in AD. Preliminary data from Harrison and colleagues (1996) study of brain tissue from seven control subjects, ten AD subjects and six subjects with

non-AD dementia did not demonstrate any significant differences in APP-695 or KPI-containing transcripts of APP mRNA between the diagnostic groups. The tissue was obtained from the Oxford Study to Investigate Memory in Ageing (OPTIMA) and was matched for age, sex, PMI and agonal state. Further, no significant differences in the ratio of KPI-encoding to KPI-lacking splice variants of APP mRNA was observed between the groups and no relationship was found between this ratio and the age of the subjects.

Johnston and colleagues (1996a) demonstrated a decrease in APP and APLP2 mRNA in the mid-temporal cortex, but not in the superior frontal cortex, in AD tissue in comparison to normal control and non-AD neurologically diseased tissue. Fourteen AD cases, nine control cases and five cases with non-AD neurological diseases, matched for age and tissue pH, were included in the study. Information on PMI was available for each case. Messenger RNA levels were measured using solution hybridisation-RNase protection assay on samples of total nucleic acid and were expressed as a function of total RNA levels. APP mRNA was present at three-fold the level of APLP2 mRNA in the control cases and KPI-containing transcripts of APP constituted 70% of total APP mRNA. A significant increase in KPI-containing transcripts was found in both regions examined in AD. Johnston and colleagues (1996a) postulate that the decreases in APP and APLP2 mRNA are confined to the mid-temporal cortex in response to the characteristically more severe pathology observed in this region compared to the frontal cortex in AD. It is conceivable that, in employing homogenised tissue, Johnston and colleagues (1996a) have masked the

neuronal decreases in KPI-containing and non-KPI transcripts of APP mRNA identified by Harrison and colleagues (1994) using ISHH.

5.2 Materials and Methods

5.2.1 Selection of Tissue

5.2.1.1 Series II Tissue

This series comprised the visual cortices of thirty-two cases, collected mainly from Oxford, but also from London, and included twelve normal control subjects, seventeen subjects with definite AD, two subjects with borderline AD and one subject with a mixed AD and multi-infarct dementia. Brain tissue from seventeen male and fifteen female subjects were included in the study. Details of all of the series II cases are presented in appendix II.

5.2.1.2 Series III Tissue - The Oxford Study to Investigate Memory in Ageing (The OPTIMA Study) Tissue

The OPTIMA Study was established in 1988, under the directorship of Dr. A.D. Smith with the aim of assembling a cohort of intensively, prospectively assessed individuals willing to be involved in research into ageing. The study of individuals recruited into OPTIMA has resulted in publications on clinical aspects of dementia, such as the use of neuroimaging in early AD (Smith *et al*, 1996a) and the predictive value of apolipoprotein E genotyping (Smith *et al*, 1996b). In addition, post-mortem tissue collected through OPTIMA has been used for mRNA studies (Harrison *et al*, 1996). In total, approximately 200 individuals have been enrolled in the OPTIMA

study. At the time of the request for tissue, approximately 90 individuals had died and in 70 of these cases frozen brain tissue was available for study.

Subjects with dementia enrolled into the OPTIMA study are assessed on the CAMDEX, a rating scale designed to measure cognitive abilities and global functioning, and receive annual haematological and biochemical screening, lumbar puncture and CT scan. The apolipoprotein E genotype is determined for all subjects. In some cases, the spouses of cognitively impaired subjects are recruited as controls, but many controls are obtained independently. To date, a remarkable 98% of individuals enrolled in the study have agreed to autopsy. Quantitative neuropathological data is available for a subset of the brains examined at autopsy.

Brain tissue from fourteen individuals with AD, eight control subjects, five individuals with borderline AD, six individuals with non-AD neurodegenerative diseases and six individuals with non-neurodegenerative conditions was selected by Dr. P.J. Harrison, Reader in Psychiatry at the University of Oxford for study in Sheffield. Blocks of tissue were collected on cork discs from the mid-hippocampus and visual cortex (Brodmann area 17) and sent to Sheffield on dry ice. No information was supplied regarding the clinical history or pathological diagnosis of the supplied tissue until the experiments and image analysis were complete.

The value of a positive control group in elucidating changes in mRNA expression specific to AD from those secondary to chronic neurological disease has been underlined by Harrison and colleagues (1994).

Unfortunately, the brains were not dissected by the same neuropathologist, nor were they all frozen according to the same protocol. The collection of frozen blocks of tissue on cork discs has both advantages and disadvantages. The tissue is exposed and unsupported on its cork disc, unlike tissue embedding in OCT. It is therefore more vulnerable to damage during freezer storage and thaws quickly once removed. The cork discs used were approximately 2.5 cm in diameter and thus it was difficult to record the case number and brain region legibly on the base. A number of blocks were difficult to identify for this reason.

The series III (the OPTIMA series) blocks were cut into eighteen μm thick sections on a Bright cryostat at -20°C with appreciable assistance from Mr. M.W. Sanders and Miss J.M. Heffernan. The histological quality of several of the tissue blocks was noted to be poor. The cryostat cut tissue was prepared as detailed in chapter 2. Details of all of the cases included in this series are presented in appendix II.

5.2.1.3 Series IV Tissue

Series IV comprised cases from both series II and the series III (the OPTIMA series) as well as cases investigated in our laboratory by two independent investigators, Dr.

A.J.L. Barton and Dr. M.H. Griffiths. Details of the series IV cases are presented in appendix II.

5.2.2 Oligodeoxynucleotide Probe Selection

Three oligodeoxynucleotide probes, APP-770, APP-insert and APP-junction were selected to examine APP expression (Figures 5.2 and 5.3). The APP-770 oligodeoxynucleotide antisense probe was directed against bases 1033 to 1089 of the cDNA sequence published by Kitaguchi and co-workers (1988) and theoretically detects APP transcripts APP-770 and APP-714. The APP-insert oligodeoxynucleotide antisense probe was directed against bases 1047 to 1076 of the APP-751 cDNA sequence published by Ponte and co-workers (1988) and theoretically detects APP mRNA transcripts APP-751, APP-770, APP-563 and APP-365. The APP-junction probe was directed against bases 975 to 989 and 1158 to 1172 of the APP-751 cDNA sequence published by Ponte and colleagues (1988). The APP-junction probe, therefore, only hybridises to APP splice variants in which the flanking regions of the KPI domain are contiguous; as in APP-695 alone (see Harrison *et al,* 1994). A sense oligodeoxynucleotide probe with the same sequence and orientation as the putative sequence of APP-695 mRNA was used to correct for non-specific binding of the APP-junction oligodeoxynucleotide antisense probe. However, when this probe was employed in series III (the OPTIMA series) hippocampus an intense signal was observed. The APP-junction sense probe when hybridised against series I and series II tissue resulted in a consistently weak signal, at the limits of detection of the system, that exhibited little variation in intensity.

Position of APP-Insert and APP-770 Oligodeoxynucleotide Probes in Relation to APP-770 mRNA

APP-770

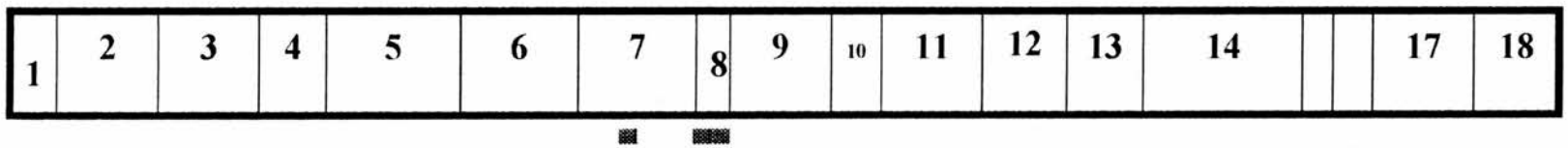

- **INSERT PROBE ANTISENSE 5'-G GGC ACA CTT CCC TTC AGT CAC ATC AAA GT-3'**
  Ponte *et al*, 1988

- **APP-770 PROBE ANTISENSE 5'-GTT TAA CAG GAT CTC GGG CAA GAG GTT CCT GGG TAG TCT TGA GTA AAC TTT GGG ACA-3'**
  Kitaguchi *et al*, 1988

Boxes represent exons (Yoshikai *et al*, 1990).

Figure 5.2

Position of APP-Junction Oligodeoxynucleotide Probe in Relation to APP-695 mRNA

APP-695

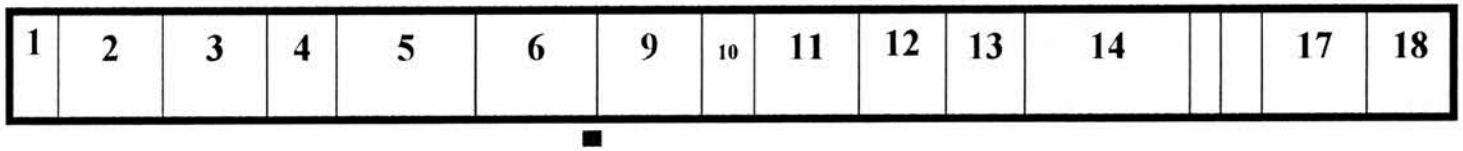

■ **JUNCTION PROBE ANTISENSE 5'-C TGC TGT TGT AGG AAC TCG AAC CAC CTC TT-3'**
Ponte *et al*, 1988

Boxes represent exons (Yoshikai *et al*, 1990).

Figure 5.3

Further, it was an order of magnitude lower in intensity than the antisense oligodeoxynucleotide probe. It was decided that the results of the APP-junction sense oligodeoxynucleotide probe should be omitted from the analysis of series III (the OPTIMA series) visual cortex. Since no sense oligodeoxynucleotide probe was available for either the APP-770 or the APP-insert oligodeoxynucleotide probes, none of the APP oligodeoxynucleotide probes employed in the study of the series III (the OPTIMA series) had a corresponding sense strand to allow for correction of the effects of non-specific binding.

5.2.3 Experimental Controls

The specificity of the APP-insert and APP-junction oligodeoxynucleotide probes has been demonstrated in our laboratory by Dr. P.J. Harrison by Northern blotting of RNA extracted from frontal cortex. The APP-insert probe detects a single band of 3.4 kb and the APP-junction probe detects a single band of 3.3 kb (Harrison *et al.*, 1994). The specificity of the APP-770 oligodeoxynucleotide probe has also been verified by Northern blotting in Professor Pearson's laboratory.

APLP2 mRNA has been demonstrated on Northern blotting to be approximately 4 kb in length, though weaker bands at approximately 3 kb and 2 kb, suggestive of cross-hybridisation with other members of the APP family, have also been described (Wasco *et al.*, 1993). Thus, it would appear that the oligodeoxynucleotide probes employed in this study do not detect APLP2. However, Northern blotting of L-APP mRNA transcripts reveals a major band of 3.4 kb (König *et al.*, 1992), suggesting

that L-APP mRNA transcripts lacking the 54 bases of exon 15 are indistinguishable on a Northern blot from APP mRNA transcripts. Thus, it is conceivable that the probes employed may not only detect the desired APP mRNA transcript, but also detect the corresponding L-APP mRNA.

5.2.4 *In Situ* Hybridisation Histochemistry

Hybridised sections were incubated for approximately 18 hours, at 36.6°C for the APP-770 oligodeoxynucleotide probe, 27°C for the APP-insert oligodeoxynucleotide probe and 27°C for the APP-junction oligodeoxynucleotide probe. The slides were then washed in 1 × SSC (4 × 15 minute washes) at 62.3°C for the APP-770 probe, 52.5°C for the APP-insert probe, and 52.5°C for the APP-junction probe. These washes were then followed by two hour long washes at room temperature, as detailed in chapter 2. Once dry, the hybridised sections were placed against film (Hyperfilm-βmax, Amersham) at room temperature for 28 days to generate autoradiograms (Figures 5.4 and 5.5). All slides were dipped in photographic emulsion (Ilford), as detailed in chapter 2, to allow cellular localisation of the ISHH signal.

5.2.5 Detection of Polyadenylated Messenger RNA in Series III (The OPTIMA Series)

Poly(A)$^+$ mRNA was measured in all of the series III (the OPTIMA series) brains for which tissue from visual cortex was available, thirty-four cases in all, in order to correct, at least partially, for differences in overall mRNA expression between the

Figure 5.4 *In situ* hybridisation histochemistry using [^{35}S]dATP labelled oligodeoxynucleotide probes performed on sections of visual cortex from the same non-AD dementia case from series III (the OPTIMA series). The images presented are direct photographs of transilluminated autoradiograms generated from this single case and hybridised with the following oligodeoxynucleotide probes. The blacker the image of the autoradiogram the greater was the exposure of the autoradiographic film to radioactivity and the more intensely labelled was the section.

A APP-junction oligodeoxynucleotide probe.

B APP-insert oligodeoxynucleotide probe.

C APP-770 oligodeoxynucleotide probe.

D Poly (dT) oligodeoxynucleotide probe.

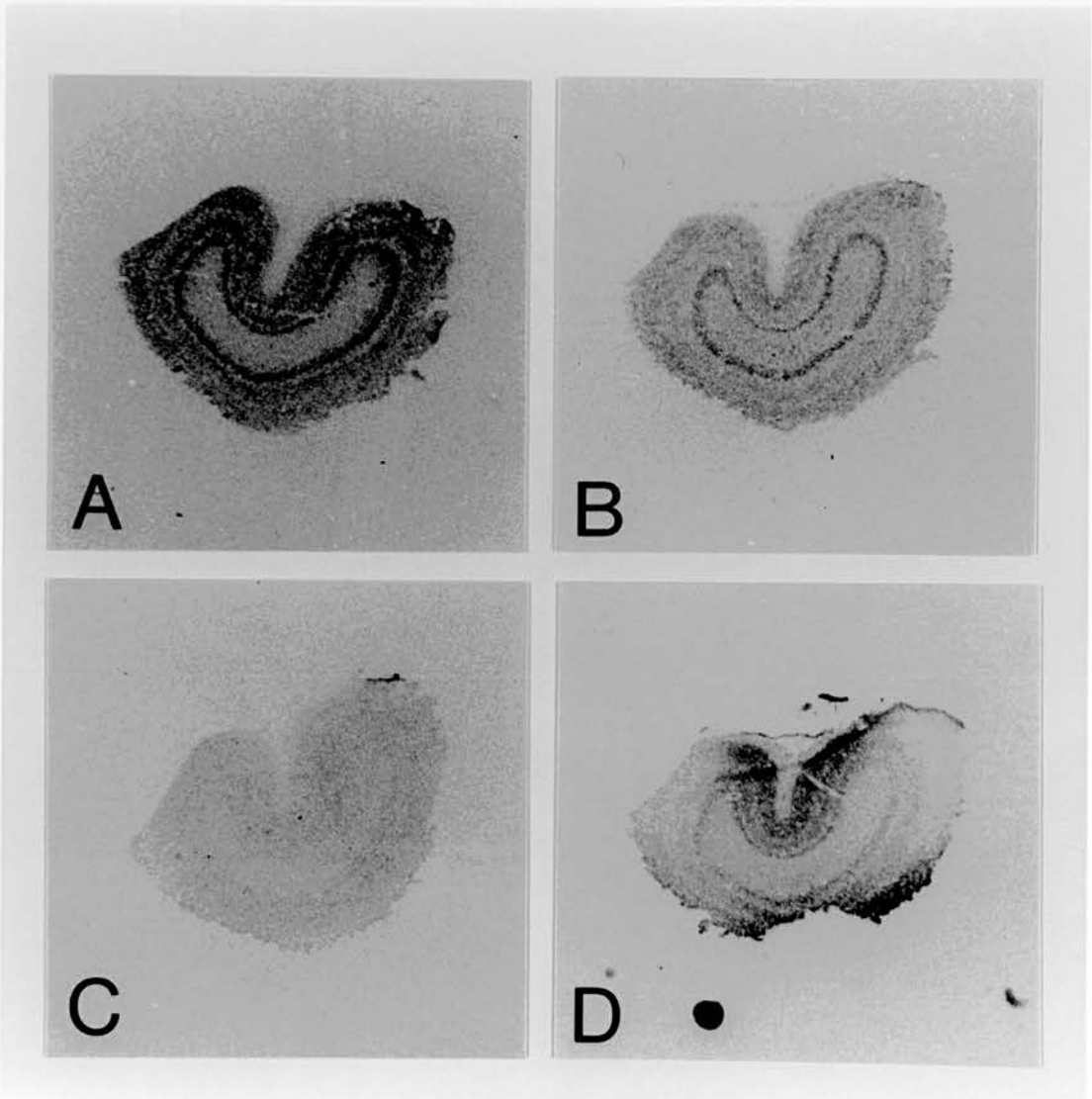
A
B
C
D

Figure 5.5 *In situ* hybridisation histochemistry using [^{35}S]dATP labelled oligodeoxynucleotide probes performed on hippocampal sections from the same non-AD dementia case from series III (the OPTIMA series). The images presented are direct photographs of transilluminated autoradiograms generated from this single case and hybridised with the following oligodeoxynucleotide probes. The blacker the image of the autoradiogram the greater was the exposure of the autoradiographic film to radioactivity and the more intensely labelled was the section.

A APP-junction oligodeoxynucleotide probe.

B APP-insert oligodeoxynucleotide probe.

C APP-770 oligodeoxynucleotide probe.

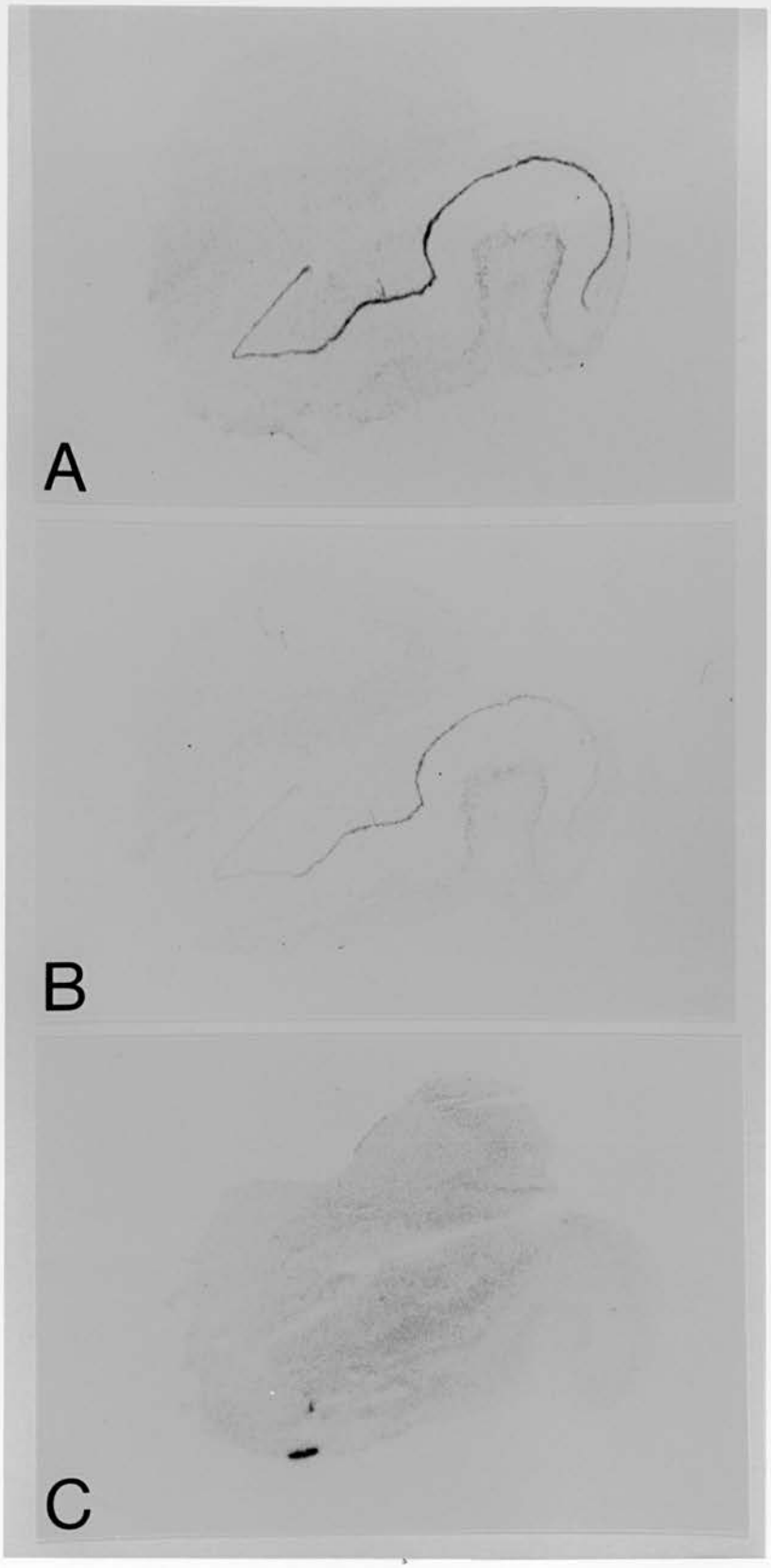
A
B
C

individual brains examined (Harrison *et al.*, 1991b, 1993). The oligodeoxynucleotide antisense probe for the detection of polyadenylated tails, the poly(dT) probe, consists of 30 thymidylate residues. A sense oligodeoxynucleotide probe, consisting of 30 adenylate residues, was synthesised to correct for non-specific binding. Ten pmoles of the poly(dT) probe was 3' labelled with 50 pmoles of [^{35}S]dTTP, since had [^{35}S]dATP been employed the radioactively labelled tail would have hybridised to the probe itself. The sense probe was 3' labelled with [^{35}S]dATP according to the standard protocol outlined in chapter 2.

Each brain was hybridised in triplicate with the poly(dT) probe. The hybridisation buffer was modified for the poly(dT) experiment as described by Harrison and colleagues (1991b). Specifically, in order to lower the required wash temperature, 20%, instead of 50%, of deionised formamide was added to the hybridisation buffer, and a 2 × SSC solution, rather than 20 × SSC solution, was employed. The sections were incubated at 25°C for 18 hours and washed, according to the standard protocol, at 35°C. Once dry, the sections were placed against film (Hyperfilm-βmax, Amersham) for 10 minutes to generate autoradiograms (Figure 5.4).

The specificity of the poly(dT) oligodeoxynucleotide probe was demonstrated by incubation of a subset of sections from visual cortex with an excess of unlabelled poly(dT) probe resulting in the abolition of signal. Similarly, pre-treatment of a subset of sections of visual cortex with ribonuclease abolished hybridisation of the

labelled oligodeoxynucleotide probe. The autoradiograms generated by the above cold displacement and ribonuclease pre-treatment were completely blank.

5.2.6 Quantification of ISHH Signal

The ISHH signal in hippocampus was assessed by outlining the stratum granulosum of the dentate gyrus and the stratum pyramidale of hippocampal fields CA1, CA3, and CA4. To analyse the ISHH signal in visual cortex, a strip of grey matter perpendicular to the cortical surface was outlined. For each section, the average intensity of light transmitted through the corresponding autoradiogram per unit area of the delineated portion of the film was obtained. The mean value of each set of three sections was then calculated and used in all subsequent calculations. The AOD, corrected where possible for non-specific binding, was calculated for each probe in the mid-hippocampus and visual cortex as described in chapter 2.

5.2.7 The Relationship between Radioactivity and Approximate Optical Density in Analysis of Series III (The OPTIMA Series)

In order to delineate the relationship between AOD and radioactivity in this system, ^{14}C microscales (Codes RPA 504 and RPA 511, Amersham) were opposed to autoradiographic film for 28 days alongside all of the oligodeoxynucleotide probes against series III (the OPTIMA series) tissue, except the poly(dT) probe against visual cortex and APP-junction probe against hippocampus. A linear relationship was demonstrated between the tissue equivalent radioactivity of the standards and AOD readings of 0.62 and below. All of the AOD readings pertaining to the

APP-770, APP-insert and APP-junction probes on series III (the OPTIMA series) tissue were within the linear range of the system. At more intense radioactive exposures the curve shouldered and then reached a plateau.

5.2.8 Statistical Analysis

All statistical analysis was performed using SPSS for Windows version 6.0. Where two groups were to be compared, a Student's *t* test was used, so long as Levene's test for homogeneity of variance was not significant ($p > 0.050$). Where Levene's test was significant, it was assumed that the requirements of the parametric test had been violated and the data was analysed using the non-parametric Mann-Whitney U.

Where the means of three or more groups were to be compared, a one way analysis of variance (ANOVA) was used. Where Levene's test for homogeneity of variance was significant, however, it was assumed that the requirements of the parametric test had not been met and the non-parametric Kruskal-Wallis one way ANOVA was used instead.

Correlation matrices, when used, were constructed using both Pearson's correlation coefficient and Spearman's rank correlation coefficient for comparison. When the results of the two tests concurred, the result was accepted. When a discrepancy was observed between the results of the two tests, the data was analysed further as detailed in the text.

5.3 Results

5.3.1 Introduction

The results in this chapter are presented in three sections corresponding to the three series of tissue employed in this part of the study. Series II comprised the visual cortices of thirty-two cases in which were examined mRNA transcripts detected by the APP-junction and APP-insert oligodeoxynucleotide probes and the ratio between KPI-encoding and KPI-lacking splice variants of APP mRNA (the insert:junction ratio). Series III (the OPTIMA series) consisted of tissue from the visual cortex and hippocampus of thirty-nine cases in which were examined mRNA transcripts detected by the poly(dT) (visual cortex only), APP-junction, APP-insert and APP-770 oligodeoxynucleotide probes and the insert:junction ratio. Series IV represented a combined data set generated specifically to allow exploration of the effect of diagnosis and the conduct of individual experiments on the insert:junction ratio.

The statistical analysis of the series III (the OPTIMA series) and series IV data was complex and performed following exhaustive consultation with biomedical statistician Miss J.M. Russell. The results of this labour are presented in detail and without apology, though many of the results generated were not significant.

The results are presented in the following order. Firstly, data relating to the APP-junction and APP-insert oligodeoxynucleotide probes and the insert:junction ratio in series II is presented, followed by the results of the correlation statistics performed on this series. Secondly, data relating to series III (the OPTIMA series) is

presented. Throughout this section, results pertaining to the visual cortex are presented first, followed by results for the dentate gyrus and hippocampal subfields CA4, CA3 and CA1, in that order. Results for poly(dT) (visual cortex only), APP-junction, APP-insert and APP-770 oligodeoxynucleotide probes are presented first, along with, where applicable, an analysis of APP-junction, APP-insert and APP-770 oligodeoxynucleotide probes when expressed as a proportion of the poly(dT) oligodeoxynucleotide probe. Data relating to the insert:junction ratio is presented along with the results of the individual oligodeoxynucleotide probes. The correlation statistics relating to series III (the OPTIMA series) are presented in the following order. Correlations between the ages and mini-mental state scores of the subjects, and neuropathology, are presented first, followed by correlations relating to the individual oligodeoxynucleotide probes and neuropathology. Next, correlations between the various oligodeoxynucleotide probes measured and tissue and demographic details are presented and finally the inter-relationships between the various oligodeoxynucleotide probes are described. Thirdly, and finally, the results of analysis of the insert:junction ratio in series IV visual cortex is presented, followed by analysis of the insert:junction ratio in the dentate gyrus and hippocampal subfields CA4, CA3 and CA1.

5.3.2 Summary of the Significant Positive, and Important Negative, Results of the Analysis of APP mRNA Expression in Tissue from Series II, III and IV

A summary of the positive findings and important negative findings is presented briefly here as a prelude to the more detailed presentation below. No effect of diagnosis on the abundance of APP-695 mRNA or that of KPI-containing transcripts of APP mRNA was apparent from analysis of series II. No effect of diagnosis on the abundance of APP-695 mRNA, KPI-containing transcripts of APP mRNA or APP-770 mRNA was apparent from analysis of series III (the OPTIMA series). The ratio between KPI-containing transcripts of APP mRNA and APP-695 mRNA, the insert:junction ratio, was also estimated for the visual cortices examined in series II, III and IV and no effect of diagnosis on this parameter was apparent.

The abundance of poly(A)$^+$ mRNA was examined in the visual cortices of series III (the OPTIMA series) and no significant difference in this parameter was identified between the four diagnostic categories examined. APP-junction, APP-insert and APP-770 mRNA levels in visual cortex were then expressed as a proportion of poly(A)$^+$ mRNA in this region and again no significant differences between the diagnostic groups was apparent.

A significant reduction in APP-695 mRNA in AD in comparison to control brains and unchanged levels of KPI-containing APP mRNA transcripts and APP-770 mRNA was identified in the dentate gyrus of series III brains (the OPTIMA series).

A significant reduction in APP-695 mRNA in the AD brains in comparison to the control or BAD brains was also found in the CA4 hippocampal subfield in series III (the OPTIMA series) in the presence of unchanged levels of the other APP transcripts measured. No effect of diagnosis on the insert:junction ratio was apparent from examination of the hippocampi in series III or IV.

Analysis of the correlation matrices prepared in the course of this study can be summarised as follows. No significant correlations were identified on analysis of series II. On analysis of series III (the OPTIMA series) a negative correlation was established between the mini-mental state score and the mean hippocampal and neocortical NFT density, the mean neocortical neuritic plaque density, the Braak score and the maximum CERAD plaque frequency. The mini-mental state score was also negatively correlated with the poly(dT) oligodeoxynucleotide probe in visual cortex. The poly(dT) probe was positively correlated with the Braak score, the mean hippocampal amyloid plaque frequency, the maximum CERAD plaque frequency, the mean neocortical neuritic plaque frequency and the mean neocortical NFT density. Both the APP-insert and APP-junction oligodeoxynucleotide probes when expressed as a proportion of the poly(dT) probe were positively correlated with the mini-mental state score. The APP-insert and APP-junction probes, when expressed as a proportion of the poly(dT) oligodeoxynucleotide probe were both negatively correlated with the mean hippocampal NFT density.

In series III (the OPTIMA series) visual cortex the APP-insert and APP-770 oligodeoxynucleotide probes were positively correlated, as were the APP-insert and APP-junction probes.

In the dentate gyrus and hippocampal subfield CA1 of series III (the OPTIMA series) the APP-insert and APP-junction oligodeoxynucleotide probes were correlated, as were the APP-insert and APP-770 oligodeoxynucleotide probes. In hippocampal subfields CA3 and CA4, however, no associations were found between the APP oligodeoxynucleotide probes.

In the visual cortex, but not in any of the other regions studied, both the APP-insert and the APP-junction oligodeoxynucleotide probes were positively correlated with tissue pH. In series II and series III (the OPTIMA series) no correlation was found between the age of the subjects and the insert:junction ratio.

Although no effect of diagnosis on the insert:junction ratio was apparent from examination of the tissue in series IV, the age of the subjects and the prosecution of the individual experiments, in visual cortex alone, did significantly affect the insert:junction ratio.

5.3.3 Series II

Since this series comprised the visual cortices from thirty-two cases, including twelve normal control subjects, seventeen subjects with definite AD, two subjects

with borderline AD and one subject with a mixed AD and multi-infarct dementia, the comparison of four diagnostic categories was possible. However, this analysis would have resulted in a significant loss of power, since there were only two borderline AD subjects and one subject with a neurological disease in addition to AD. Therefore, the borderline AD cases and the mixed AD and multi-infarct dementia case, were excluded from the analysis and a Students *t* test was used to compare the control subjects with the AD subjects. Details of all of the series II cases are presented in appendix II and are summarised in tables 5.1 and 5.2.

The cases used in this study have been examined previously and the results have been published (Wighton-Benn *et al.*, 1995). However, since publication of this work, it has become clear that one of the control cases included in the original study was unsuitable by virtue of co-existing neurological disease. This case has therefore been excluded from the analysis.

The APP-junction and APP-insert antisense oligodeoxynucleotide probes were used to examine this series. The APP-770 oligodeoxynucleotide antisense probe was not available at the time this series was examined. The mean AOD of the APP-junction sense oligodeoxynucleotide probe proved to be 0.01 for both the AD and control cases examined. In view of the reassuringly uniform and universally low signal attributable to this probe, this value was not subtracted from the AOD of the APP-junction antisense oligodeoxynucleotide probe for either the AD or control

Demographic and Agonal State Score Details of Series II Cases

Diagnosis	Number of cases	Sex	Age in Years (mean ± SD)	Agonal State Score (mean ± SD)
Normal Controls	12	Male = 7 Female = 5	77.2 ± 11.2 (n = 12)	2.0 ± 1.2 (n = 7)
Alzheimer's disease	17	Male = 9 Female = 8	83.8 ± 7.1 (n = 17)	2.5 ± 1.2 (n = 12)
Borderline Alzheimer's disease	2	Female = 2	85 and 91 years (n = 2)	No data available
Alzheimer's disease and Multi-infarct dementia	1	Male = 1	83 years (n = 1)	4 (n = 1)

Table 5.1

Details of Post-Mortem Delay and Storage of Series II Brain Tissue

Diagnosis	Post-Mortem Delay in Hours (mean ± SD)	Storage in Days of Tissue as a Block (mean ± SD)	Storage in Days of Cryostat Cut Tissue (mean ± SD)	Total Storage Time of Tissue in Days (mean ± SD)
Normal Controls	33.1 ± 13.6 (n = 9)	253.8 ± 172.8 (n = 12)	741.6 ± 326.8 (n = 12)	978.8 ± 258.6 (n = 12)
Alzheimer's disease	34.4 ± 17.2 (n = 16)	402.9 ± 249.6 (n = 17)	664.8 ± 298.6 (n = 17)	1067.6 ± 317.6 (n = 17)
Borderline Alzheimer's Disease	42 (n = 1)	455 and 287 days (n = 2)	484 and 359 days (n = 2)	939 and 646 days (n = 2)
Alzheimer's disease and Multi-infarct dementia	16 (n = 1)	80 days (n = 1)	132 days (n = 1)	1408 days (n = 1)

Table 5.2

cases. Autoradiograms generated from the analysis of series II visual cortex are not presented.

No significant difference in age was identified between the two diagnostic groups using the non-parametric two-tailed Mann-Whitney U test corrected for ties. Using a students *t* test, no significant differences were found between the two groups in terms of agonal state score, PMI, storage of the tissue as a block, storage of the tissue as cryostat cut sections or total tissue storage time. No significant differences were observed between the two groups in the AOD of either the APP-junction or APP-insert probes using a Student's *t* test (Figure 5.6). The ratio of the AOD of the APP-junction probe to the AOD of the APP-insert probe, the insert:junction ratio, was not significantly different between the two groups using a students *t* test (Figure 5.7).

All thirty-two cases were included in a correlation matrix comprising twenty-one cells, of which two cells yielded statistically significant Pearson's correlation coefficients ($p < 0.050$) (Table 5.3). A Pearson's correlation coefficient of $p = 0.050$ was obtained in a third cell. An identical Spearman's correlation matrix was performed for comparison.

A significant, positive correlation was identified between the AOD of the APP-insert probe and the insert:junction ratio using both parametric ($p < 0.001$) and non-parametric ($p < 0.001$) tests. A weaker, negative, Pearson's correlation

Figure 5.6 APP mRNA Expression in the Visual Cortex of Series II Alzheimer's Diseased Versus Control Brains

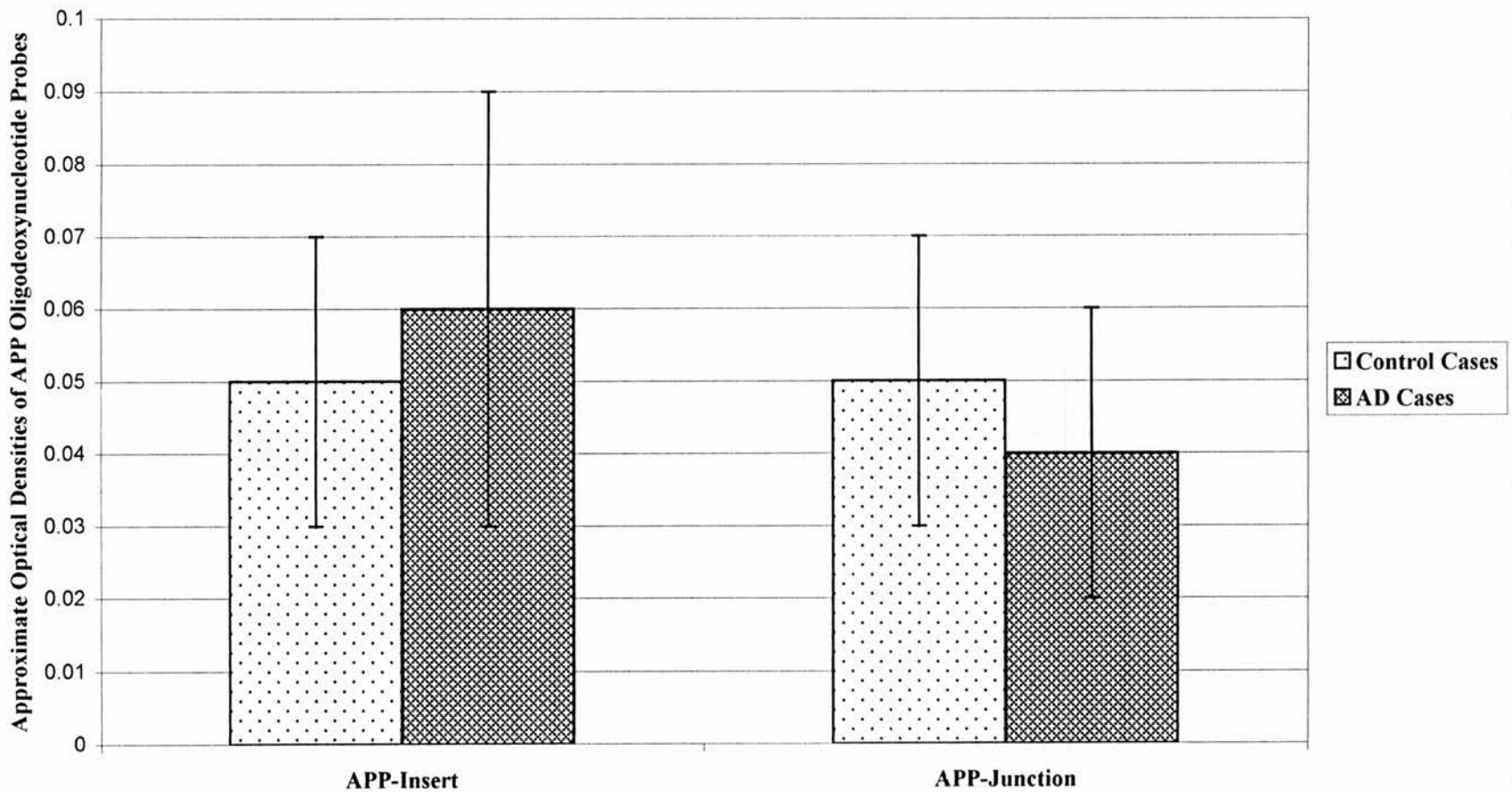

Figure 5.7 APP-Insert to APP-Junction Ratio in Series II Visual Cortex in Alzheimer's Diseased Versus Control Brains

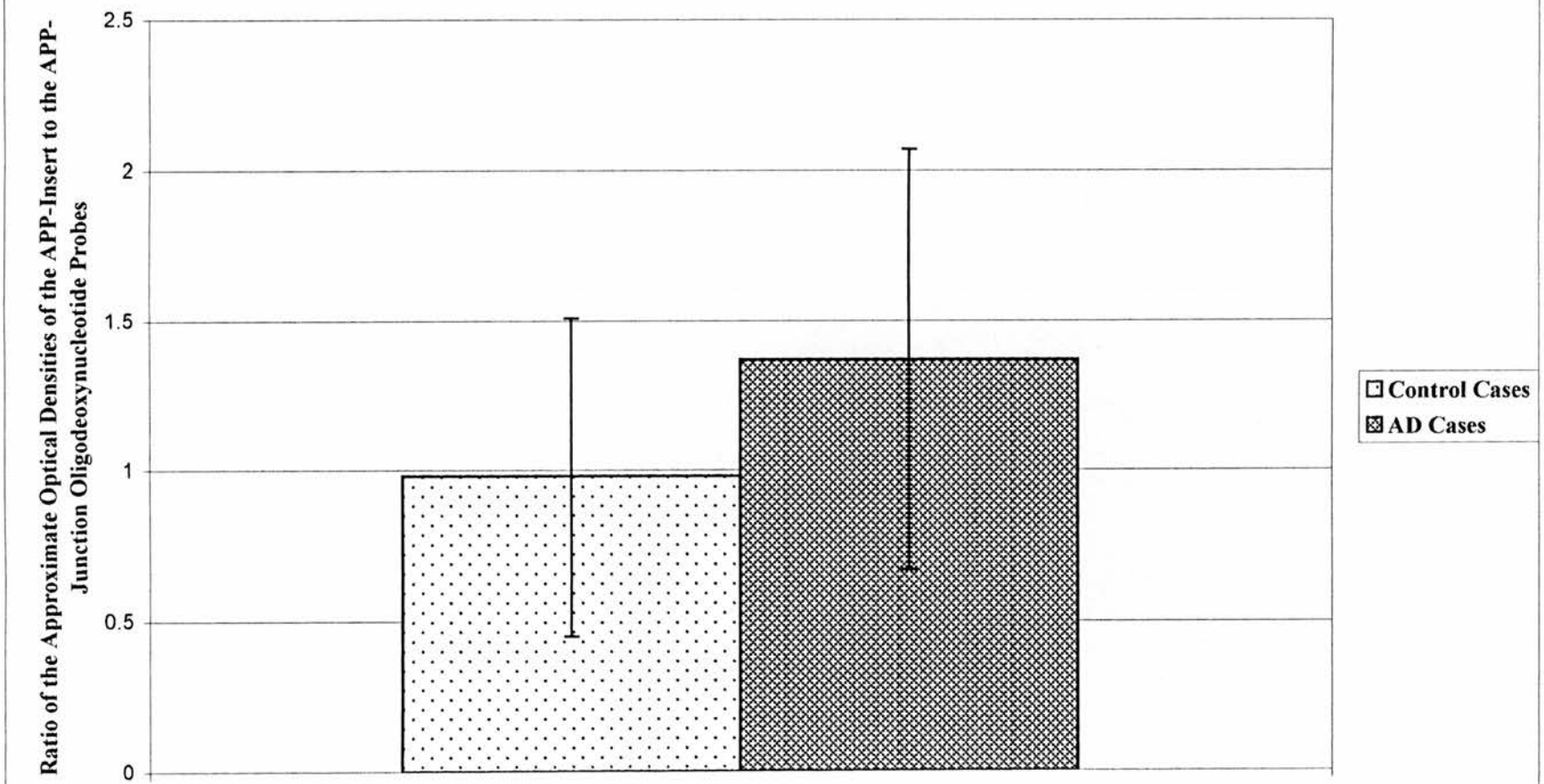

Table 5.3 Pearson's Correlation Coefficients for APP Data on Series II (Visual Cortex)

	Age	Diagnosis	Agonal State Score	Post Mortem Delay	Block Storage Time	Section Storage Time	Insert: Junction Ratio	APP-Junction Probe
APP-Insert Probe	0.165 (n = 32) p = 0.367	0.154 (n = 32) p = 0.401	0.064 (n = 20) p = 0.787	0.368 (n = 27) p = 0.059	-0.215 (n = 32) p = 0.236	0.180 (n = 32) p = 0.323	0.676 (n = 30) **p = 0.000**	0.304 (n = 30) p = 0.102
APP-Junction Probe	-0.111 (n = 30) p = 0.558	-0.190 (n = 30) p = 0.315	-0.155 (n = 18) p = 0.540	0.319 (n = 25) p = 0.120	-0.155 (n = 30) p = 0.413	0.102 (n = 30) p = 0.590	-0.403 (n = 30) **p = 0.027**	
Insert: Junction Ratio	0.361 (n = 30) **p = 0.050**	0.293 (n = 30) p = 0.116	0.200 (n = 18) p = 0.427	0.134 (n = 25) p = 0.524	-0.082 (n = 30) p = 0.668	-0.024 (n = 30) p = 0.901		

coefficient was obtained between the AOD of the APP-junction probe and the insert:junction ratio ($p = 0.027$), though non-parametric analysis was not significant ($p = 0.073$). Scatter diagrams of the AOD of the APP-junction probe and the AOD of the APP-insert probe plotted against the insert:junction ratio confirmed that this ratio is more heavily influenced by the AOD of the APP-insert probe than that of the APP-junction probe (Figures 5.8 and 5.9).

Finally, the insert:junction ratio was correlated with the age of the subjects in the visual cortex of series II using Pearson's correlation coefficient ($p = 0.050$), but not using Spearman's rank correlation ($p = 0.133$). A scatter diagram confirmed the positive correlation between these two parameters implying that the non-parametric test merely lacked the statistical power to demonstrate this correlation (Figure 5.10).

However, since in a matrix of twenty-four cells a minimum of four significant findings would be expected if the variables were meaningfully related, two significant cells are no more than would be predicted to occur by chance.

Figure 5.8 Approximate Optical Density of the APP-Junction Oligodeoxynucleotide Probe Plotted Against the APP-Insert to APP-Junction Ratio in Series II Visual Cortex

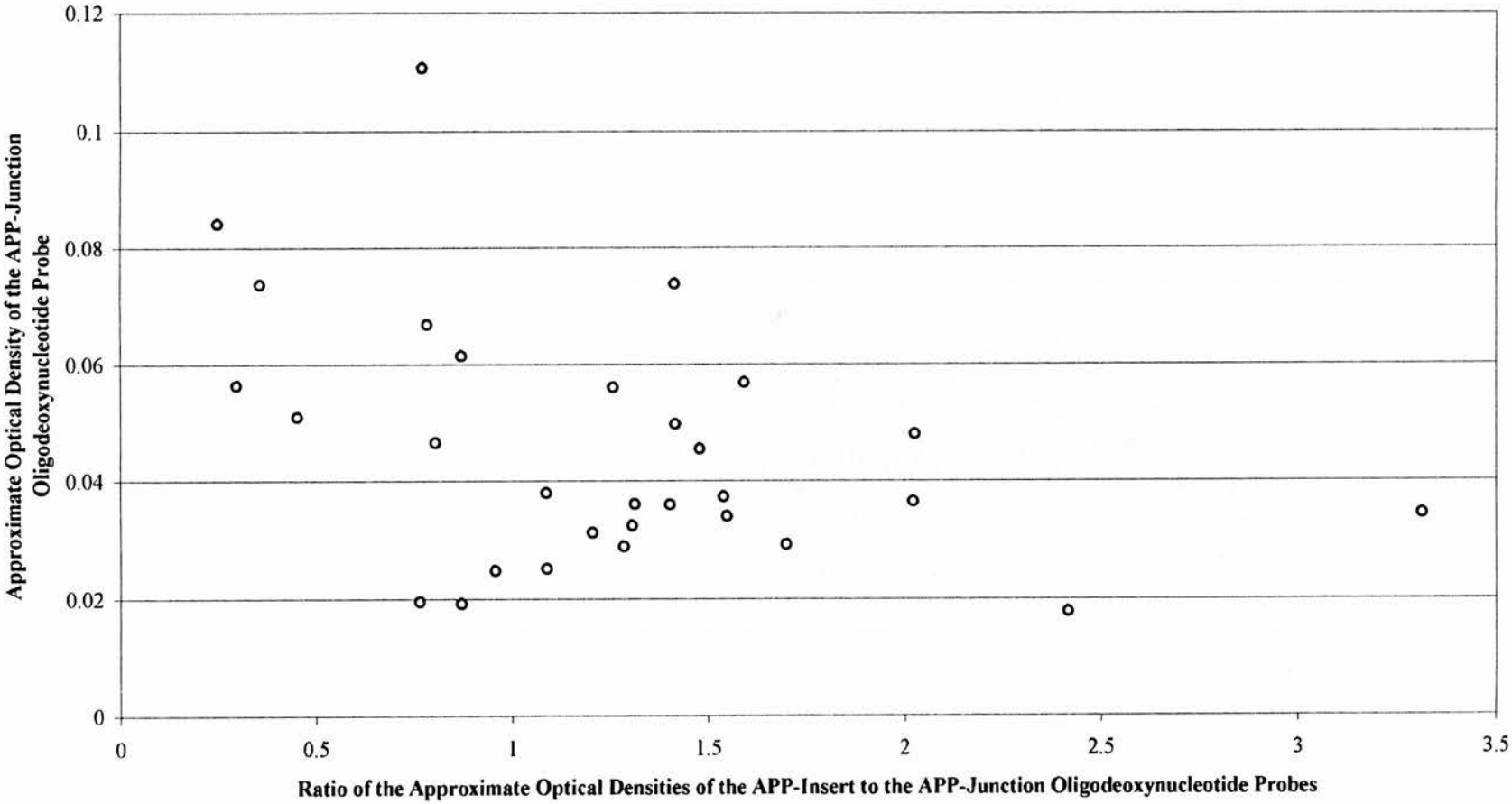

Figure 5.9 Approximate Optical Density of the APP-Insert Oligodeoxynucleotide Probe Plotted Against the APP-Insert to APP-Junction Ratio in Series II Visual Cortex

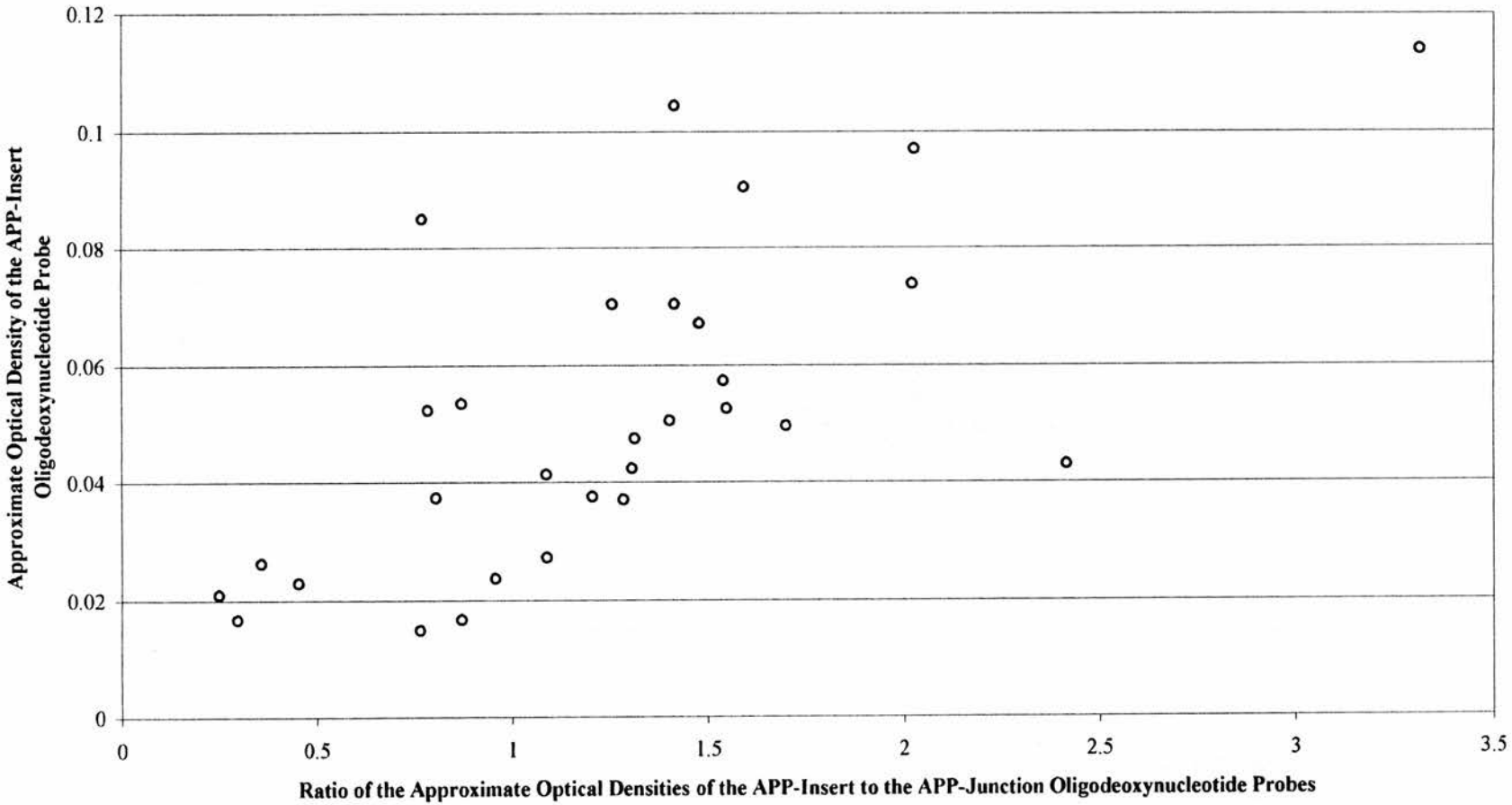

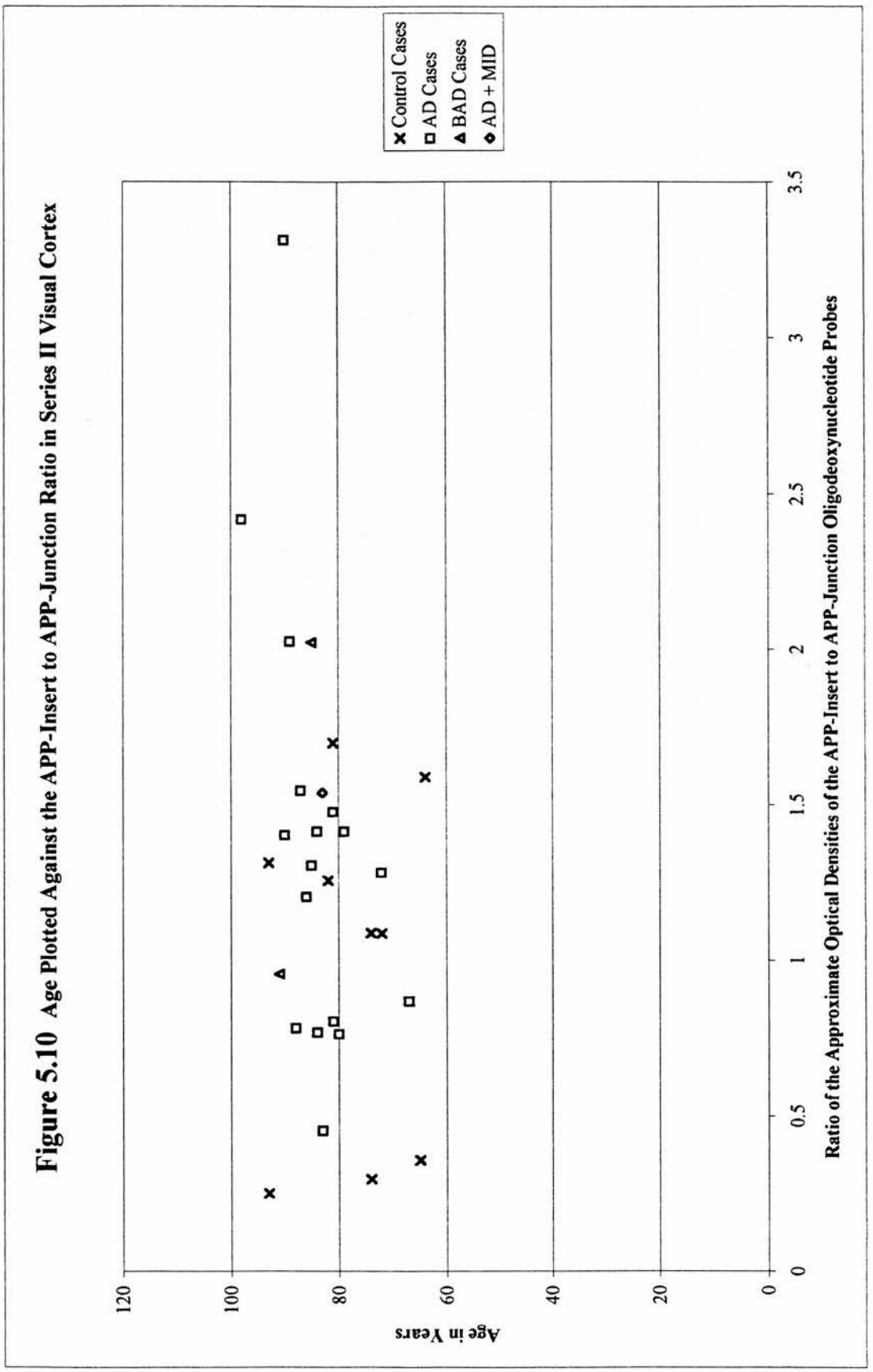

Figure 5.10 Age Plotted Against the APP-Insert to APP-Junction Ratio in Series II Visual Cortex

5.3.4 Series III - The OPTIMA Series

5.3.4.1 Introduction

Series III (the OPTIMA series) comprised tissue representative of five diagnostic categories: normal controls, definite AD, borderline AD, non-AD neurodegenerative dementias and non-neurodegenerative dementias. Details of all of the series III cases are presented in the appendix II. The demographic, clinical and storage details of this tissue is presented in table 5.4. The data set comprised thirty-nine cases in all, twenty-one female and eighteen male subjects. Female subjects were over-represented in the non-AD neurodegenerative disease group (five female subjects and one male) and under-represented in the control group (three female subjects and five male). Otherwise the sex ratio of the diagnostic groups was acceptable. The neuropathological details available for series III cases are presented in table 5.5.

The borderline AD grouping represents the smallest number of cases: three male and two female subjects. The possibility of combing this group with the AD group was rejected, however, following examination of a series of boxplots depicting the neuropathological measures made on these cases (Figures 5.11 to 5.15). Boxplots of the mean neocortical and mean hippocampal neuritic plaque density, the mean neocortical and mean hippocampal neurofibrillary tangle density and the maximum CERAD plaque frequency suggested that the fourteen definite AD and five borderline AD cases were from different populations. A decision was therefore made to retain the distinction between the AD and borderline AD cases.

Demographic, Clinical and Storage Details of Series III (OPTIMA) Tissue

Diagnosis	Number of Cases	Sex	Age in years (mean ± SD)	Post-Mortem Delay in hours (mean ± SD)	Mini-Mental State Score (mean ± SD)	Storage Time in years (mean ± SD)
Normal Controls	8	Male=5 Female=3	76.9 ± 7.5 (n=8)	38.9 ± 18.4 (n=8)	27.4 ± 2.8 (n=7)	3.1 ± 1.1 (n=8)
Alzheimer's disease	14	Male=6 Female=8	77.7 ± 8.0 (n=14)	35.4 ± 8.3 (n=13)	5.1 ± 7.4 (n=10)	4.6 ± 1.7 (n=14)
Borderline Alzheimer's disease	5	Male=3 Female=2	80.2 ± 9.8 (n=5)	30.6 ± 16.0 (n=5)	19.4 ± 5.7 (n=5)	3.4 ± 1.3 (n=5)
Non-Alzheimer's Neurodegenerative disease	6	Male=1 Female=5	82.3 ± 6.5 (n=6)	26.5 ± 17.2 (n=6)	8.5 ± 3.4 (n=4)	4.2 ± 1.9 (n=6)
Non-Neurodegenerative disease	6	Male=3 Female=3	80.3 ± 37.9 (n=6)	34.8 ± 20.6 (n=6)	7.3 ± 6.4 (n=6)	4.3 ± 1.6 (n=6)

Table 5.4

Neuropathological Details of Series III (OPTIMA) Tissue

Diagnosis	pH of Tissue (Mean ± SEM)	CERAD maximum plaque frequency (Mean ± SD)	Braak Score Mean ± SD	Amyloid Plaques in HC Mean ± SD	Neuritic Plaques in HC Mean ± SD	NFTs in HC Mean ± SD	NFTs in Cortex Mean ± SD	Neuritic Plaques in Cortex Mean ± SD
Normal Controls	6.6 ± 0.4 (n=6)	0.4 ± 1.1 (n=7)	1.0 ± 0.9 (n=5)	(n=2) Both=0	(n=2) Both=0	(n=2) Both=0	0.6 ± 0.8 (n=5)	0.7 ± 1.5 (n=5)
Alzheimer's disease	6.6 ± 0.3 (n=11)	4.8 ± 0.6 (n=13)	5.4 ± 0.6 (n=11)	2.6 ± 2.2 (n=9)	0.7 ± 0.9 (n=9)	5.6 ± 3.7 (n=9)	19.1 ± 14.2 (n=12)	14.3 ± 7.1 (n=12)
Borderline Alzheimer's disease	6.6 ± 0.4 (n=5)	2.0 ± 1.4 (n=5)	2.1 ± 1.2 (n=4)	(n=2) Both=0	(n=2) Both=0	(n=2) Both=0	0.2 ± 0.2 (n=4)	2.8 ± 1.8 (n=4)
Non-Alzheimer's Neurodegenerative disease	6.9 ± 0.2 (n=5)	0.5 ± 0.6 (n=4)	2.1 ± 1.4 (n=4)	(n=2) Both=0	(n=2) Both=0	(n=2) (0, 6.2)	0.2 ± 0.2 (n=4)	1.0 ± 1.1 (n=4)
Non-Neurodegenerative disease	6.7 ± 0.4 (n=6)	0.5 ± 1.2 (n=6)	2.3 ± 0.4 (n=5)	(n=3) All=0	(n=3) All=0	(n=3) All=0	0.8 ± 0.8 (n=5)	2.3 ± 4.9 (n=5)

Table 5.5

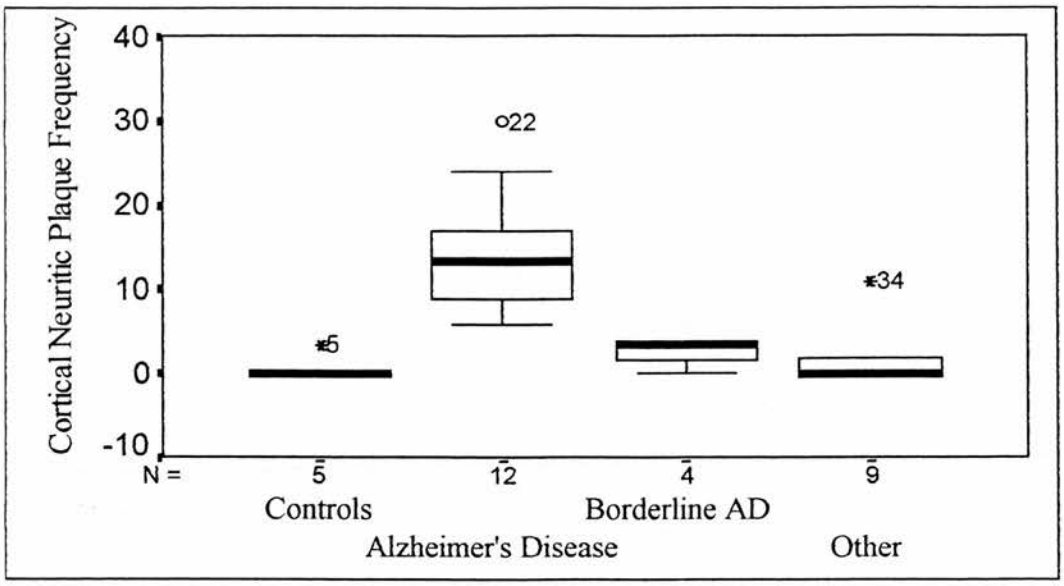

Figure 5.11 Boxplot Depicting the Mean Neocortical Neuritic Plaque Frequency for the Four Diagnostic Groups Examined in Series III (OPTIMA)

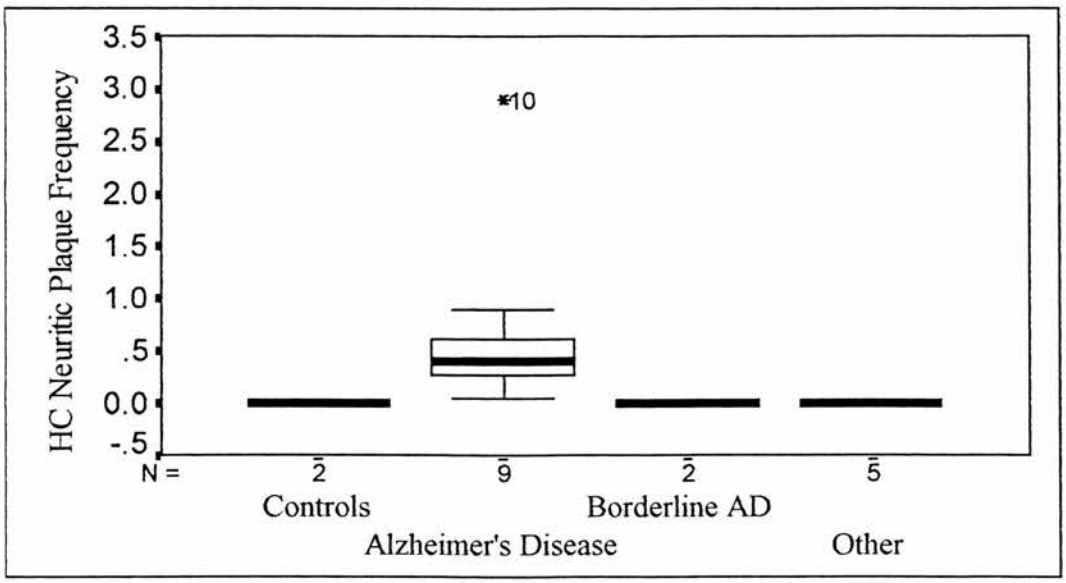

Figure 5.12 Boxplot Depicting the Mean Hippocampal Neuritic Plaque Frequency for the Four Diagnostic Groups Examined in Series III (OPTIMA)

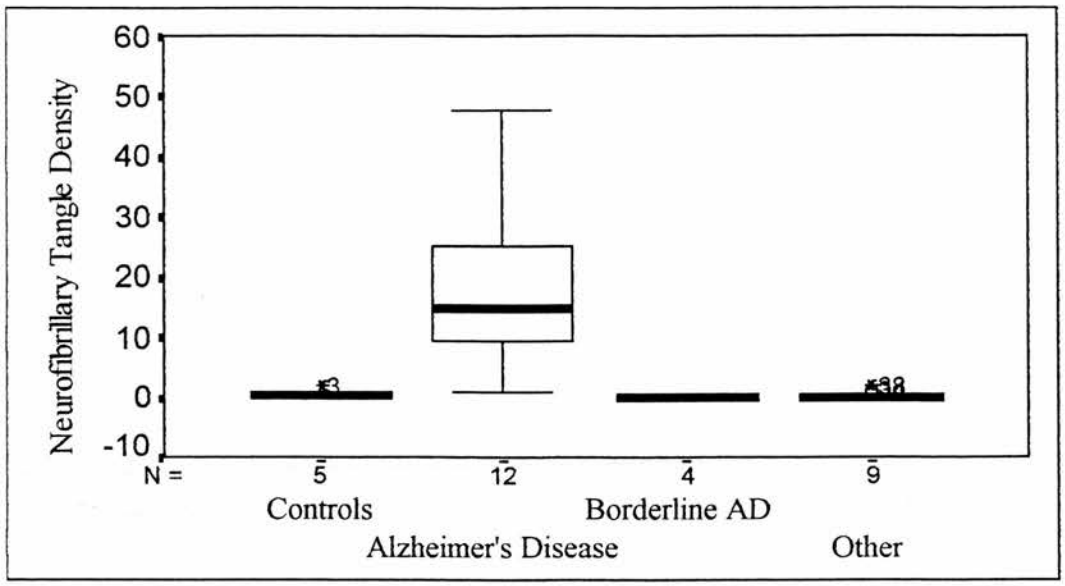

Figure 5.13 Boxplot Depicting the Mean Neocortical Neurofibrillary Tangle Density for the Four Diagnostic Groups Examined in Series III (OPTIMA)

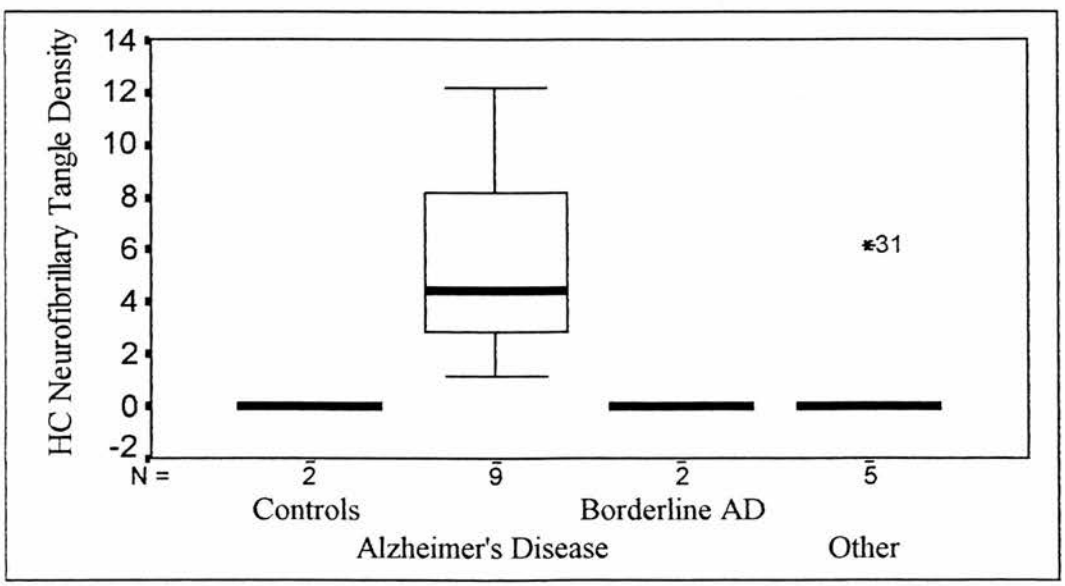

Figure 5.14 Boxplot Depicting the Mean Hippocampal Neurofibrillary Tangle Density for the Four Diagnostic Groups Examined in Series III (OPTIMA)

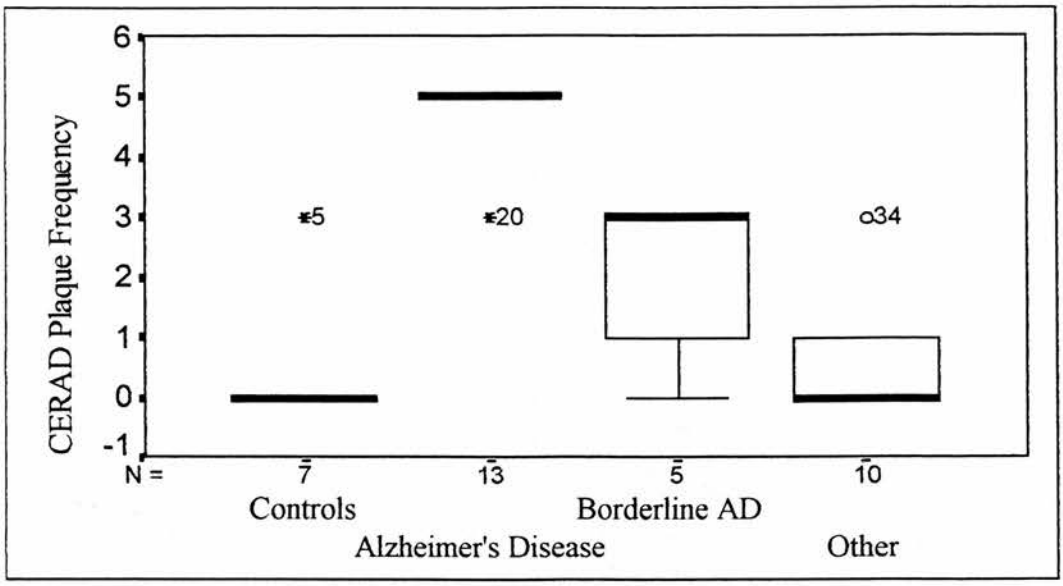

Figure 5.15 Boxplot Depicting the Maximum CERAD Plaque Frequency (0-5) for the Four Diagnostic Groups Examined in Series III (OPTIMA)

The six non-AD neurodegenerative dementia cases comprised brains from individuals who had suffered from Parkinson's disease, Pick's disease, Huntington's chorea and progressive supranuclear palsy. The six non-neurodegenerative dementia cases comprised brains from individuals who had suffered from multi-infarct dementia and glioma. These latter two diagnostic categories were small, and since data on any specific probe was not always available for all of the cases in the series, the number of cases from these groups, for any one probe, was sometimes reduced further. Moreover, both groups were heterogeneous and included in order to provide information from a positive control group about the non-specific effects of a dementing illness. It was decided that combining these two groups would serve this aim equally well and, importantly, would improve the power of the analysis. The loss of data would be minimal, since the groups did not represent pure diagnostic categories and, further, on examination of the available demographic and neuropathological data for the two groups, no significant differences were identified. The non-AD neurodegenerative and non-neurodegenerative dementia groups were, therefore, amalgamated into a non-AD dementia group for all subsequent analysis of the data.

No statistically significant differences were found between the four diagnostic categories in terms of age, PMI, freezer storage of the tissue in years or brain pH, using a one way ANOVA ($p > 0.050$).

5.3.4.2 Analysis of Polyadenylated Messenger RNA in Series III (The OPTIMA Series) Visual Cortex

The AOD of the poly(dT) oligodeoxynucleotide probe was measured in the visual cortex of series III (the OPTIMA series) tissue. No significant differences in the AOD of this probe were identified between the four diagnostic groups using a one way ANOVA.

5.3.4.3 Analysis of the APP-Junction, APP-Insert and APP-770 Oligodeoxynucleotide Probes in Series III (The OPTIMA Series) Visual Cortex

The AOD of the probes were calculated and used in all subsequent analysis. No significant differences were observed between the four diagnostic groups in the AOD of the APP-junction probe in visual cortex using a one way analysis of variance (ANOVA) (Figure 5.16). However, Levene's test for homogeneity of variance was significant ($p = 0.026$) implying that the requirements of the one way ANOVA had not been met. Consequently, a Kruskal-Wallis one way ANOVA was performed which did not reveal any significant differences in the AOD of the APP-junction oligodeoxynucleotide probe between the four diagnostic groups.

No significant differences were found between the four diagnostic categories in the AOD of the APP-insert or APP-770 oligodeoxynucleotide probes in visual cortex using a one way ANOVA (Figure 5.16).

Figure 5.16 APP mRNA Expression in Series III (OPTIMA) Visual Cortex in Diseased Versus Control Brains

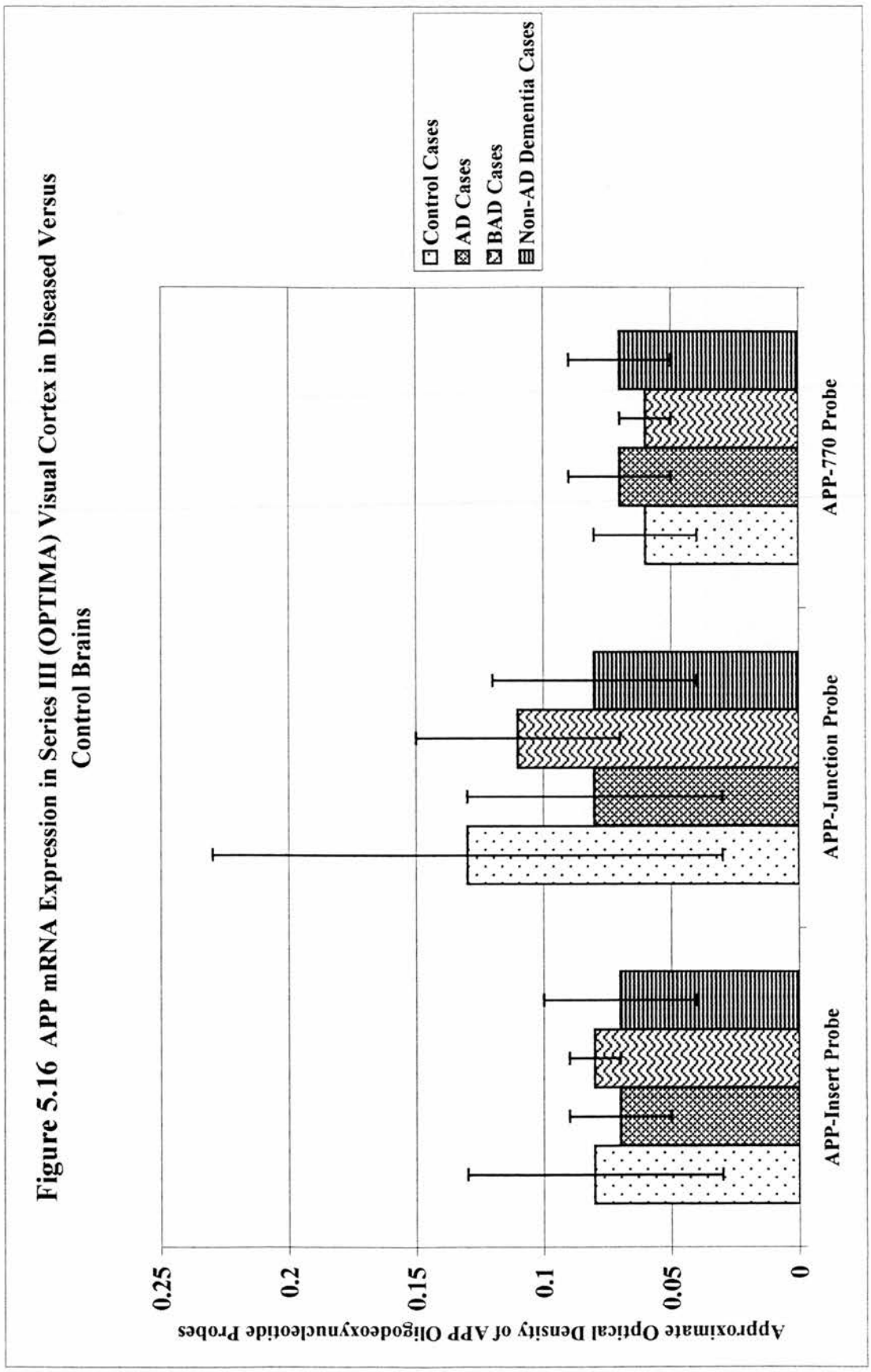

For each case, the AOD of the APP-junction, APP-insert and APP-770 probes, in visual cortex, was expressed as a proportion of the AOD of the poly(dT) probe in this region (Figure 5.17). Using a one way ANOVA, no significant differences were observed, between the four diagnostic categories, when the APP-770 oligodeoxynucleotide probe or the APP-junction oligodeoxynucleotide were expressed in this way. However, Levene's test for homogeneity of variance revealed that the requirements of the one way ANOVA were not met for the AOD of the APP-insert oligodeoxynucleotide probe when expressed as a proportion of the AOD of the poly(dT) probe and a Kruskal-Wallis one way ANOVA was performed, confirming that there were no statistically significant differences in the APP-insert to poly(dT) ratio between the four diagnostic groups.

No significant differences were found, using a one way ANOVA, between the four diagnostic groups, in the insert:junction ratio, in the visual cortex, of series III (the OPTIMA series) brains (Figure 5.18).

Figure 5.17 APP mRNA Expression as a Proportion of Poly(A)$^+$ mRNA Expression in Series III (OPTIMA) Visual Cortex in Diseased Versus Control Brains

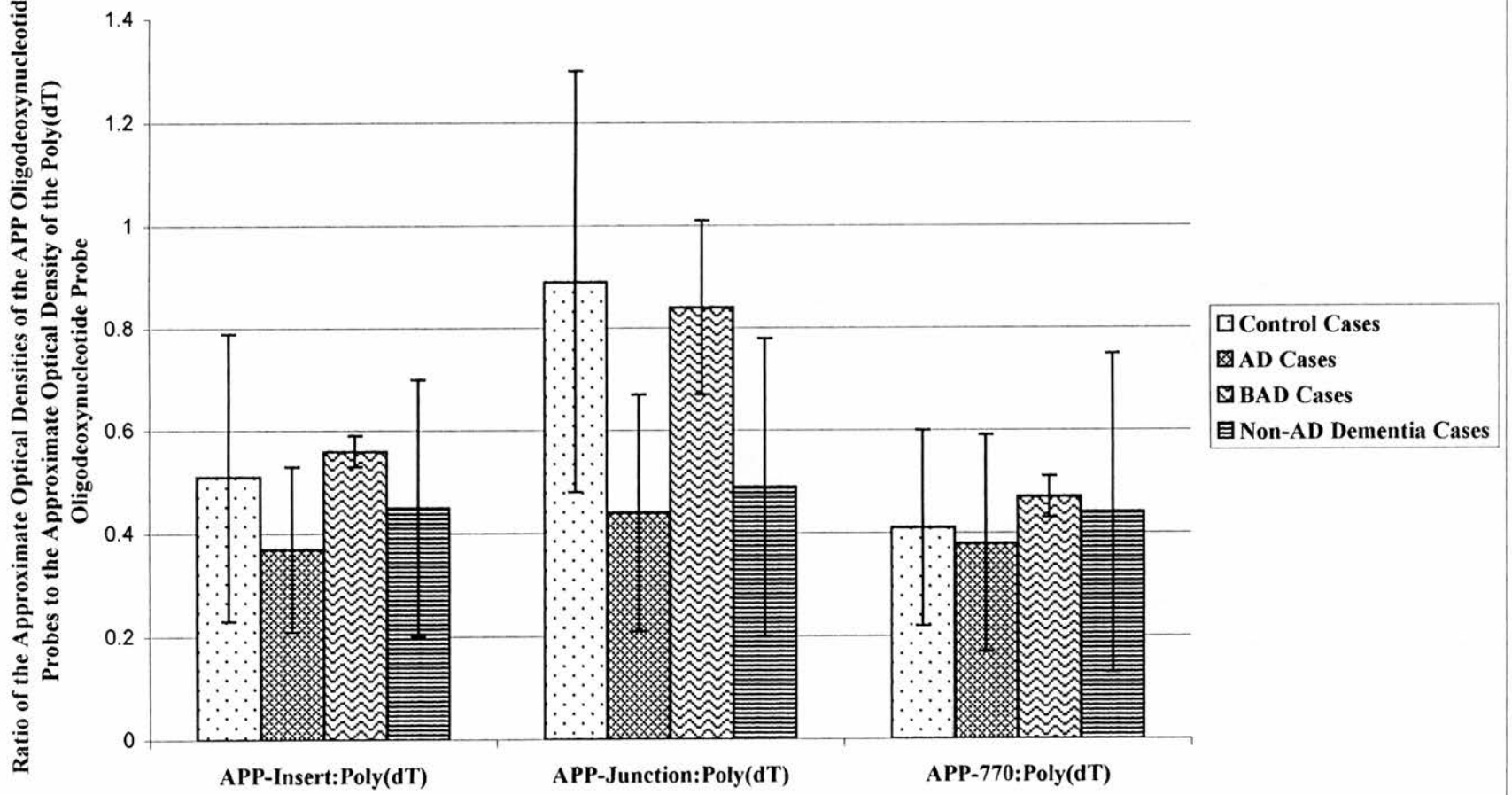

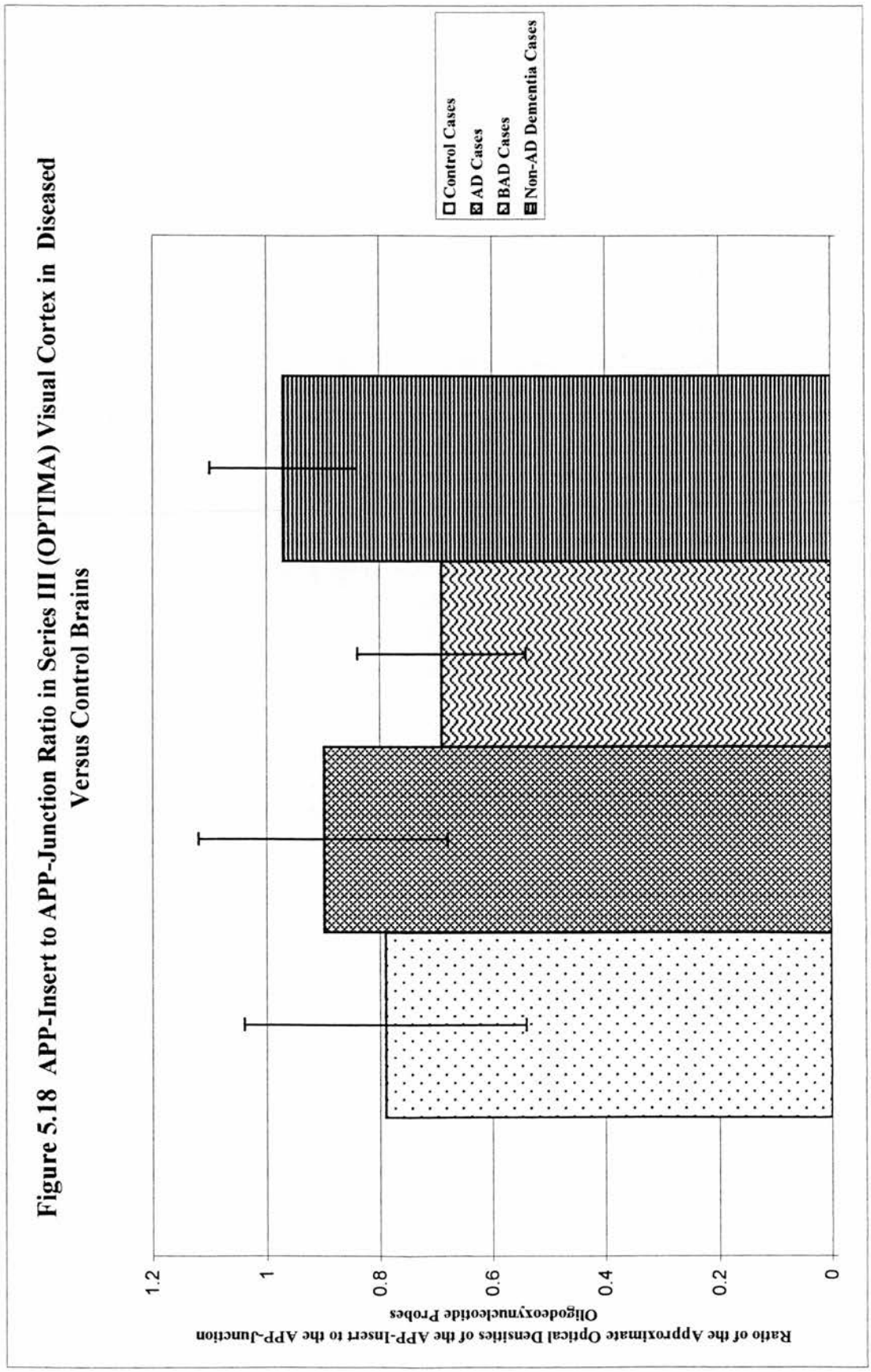

Figure 5.18 APP-Insert to APP-Junction Ratio in Series III (OPTIMA) Visual Cortex in Diseased Versus Control Brains

5.3.4.4 Analysis of the APP-Junction, APP-Insert and APP-770 Oligodeoxynucleotide Probes in Series III (The OPTIMA Series) Hippocampus

5.3.4.4.1 The APP-770 Oligodeoxynucleotide Probe in Series III (The OPTIMA Series) Hippocampus

The boundaries of the dentate gyrus and the hippocampal CA subfields could not be identified using the APP-770 oligodeoxynucleotide probe and a global measure of the AOD of this probe, in the hippocampus overall, was made. No significant differences between the four diagnostic groups in the AOD of the APP-770 oligodeoxynucleotide probe in the hippocampus were observed using a Kruskal-Wallis one way ANOVA (Figure 5.19).

5.3.4.4.2 The APP-Junction Oligodeoxynucleotide Probe in Series III (The OPTIMA Series) Hippocampus

The APP-junction oligodeoxynucleotide probe was measured over the dentate gyrus and CA4, CA3 and CA1 subfields of the hippocampus. The AOD of this probe varied significantly between the four diagnostic groups in the dentate gyrus ($p = 0.034$) and CA4 ($p = 0.016$), but not in CA3 or CA1, using a one way ANOVA (Figure 5.20). Tukey's Honestly Significant Difference test (significance level $p = 0.050$) was used to determine where the differences, identified between the diagnostic groups in dentate gyrus and CA4, lay. In the dentate gyrus the AOD of the APP-junction oligodeoxynucleotide probe was significantly higher in the control

Figure 5.19 APP-770 mRNA Expression in Series III (OPTIMA) Hippocampus in Diseased Versus Control Brains

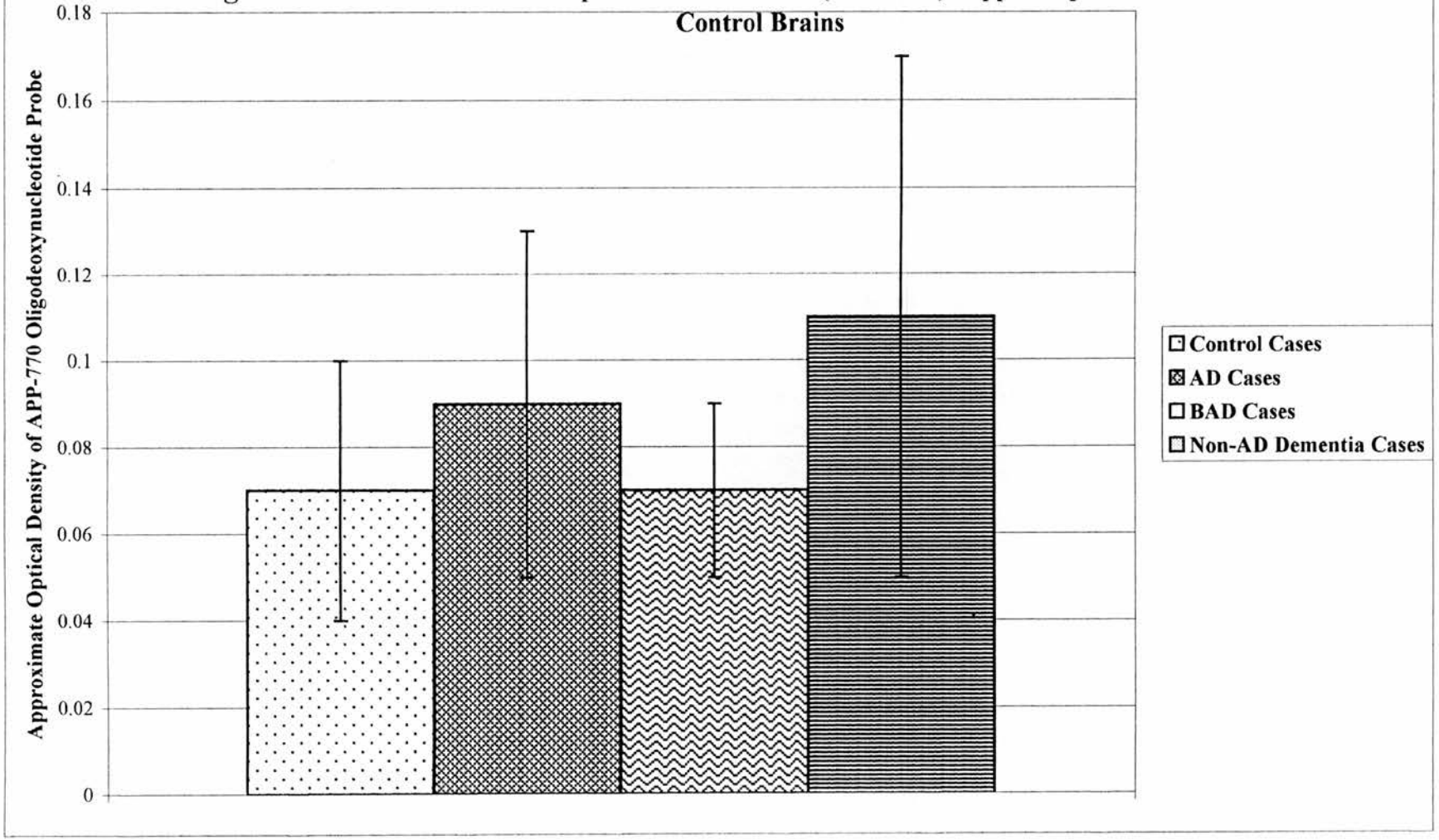

Figure 5.20 APP-Junction mRNA Expression in Series III (OPTIMA) Hippocampus in Diseased Versus Control Brains

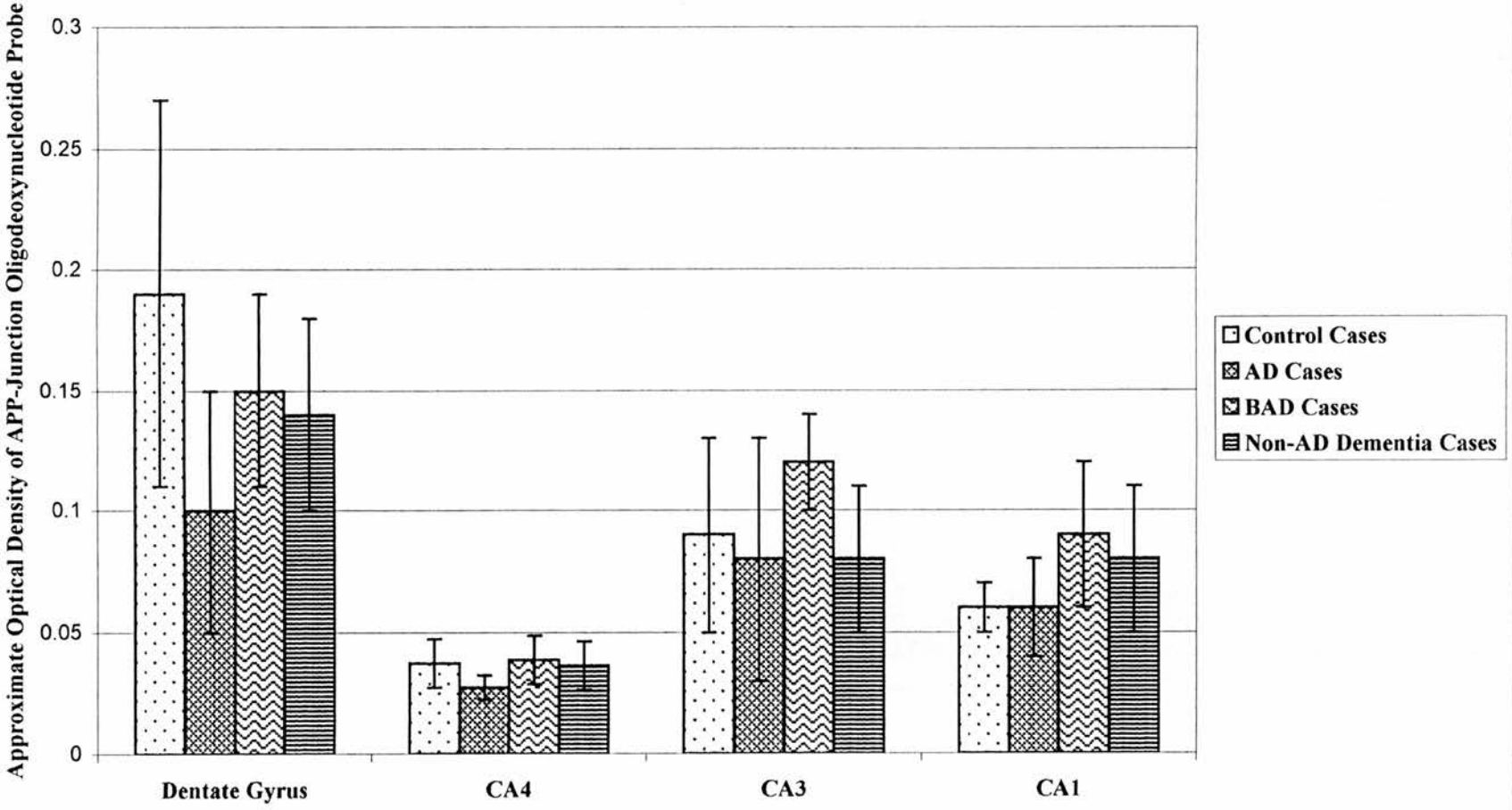

subjects in comparison to the AD subjects, while in CA4, the AOD of the APP-junction oligodeoxynucleotide probe was significantly higher in the control and borderline subjects, than in the AD subjects.

5.3.4.4.3 The APP-Insert Oligodeoxynucleotide Probe in Series III (The OPTIMA Series) Hippocampus

No significant differences between the four diagnostic groups in the CA4, CA3 or CA1 hippocampal fields was detected for the APP-insert oligodeoxynucleotide probe using a one way ANOVA (Figure 5.21). The non-parametric Kruskal-Wallis one way ANOVA was required to establish that there were no significant differences between the four diagnostic groups in the AOD of the APP-insert oligodeoxynucleotide probe in the dentate gyrus.

5.3.4.4.4 The Insert to Junction Ratio in Series III (The OPTIMA Series) Hippocampus

Finally, the insert:junction ratio was calculated, as above, for the dentate gyrus and hippocampal fields CA4, CA3 and CA1 of series III (the OPTIMA series) tissue. No significant differences were identified between the diagnostic groups in the insert:junction ratio in any of the regions analysed using one way ANOVA (Figure 5.22).

Figure 5.21 **APP-Insert mRNA Expression in Series III (OPTIMA) Hippocampus in Diseased Versus Control Brains**

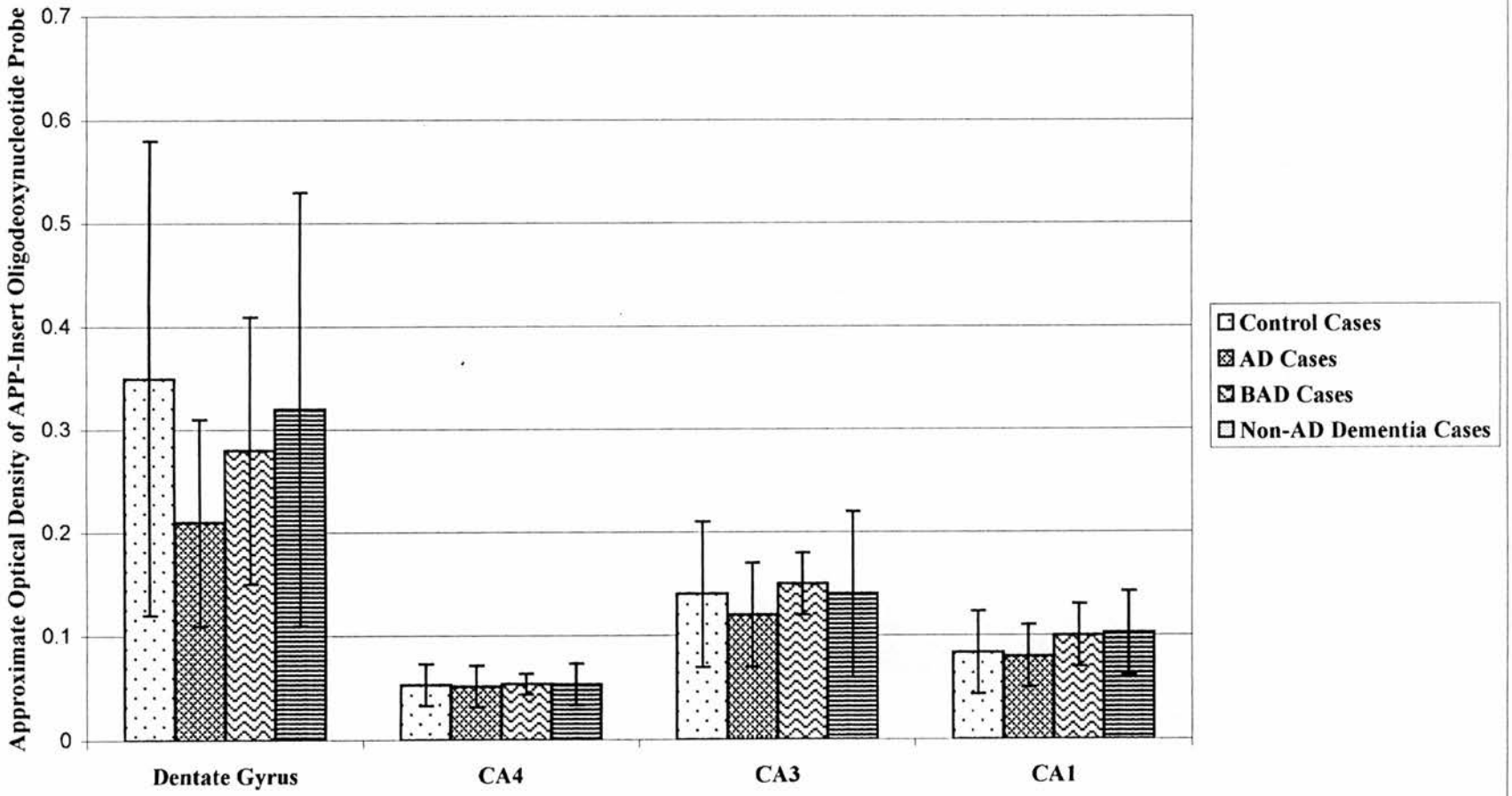

Figure 5.22 APP-Insert to APP-Junction Ratio in Series III (OPTIMA) Hippocampus in Diseased Versus Control Brains

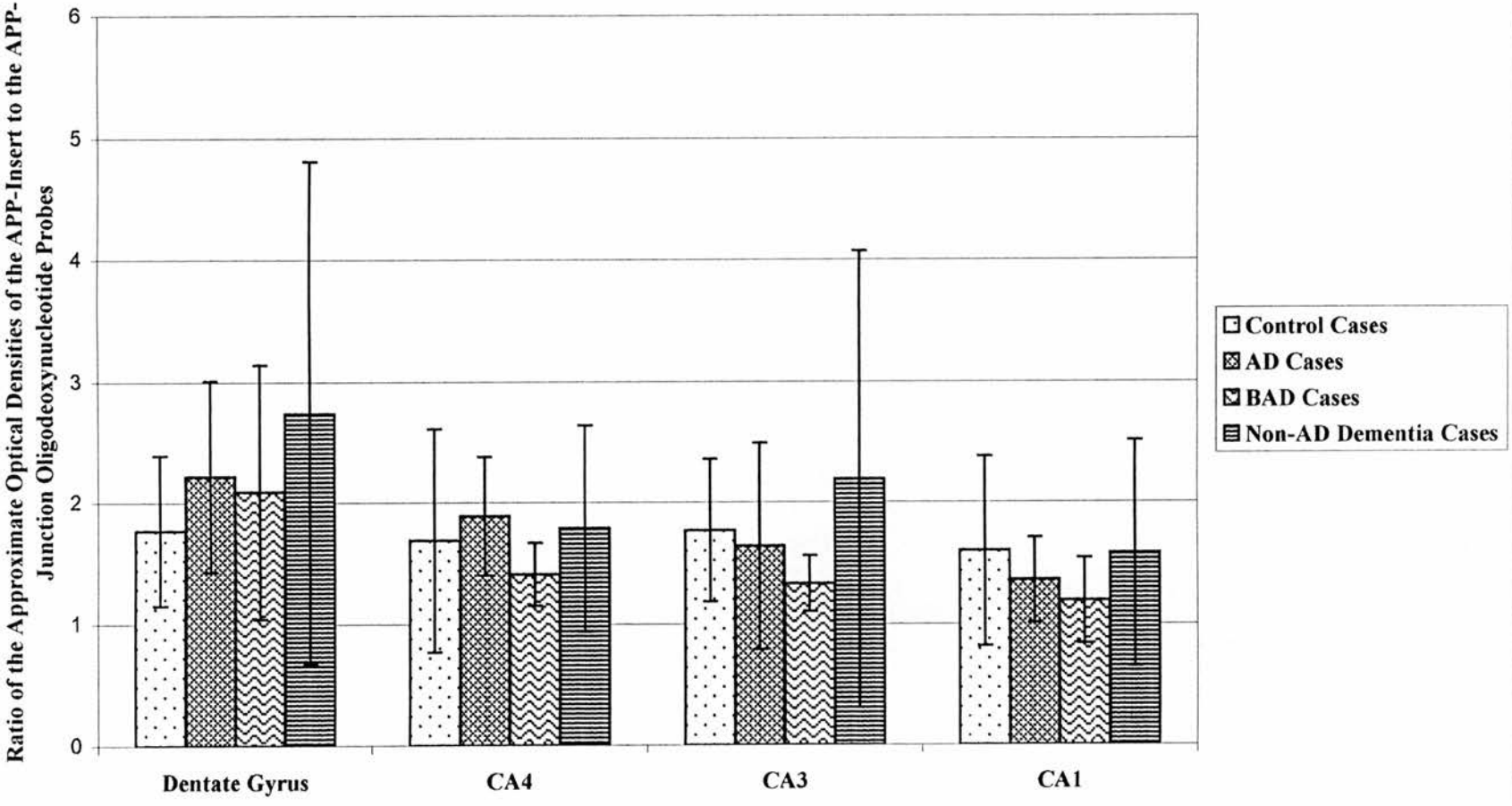

5.3.4.5 Significant Correlations Identified on Analysis of Series III (The OPTIMA Series) Data

5.3.4.5.1 Introduction

A series of correlation matrices were constructed to examine the series III (the OPTIMA series) data. In each case, a Pearson's correlation matrix and a Spearman's rank correlation matrix were prepared, and the two compared. Where p values are presented in the text they relate to the Pearson's correlation matrix, unless otherwise stated.

5.3.4.5.2 Correlations Identified Between the Age and Mini-Mental State Scores of the Subjects and Neuropathology

A Pearson's correlation matrix, consisting of 14 cells, was constructed to examine the relationship(s), if any, between the age and mini-mental state scores of the subjects and the 7 neuropathological parameters examined for each case (Table 5.6). Six significant correlations, ($p < 0.050$), were identified. Since the probability of generating three, or more, significant findings in a matrix of 15 cells by chance is $p = 0.036$, the association between the above variables is likely to be a real one. All but one of the significant correlations identified in the Pearson's correlation matrix, were confirmed on non-parametric analysis of the data.

Five of the six significant correlations identified on parametric analysis (four of which had p values less than 0.010) related to correlations between the score on mini-mental state examination and neuropathological findings. The mean

Table 5.6 Pearson's Correlation Coefficients for Series III (OPTIMA) Data							
	Maximum CERAD Plaque Frequency	**Braak Score**	**Mean HC Amyloid Plaque Frequency**	**Mean HC Neuritic Plaque Frequency**	**Mean HC NFT Density**	**Mean Neocortical NFT Density**	**Mean Neocortical Neuritic Plaque Density**
Age	-0.007 (n = 35) p = 0.967	-0.054 (n = 29) p = 0.783	0.004 (n = 18) p = 0.987	0.118 (n = 18) p = 0.641	0.038 (n = 18) p = 0.882	-0.366 (n = 30) **p = 0.047**	0.014 (n = 30) p = 0.942
Mini-Mental State Score	-0.516 (n = 32) **p = 0.003**	-0.590 (n = 26) **p = 0.002**	-0.400 (n = 15) p = 0.139	-0.354 (n = 15) p = 0.195	-0.572 (n = 15) **p = 0.026**	-0.596 (n = 27) **p = 0.001**	-0.523 (n = 27) **p = 0.005**

neocortical neuritic plaque density, the mean neocortical neurofibrillary tangle density, the maximum CERAD plaque frequency and the Braak score, were all negatively correlated with the score on mini-mental state examination with a p value of less than 0.010. The mean hippocampal neurofibrillary tangle density was correlated with the score on mini-mental state examination with a p value of 0.026. The mean hippocampal neuritic and amyloid plaque frequencies, however, were not correlated with the mini-mental state scores.

The final significant correlation was between age and mean neocortical neurofibrillary tangle density (-0.366; $p = 0.047$). Unlike all of the other significant findings in the Pearson's correlation matrix, this correlation could not be replicated on non-parametric analysis of the data and, moreover, suggested that as the included subjects increased in age their mean neocortical neurofibrillary tangle density fell. A scatter plot (Figure 5.23) revealed two outlying values as likely to be responsible for the parametric correlation between these two variables and, thus, this significant finding was disregarded.

No significant correlations were identified between the ages and mini-mental state scores of the subjects or between the pH, PMI and duration of storage of the tissue using either parametric or non-parametric tests. (Correlation matrices not presented.)

5.3.4.5.3 Correlations Between the APP-Insert, APP-Junction, APP-770 and Poly(dT) Oligodeoxynucleotide Probes in the Visual Cortex and Neuropathology

Data on correlations between the APP and poly(dT) probes in visual cortex and neuropathology, were sought using a Pearson's correlation matrix comprising 56 cells, of which three were significant (Table 5.7; pages 247 and 248). The Spearman's correlation matrix is presented for comparison, since three entirely different cells proved significant on non-parametric analysis (Table 5.8; pages 249 and 250).

On parametric analysis, the first significant finding related to the AOD of the APP-junction probe in visual cortex, which was correlated with the mean hippocampal neuritic plaque frequency, with a value of 0.551 and a probability of $p = 0.027$. This correlation was not confirmed using Spearman's rank correlation, and it became apparent on examination of a scatter diagram that it was likely that a single massively outlying value was responsible for the significant correlation identified using the parametric test (Figure 5.24). This correlation was, therefore, regarded as spurious.

The second significant correlation on parametric analysis related to the insert:poly(dT) ratio in visual cortex, which was negatively correlated (-0.544) with the mean hippocampal neurofibrillary tangle density with a p value of 0.036. Spearman's rank correlation revealed a correlation coefficient of –0.504 and a p

Table 5.7 Pearson's Correlation Coefficients for Series III (OPTIMA) Visual Cortex Data							
	Maximum CERAD Plaque Frequency	**Braak Score**	**Mean HC Amyloid Plaque Frequency**	**Mean HC Neuritic Plaque Frequency**	**Mean HC NFT Density**	**Mean Neocortical NFT Density**	**Mean Neocortical Neuritic Plaque Density**
APP-Insert Probe	-0.063 (n = 31) p = 0.736	-0.084 (n = 27) p = 0.676	0.228 (n = 16) p = 0.397	0.397 (n = 16) p = 0.128	-0.214 (n = 16) p = 0.426	-0.079 (n = 27) p = 0.695	-0.049 (n = 27) p = 0.810
APP-Junction Probe	0.003 (n = 31) p = 0.986	-0.076 (n = 27) p = 0.705	0.337 (n = 16) p = 0.202	0.551 (n = 16) **p = 0.027**	-0.198 (n = 16) p = 0.463	-0.037 (n = 27) p = 0.855	-0.040 (n = 27) p = 0.842
APP-770 Probe	0.087 (n = 29) p = 0.653	0.019 (n = 26) p = 0.928	-0.017 (n = 15) p = 0.459	-0.017 (n = 15) p = 0.953	-0.320 (n = 15) p = 0.245	0.026 (n = 26) p = 0.900	0.049 (n = 26) p = 0.811
Insert: Junction Ratio	-0.026 (n = 31) p = 0.891	0.110 (n = 27) p = 0.585	-0.111 (n = 16) p = 0.681	-0.326 (n = 16) p = 0.217	0.119 (n = 16) p = 0.662	-0.064 (n = 27) p = 0.750	0.169 (n = 27) p = 0.399
Poly(dT) Probe	0.270 (n = 29) p = 0.157	0.076 (n =26) p = 0.712	0.325 (n = 15) p = 0.237	0.350 (n = 15) p = 0.200	0.373 (n = 15) p = 0.171	0.291 (n = 26) p = 0.149	0.284 (n = 26) p = 0.160

Table 5.7 Pearson's Correlation Coefficients for Series III (OPTIMA) Visual Cortex Data							
	Maximum CERAD Plaque Frequency	**Braak Score**	**Mean HC Amyloid Plaque Frequency**	**Mean HC Neuritic Plaque Frequency**	**Mean HC NFT Density**	**Mean Neocortical NFT Density**	**Mean Neocortical Neuritic Plaque Density**
APP-Insert Probe: Poly(dT) Probe	-0.366 (n = 29) p = 0.051	-0.262 (n = 26) p = 0.197	-0.311 (n = 15) p = 0.260	-0.153 (n = 15) p = 0.586	-0.544 (n = 15) **p = 0.036**	-0.370 (n = 26) p = 0.063	-0.356 (n = 26) p = 0.075
APP-Junction Probe: Poly(dT) Probe	-0.193 (n = 29) p = 0.315	-0.266 (n = 26) p = 0.189	-0.232 (n = 15) p = 0.406	0.009 (n = 15) p = 0.976	-0.520 (n = 15) **p = 0.047**	-0.321 (n = 26) p = 0.110	-0.299 (n = 26) p = 0.138
APP-770 Probe: Poly(dT) Probe	-0.214 (n = 28) p = 0.273	-0.141 (n = 25) p = 0.502	-0.405 (n = 14) p = 0.151	-0.295 (n = 14) p = 0.306	-0.429 (n = 14) p = 0.126	-0.274 (n = 25) p = 0.186	-0.271 (n = 25) p = 0.190

Table 5.8 Spearman's Correlation Coefficients for Series III (OPTIMA) Visual Cortex Data							
	Maximum CERAD Plaque Frequency	**Braak Score**	**Mean HC Amyloid Plaque Frequency**	**Mean HC Neuritic Plaque Frequency**	**Mean HC NFT Density**	**Mean Neocortical NFT Density**	**Mean Neocortical Neuritic Plaque Density**
APP-Insert Probe	0.010 (n = 31) p = 0.956	-0.079 (n = 27) p = 0.697	-0.085 (n = 16) p = 0.755	-0.099 (n = 16) p = 0.715	-0.190 (n = 16) p = 0.480	0.084 (n = 27) p = 0.678	0.040 (n = 27) p = 0.842
APP-Junction Probe	-0.010 (n = 31) p = 0.959	-0.132 (n = 27) p = 0.513	-0.142 (n = 16) p = 0.601	-0.116 (n = 16) p = 0.668*	-0.178 (n = 16) p = 0.509	0.086 (n = 27) p = 0.670	-0.065 (n = 27) p = 0.746
APP-770 Probe	0.115 (n = 29) p = 0.551	-0.018 (n = 26) p = 0.930	-0.316 (n = 15) p = 0.251	-0.389 (n = 15) p = 0.151	-0.324 (n = 15) p = 0.239	0.186 (n = 26) p = 0.362	0.139 (n = 26) p = 0.499
Insert: Junction Ratio	0.021 (n = 31) p = 0.913	0.129 (n = 27) p = 0.521	0.118 (n = 16) p = 0.664	0.072 (n = 16) p = 0.790	0.086 (n = 16) p = 0.752	-0.018 (n = 27) p = 0.929	0.092 (n = 27) p = 0.648
Poly(dT) Probe	0.398 (n = 29) **p = 0.033**	0.236 (n =26) p = 0.246	0.285 (n = 15) p = 0.304	0.211 (n = 15) p = 0.450	0.429 (n = 15) p = 0.110	0.424 (n = 26) **p = 0.031**	0.476 (n = 26) **p = 0.014**

Table 5.8 Spearman's Correlation Coefficients for Series III (OPTIMA) Visual Cortex Data							
	Maximum CERAD Plaque Frequency	**Braak Score**	**Mean HC Amyloid Plaque Frequency**	**Mean HC Neuritic Plaque Frequency**	**Mean HC NFT Density**	**Mean Neocortical NFT Density**	**Mean Neocortical Neuritic Plaque Density**
APP-Insert Probe: Poly(dT) Probe	-0.322 (n = 29) p = 0.088	-0.153 (n = 26) p = 0.456	-0.196 (n = 15) p = 0.485	-0.114 (n = 15) p = 0.685	-0.504 (n = 15) p = 0.055*	-0.204 (n = 26) p = 0.318	-0.331 (n = 26) p = 0.098
APP-Junction Probe: Poly(dT) Probe	-0.307 (n = 29) p = 0.106	-0.309 (n = 26) p = 0.125	-0.341 (n = 15) p = 0.214	-0.263 (n = 15) p = 0.343	-0.497 (n = 15) p = 0.059*	-0.224 (n = 26) p = 0.272	-0.312 (n = 26) p = 0.120
APP-770 Probe: Poly(dT) Probe	-0.181 (n = 28) p = 0.358	-0.048 (n = 25) p = 0.818	-0.294 (n = 14) p = 0.307	-0.256 (n = 14) p = 0.378	-0.448 (n = 14) p = 0.108	-0.125 (n = 25) p = 0.552	-0.234 (n = 25) p = 0.261

* Denotes cells where Pearson's correlation coefficient is significant

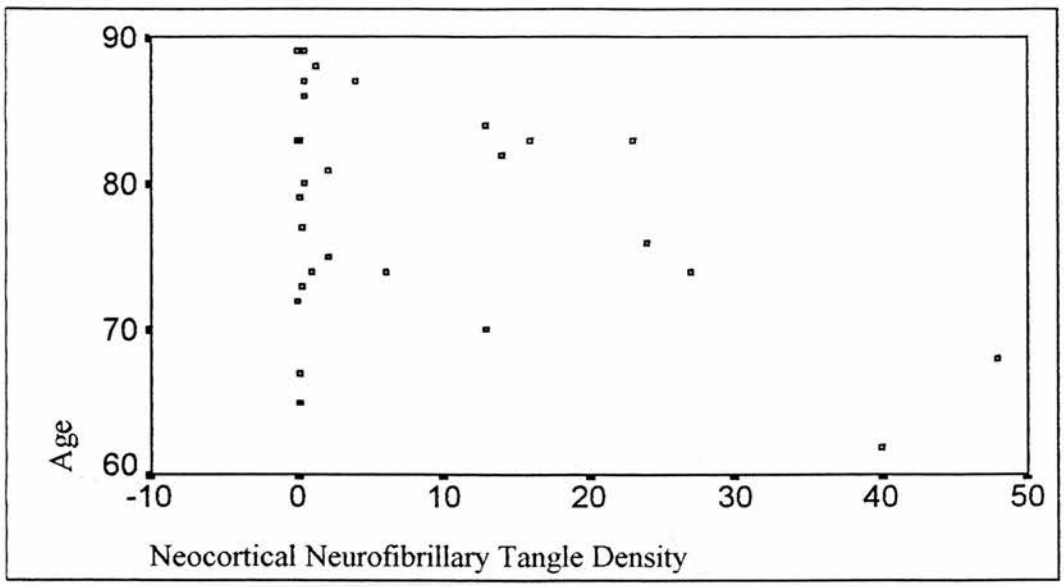

Figure 5.23 Age Plotted Against the Mean Neocortical Neurofibrillary Tangle Density for Series III (OPTIMA) Cases

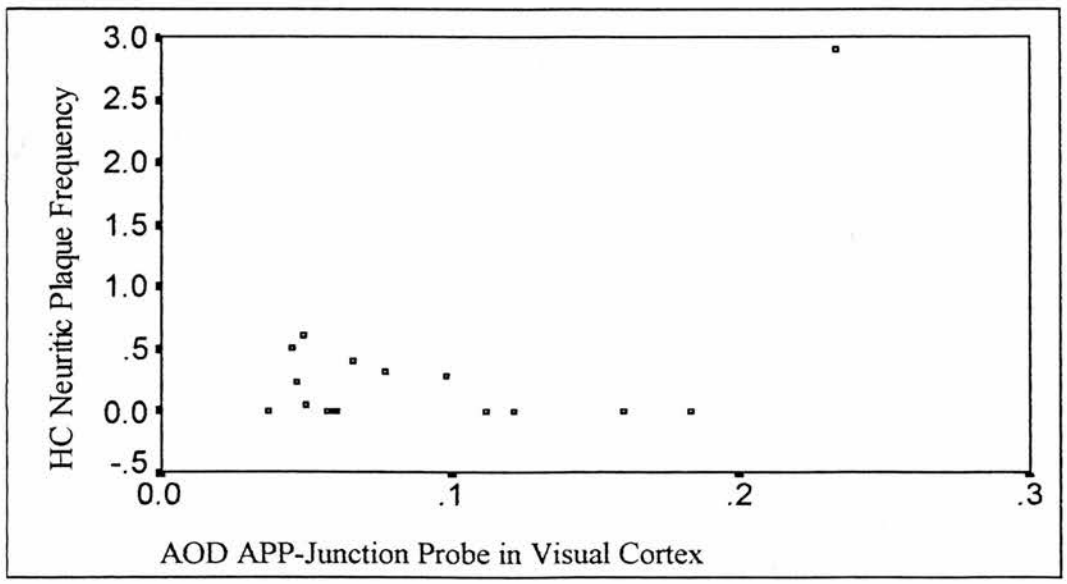

Figure 5.24 The Approximate Optical Density of the APP-Junction Oligodeoxynucleotide Probe in the Visual Cortex Plotted Against the Mean Hippocampal Neuritic Plaque Frequency for Series III (OPTIMA) Cases

value of 0.055, suggesting that the non-parametric test simply lacked the power to identify the correlation between these two variables.

Finally, the third significant correlation on parametric analysis related to the junction:poly(dT) ratio in visual cortex, which was also negatively correlated (-0.520) with the mean hippocampal neurofibrillary tangle density with a p value of 0.047. Non-parametric analysis revealed a negative correlation of -0.497 with a p value of 0.059, suggesting that, again, Spearman's rank correlation lacked the power to identify the correlation between these two variables.

Non-parametric analysis of the data revealed that the AOD of the poly(dT) probe in visual cortex was correlated with the maximum CERAD plaque frequency, mean neocortical neuritic plaque density and mean neocortical neurofibrillary tangle density. These findings were not confirmed on parametric analysis of the data. However, scrutiny of the data revealed two extreme values for the AOD of the poly(dT) oligodeoxynucleotide probe. When these two outlying values were removed, the CERAD plaque frequency was found to be correlated with the AOD of the poly(dT) probe using both tests with a p value of less than 0.010 for both, suggesting that these extreme values had masked the parametric correlation between these two variables. Further, exclusion of these two values revealed a correlation between the AOD of the poly(dT) probe and the mean neocortical neuritic plaque density with a p value of 0.003 for the parametric test and 0.002 for the non-parametric test. Similarly, on the removal of these two values, the mean

neocortical neurofibrillary tangle density and AOD of the poly(dT) probe were correlated with a p value of 0.005 on the parametric test and a p value of 0.002 on the non-parametric test.

As a precaution, parametric and non-parametric analysis of the relationship between the AOD of the poly(dT) probe and the remaining neuropathological parameters was repeated following exclusion of these two extreme values for the AOD of the poly(dT) oligodeoxynucleotide probe. The correlation between the Braak score and the AOD of the poly(dT) probe then became significant, ($p < 0.030$), using both parametric and non-parametric tests. The mean hippocampal amyloid plaque frequency and the mean hippocampal neuritic plaque frequency were also significantly correlated with the AOD of the poly(dT) probe ($p < 0.030$) by parametric analysis alone. Examination of a scatter diagram (Figure 5.25) of the mean hippocampal amyloid plaque frequency and the AOD of the poly(dT) probe suggested that the two were indeed correlated but that Spearman's rank correlation ($p = 0.108$) simply lacked the power to establish the relationship. The mean hippocampal neuritic plaque frequency, however, did not appear to be correlated with the AOD of the poly(dT) probe on scrutiny of a scatter diagram (Figure 5.26).

In conclusion, 3 significant Pearson's correlation coefficient's in a total matrix of 56 cells is less than would have been predicted to occur by chance and, overall, a significant relationship, between the AOD of the probes measured and neuropathology would appear unlikely. However, 3 of the 7 neuropathological

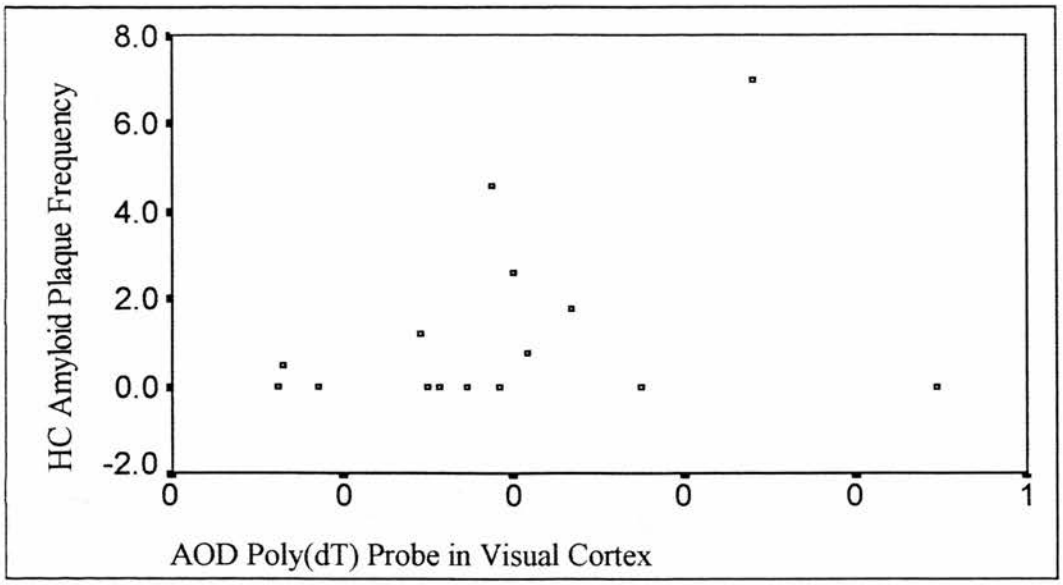

Figure 5.25 The Approximate Optical Density of the Poly(dT) Oligodeoxynucleotide Probe in the Visual Cortex Plotted Against the Mean Hippocampal Amyloid Plaque Frequency for Series III (OPTIMA) Cases

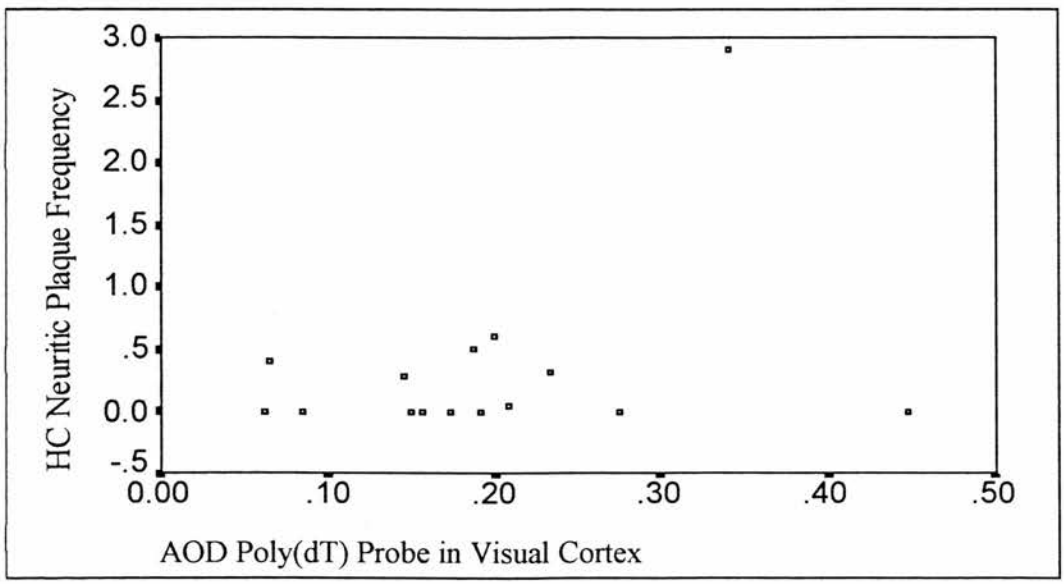

Figure 5.26 The Approximate Optical Density of the Poly(dT) Oligodeoxynucleotide Probe in the Visual Cortex Plotted Against the Mean Hippocampal Neuritic Plaque Frequency for Series III (OPTIMA) Cases

parameters measured, were positively correlated with the AOD of the poly(dT) probe on a Spearman's correlation matrix. Parametric statistical techniques are notoriously sensitive to extreme values, and when two outlying values for the AOD of the poly(dT) probe were excluded from the analysis, parametric testing of the above relationships became significant in concordance with the non-parametric analysis and a fourth correlation, significant on both parametric and non-parametric testing, was revealed. Moreover, the clustering of significant findings in a matrix of 56 cells suggests that the abundance of poly(A)$^+$ mRNA in visual cortex in AD and normal control brains, is meaningfully related to the severity of both neocortical and hippocampal pathology, as measured in this study. Removal of the outlying values for the AOD of the poly(dT) oligodeoxynucleotide probe results in the identification of eight significant cells in the parametric matrix of 56 cells. It is noteworthy that the probability of generating 8 significant cells in a matrix of 70 cells is $p = 0.023$. It is also curious that the AOD of both the insert and junction probes in visual cortex when expressed as a proportion of the AOD of poly(dT) probe, were negatively correlated with the average hippocampal neurofibrillary tangle density, suggesting that these ratios may reflect, indirectly, hippocampal neuritic pathology.

5.3.4.5.4 Correlations Between the APP-Insert, APP-Junction and APP-770 Oligodeoxynucleotide Probes in the Dentate Gyrus and Neuropathology

A Pearson's correlation matrix of 28 cells (Table 5.9), prepared to examine the relationship between the APP oligodeoxynucleotide probes in dentate gyrus and

Table 5.9 Pearson's Correlation Coefficients for Series III (OPTIMA) Hippocampal Dentate Gyrus Data							
	Maximum CERAD Plaque Frequency	**Braak Score**	**Mean HC Amyloid Plaque Frequency**	**Mean HC Neuritic Plaque Frequency**	**Mean HC NFT Density**	**Mean Neocortical NFT Density**	**Mean Neocortical Neuritic Plaque Density**
APP-770 Probe (Whole HC)	-0.189 (n = 23) p = 0.387	-0.112 (n = 19) p = 0.648	-0.372 (n = 11) p = 0.259	-0.342 (n = 11) p = 0.304	-0.480 (n = 11) p = 0.135	-0.072 (n = 19) p = 0.768	-0.365 (n = 19) p = 0.125
APP-Insert Probe	-0.274 (n = 25) p = 0.185	-0.255 (n = 21) p = 0.265	-0.074 (n = 11) p = 0.828	-0.026 (n = 11) p = 0.940	-0.439 (n = 11) p = 0.176	-0.139 (n = 21) p = 0.547	-0.303 (n = 21) p = 0.182
APP-Junction Probe	-0.396 (n = 22) p = 0.069	-0.282 (n = 18) p = 0.256	-0.156 (n = 11) p = 0.647	-0.092 (n = 11) p = 0.789	-0.501 (n = 11) p = 0.116	-0.064 (n = 18) p = 0.802	-0.488 (n = 18) **p = 0.040**
Insert: Junction Ratio	-0.163 (n = 22) p = 0.470	-0.151 (n = 18) p = 0.551	0.003 (n = 11) p = 0.993	0.018 (n = 11) p = 0.957	-0.236 (n = 11) p = 0.485	-0.171 (n = 18) p = 0.497	-0.152 (n = 18) p = 0.547

neuropathology, revealed only one significant finding. The AOD of the APP-junction probe in dentate gyrus was negatively correlated with the mean neocortical neuritic plaque density (-0.488), with a p value of 0.040, using the parametric test. Spearman's rank correlation resulted in a correlation coefficient of -0.424 and a p value of 0.080, for the same two variables, suggesting that the non-parametric test lacked the power to establish this correlation.

However, one significant finding out of 28 cells is less than would have been predicted to occur by chance, implying that the abundance of the mRNA species detected by the APP-insert, APP-junction and APP-770 oligodeoxynucleotide probes in dentate gyrus, or the insert:junction ratio, are unrelated to neuropathological severity as measured in this study.

5.3.4.5.5 Correlations Between the APP-Insert, APP-Junction and APP-770 Oligodeoxynucleotide Probes in CA4 and Neuropathology

A Pearson's correlation matrix of 21 cells was used to examine the relationship between the APP probes and neuropathology in CA4 (Table 5.10). Both parametric and non-parametric tests concurred and the only significant finding was a negative correlation between the AOD of the APP-junction oligodeoxynucleotide probe and the maximum CERAD plaque frequency ($p = 0.014$). One significant finding is less than would have been predicted to occur by chance, suggesting that neither the abundance of the APP mRNA species measured in CA4, nor the insert:junction ratio, are meaningfully related to the neuropathological severity as measured in this study.

Table 5.10 Pearson's Correlation Coefficients for Series III (OPTIMA) Hippocampal CA4 Data							
	Maximum CERAD Plaque Frequency	**Braak Score**	**Mean HC Amyloid Plaque Frequency**	**Mean HC Neuritic Plaque Frequency**	**Mean HC NFT Density**	**Mean Neocortical NFT Density**	**Mean Neocortical Neuritic Plaque Density**
APP-Insert Probe	-0.076 (n = 25) p = 0.719	-0.214 (n = 21) p = 0.352	-0.041 (n = 11) p = 0.904	-0.017 (n = 11) p = 0.959	-0.439 (n = 11) p = 0.177	-0.174 (n = 21) p = 0.452	0.046 (n = 21) p = 0.843
APP-Junction Probe	0.516 (n = 22) **p = 0.014**	-0.435 (n = 18) p = 0.071	-0.402 (n = 11) p = 0.220	-0.358 (n = 11) p = 0.279	-0.427 (n = 11) p = 0.190	-0.351 (n = 18) p = 0.153	-0.442 (n = 18) p = 0.067
Insert: Junction Ratio	0.016 (n = 22) p = 0.946	-0.113 (n = 18) p = 0.656	0.121 (n = 11) p = 0.724	0.125 (n = 11) p = 0.713	-0.203 (n = 11) p = 0.549	-0.143 (n = 18) p = 0.570	0.030 (n = 18) p = 0.906

5.3.4.5.6 Correlations Between the APP-Insert, APP-Junction and APP-770 Oligodeoxynucleotide Probes in CA3 and Neuropathology

No significant correlations were observed, between the neuropathological parameters measured and the APP probes and insert:junction ratio in CA3, on a Pearson's correlation matrix of 21 cells (Table 5.11). However, the non-parametric matrix suggested a correlation between the insert:junction ratio and the maximum CERAD plaque frequency of –0.586 ($p = 0.035$). Examination of a scatter diagram (Figure 5.27) did not support this correlation and it was, thus, disregarded. It would appear that, in CA3, neither the abundance of the APP mRNA species measured, nor the insert:junction ratio, are meaningfully related to the severity of neuropathology as assessed in this study.

5.3.4.5.7 Correlations Between the APP-Insert, APP-Junction and APP-770 Oligodeoxynucleotide Probes in CA1 and Neuropathology

No significant correlations were observed, using either the parametric or non-parametric tests, between the neuropathological parameters measured and the abundance of mRNA species identified by the APP-insert, APP-junction or APP-770 probes, or the insert:junction ratio, in CA1 (Table 5.12).

Table 5.11 Pearson's Correlation Coefficients for Series III (OPTIMA) Hippocampal CA3 Data							
	Maximum CERAD Plaque Frequency	**Braak Score**	**Mean HC Amyloid Plaque Frequency**	**Mean HC Neuritic Plaque Frequency**	**Mean HC NFT Density**	**Mean Neocortical NFT Density**	**Mean Neocortical Neuritic Plaque Density**
APP-Insert Probe	-0.173 (n = 20) p = 0.466	-0.242 (n = 16) p = 0.366	-0.199 (n = 9) p = 0.607	-0.203 (n = 9) p = 0.600	-0.141 (n = 9) p = 0.718	-0.243 (n = 16) p = 0.363	-0.0002 (n = 16) p = 0.999
APP-Junction Probe	0.101 (n = 17) p = 0.700	0.217 (n = 13) p = 0.477	0.496 (n = 8) p = 0.212	0.527 (n = 8) p = 0.180	0.195 (n = 8) p = 0.643	0.024 (n = 13) p = 0.939	0.449 (n = 13) p = 0.124
Insert: Junction Ratio	-0.276 (n = 17) p = 0.283	-0.231 (n = 13) p = 0.447	-0.256 (n = 8) p = 0.541	-0.269 (n = 8) p = 0.519	-0.120 (n = 8) p = 0.778	-0.215 (n = 13) p = 0.481	-0.237 (n = 13) p = 0.436

Table 5.12 Pearson's Correlation Coefficients for Series III (OPTIMA) Hippocampal CA1 Data							
	Maximum CERAD Plaque Frequency	**Braak Score**	**Mean HC Amyloid Plaque Frequency**	**Mean HC Neuritic Plaque Frequency**	**Mean HC NFT Density**	**Mean Neocortical NFT Density**	**Mean Neocortical Neuritic Plaque Density**
APP-Insert Probe	-0.258 (n = 22) p = 0.246	-0.157 (n = 18) p = 0.535	-0.084 (n = 10) p = 0.817	-0.092 (n = 10) p = 0.800	-0.018 (n = 10) p = 0.961	-0.281 (n = 18) p = 0.258	-0.136 (n = 18) p = 0.592
APP-Junction Probe	-0.044 (n = 20) p = 0.855	-0.003 (n = 16) p = 0.990	-0.105 (n = 9) p = 0.788	-0.105 (n = 9) p = 0.788	-0.105 (n = 9) p = 0.788	-0.138 (n = 16) p = 0.610	-0.099 (n = 16) p = 0.715
Insert: Junction Ratio	-0.249 (n = 19) p = 0.304	-0.124 (n = 15) p = 0.658	0.065 (n = 9) p = 0.867	0.065 (n = 9) p = 0.867	0.065 (n = 9) p = 0.867	-0.120 (n = 15) p = 0.477	-0.174 (n = 15) p = 0.535

5.3.4.5.8 Correlations Between the APP-Insert, APP-Junction, APP-770 and Poly(dT) Oligodeoxynucleotide Probes and Demographic and Tissue Details in Visual Cortex

A Pearson's correlation matrix of forty cells was prepared to examine the relationship(s), if any, between the APP and poly(dT) oligodeoxynucleotide probes, and the age and mini-mental state scores of the subjects, and the pH, PMI and storage of the tissue (Table 5.13). This matrix generated five significant correlations ($p < 0.050$). The probability of generating five significant correlations from forty cells is $p = 0.048$, therefore, a real relationship between the parameters measured and the oligodeoxynucleotide probes analysed is likely.

The Pearson's correlation matrix identified two significant correlations that related to the pH of the tissue used. Tissue pH was correlated with both the AOD of the APP-junction oligodeoxynucleotide probe ($p = 0.003$) and AOD of the APP-insert oligodeoxynucleotide probe ($p = 0.001$) measured in the visual cortex. Non-parametric analysis confirmed both of these relationships. No correlation was observed between the insert:junction ratio in visual cortex and the tissue pH.

The three remaining significant Pearson's correlations related to the scores on mini-mental state examination. Firstly, the AOD of the APP-junction oligodeoxynucleotide probe was found to be positively correlated with the mini-mental state score, on parametric analysis alone ($p = 0.047$). A scatter diagram (Figure 5.28) of the data revealed two outlying values that when removed resulted in

Table 5.13 Pearson's Correlation Coefficients for Series III (OPTIMA) Visual Cortex Data					
	Age	**Mini-Mental State Score**	**Tissue pH**	**Post-Mortem Delay**	**Storage**
APP-Insert Probe	-0.079 (n = 35) p = 0.653	0.302 (n = 28) p = 0.119	0.573 (n = 29) **p = 0.001**	-0.232 (n = 34) p = 0.188	0.074 (n = 35) p = 0.673
APP-Junction Probe	-0.142 (n = 34) p = 0.425	0.379 (n = 28) **p = 0.047**	0.540 (n = 28) **p = 0.003**	-0.082 (n = 33) p = 0.649	-0.006 (n = 34) p = 0.971
APP-770 Probe	0.162 (n = 33) p = 0.366	-0.211 (n = 26) p = 0.301	0.232 (n = 27) p = 0.244	0.151 (n = 32) p = 0.410	0.076 (n = 33) p = 0.675
Insert: Junction Ratio	0.251 (n = 34) p = 0.153	-0.348 (n = 28) p = 0.069	-0.220 (n = 28) p = 0.260	-0.086 (n = 33) p = 0.634	0.182 (n = 34) p = 0.302
Poly(dT) Probe	-0.098 (n = 33) p = 0.586	-0.360 (n = 27) p = 0.065	0.165 (n = 28) p = 0.402	-0.106 (n = 32) p = 0.562	0.235 (n = 33) p = 0.188
APP-Insert Probe: Poly(dT) Probe	0.045 (n = 33) p = 0.803	0.482 (n = 27) **p = 0.011**	0.325 (n = 28) p = 0.092	-0.061 (n = 32) p = 0.740	-0.135 (n = 33) p = 0.452
APP-Junction Probe: Poly(dT) Probe	-0.001 (n = 32) p = 0.995	0.534 (n = 27) **p = 0.004**	0.352 (n = 27) p = 0.071	0.054 (n = 31) p = 0.775	-0.173 (n = 32) p = 0.345
APP-770 Probe: Poly(dT) Probe	0.269 (n = 32) p = 0.137	0.134 (n = 26) p = 0.512	0.026 (n = 27) p = 0.898	0.201 (n = 31) p = 0.277	-0.092 (n = 32) p = 0.616

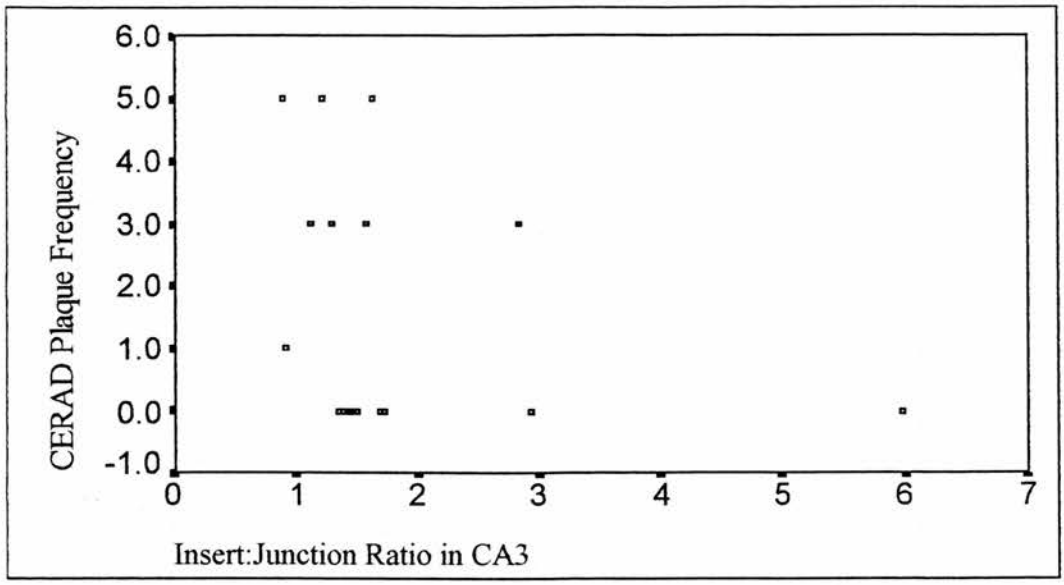

Figure 5.27 The Insert:Junction Ratio in Hippocampal Subfield CA3 Plotted Against the Maximum CERAD Plaque Frequency for Series III (OPTIMA) Cases

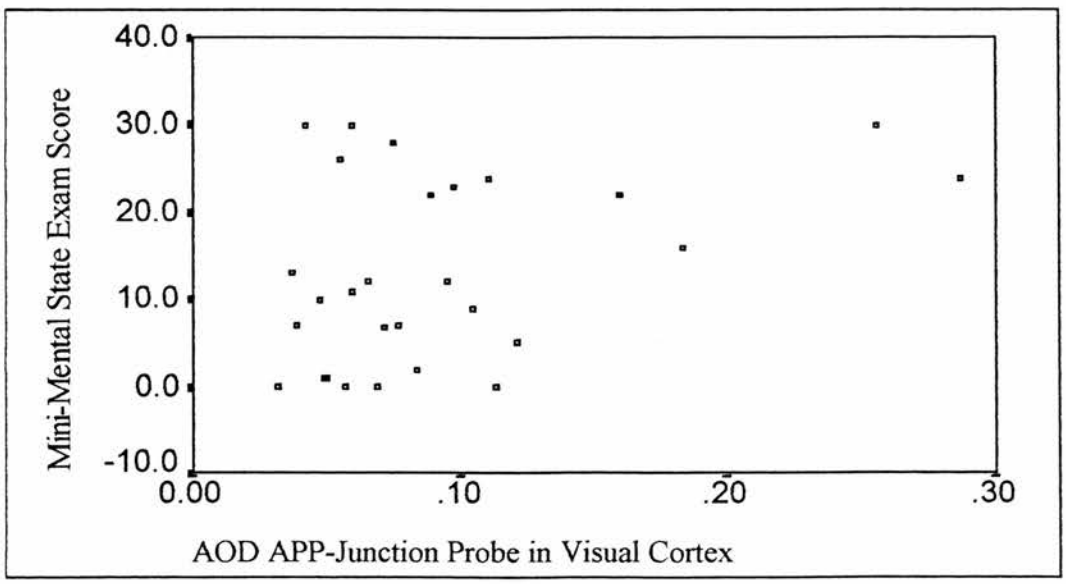

Figure 5.28 The Approximate Optical Density of the APP-Junction Oligodeoxynucleotide Probe in the Visual Cortex Plotted Against the Mini-Mental State Examination Score for Series III (OPTIMA) Cases

a loss of significance of the parametric test. Secondly, the insert:poly(dT) ratio was positively correlated with the mini-mental state score using both parametric ($p = 0.011$) and non parametric ($p = 0.009$) tests. The third significant Pearson's correlation related to the junction:poly(dT) ratio, which was positively correlated with the mini-mental state score on parametric analysis of the data only ($p = 0.018$). Since Spearman's correlation coefficient was found to be approaching significance ($p = 0.054$), it is likely that the non-parametric test merely lacked the power to demonstrate this relationship definitively.

On non-parametric analysis only, the AOD of the poly(dT) probe was negatively correlated with the mini-mental state score ($p = 0.014$). Analysis of a scatter diagram (Figure 5.29) suggested that an outlying value was responsible for the lack of significance of the parametric result ($p = 0.065$) and it was, therefore, concluded that the AOD of the poly(dT) probe was correlated with the mini-mental state score in the visual cortex. It is likely that the correlations identified between the insert:poly(dT) ratio and junction:poly(dT) ratio, and the mini-mental state score, in reality reflects the negative correlation established between the AOD of the poly(dT) probe in visual cortex and the score on mini-mental state examination.

5.3.4.5.9 Correlations Between the APP-Insert, APP-Junction and APP-770 Oligodeoxynucleotide Probes and Demographic and Tissue Details in Dentate Gyrus and Hippocampal Fields CA4, CA3 and CA1

A Pearson's correlation matrix of 20 cells was prepared examining the relationship(s) between the above probes in the dentate gyrus and the age, mini-mental state score, tissue pH, PMI and tissue storage of the cases used (Table 5.14). Only one significant finding was obtained. The AOD of the APP-junction probe was correlated with the mini-mental state score ($p=0.042$). Spearman's rank correlation did not achieve significance ($p=0.073$), but was, however, close enough to suggest that the two variables were indeed correlated but that the non-parametric test lacked the power to demonstrate this association.

No significant correlations were found, using either parametric or non-parametric tests, between the age and mini-mental state of the subjects or the pH, PMI or storage of the tissue, and the above probes, in CA4 (Table 5.15). In CA3 (Table 5.16), the AOD of the APP-junction probe was correlated with the mini-mental state score using Spearman's rank correlation ($p=0.041$). The parametric test, however, did not achieve significance ($p=0.055$). Examination of a scatter diagram (Figure 5.30) of these two variables suggested a correlation between the two that was masked by an outlying value distorting the parametric test. No significant correlations were found in CA1 between the APP probes and the age, mini-mental state scores of the subjects or the pH, PMI or storage of the tissue (Table 5.17).

Table 5.14 Pearson's Correlation Coefficients for Series III (OPTIMA) Hippocampal Dentate Gyrus Data					
	Age	**Mini-Mental State Score**	**Tissue pH**	**Post-Mortem Delay**	**Storage**
APP-770 Probe (Whole HC)	-0.079 (n = 27) p = 0.696	-0.073 (n = 22) p = 0.746	0.267 (n = 26) p = 0.187	-0.319 (n = 26) p = 0.112	-0.136 (n = 27) p = 0.500
APP-Insert Probe	0.044 (n = 29) p = 0.819	0.250 (n = 24) p = 0.239	0.125 (n = 26) p = 0.542	0.130 (n = 28) p = 0.508	-0.184 (n = 29) p = 0.339
APP-Junction Probe	-0.310 (n = 25) p = 0.132	0.447 (n = 21) **p = 0.042**	0.360 (n = 23) p = 0.092	-0.103 (n = 24) p = 0.632	-0.251 (n = 25) p = 0.226
Insert: Junction Ratio	0.164 (n = 25) p = 0.434	-0.102 (n = 21) p = 0.659	-0.134 (n = 23) p = 0.544	0.247 (n = 24) p = 0.245	0.032 (n = 25) p = 0.881

Table 5.15 Pearson's Correlation Coefficients for Series III (OPTIMA) Hippocampal CA4 Data					
	Age	**Mini-Mental State Score**	**Tissue pH**	**Post-Mortem Delay**	**Storage**
APP-Insert Probe	0.170 (n = 29) p = 0.378	0.204 (n = 24) p = 0.340	0.060 (n = 26) p = 0.770	0.241 (n = 28) p = 0.217	0.115 (n = 29) p = 0.551
APP-Junction Probe	-0.269 (n = 25) p = 0.193	0.373 (n = 21) p = 0.096	0.138 (n = 23) p = 0.530	-0.182 (n = 24) p = 0.395	0.053 (n = 25) p = 0.800
Insert: Junction Ratio	0.256 (n = 25) p = 0.216	-0.021 (n = 21) p = 0.929	-0.073 (n = 23) p = 0.739	0.308 (n = 24) p = 0.143	0.073 (n = 25) p = 0.730

Table 5.16 Pearson's Correlation Coefficients for Series III (OPTIMA) Hippocampal CA3 Data					
	Age	**Mini-Mental State Score**	**Tissue pH**	**Post-Mortem Delay**	**Storage**
APP-Insert Probe	0.232 (n = 23) p = 0.286	0.206 (n = 19) p = 0.397	0.135 (n = 21) p = 0.558	0.283 (n = 23) p = 0.191	-0.109 (n = 23) p = 0.621
APP-Junction Probe	-0.166 (n = 19) p = 0.498	0.236 (n = 16) p = 0.379	0.459 (n = 18) p = 0.055	-0.006 (n = 19) p = 0.982	0.100 (n = 19) p = 0.683
Insert: Junction Ratio	0.167 (n = 19) p = 0.495	-0.050 (n = 16) p = 0.853	-0.255 (n = 18) p = 0.307	0.258 (n = 19) p = 0.286	0.029 (n = 19) p = 0.907

Table 5.17 Pearson's Correlation Coefficients for Series III (OPTIMA) Hippocampal CA1 Data					
	Age	**Mini-Mental State Score**	**Tissue pH**	**Post-Mortem Delay**	**Storage**
APP-Insert Probe	0.272 (n = 25) p = 0.188	0.098 (n = 21) p = 0.673	0.049 (n = 23) p = 0.825	0.072 (n = 25) p = 0.733	0.033 (n = 25) p = 0.876
APP-Junction Probe	0.023 (n = 22) p = 0.918	-0.092 (n = 20) p = 0.699	-0.044 (n = 21) p = 0.850	-0.080 (n = 22) p = 0.723	-0.070 (n = 22) p = 0.759
Insert: Junction Ratio	0.209 (n = 21) p = 0.364	0.144 (n = 19) p = 0.558	0.065 (n = 20) p = 0.786	0.063 (n = 21) p = 0.787	0.104 (n = 21) p = 0.655

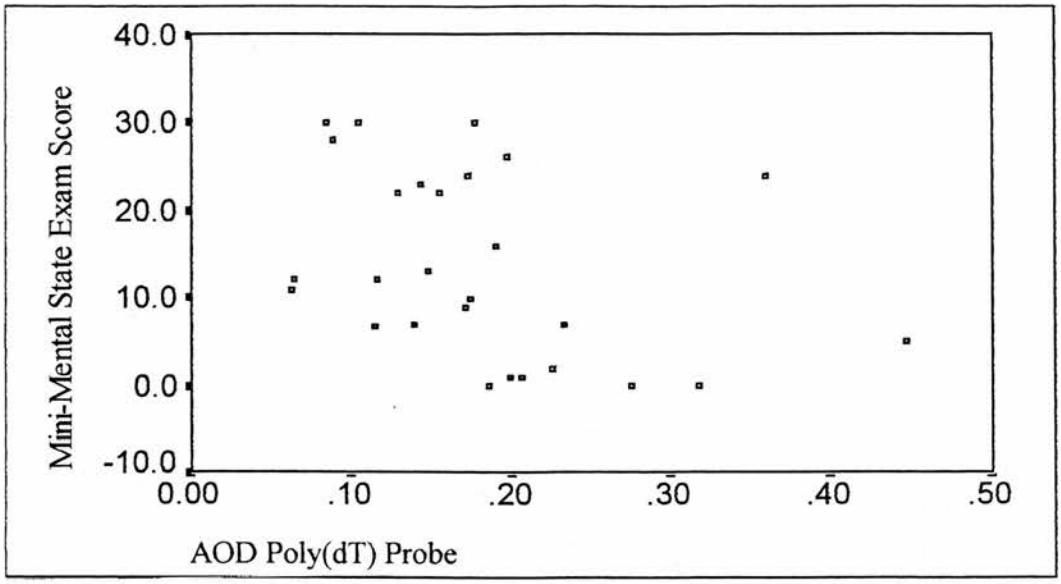

Figure 5.29 The Approximate Optical Density of the Poly(dT) Oligodeoxynucleotide Probe in the Visual Cortex Plotted Against the Mini-Mental State Examination Score for Series III (OPTIMA) Cases

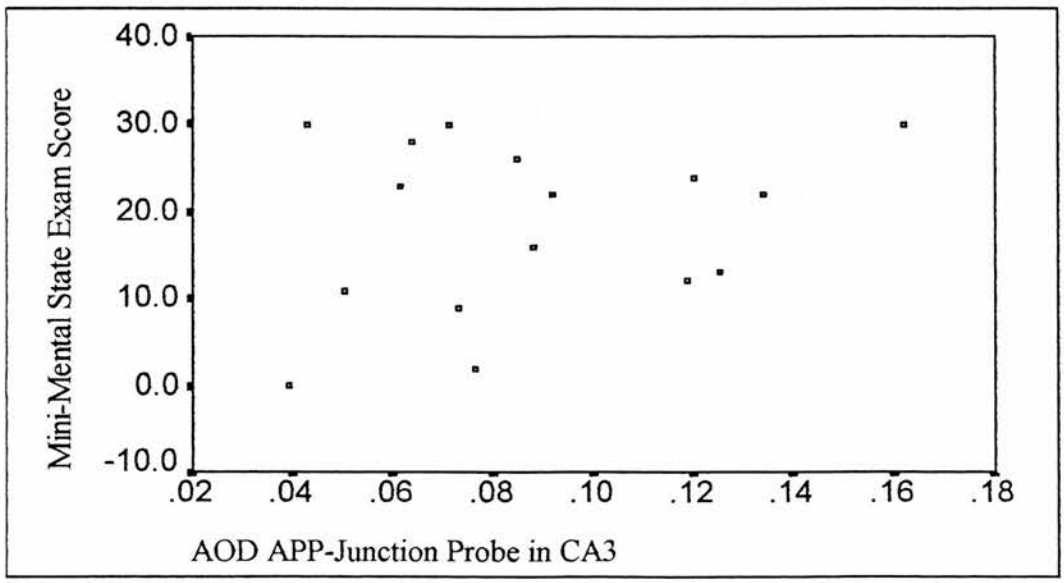

Figure 5.30 The Approximate Optical Density of the APP-Junction Oligodeoxynucleotide Probe in Hippocampal Subfield CA3 and the Mini-Mental State Examination Score for Series III (OPTIMA) Cases

In total, a Pearson's correlation matrix of 65 cells was generated, to examine the relationship between the APP probes and the age and mini-mental state scores of the subjects and the pH, PMI and storage of the tissue, in the dentate gyrus and hippocampal fields CA4, CA3 and CA1. Only one significant finding was observed: less than would have been predicted to occur by chance. It would appear that the abundance of the mRNA species detected by the APP probes used in this study in the dentate gyrus, CA4, CA3 or CA1 are not significantly affected by the age or mini-mental state scores of the subjects studied, or by the pH, PMI or duration of storage of the tissue.

5.3.4.5.10 Correlations Between the APP-Insert, APP-Junction, APP-770 and Poly(dT) Oligodeoxynucleotide Probes in Visual Cortex

A Pearson's correlation matrix of 28 cells (Table 5.18), constructed to examine the inter-relationship(s), if any, between the APP-insert, APP-junction and APP-770 oligodeoxynucleotide probes and the poly(dT) probe, in the visual cortex, generated fifteen significant correlations ($p < 0.050$). The relationship between the probes is unlikely to be due to chance, since the probability of obtaining 5 significant correlations in a matrix of 30 cells is $p = 0.016$.

The most striking finding in the visual cortex is the correlation between the AOD of the APP-insert oligodeoxynucleotide probe and the AOD of the APP-junction oligodeoxynucleotide probe with a Pearson's correlation coefficient of 0.905 and a p value of < 0.001. Non-parametric analysis resulted in a p value of < 0.001 also. The

Table 5.18 Pearson's Correlation Coefficients for Series III (OPTIMA) Visual Cortex Data								
	APP-Insert Probe	**APP-Junction Probe**	**APP-770 Probe**	**Insert: Junction Ratio**	**Poly(dT) Probe**	**APP-Insert Probe: Poly(dT) Probe**	**APP-Junction Probe: Poly(dT) Probe**	**APP-770 Probe: Poly(dT) Probe**
APP-Insert Probe	1.000 (n = 35) p =	0.905 (n = 34) **p = 0.000**	0.418 (n = 33) **p = 0.016**	-0.376 (n = 34) **p = 0.028**	0.352 (n = 33) **p = 0.045**	0.449 (n = 33) **p = 0.009**	0.686 (n = 32) **p = 0.000**	-0.085 (n = 32) p = 0.643
APP-Junction Probe	0.905 (n = 34) **p = 0.000**	1.000 (n = 34) p =	0.300 (n = 32) p = 0.095	-0.678 (n = 34) **p = 0.000**	0.229 (n = 32) p = 0.208	0.278 (n = 32) p = 0.123	0.790 (n = 32) **p = 0.000**	-0.209 (n = 31) p = 0.260
APP-770 Probe	0.418 (n = 33) **p = 0.016**	0.300 (n = 32) p = 0.095	1.000 (n = 33) p =	0.011 (n = 32) p = 0.952	0.282 (n = 32) p = 0.118	0.144 (n = 32) p = 0.432	0.230 (n = 31) p = 0.212	0.376 (n = 32) **p = 0.034**
Insert: Junction Ratio	-0.376 (n = 34) **p = 0.028**	-0.678 (n = 34) **p = 0.000**	0.011 (n = 32) p = 0.952	1.000 (n = 34) p =	-0.156 (n = 32) p = 0.394	-0.006 (n = 32) p = 0.972	-0.555 (n = 32) **p = 0.001**	0.225 (n = 31) p = 0.224
Poly(dT) Probe	0.352 (n = 33) **p = 0.045**	0.229 (n = 32) p = 0.208	0.282 (n = 32) p = 0.118	-0.156 (n = 32) p = 0.394	1.000 (n = 33) p =	-0.581 (n = 33) **p = 0.000**	-0.371 (n = 32) **p = 0.036**	-0.672 (n = 32) **p = 0.000**

Table 5.18 Pearson's Correlation Coefficients for Series III (OPTIMA) Visual Cortex Data								
	APP-Insert Probe	**APP-Junction Probe**	**APP-770 Probe**	**Insert: Junction Ratio**	**Poly(dT) Probe**	**APP-Insert Probe: Poly(dT) Probe**	**APP-Junction Probe: Poly(dT) Probe**	**APP-770 Probe: Poly(dT) Probe**
APP-Insert Probe: Poly(dT) Probe	0.449 (n = 33) **p = 0.009**	0.278 (n = 32) p = 0.123	0.144 (n = 32) p = 0.432	-0.006 (n = 32) p = 0.972	-0.581 (n = 33) **p = 0.000**	1.000 (n = 33) p =	0.636 (n = 32) **p = 0.000**	0.705 (n = 32) **p = 0.000**
APP-Junction Probe: Poly(dT) Probe	0.686 (n = 32) **p = 0.000**	0.790 (n = 32) **p = 0.000**	0.230 (n = 31) p = 0.212	-0.555 (n = 32) **p = 0.001**	-0.371 (n = 32) **p = 0.036**	0.636 (n = 32) **p = 0.000**	1.000 (n = 32) p =	0.258 (n = 31) p = 0.160
APP-770 Probe: Poly(dT) Probe	-0.085 (n = 32) p = 0.643	-0.209 (n = 31) p = 0.260	0.376 (n = 32) **p = 0.034**	0.225 (n = 31) p = 0.224	-0.672 (n = 32) **p = 0.000**	0.705 (n = 32) **p = 0.000**	0.258 (n = 31) p = 0.160	1.000 (n = 32) p =

AOD of the APP-insert probe was also positively correlated with the AOD of the APP-770 probe on both parametric ($p = 0.016$), and non-parametric ($p < 0.001$), analysis. The AOD of the APP-junction oligodeoxynucleotide probe was significantly correlated with the AOD of the APP-770 oligodeoxynucleotide probe by non-parametric analysis only ($p = 0.003$). Parametric analysis revealed a p value of 0.095 and examination of a scatter diagram (Figure 5.31) suggested that two outlying values were responsible for the non-significance of the Pearson's correlation coefficient.

The AOD of the APP-junction probe was negatively correlated with the insert:junction ratio by both parametric (-0.678; $p < 0.001$) and non-parametric (-0.653; $p < 0.001$) analysis. The AOD of the APP-insert oligodeoxynucleotide probe was significantly negatively correlated to the insert:junction ratio by parametric analysis alone (-0.376; $p = 0.028$). Non-parametric analysis revealed a p value of 0.099 suggesting that Spearman's rank correlation lacked the statistical power to identify this correlation. Thus, it would appear that in visual cortex the APP-junction oligodeoxynucleotide probe influences the insert:junction ratio to a greater degree than does the APP-insert oligodeoxynucleotide probe. Further, since these two probes are highly correlated, an increase in the AOD of the APP-insert oligodeoxynucleotide probe is associated with an increase in the AOD of the APP-junction oligodeoxynucleotide probe and a lowering of the insert:junction ratio, hence the negative correlation between the AOD of the APP-insert probe and the insert:junction ratio.

The AOD of the APP-insert oligodeoxynucleotide probe was correlated with the AOD of the poly(dT) probe by parametric analysis alone (0.352; $p = 0.045$). Non-parametric analysis of this correlation revealed a p value of 0.112, suggesting that the non-parametric test lacked the power to establish this correlation.

Both the AOD of the APP-insert oligodeoxynucleotide probe (0.449; $p = 0.009$) and the AOD of the poly(dT) oligodeoxynucleotide probe (-0.581; $p < 0.001$) were correlated with the insert:poly(dT) ratio. Non-parametric analysis confirmed both of these results. Both of these probes would appear to influence the ratio between them to approximately the same degree.

The AOD of the APP-insert oligodeoxynucleotide probe (0.686; $p < 0.001$) and the AOD of the APP-junction oligodeoxynucleotide probe (0.790; $p < 0.001$) are both correlated with the junction:poly(dT) ratio. The Spearman's rank correlation matrix confirmed the above two results. The strong correlation between the AOD of the APP-insert and APP-junction oligodeoxynucleotide probes probably accounts for the correlation between the AOD of the APP-insert oligodeoxynucleotide probe with the junction:poly(dT) ratio. The AOD of the poly(dT) probe correlates with the APP-770:poly(dT) ratio on both parametric (-0.672; $p < 0.001$), and non-parametric (-0.810; $p < 0.001$) analysis, suggesting that the AOD of the poly(dT) probe is the major determinant of the ratio. The AOD of the APP-770 oligodeoxynucleotide probe, was correlated with the APP-770:poly(dT) ratio on parametric analysis alone (0.376; $p = 0.034$). Examination of a scatter plot (Figure 5.32) suggested two

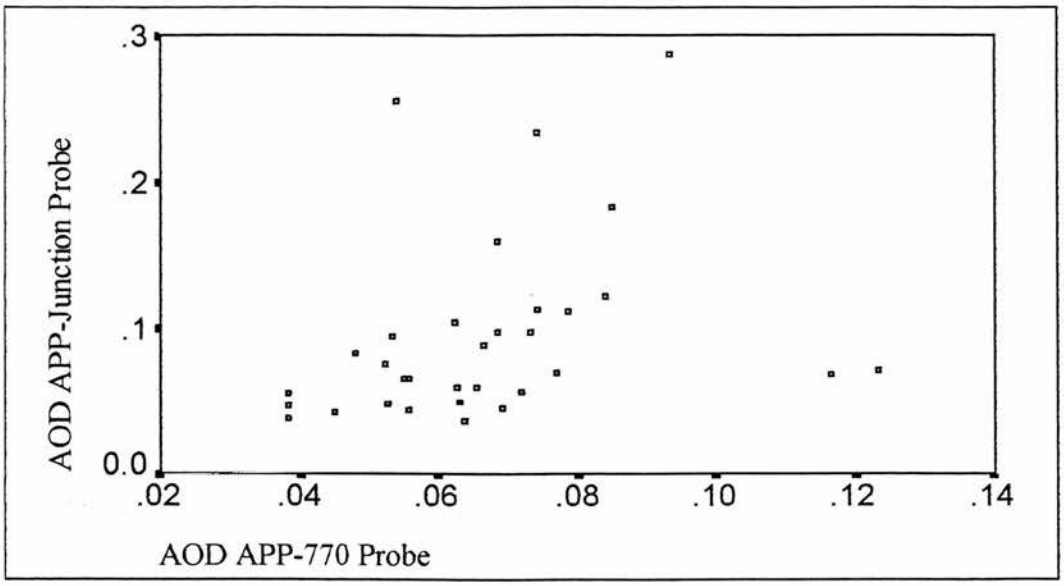

Figure 5.31 The Approximate Optical Density of the APP-770 Oligodeoxynucleotide Probe Plotted Against the Approximate Optical Density of the APP-Junction Oligodeoxynucleotide Probe in Series III (OPTIMA) Visual Cortex

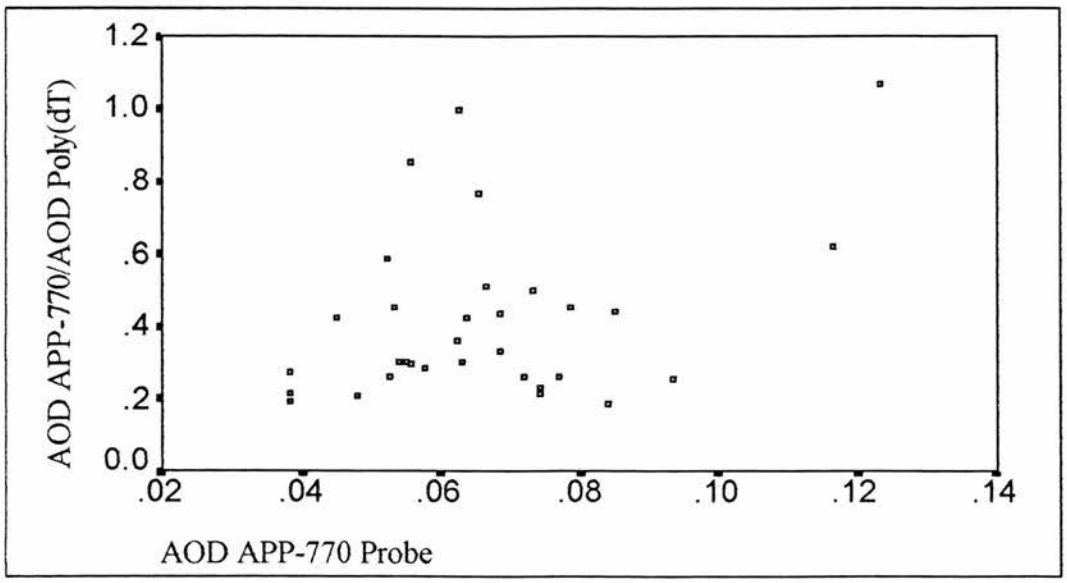

Figure 5.32 The Approximate Optical Density of the APP-770 Oligodeoxynucleotide Probe Plotted Against the Approximate Optical Density of the APP-770 Oligodeoxynucleotide Probe Expressed as a Proportion of the Approximate Optical Density of the Poly(dT) Oligodeoxynucleotide Probe in Series III (OPTIMA) Visual Cortex

outlying values as being responsible for the parametric correlation and the finding was disregarded.

The insert:poly(dT) ratio was positively correlated with both the junction:poly(dT) ratio and the APP-770:poly(dT) ratio on both parametric ($p < 0.001$) and non-parametric ($p < 0.001$) analysis, probably as a result of the common denominator of the AOD of poly(dT) probe and the correlations between the AOD of the APP-insert, APP-junction and APP-770 probes.

The junction:poly(dT) ratio was negatively correlated with both the insert:junction ratio (-0.555; $p = 0.001$) and the AOD of the poly(dT) probe (-0.371; $p = 0.036$). Non-parametric analysis confirmed the above two observations ($p = 0.002$ for each).

Finally, the APP-770:poly(dT) ratio was positively correlated with the junction:poly(dT) ratio by non-parametric analysis alone ($p = 0.006$). Parametric analysis revealed a p value of 0.160 and examination of a scatter diagram (Figure 5.33) suggested that two outlying values were responsible for the non-significance of the parametric test. Again the common denominator of the AOD of the poly(dT) probe and the correlation between the AOD of the APP-junction and APP-770 probes is likely to be responsible for this finding.

5.3.4.5.11 Correlations Between the APP-Insert, APP-Junction and APP-770 Oligodeoxynucleotide Probes in Dentate Gyrus

A Pearson's correlation matrix of 6 cells was constructed to examine the inter-relationship(s), if any, between the APP-insert, APP-junction and APP-770 oligodeoxynucleotide probes in the dentate gyrus (Table 5.19).

The AOD of the APP-insert oligodeoxynucleotide probe was highly correlated with the AOD of the APP-junction oligodeoxynucleotide probe in this region, using both parametric and non-parametric tests ($p = 0.001$). The AOD of the APP-insert oligodeoxynucleotide probe was also highly correlated with the AOD of the APP-770 oligodeoxynucleotide probe using both parametric ($p = 0.006$), and non-parametric ($p = 0.003$), tests. Finally, the AOD of the APP-insert oligodeoxynucleotide probe was highly correlated with the insert:junction ratio using both parametric ($p < 0.001$) and non-parametric ($p = 0.004$) tests. In contrast to the visual cortex, the AOD of the APP-junction probe was not correlated with the insert:junction ratio suggesting that in the dentate gyrus the AOD of the APP-insert oligodeoxynucleotide probe dominates this ratio. Further, since the probability of obtaining 3 significant findings in a sample of 10 cells is $p = 0.012$, the correlations identified, between the APP oligodeoxynucleotide probes and the insert:junction ratio in the dentate gyrus, is unlikely to be due to chance.

Table 5.19 Pearson's Correlation Coefficients for Series III (OPTIMA) Hippocampal Dentate Gyrus Data				
	APP-770 Probe (Whole HC)	**APP-Insert Probe**	**APP-Junction Probe**	**Insert:Junction Ratio**
APP-770 Probe (Whole HC)	1.000 (n = 27) p =	0.512 (n = 27) **p = 0.006**	0.255 (n = 24) p = 0.230	0.343 (n = 24) p = 0.100
APP-Insert Probe	0.512 (n = 27) **p = 0.006**	1.000 (n = 29) p =	0.642 (n = 25) **p = 0.001**	0.669 (n = 25) **p = 0.000**
APP-Junction Probe	0.255 (n = 24) p = 0.230	0.642 (n = 25) **p = 0.001**	1.000 (n = 25) p =	-0.136 (n = 25) p = 0.515
Insert:Junction Ratio	0.343 (n = 24) p = 0.100	0.669 (n = 25) **p = 0.000**	-0.136 (n = 25) p = 0.515	1.000 (n = 25) p =

5.3.4.5.12 Correlations Between the APP-Insert, APP-Junction and APP-770 Oligodeoxynucleotide Probes in CA4

A Pearson's correlation matrix of 6 cells was constructed to examine the inter-relationship(s), if any, between the APP-insert, APP-junction and APP-770 oligodeoxynucleotide probes and the insert:junction ratio in CA4 (Table 5.20). The Pearson's correlation matrix revealed two significant correlations. The AOD of the APP-insert oligodeoxynucleotide probe was positively correlated (0.813; $p < 0.001$), and the AOD of the APP-junction oligodeoxynucleotide probe was negatively correlated (-0.627; $p = 0.001$), with the insert:junction ratio. Both correlations were confirmed using the non-parametric test. The APP-junction and APP-insert oligodeoxynucleotide probes would appear to influence the insert:junction ratio to approximately the same degree.

Since the probability of generating 2 significant findings in a sample of 5 cells, is $p = 0.023$, the associations identified between the APP probes and the insert:junction ratio is likely to be significant.

5.3.4.5.13 Correlations Between the APP-Insert, APP-Junction and APP-770 Oligodeoxynucleotide Probes in CA3

A Pearson's correlation matrix of 6 cells was constructed to examine the inter-relationship(s), if any, between the APP-insert, APP-junction and APP-770 oligodeoxynucleotide probes and the insert:junction ratio in CA3 (Table 5.21). Only one significant finding was observed in the Pearson's correlation matrix: the AOD of

Table 5.20 Pearson's Correlation Coefficients for Series III (OPTIMA) Hippocampal CA4 Data				
	APP-770 Probe (Whole HC)	**APP-Insert Probe**	**APP-Junction Probe**	**Insert:Junction Ratio**
APP-770 Probe (Whole HC)	1.000 (n = 27) p =	0.249 (n = 27) p = 0.211	-0.079 (n = 24) p = 0.715	0.159 (n = 24) p = 0.459
APP-Insert Probe	0.249 (n = 27) p = 0.211	1.000 (n = 29) p =	-0.084 (n = 25) p = 0.688	0.813 (n = 25) **p = 0.000**
APP-Junction Probe	-0.079 (n = 24) p = 0.715	-0.084 (n = 25) p = 0.688	1.000 (n = 25) p =	-0.627 (n = 25) **p = 0.001**
Insert:Junction Ratio	0.159 (n = 24) p = 0.459	0.813 (n = 25) **p = 0.000**	-0.627 (n = 25) **p = 0.001**	1.000 (n = 25) p =

Table 5.21 Pearson's Correlation Coefficients for Series III (OPTIMA) Hippocampal CA3 Data				
	APP-770 Probe (Whole HC)	**APP-Insert Probe**	**APP-Junction Probe**	**Insert:Junction Ratio**
APP-770 Probe (Whole HC)	1.000 (n = 27) p =	0.188 (n = 21) p = 0.414	-0.142 (n = 18) p = 0.574	0.163 (n = 18) p = 0.518
APP-Insert Probe	0.188 (n = 21) p = 0.414	1.000 (n = 23) p =	0.307 (n = 19) p = 0.201	0.684 (n = 19) **p = 0.001**
APP-Junction Probe	-0.142 (n = 18) p = 0.574	0.307 (n = 19) p = 0.201	1.000 (n = 19) p =	-0.437 (n = 19) p = 0.061
Insert:Junction Ratio	0.163 (n = 18) p = 0.518	0.684 (n = 19) **p = 0.001**	-0.437 (n = 19) p = 0.061	1.000 (n = 19) p =

the APP-insert oligodeoxynucleotide probe was positively correlated with the insert:junction ratio ($p = 0.001$). The result was confirmed by non-parametric analysis of the data.

The Spearman's rank correlation matrix, identified a further significant correlation: the AOD of the APP-junction probe was significantly negatively correlated with the insert:junction ratio ($p = 0.023$). Examination of a scatter diagram (Figure 5.34) did not support a correlation between these two variables.

In conclusion, it would appear that no significant inter-relationships exist between the APP oligodeoxynucleotide probes examined and the insert:junction ratio in hippocampal field CA3.

5.3.4.5.14 Correlations Between the APP-Insert, APP-Junction and APP-770 Oligodeoxynucleotide Probes in CA1

A Pearson's correlation matrix of 6 cells was constructed to examine the inter-relationship(s), if any, between the APP-insert, APP-junction and APP-770 oligodeoxynucleotide probes and the insert:junction ratio in CA1 (Table 5.22). Four significant correlations were identified, suggesting that the abundance of the mRNA species identified by the APP-insert, APP-junction and APP-770 probes, and the insert:junction ratio, in this region are meaningfully related.

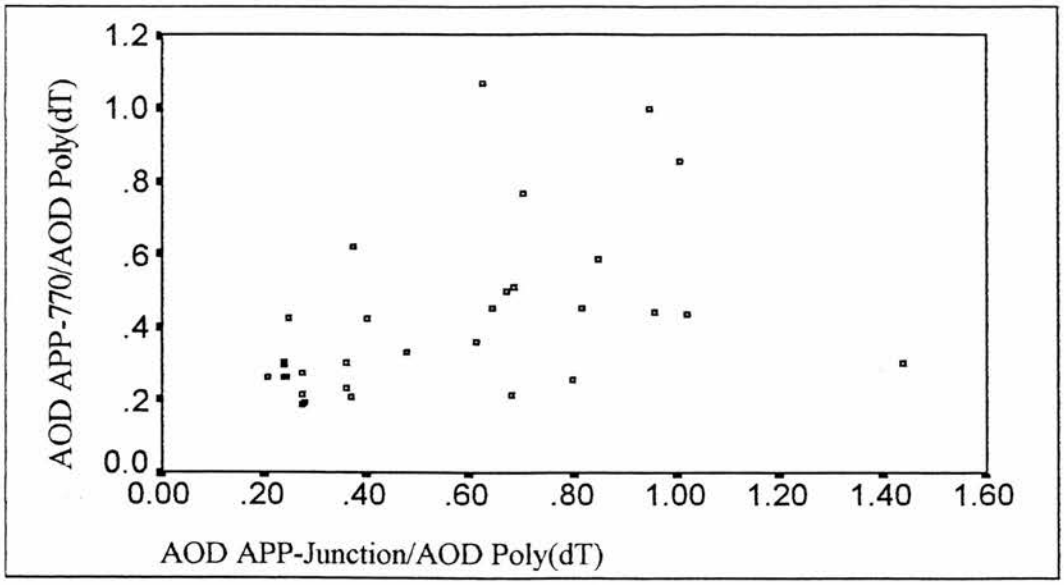

Figure 5.33 The Approximate Optical Density of the APP-Junction Oligodeoxynucleotide Probe when Expressed as a Proportion of the Approximate Optical Density of the Poly(dT) Oligodeoxynucleotide Probe Plotted Against the Approximate Optical Density of the APP-770 Oligodeoxynucleotide Probe when Expressed as a Proportion of the Approximate Optical Density of the Poly(dT) Oligodeoxynucleotide Probe in Series III (OPTIMA) Visual Cortex

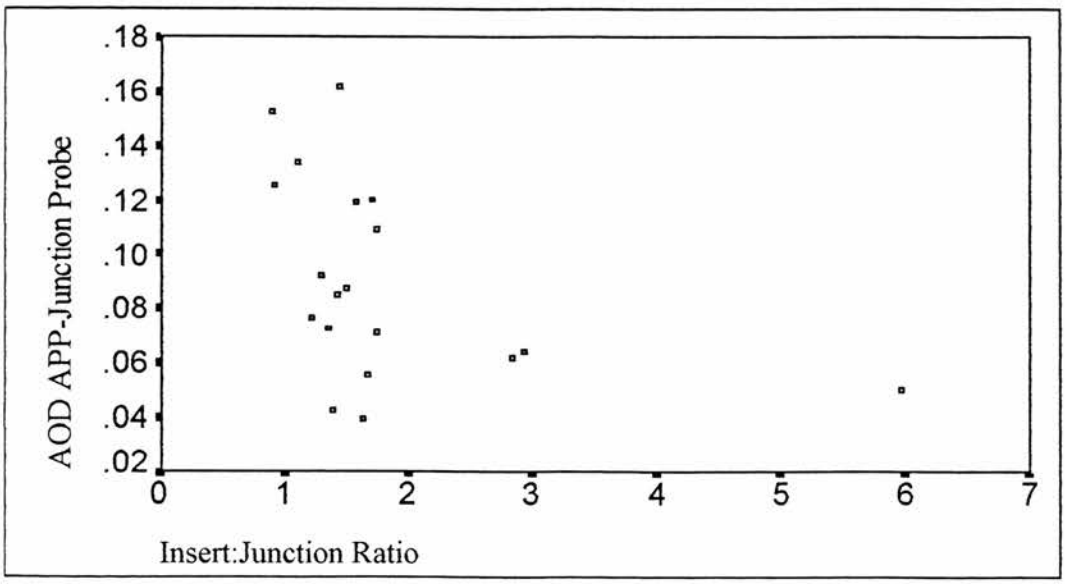

Figure 5.34 The Insert:Junction Ratio Plotted Against the Approximate Optical Density of the APP-Junction Oligodeoxynucleotide Probe in Hippocampal Subfield CA3 for Series III (OPTIMA) Cases

Table 5.22 Pearson's Correlation Coefficients for Series III (OPTIMA) Hippocampal CA1 Data				
	APP-770 Probe (Whole HC)	**APP-Insert Probe**	**APP-Junction Probe**	**Insert:Junction Ratio**
APP-770 Probe (Whole HC)	1.000 (n = 27) p =	0.458 (n = 23) **p = 0.028**	0.006 (n = 21) p = 0.979	0.486 (n = 20) **p = 0.030**
APP-Insert Probe	0.458 (n = 23) **p = 0.028**	1.000 (n = 25) p =	0.512 (n = 21) **p = 0.018**	0.555 (n = 21) **p = 0.009**
APP-Junction Probe	0.006 (n = 21) p = 0.979	0.512 (n = 21) **p = 0.018**	1.000 (n = 22) p =	-0.397 (n = 21) p = 0.075
Insert:Junction Ratio	0.486 (n = 20) **p = 0.030**	0.555 (n = 21) **p = 0.009**	-0.397 (n = 21) p = 0.075	1.000 (n = 21) p =

The AOD of the APP-insert oligodeoxynucleotide probe was positively correlated with the AOD of the APP-junction oligodeoxynucleotide probe ($p = 0.018$). Non-parametric analysis revealed a p value of 0.111, suggesting that the non-parametric test lacked the power to establish this correlation. The AOD of the APP-insert oligodeoxynucleotide probe was also positively correlated with the AOD of the APP-770 probe ($p = 0.028$) and this result was confirmed on non-parametric analysis ($p = 0.020$).

The AOD of the APP-insert oligodeoxynucleotide probe was positively correlated with the insert:junction ratio (0.009) and this finding was confirmed on non-parametric analysis of the data. The AOD of the APP-770 oligodeoxynucleotide probe was positively correlated with the insert:junction ratio by parametric analysis alone ($p = 0.030$) and examination of a scatter diagram (Figure 5.35) revealed two outlying values as the likely source of the parametric correlation.

The AOD of the APP-junction oligodeoxynucleotide probe was negatively correlated with the insert:junction ratio on non-parametric analysis alone: examination of a scatter diagram (Figure 5.36) suggested that the two were not, in fact, correlated.

Thus, in hippocampal field CA1, as in the dentate gyrus, the AOD of the APP-insert oligodeoxynucleotide probe appears to dominate the insert:junction ratio.

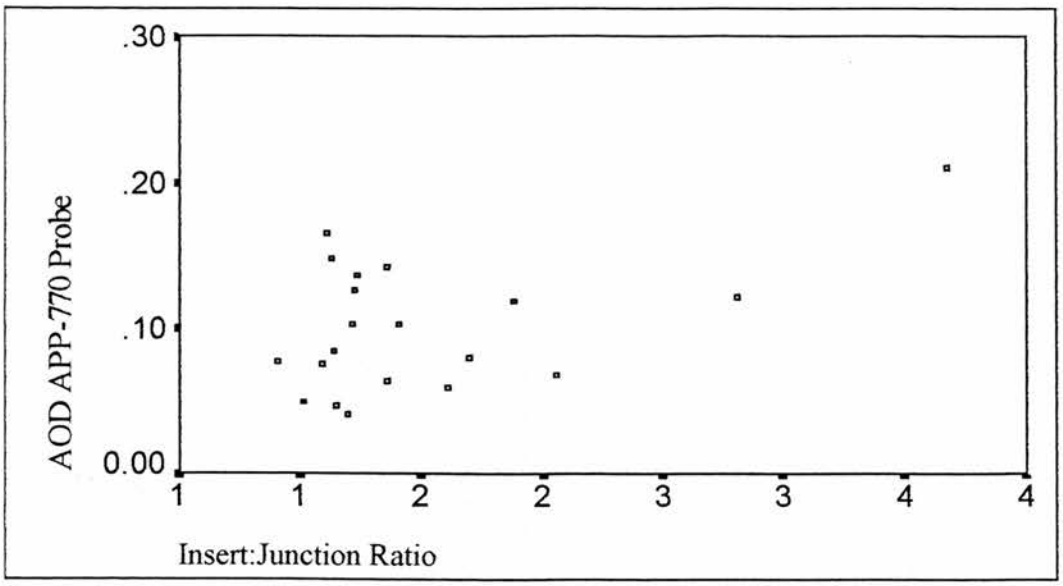

Figure 5.35 The Insert:Junction Ratio Plotted Against the Approximate Optical Density of the APP-770 Oligodeoxynucleotide Probe in Hippocampal Subfield CA1 for Series III (OPTIMA) Cases

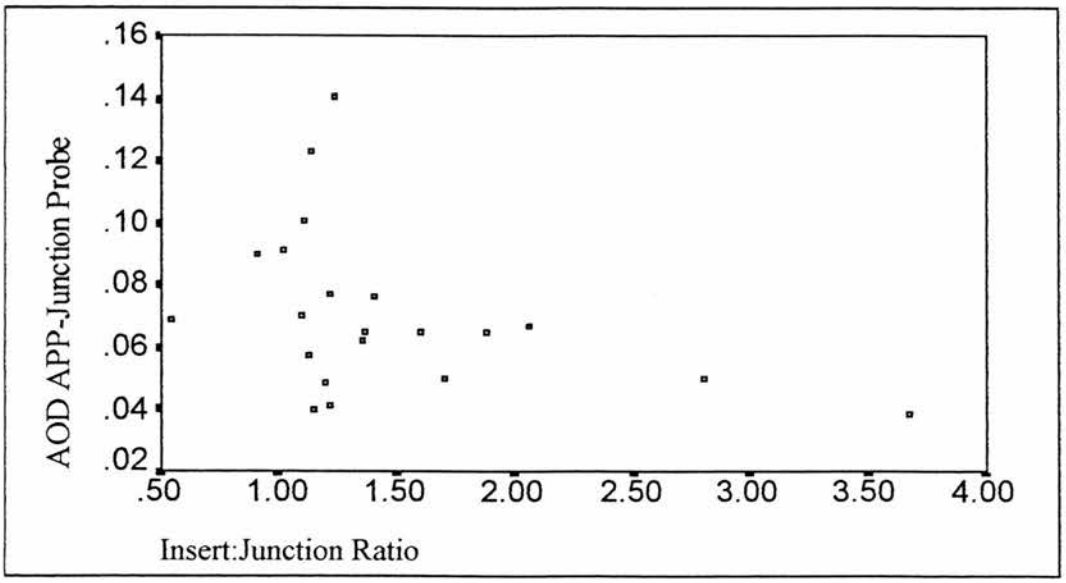

Figure 5.36 The Insert:Junction Ratio Plotted Against the Approximate Optical Density of the APP-Junction Oligodeoxynucleotide Probe in Hippocampal Subfield CA1 for Series III (OPTIMA) Cases

5.4.4 Series IV

5.4.4.1 Introduction

Analysis of series III (the OPTIMA series) led to the conclusion that the AOD of both the APP-insert and APP-junction oligodeoxynucleotide probes were correlated with agonal state. The insert:junction ratio, however, did not correlate with agonal state, implying that these two probes are equally affected by agonal state factors. This finding suggested that the insert:junction ratio could be of use where information regarding agonal state was absent, or inadequate.

Data generated by two other scientists, Dr. A.J.L. Barton and Dr. M.H. Griffiths, was combined with the data already generated during the course of this study to allow analysis of the insert:junction ratio in the visual cortex, dentate gyrus and hippocampal fields CA4, CA3 and CA1 of a larger number of normal and Alzheimer diseased brains.

A simple, two way ANOVA study, was designed, which would allow examination of the relative importance of diagnosis and the conduct of the individual experiments in determining the insert:junction ratio. To accommodate this study design, cases belonging to ambiguous diagnostic categories were removed from the four different data sets used, generating two groups of subjects: normal control subjects and subjects with unequivocal AD. To simplify interpretation of the results, an equal number of matched control and AD cases were selected from each data set for each brain area to be studied.

Control and AD cases where the insert:junction ratio had been measured in multiple brain areas were preferred, since they minimised inconsistency of case mix across the brain areas analysed. Similarly, as far as was possible, the cases selected from each individual data set were held constant across the different brain areas. Where a raw data set included an unequal number of control and AD subjects for a particular brain area, those where demographic details or information about PMI were missing, were excluded. If necessary, cases were then excluded with a view to matching the control and AD cases selected from each data set for sex, age and PMI. When it was no longer possible to exclude cases by these criteria, and the numbers of control and AD subjects remained unequal, subjects were randomly removed from the analysis. Demographic details, PMI and diagnosis of all of the cases included in this analysis, labelled series IV, are presented in appendix II. For each brain region the effects of diagnosis and experiment number on the insert:junction ratio was assessed. Subsequently, the age and sex of the subjects, and the PMI of the tissue employed, were included in the analysis and any discrepancies between the two analytical models analysed. However, since the control and AD cases included in this analysis were matched for age and PMI, extreme values of these variables tended to be excluded from the analysis. It was, therefore, impossible to assess the effects of age and PMI on the insert:junction ratio. Further, the total number of cases that could be analysed in this way remained relatively small. In order to increase the power of the analysis and examine the effects of age and PMI, the remaining control and AD cases belonging to the four series were included in a second statistical analysis effectively widening the range of ages and tissue post-mortem delay analysed. The

cases included in this second, unmatched analysis are listed under the appropriate brain area and marked with an asterisk.

The effect of age on the insert:junction ratio was of particular interest since a previous study conducted in Professor Pearson's laboratory (Heffernan, 1996) had demonstrated a significant positive relationship between the insert:junction ratio and age in a series of thirteen neurologically normal individuals whose ages varied from eighteen to ninety-three years.

The unmatched series were examined using a customised, sequential, two way ANOVA. The order of entry of the terms in the model was determined in advance and was fixed. Previous, thorough analysis suggested that the insert:junction ratio in the visual cortex and hippocampus was unlikely to be significantly affected by diagnosis, therefore, terms including the variables age, experiment number, PMI and sex were included before terms including the variable diagnosis. This model effectively excluded the effects of all other variables on the insert:junction ratio before considering the effects of diagnosis and lowered the probability of demonstrating a significant effect of diagnosis on the insert:junction ratio: a premeditated bias in the conduct of the analysis. Information on PMI was unavailable for some of the cases included in the unmatched series and where this occurred this variable was excluded from the analysis initially and then included to observe any alteration in the results.

5.4.4.2 Insert:Junction Ratio in Series IV Visual Cortex

Data from three independent experiments was combined to provide data on the insert:junction ratio in normal and Alzheimer diseased visual cortex. Fourteen cases from Dr. Barton's experiment, fourteen series III (the OPTIMA series) cases and twenty cases from series II, forty-eight cases in all, were included in the analysis (Table 5.23). Summarised demographic and post-mortem details of these cases are presented in table 5.24. Those cases marked with an asterisk represent those cases excluded from the matched series and subsequently included in the unmatched series.

The matched series was analysed first. Dr. Barton's control cases were significantly younger than her AD cases ($p = 0.010$), though there was no significant difference in PMI between her two diagnostic categories. No significant differences were identified between the control and AD cases selected from series II in terms of age and PMI, nor were any such differences identified between the control and AD cases selected from series III (the OPTIMA series).

The Cochran test for non-homogeneity of variance performed on the combined data set in visual cortex was significant ($p < 0.050$), suggesting that the requirements of the two way ANOVA had not been met. The data was transformed by raising the insert:junction ratio in visual cortex to the power of 0.1, whereupon the Cochran test became non-significant. A two way ANOVA performed on the combined, transformed data set revealed a significant effect of experiment number ($p = 0.011$),

Table 5.23 Series IV Visual Cortex		
Dr. Barton's Cases	**Series II Cases**	**Series III Cases (OPTIMA)**
107	S1	*C3452
109	S14	*C3970
1013	S20	C4017
1016	S23	C4295
1028	*S25	1174/91
1043	S27	*1250/91
1053	S28	1313/91
1063	S40	1381/91
1073	*S41	*1125/92
1078	*S42	1438/92
1079	S44	1127/93
1080	S46	1165/93
1081	S51	1306/93
1084	S53	1182/94
	*S65	1234/94
	S66	1252/94
	S69	1274/94
	S74	1340/94
	S78	*1445/94
	*S80	
	S82	
	S90	
	S96	
	*S100	
	H53	
	H81	

* Denotes cases added to series for unmatched analysis only.

Table 5.24 Series IV Visual Cortex - Matched Cases

Demographic and Post-Mortem Details of Cases Selected from Dr. A.J.L. Barton's Experiment

Diagnosis	Number of Cases	Sex	Age mean ± SD	Post-Mortem Delay in Hours mean ± SD
Controls	7	Male = 6 Female = 1	66.7 ± 8.7 (n = 7)	37.7 ± 30.7 (n = 7)
AD	7	Male = 3 Female = 4	81.3 ± 9.1 (n = 7)	34.1 ± 26.4 (n = 7)

Demographic and Post-Mortem Details of Cases Selected from Series II

Diagnosis	Number of Cases	Sex	Age mean ± SD	Post-Mortem Delay in Hours mean ± SD
Controls	10	Male = 5 Female = 5	76.5 ± 10.6 (n = 10)	35.7 ± 14.4 (n = 7)
AD	10	Male = 5 Female = 5	83.0 ± 7.0 (n = 10)	34.1 ± 18.1 (n = 10)

Demographic and Post-Mortem Details of Cases Selected from Series III - (OPTIMA Series)

Diagnosis	Number of Cases	Sex	Age mean ± SD	Post-Mortem Delay in Hours mean ± SD
Controls	7	Male = 5 Female = 2	77.4 ± 7.9 (n = 7)	38.7 ± 19.9 (n = 7)
AD	7	Male = 5 Female = 2	75.3 ± 8.3 (n = 7)	39.3 ± 8.5 (n = 7)

but no effect of diagnosis ($p = 0.050$), on the insert:junction ratio (Figure 5.37). The ages of the subjects and the PMI of the tissue were then added to the model as covariates and the sex of the subjects included in the model as a factor. Only forty-five cases were analysed, since PMI data was absent for three cases. The Cochran test was non-significant. A significant effect was demonstrated for experiment number ($p = 0.013$), but not for diagnosis ($p = 0.259$), on the insert:junction ratio in visual cortex. A significant interaction was also demonstrated between diagnosis and sex ($p = 0.029$) for the transformed insert:junction ratio. Analysis of the data revealed that the mean, transformed insert:junction ratio was 0.98 for both the thirteen male AD and sixteen male control cases and, moreover, the dispersion of the insert:junction ratio was similar in these two groups (standard deviations of 0.04 and 0.05 respectively). However, the mean, transformed insert:junction ratio of the eleven female AD cases was 1.02 with a standard deviation of 0.06, whereas the mean, transformed insert:junction ratio of the eight female control cases was 0.94 with a standard deviation of 0.05. Thus, though there is no significant effect of sex or diagnosis alone on the transformed insert:junction ratio, female AD and control cases do behave differently from their male counterparts in terms of transformed insert:junction ratio, for reasons that are unclear. Understandably, the effect of age and PMI in predicting the insert:junction ratio was not significant in this carefully matched series.

Data on the insert:junction ratio in the visual cortex of six additional cases from series II and five additional cases from series III (the OPTIMA series) was then

Figure 5.37 APP-Insert to APP-Junction Ratio in Series IV Visual Cortex in Alzheimer's Diseased Versus Control Brains (Matched Series)

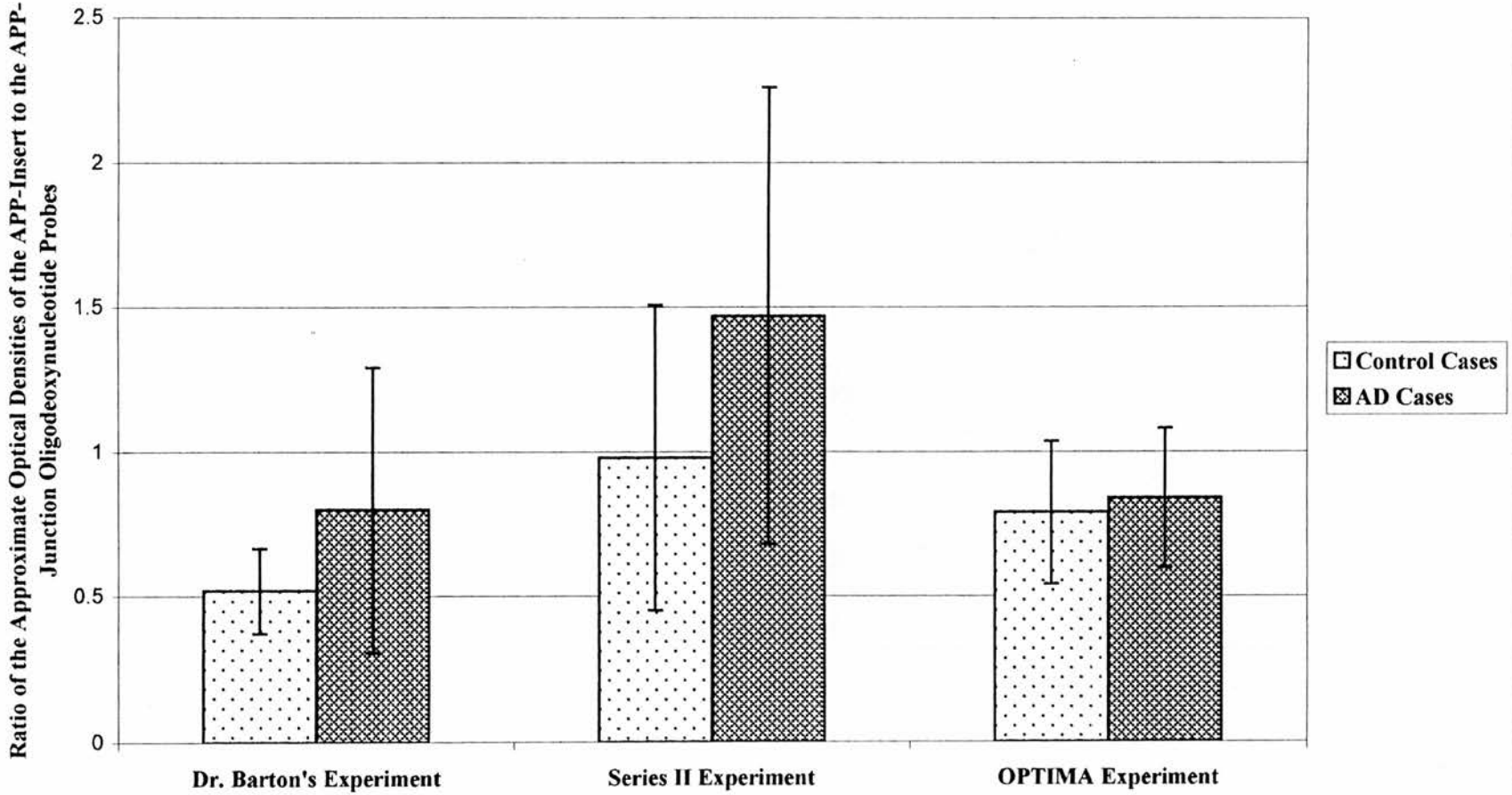

added to the series. No additional cases were available from Dr. A.J.L. Barton's series. These cases are marked by an asterisk in table 5.23.

The insert:junction ratio was examined in the visual cortex of the fifty-nine unmatched series IV cases using the customised, sequential, two way ANOVA. However, the Cochran test for non-homogeneity of variance was significant suggesting that the requirements of the two way ANOVA had not been met. Therefore, the data was transformed, as above, by raising the insert:junction ratio to the power of 0.1, whereupon the Cochran test became non-significant. The covariate PMI was excluded from the analysis initially, since this information was not available for five of the cases included in the study. A significant effect on the transformed insert:junction ratio was demonstrated for age ($p < 0.001$) and experiment number ($p = 0.008$), but not for diagnosis ($p = 0.229$). The terms 'age and diagnosis' ($p = 0.047$), 'diagnosis and sex' ($p = 0.014$) and 'age, diagnosis and sex' ($p = 0.013$), also had significant effects on the transformed insert:junction ratio. In the unmatched series the AD cases tended to be older (mean ± standard deviation = 81.7 ± 8.4 years) than the controls (mean ± standard deviation = 73.9 ± 10.1 years) and, of course, age is strongly positively correlated with the transformed insert:junction ratio. Analysis of the cohort by diagnosis and sex revealed that, inexplicably, while the male AD cases were older (mean ± standard deviation = 78.5 ± 7.0 years) than the male controls (mean ± standard deviation = 72.4 ± 10.6 years) the mean, transformed insert:junction ratio of the two groups was equal (0.98) and their dispersion was similar (standard deviation of control cases = 0.05; standard

deviation of AD cases = 0.04). The female AD cases were also older (mean ± standard deviation = 83.7 ± 9.0 years) than the female control cases (mean ± standard deviation = 77.0 ± 9.0 years) however, the mean, transformed insert:junction ratio differed between the two groups (mean ± standard deviation of AD cases = 1.02 ± 0.05; mean ± standard deviation of control cases = 0.94 ± 0.05). Thus, females with AD behave differently in terms of transformed insert:junction ratio than do males with AD, for reasons that are unclear. When the analysis was repeated including PMI in the model, only the terms 'age' ($p < 0.000$), 'trial' ($p = 0.011$) and 'age and sex' ($p = 0.027$) were significant. The Cochran test was not significant.

5.4.4.3 Insert:Junction Ratio in Series IV Hippocampus

5.4.4.3.1 Insert:Junction Ratio in Series IV Dentate Gyrus

A total of thirty-eight cases were used to analyse the effect of diagnosis and experiment number on the insert:junction ratio in the dentate gyrus. The cases comprised fourteen cases from Dr. Barton's series, twelve cases from series III (the OPTIMA series) and twelve cases from Dr. Griffiths's series (Table 5.25). Summarised demographic and post-mortem details of the cases used are presented in table 5.26. Those cases marked with an asterisk represent those cases excluded from the matched series and subsequently included in the unmatched series. The cases selected from each series for the matched analysis did not differ significantly in terms of age or PMI.

Table 5.25 Series IV Dentate Gyrus		
Dr. Barton's Cases	**Dr. Griffiths's Cases**	**Series III Cases (OPTIMA)**
109	835	C4017
1011	986	C4295
1013	1010	1174/91
1028	1015	1381/91
*1043	1022	1438/92
1045	1029	1127/93
1053	1050	1306/93
1058	1289	1182/94
1063	*1419	1234/94
*1066	1590	*1252/94
1072	1639	1274/94
1073	1790	1340/94
1074	7292	*1445/94
1078		1004/95
1079		
1080		
*1081		

* Denotes cases added to series for unmatched analysis only.

Table 5.26 Series IV Dentate Gyrus - Matched Cases

Demographic and Post-Mortem Details of Cases Selected from Dr. A.J.L. Barton's Experiment

Diagnosis	Number of Cases	Sex	Age Mean ± SD	Post-Mortem Delay in Hours mean ± SD
Controls	7	Male = 4 Female = 3	72.1 ± 15.3 (n = 7)	38.7 ± 30.4 (n = 7)
AD	7	Male = 4 Female = 3	78.3 ± 9.3 (n = 7)	34.1 ± 26.3 (n = 7)

Demographic and Post-Mortem Details of Cases Selected from Dr. M.H. Griffiths's Experiment

Diagnosis	Number of Cases	Sex	Age mean ± SD	Post-Mortem Delay in Hours mean ± SD
Controls	6	Male = 4 Female = 2	79.2 ± 7.5 (n = 6)	34.2 ± 15.3 (n = 6)
AD	6	Male = 1 Female = 5	80.2 ± 4.8 (n = 6)	37.3 ± 20.3 (n = 6)

Demographic and Post-Mortem Details of Cases Selected from Series III - (OPTIMA Series)

Diagnosis	Number of Cases	Sex	Age mean ± SD	Post-Mortem Delay in Hours mean ± SD
Controls	6	Male = 4 Female = 2	75.8 ± 7.4 (n = 6)	38.0 ± 21.7 (n = 6)
AD	6	Male = 4 Female = 2	77.0 ± 6.0 (n = 6)	38.7 ± 9.0 (n = 6)

The Cochran test for used to analyse the matched series for non-homogeneity of variance and was not significant ($p = 0.910$). A two way ANOVA did not demonstrate any significant effects of diagnosis or experiment number, nor any interaction between the two, on the insert:junction ratio in the dentate gyrus of series IV (Figure 5.38). The inclusion of sex, as a factor, and age and PMI, as covariates, did not alter the conclusions of the two way ANOVA in the dentate gyrus.

Three cases from Dr. Barton's series, one case from Dr. Griffiths's series and two cases from series III (the OPTIMA series) were added to examine the effects of age and PMI on the insert:junction ratio in dentate gyrus. The customised, sequential, two way ANOVA was used to examine the forty-four cases unmatched cases. The covariate PMI was not included initially since this data was not available for one case. The Cochran test was not significant. The term 'age and diagnosis' was the only one to achieve significance ($p = 0.010$). The procedure was then repeated including PMI as a covariate. The Cochran test for non-homogeneity of variance was not significant and the terms 'age and diagnosis' and 'age, diagnosis and trial' achieved significance ($p = 0.017$ and $p = 0.037$ respectively). On a scatter diagram (Figure 5.39) it was clear that the youngest controls tended to have the lowest insert:junction ratios and the AD cases tended to be older (mean ± standard deviation = 78.3 ± 7.98 years) than the controls (mean ± standard deviation = 73.6 ± 11.1 years). Furthermore, in this unmatched series the youngest subgroup represents the control subjects in Dr. Barton's experiment (mean ± standard deviation = 70.8 ±

Figure 5.38 APP-Insert to APP-Junction Ratio in Series IV Dentate Gyrus in Alzheimer's Diseased Versus Control Brains (Matched Series)

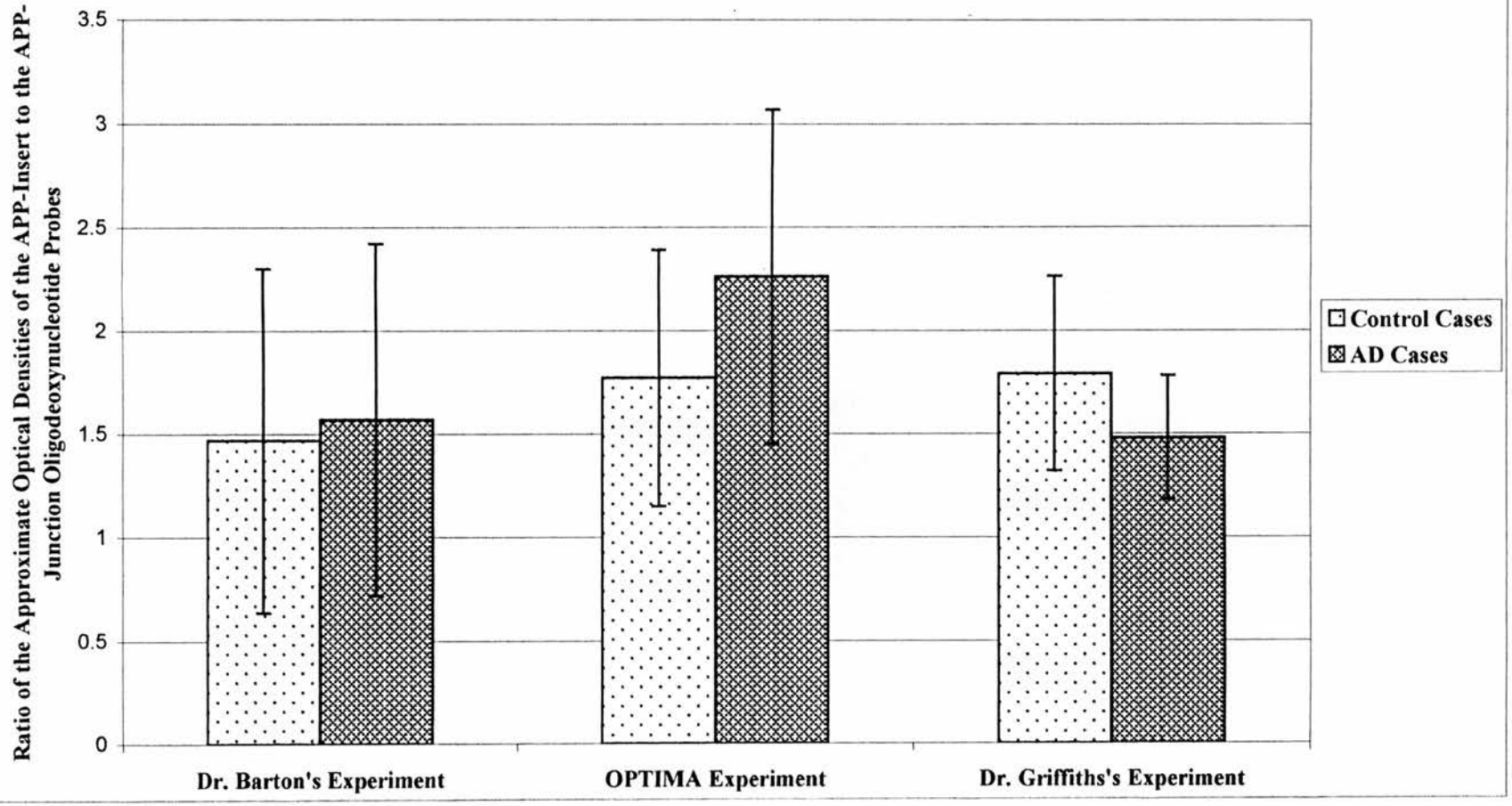

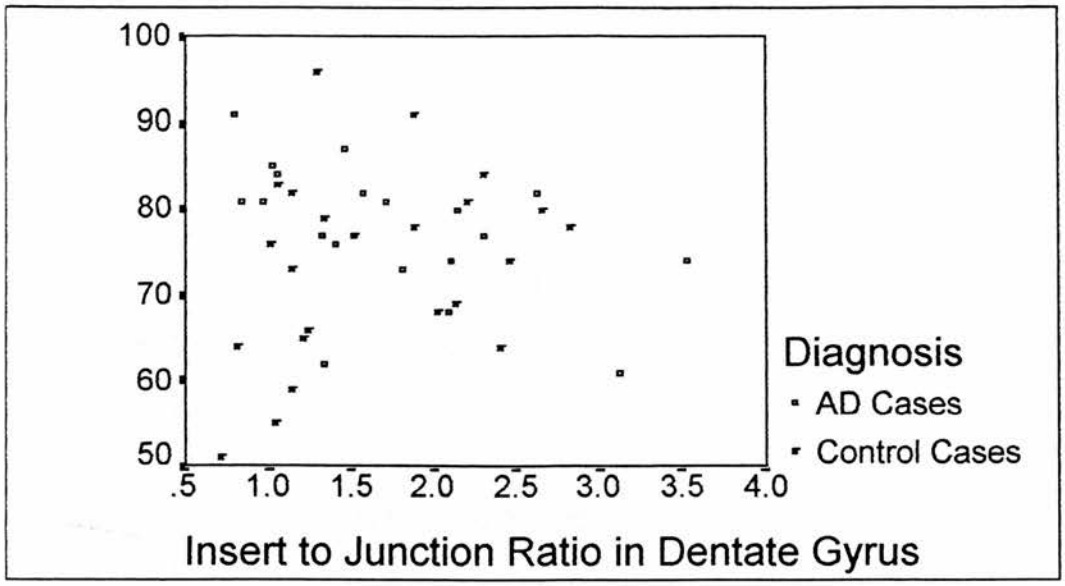

5.39 Age Plotted Against the APP-Insert to APP-Junction Ratio in the Dentate Gyrus of Series IV Alzheimer Diseased and Control Brains (Unmatched Series)

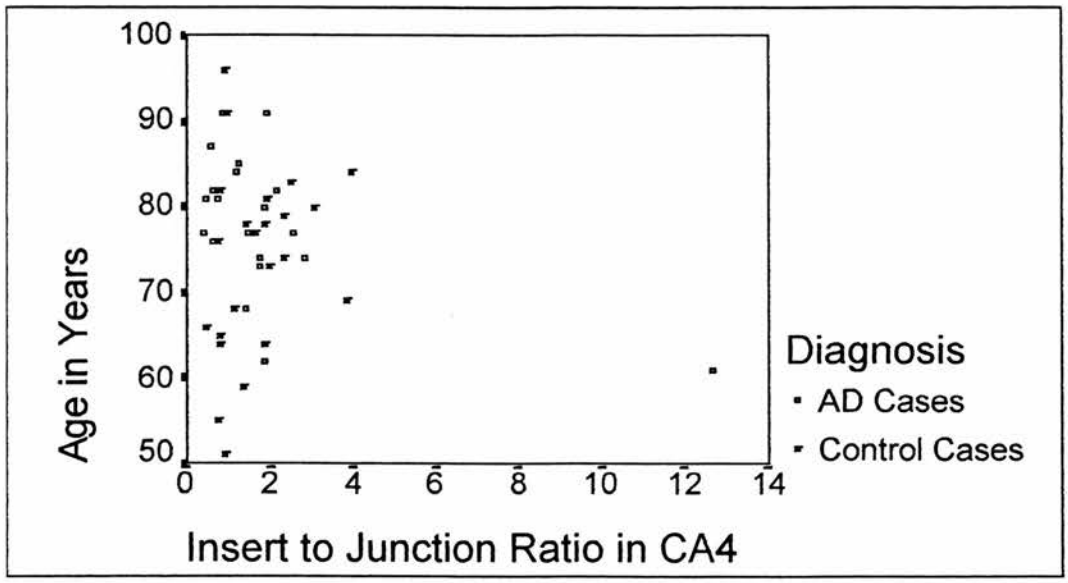

Figure 5.41 Age Plotted Against the APP-Insert to APP-Junction Ratio in Hippocampal Subfield CA4 of Series IV Alzheimer Diseased and Control Brains (Unmatched Series)

12.9 years), while the oldest subgroup is the AD subjects in Dr. Griffiths's experiment (mean ± standard deviation = 80.2 ± 4.8 years). It is likely that it is this discrepancy in ages between the subgroups that is responsible for the significant effect of 'age, diagnosis and trial' on the insert:junction ratio.

5.4.4.3.2 Insert:Junction Ratio in Series IV Hippocampal CA4 Field

The insert:junction ratio in CA4 was analysed using fourteen cases from Dr. Barton's series, twelve cases from series III (the OPTIMA series) and ten cases from Dr. Griffiths's series, a total of thirty-six cases (Table 5.27). Summarised demographic and post-mortem details of these cases are presented in table 5.28. Those cases marked with an asterisk represent those cases excluded from the matched series and subsequently included in the unmatched series. The cases selected from each series for the matched analysis did not differ significantly in terms of age or PMI.

On analysis of the matched series the Cochran test was significant ($p < 0.001$), suggesting that the requirements of the two way ANOVA were not met. The insert:junction ratio in CA4 was transformed by raising each value to the power of negative 0.7. The Cochran test on the transformed data was not significant ($p > 0.082$). No significant effect of diagnosis (Figure 5.40) or experiment number on the transformed insert:junction ratio in CA4, nor any significant interaction between the two, was demonstrated using the two way ANOVA. The inclusion of sex, as a factor, and age and PMI, as covariates, resulted in the term 'sex, diagnosis and experiment number' achieving significance ($p = 0.044$). Analysing the transformed

Table 5.27 Series IV Hippocampal CA4		
Dr. Barton's Cases	**Dr. Griffiths's Cases**	**Series III Cases (OPTIMA)**
109	835	C4017
1011	986	C4295
1013	*1010	1174/91
1028	1015	1381/91
*1043	1022	1438/92
1045	1029	1127/93
1053	1050	1306/93
1058	1289	1182/94
1063	*1419	1234/94
*1066	1639	*1252/94
1072	1790	1274/94
1073	7292	1340/94
1074		*1445/94
1078		1004/95
1079		
1080		
*1081		

* Denotes cases added to series for unmatched analysis only.

Table 5.28 Series IV Hippocampal CA4 - Matched Cases

Demographic and Post-Mortem Details of Cases Selected from Dr. A.J.L. Barton's Experiment

Diagnosis	Number of Cases	Sex	Age Mean ± SD	Post-Mortem Delay in Hours mean ± SD
Controls	7	Male = 4 Female = 3	72.1 ± 15.3 (n = 7)	38.7 ± 30.4 (n = 7)
AD	7	Male = 4 Female = 3	78.3 ± 9.3 (n = 7)	34.1 ± 26.3 (n = 7)

Demographic and Post-Mortem Details of Cases Selected from Dr. M.H. Griffiths's Experiment

Diagnosis	Number of Cases	Sex	Age mean ± SD	Post-Mortem Delay in Hours Mean ± SD
Controls	5	Male = 3 Female = 2	78.2 ± 8.0 (n = 5)	39.4 ± 9.4 (n = 5)
AD	5	Male = 1 Female = 4	80.0 ± 5.3 (n = 5)	37.2 ± 22.7 (n = 5)

Demographic and Post-Mortem Details of Cases Selected from Series III - (OPTIMA Series)

Diagnosis	Number of Cases	Sex	Age mean ± SD	Post-Mortem Delay in Hours mean ± SD
Controls	6	Male = 4 Female = 2	75.8 ± 7.4 (n = 6)	38.0 ± 21.7 (n = 6)
AD	6	Male = 4 Female = 2	77.0 ± 6.0 (n = 6)	38.7 ± 9.0 (n = 6)

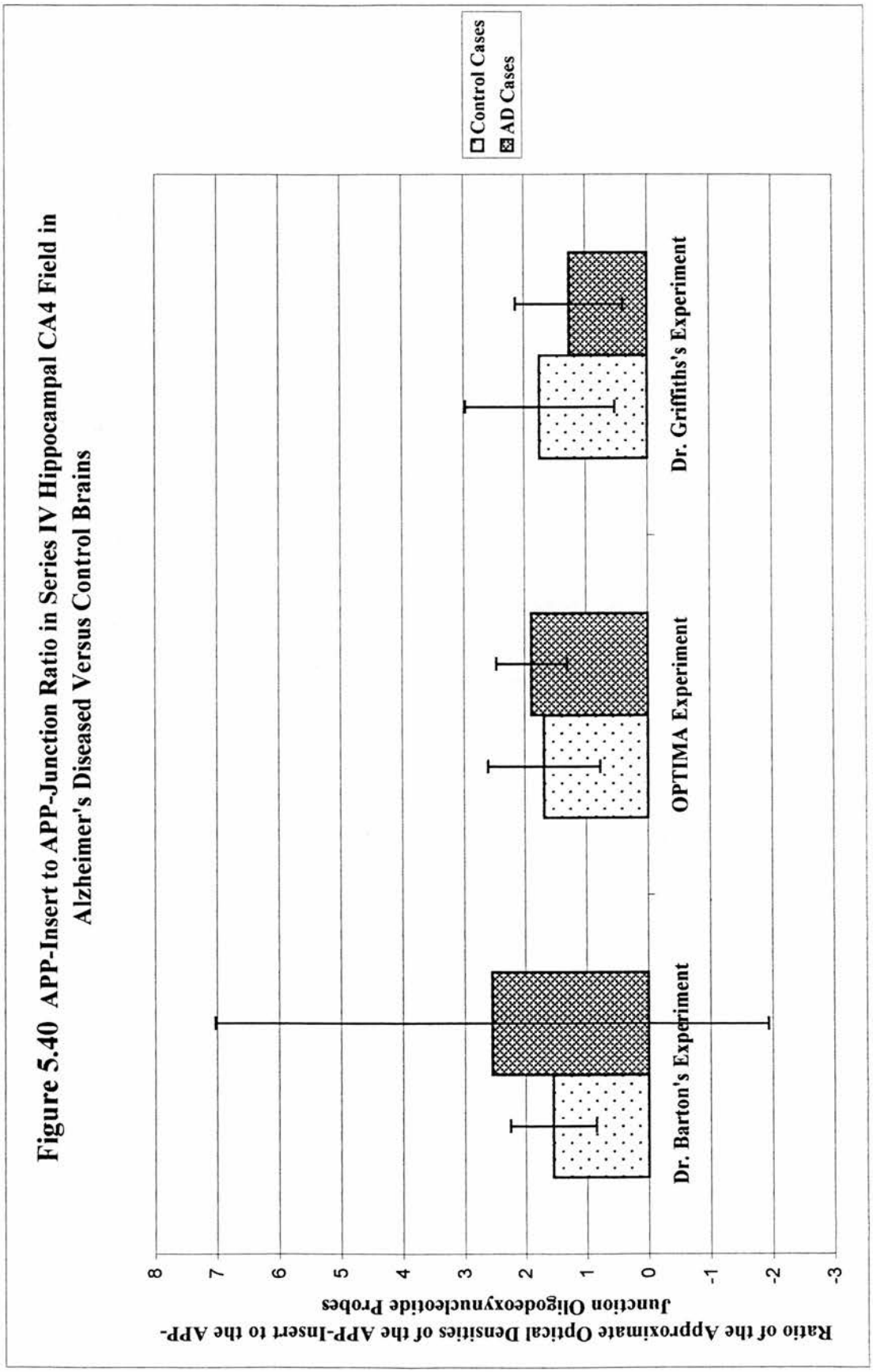

Figure 5.40 APP-Insert to APP-Junction Ratio in Series IV Hippocampal CA4 Field in Alzheimer's Diseased Versus Control Brains

insert:junction ratio by experiment number, diagnosis and sex revealed that the subgroup with the highest transformed insert:junction ratio was the female AD subjects in Dr. Barton's experiment (mean ± standard deviation = 1.40 ± 0.30), while the subgroup with the lowest transformed insert:junction ratio was the female control subjects in the series III (the OPTIMA series) experiment (mean ± standard deviation = 0.54 ± 0.12). The term 'sex, diagnosis and experiment number' resulted in subgroups of subjects that behave differently from one another in terms of transformed insert:junction ratio.

Three cases were added from Dr. Barton's series, two cases from series III (the OPTIMA series) and two cases from Dr. Griffiths's series in order to examine the effect of age and PMI on the insert:junction ratio in CA4. This unmatched series of forty-three cases were analysed using the customised, sequential, two way ANOVA. PMI was excluded from the model initially since this would have resulted in the loss of one case for which no data on PMI was available. The Cochran test was significant for the insert:junction ratio in CA4 and the insert:junction ratio was therefore transformed by raising each value to the power of negative 0.7: the same transformation as was performed on the matched series. Unfortunately, the Cochran test remained significant for the insert:junction ratio transformed in this way. Examination of a scatter diagram of the insert:junction ratio in CA4 plotted against age revealed a massively outlying value for the insert:junction ratio among Dr. Barton's cases (Figure 5.41). On exclusion of this case, transforming the remaining insert:junction ratios in CA4 by logging to the base 10 resulted in homogeneity of

variance as analysed by the Cochran test. PMI was excluded from the analysis initially, since this information was not available for one case. Using the customised, sequential, two way ANOVA none of the variables examined had a significant effect on the transformed insert:junction ratio in CA4. When PMI was added to the model as a covariate, two terms, 'PMI and experiment number' and 'age, diagnosis and experiment number', achieved significance ($p = 0.022$ and $p = 0.026$ respectively). While the mean PMI was similar for all three experiments, Dr. Barton's experiment showed the greatest dispersion in PMI exhibiting both the longest and shortest PMIs in the series and the lowest mean transformed insert:junction ratio. The mean PMI of series III (the OPTIMA series) (mean ± standard deviation = 38.00 ± 15.18) was similar to that of Dr. Griffiths's series (mean ± standard deviation = 34.58 ± 17.52) and the dispersion of PMIs was similar in both. The mean transformed insert:junction ratios calculated for these two series, however, were very different (series III (the OPTIMA series) mean ± standard deviation = 0.22 ± 0.18; Dr. Griffiths's series mean ± standard deviation = 0.12 ± 0.30). Thus, similar values for PMI are associated with different transformed insert:junction ratios in experiments carried out by different researchers.

The significance of the term 'age, diagnosis and experiment number' was examined in the unmatched series. The transformed insert:junction ratio in CA4 of AD series III (OPTIMA) cases was higher than that for control series III cases. In contrast, in Dr. Barton and Dr. Griffiths's experiments, the transformed insert:junction ratio was lower in the AD cases than the controls. Further, the AD and control cases included

in series III (the OPTIMA series) are well matched in terms of age, while in the other two experiments the AD cases are older than the controls. Thus, in series III (the OPTIMA series), cases of similar ages, but different diagnostic groups, differ in their transformed insert:junction ratio, unlike cases of a similar age in either of the other two experiments.

5.4.4.3.3 Insert:Junction Ratio in Series IV Hippocampal CA3 Field

A total of thirty-two cases were processed in a two way ANOVA to examine the insert:junction ratio in CA3. Fourteen cases from Dr. Barton's Series, eight cases from series III (the OPTIMA series) and ten Cases from Dr. Griffiths's series were included. The case numbers of the brains selected from each series are presented in table 5.29 and the demographic and post-mortem details of the cases used are summarised in table 5.30. Those cases marked with an asterisk represent those cases excluded from the matched series and subsequently included in the unmatched series. The matched control and AD cases, selected from each series, did not differ significantly in age or PMI.

The Cochran test was not significant for the insert:junction ratio of this matched series, suggesting that the requirements of the two way ANOVA were satisfied. No significant effects of diagnosis (Figure 5.42) or experiment number could be demonstrated on the insert:junction ratio in CA3, nor any significant interaction between these factors, using this test. The inclusion of the age of the subjects, their

Table 5.29 Series IV Hippocampal CA3		
Dr. Barton's Cases	**Dr. Griffiths's Cases**	**Series III Cases (OPTIMA)**
109	835	C4017
1011	986	1174/91
1013	*1010	1381/91
1028	1015	1127/93
*1043	1022	1306/93
1045	1029	1182/94
1053	1050	*1234/94
1058	1289	1274/94
1063	1639	*1340/94
*1066	1790	1004/95
1072	7292	
1073		
1074		
1078		
1079		
1080		

* Denotes cases added to series for unmatched analysis only.

Table 5.30 Series IV Hippocampal CA3 - Matched Cases

Demographic and Post-Mortem Details of Cases Selected from Dr. A.J.L. Barton's Experiment

Diagnosis	Number of Cases	Sex	Age Mean ± SD	Post-Mortem Delay in Hours mean ± SD
Controls	7	Male = 4 Female = 3	72.1 ± 15.3 (n = 7)	38.7 ± 30.4 (n = 7)
AD	7	Male = 4 Female = 3	78.3 ± 9.3 (n = 7)	34.1 ± 26.3 (n = 7)

Demographic and Post-Mortem Details of Cases Selected from Dr. M.H. Griffiths's Experiment

Diagnosis	Number of Cases	Sex	Age mean ± SD	Post-Mortem Delay in Hours Mean ± SD
Controls	5	Male = 3 Female = 2	78.2 ± 8.0 (n = 5)	39.4 ± 9.4 (n = 5)
AD	5	Male = 1 Female = 4	80.0 ± 5.3 (n = 5)	37.2 ± 22.7 (n = 5)

Demographic and Post-Mortem Details of Cases Selected from Series III - (OPTIMA Series)

Diagnosis	Number of Cases	Sex	Age mean ± SD	Post-Mortem Delay in Hours Mean ± SD
Controls	4	Male = 2 Female = 2	76.2 ± 7.5 (n = 4)	42.0 ± 24.6 (n = 4)
AD	4	Male = 2 Female = 2	76.0 ± 6.3 (n = 4)	39.2 ± 11.5 (n = 4)

Figure 5.42 APP-Insert to APP-Junction Ratio in Series IV Hippocampal CA3 Field in Alzheimer's Diseased Versus Control Brains

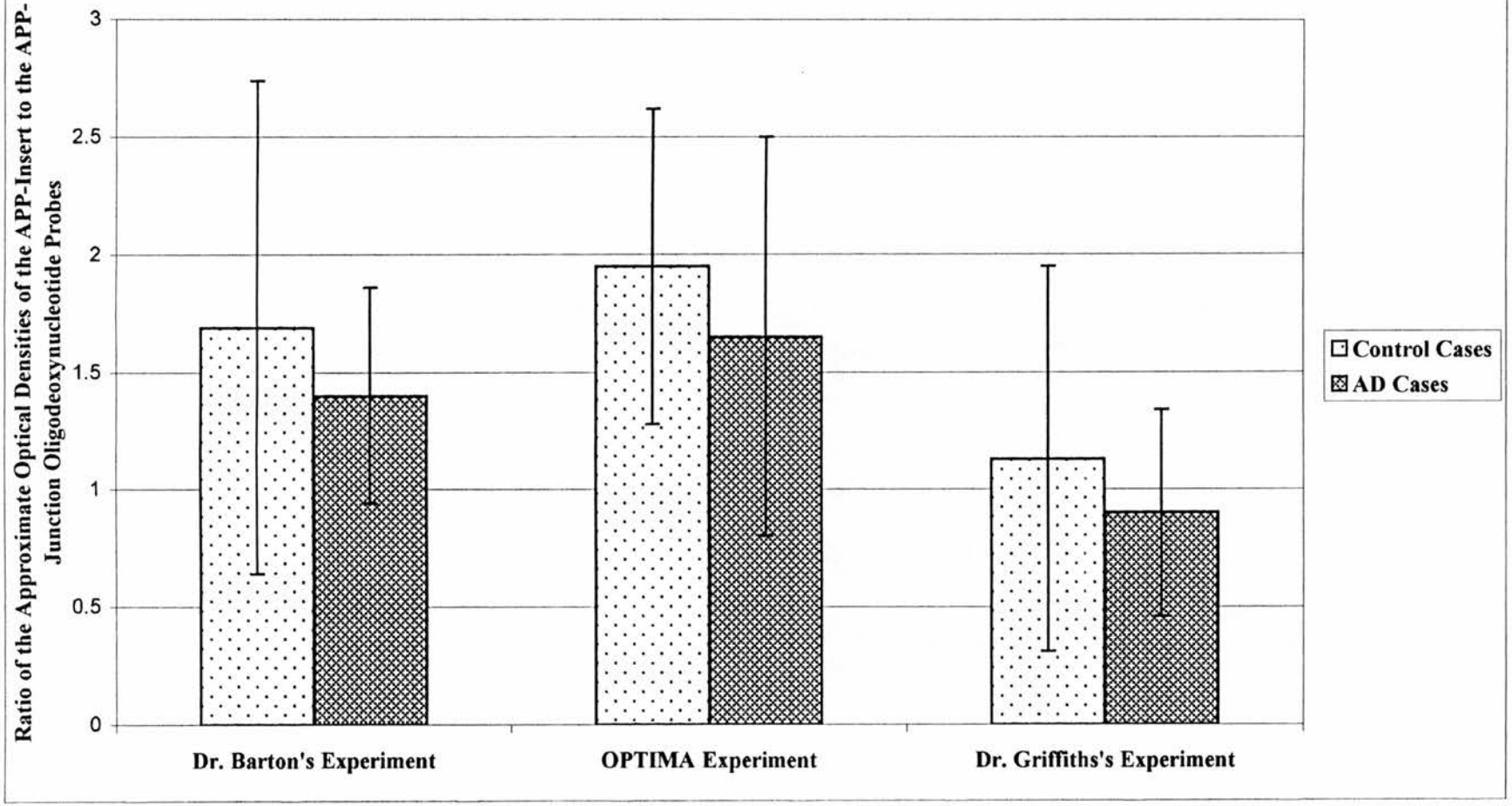

sex, and the tissue PMI, in analysing the insert:junction ratio in CA3 did not alter the conclusions of the two way ANOVA.

Two cases were added from Dr. Barton's series, one case from Dr. Griffiths's series and two cases from series III (the OPTIMA series) in order to examine the effects of age and PMI on an unmatched series. The Cochran test was not significant. A complete data set was available for all thirty-seven cases and therefore the customised, sequential two way ANOVA was performed to examine the effects of age, experiment number, sex, PMI and diagnosis, or any interaction between these variables, on the insert:junction ratio in CA3. The only term to achieve significance was 'age and diagnosis' ($p = 0.042$). On closer inspection of the data, it appeared that the older AD subjects tended to have lower insert:junction ratios than younger AD subjects but this was not true for the control subjects for whom no pattern in relation to age could be discerned. Thus, for reasons that are unclear, elderly AD and control subjects appear to behave differently in terms of their insert:junction ratio.

5.4.4.3.4 Insert:Junction Ratio in Series IV Hippocampal CA1 Field

The insert:junction ratio in CA1 was analysed in twenty-six cases in total, eight cases from Dr. Barton's series, eight cases from series III (the OPTIMA series) and ten cases from Dr. Griffiths's series. The case numbers of the brains selected from each series are presented in table 5.31 and the demographic and post-mortem details of the cases used are summarised in table 5.32. Those cases marked with an asterisk represent those cases excluded from the matched series and subsequently included in

Table 5.31 Series IV Hippocampal CA1		
Dr. Barton's Cases	**Dr. Griffiths's Cases**	**Series III Cases (OPTIMA)**
1028	**835**	**1174/91**
1045	**986**	**1381/91**
1053	***1010**	**1438/92**
1058	**1022**	**1127/93**
1063	**1029**	**1306/93**
***1066**	**1050**	**1182/94**
***1072**	**1289**	***1234/94**
***1074**	***1419**	**1274/94**
1078	**1639**	***1340/94**
1079	**1590**	**1004/95**
1080	**1790**	
	7292	

* Denotes cases added to series for unmatched analysis only.

Table 5.32 Series IV Hippocampal CA1 - Matched Series

Demographic and Post-Mortem Details of Cases Selected from Dr. A.J.L. Barton's Experiment

Diagnosis	Number of Cases	Sex	Age Mean ± SD	Post-Mortem Delay in Hours mean ± SD
Controls	4	Male = 2 Female = 2	71.2 ± 19.0 (n = 4)	32.5 ± 24.8 (n = 4)
AD	4	Male = 2 Female = 2	79.5 ± 13.0 (n = 4)	19.8 ± 14.1 (n = 4)

Demographic and Post-Mortem Details of Cases Selected from Dr. M.H. Griffiths's Experiment

Diagnosis	Number of Cases	Sex	Age mean ± SD	Post-Mortem Delay in Hours Mean ± SD
Controls	5	Male = 3 Female = 2	78.2 ± 8.0 (n = 5)	39.4 ± 9.4 (n = 5)
AD	5	Male = 1 Female = 4	80.8 ± 5.0 (n = 5)	40.0 ± 21.5 (n = 5)

Demographic and Post-Mortem Details of Cases Selected from Series III - (OPTIMA Series)

Diagnosis	Number of Cases	Sex	Age mean ± SD	Post-Mortem Delay in Hours Mean ± SD
Controls	4	Male = 2 Female = 2	76.2 ± 7.5 (n = 4)	42.0 ± 24.6 (n = 4)
AD	4	Male = 2 Female = 2	74.0 ± 4.9 (n = 4)	40.0 ± 11.3 (n = 4)

the unmatched series. The control and AD cases selected from each series did not differ significantly in terms of age or PMI.

On analysis of the matched series, the Cochran test for homogeneity of variance was significant ($p < 0.05$) for the insert:junction ratio in CA1, suggesting that the requirements of the two way ANOVA were not met. The log 10 of the insert:junction ratio in CA1 was calculated in an attempt to compress the scale and normalise the data. The Cochran test performed on the log 10 (insert:junction ratio) was not significant, and a two way ANOVA did not demonstrate any significant effects of diagnosis (Figure 5.43) or experiment number on the insert:junction ratio in CA1, nor any significant interaction between the two. The inclusion of the age of the subjects, their sex, or the PMI of the tissue did not alter the findings, using this model, in CA1.

Three cases were added from Dr. Barton's series, two cases from series III (the OPTIMA series) and two cases from Dr. Griffiths's series and a customised, sequential two way ANOVA was performed on the thirty-three unmatched cases with data for the insert:junction ratio in CA1. The Cochran test was significant ($p = 0.001$) therefore the insert:junction ratio in CA1 was transformed according to the formula 1/insert:junction ratio. The Cochran test performed on the transformed data was non-significant and no significant effects of age, sex, experiment number, PMI or diagnosis on the transformed insert:junction ratio were apparent using this model in this region.

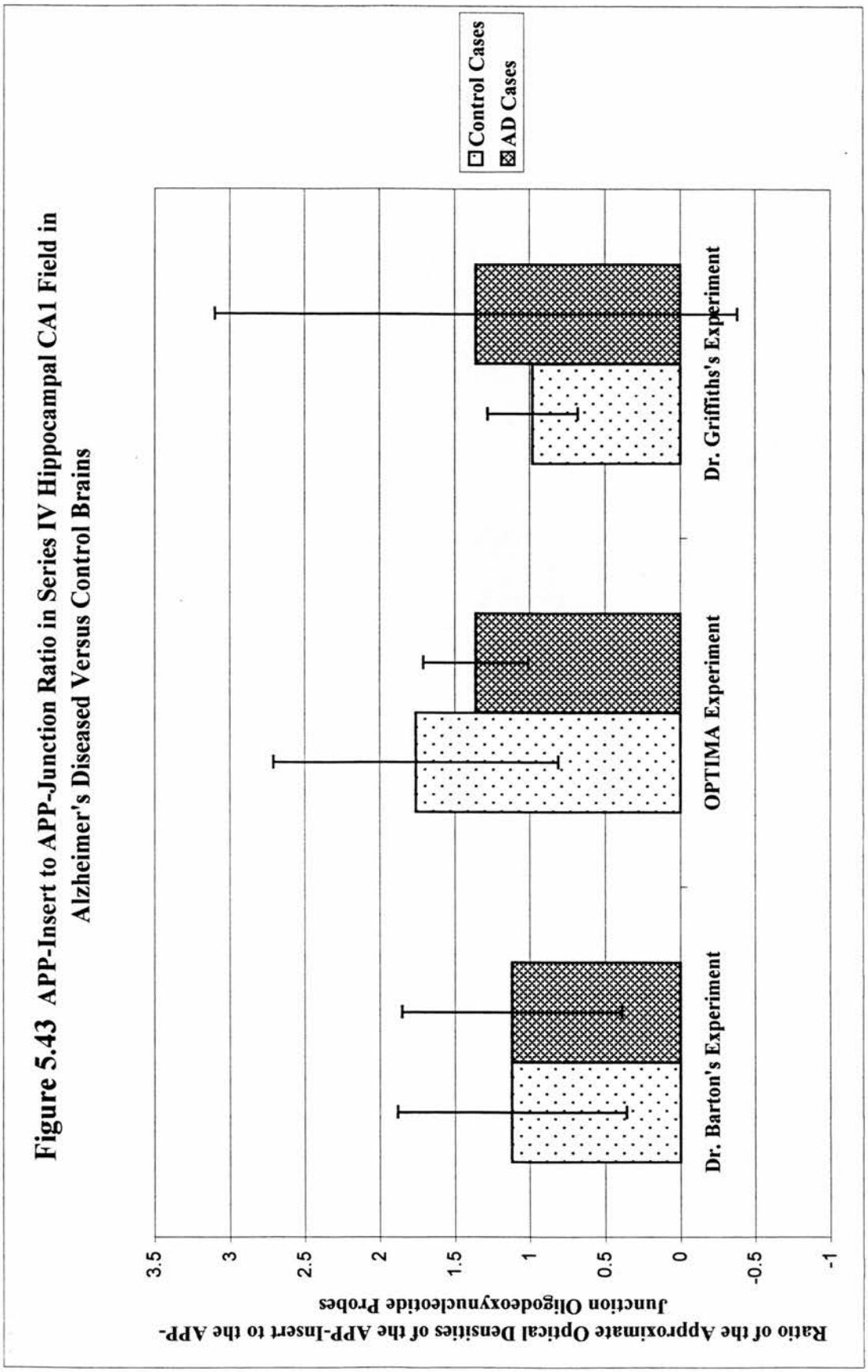

Figure 5.43 APP-Insert to APP-Junction Ratio in Series IV Hippocampal CA1 Field in Alzheimer's Diseased Versus Control Brains

5.4 Discussion

The importance of APP to the pathogenesis of AD is undisputed: a number of mutations in the APP gene are associated with FAD (Goate *et al.*, 1991; Chartier-Harlin *et al.*, 1991; Murrell *et al.*, 1991; Mullan *et al.*, 1992; Hendriks *et al.*, 1992). FAD is generally associated with an early age of onset, but only 5 to 10% of all AD cases present below the age of 60 years (Sandbrink *et al.*, 1996). Clearly, therefore, since the above mutations represent a minority of FAD, mutations in the APP gene explain a minute proportion of all AD cases. Of course, it is not the abnormality in the APP gene *per se*, but an increase in the production of β-amyloid, the major protein constituent of the plaque and meningovascular amyloid deposits which characterise AD, that is believed to be fundamental to the development of AD (Citron *et al.*, 1992). Clearly, there are other mechanisms by which β-amyloid levels might be increased. The abundance or stability of APP mRNA might be enhanced, for example, or the efficiency with which APP mRNA is translated might be increased. Abnormalities in the APP peptide which promote its amyloidogenic cleavage or aberrant processing of normal APP, or any combination of the above, might result in the increased levels of β-amyloid assumed to be necessary for the development of AD.

APP mRNA levels are increased in Down's syndrome consistent with the 50% increase in gene dosage associated with trisomy 21 (Tanzi *et al.*, 1987) and are believed to be responsible for the early appearance of the pathological stigmata of AD in patients with this condition. There is other evidence that increased APP

mRNA levels are toxic. Fibroblast cell lines derived from affected members of a Canadian FAD pedigree that shows strong linkage to chromosome 14, exhibit an increase in APP mRNA (Querfurth *et al.*, 1995) and elevated APP mRNA levels are observed in transgenic mice exhibiting AD-like pathology (Rockenstein *et al.*, 1995). Further, severe degeneration of post-mitotic murine embryonal carcinoma PC12 neurons that exhibit increased APP mRNA and peptide has been demonstrated (Yoshikawa *et al.*, 1992). Thus, the hypothesis that the neuropathology of AD originated from a modest, protracted, increase in APP mRNA levels was compelling, since it was both biologically plausible (Jacobsen, 1991) and experimentally testable.

Crucial to the analysis of APP mRNA expression in AD, is the determination of the upper and lower limits of APP mRNA in normal human brain, since it is conceivable that subtle alterations in APP mRNA expression over decades might be implicated in the pathophysiology of the disease (Jacobsen *et al.*, 1991). Unfortunately, APP mRNA levels appear to be extremely variable in normal human brain. Oyama and co-workers (1993) studied thirty-seven brains obtained at autopsy from elderly individuals, four of whom were diagnosed as suffering from AD diagnosed as typical on clinical and pathological grounds. The authors noted a marked individual variability in APP mRNA levels among the brains examined, for reasons they were unable to fully explain. Harrison and colleagues (1994) have also commented on the marked brain to brain variability in APP mRNA and hence the difficulty in identifying disease related alterations in the expression of these mRNA species. Ebstein and co-workers (1996), in their study of lymphocytes harvested from

sixty-four cognitively intact subjects ranging from twenty to ninety-one years of age, provide indirect evidence in support of the variability of brain APP mRNA expression in normal brain. The authors documented a ten fold variation in individual APP-751 mRNA levels in subjects less than fifty-five years old. Thus, given the wide variation in normal APP mRNA levels, large numbers of control subjects are needed to generate statistically meaningful results and to avoid generating false positive and false negative findings (Harrison *et al.*, 1996). However, despite this, APP mRNA expression has generally been studied in normal, post-mortem, human brain using small numbers of cases. For example, Cohen and colleagues (1988), Goedert (1987), Neve and co-workers (1990), Harrison and co-workers (1991d; 1994), Rockenstein and co-workers (1995) and Johnston and colleagues (1996b) all employed five or less control subjects in their analysis. Further, any differences in APP mRNA expression between diseased and normal brain tissue are likely to be modest, necessitating the recruitment and investigation of large numbers of diseased as well as control subjects. While Robinson and colleagues (1994) employed forty-two AD cases in a Northern blotting study, most studies employ far less cases (Cohen *et al.*, 1988; Goedert 1987; Neve *et al.*, 1990; Harrison *et al.*, 1991d; Rockenstein *et al.*, 1995). In addition, though the importance of controlling for pre-mortem variables (Harrison *et al.*, 1994) and post-mortem handling (Burke *et al.*, 1991) when analysing APP mRNA levels has been demonstrated, not all studies take agonal state (Robinson *et al.*, 1994) or PMI (Robinson *et al.*, 1994) into account.

Other challenges to the accurate assessment of APP mRNA levels in AD present themselves. Firstly, studies employing human post-mortem brain tissue encompass subjects at varying stages of AD, a disease that occupies a neuropathological spectrum (Braak and Braak, 1991). Rarely is the severity of disease of included subjects known, nor is it likely that they represent a homogeneous group of equally affected individuals, such that studies may vary greatly in their case mix. Further, accurate diagnosis of AD depends on the adequate exclusion of complicating pathologies, the application of recognised diagnostic criteria and neuropathological precision. Secondly, the value of the concomitant use of a measure of overall gene expression to help identify those mRNA species differentially affected by the disease process, as opposed to those that are simply altered in tandem with changes in total gene expression, have been underlined by Harrison and co-workers (1991b). Ideally, ISHH studies of specific mRNAs should be complemented by an assessment of the abundance of polyadenylated mRNA.

Thirdly, the effect of age on APP mRNA expression remains controversial. Some workers have attempted to study the effects of age on the individual splice variants of APP mRNA. Harrison and colleagues (1994) found no association between age and APP mRNA expression in the frontal cortex of eleven AD and four control subjects on whom data was available regarding age, PMI and pre-mortem course. Similarly, Jacobsen and co-workers (1991) failed to establish any effect of age on APP mRNA expression. However, though these workers did include an internal control to allow better comparison of tissue derived from different samples, they did

not control for the effects of PMI or agonal state. Robinson and co-workers (1994) documented a trend for neuronal transcription of the neurofilament light subunit and major transcripts of APP to decline with age in both AD and control subjects: a finding that was most significant and consistent for APP-695. Robinson and colleagues (1994), however, did not take agonal state factors into account in their analysis.

Other workers have examined the relationship between KPI-encoding and KPI-lacking splice variants of APP mRNA with age. Koo and colleagues (1990) demonstrated that KPI-encoding APP mRNA species predominated over non-KPI APP mRNA species in aged controls and AD sufferers, while in young adult controls the abundance of KPI-containing and non-KPI APP mRNA transcripts was approximately equal. Tanaka and co-workers (1992) demonstrated an increase in the ratio of KPI-encoding to KPI-lacking splice variants of APP mRNA with age in the frontal cortex of eight AD and seven control subjects, though the AD subjects exhibited this change in ratio at an earlier age than the control subjects. These workers also documented a positive correlation between age and this ratio in grey matter from control, but not AD, frontal cortex (Tanaka *et al.*, 1993). However, tissue from only six control and five AD subjects were examined in this study. Heffernan (1996) examined the relationship between KPI-encoding and KPI-lacking splice variants of APP mRNA in the hippocampus, temporal cortex and visual cortex of a series of normal human post-mortem brains from thirteen individuals aged between eighteen and ninety-three years at death. The ratio between KPI-encoding

and KPI-lacking splice variants of APP mRNA was positively correlated with age in the visual cortex only. Harrison and colleagues (1994) found no association between the ratio of KPI-encoding and KPI-lacking splice variants of APP mRNA and age in their ISHH study of frontal cortex. Ebstein and co-workers (1996), in their analysis of lymphocytes from AD and control donors, found APP-751 mRNA to be positively correlated with age in their sixty-four control subjects aged twenty-one to ninety-one years. APP-751 mRNA levels in their nineteen AD cases were equivalent to those in an age-matched control group. The ratio of APP-751 to APP-770 mRNA in the AD subjects, however, was lower than that in the age matched controls due to an increase in APP-770 mRNA in AD over and above that seen in the age matched control subjects. Thus, Ebstein and colleagues (1996) conclude that KPI-containing transcripts of APP mRNA increase with age. In conclusion, it would appear wise to age-match control and diseased subjects to eliminate the potentially confounding effect of age on APP mRNA levels.

The fourth consideration concerns the cerebral region studied. Clearly, APP mRNA expression studies that employ different brain areas are not comparable. The brain has been described as a multi-organ organ (Wisniewski, 1993), limiting the extent to which the findings in one brain area can be extrapolated to another. The extent of neuronal loss in AD is variable and may be region-specific, altering the ratio of neuronal to non-neuronal cells in the disease (Neve *et al.*, 1990). Of course, cellular composition is crucial to the interpretation of APP mRNA expression studies. L-APP transcripts, for example, are not expressed in neurons (Sandbrink *et al.*,

1994a; Sandbrink *et al.*, 1997), but are otherwise ubiquitous (Sandbrink *et al.*, 1994b). Techniques that employ homogenised tissue may include reactive astrocytes, microglia and endothelial cells as well as varying numbers and types of neurons. Therefore, studies may not be comparing like with like when they examine equal volumes of AD and control brain tissue, as in the 1993 study of Oyama and co-workers, for example. Further, neurons may not themselves be uniform in their expression of the alternative splice forms of APP (Jacobsen *et al.*, 1991).

Fifthly, are technical considerations such as the availability of suitable tissue and its appropriate processing and storage. Human, post-mortem brain tissue is precious: it requires the co-operation and goodwill of the donor and their family and its handling, storage and processing represents a considerable investment in time and money. Experimental variables, such as the efficiency of oligodeoxynucleotide probe labelling, render it impossible to compare the intensity of ISHH between cerebral regions directly, making statistical analysis imperative. Exclusion of the non-specific effects of a dementing illness requires the analysis of a positive control group of non-AD dementia sufferers, the value of which has been discussed by Harrison and co-workers (1994). Ideally these individuals should be a homogeneous group of non-AD dementia sufferers (Pearson *et al.*, 1992). Finally, the importance of the application of complementary techniques that examine individual or sub-populations of cells in reaching a comprehensive understanding of APP mRNA expression is obvious. Indeed, the study of selected types of neurons, such as olfactory neuroblasts (Wolozin *et al.*, 1993), as well as non-neuronal cells (Ebstein *et*

al., 1996), from AD donors, has contributed to AD research in this way. In addition primate and rat brains (Koo *et al.*, 1990; Chao *et al.*, 1994;) and human (Querfurth *et al.*, 1995) and rat (Sandbrink *et al.*, 1997) cell lines have been studied in an attempt to further our understanding of the pathophysiological processes underlying AD.

The neuropathological stigmata of AD are not uniformly distributed in brain (Pearson and Powell, 1989), and the particular vulnerability of certain brain areas to the pathological changes characteristic of the disease is unexplained, hence the interest in regional variations in APP mRNA expression in health and disease. Goedert (1987) observed little regional variation in APP mRNA expression in his study of human, control brains. Johnston and co-workers (1996a), however, observed regional differences in the levels of APP and APLP2 mRNA, and in APP splicing, in their study of three control, post-mortem, human brains. Their data suggests that APP, APLP2 and KPI-containing APP mRNA transcripts are most abundantly expressed in the temporal cortex, are intermediately expressed in the occipital cortex and are least abundant in the cerebellum; an area relatively spared from the ravages of AD. Johnson and colleagues (1989) analysed APP-751 and APP-695 mRNA expression in the neocortex, hippocampus and cerebellum of nine AD and ten control subjects. They found APP-751 mRNA to be unchanged in the disease while APP-695 mRNA was decreased selectively in the hippocampus and neocortex in AD. However, none of the three studies described above (Goedert, 1987; Johnston *et al.*, 1996a; Johnson *et al.*, 1989) included tissue obtained from individuals whose pre-mortem condition was known. It is conceivable that in some

cerebral regions mRNA is more vulnerable to the effects of a poor agonal state than it is in other brain areas (Harrison *et al.*, 1995).

Numerous studies have examined the abundance of individual splice variants of APP mRNA in AD. However, few satisfactorily control for all of the confounding variables now known to influence APP mRNA levels. Two studies, superior in their prosecution, are worthy of note. Harrison and co-workers (1994) examined the frontal cortex in eleven AD, four control and six non-AD dementia subjects using ISHH. They normalised KPI-containing and non-KPI APP mRNA levels to the abundance of polyadenylated mRNA is this region and documented a decrease in both in comparison to the control and non-AD dementia subjects. This study attended partially to potentially confounding agonal state factors and the tissue specimens were obtained at rapid autopsy; however, by the authors' admission the control group was small.

The impressive study of Johnston and co-workers (1996a) employs a novel solution hybridisation-RNase protection assay and represents an attempt to control for all of the factors now known to influence APP mRNA levels. Fourteen AD, nine control subjects and five individuals afflicted with non-AD neurological diseases were included in the analysis. The cases were matched for both pH and age, and information was available regarding PMI. Total APP and APLP2 mRNA levels were reduced in the mid-temporal, but not superior frontal, cortex in AD tissue in comparison to the other two groups examined. However, the proportion of APP

mRNA that was KPI-encoding was increased in both cortical areas in AD. There are two important caveats regarding interpretation of this study. Firstly, this study represents the findings in a heterogeneous cellular mix and, thus, is not directly comparable with the study by Harrison and co-workers (1994). Secondly, the mRNA species measured are expressed as a proportion of total RNA levels, rather than as a proportion of all polyadenylated mRNA species as in Harrison and colleagues (1994) study. Since mRNA represents between only three and five per cent of all cellular RNA, Johnston and co-workers (1996a) method may have been less sensitive and, thus, unable to detect the reduction in APP mRNA levels in frontal cortex identified by Harrison and co-workers (1994). Alternatively, the frontal cortices in the cases studied by Johnston and colleagues (1996a) may have been less severely diseased than those employed by Harrison and co-workers (1994). However, crucially, neither of these studies support the hypothesis that APP mRNA levels are elevated in AD.

In this thesis a consistent picture of APP mRNA expression in AD, BAD and non-AD dementia brains, in comparison to control brains, emerges, and suggests that the hippocampus and neocortex are differentially affected by the disease processes studied. Therefore, as suspected, it appears inadvisable to extrapolate the findings obtained from the study of one cerebral area to another.

The examination of series II control and AD visual cortices failed to find any effect of diagnosis on the abundance of APP-695 mRNA or that of KPI-containing transcripts of APP mRNA. This finding was reproduced on examination of the

visual cortices in series III (the OPTIMA series), that included not only AD and control brains, but those from individuals who had suffered from BAD and non-AD dementias during life. The analysis of APP mRNA expression was extended in series III to include examination of APP-770 mRNA expression, which was also unaffected by diagnostic group. The ratio between KPI-containing transcripts of APP mRNA and non-KPI APP mRNA, the insert:junction ratio, was also estimated for the visual cortices examined in series II and III, and in neither study was there any effect of diagnosis on this parameter. The insert:junction ratio was also examined in series IV visual cortices in AD brains in comparison to control brains and no significant effect of diagnosis on the insert:junction ratio was apparent.

The abundance of poly(A)$^+$ mRNA was examined in the visual cortices of series III (the OPTIMA series) and no significant difference in this parameter was identified between the four diagnostic categories. The APP-junction, APP-insert and APP-770 oligodeoxynucleotide probes in visual cortex were then expressed as a proportion of poly(A)$^+$ mRNA in this region and again no significant differences between the diagnostic groups was apparent.

APP mRNA expression in the hippocampus in AD in comparison to control brain tissue was examined in series I brains (see chapter 4). Total APP mRNA was significantly reduced in the dentate gyrus of AD hippocampus in comparison with control hippocampus in the presence of unchanged levels of poly(A)$^+$ mRNA in this region. No significant differences in total APP mRNA expression were identified in

the CA4 and CA3 subfields of the hippocampi studied in series I. A reduction in total APP mRNA expression was confirmed in the dentate gyrus of series III brains (the OPTIMA series) in the form of a significant reduction in APP-695 mRNA in AD in comparison to control brains and unchanged levels of KPI-containing APP and APP-770 mRNA. A significant reduction in APP-695 mRNA in the AD brains in comparison to the control or BAD brains was also found in the CA4 hippocampal subfield in series III in the presence of unchanged levels of the other APP mRNA transcripts measured. No effect of diagnosis on the insert:junction ratio was apparent from examination of the hippocampi in series I, III or IV. Thus, it can be concluded unequivocally from this study that, though increased APP mRNA levels are associated with the neuropathological stigmata of AD (Tanzi *et al.*, 1987), increased APP mRNA levels are not a feature of Alzheimer diseased visual cortex or hippocampus. Indeed, in the dentate gyrus and hippocampal subfield CA4, APP-695 mRNA was reduced in AD tissue in comparison to tissue from control, BAD or non-AD dementia subjects.

Analysis of the correlation matrices prepared in the course of this study can be summarised as follows. No significant correlations were identified on analysis of series II, since two significant findings ($p < 0.050$) and one finding of $p = 0.050$ is less than would have been predicted to occur by chance. However, it is noteworthy that one of the two significant findings identified on examination of series II had a p value of less than 0.001. On consultation with biomedical statistician, Miss J.M. Russell, the determination of the statistical significance of this finding, a complex

and inexact undertaking, was deemed beyond the scope of this thesis. No correlation statistics were performed on series IV, since this series was compiled specifically to examine the effects of diagnosis and experimental variables on the insert:junction ratio. Thus, further statistical analysis of this data set was not appropriate. Series III (the OPTIMA series) benefited from the inclusion of tissue from cerebral areas differentially involved in the disease processes studied and from the unparalleled demographic, neuropathological and tissue details available. A previous study of OPTIMA derived tissue (Nagy *et al.*, 1995) documented a highly positive correlation between the extent of cognitive decline and the severity of neuropathological change. This finding was replicated in series III (the OPTIMA series). A negative correlation was established between the mini-mental state score and the mean hippocampal and neocortical NFT density, the mean neocortical neuritic plaque density, the Braak score and the maximum CERAD plaque frequency. Thus, despite the relatively crude nature of the mini-mental state examination, the score does appear to reflect the degree of underlying pathology.

The mini-mental state score was also negatively correlated with the AOD of the poly(dT) oligodeoxynucleotide probe in visual cortex, suggesting that the more plentiful were polyadenylated species of mRNA in this region the poorer was cognitive function. The abundance of polyadenylated mRNA in visual cortex was also correlated with both neocortical and hippocampal pathological severity, since the AOD of the poly(dT) probe was positively correlated with the Braak score, the mean hippocampal amyloid plaque frequency, the maximum CERAD plaque

frequency, the mean neocortical neuritic plaque frequency and the mean neocortical NFT density. In contrast, when the AOD of the APP-insert and APP-junction oligodeoxynucleotide probes were expressed as a proportion of the AOD of the poly(dT) probe both were positively correlated with the mini-mental state score. This correlation cannot be explained simply as a result of the negative correlation identified between the mini-mental state score and the AOD of the poly(dT) oligodeoxynucleotide probe, since in both cases the correlation is slightly stronger than that between the mini-mental state score and the AOD of the poly(dT) oligodeoxynucleotide probe, and of considerably more compelling significance. It would appear that the greater the proportion of polyadenylated mRNA in visual cortex that is detected by the APP-insert and APP-junction oligodeoxynucleotide probes then the more robust is cognitive function. In further support of this contention is the negative correlation between the AOD of the APP-insert and APP-junction oligodeoxynucleotide probes, when expressed as a proportion of the AOD of the poly(dT) oligodeoxynucleotide probe, and the mean hippocampal NFT density. It would appear that the greater the proportion of the polyadenylated mRNA in visual cortex that is detected by the APP-insert and APP-junction oligodeoxynucleotide probes then the less severe is hippocampal pathology. It would appear that increasing pathological severity is associated with up-regulation of some mRNAs, but not the major APP mRNA transcripts of APP-695, APP-751 and APP-770. Indeed, it is noteworthy that the abundance of the mRNA species identified by the APP-insert, APP-junction and APP-770 oligodeoxynucleotide

probes alone was unhelpful in predicting pathological severity as measured by the seven parameters employed in this study in any of the cerebral regions examined.

Initially, the above cohesive cluster of results in the visual cortex proved perplexing, however, on closer scrutiny a plausible explanation of these findings emerged. Polyadenylated mRNA would be expected to be increased in AD, despite neuronal losses, consequent upon the gliosis that is characteristic of the disease (Frederickson, 1992). It is likely that the AOD of the poly(dT) oligodeoxynucleotide probe is a measure, in part, of the extent of gliosis and hence disease progression. The proportion of polyadenylated mRNA that is APP-695 mRNA, in contrast, would be expected to fall in AD, since this splice variant of APP is the predominant form in neurons (Sandbrink *et al.*, 1997). Thus, a smaller ratio between the AOD of the APP-junction and poly(dT) oligodeoxynucleotide probes would be expected to be associated with increased pathology and poorer cognitive function. In health, the ratio between the AOD of the APP-junction and poly(dT) oligodeoxynucleotide probes would be predicted to be larger, since APP-695 mRNA should be more abundant and polyadenylated mRNA less so. Of course, in the visual cortex the AOD of the APP-junction and APP-insert oligodeoxynucleotide probes are highly correlated, hence the association between the AOD of the APP-insert oligodeoxynucleotide probe, when expressed as a proportion of the AOD of the poly(dT) oligodeoxynucleotide probe, and pathology and cognitive function. No significant differences in the AOD of the poly(dT) oligodeoxynucleotide probe were identified between the four diagnostic groups studied, yet this parameter proved

positively correlated with five of the seven neuropathological measures employed in this study. It is likely that diagnostic group is too crude an approximation of pathology and, in addition, twenty-seven cases were available in which to study the association between the AOD of the poly(dT) oligodeoxynucleotide and pathology, a marked increase in the power of the analysis when compared to identifying a relationship between the AOD of this oligodeoxynucleotide probe and diagnostic group.

The association between the APP-insert and APP-770 oligodeoxynucleotide probes in visual cortex is understandable given that the APP-770 probe theoretically detects APP-714 and APP-770 mRNAs, while the APP-insert probe detects APP-770, APP-751, APP-563 and APP-365 mRNAs. However, the strong correlation between the APP-insert and APP-junction probes in this region cannot be dismissed so easily. It would appear that in healthy and diseased visual cortex the abundance of the APP mRNA species detected by the APP-junction and APP-insert oligodeoxynucleotide probes are highly inter-dependent. Further, since the two are positively correlated, changes in the relative abundance of the mRNA species identified by the APP-junction and APP-insert oligodeoxynucleotide probes must result from alterations in transcription and/or mRNA degradation and not from alternative splicing of heterogeneous nuclear APP RNA.

In the dentate gyrus and hippocampal subfield CA1, as in the visual cortex of this series, the APP-insert and APP-junction oligodeoxynucleotide probes were

correlated, as were the APP-insert and APP-770 oligodeoxynucleotide probes. In hippocampal subfields CA3 and CA4, however, no associations were found between the AOD of the APP oligodeoxynucleotide probes examined.

In the visual cortex, but not in any of the other regions studied, both the APP-insert and the APP-junction oligodeoxynucleotide probes were positively correlated with tissue pH, and to a similar degree (0.573; $p = 0.001$ and 0.540; $p = 0.003$ respectively). It is unclear why in the visual cortex alone these two APP oligodeoxynucleotide probes would appear sensitive to pH. However, this association underlines the need to control for agonal state factors when measuring APP mRNA levels and probably explains, in part, the highly variable nature of APP mRNA levels (Oyama *et al.*, 1993; Harrison *et al.*, 1994; Ebstein *et al.*, 1996). In contrast, the use of the insert:junction ratio is supported by this study, since as both probes are equally affected by pH the resulting ratio is immune to its effects.

A ratio is a dimensionless pure number whose units are immaterial (Bland and Altman, 1996). On analysis of series III the APP-junction oligodeoxynucleotide probe was negatively correlated with the insert:junction ratio in the visual cortex with a value of -0.678 and a p value of $p < 0.001$. The APP-insert oligodeoxynucleotide probe was also negatively correlated with the insert:junction ratio with a value of -0.376 and a p value of $p = 0.028$ in this region. Thus, it would appear that in the visual cortex the value of the insert:junction ratio in health and disease is dominated by the value of the APP-junction oligodeoxynucleotide probe.

Conversely, in the dentate gyrus and hippocampal subfield CA1, areas particularly susceptible to the pathological changes characteristic of AD, the insert:junction ratio appears to be dominated, in health and disease, by the value of the APP-insert oligodeoxynucleotide probe. In hippocampal subfield CA4, the APP-insert oligodeoxynucleotide probe was positively correlated (0.813; $p < 0.001$) and the APP-junction oligodeoxynucleotide probe negatively correlated (-0.627; $p=0.001$) with the insert:junction ratio. Thus, it would appear that both oligodeoxynucleotide probes influence the value of the insert:junction ratio to the same degree in this region. In hippocampal subfield CA3 no relationships were found between the value of any of the APP oligodeoxynucleotide probes measured and the insert:junction ratio. Therefore, intriguingly, the major determinant of the insert:junction ratio did differ between the two cerebral regions studied. This finding implies that the insert:junction ratio in the visual cortex is relatively resistant to alterations in the abundance of KPI-encoding transcripts of APP mRNA and vulnerable to changes in APP-695 mRNA. The insert:junction ratio in the dentate gyrus and hippocampal subfield CA1, however, would be predicted to be selectively vulnerable to changes in KPI-encoding APP mRNA levels and relatively impervious to changes in APP-695 mRNA.

No effect of diagnosis on the insert:junction ratio could be discerned on examination of the visual cortices in series II and III or the hippocampi in series I and III. Series IV was compiled specifically to examine the relative importance of diagnosis and experimental variables on the insert:junction ratio in a larger series of brains. No

significant differences, in terms of agonal state, were identified between the diagnostic groups examined in series II and III, however, the data available on pre-mortem course was inadequate for some of the cases included in series IV, therefore, the insert:junction ratio alone was analysed. Experimental variables were found to significantly influence the insert:junction ratio in the visual cortex alone of series IV. In none of the areas examined was the insert:junction ratio correlated with diagnosis.

In order to increase the power of the analysis of series IV, and to examine the effects of age and PMI, the remaining cases in the series were included in a subsequent unmatched analysis. The intention was to widen the range of ages over which the insert:junction ratio was examined and in this regard the analysis was successful. Series II comprised cases aged from sixty-four to ninety-eight years and series III (the OPTIMA series) comprised cases aged between sixty-two to ninety-one years. The range of ages of the subjects studied in series IV was similar for all cerebral areas, fifty-one to ninety-eight years for the visual cortex and fifty-one to ninety-six for the other regions studied. In the visual cortex of series IV (Figure 5.44), but not the dentate gyrus or hippocampal subfields CA4, CA3 or CA1, the insert:junction ratio was correlated with the age of the examined subjects. The identification of this correlation in visual cortex alone is unexplained, but replicates the findings of Heffernan (1996) who established this correlation in the visual cortex, but not the hippocampus, in a series of normal controls aged between eighteen and ninety-three years. However, the visual cortex data set comprised the largest number of cases,

Figure 5.44 Age Plotted Against the APP-Insert to APP-Junction Ratio in the Visual Cortex of Series IV Alzheimer Diseased and Control Brains

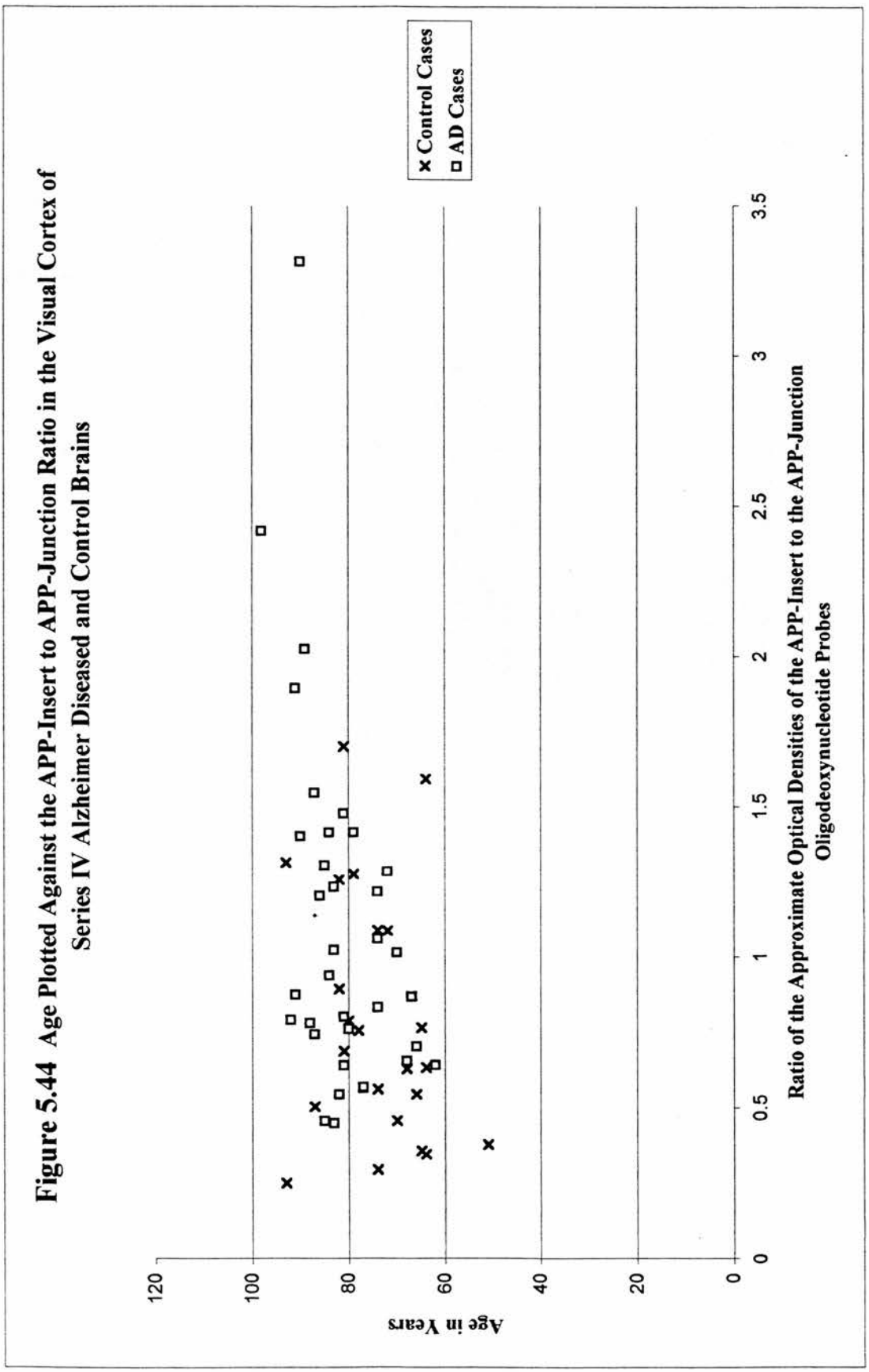

fifty-nine, while the number of cases studied in the dentate gyrus and hippocampal subfields CA4, CA3 and CA1 was forty-four, forty-three, thirty-seven and thirty-three respectively. In any event, the increase identified in the insert:junction ratio in the visual cortex with age implies that KPI-encoding and non-KPI APP mRNA transcripts must either both decrease or both increase in this region with age, since in visual cortex the mRNA species detected by the APP-junction and APP-insert oligodeoxynucleotide probes are positively correlated in healthy and diseased tissue. Thus, the increase documented in the insert:junction ratio with age in the visual cortices of series IV may be due to an increase in the mRNA species detected by both the APP-insert and the APP-junction oligodeoxynucleotide probes that is far more significant for the APP-insert oligodeoxynucleotide probe or, alternatively, to a decrease in the mRNA species detected by both probes that is far more marked for the species detected by the APP-junction oligodeoxynucleotide probe. Since information on pre-mortem course was incomplete for the series it was not possible to analyse the individual transcripts of APP mRNA. However, the finding that KPI-encoding splice variants of APP mRNA increase relative to non-KPI APP mRNA transcripts with age hints that this predominance of KPI-encoding APP mRNA is amyloidogenic, since age is a risk factor for AD. It may be that the balance between these two forms of APP mRNA is crucially altered with age in favour of amyloidogenesis.

Clearly the use of age-matched controls in the study of AD is to be applauded, however, this does artificially truncate the age range over which APP mRNA levels

are studied and may be, in part, responsible for the failure to identify the correlation between the insert:junction ratio and age in some studies. This is likely to be consolidated by the small numbers of cases employed by most workers.

This thesis represents the analysis of a large series of human post-mortem brains: a total of one hundred and thirty-nine cases were examined in the course of the work on APP mRNA expression, and thirty-nine cases were included in the series III (the OPTIMA series) study alone. Thus, it represents a large and comprehensive analysis of APP mRNA in human brain. The diagnosis of AD was made on clinical history and was confirmed neuropathologically. Further, all of the experiments described in this thesis were performed at a single centre, in a blind and uniform manner, and variables known to confound the measurement of APP mRNA, such as age of the individual at death, tissue pH and PMI, were matched. Where possible, polyadenylated mRNA was estimated as a measure of overall gene expression in order to identify gene specific effects. The analysis of the ISHH experiments was conducted with particular care: ^{14}C microscales were used to demonstrate that the hybridisation signal generated could be meaningfully analysed and the image analysis system employed was dedicated to the analysis of a single experiment until its completion. The statistical analysis of the data was thorough and achieved with the extensive assistance of a professional biomedical statistician. Nevertheless, a number of deficiencies in the design and prosecution of this study remain. Firstly, the tissue employed in this thesis was obtained, fortuitously, from a restricted number of sources and was handled by relatively few neuropathologists; even so, not

all of the tissue was dealt with identically. For example, tissue blocks from series I and II were fully embedded in OCT embedding compound on a dry ice and alcohol slurry, while tissue blocks from series III (the OPTIMA series) were mounted unsupported on cork discs with the embedding compound. The series III tissue was, thus, less well protected during storage and more vulnerable to thawing. Secondly, while the inclusion of a positive control group for comparison in series III is an advance, the group was non-homogeneous. Thirdly, the choice of cortical areas examined obviously restricts the applicability of the findings of this study. However, the consistent nature of the findings is reassuring and suggests that the two cerebral areas studied are differentially affected by the disease processes examined.

The APP gene bears a stress-inducible heat shock control element in its promoter region (Salbaum *et al.*, 1988) and, like the heat shock genes, its expression is up-regulated in response to cAMP (Gegelashvili *et al.*, 1996). APP is known to be induced in response to stress *in vitro* (Abe *et al.*, 1991a) and *in vivo* (Siman *et al.*, 1989). Indeed, APP synthesis and turnover increases rapidly in response to brain injury and it is postulated that its function is either to protect or repair damaged neurons (Bowes *et al.*, 1994). Since the abnormal intracellular proteins that characterise AD are a known stimulus to the heat shock proteins, it is curious that APP is not up-regulated in AD. However, Abe and co-workers (1991b) have demonstrated that the induction of APP in response to stress is not absolute, confirming the complexity of the control of APP expression. Indeed, Harrison and colleagues (1994) demonstrated a negative correlation between the abundance of

APP-695 mRNA and that of a stress-inducible 70 kDa heat shock protein mRNA (hsx70 mRNA) in the frontal cortex of control, AD and non-AD dementia brains.

Wolozin and colleagues (1993) studied olfactory neuroblasts from AD donors and controls and found good agreement between APP mRNA and protein levels and no significant disease-related differences in levels of APP mRNA or protein between the two groups. These findings imply that, in AD, APP mRNA is translated with an efficiency typical of that in normal cells, however, generalisation of these *in vitro* conclusions may be unwise. Olfactory neuroblasts do express many neuronal proteins, but, unlike neurons, synthesise predominantly APP-770 and APP-751 mRNA and protein, rather than APP-695 mRNA and protein. The authors do, however, conclude that APP mRNA levels are less important in the pathophysiology of AD than was originally thought and with this I would concur.

The fact that brain APP mRNA levels are unaltered in AD, does not, of course, guarantee that translation of all of the splice variants of APP mRNA is accurate in AD and proceeds with an efficiency equal to that in control tissue. Nor does it ensure that the resulting peptide is delivered to the correct intracellular compartment in the disease. Abundant APP, as a result of improved efficiency of translation of APP mRNA or depressed post-translational catabolism of the nascent protein, might lead to the enhanced production of toxic carboxyl terminal β-amyloid containing derivatives of APP and β-amyloid (Fraser *et al.*, 1996; Yoshikawa *et al.*, 1992; Rogers *et al.*, 1992). It is clear, however, that β-amyloid production can be enhanced

without such an increase in the APP peptide (Reaume *et al.*, 1996). The amyloidogenic and non-amyloidogenic processing pathways of APP are linked *in vivo* (Reaume *et al.*, 1996), probably through competition for substrate (Gandy and Greengard, 1994). Thus, alterations in the metabolic fate of a normal amount of APP peptide could conceivably result in an increase in the production of β-amyloid. Abnormal trafficking of the APP peptide, for example, such that exposure to the usual spectrum of proteases does not occur, failure of one or more of the components of the usual degradative pathway or the use of an alternative, or usually little used, processing pathway might all increase β-amyloid synthesis. Alternatively, abnormalities in the APP peptide itself might lead to the production of metabolically disruptive metabolites (Nixon and Cataldo, 1994), as well as interfering with the hypothesised functions of APP, such as its role in the cell membrane (Okamoto *et al.*, 1995) and in cell adhesion (Moya *et al.*, 1994).

There is evidence that the balance between KPI-containing and KPI-lacking isoforms of the APP peptide is disrupted in AD in the form of an increase in the proportion of KPI-containing forms. Further, there is reason to believe that this disturbance might promote amyloidogenesis. Moir and co-workers (1998) have documented a significant increase in the proportion of KPI-containing isoforms of APP in APP purified from the soluble subcellular fraction of AD brains in comparison to control brains. Transgenic mice that exhibit a selective, moderate, neuronal over-expression of APP-751 mRNA and protein develop hippocampal and cortical extracellular β-amyloid immunoreactive deposits (Quon *et al.*, 1991). In contrast, preliminary

data suggests that such mice over-expressing the APP-695 mRNA and protein do not exhibit such pathology (Quon *et al.*, 1991). KPI-containing isoforms of the APP peptide have been documented to impair α secretase cleavage of APP (Ho *et al.*, 1996) and to form complexes with proteolytic peptides, thus potentially altering the spectrum of proteases available to cleave APP. A metabolically relevant interaction between KPI-containing isoforms of APP and lysosomal enzymes has also been proposed (Benowitz *et al.*, 1989). Of course, a relative deficiency of non-KPI APP protein species might also interfere with the neuroprotective functions proposed for α secretase cleaved APP-695 protein (Jin *et al.*, 1994).

An alteration in the ratio of KPI-encoding to non-KPI APP mRNA species might underlie any change in the ratio of KPI-containing to KPI-lacking APP isoforms in AD. However, this study does not support an alteration in the ratio of KPI-containing transcripts of APP mRNA relative to non-KPI APP mRNA in the disease. KPI-encoding APP mRNA transcripts do, however, increase relative to APP-695 mRNA transcripts with age in the visual cortex. This increase in ratio might be one mechanism whereby age predisposes to AD and further supports the belief that an increase in KPI-containing APP isoforms is a risk factor for AD. In addition, a relative increase in KPI-containing APP mRNA would be predicted to selectively alter the insert:junction ratio in the dentate gyrus and hippocampal subfield CA1, the insert:junction ratio in the visual cortex being resistant to such changes. Thus, the dentate gyrus and hippocampal subfield CA1, would be expected to exhibit greater pathology than the visual cortex should the balance of

KPI-containing to KPI-lacking isoforms of APP be important in the pathophysiology of AD, and indeed they do.

The genetic abnormalities underlying the majority, if not all, of the forms of AD inherited in an autosomal dominant fashion with complete penetrance have now been identified (Sandbrink *et al.*, 1996). Given the evidence, exploration of APP mRNA levels in AD was an obvious and compelling research topic, however, this study implies that further investigation of APP transcription in AD is likely to prove fruitless and would be ill advised. In AD it would appear that abnormalities at the level of the efficiency of translation of KPI-encoding transcripts of APP mRNA, at the earliest, result in the proposed increase in KPI-containing isoforms of the APP peptide hypothesised to be crucial to enhanced β-amyloid production. The most profitable avenues for future research in AD would seem to be determination of the abundance of KPI-containing and non-KPI isoforms of the APP peptide in neurons and investigation of the cellular handling of these nascent APP forms.

Chapter 6

Ubiquitin-Dependent Non-Lysosomal Proteolysis is not Enhanced in Established Alzheimer's Disease

6.1 Introduction

Ubiquitin is a seventy-six amino acid polypeptide first identified during the isolation and characterisation of thymopoietin I and II from bovine thymus (Goldstein *et al.*, 1975). The newly discovered polypeptide was originally labelled ubiquitous immunopoietic polypeptide, since it was capable of inducing differentiation of not only pro-thymocytes, but also B cells, and appeared to be universally represented in living cells. Ubiquitin is found not only in all animal cells, but also in yeast, bacteria and higher plants (Goldstein *et al.*, 1975), and, indeed, has been shown to be fully conserved between the two orders of mammals from cattle to man (Schlesinger and Goldstein, 1975). The rigorous conservation of ubiquitin over this immense evolutionary time span hints at its vital role within cells (Goldstein *et al.*, 1975; St John *et al.*, 1986). In evolutionary terms, the appearance of ubiquitin antedates even such early developments as karyon formation that occurred far in advance of the regulation of cells by nerve networks and endocrine signals (Goldstein *et al.*, 1975).

Ubiquitin is found in the cytoplasm and the nucleus (Lund *et al.*, 1985) and has been implicated in both lysosomal and non-lysosomal proteolysis (Gropper *et al.*, 1991; Ciechanover *et al.*, 1984a). Within eukaryotic cell nuclei 10% of histone H2A and 1-2% of histone H2B are ubiquitinated at a defined lysine residue (Morimoto *et al.*,

1993). Ubiquitinated histones are preferentially associated with transcribed genes, implying that ubiquitin-mediated proteolysis of chromosomal proteins may be involved in the regulation of gene expression (Ciechanover *et al.*, 1984a), though this remains controversial (Morimoto *et al.*, 1993). Indeed, the slow turnover of histones suggests that the function of ubiquitin conjugation of histones may be unrelated to proteolysis (Finley *et al.*, 1984). Cytoplasmic ubiquitin is part of the ATP-dependent ubiquitin/25S proteasome system that is the major means of disposing of abnormal and short-lived intracellular protein (Ciechanover *et al.*, 1984a). A functional ubiquitin conjugating system also appears to be necessary for lysosomal biogenesis and maturation (Lenk *et al.*, 1992; Löw *et al.*, 1993) and for the enhanced degradation of endogenous long-lived proteins by lysosomal autophagy that is induced in response to cellular stress (Gropper *et al.*, 1991).

The efficient removal of abnormal and expired proteins is crucial to cellular survival, especially so for post-mitotic, terminally differentiated cells like neurons that cannot dilute out unwanted proteins through division and replication. The intracellular precipitation of abnormal proteins could conceivably interfere with protein synthesis, intracellular transport and the assembly of ribosomes and other macromolecular complexes (Bond and Schlesinger, 1985), and embarrass dynamic fibrous structures such as chromatin and the cytoskeleton (Finley *et al.*, 1984). Of course, immunochemical and histochemical studies have demonstrated that neurons are rich in lysosomes and lysosomal enzymes (Nixon *et al.*, 1992) whose constitutive function is proteolysis (Ciechanover *et al.*, 1984a). However, it is only under conditions of nutritional deprivation that significant degradation of short-lived and

abnormal proteins is carried out by these organelles (Ciechanover *et al.*, 1984a). Under basal metabolic conditions it is clear that the degradation of the majority of such proteins is non-lysosomal (Ciechanover *et al.*, 1984b). Cells from the mouse mammary cell line, ts85, that bear a mutant, thermolabile ubiquitin-activating enzyme, fail to degrade abnormal and otherwise short-lived proteins at non-permissive temperatures (Finley *et al.*, 1984). Studies of this mutant imply that the contribution of ubiquitin-independent proteolysis to the breakdown of short-lived and aberrant proteins is no more than 10% and probably less (Ciechanover *et al.*, 1984b).

Ubiquitin is an essential component of non-lysosomal, ATP-dependent proteolysis. The carboxyl terminal glycine residue of ubiquitin is conjugated to a wide variety of substrate proteins through an isopeptide bond with the ε-amino groups of lysine residues in the substrate (Ciechanover *et al.*, 1984a). St John and co-workers (1986) hypothesise that the requirement that ubiquitin interact with many different proteins has prohibited mutations which might interfere with this capacity, resulting in the extreme amino acid conservation exhibited by ubiquitin. One or more ubiquitin molecules may be conjugated to a single protein molecule in preparation for its proteolytic degradation (Bond and Schlesinger 1985). This process has an absolute requirement for metabolic energy (Ciechanover *et al.*, 1984a). It is believed that ATP is needed, not for what is essentially an exothermic reaction in thermodynamic terms, but to fuel the precise nature of such protein degradation (Ciechanover *et al.*, 1984a). ATP is also required for the enzymatic degradation of the protein moiety of the ubiquitin-protein conjugate (Hershko *et al.*, 1984).

Ubiquitin is a member of the multi-gene, heat shock protein family (Bond and Schlesinger, 1985; Finley and Varshavsky, 1985; Nowak *et al.*, 1990). The heat shock proteins are produced by cells on exposure to thermal stress, and in response to viral infection, amino acid analogues, DNA damage, ethanol and heavy metals (Mosser *et al.*, 1990; Ananthan *et al.*, 1986). The cells react by increasing the amount, or activity, of a transcription factor that is specific for the heat shock genes and the metabolic effort of the cell is re-directed to the production of the heat shock proteins (Bond and Schlesinger 1985). Kinouchi and colleagues (1993) draw attention to the substantial body of evidence in support of a protective role for the heat shock proteins in cellular injury (see also Kiang and Tsokos, 1996 for review). Kiang and Tsokos (1996) favour the 70 kDa heat shock proteins (Hsp70) as the likely mediators of this protective effect. Induction of Hsp70 heat shock proteins in neurons is associated with the acquisition of tolerance against subsequent injury (see Kiang and Tsokos, 1996 for review). However, the unique induction kinetics demonstrated for different members of the heat shock protein family suggests that other heat shock proteins are necessary for this effect (Higashi *et al.*, 1994). It is likely that several classes of heat shock proteins act in concert in response to cellular stress (Kinouchi *et al.*, 1993; Higashi *et al.*, 1994). Further, the profile of heat shock protein induction may be organ specific following a comparable stress (Nowak *et al.*, 1990). The induction of ubiquitin in response to stresses as diverse as ischaemia and hyperthermia occurs largely in concert with the induction of Hsp70 *in vivo* in rodent brain, though Hsp70 is more readily detected than ubiquitin in this model in response to hyperthermia (Nowak *et al.*, 1990). The inclusion of the ubiquitin genes in the heat shock regulon is not unexpected. Heat stress particularly, would be predicted to

result in an increase in the production of misfolded and denatured proteins that increase the demands on the proteolytic capacity of the cell (Bond and Schlesinger, 1985).

The final common pathway that results in activation of the heat shock genes appears to be the accumulation of abnormal protein forms in response to an unphysiological milieu (Ananthan *et al.*, 1986). Ananthan and co-workers (1986) demonstrated that denatured, but not native, proteins microinjected into *Xenopus* oocytes resulted in the activation of transcription of the heat shock genes. The key regulatory protein in the heat shock response is believed to be the heat shock factor (HSF) which binds to a highly conserved *cis*-acting sequence, the heat shock element, that is present in the promoters of heat-induced genes. This heat shock element is composed of three repeats of a five base module nGAAn (See Wu *et al.*, 1990 for review). HSF not only pre-exists, but is pre-localised to the nucleus, thus minimising the delay in initiating heat shock transcription in response to stress, though how HSF is directed to, and maintained, in this cellular compartment is unknown (Westwood *et al.*, 1991). On heat shock, HSF undergoes oligomerisation from an inactive monomer to an active multimer (Westwood *et al.*, 1991). This transformation may be as a result of heat-induced phosphorylation of HSF (Larson *et al.*, 1988) or, alternatively, the fourth leucine zipper motif, unique to mammalian HSF, could be involved in intermolecular and intramolecular interactions that determine the oligomerisation state of HSF (Westwood *et al.*, 1991). It is conceivable that the oligomeric form of HSF affords better contact with the triplicated nGAAn module of the heat shock element than monomeric HSF (Westwood *et al.*, 1991). However, high levels of

DNA-binding of HSF are insufficient to induce heat shock transcription and a constitutive heat shock element binding factor also appears to be involved in the regulation of heat shock transcription (Liu *et al.*, 1993). Crucially, HSF also binds to loci repressed during heat shock suggesting a role for this factor in the repression of normal gene activity during heat shock (Westwood *et al.*, 1991).

Evidence exists in support of four theories concerning the activation of cryptic, monomeric non-DNA binding HSF, in response to an accumulation of abnormal intracellular protein, that account for the homeostatic nature of the heat shock response. Firstly, it is proposed that the unphysiological milieu alters the conformation of HSF directly, resulting in its activation (Mosser *et al.*, 1990). Secondly, Ananthan and colleagues (1986) hypothesise that while HSF exists predominantly in an inactive form in unstressed cells, the active form is present, but is labile. On heat shock, denatured proteins amass and are degraded in preference to the labile, active form of HSF, which accumulates and activates the heat shock genes. Thirdly, it is suggested that HSF in unstressed cells may be prevented from adopting its active, DNA-binding form because it is held in a complex with Hsp70 (Abravaya *et al.*, 1992). On heat shock, a pool of denatured and malfolded proteins accumulate and compete with HSF for binding to Hsp70 (Abravaya *et al.*, 1992; Mosser *et al.*, 1990). The released HSF oligomerises and acquires DNA-binding and transcriptional activity (Abravaya *et al.*, 1992). Finally, Munro and Pelham (1985) advance the theory that during heat shock the demands on the ubiquitin proteolytic system are so great that there is a failure to ubiquitinate a critical factor, perhaps even

HSF itself, and that this non-ubiquitinated factor promotes transcription of the heat shock genes.

Abnormal protein conformations in the form of NFTs, amyloid plaques and meningovascular amyloid characterise AD. In AD, antibodies directed against ubiquitin strongly stain NFTs, the distended neurites associated with senile plaques and a subset of neuronal processes, distinct from senile plaques or NFTs, suggesting that these structures are highly ubiquitinated (Perry *et al.*, 1987). Why such substrate proteins are not subsequently degraded is unclear (Perry *et al.*, 1987). Mori and co-workers (1987) observe that tangle-bearing neurons are actively ubiquitinating them and postulate that at some stage in the degenerating process such neurons should exhibit expression of the heat shock proteins in response to the accumulation of abnormal protein. Indeed, Harrison and co-workers (1993) documented an increase in the mRNA of a specific 70 kDa heat shock protein, hsx70, in frontal cortex white matter in AD and non-AD dementias. Importantly, the authors found no correlation in this study between hsx70 mRNA levels and agonal state factors such as coma and pyrexia (Harrison *et al.*, 1993).

This study aimed to examine the expression of ubiquitin, using ISHH, in two brain areas differentially affected by AD: the visual cortex and the hippocampus. It was hypothesised that ubiquitin up-regulation would be an early feature of Alzheimer diseased cells in response to the increase in aberrant protein forms that is characteristic of the disease. AD progression, it was proposed, would be associated with failure of the ATP-dependent non-lysosomal pathway and a fall in ubiquitin

mRNA levels. It would appear likely that failure of a system that displays such striking evolutionary conservation as the ubiquitin proteolytic pathway, would severely compromise the capacity of an organism to withstand cellular stress (Heydari *et al.*, 1993). Indeed, genetic evidence supports the view that an intact ubiquitin conjugating system is essential for cellular survival (Wu *et al.*, 1981).

6.2 Materials and Methods

6.2.1 Introduction

These experiments were performed with the assistance of Miss J.M. Heffernan and Mr. M.W. Sanders on brains from series III (the OPTIMA series) as detailed in chapter 2. Details of all of the cases used are presented in appendix II. Summarised demographic and post-mortem information is presented in the tables relating to the OPTIMA tissue, tables 5.4 and 5.5 on pages 226 and 227 respectively. The brains were prepared and hybridised as described in chapter 2.

6.2.2 Oligodeoxynucleotide Probe Selection

The human genome contains numerous copies of the ubiquitin sequence (Wiborg *et al.*, 1985). Three bands, corresponding to splice variants of ubiquitin mRNA of 651, 1100 and 2500 nucleotides long, that are labelled ubiquitin A, ubiquitin B and ubiquitin C respectively, are visible on Northern blotting of poly(A)$^+$ mRNA extracted from human brain (Wiborg *et al.*, 1985; Lund *et al.*, 1985). Ubiquitin A encodes one, ubiquitin B three and ubiquitin C nine copies of ubiquitin. At least two splice variants of ubiquitin A mRNA exist that code for a single sequence of ubiquitin fused at its carboxyl terminus to a non-ubiquitin peptide sequence (Lund *et al.*, 1985; Salvesen *et al.*, 1987). Lund and co-workers (1985) identified a 516 base pair cDNA corresponding to amino acids five to seventy-six of the ubiquitin

sequence, an eighty amino acid carboxyl terminal extension, a 3' untranslated region and a poly(A)$^+$ tail. This carboxyl tail extension is unique to ubiquitin A and suggests that this isoform is synthesised as a precursor. Salvesen and colleagues (1987) isolated a different, smaller cDNA clone encoding residues forty to seventy-six of ubiquitin along with a carboxyl terminal extension. Salvesen and co-workers (1987) sequence of ubiquitin A differs at only one base from a region of the sequence, published by Wiborg and co-workers (1985), encoding the nomeric form of ubiquitin, ubiquitin C. The ubiquitin C gene is highly unusual. Firstly, it encodes a polypeptide containing nine direct repeats of the ubiquitin sequence, uninterrupted by spacer sequences, and, secondly, there are no introns in the coding region. Thus, for the first eight repeats of the ubiquitin sequence in ubiquitin C, the terminal glycine of one sequence is followed immediately by the first amino acid, methionine, of the next ubiquitin sequence. The ubiquitin B gene, containing three head to tail repeats of the ubiquitin sequence, was isolated and characterised by Baker and Board (1987a), along with two processed ubiquitin B pseudogenes. The existence of a third ubiquitin B processed pseudogene (Baker and Board, 1987b) and a ubiquitin B tetrameric non-processed pseudogene (Cowland *et al.*, 1988) has been demonstrated.

The region of maximum homology between the ubiquitin A sequence characterised by Lund and co-workers (1985) and the other three ubiquitin sequences was identified. However, since any thirty nucleotide sequence within this region contained a minimum of six mismatches between this ubiquitin A sequence and the other three splice variants of ubiquitin mRNA, it was necessary to design two oligodeoxynucleotide probes to ensure that all known forms of human ubiquitin mRNA were detected. A sense oligodeoxynucleotide probe, with a base sequence identical to the mRNA region of interest and in the same orientation, was designed

for each of the antisense oligodeoxynucleotide probes.

The main oligodeoxynucleotide probe, labelled ubiquitin C, was designed to hybridise to ubiquitin mRNA of all three known molecular weights. The ubiquitin C oligodeoxynucleotide probe was directed against bases 168 to 198 of the sequence published by Wiborg and co-workers (1985) and, with two mismatches, to bases 168 to198 of the sequence published by Baker and Board (1987a). The ubiquitin C oligodeoxynucleotide probe also matched bases 53 to 82 of the ubiquitin A sequence published by Salvesen and colleagues (1987) with one mismatch. The second oligodeoxynucleotide probe, designed to hybridise to the ubiquitin A sequence of Lund and colleagues (1985) alone, was directed against bases 136 to 165 of their published sequence. This oligodeoxynucleotide probe was labelled ubiquitin A. The two oligodeoxynucleotide probes were as follows:

Ubiquitin C Antisense GGT GGA CTC TTT CTG GAT GTT GTA GTC AGA

Ubiquitin A Antisense CTG GAA GAT GGA CTG ACT TTG TCT GAC TAC

6.2.3 Experimental Controls

Dr. P.R. Heath demonstrated the specificity of the ubiquitin C and ubiquitin A oligodeoxynucleotide probes using Northern blotting with a [^{32}P]dATP-labelled probe hybridised to 25 µg total RNA extracted from the frontal cortex of a control subject (Figure 6.1). The ubiquitin C oligodeoxynucleotide probe detected three bands of approximately 2.5, 1.35 and less than one kilobase, and the ubiquitin A oligodeoxynucleotide probe detected a single band of less than one kilobase, in keeping with published data (Wiborg *et al.*, 1985; Lund *et al.*, 1985).

Figure 6.1 Northern blot performed by Dr. P.R. Heath demonstrating the specificity of the ubiquitin C and ubiquitin A oligodeoxynucleotide probes. The oligodeoxynucleotide probes were labelled with [^{32}P]-dATP and hybridised to 25 µg total RNA extracted from the frontal cortex of a neurologically normal control.

Lane 1	RNA molecular weight ladder (Gibco BRL).
Lane 2	Sample total RNA.
Lane 3	Sample total RNA.
Lane 4	[^{32}P]-dATP labelled ubiquitin C oligodeoxynucleotide probe.
Lane 5	[^{32}P]-dATP labelled ubiquitin C oligodeoxynucleotide probe.
Lane 6	[^{32}P]-dATP labelled ubiquitin A oligodeoxynucleotide probe.
Lane 7	[^{32}P]-dATP labelled ubiquitin A oligodeoxynucleotide probe.

The open triangles on the right of the photograph indicate the position of the observed bands.

The ubiquitin C oligodeoxynucleotide probe detected three bands of approximately 2.5, 1.35 and less than 1.35 kilobases.

The ubiquitin A oligodeoxynucleotide probe detected a single band of less than 1.35 kilobases.

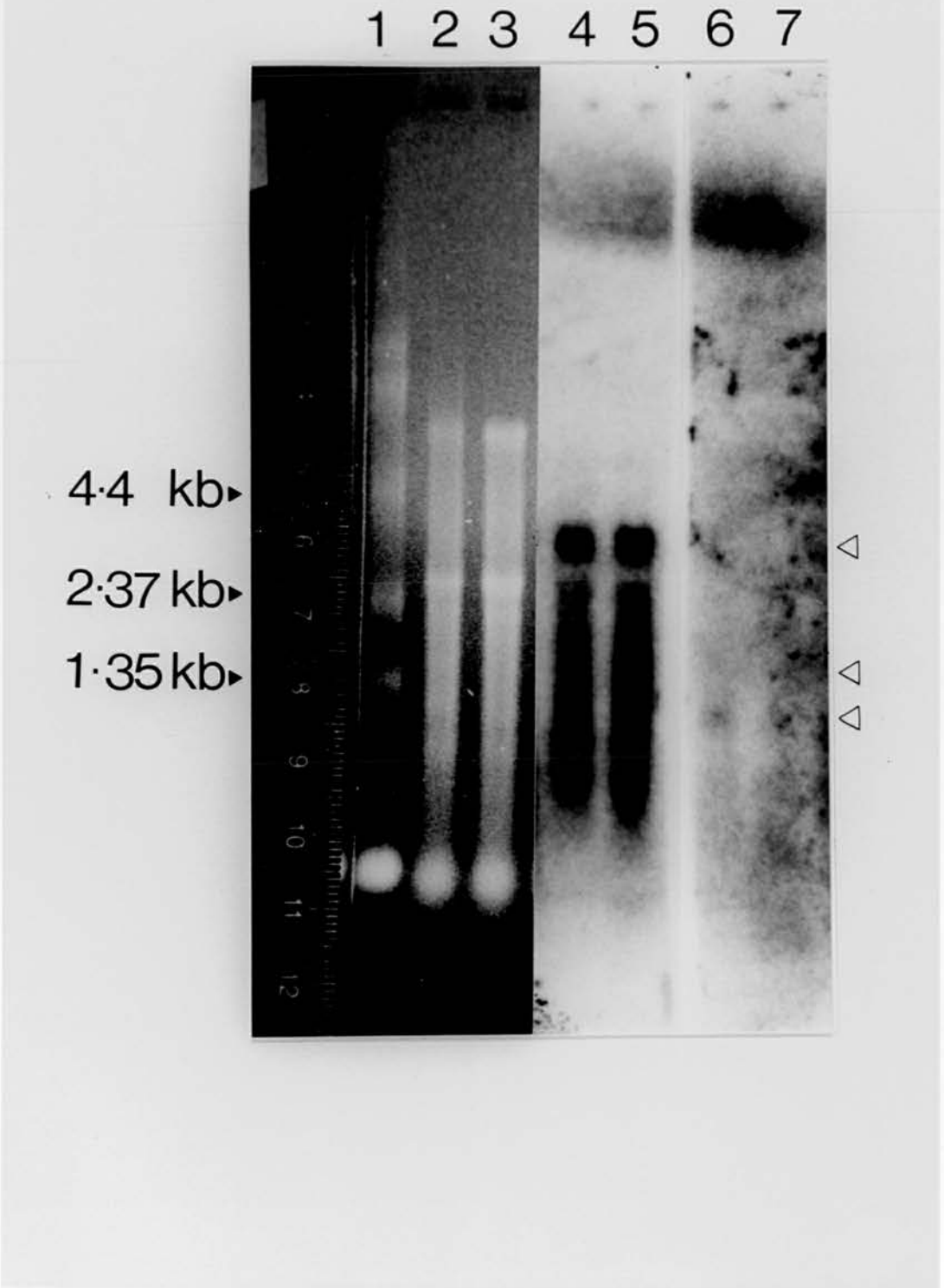
1 2 3 4 5 6 7
4·4 kb
2·37 kb
1·35 kb

In situ hybridisation histochemistry of the series III (the OPTIMA series) visual cortex and hippocampus with the ubiquitin C and ubiquitin A antisense oligodeoxynucleotide probes was accompanied by concurrent hybridisation of adjacent sections with the sense oligodeoxynucleotide probes for ubiquitin C (Figure 6.2) and ubiquitin A (Figure 6.3). The addition of 100-fold excess of unlabelled probe and pre-treatment of sections with ribonuclease led, in both cases, to the abolition of signal for the ubiquitin C and ubiquitin A antisense oligodeoxynucleotide probes. The autoradiograms generated by the above cold displacement and ribonuclease pre-treatment experiments were completely blank (data not shown).

6.2.4 *In Situ* Hybridisation Histochemistry

The hybridised sections were incubated for approximately 18 hours at 26°C for both the ubiquitin C and the ubiquitin A oligodeoxynucleotide probes. The slides were then washed in 1 × SSC (4 × 15 minute washes) at 51.5°C for both oligodeoxynucleotide probes. These washes were then followed by 2 × 60 minute washes at room temperature. Once dry, the hybridised sections were placed against film (Hyperfilm-βmax, Amersham) at room temperature for between 52 and 79 days to generate autoradiograms (Figures 6.2 and 6.3).

6.2.5 Quantification of ISHH Signal

Quantitative assessment of ISHH signal, reflecting the abundance of the mRNAs detected by the ubiquitin C and ubiquitin A oligodeoxynucleotide probes, was made on the autoradiograms using an image analysis system (Seescan Plc, Cambridge). Grain counting over individual neurons was not attempted. Mean grey density was calculated, blind to case details, over the stratum granulosum of the dentate gyrus and over the stratum pyramidale of hippocampal fields CA1, CA3 and CA4. In the

Figure 6.2 *In situ* hybridisation histochemistry using [^{35}S]dATP labelled oligodeoxynucleotide probes performed on sections of visual cortex from the same case of non-AD dementia from series III (the OPTIMA series). The images presented are direct photographs of transilluminated autoradiograms generated from this single case and hybridised with the following oligodeoxynucleotide probes. The blacker the image of the autoradiogram the greater was the exposure of the autoradiographic film to radioactivity and the more intensely labelled was the section.

A Ubiquitin C antisense oligodeoxynucleotide probe.

B Ubiquitin C sense oligodeoxynucleotide probe.

C Ubiquitin A antisense oligodeoxynucleotide probe.

D Ubiquitin A sense oligodeoxynucleotide probe.

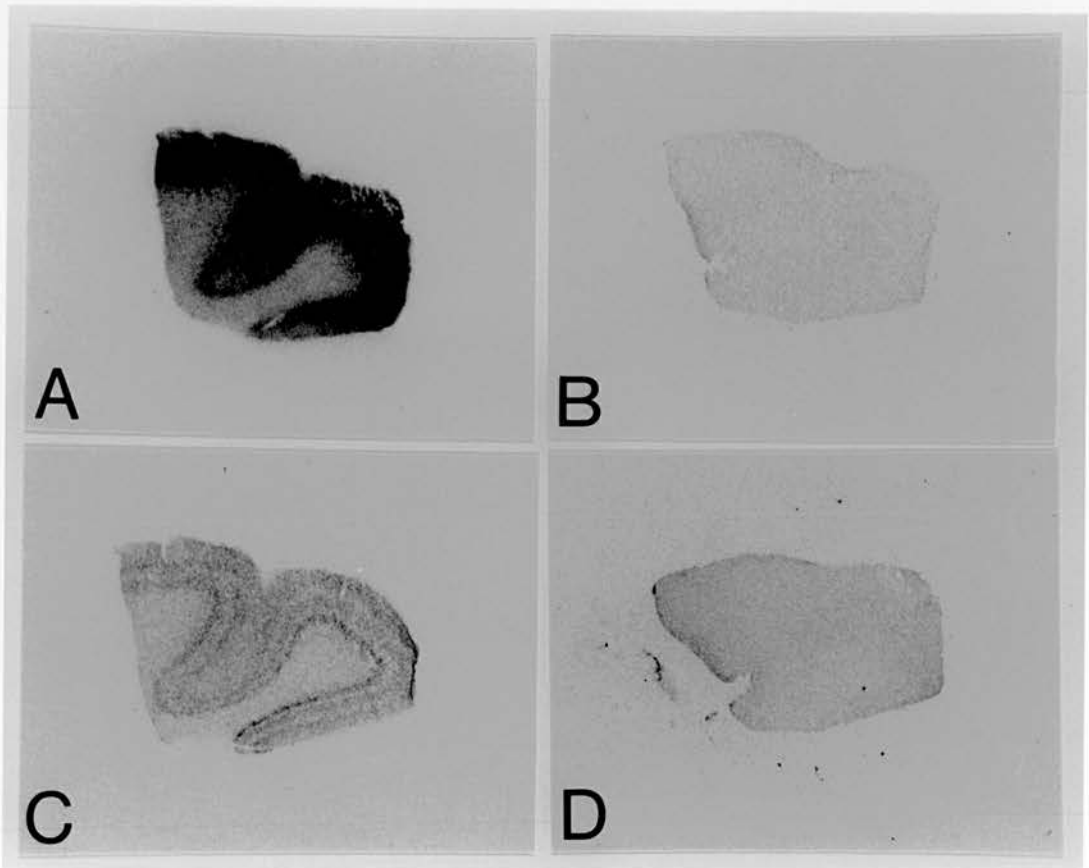
A
B
C
D

Figure 6.3 *In situ* hybridisation histochemistry using [^{35}S]dATP labelled oligodeoxynucleotide probes performed on hippocampal sections from the same case of borderline AD from series III (the OPTIMA series). The images presented are direct photographs of transilluminated autoradiograms generated from this single case and hybridised with the following oligodeoxynucleotide probes. The blacker the image of the autoradiogram the greater was the exposure of the autoradiographic film to radioactivity and the more intensely labelled was the section.

A Ubiquitin C antisense oligodeoxynucleotide probe.

B Ubiquitin C sense oligodeoxynucleotide probe.

C Ubiquitin A antisense oligodeoxynucleotide probe.

D Ubiquitin A sense oligodeoxynucleotide probe.

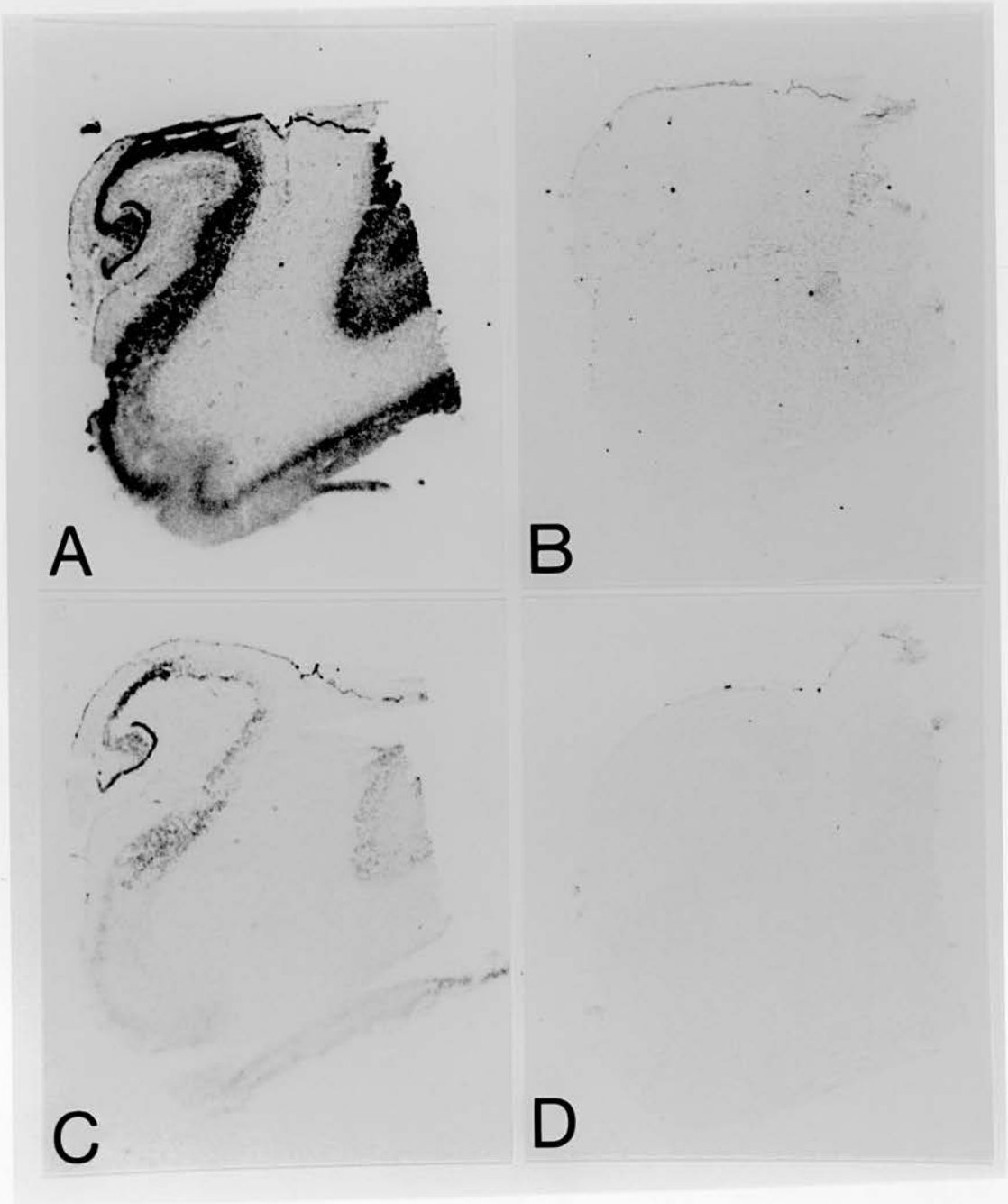
A
B
C
D

visual cortex a strip of tissue perpendicular to the cortical surface was selected for measurement of the mean grey density. Areas of the tissue where the stria of Gennari were visible were preferred. The mean value from each set of triplicates was used for all subsequent calculations.

6.2.6 Statistical Analysis

All statistical analysis was performed using SPSS for Windows version 6.0. A one way ANOVA was used to analyse the four diagnostic groups. Where Levene's test for homogeneity of variance was not significant, it was assumed that the requirements of the one way ANOVA had been met. Where Levene's test was significant, it was assumed that the requirements for the parametric test had been violated and the data was examined using the non-parametric Kruskal-Wallis one way ANOVA.

Correlation matrices were constructed using both Pearson's correlation coefficient and Spearman's rank correlation coefficient. When the two tests were in agreement, the result was accepted, when a discrepancy was observed, the data was analysed further, as detailed in the text.

6.2.7 The Relationship between Radioactive Exposure and Greyness of Radiographic Film

^{14}C microscales were opposed to the radiographic films alongside sections from all four of the ubiquitin experiments performed in this study, allowing examination of the relationship between exposure of the film to radioactivity and its resulting greyness. The ^{14}C microscales were supplied complete with information regarding the absolute radioactivity contained within each active layer of the polymer. The

estimated tissue equivalent radioactivity (ETR) was also supplied for each active layer of the polymer. This value is an estimate of the radioactivity inherent in an apparently equally radioactive tissue sample, adjusted for the autoabsorptive nature of tissue. A series of calibration curves were constructed depicting the relationship between the radioactivity inherent in the ^{14}C microscales and the corresponding greyness of the exposed radiographic films. The ETR, rather than the absolute radioactivity, of the ^{14}C microscales was used to construct these curves, since it was hoped that they might ultimately be used to estimate the radioactivity inherent in the ISHH sections used in this study. Clearly, to use the absolute radioactivity to construct the calibration curves would be to underestimate the radioactivity inherent in the ISHH tissue sections.

Traditionally, the greyness of an autoradiographic film, as measured by specialised image analysis equipment, has been converted to an optical density reading; the optical density of a direct autoradiogram being linearly related to its exposure to radioactivity over a limited range (Laskey, 1993). However, it was clear from the calibration curves generated during this study that there was considerable spread of the data about the line of best fit relating optical density to radioactive exposure. In addition, at low levels of radioactive exposure, such as when tissue sections hybridised with the sense oligodeoxynucleotide probes were opposed to radiographic film, the relationship between optical density and radioactive exposure clearly ceased to be linear.

Using the traditional formula, the correction of antisense AOD readings for non-specific binding using the AOD of the corresponding sense oligodeoxynucleotide probe is also problematic. Since the difference between the log of two numbers is the log of their ratio (Bland and Altman, 1996), the expanded traditional formula for negative optical density, corrected for non-specific binding, takes the following form:

$$-\text{Optical density} = \log 10\left(\frac{255}{\text{mean grey level antisense}}\right) - \log 10\left(\frac{255}{\text{mean grey level sense}}\right)$$

$$-\text{Optical density} = \log 10\left(\frac{255/\text{mean grey level antisense}}{255/\text{mean grey level sense}}\right)$$

$$-\text{Optical density} = \log 10\left(\frac{255 \times \text{mean grey level sense}}{255 \times \text{mean grey level antisense}}\right)$$

$$-\text{Optical density} = \log 10\left(\frac{\text{mean grey level sense}}{\text{mean grey level antisense}}\right)$$

$$-\text{Optical density} = \log 10(\text{mean grey level sense}) - \log 10(\text{mean grey level antisense})$$

Thus, according to the above formula it appears that it is not necessary to calculate the optical density of the sense and antisense oligodeoxynucleotide probes individually.

6.2.8 An Improved Formula Relating Radioactive Exposure to Greyness of Radiographic Film

In the course of this study an alternative formula was devised relating radioactive exposure to the consequent greyness of radiographic film. In three out of the four ubiquitin experiments performed this resulted in improved adherence of the data to the line of best fit and in two increased the range over which radioactive exposure and greyness of film were linearly related. The mean grey level obtained for each radioactive layer of the polymer was subtracted from the mean grey level assigned to incident light (assumed to be pure white light with a greyness of 255) and the resulting value was logged to the base 10. A linear relationship was obtained between this value and the log10(ETR). Thus, the formula is as follows:

$$\log10(\text{ETR}) = \log10(255 - \text{mean grey level})$$

Thus, the antilog of log10(255 - mean grey level) gives an estimate of the strength of radioactivity found in each section, whether hybridised with a sense or antisense oligodeoxynucleotide probe, and correction for non-specific binding using this formula is accurate and intuitive.

The application of the alternative formula, and its comparison with the traditional formula, to each of the ubiquitin experiments is detailed below.

6.2.9 Application of the Alternative Formula to the Analysis of the Ubiquitin Oligodeoxynucleotide Probes

6.2.9.1 The Ubiquitin C Oligodeoxynucleotide Probe in the Visual Cortex

Alongside the sections of visual cortex hybridised with the ubiquitin C oligodeoxynucleotide probe were ^{14}C microscales RPA 504 and RPA 511. Image analysis of the autoradiogram generated by the ^{14}C microscales resulted in a mean grey level for each radioactive layer of the polymer from which was calculated its corresponding AOD. The ETR for each layer of the polymer was plotted against the AOD generating a straight line graph with the equation $y = 189.38x + 3.97$ (Figure 6.4). On inspection of the points plotted it was clear that there was considerable spread of the data about this line of best fit and, at low AOD readings especially, the points plotted fell sharply away from this line. The mean grey level for each layer of the polymer was substituted into the alternative formula: log10(255 - mean grey level) and the resulting value plotted against the log10(ETR). When transformed in this way, the points adhered closely to a line of best fit with the equation $y = 1.3x - 0.87$ (Figure 6.5). The straight line fit of the data was highly significant ($p < 0.001$). Further, R^2, a summary measure of goodness of fit, was larger (0.999) for the alternative formula than for the traditional formula (0.987), confirming that the alternative formula was superior. It was decided, therefore, to use the alternative formula to convert the raw mean grey levels obtained for the ubiquitin C sense and antisense oligodeoxynucleotide probes in the visual cortex to a log10(ETR) reading. The antilog of this value, giving an estimate of the radioactivity inherent in the section, the ETR, was obtained for all of the sense and antisense mean grey levels.

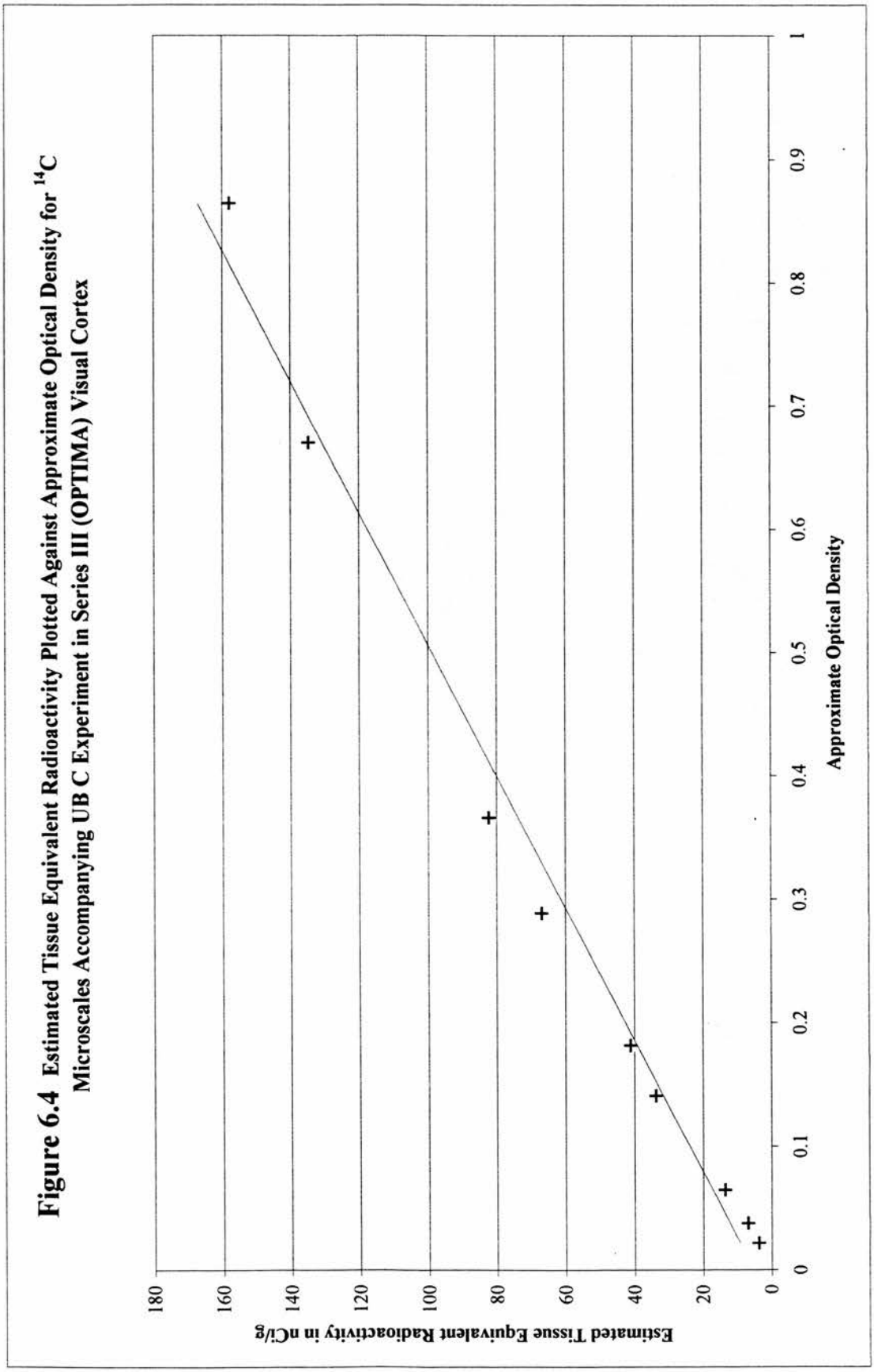

Figure 6.4 Estimated Tissue Equivalent Radioactivity Plotted Against Approximate Optical Density for ^{14}C Microscales Accompanying UB C Experiment in Series III (OPTIMA) Visual Cortex

Figure 6.5 Log10(Tissue Equivalent Radioactivity) Plotted Against Log10(255-Mean Grey Level) for ^{14}C Microscales Accompanying UB C Experiment in Series III (OPTIMA) Visual Cortex

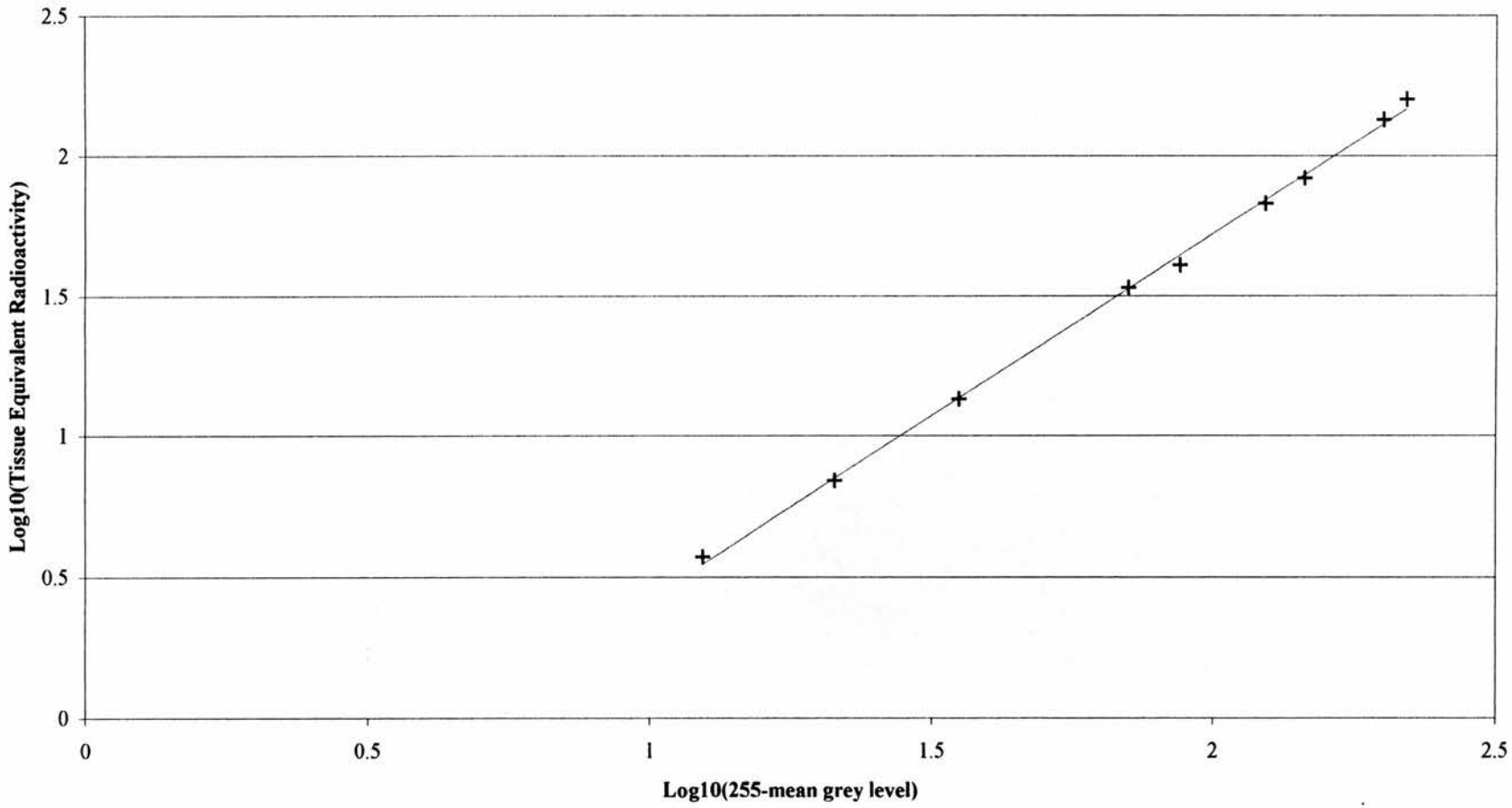

The antisense sections were then corrected for non-specific binding by subtracting the sense ETR from the antisense ETR.

A problem was encountered in analysis of the ubiquitin C antisense oligodeoxynucleotide probe in the visual cortex. Radioactive exposure eventually saturates radiographic film so that further radioactive decay has no effect on its greyness. A number of visual cortex sections hybridised with the ubiquitin C antisense oligodeoxynucleotide probe were so intensely radioactive as to lie beyond the linear portion of the graph. Two control cases, two BAD, one AD and one non-AD dementia case were in this category. The radioactivity of these sections was, therefore, underestimated whichever formula was applied. However, fortuitously, the cases to which this applied were representative of each of the diagnostic groups studied.

6.2.9.2 The Ubiquitin C Oligodeoxynucleotide Probe in the Hippocampus

The raw mean grey levels obtained from the analysis of ^{14}C microscales RPA 504 and RPA 511 opposed to autoradiographic film alongside the hippocampal sections hybridised with the ubiquitin C oligodeoxynucleotide probe, were converted to AOD readings and plotted against the corresponding ETR for each active layer of the polymer, as above (Figure 6.6). Using this formula, the most intensely radioactive layer of the microscales fell well beyond the portion of the graph in which radioactive exposure and AOD were linearly related. Using the alternative formula, however, this reading could be accommodated in the linear portion of the graph (Figure 6.7). The AOD and log10(255 - mean grey level) readings plotted,

Figure 6.6 Estimated Tissue Equivalent Radioactivity Plotted Against Approximate Optical Density for ^{14}C Microscales Accompanying UB C Experiment in Series III (OPTIMA) Hippocampus

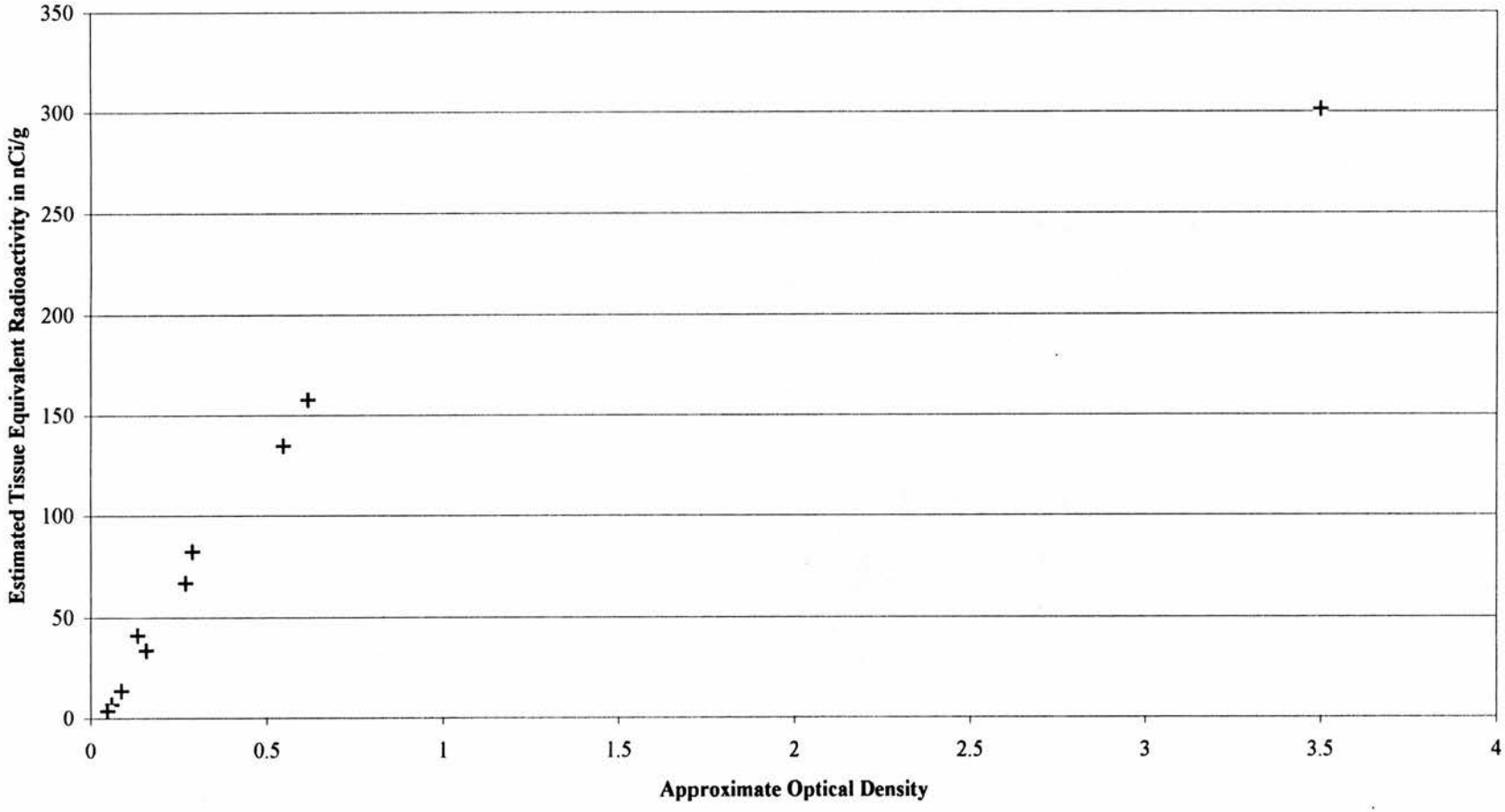

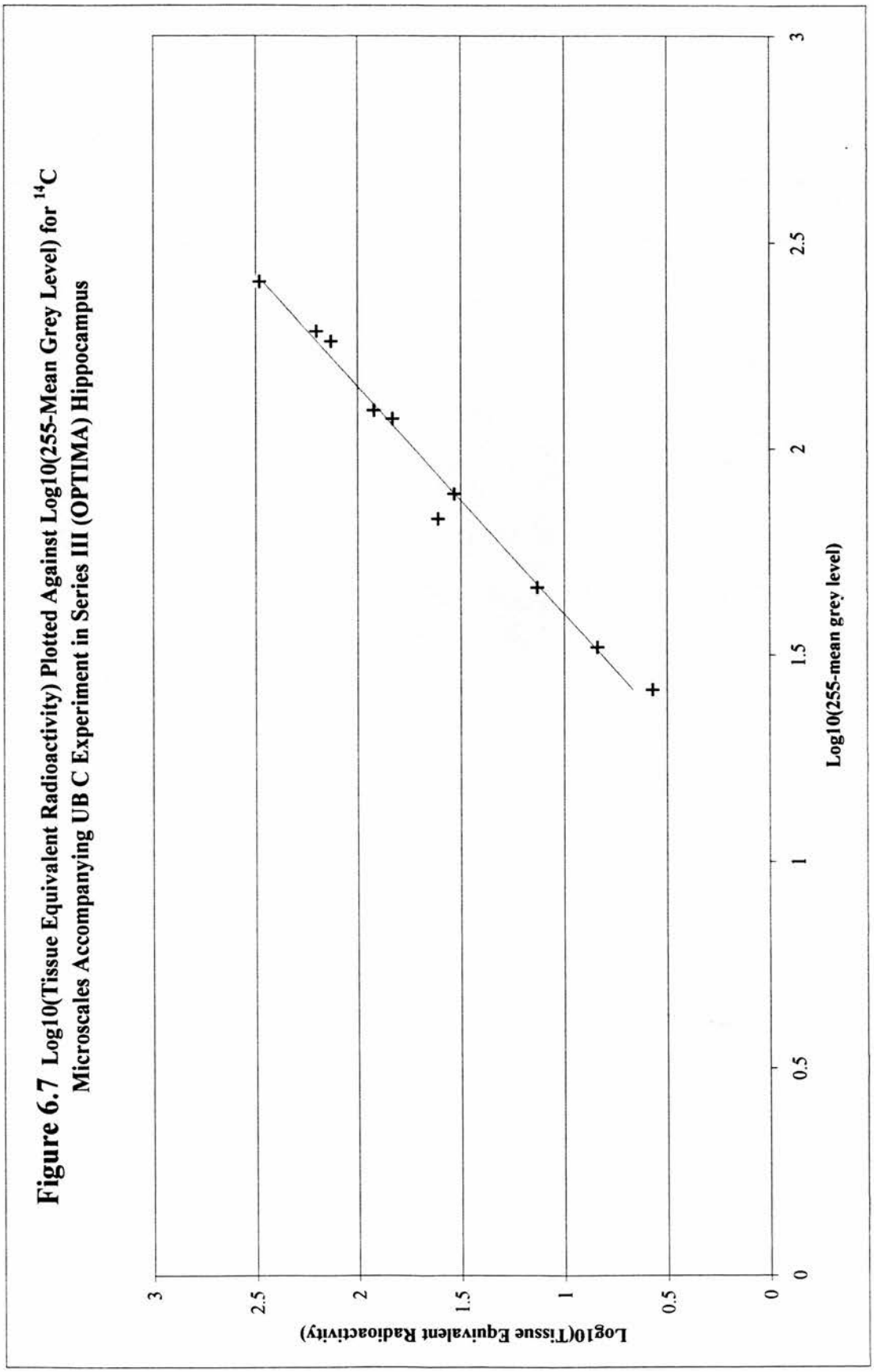

Figure 6.7 Log10(Tissue Equivalent Radioactivity) Plotted Against Log10(255-Mean Grey Level) for ^{14}C Microscales Accompanying UB C Experiment in Series III (OPTIMA) Hippocampus

corresponded to mean grey level values of between 0.08 and 228.85 in each case. The equation for the line of best fit for the graph depicting the alternative formula was $y = 1.81x-1.9$ (Figure 6.7). R^2 was 0.983 with a probability of $p < 0.001$. Thus, the straight line fit of this data is highly significant. It would appear that the division required by the traditional formula exaggerates small changes in mean grey level that are minimised using the alternative formula in which the mean grey level is subtracted from the incident light. It was decided that the alternative formula, given its larger range, should be used in the analysis of the ubiquitin C oligodeoxynucleotide probe in the hippocampus.

It should be noted, however, that using either formula, eleven of the available sense readings fell beyond the linearity of the graph. It was, therefore, impossible to correct accurately for non-specific binding using a case-specific sense strand. A global reading for non-specific binding, calculated from the cases where the log10(255 - mean grey level) of the sense section did fall within the linear part of the graph, would have resulted in the same value being subtracted from each antisense reading. As there appeared to be no merit in this, the ubiquitin C probe in hippocampus was not corrected for non-specific binding. However, given that the tissue sections hybridised with the sense ubiquitin C oligodeoxynucleotide probe produced autoradiograms that were universally and uniformly pale, this was deemed acceptable. In addition, despite the larger range of the alternative formula, one hippocampal section hybridised with the ubiquitin C antisense oligodeoxynucleotide probe remained too intensely stained to be accommodated within the linear portion of the graph.

6.2.9.3 The Ubiquitin A Oligodeoxynucleotide Probe in the Visual Cortex

Unfortunately, only the ^{14}C microscale Code RPA 504, composed of layers of ^{14}C polymer of actual radioactivity of between 104 to 0.1 nCi/g, was available for the ubiquitin A experiment in the visual cortex. A linear relationship was demonstrated both between the AOD and the ETR using the traditional formula (Figure 6.8) and between the log10(255-mean grey level) and log10(ETR) using the alternative formula (Figure 6.9). The range over which these relationships remained linear was similar for both formulae and all of the sense and antisense readings obtained from the ubiquitin A experiment in visual cortex could be accommodated within the linear portions of both graphs. However, using the traditional formula the equation of the line was $y = 136.15x + 5.36$, R^2 was 0.980 and the significance was $p = 0.001$. Using the alternative formula, the equation of the line was $y = 1.33x - 1.03$, R^2 was 0.998 and the significance was $p < 0.001$. Thus, the alternative formula was judged to be superior. The alternative formula was used to convert all of the antisense and sense mean grey levels to log10(255 - mean grey level) and the antisense ETR readings were then corrected for non-specific binding, as above.

6.2.9.4 The Ubiquitin A Oligodeoxynucleotide Probe in the Hippocampus

Plotting of AOD against ETR for the ^{14}C microscales accompanying the UB A experiment in the hippocampus generated a straight line with the equation $y = 211.62x + 6.44$ (Figure 6.10). R^2 for this line of best fit was 0.992 and the significance was $p < 0.001$.

Figure 6.8 Estimated Tissue Equivalent Radioactivity Plotted Against Approximate Optical Density for ^{14}C Microscales Accompanying UB A Experiment in Series III (OPTIMA) Visual Cortex

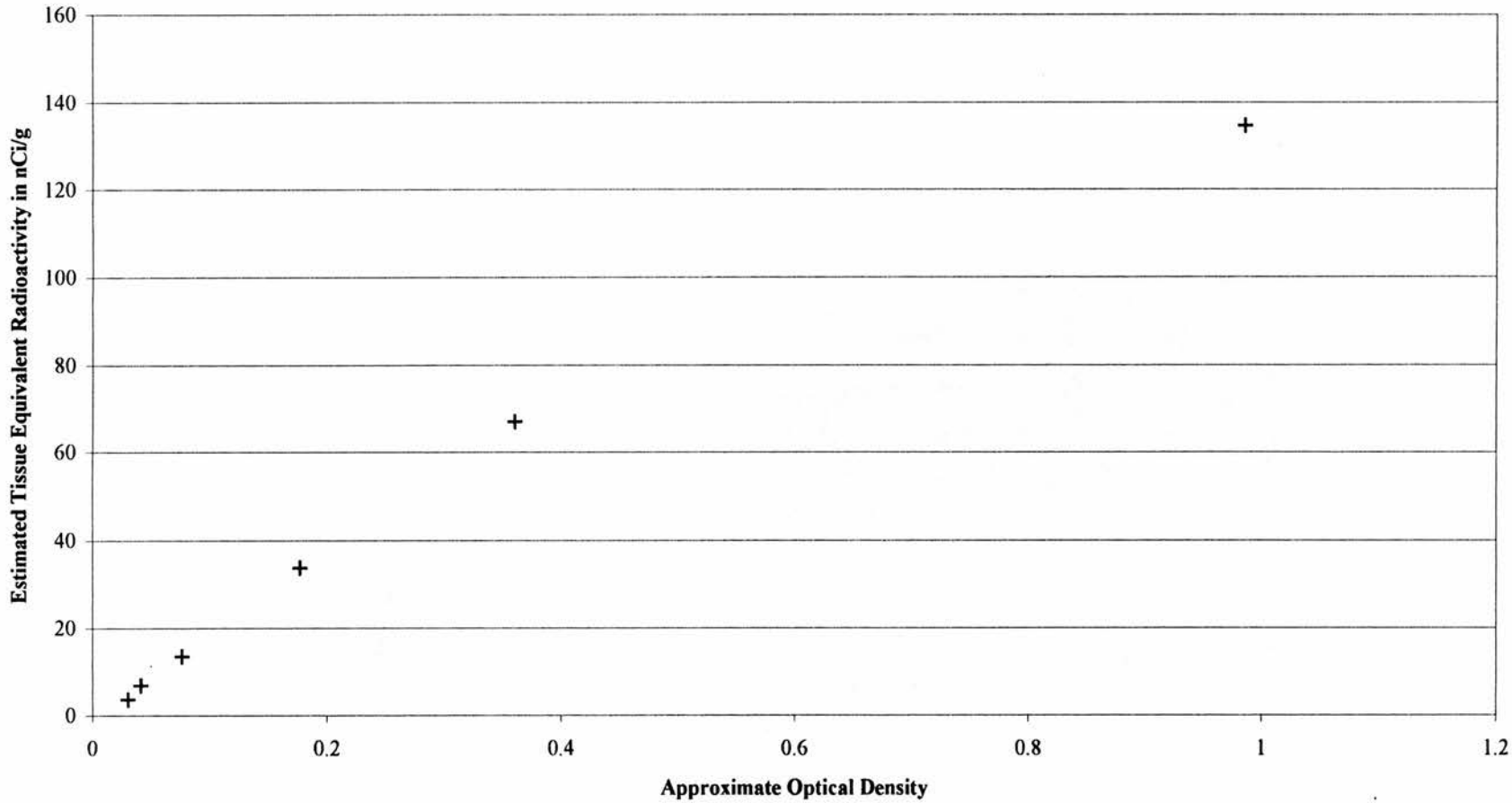

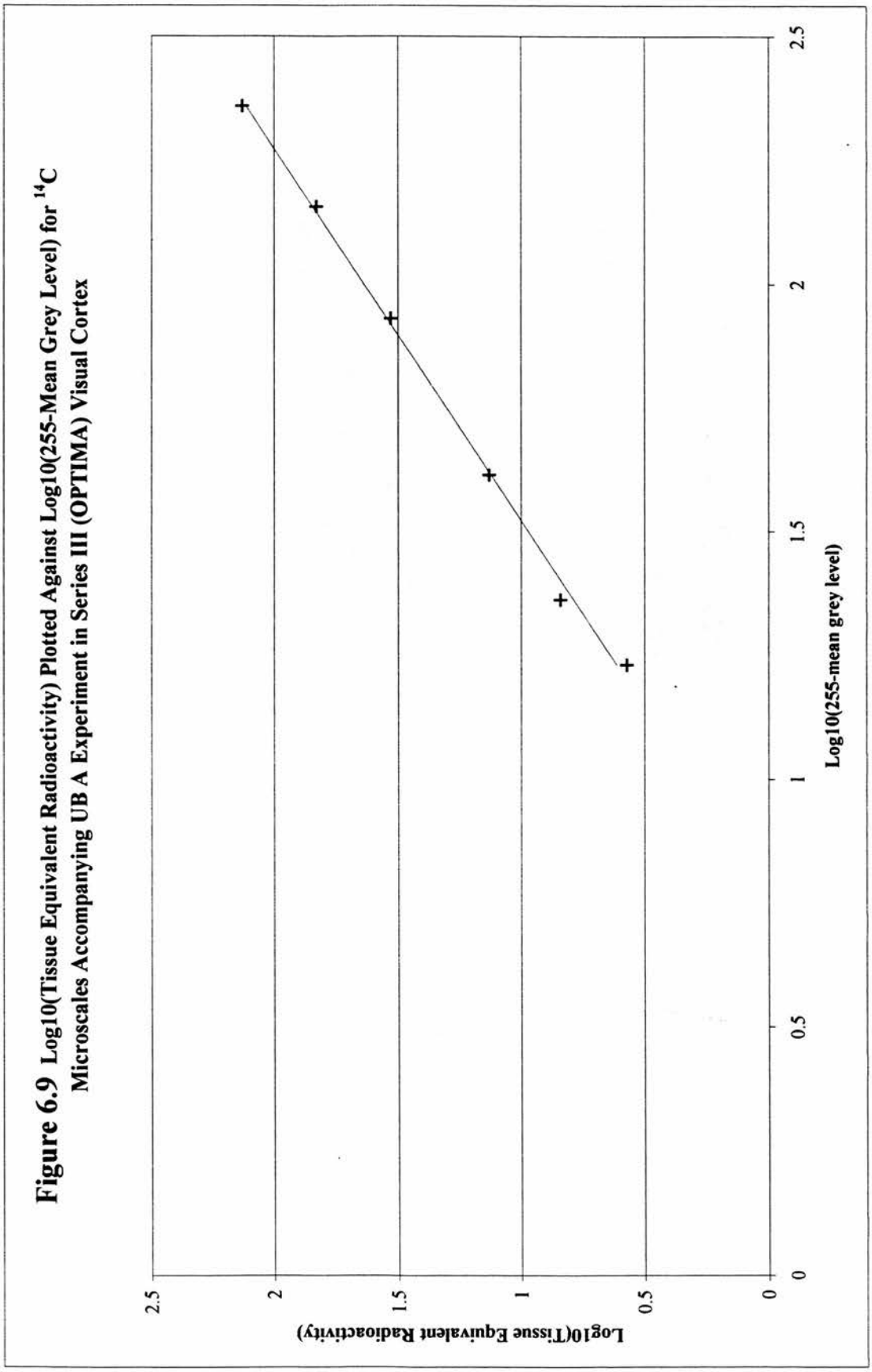

Figure 6.9 Log10(Tissue Equivalent Radioactivity) Plotted Against Log10(255-Mean Grey Level) for ^{14}C Microscales Accompanying UB A Experiment in Series III (OPTIMA) Visual Cortex

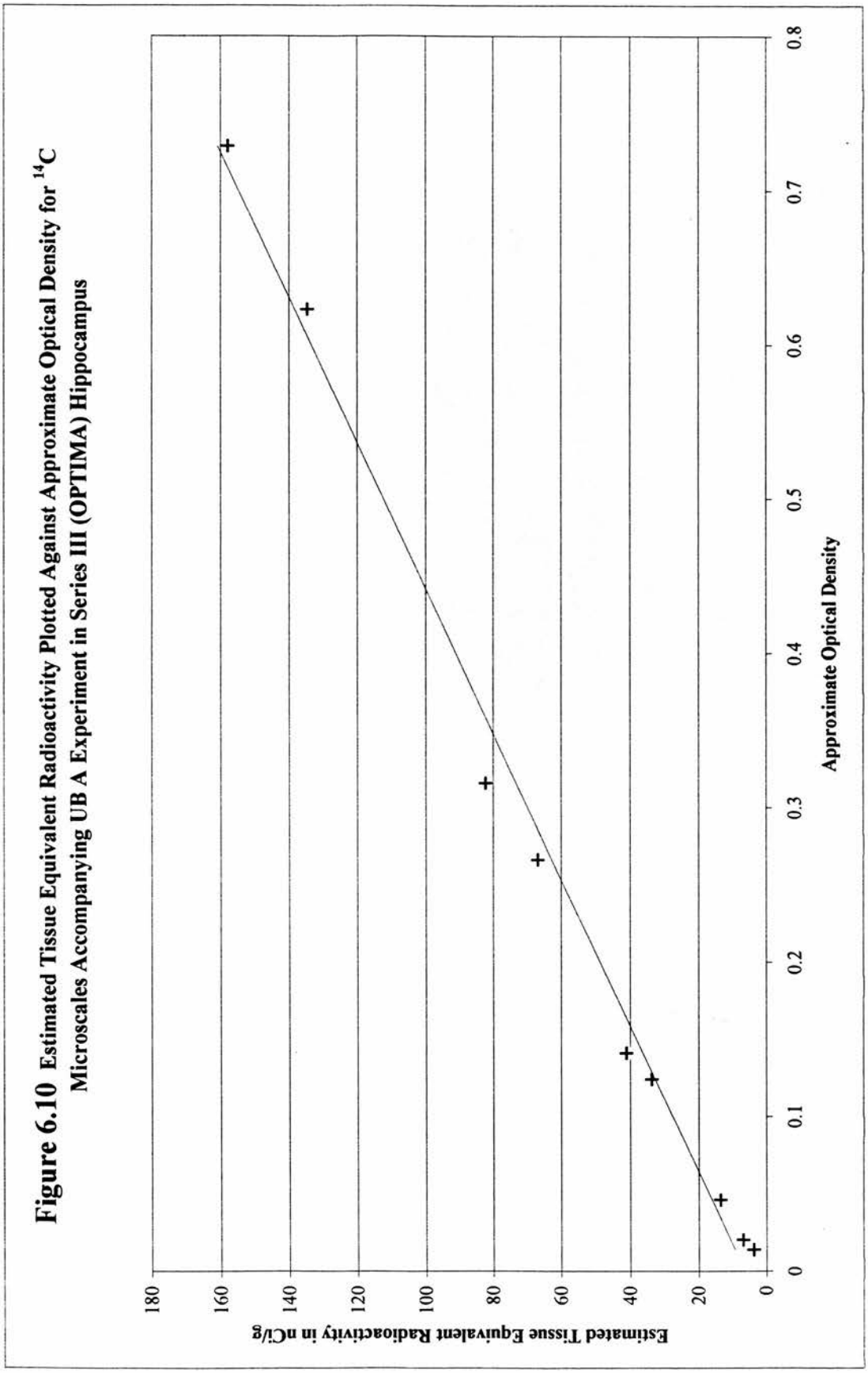

Figure 6.10 Estimated Tissue Equivalent Radioactivity Plotted Against Approximate Optical Density for ^{14}C Microscales Accompanying UB A Experiment in Series III (OPTIMA) Hippocampus

The value of log10(255 - mean grey level) was plotted against log10(ETR) and generated a straight line graph with the equation $y = 1.10x - 0.04$ (Figure 6.11). R^2 for this line of best fit was 0.995 and the significance was $p < 0.001$, suggesting that the alternative formula was superior. The linear portion of the two graphs covered an equal range. The alternative formula was, therefore, used in the analysis of the ubiquitin A oligodeoxynucleotide probe in the hippocampus.

One section labelled with the ubiquitin A sense oligodeoxynucleotide probe was too pale to be accommodated within the linear portion of either scale and four cases labelled with antisense probe did not have a section labelled with the corresponding sense oligodeoxynucleotide probe. Therefore, an average mean grey level was calculated for the sections hybridised with ubiquitin A sense oligodeoxynucleotide probe. This value was used to correct for non-specific binding in those four cases that lacked a corresponding sense section and the one case whose sense section was too pale to be converted accurately to an ETR. In hippocampal subfield CA4, the sense ETR was greater than the antisense ETR for four of the studied cases. In these cases the antisense ETR was recorded as zero, since subtracting the sense ETR from the antisense ETR would otherwise have resulted in a negative value for the ETR of the sample sections. Three antisense readings, corrected for non-specific binding, were too dark to be accommodated on the linear portion of the graph. These cases included a control case, a BAD case and an AD case. Since only three cases were involved and three of the four diagnostic groups represented, it was accepted that the radioactivity inherent in these sections would be underestimated using either formula.

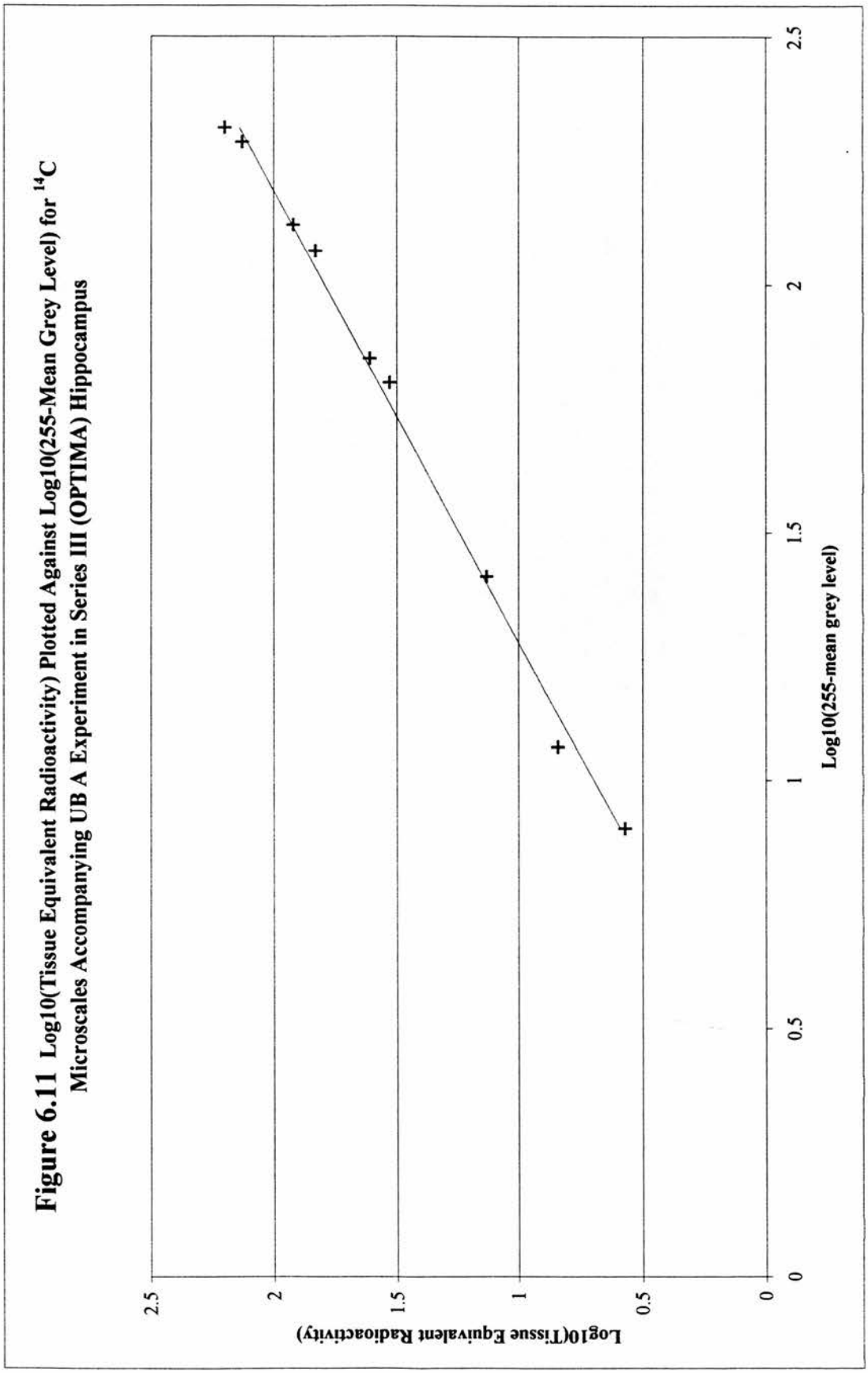

Figure 6.11 Log10(Tissue Equivalent Radioactivity) Plotted Against Log10(255-Mean Grey Level) for ^{14}C Microscales Accompanying UB A Experiment in Series III (OPTIMA) Hippocampus

6.3 Results

6.3.1 Introduction

The ETR of the ubiquitin C and ubiquitin A oligodeoxynucleotide probes did not vary significantly with the sex of the subjects.

6.3.2 Analysis of the Ubiquitin C and Ubiquitin A Oligodeoxynucleotide Probes in the Visual Cortex

No significant differences in the ETR of the ubiquitin C oligodeoxynucleotide probe were identified in visual cortex between the four diagnostic groups using a one way ANOVA (Figure 6.12). The Levene test for homogeneity of variance was not significant.

The ETR of the ubiquitin A oligodeoxynucleotide probe in visual cortex was compared between the four diagnostic groups using a one way ANOVA. No significant differences were observed between the groups (Figure 6.13). The Levene test for homogeneity of variance was not significant.

6.3.3 Analysis of the Ubiquitin C and Ubiquitin A Oligodeoxynucleotide Probes in the Hippocampus

A one way ANOVA was performed to examine the ETR of the ubiquitin C oligodeoxynucleotide probe in the hippocampus (Figure 6.14). No significant differences were observed between the four diagnostic groups in the ETR of this oligodeoxynucleotide probe in hippocampal subfields CA4 and CA1. In the dentate

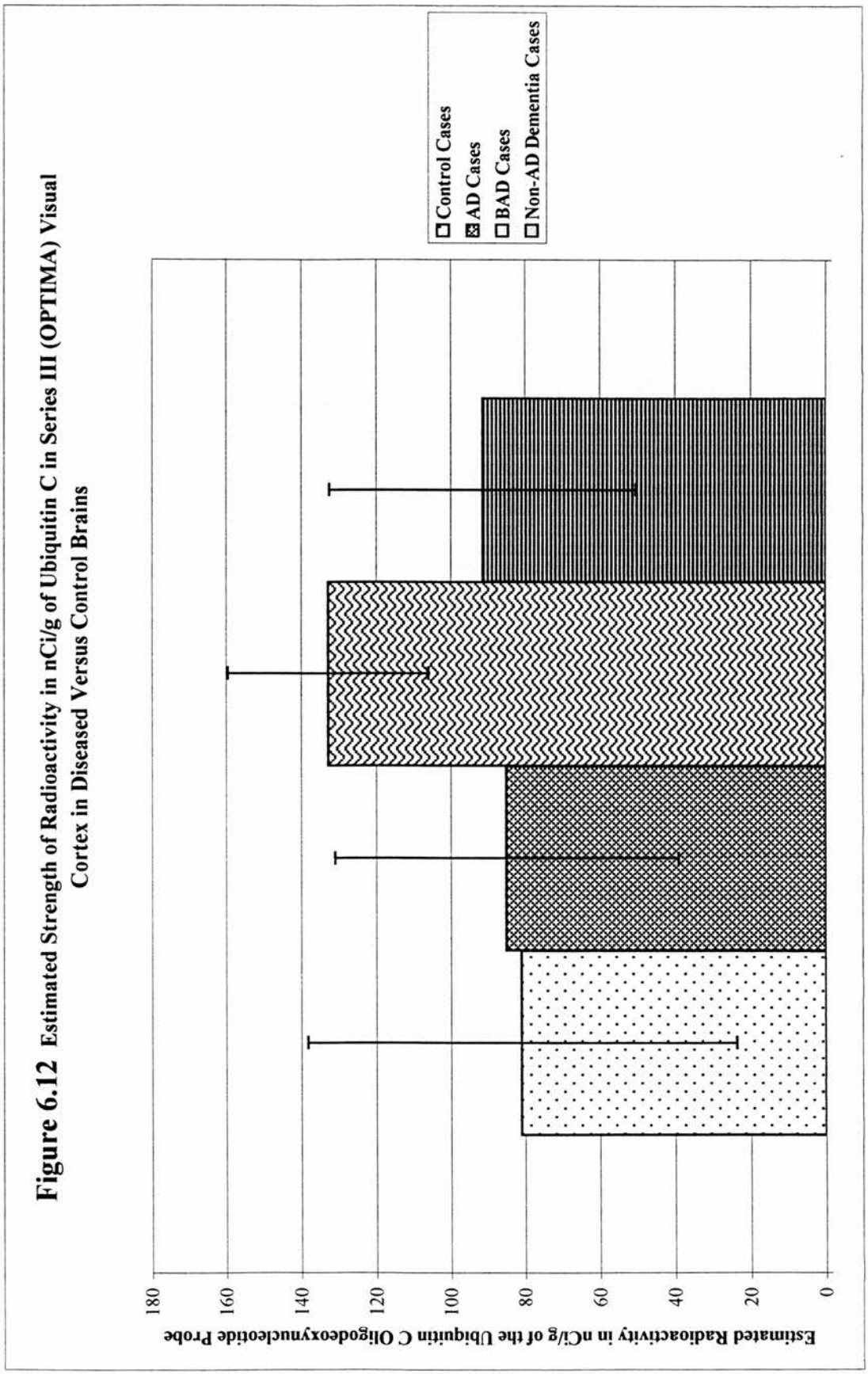

Figure 6.12 Estimated Strength of Radioactivity in nCi/g of Ubiquitin C in Series III (OPTIMA) Visual Cortex in Diseased Versus Control Brains

Figure 6.13 Estimated Strength of Radioactivity in nCi/g of Ubiquitin A in Series III (OPTIMA) Visual Cortex in Diseased Versus Control Brains

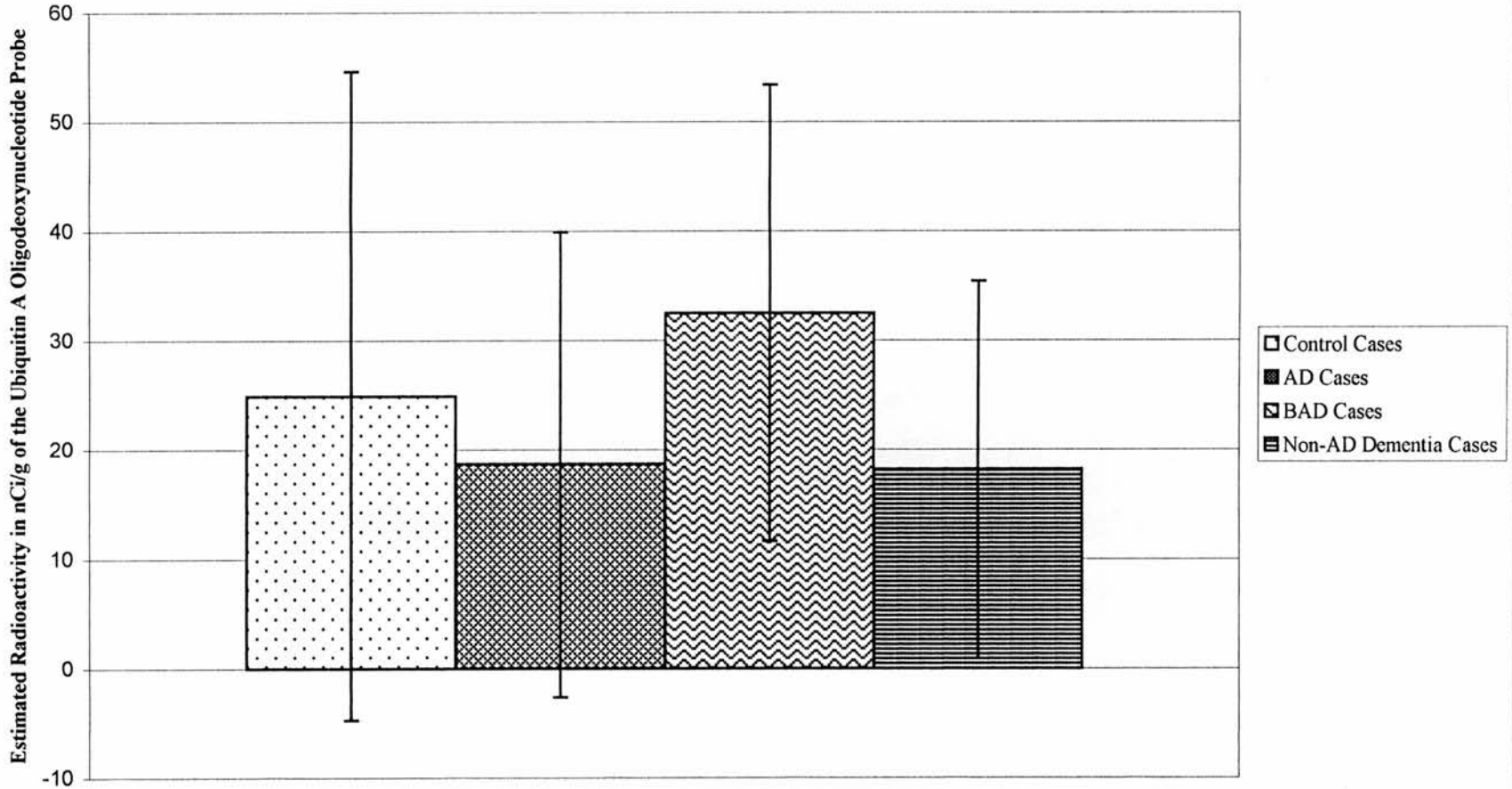

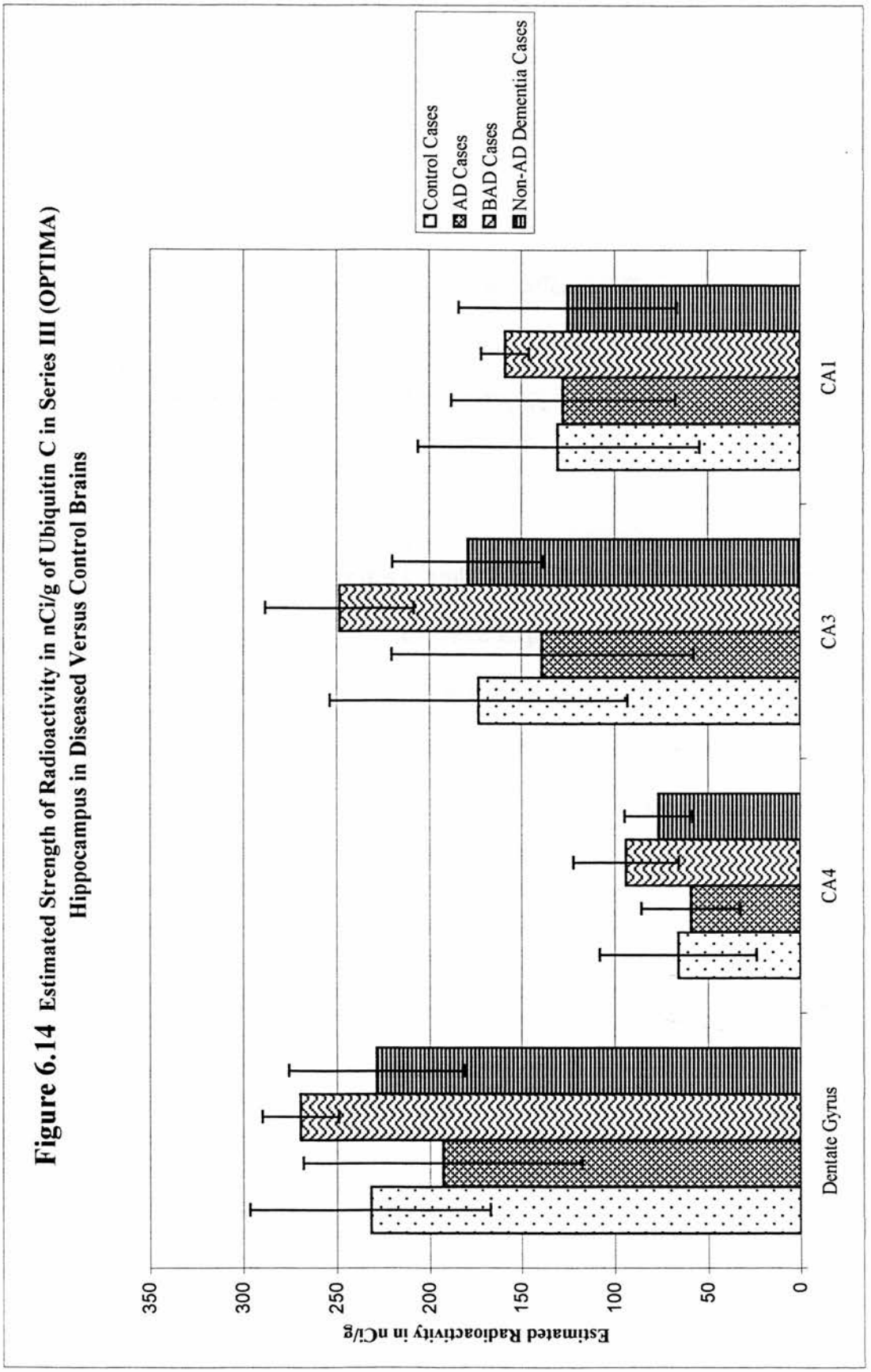

Figure 6.14 Estimated Strength of Radioactivity in nCi/g of Ubiquitin C in Series III (OPTIMA) Hippocampus in Diseased Versus Control Brains

gyrus and hippocampal subfield CA3, however, the Levene test for homogeneity of variance was significant, suggesting that the requirements of the one way ANOVA had not been met. In each case the non-parametric Kruskal-Wallis one way ANOVA was not significant.

A one way ANOVA failed to demonstrate any significant differences between the four diagnostic groups in the ETR of the ubiquitin A oligodeoxynucleotide probe in the any of the hippocampal regions examined (Figure 6.15). The Levene test for homogeneity of variance was not significant.

6.3.4 Analysis of the Ubiquitin C and Ubiquitin A Oligodeoxynucleotide Probes in the Visual Cortex when Expressed as a Ratio with the Poly(dT) Oligodeoxynucleotide Probe

The AOD of the poly(dT) oligodeoxynucleotide probe had been measured in series III (the OPTIMA series) visual cortex and the ETR of the ubiquitin C and A oligodeoxynucleotide probes in the visual cortex were expressed as a ratio of the AOD of all polyadenylated mRNA in this region (Figure 6.16). It was considered legitimate to do this, since though the units are different, the numerator was consistently AOD units and the denominator was consistently ETR units, and the ratio was not to be used in any subsequent calculations. The ubiquitin C/poly(dT) ratio differed significantly between the four diagnostic groups ($p = 0.035$). The Levene test for homogeneity of variance was not significant. Tukey's honestly significant difference test was applied and indicated that the ubiquitin C/poly(dT) ratio in the BAD cases was significantly higher than this ratio in the control or AD

Figure 6.15 Estimated Strength of Radioactivity in nCi/g of Ubiquitin A in Series III (OPTIMA) Hippocampus in Diseased Versus Control Brains

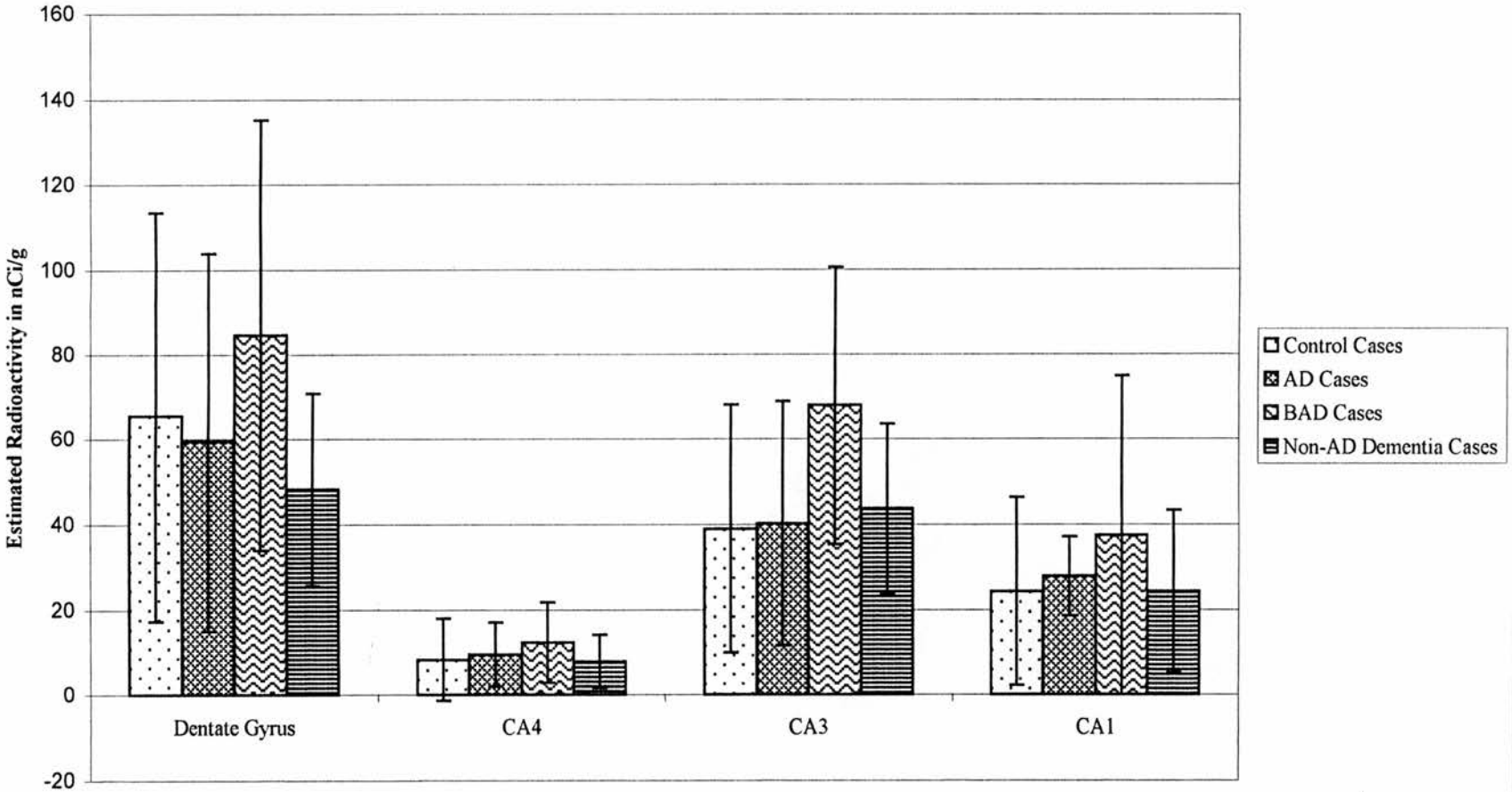

Figure 6.16 Ubiquitin C mRNA Expression as a Proportion of Poly(A)+ mRNA Expression in Series III (OPTIMA) Visual Cortex in Diseased Versus Control Brains

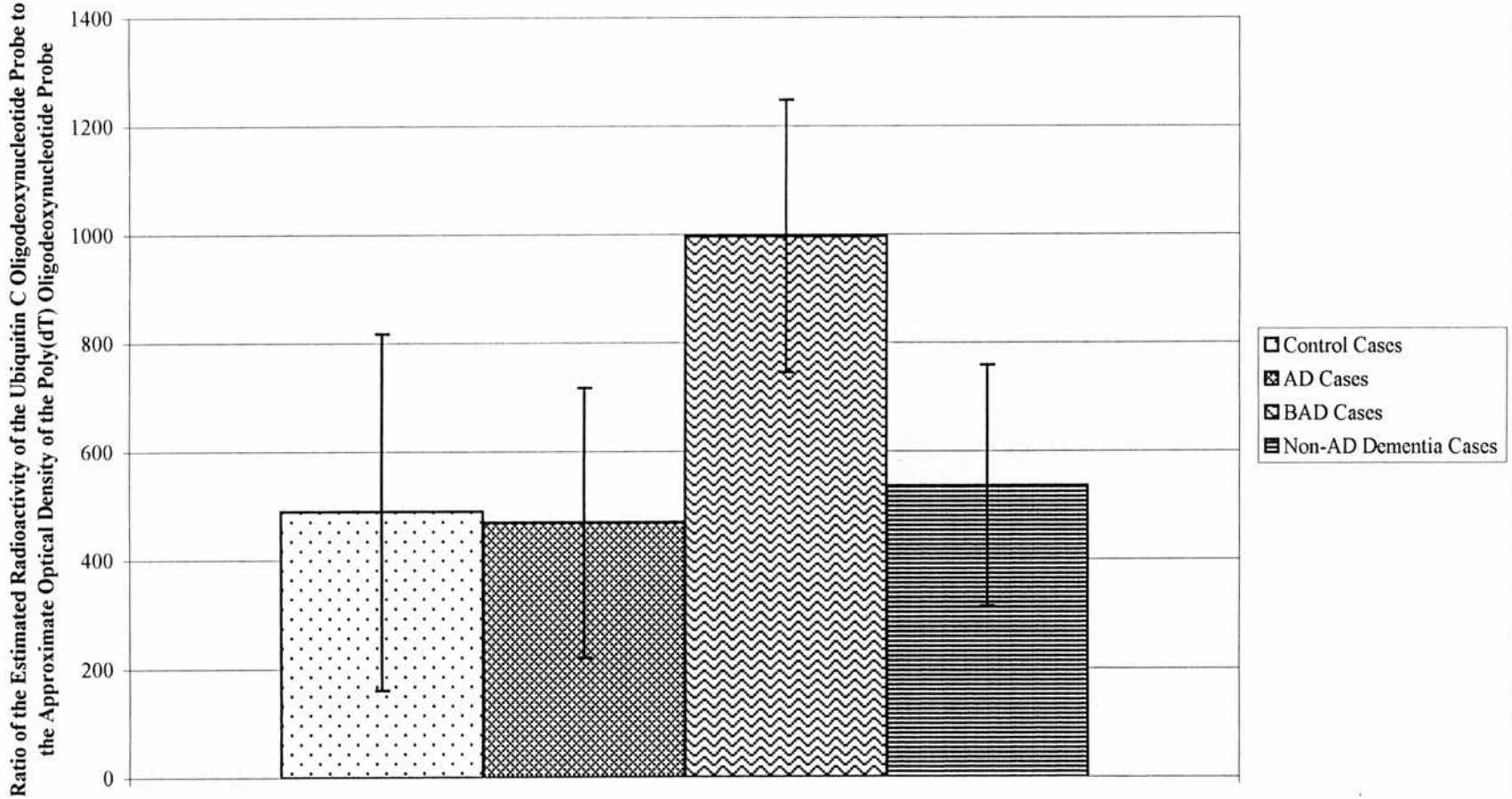

cases (Figure 6.16). The ubiquitin A/poly(dT) ratio, however, did not differ significantly between the four diagnostic groups. The Levene test for homogeneity of variance was not significant for the ubiquitin A/poly(dT) ratio in the visual cortex (Figure 6.17).

6.3.5 Correlations Identified on Analysis of the Ubiquitin Oligodeoxynucleotide Probes

6.3.5.1 Correlations Involving the Ubiquitin C and Ubiquitin A Oligodeoxynucleotide Probes in the Visual Cortex

A correlation matrix comprising thirty-three cells was prepared to examine the relationships, if any, between the ETR of the ubiquitin C and ubiquitin A oligodeoxynucleotide probes in the visual cortex and the age and mini-mental state scores of the subjects, the PMI, pH, storage and severity of neuropathology of the tissue, and the abundance of mRNAs detected by the APP-695, APP-insert, APP-770 and poly(dT) oligodeoxynucleotide probes. A Spearman's rank correlation matrix was prepared for comparison. Correlations, discussed below, were identified between the ETR of the ubiquitin A oligodeoxynucleotide probe, in visual cortex, and both tissue pH and mean hippocampal neuritic plaque frequency. However, no significant correlations were identified between the ETR of the ubiquitin A or C probes and the age and mini-mental state scores of the subjects or between these probes and the PMI and storage of the tissue. No significant correlations were identified between these probes and any neuropathological measure apart from that with the mean hippocampal neuritic plaque frequency referred to above. Therefore, correlation statistics relating only to associations between the various

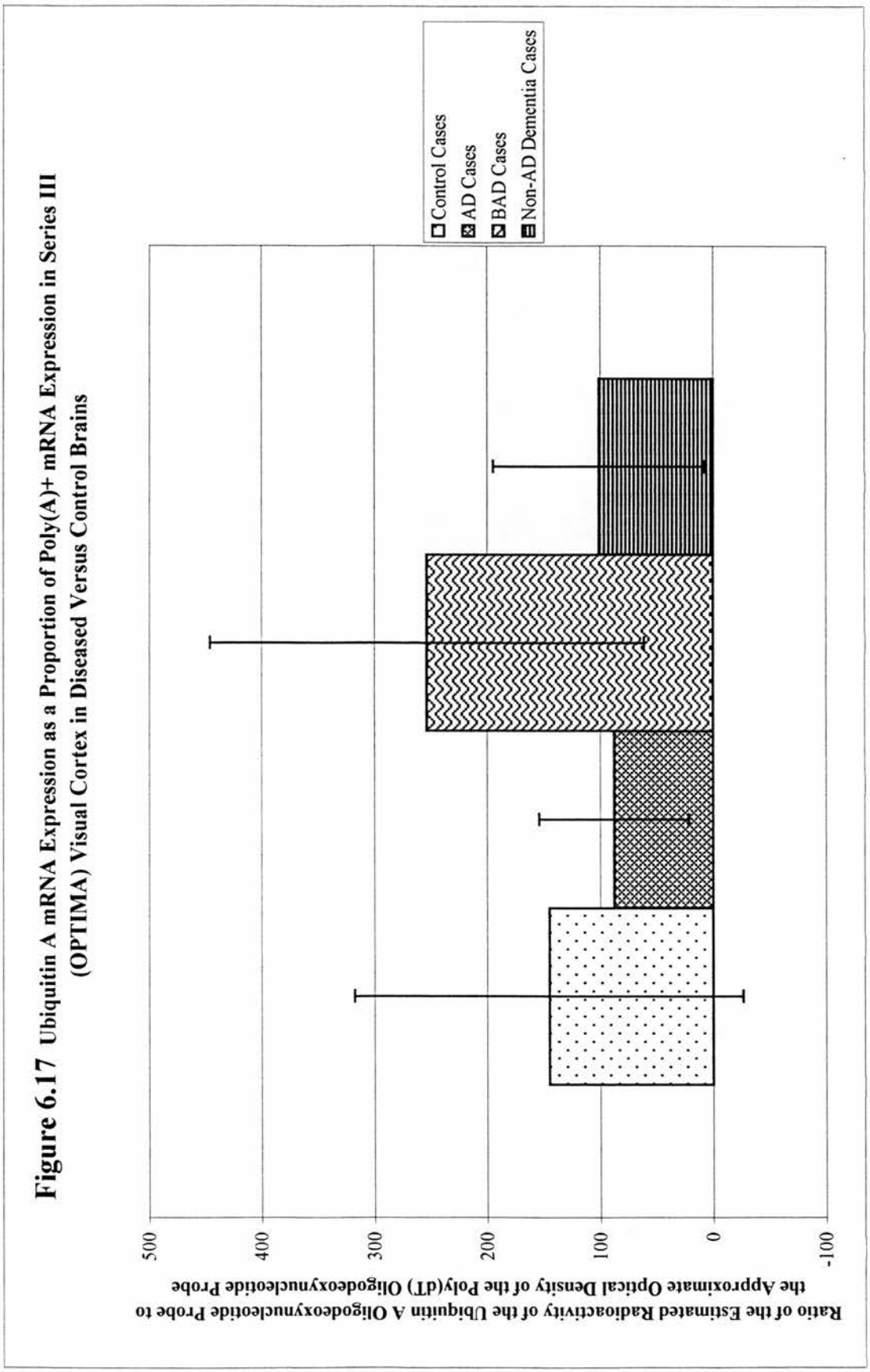

Figure 6.17 Ubiquitin A mRNA Expression as a Proportion of Poly(A)+ mRNA Expression in Series III (OPTIMA) Visual Cortex in Diseased Versus Control Brains

oligodeoxynucleotide probes measured are presented in tables 6.1 and 6.2. Data regarding correlations between the ubiquitin C and ubiquitin A oligodeoxynucleotide probes are presented in both correlation tables for ease of reference.

Both the parametric and non-parametric tests concurred that the ETR of the ubiquitin C oligodeoxynucleotide probe was positively correlated with the AOD of the APP-695 probe (0.813; $p < 0.001$), the AOD of the APP-insert probe (0.810; $p < 0.001$) and the ETR of the ubiquitin A probe (0.868; $p < 0.001$). On non-parametric analysis alone, the ETR of the ubiquitin C probe was positively correlated with the AOD of the APP-770 probe (0.387; $p = 0.029$). Examination of a scatter diagram suggested that these two probes were indeed correlated and that one extreme value was responsible for the non-significance of the parametric test (Figure 6.18).

The parametric and non-parametric tests concurred that the ETR of the ubiquitin A probe was positively correlated with the AOD of the APP-695 probe (0.865; $p < 0.001$) and the AOD of the APP-insert probe (0.839; $p < 0.001$). Examination of a scatter diagram suggested that the ETR of the ubiquitin A probe and the AOD of the APP-770 probe were correlated and that three markedly outlying values were responsible for the non-significance of the parametric test (Figure 6.19). On parametric analysis alone, the ETR of the ubiquitin A probe in the visual cortex was positively correlated with the pH of the tissue (0.400; $p = 0.035$). A scatter diagram revealed that that two were indeed correlated and that the non-significance of the non-parametric test (0.348; $p = 0.070$) was probably due to the relative lack of power

Table 6.1 Pearson's Correlation Coefficients for Series III (OPTIMA) Correlations with the Ubiquitin C Oligodeoxynucleotide Probe

	APP-Insert Probe	APP-Junction Probe	Ubiquitin A Probe
Dentate Gyrus	0.611 (n = 25) **p = 0.001**	0.681 (n = 24) **p = 0.000**	0.823 (n = 26) **p = 0.000**
CA4	0.273 (n = 25) p = 0.187	0.275 (n = 24) p = 0.194	0.607 (n = 26) **p = 0.001**
CA3	0.420 (n = 20) p = 0.066	0.751 (n = 18) **p = 0.000**	0.902 (n = 22) **p = 0.000**
CA1	0.534 (n = 19) **p = 0.018**	0.279 (n = 18) p = 0.262	0.517 (n = 21) **p = 0.016**
Visual Cortex	0.810 (n = 32) **p = 0.000**	0.813 (n = 31) **p = 0.000**	0.868 (n = 32) **p = 0.016**

Table 6.2 Pearson's Correlation Coefficients for Series III (OPTIMA) Correlations with the Ubiquitin A Oligodeoxynucleotide Probe			
	APP-Insert Probe	**APP-Junction Probe**	**Ubiquitin A Probe**
Dentate Gyrus	0.714 (n = 23) **p = 0.000**	0.701 (n = 22) **p = 0.000**	0.823 (n = 26) **p = 0.000**
CA4	0.160 (n = 23) p = 0.465	0.283 (n = 22) p = 0.201	0.607 (n = 26) **p = 0.001**
CA3	0.557 (n = 19) **p = 0.013**	0.726 (n = 17) **p = 0.001**	0.902 (n = 22) **p = 0.000**
CA1	0.512 (n = 19) **p = 0.025**	0.786 (n = 18) **p = 0.000**	0.517 (n = 21) **p = 0.016**
Visual Cortex	0.839 (n = 34) **p = 0.000**	0.865 (n = 33) **p = 0.000**	0.868 (n = 32) **p = 0.016**

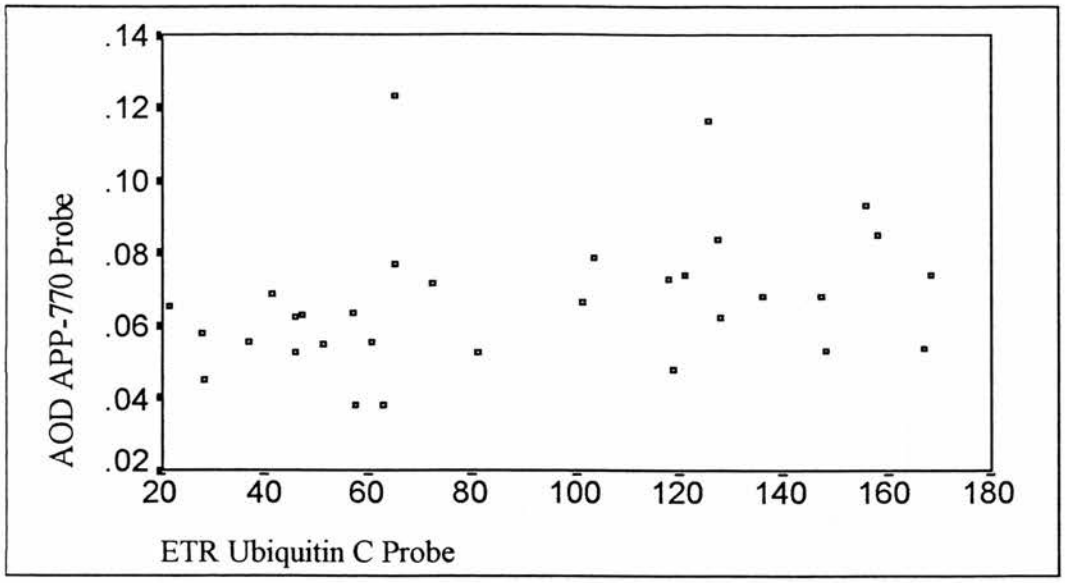

Figure 6.18 The Estimated Tissue Radioactivity of the Ubiquitin C Oligodeoxynucleotide Probe Plotted Against the Approximate Optical Density of the APP-770 Oligodeoxynucleotide Probe in Series III (OPTIMA) Visual Cortex

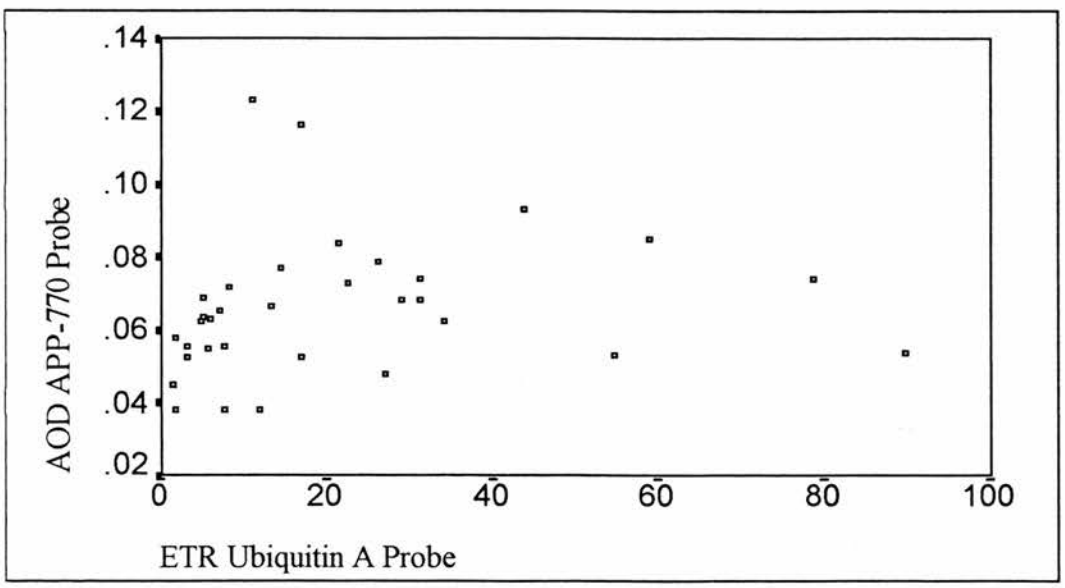

Figure 6.19 The Estimated Tissue Radioactivity of the Ubiquitin A Oligodeoxynucleotide Probe Plotted Against the Approximate Optical Density of the APP-770 Oligodeoxynucleotide Probe in Series III (OPTIMA) Visual Cortex

of this test (Figure 6.20). A correlation between the ETR of the ubiquitin A probe and the mean hippocampal neuritic plaque frequency, on parametric analysis alone, was disregarded on scrutiny of a scatter diagram (Figure 6.21). Seven cells were significant in the matrix of thirty-three cells, a finding that is unlikely to be due to chance, since the probability of obtaining five significant cells in a matrix of thirty cells is $p = 0.016$.

6.3.5.2 Correlations Involving the Ubiquitin C and Ubiquitin A Oligodeoxynucleotide Probes in the Hippocampus

A Pearson's correlation matrix comprising thirty-one cells was constructed to examine the relationships, if any, between the ETR of the ubiquitin C and ubiquitin A oligodeoxynucleotide probes in the dentate gyrus and the age and mini-mental state scores of the subjects, the PMI, pH, storage and severity of neuropathology of the tissue, and the abundance of the mRNAs detected by the APP-695, APP-insert and APP-770 probes. An identical Spearman's rank correlation matrix was constructed for comparison. Apart from a significant correlation, discussed below, between the ETR of the ubiquitin C oligodeoxynucleotide probe, in dentate gyrus, and the mean hippocampal NFT density, no other significant correlations were identified between the ETR of the ubiquitin C and A probes in this region and the age and mini-mental state scores of the subjects, the PMI, pH and storage of the tissue or any other neuropathological parameter. Therefore, correlation statistics relating only to associations between the various oligodeoxynucleotide probes measured are presented in tables 6.1 and 6.2. Data regarding correlations between

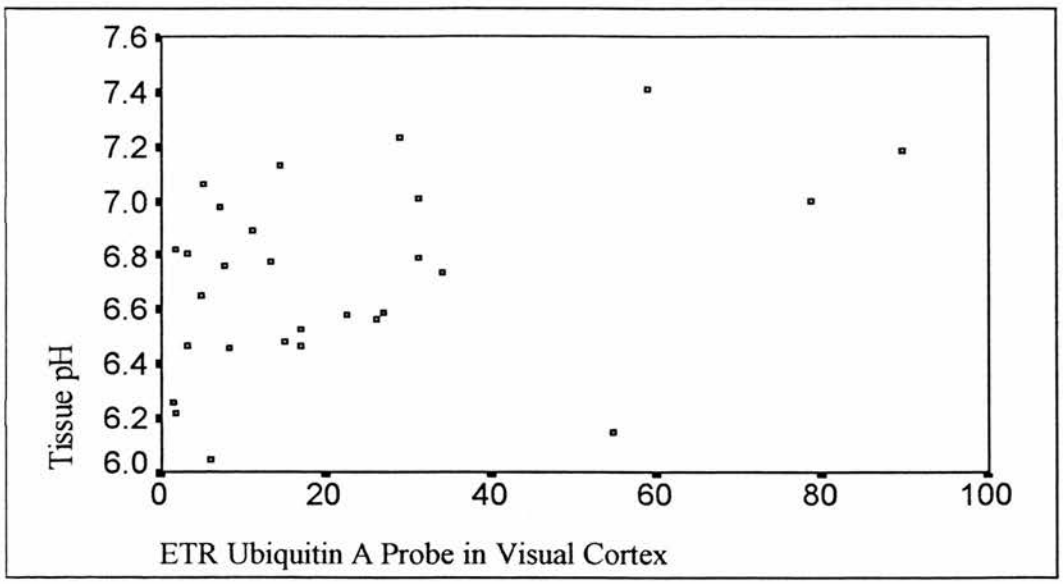

Figure 6.20 The Estimated Tissue Radioactivity of the Ubiquitin A Oligodeoxynucleotide Probe in the Visual Cortex Plotted Against Tissue pH for Series III (OPTIMA) Cases

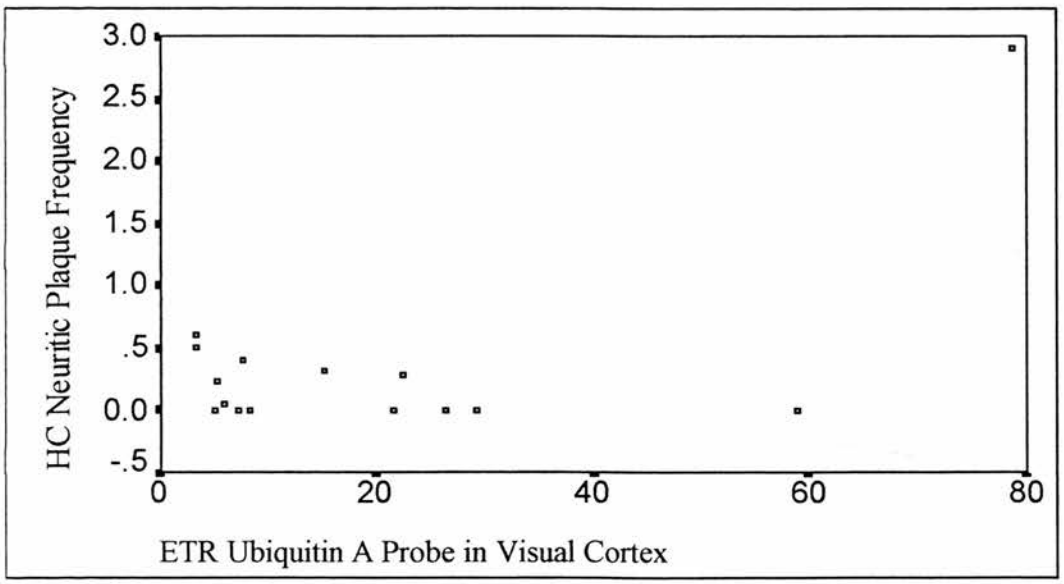

Figure 6.21 The Estimated Tissue Radioactivity of the Ubiquitin A Oligodeoxynucleotide Probe in the Visual Cortex Plotted Against the Mean Hippocampal Neuritic Plaque Frequency for Series III (OPTIMA) Cases

the ubiquitin C and ubiquitin A oligodeoxynucleotide probes are presented in both correlation tables for ease of reference.

Parametric and non-parametric tests concurred that the ETR of the ubiquitin C and ubiquitin A oligodeoxynucleotide probes were positively correlated in the dentate gyrus ($p < 0.001$). The ubiquitin C probe was correlated with both APP-695 ($p < 0.001$) and APP-insert ($p = 0.001$) oligodeoxynucleotide probes on both parametric and non-parametric analysis. An additional significant parametric correlation between the mean hippocampal NFT density and the ETR of the ubiquitin C oligodeoxynucleotide probe in this region (Pearson's $p = 0.020$; Spearman's $p = 0.186$) was discounted on examination of a scatter diagram (Figure 6.22). The ubiquitin A oligodeoxynucleotide probe in the dentate gyrus positively correlated with the abundance of APP-695 mRNA ($p < 0.001$) and APP-insert ($p < 0.001$) on both parametric and non-parametric tests. Six significant findings in a correlation matrix of thirty-one cells is likely to be significant, since the probability of obtaining five significant cells in a matrix of thirty-five cells is $p = 0.029$.

A similar Pearson's correlation matrix and Spearman's rank correlation matrix were prepared for hippocampal subfields CA4, CA3 and CA1.

No significant correlations were identified between the ETR of the ubiquitin C and A oligodeoxynucleotide probes, in hippocampal subfields CA4, CA3 and CA1, and the age and mini-mental state scores of the subjects or the PMI, pH, storage and severity

of neuropathology of the tissue. Therefore, only correlation statistics relating to the various oligodeoxynucleotide probes examined are presented in tables 6.1 and 6.2.

The ubiquitin C and ubiquitin A oligodeoxynucleotide probes were correlated on both parametric and non-parametric tests in hippocampal subfields CA4, CA3 and CA1 ($p < 0.020$). In CA4 this was the only significant finding. Using both parametric and non-parametric statistics the ETR of the ubiquitin C oligodeoxynucleotide probe was positively correlated with the AOD of the APP-insert probe ($p = 0.018$) in hippocampal subfield CA1, while in CA3 the ubiquitin C probe was correlated with the APP-695 oligodeoxynucleotide probe ($p < 0.001$). Non-parametric analysis suggested that the ubiquitin C oligodeoxynucleotide probe in CA3 was also correlated with APP-insert ($p = 0.016$) though the parametric test was not significant ($p = 0.066$). Examination of a scatter diagram suggested that the two were indeed correlated and that a single outlying value was responsible for the non-significance of the parametric test (Figure 6.23).

In hippocampal subfield CA1 the abundance of ubiquitin A mRNA was positively correlated with the abundance of APP-695 mRNA ($p < 0.001$) and APP-insert mRNA ($p = 0.025$) on both parametric and non-parametric analysis.

The correlation statistics relating to hippocampal subfields CA4, CA3 and CA1 suggest that the number of significant cells are no more than would have been expected to occur by chance.

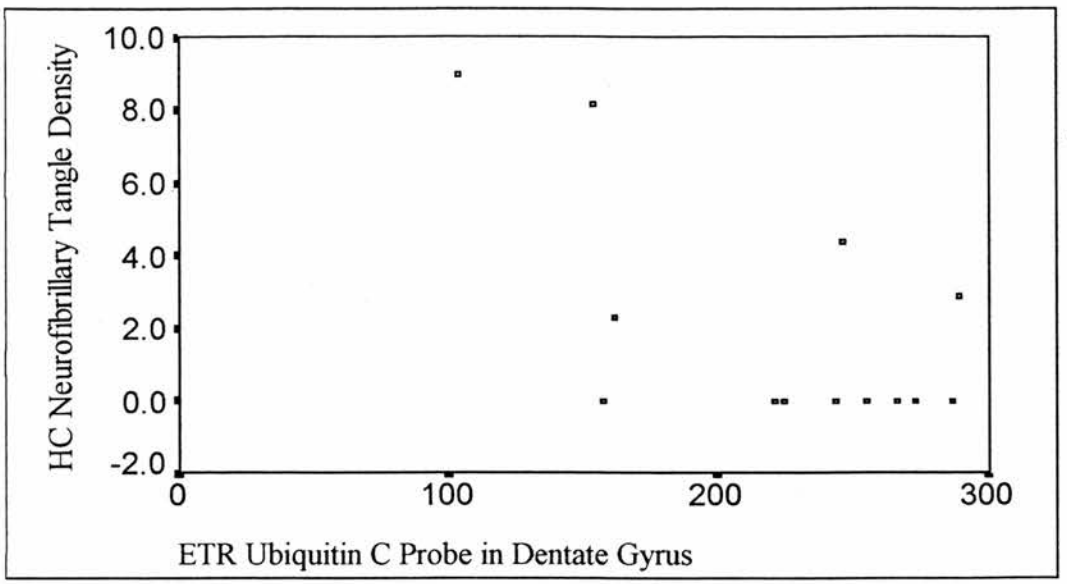

Figure 6.22 The Estimated Tissue Radioactivity of the Ubiquitin C Oligodeoxynucleotide Probe in Dentate Gyrus Plotted Against the Mean Hippocampal Neurofibrillary Tangle Density for Series III (OPTIMA) Cases

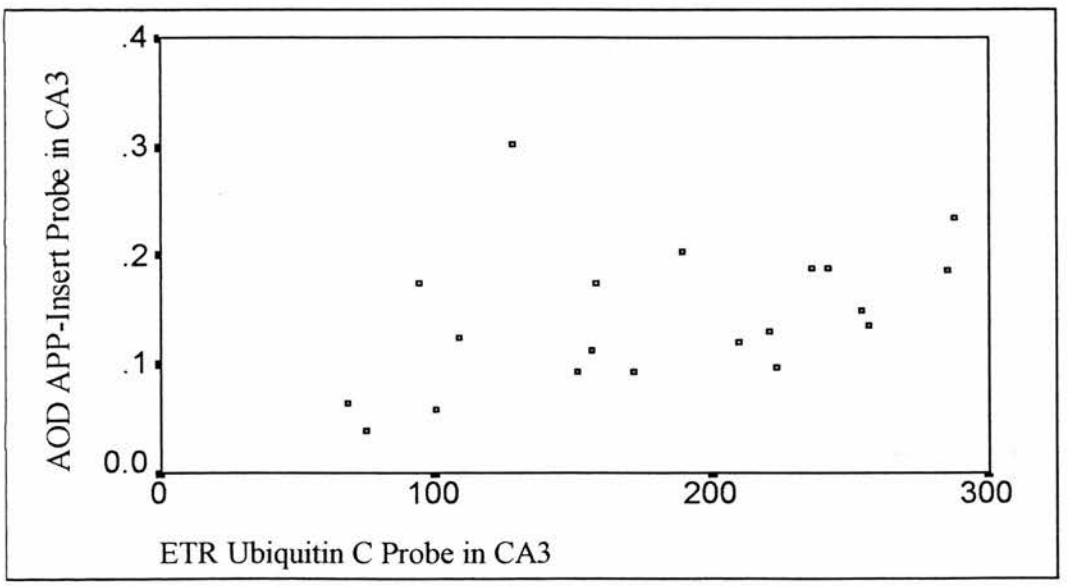

Figure 6.23 The Estimated Tissue Radioactivity of the Ubiquitin C Oligodeoxynucleotide Probe in Hippocampal Subfield CA3 Plotted Against the Mean Hippocampal Neurofibrillary Tangle Density for Series III (OPTIMA) Cases

6.4 Discussion

The ^{14}C microscales were used consistently during the analysis of ubiquitin mRNA by ISHH in the visual cortex and hippocampus, allowing the relationship between exposure of the films to radioactivity and their resulting greyness to be methodically explored. Subsequently, the conversion of the mean grey levels to optical density readings was abandoned in favour of a demonstrably superior alternative transformation. The alternative formula used to generate an estimate of the radioactivity inherent in the hybridised tissue sections involved transforming mean grey levels as follows: log10(255 - mean grey level). Mean grey levels transformed in this way were linearly related to the log10(ETR). Importantly, the range over which the alternatively transformed mean grey levels were linearly related to the log10(ETR) was equal, or superior, to the range over which optical density was linearly related to the ETR. Moreover, using the alternative formula scatter of the data about the line of best fit relating log10(255 - mean grey level) to log10(ETR) was minimal. Obtaining the antilog of the log10(ETR) was simple and allowed an estimate of the radioactivity inherent in the section, the parameter of interest, to be made directly, in contrast to the circuitous estimation of optical density. Further, the radioactivity inherent in sections hybridised with antisense and sense oligodeoxynucleotide probes could be estimated identically and correction for non-specific binding was simple and intuitive. However, this promising, alternative transformation needs to be tested further in order to establish its limitations and wider applicability.

No significant differences were observed in the expression of ubiquitin mRNA in the hippocampus or visual cortex of the control, BAD, AD and non-AD dementia cases studied. However, when the ETR of the ubiquitin C oligodeoxynucleotide probe was expressed as a proportion of all polyadenylated mRNA in the visual cortex, a significantly higher proportion of the polyadenylated mRNA in the BAD cases was accounted for by ubiquitin mRNA than in the AD or control cases. The ubiquitin C probe detects ubiquitin mRNA of all three known molecular weights, though theoretically not the alternative sequence for ubiquitin A published by Lund and colleagues (1985). No significant differences in the ubiquitin A/poly(dT) ratio in the visual cortex were observed between the diagnostic groups. Presumably the ubiquitin A oligodeoxynucleotide probe detects such a small proportion of ubiquitin mRNA that any change in relation to the abundance of all polyadenylated mRNA would be negligible.

The BAD cases lack the definitive pathological stigmata of AD and in all probability represent an early stage in the progression of the disease. Furthermore, the visual cortex represents an area relatively spared in AD that would be expected to show far less pathological involvement than the hippocampus at all stages of the disease. Thus, it would appear that the up-regulation of the ubiquitin system in response to an accumulation of abnormal protein is a feature of early AD: even in the visual cortex in established disease ubiquitin mRNA has returned to control levels. Such up-regulation of ubiquitin mRNA would be difficult to study, since the earliest, pre-clinical stages of AD rarely reach medical attention and a slight deterioration in cognitive ability, especially in individuals with a high pre-morbid intellect, is

notoriously difficult to document with certainty. The examination of the brains of individuals who have suffered from Down's syndrome during life would afford an opportunity to examine ubiquitin expression in at risk groups of neurons destined to develop the pathological stigmata of AD. It would be of interest to investigate whether other members of the heat shock regulon, including APP, are increased in such cells. The increase in ubiquitin mRNA would appear to be occurring even before a definitive neuropathological diagnosis of AD can be made, presumably in response to an, as yet, invisible accumulation of abnormal intracellular protein. The increase in ubiquitin mRNA relative to polyadenylated mRNA in the visual cortex may signal the incipient failure of intracellular ATP-dependent proteolysis. Similar subtle alterations have been identified in the parallel lysosomal proteolytic system in apparently healthy neurons, a sign of metabolic dysfunction that is believed to signal future cellular degeneration (Nixon *et al.*, 1992).

The importance of a functional stress response to cellular survival is underlined by Heydari and co-workers (1993) who examined the ability of hepatocytes isolated from young and aged rats to express heat shock proteins in response to a thermal stress. The authors documented an age-related decline in heat shock transcription as a result of a decreased binding of HSF to the heat shock element. Caloric restriction of the aged rats, a practice consistently demonstrated to retard the effects of ageing in mammals, reversed this age-related decline in heat shock transcription. Further evidence of the key role of the heat shock proteins, and ubiquitin in particular, in neuronal survival, is the role of ubiquitin in ischaemic tolerance (Kato *et al.*, 1993). Survival of gerbil hippocampal neurons following ischaemia parallels the recovery of

ubiquitin immunoreactivity. Neurons in hippocampal subfield CA1 that are destined to die following ischaemia, never recover ubiquitin immunoreactivity, whereas CA1 cells pre-treated with sub-lethal ischaemia recover ubiquitin immunoreactivity and survive. Even more cogent is the fact that the toxic effects of β-amyloid on rat pheochromocytoma PC12 cells can be attenuated by prior exposure of the cell cultures to heat shock (Behl and Schubert, 1993).

The unusual genomic arrangement of ubiquitin C in which identical polypeptide sequences are tandemly repeated in a single mRNA reading frame, suggests that ubiquitin C is translated as a polyubiquitin precursor that is post-translationally modified (Lund *et al.*, 1985). Such a design allows for the rapid production of ubiquitin in response to stress (Bond and Schlesinger, 1985). It is conceivable that the primary product, polyubiquitin, may have a function distinct from the monomeric form of ubiquitin in cellular metabolism (St John *et al.*, 1986). Significantly, it was not possible to employ a single oligodeoxynucleotide probe to detect all four known splice variants of ubiquitin mRNA. Even the region of greatest homology in the alternative ubiquitin A mRNA sequence detailed by Lund and co-workers (1985). could not be accommodated by the probe chosen to detect the other three known splice variants. Given the rigorous conservation to which the ubiquitin genes are subject (Goldstein *et al.*, 1975) it is possible that the alternative ubiquitin A sequence evolved at a slightly different stage of evolution. As such, it may serve a different function and be subject to different transcriptional controls. Indeed, ubiquitin A is a fusion protein (Lund *et al.*, 1985; Salvesen *et al.*, 1987) that may be biologically active in its own right (Lund *et al.*, 1985). There is evidence that the ubiquitin yeast

genes, UBI1, UBI2, UBI3 and UBI4, are differentially controlled. UBI4, the yeast polyubiquitin gene, is dramatically induced in response to starvation, heat shock or the DNA damageing agents, 4-nitroquinoline 1-oxide and methylmethane sulfonate, but these stresses variably affect transcription of the other three ubiquitin genes (Fraser *et al.*, 1991). This study would support a functional distinction between ubiquitin C and B and ubiquitin A, since only the ubiquitin mRNA identified by the probe derived from the ubiquitin A sequence published by Lund and colleagues (1985), in visual cortex, is significantly positively correlated with tissue pH.

The APP gene promoter contains a stress-inducible heat shock element (Salbaum *et al.*, 1988) and immunochemical studies of APP expression in rats following brain damage by kainic acid injection, suggest that APP is a rapid reactive protein involved in brain damage and repair (Kawarabayashi *et al.*, 1991). The association demonstrated between the APP and the ubiquitin C and ubiquitin A oligodeoxynucleotide probes in the visual cortex and dentate gyrus in this study, suggests that transcriptional control of these genes is intimately related and is further evidence that APP is a member of the heat shock protein superfamily.

Under normal metabolic conditions non-lysosomal ATP-dependent proteolysis is responsible for the degradation of the majority of short-lived and abnormal proteins. It is primarily when the cell is depleted of energy that a significant amount of lysosomal degradation of intracellular protein takes place (Ciechanover *et al.*, 1984a). The central nervous system is particularly vulnerable to metabolic stress given its high energy requirements (Tytell *et al.*, 1993). Positron emission

tomography performed on patients suffering from clinically diagnosed AD has been used to measure regional cerebral glucose metabolism, an index of neuronal activity, and has demonstrated that it is significantly reduced in comparison to that of controls (Foster *et al.*, 1984). Posterior parietotemporal areas were primarily affected, though medial temporal lobe structures were not assessed in this study. Marked metabolic abnormalities were identified even in those patients with mild cognitive impairment, suggesting that cortical metabolic dysfunction can be severe before it is clinically evident (Foster *et al.*, 1984). Analysis of oxygen metabolism in AD has revealed similar evidence of hypometabolism. Reduced oxygen consumption is apparent in the parietal and adjoining areas of the posterior temporal cortex and anterior occipital cortex first, with involvement of the frontal cortex in advanced disease (Bench *et al.*, 1990). This progression of functional deficits, as identified by *in vivo* imageing techniques, mirrors the neuropathological advance of the disease as described by Pearson and Powell (1989). Further, the efficiency of ubiquitination and ubiquitin-mediated degradation of substrate proteins has been demonstrated to be impaired by glycation, a common post-translational modification that increasingly occurs in *in vivo* with advancing age (Takizawa *et al.*, 1993). Thus, age may itself predispose to a deterioration in ubiquitin dependent proteolysis.

The poverty of cellular energy that is a feature of AD (see Bowling and Beal, 1995 for review) may be compounded in the elderly by mitochondrial genome deletions: a phenomenon that is particularly common in tissues, such as the nervous system, that have high energy requirements (Cortopassi *et al.*, 1992). Further, under conditions of cellular stress, the metabolic effort of the cell is re-directed towards the production

of the products of the heat shock genes and the products of other genes are suppressed, potentially compounding the metabolic embarrassment of the cell.

There is evidence for early lysosomal dysfunction in AD. At-risk, but apparently healthy, populations of neurons in the disease exhibit modest lysosomal abnormalities in comparison with the advanced lysosomal disruption seen in overtly abnormal neurons (Nixon *et al.*, 1992). Lysosomes and lysosome-related organelles have been observed to accumulate in at-risk pyramidal neurons of the neocortex and hippocampus that are free of neurofibrillary pathology on thioflavin staining and show no apparent atrophy or chromatolytic changes on Nissl staining (Nixon *et al.*, 1992), suggesting increased lysosomal activity. Further, Cataldo, Mann and Nixon have observed alterations in the lysosomal system of at-risk neurons in the brains of sufferers from Down's syndrome at a time when only diffuse deposits of β-amyloid can be detected and neurofibrillary tangles are few (Nixon *et al.*, 1992). The pyramidal cells of the hippocampus and neocortex appear to be particularly vulnerable to the accumulation of cellular debris, since they show the greatest accumulation of lipofuscin during ageing (Cataldo *et al.*, 1994). Thus, the effects of AD might be predicted to be most conspicuous in these cells (Cataldo *et al.*, 1994).

Significantly, in diseases where the lysosomal system is involved at an early stage, Nixon and Cataldo (1993) believe that the primary abnormality is frequently linked either to lysosomal dysfunction or to the production of large quantities of a digestion-resistant substrate that accumulates within lysosomes. Punctate concentrations of APP have been demonstrated immunochemically in pyramidal

cells of the neocortex, especially those in associative regions, in normal brain (Benowitz *et al.*, 1989). The pyramidal cells of hippocampal subfield CA1 also show intense punctate concentrations of APP in normal brain (Benowitz *et al.*, 1989). Thus, the cerebral regions involved are those most vulnerable to the pathological changes associated with AD. Further, electron microscopy has confirmed that these dense concentrations of APP are contained within secondary lysosomes (Benowitz *et al.*, 1989). Mayer and co-workers (1992) have described the lysosome as a bioreactor for the production of β-amyloid and lysosomal internalisation, partial degradation and subsequent exocytosis of substrate has been indirectly demonstrated in cell culture (Buktenica *et al.*, 1987). Undoubtedly the hypometabolism that is characteristic of AD (see Bowling and Beal, 1995 for review) compromises ATP-dependent non-lysosomal proteolysis and results in increased reliance on lysosomal degradation of intracellular proteins. Enhanced lysosomal activity might be predicted to result in increased amyloidogenic processing of APP and potentially to the extrusion of β-amyloid and β-amyloid-containing peptides into the extracellular space. The results of this study suggest that further investigation of proteolytic mechanisms in AD would be worthwhile, especially since lysosomotropic agents have been shown to reduce β-amyloid production in cell cultures, raising the possibility of therapeutic intervention in the disease process (Shoji *et al.*, 1992).

Concluding Remarks

Any attempt to weave the findings of this thesis into a cohesive whole that underpins AD is to overstate the significance of the data. The possibility that APP mRNA was increased in AD was a biologically plausible and eminently testable hypothesis that merited careful study. However, comprehensive analysis of APP mRNA levels in a large, well-matched series, controlled for known confounding variables, demonstrated that this hypothesis was false. The probable functional association between the heterotrimeric G protein, Goα, and APP, and the tentative conclusion that ubiquitin mRNA is up-regulated in pre-clinical AD, offer tantalising glimpses of the pathophysiology of the disease, but do not significantly alter our understanding of it, while the RT-PCR study proved wholly inconclusive. The relative poverty of significant findings unearthed by this study is disappointing, though the definitive exclusion of an up-regulation of APP mRNA in AD is a profoundly important negative result.

This study illustrates that despite the proven ability of techniques like *in situ* hybridisation histochemistry and the polymerase chain reaction to contribute to our understanding of complex, multi-factorial diseases such as Alzheimer's disease, there is no guarantee that a promising study, however meticulously prosecuted, will reveal illuminating results. A genuine interest in the research question posed is helpful in weathering such scientific disappointments.

The study of mRNA levels, especially APP mRNA levels, in AD has evolved to its current level of sophistication. Early studies simply could not have anticipated the capricious nature of APP mRNA levels or controlled for the variety of factors now known to confound their measurement. Thus, the prosecution of this study benefited from the insights generated by earlier studies of APP mRNA levels in human brain. Further, the laboratory in which this research was performed is dedicated to the study of human neuropsychiatric diseases using primarily post-mortem brain tissue and is actively engaged in addressing the difficulties inherent in such work. Without large numbers of superior tissue samples, expert neuropathological verification of diagnosis, the availability of a positive control group and detailed clinical and demographic information it would not have been possible to identify the increase in ubiquitin C/poly(dT) mRNA levels in borderline AD. Similarly, it would not have been possible to demonstrate that the insert:junction ratio in the visual cortex is relatively immune to the effects of agonal state without data on tissue pH.

At the beginning of a project such as this it is difficult to conceive of its scale and complexity. Indeed, it would not have been possible, at the start, to envisage abandoning the traditional method of quantifying autoradiographic greyness using optical density. Moreover, basic laboratory skills can seem obvious to the experienced and naturally inclined, but may appear obscure and unnecessarily complicated to the novice, and the pace of laboratory research can seem slow, painfully so initially, to the clinician ignorant of the complexity of the endeavour. Further, the de-skilled clinician can be tempted to cling to tasks at which they are competent, especially when they can be legitimised as pressing or urgent, and

would appear prudent to reserve the analysis of such tissue, with all its attendant difficulties, for the resolution of crucially important, highly specific and carefully framed research questions likely to be impervious to other approaches.

Appendix I

Solutions

All chemicals employed in the preparation of the following solutions were of molecular biology grade.

Agarose Gel Loading Buffer
A 6 × concentration of loading gel buffer was prepared by combining a solution of 30% glycerol in purified deionised water with 0.25% of bromophenol blue.

100% Deionised Formamide
Five grams of BioRad AG 501 - X8, 20 - 50 mesh ion exchange resin was added to 50 ml formamide. The solution was stirred for 30 minutes at room temperature and then filtered twice through Whatman No 1 filter paper.

Denhardt's Solution
For 500 ml of a 50 × Denhardt's solution, 5 g ficoll, 5 g polyvinylpyrrolidone and 5 g bovine serum albumin were dissolved in autoclaved, DEPC treated water to achieve a final volume of 500 ml. The solution was then filtered through a disposable Nalgene filter.

Disodium Ethylene Diamine Tetraacetate (EDTA)
For 1 litre of the solution, 37.22 g EDTA was dissolved in 800 ml autoclaved, DEPC treated water with vigorous stirring. The pH was adjusted to 8.0 with solid pellets of sodium hydroxide and autoclaved, DEPC treated water added to give a final volume of 1 litre.

Gelatin/Chrome Alum Subbing Solution for Glass Slides
For 500 ml of a 1% gelatin and 0.05% chromic potassium sulphate subbing solution, 5g gelatin and 250 mg chrome alum were dissolved in 500 ml purified, deionised water with gentle heat. When dissolved, the solution was filtered through Whatman No 1 filter paper. When the solution was cool, racks of slides were dipped into the subbing solution for a few seconds, removed, drained and blotted. The slides were then dried in a 40°C oven overnight.

Hybridisation Buffer
For 50 ml:

10 ml	20 × SSC
1 ml	50 × Denhardt's solution
0.5 ml	0.1 M disodium ethylene diamine tetraacetate (EDTA)
1 ml	denatured herring/salmon sperm DNA
5 mg	yeast tRNA
5 mg	poly A
25 ml	deoinised formamide
5 g	dextran sulphate

The yeast tRNA and poly A are obtained commercially as salts (Sigma) and diluted to a concentration of 10 mg/ml on arrival.

The above reagents, except the dextran sulphate, were combined. The dextran sulphate was then gradually added, while stirring the solution over a gentle heat. When dissolved, the solution was made up to 50 ml with 20 mM phosphate buffer.

Phosphate Buffered Saline
Tablets of phosphate buffered saline containing 137 mM sodium chloride, 2.7 mM potassium chloride and 10 mM phosphate buffer were bought commercially (Sigma). To produce 200 ml phosphate buffered saline one tablet was dissolved in 200 ml purified, deionised water.

Ribonuclease Pre-Treatment Solution
Two hundred ml of ribonuclease solution was prepared as follows. Four hundred µl RNase A solution (Sigma 10 mg/ml), 2 ml 1 M tris (hydroxymethyl) aminomethane (tris) hydrochloride at a pH of 8.0, 1 ml 0.2 M EDTA at a pH of 8.0, 5.8 g sodium chloride and 2 µl RNase T1 (Sigma 100 units/µl) were combined. The solution was made up to a final volume of 200 ml with purified, autoclaved water. The tissue sections were incubated in this solution for 60 minutes at 37°C and then pre-treated and stored as usual.

Sodium Thiosulphate Fixative
For a 30% weight by volume solution of sodium thiosulphate, 300 g of sodium thiosulphate was dissolved in purified, deionised water and made up to a final volume of 1 litre.

Standard Citrate Saline (SSC)
To prepare 1 litre of SSC, 175.3 g sodium chloride and 88.2 g sodium citrate were dissolved in 800 ml autoclaved, DEPC treated water. The pH was adjusted to 7.0 with hydrochloric acid. Autoclaved, DEPC treated water was then added to bring the final volume to one litre.

STE Buffer
To prepare this buffer 0.1 M of sodium chloride, 10 mM of tris chloride and 1 mM of EDTA were dissolved in purified, deionised water to a final volume of one litre. Both of the latter solutions were at a pH of 8.0.

Triethanolamine Hydrochloride (TEA) with Acetic Anhydride
For 250 ml of TEA, 4.625 g TEA and 2.25 g sodium chloride were made up to 250 ml with purified, deionised water. The pH was adjusted to 8.0 with a 10 M solution of sodium hydroxide. Finally, 0.625 ml of acetic anhydride was added immediately prior to use.

Tris Borate EDTA Buffer (TBE)

For 1 litre of 5 × TBE buffer, 54 g tris, 27.5 g boric acid and 20 ml of 0.5 M EDTA at a pH of 8.0 were dissolved in purified, deionised water to a final volume of 1 litre.

Appendix II

Series I Cases						
Case Number	**Diagnosis**	**Sex**	**Age**	**Post Mortem Delay in Hours**	**Agonal State Score**	**Total Storage Time in Days***
S1	Control	Female	82	50		864 (84)
S4	AD	Female	79	31		857 (84)
S11	AD	Female	77	68	2	836 (70)
S12	Control	Male	68	21	3	768 (3)
S14	Control	Female	93			873 (111)
S15	Control	Male	94	27	2	884 (122)
S17	AD	Male	89	29	3	879 (128)
S20	AD	Female	80	20	3	1011 (248)
S23	Control	Female	74	35	1	887 (135)
S25	AD	Female	86	18		1291 (539)
S27	AD	Female	89	3	4	1032 (281)
S28	AD	Male	83	17	2	859 (471)
S29	BAD	Female	71	43		800 (52)
S34	AD	Female	80	17		793 (47)
S40	Control	Female	65	24		669 (306)
S41	AD	Male	88			663 (330)
S42	AD	Male	81	60		768 (430)
S44	AD	Female	90	40	3	744 (406)
S46	AD	Male	79	69	1	793 (447)
S51	Control	Male	74	34		525 (213)
S53	AD	Female	90	46	4	752 (459)
S56	Control	Female	74			662 (363)
S57	Control	Male	89			675 (567)
S61	AD	Male	78	45	3.5	783 (499)
S65	AD	Male	72	19		473 (190)
S66	AD	Female	87	42	2	530 (251)
S67	BAD	Male	79	50	4	448 (174)
S69	Control	Male	93	22	2	887 (610)

Series I Cases						
Case Number	**Diagnosis**	**Sex**	**Age**	**Post Mortem Delay in Hours**	**Agonal State Score**	**Total Storage Time in Days**
S74	Control	Female	67	25	1	516 (248)
S78	AD	Male	67	30	3.5	1355 (1131)
S79	BAD	Female	91	42		684 (462)
S80	AD	Female	98	40	1	585 (362)
S82	AD	Male	81	36	2	545 (333)
S83	AD	Female	84	48	3.5	587 (374)
S89	AD+PD	Female	98	58	3	731 (590)
S90	Control	Male	81			362 (223)
S92	BAD	Female	85			391 (287)
S96	Control	Male	72		4	408 (215)
S100	AD	Male	85	24		387 (202)
H12	AD	Female	44	27	2	1557 (147)
H53	AD	Male	84	38	1	1458 (106)
H71	Control	Male	69	70	4	1333 (33)
H81	Control	Male	64	60	1	1242 (48)
H94	AD+MID	Male	83	16	4	1153 (80)
H95	AD	Female	59	9	4	989 (21)

*The first figure denotes the total storage time of the tissue. The figure in brackets represents the duration of storage of the tissue as an uncut block, the remaining days being storage of the tissue as cryostat cut sections.

Series II Cases						
Case Number	**Diagnosis**	**Sex**	**Age**	**Post Mortem Delay in Hours**	**Agonal State Score**	**Total Storage Time in Days**
S1	Control	Female	82	50		1119
S12	Control	Male	68	21	3	1023
S14	Control	Female	93			1128
S15	Control	Male	94	27	2	1039
S20	AD	Female	80	20	3	1266
S23	Control	Female	74	35	1	1142
S25	AD	Female	86	18		1546
S27	AD	Female	89	3	4	1287
S28	AD	Male	83	17	2	1114
S40	Control	Female	65	24		924
S41	AD	Male	88			918
S42	AD	Male	81	60		1023
S44	AD	Female	90	40	3	999
S46	AD	Male	79	69	1	1030
S51	Control	Male	74	34		680
S53	AD	Female	90	46	4	1007
S65	AD	Male	72	19		728
S66	AD	Female	87	42	2	785
S69	Control	Male	93	22	2	1142
S74	Control	Female	67	25	1	771
S78	AD	Male	67	30	3.5	1610
S79	BAD	Female	91	42		939
S80	AD	Female	98	40	1	840
S82	AD	Male	81	36	2	800
S83	AD	Female	84	48	3.5	842
S90	Control	Male	81			617
S92	BAD	Female	85			646
S96	Control	Male	72		4	663

Series II Cases						
Case Number	**Diagnosis**	**Sex**	**Age**	**Post Mortem Delay in Hours**	**Agonal State Score**	**Total Storage Time in Days**
S100	AD	Male	85	24		642
H53	AD	Female	84	38	1	1713
H81	Control	Male	64	60	1	1497
H94	AD+MID	Male	83	16	4	1408

Series III – The OPTIMA Series						
Case Number	**Diagnosis**	**Sex**	**Age**	**Post Mortem Delay in Hours**	**Tissue pH**	**Total Storage Time in Years**
C3031	Non-AD Neurodeg Disorder	Female	77	16		6
C3452	AD	Female	83	29	6.47	6
C3630	Non-Neurodeg Disorder	Male	75	8	7.41	5
C3965	Non-Neurodeg Disorder	Female	67	22	6.76	5
C3970	AD	Female	87	39		5
C4017	AD	Male	82	36	7.00	5
C4227	Non-AD Neurodeg Disorder	Female	88	14	6.79	5
C4295	AD	Male	84	36	6.05	5
1026/90	AD	Male	76	30	6.69	5
1123/91	BAD	Male	73	38	6.57	4
1174/91	Control	Female	81	78	6.57	4
1250/91	AD	Female	74	30	6.81	4
1313/91	AD	Female	83	44	6.48	4
1366/91	Non-Neurodeg Disorder	Male	88	28	6.46	4
1381/91	AD	Male	74	56	6.58	4
1009/92	Non-Neurodeg Disorder	Male	83	42	6.65	3
1020/92	Non-AD Neurodeg Disorder	Female	83	13	7.06	3
1027/92	BAD	Male	67	55	7.23	3
1125/92	AD	Female	70	22		4
1274/92	Control	Male	79	29	6.98	3

Series III – The OPTIMA Series						
Case Number	**Diagnosis**	**Sex**	**Age**	**Post Mortem Delay in Hours**	**Tissue pH**	**Total Storage Time in Years**
1309/92	Control	Female	73	40	6.22	3
1436/92	BAD	Female	89	24	6.48	3
1438/92	AD	Male	74	39	6.53	3
1127/93	Control	Male	65	24		2
1135/93	Non-AD Neurodeg Disorder	Female	86	50	6.82	2
1165/93	Control	Male	87	43		2
1214/93	Non-Neurodeg Disorder	Female	86	41	6.89	2
1306/93	AD	Female	68	30	6.59	2
1431/93	Non-AD Neurodeg Disorder	Male	72	19	6.74	2
1034/94	BAD	Male	89	16	6.78	1
1182/94	Control	Female	80	37	6.47	1
1234/94	Control	Male	82	43	6.26	1
1252/94	AD	Male	62	34	7.01	1
1315/94	BAD	Female	83	20	6.15	1
1340/94	Control	Male	68	17	7.19	1
1376/94	Non-Neurodeg Disorder	Female	83	68	6.30	1
1445/94	AD	Female	91			1
1004/95	AD	Female	80	35	6.70	1
1145/95	Non-AD Neurodeg Disorder	Female	88	47	7.13	1

Series IV Cases				
Details of Cases Selected from Series II (Visual Cortex)				
Case Number	**Diagnosis**	**Sex**	**Age**	**Post-Mortem Delay in Hours**
S1	Control	Female	82	50
S14	Control	Female	93	
S20	AD	Female	80	20
S23	Control	Female	74	35
S25	AD	Female	86	18
S27	AD	Female	89	3
S28	AD	Male	83	17
S40	Control	Female	65	24
S41	AD	Male	88	
S42	AD	Male	81	60
S44	AD	Female	90	40
S46	AD	Male	79	69
S51	Control	Male	74	34
S53	AD	Female	90	46
S65	AD	Male	72	19
S66	AD	Female	87	42
S69	Control	Male	93	22
S74	Control	Female	67	25
S78	AD	Male	67	30
S80	AD	Female	98	40
S82	AD	Male	81	36
S90	Control	Male	81	
S96	Control	Male	72	
S100	AD	Male	85	24
H53	AD	Male	84	38
H81	Control	Male	64	60

Series IV Cases				
Details of Cases Selected from Series III (OPTIMA Series) (Visual Cortex, Dentate Gyrus and Hippocampal Fields CA4, CA3 and CA1)				
Case Number	**Diagnosis**	**Sex**	**Age**	**Post-Mortem Delay in Hours**
C3452	AD	Female	83	29
C3970	AD	Female	87	39
C4017	AD	Male	82	36
C4295	AD	Male	84	36
1174/91	Control	Female	81	78
1250/91	AD	Female	74	30
1313/91	AD	Female	83	44
1381/91	AD	Male	74	56
1125/92	AD	Female	70	22
1438/92	AD	Male	74	39
1127/93	Control	Male	65	24
1165/93	Control	Male	87	43
1306/93	AD	Female	68	30
1182/94	Control	Female	80	37
1234/94	Control	Male	82	43
1252/94	AD	Male	62	34
1274/94	Control	Male	79	29
1340/94	Control	Male	68	17
1445/94	AD	Female	91	
1004/95	AD	Female	80	35

Series IV Cases				
Details of Cases Selected from Dr. A.J.L. Barton's Experiment (Visual Cortex, Dentate Gyrus and Hippocampal Fields CA4, CA3 and CA1)				
Case Number	**Diagnosis**	**Sex**	**Age**	**Post-Mortem Delay in Hours**
107	AD	Female	92	11
109	AD	Male	77	35
1011	AD	Female	76	39
1013	AD	Male	77	86
1016	AD	Female	66	40
1028	AD	Female	91	6
1043	Control	Male	66	7
1045	Control	Female	96	68
1053	AD	Male	85	38
1058	AD	Male	61	12
1063	AD	Female	81	23
1066	Control	Female	73	24
1072	Control	Female	83	27
1073	Control	Male	78	94
1074	Control	Male	59	20
1078	Control	Male	64	22
1079	Control	Female	74	11
1080	Control	Male	51	29
1081	Control	Male	64	60
1084	Control	Male	70	41

Series IV Cases				
Details of Cases Selected from Dr. M.H. Griffiths's Experiment (Dentate Gyrus and Hippocampal Fields CA4, CA3 and CA1)				
Case Number	**Diagnosis**	**Sex**	**Age**	**Post-Mortem Delay in Hours**
835	Control	Male	77	48
986	Control	Male	78	42
1010	Control	Male	84	8
1015	AD	Female	77	24
1022	Control	Male	69	28
1029	AD	Female	81	17
1050	AD	Male	82	75
1289	AD	Female	87	31
1419	Control	Male	55	24
1590	AD	Female	81	38
1639	Control	Female	91	48
1790	AD	Female	73	39
7292	Control	Female	76	31

References

Abe, K., St.George-Hyslop, P.H., Tanzi, R.E., & Kogure, K. (1991a). Induction of amyloid precursor protein mRNA after heat shock in cultured human lymphoblastoid cells. Neuroscience Letters, 125, 169-171.

Abe, K., Tanzi, R.E., & Kogure, K. (1991b). Induction of HSP70 mRNA after transient ischemia in gerbil brain. Neuroscience Letters, 125, 166-168.

Abravaya, K., Myers, M.P., Murphy, S.P., & Morimotot, R.I. (1992). The human heat shock protein hsp70 interacts with HSF, the transcription factor that regulates heat shock gene expression. Genes and Development, 6, 1153-1164.

Adams, C. (1997). Alzheimer's disease research: A game of connect the dots. Gerontology, 43, 8-19.

Aisen, P.S. & Davis, K.L. (1994). Inflammatory mechanisms in Alzheimer's disease: Implications for therapy. Am J Psychiatry, 151, 1105-1113.

Akiyama, H. & McGeer, P.L. (1990). Brain microglia constitutively express β-2 integrins. Journal of Neuroimmunology, 30, 81-93.

Aldridge, J. (1993). The principles of image analysis. Quantitative Neuropathology, Cambridge 2.4.93, 2-16.(abstract)

Alzheimer, A. (1987). About a Peculiar Disease of the Cerebral Cortex (Uber eine eigenartige Erkrankung der Hirnrinde. Allgemeine Zeitschrift fur Psychiatrie und Psychisch-Gerichtliche Medizin 64:146-148, 1907). Alzheimer Disease and Associated Disorders, 1, 7-8.

Ananthan, J., Goldberg, A.L., & Voellmy, R. (1986). Abnormal Proteins Serve as Eukaryotic Stress Signals and Trigger the Activation of Heat Shock Genes. Science, 232, 522-524.

Anderson, J.P., Chen, Y., Kim, K.S., & Robakis, N.K. (1992). An alternative secretase cleavage produces soluble Alzheimer amyloid precursor protein containing a ptentially amyloidogenic sequene. Journal of Neurochemistry, 59, 2328-2331.

Babila, T., Schaad, N.C., & Klein, D.C. (1992). Rat pineal Gsα, Giα and Goα: relative abundance and development. Brain Research, 572, 232-235.

Baker, R.T. & Board, P.G. (1987a). The human ubiquitin gene family: structure of a gene and pseudogenes from the Ub B subfamily. Nucleic Acids Research, 15, 443-463.

Baker, R.T. & Board, P.G. (1987b). Nucleotide sequence of a human ubiquitin Ub B processed pseudogene. Nucleic Acids Research, 15, 4352

Ballard, C., Coope, B., Oyebode, F., & Wilcock, G. (1997). Depression in dementia sufferers-comparison of diagnostic criteria. JAGS, 45, 123-124.

Bargmann, C. & Weinberg, R.A. (1988). Oncogenic activation of the neu-encoded receptor protein by point mutation and deletion. EMBO, 7, 2043-2052.

Barrow, C.J. & Zagorski, M.G. (1991). Solution structures of β peptide and its constituent fragments: Relation to amyloid deposition. Science, 253, 179-182.

Barton, A.J.L. Studies of Gene Expression in the Central Nervous System in Relation to Alzheimer's Disease. PhD thesis submitted 1991 to the University of London.

Barton, A.J.L., Pearson, R.C.A., Najlerahim, A., & Harrison, P.J. (1993). Pre- and postmortem influences on brain RNA. Journal of Neurochemistry, 61, 1-11.

Behl, C. & Schubert, D. (1993). Heat shock partially protects rat pheochromocytoma PC12 cells from amyloid β peptide toxicity. Neuroscience Letters, 154, 1-4.

Bench, C.J., Dolan, R.J., Friston, K.J., & Frackowiak, R.S.J. (1990). Positron emission tomography in the study of brain metabolism in psychiatric and neuropsychiatric disorders. British Journal of Psychiatry, 157, 82-95.

Benesch, C.G., McDaniel, K.D., Cox, C., & Hamill, R.W. (1993). End-stage Alzheimer's disease. Arch Neurol, 50, 1309-1315.

Benowitz, L.I., Rodriguez, W., Paskevich, P., Mufson, E.J., Schenk, D., & Neve, R.L. (1989). The Amyloid Precursor Protein Is Concentrated in Neuronal Lysosomes in Normal and Alzheimer Disease Subjects. Experimental Neurology, 106, 237-250.

Bertrand, P., Sanford, J., Rudolph, U., Codina, J., & Birnbaumer, L. (1990). At least three alternatively spliced mRNAs encoding two α_subunits of the Go GTP-binding protein can be expressed in a single tissue. The Journal of Biological Chemistry, 265, 18576-18580.

Birnbaumer, L. (1992). Receptor-to-effector signaling through G proteins: Roles for bgamma dimers as well as a subunits. Cell, 71, 1069-1072.

Bland, J.M. & Altman, D.G. (1996). Transformations, means and confidence intervals. British Medical Journal, 312, 1079

Bond, U. & Schlesinger, M.J. (1985). Ubiquitin is a heat shock protein in chicken embryo fibroblasts. Molecular and Cellular Biology, 5, 949-956.

Bonkale, W.L., Fastbom, J., Wiehager, B., Ravid, R., Winblad, B., & Cowburn, R.F. (1996). Impaired G-protein-stimulated adenylyl cyclase activity in Alzheimer's disease brain is not accompanied by reduced cyclic-AMP-dependent protein kinase A activity. Brain Research, 737, 155-161.

Bourtchuladze, R., Frenguelli, B., Blendy, J., Cioffi, D., Schutz, G., & Silva, A.J. (1994). Deficient long-term memory in mice with a targeted mutation of the cAMP-responsive element-binding protein. Cell, 79, 59-68.

Bowen, D.M., Smith, C.B., White, P., & Davison, A.N. (1976). Neurotransmitter-related enzymes and indices of hypoxia in senile dementia and other abiotrophies. Brain, 99, 459-496.
Bowes, M.P., Masliah, E., Otero, D.A.C., Zivin, J.A., & Saitoh, T. (1994). Reduction of neurological damage by a peptide segment of the amyloid b/A4 protein precursor in a rabbit spinal cord ischemia model. Exp Neurol, 129, 112-119.

Bowling, A.C. & Beal, M.F. (1995). Bioenergetic and oxidative stress in neurodegenerative diseases. Life Sciences, 56, 1151-1171.

Boyles, J.K., Pitas, R.E., Wilson, E., Mahley, R.W., & Taylor, J.M. (1985). Apolipoprotein E associated with astrocytic glia of the central nervous system and with nonmyelinating glia of the peripheral nervous system. Journal of Clinical Investigation, 76, 1501-1513.

Braak, E., Braak, H., & Mandelkow, E.M. (1994). A sequence of cytoskeleton changes related to the formation of neurofibrillary tangles and neuropil threads. Acta Neuropathol (Berl), 87, 554-567.

Braak, H. & Braak, E. (1991). Neuropathological stageing of Alzheimer-related changes. Acta Neuropathol, 82, 239-259.

Bray, P., Carter, A., Simons, C., Guo, V., Puckett, C., Kamholz, J., Spiegel, A., & Nirenberg, M. (1986). Human cDNA clones for four species of Gαs signal transduction protein. Proc Natl Acad Sci USA, 83, 8893-8897.

Brayne, C. (1993). Research and Alzheimer's disease: an epidemiological perspective. Psychological Medicine, 23, 287-296.

Breitner, J.C.S., Welsh, K.A., Helms, M.J., Gaskell, P.C., Gau, A.A., Roses, A.D., Pericak-Vance, M.A., & Saunders, A.M. (1995). Delayed onset of Alzheimer's disease with nonsteroidal anti-inflammatory and histamine H2 blocking drugs. Neurobiology of Aging, 16, 523-530.

Breitner, J.C.S. & Folstein, M.F. (1984). Familial Alzheimer dementia: a prevalent disorder with specific clinical features. Psychological Medicine, 14, 63-80.

Brenner, D.E., Kukull, W.A., Stergachis, A., van Belle, G., Bowen, J.D., McCormick, W.C., Teri, L., & Larson, E.B. (1994). Postmenopausal estrogen replacement therapy and the risk of Alzheimer's disease: A population-based case-control study. Am J Epidemiol, 140, 262-267.

Brunden, K.R., Windebank, A.J., & Poduslo, J.F. (1990). Catabolic regulation of the expression of the major myelin glycoprotein by schwann cells in culture. Journal of Neurochemistry, 54, 459-466.

Buktenica, S., Olenick, S.J., Salgia, R., & Frankfater, A. (1987). Degradation and regurgitation of extracellular proteins by cultured mouse peritoneal macrophages and baby hamster kidney fibroblasts. Kinetic evidence that the transfer of proteins to lysosomes is not irreversible. The Journal of Biological Chemistry, 262, 9469-9476.

Burke, W.J., O'Malley, K.L., Chung, H.D., Harmon, S.K., Miller, J.P., & Berg, L. (1991). Effect of pre- and postmortem variables on specific mRNA levels in human brain. Molecular Brain Research, 11, 37-41.

Burns, A. (1990). Cranial computerised tomography in dementia of the Alzheimer type. British Journal of Psychiatry, 157, 10-15.

Burns, A., Jacoby, R., & Levy, R. (1990a). Psychiatric phenomena in Alzheimer's disease. III: Disorders of mood. British Journal of Psychiatry, 157, 81-86.

Burns, A., Jacoby, R., & Levy, R. (1990b). Psychiatric phenomena in Alzheimer's disease. IV: Disorders of behaviour. The British Journal of Psychiatry, 157, 86-94.

Buxbaum, J.D., Oishi, M., Chen, H.I., Pinkas-Kramarski, R., Jaffe, E.A., Gandy, S.E., & Greengard, P. (1992). Cholinergic agonists and interleukin 1 regulate processing and secretion of the Alzheimer β/A4 amyloid protein precursor. Proc Natl Acad Sci USA, 89, 10075-10078.

Buxbaum, J.D., Ruefli, A.A., Parker, C.A., Cypess, A.M., & Greengard, P. (1994). Calcium regulates processing of the Alzheimer amyloid protein precursor in a protein-kinase C-independent manner. Proc Natl Acad Sci USA, 91, 4489-4493.

Campbell, S.K., Switzer, R.C., & Martin, T.L. (1987). Alzheimer's plaques and tangles: a controlled and enhanced silver-staining method. Soc Neurosci Abstr, 13, 678

Candy, J.M., Klinowski, J., Perry, R.H., Perry, E.K., Fairbairn, A., Oakley, A.E., Carpenter, T.A., Atack, J.R., Blessed, G., & Edwardson, J.A. (1986). Aluminosilicates and senile plaque formation in Alzheimer's disease. The Lancet, February 15, 354-356.

Cataldo, A.M., Hamilton, D.J., & Nixon, R.A. (1994). Lysosomal abnormalities in degenerating neurons link neuronal compromise to senile plaque development in Alzheimer's disease. Brain Research, 640, 68-80.

Chao, H.M., Spencer, R.L., Frankfurt, M., & McEwen, B.S. (1994). The effects of aging and hormonal manipulation on amyloid precursor protein APP695 mRNA expression in the rat hippocampus. J Neuroendocrinol, 6, 517-521.

Chartier-Harlin, M., Crawford, F., Houlden, H., Warren, A., Hughes, D., Fidani, L., Goate, A., Rossor, M., Roques, P., Hardy, J., & Mullan, M. (1991). Early-onset Alzheimer's disease caused by mutations at codon 717 of the β-amyloid precursor protein gene. Nature, 353, 844-846.

Checler, F. (1995). Processing of the β-amyloid precursor protein and its regulation in Alzheimer's disease. Journal of Neurochemistry, 65, 1431-1444.

Chen, W., Goldstein, J.L., & Brown, M.S. (1990). NPXY, a Sequence Often Found in Cytoplasmic Tails, Is Required for Coated Pit-Mediated Internalization of the Low Density Lipoprotein Receptor. The Journal of Biological Chemistry, 265, 3116-3123.

Chomczynski, P. & Sacchi, N. (1987). Single-step method of RNA isolation by acid guanidinium thiocyanate-phenol-chloroform extraction. Analytical Biochemistry, 162, 156-159.

Christensen, H., Maltby, N., Jorm, A.F., Creasey, H., & Broe, G.A. (1992). Cholinergic 'blockade' as a model of the cognitive deficits in Alzheimer's disease. Brain, 115, 1681-1699.

Ciechanover, A., Finley, D., & Varshavsky, A. (1984a). The Ubiquitin-Mediated Proteolytic Pathway and Mechanisms of Energy-Dependent Intracellular Protein Degradation. Journal of Cellular Biochemistry, 24, 27-53.

Ciechanover, A., Finley, D., & Varshavsky, A. (1984b). Ubiquitin Dependence of Selective Protein Degradation Demonstrated in the Mammalian Cell Cycle Mutant ts85. Cell, 37, 57-66.

Citron, M., Oltersdorf, T., Haass, C., McConlogue, L., Hung, A.Y., Seubert, P., Vigo-Pelfrey, C., Lieberburg, I., & Selkoe, D.J. (1992). Mutation of the β-amyloid precursor protein in familial Alzheimer's disease increases β-protein production. Nature, 360, 672-674.

Clark, M.J., Gagnon, J., Williams, A.F., & Barclay, A.N. (1985). MRC OX-2 antigen: a lymphoid/neuronal membrane glycoprotein with a structure like a single immunoglobulin light chain. The EMBO Journal, 4, 113-118.

Codina, J., Hildebrandt, J.D., Sekura, R.D., Birnbaumer, M., Bryan, J., Manclark, C.R., Iyengar, R., & Birnbaumer, L. (1984). N_S and N_i, the stimulatory and inhibitory regulatory components of adenylyl cyclases Purification of the human erythrocyte proteins without the use of activating regulatory ligands. The Journal of Biological Chemistry, 259, 5871-5886.

Cohen, M.L., Golde, T.E., Usiak, M.F., Younkin, L.H., & Younkin, S.G. (1988). In situ hybridization of nucleus basalis neurons shows increased β-amyloid mRNA in Alzheimer disease. Proc Natl Acad Sci USA, 85, 1227-1231.

Cole, G.M., Huynh, T.V., & Saitoh, T. (1989). Evidence for Lysosomal Processing of Amyloid β-Protein Precursor in Cultured Cells. Neurochemical Research, 14, 933-939.

Cooper, D.M.F., Boyajian, C.L., Goldsmith, P.K., Unson, C.G., & Spiegel, A. (1990). Differential expression of low molecular weight form of Gs-α in neostriatum and cerebellum: correlation with expression of calmodulin-independent adenylyl cyclase. Brain Research, 523, 143-146.

Corder, E.H., Saunders, A.M., Strittmatter, W.J., Schmechel, D.E., Gaskell, P.C., Small, G.W., Roses, A.D., Haines, J.L., & Pericak-Vance, M.A. (1993). Gene Dose of Apolipoprotein E Type 4 Allele and the Risk of Alzheimer's Disease in Late Onset Families. Science, 261, 921-923.

Cortopassi, G.A., Shibata, D., Soong, N.-W., & Arnheim, N. (1992). A pattern of accumulation of a somatic deletion of mitochondrial DNA in aging human tissues. Proc Natl Acad Sci, 89, 7370-7374.

Cotman, C.W. & Anderson, A.J. (1995). A potential role for apoptosis in neurodegeneration and Alzheimer's disease. Molecular Neurobiology, 10, 19-45.

Cotman, C.W., Pike, C.J., & Copani, A. (1992). β-amyloid neurotoxicity: A discussion of in vitro findings. Neurobiology of Aging, 13, 587-590.

Cotman, C.W., Pike, C.J., & Cummings, B.J. (1993). Adaptive versus pathological plasticity possible contributions to age-related dementia. Advances in Neurology, 59, 35-45.

Cowburn, R.F., O'Neill, C., Ravid, R., Alafuzoff, I., Winblad, B., & Fowler, C.J. (1992). Adenylyl cyclase activity in postmortem human brain: evidence of altered G protein mediation in Alzheimer's disease. Journal of Neurochemistry, 58, 1409-1419.

Cowland, J.B., Wiborg, O., & Vuust, J. (1988). Human ubiquitin genes: one member of the UbB gene subfamily is a tetrameric non-processed pseudogene. FEB, 231, 187-191.

Das, H.K., McPherson, J., Bruns, G.A.P., Karathanasis, S.K., & Breslow, J.L. (1985). Isolation, Characterization, and Mapping to Chromosome 19 of the Human Apolipoprotein E Gene. The Journal of Biological Chemistry, 260, 6240-6247.

Davis, J.B. (1996). Oxidative mechanisms in β-amyloid cytotoxicity. Neurodegeneration, 5, 441-444.

Davis, J.B., McMurray, H.F., & Schubert, D. (1992). The amyloid beta-protein of Alzheimer's diseaseis chemotactic for mononuclear phagocytes. Biochemical and Biophysical Research Communications, 189, 1096-1100.

Davis, L.G., Dibner, M.D. & Batty, J.F. (1986). Basic Methods in Molecular Biology. New York: Elsevier.

de Sauvage, F. & Octave, J. (1989). A novel mRNA of the A4 amyloid precursor gene coding for a possibly secreted protein. Science, 245, 651-653.

Department of Health. (1997). A handbook on the mental health of older people. London: Department of Health.

Dib, K., Delemer, B., El Jamali, A., Haye, B., Jacquemin, C., & Corrèze, C. (1994). 12-O-tetradeconoyl-phorbol-13-acetate (TPA) counteracts the cAMP up-regulation of the expression of the stimulatory guanine nucleotide binding protein (Gsα) and Gsα messenger RNA in cultured pig thyroid cells. Molecular and Cellular Endocrinology, 99, 229-235.

Ebly, E.M., Parhad, I.M., Hogan, D.B., & Fung, T.S. (1994). Prevalence and types of dementia in the very old: Results from the Canadian Study of Health and Aging. Neurology, 44, 1593-1600.

Ebstein, R.P., Nemanov, L., Lubarski, G., Dano, M., Trevis, T., & Korczyn, A.D. (1996). Changes in expression of lymphocyte amyloid precursor protein mRNA isoforms in normal aging and Alzheimer's disease. Molecular Brain Research, 35, 260-268.

Efthimiopoulos, S., Felsenstein, K.M., Sambamurti, K., Robakis, N.K., & Refolo, L.M. (1994). Study of the phorbol ester effect on Alzheimer amyloid precusor protein processing: Sequence requirements and involvement of a cholera toxin sensitive protein. Journal of Neuroscience Research, 38, 81-90.

Eikelenboom, P. & Stam, F.C. (1982). Immunoglobulins and complement factors in senile plaques-an immunoperoxidase study. Acta Neuropathologica, 57, 239-242.

Enomoto, K. & Asakawa, T. (1986). Inhibition of catalytic unit of adenylate cyclase and activation of GTPase of N_i protein by β gamma-subunits of GTP-binding proteins. FEBS Letters, 202, 63-68.

Ernst, R.L. & Hay, J.W. (1994). The US economic and social costs of Alzheimer's disease revisited. Am J Public Health, 84, 1261-1264.

Estus, S., Golde, T.E., Kunishita, T., Blades, D., Lowery, D., Eisen, M., Usiak, M., Qu, X., Tabira, T., Greenberg, B.D., & Younkin, S.G. (1992). Potentially amyloidogenic, carboxyl-terminal derivatives of the amyloid precursor protein. Science, 255, 726-728.

Etcheberrigaray, R., Ito, E., Kim, C.S., & Alkon, D.L. (1994). Soluble β-amyloid induction of Alzheimer's phenotype for human fibroblast K^+ channels. Science, 264, 276-279.

Ewald, D.A., Sternweis, P.C., & Miller, R.J. (1988). Guanine nucleotide-binding protein G_o-induced coupling of neuropeptide Y receptors to Ca^{2+} channels in sensory neurons. Proc Natl Acad Sci, 85, 3633-3637.

Feldman, A.M., Cates, A.E., Bristow, M.R., & Van Dop, C. (1989). Altered Expression of α-subunits of G Proteins in Failing Human Hearts. Journal of Mol Cell Cardiol, 21, 359-365.

Ferré, F., Marchese, A., Pezzoli, P., Griffin, S., Buxton, E. & Boyer, V. (1994). Quantitative PCR: An overview. In K.B. Mullis, F. Ferré & R.A. Gibbs (Eds.). The Polymerase Chain Reaction (pp. 67-88). Cambridge, MA: Birkhäuser Boston

Finley, D., Ciechanover, A., & Varshavsky, A. (1984). Thermolability of ubiquitin-activating enzyme from the mammalian cell cycle mutant ts85. Cell, 37, 43-55.

Finley, D. & Varshavsky, A. (1985). The ubiquitin system: Functions and mechanisms. Trends Biochem, 10, 343-346.

Foster, N.L., Chase, T.N., Mansi, L., Brooks, R., Fedio, P., Patronas, N.J., & Di Chiro, G. (1984). Cortical abnormalities in Alzheimer's disease. Ann Neurol, 16, 649-654.

Fowler, C.J., Cowburn, R.F., & O'Neill, C. (1992). Brain Signal Transduction Disturbances in Neurodegenerative Disorders Mini Review. Cellular Signalling, 4, 1-9.

Frackowiak, J., Zoltowska, A., & Wisniewski, H.M. (1994). Non-fibrillar b-amyloid protein is associated with smooth muscle cells of vessel walls in Alzheimer disease. J Neuropathol Exp Neurol, 53, 637-645.

Frank, D.A. & Greenberg, M.E. (1994). CREB: A mediator of long-term memory from mollusks to mammals. Cell, 79, 5-8.

Fraser, J., Luu, G.A., Neculcea, J., Thomas, D.Y., & Storms, R.K. (1991). Ubiquitin gene expression: response to environmental changes. Current Genetics, 20, 17-23.

Fraser, S.P., Suh, Y.-H., Chong, Y.H., & Djamgoz, M.B.A. (1996). Membrane currents induced in Xenopus oocytes by the C-terminal fragment of the β-amyloid precursor protein. Journal of Neurochemistry, 66, 2034-2040.

Frederickson, R.C.A. (1992). Astoglia in Alzheimers's disease. Neurobiology of Aging, 13, 239-253.

Frisoni, G.B., Geroldi, C., Bianchetti, A., Trabucchi, M., Govoni, S., Franceschini, G., & Calabresi, L. (1994). Apolipoprotein E ×4 allele frequency in vascular dementia and Alzheimer's disease. Stroke, 25, 1703

Frucht, S.J., Teplow, D.A., Selkoe, D.J., & Koo, E.H. (1992). Biochemical similarities between diffuse plaque and senile plaque amyloid. J Neuropathol Exp Neurol, 51, 369

Galasko, D., Hansen, L.A., Katzman, R., Wiederholt, W., Masliah, E., Terry, R., Hill, L.R., Lessin, P., & Thal, L.J. (1994). Clinical-neuropathological correlations in Alzheimer's disease and related dementias. Arch Neurol, 51, 888-895.

Games, D., Adams, D., Alessandrini, R., Barbour, R., Berthelette, P., Blackwell, C., Carr, T., Clemens, J., Donaldson, T., Gillespie, F., Guido, T., Hagopian, S., Johnson-Wood, K., Khan, K., Lee, M., Leibowitz, P., Lieberburg, I., Little, S., Masliah, E., McConlogue, L., Montoya-Zavala, M., Mucke, L., Paganini, L., Penniman, E., Power, M., Schenk, D., Seubert, P., Snyder, B., Soriano, F., Tan, H., Vitale, J., Wadsworth, S., Wolozin, B., & Zhao, J. (1995). Alzheimer-type neuropathology in transgenic mice overexpressing V717F β-amyloid precursor protein. Nature, 373, 523-527.

Gandy, S. & Greengard, P. (1994). Regulated cleavage of the Alzheimer amyloid precursor protein: Molecular and cellular basis. Biochimie, 76, 300-303.

Geaney, D.P. & Abou-Saleh, M.T. (1990). The use and applications of single-photon emission computerised tomography in dementia. British Journal of Psychiatry, 157, 66-75.

Gegelashvili, G., Bock, E., Schousboe, A., & Linnemann, D. (1996). Two types of amyloid precursor protein (APP) mRNA in rat glioma cell lines: Upregulation via cyclic AMP-dependent pathway. Molecular Brain Research, 37, 151-156.

Gelfand, D.H. & White, T.J. (1990). Thermostable DNA Polymerases. In M.A. Innis, D.H. Gelfand, J.J. Sninsky & T.J. White (Eds.). PCR Protocols A Guide to Methods and Applications (pp. 129-141). London: Academic Press Inc. Harcourt Brace Jovanovich, Publishers

Gentleman, S.M., Graham, D.I., & Roberts, G.W. (1993). Molecular pathology of head trauma: altered βAPP metabolism and the aetiology of Alzheimer's disease. Progress in Brain Research, 96, 237-245.

Giaccone, G., Tagliavini, F., Linoli, G., Bouras, C., Frigerio, L., Frangione, B., & Bugiani, O. (1989). Down patients: extracellular preamyloid deposits precede neuritic degeneration and senile plaques. Neuroscience Letters, 97, 232-238.

Gilliland, G., Perrin, S. & Bunn, H.F. (1990). Competitive PCR for Quantitation of mRNA. In M.A. Innis, D.H. Gelfand, J.J. Sninsky & T.J. White (Eds.). PCR Protocols A Guide to Methods and Applications (pp. 60-69). London: Academic Press, Inc. Harcourt Brace Jovanovich, Publishers

Gilman, A.G. (1987). G Proteins: Transducers of Receptor-Generated Signals. Annu Rev Biochem, 56, 615-649.

Glenner, G.G. & Wong, C.W. (1984). Alzheimer's disease: Initial report of the purification and characterization of a novel cerebrovascular amyloid protein. Biochemical and Biophysical Research Communications, 120, 885-890.

Goate, A., Chartier-Harlin, M., Mullan, M., Brown, J., Crawford, F., Fidani, L., Giuffra, L., Haynes, A., Irving, N., James, L., Mant, R., Newton, P., Rooke, K., Roques, P., Talbot, C., Pericak-Vance, M., Roses, A., Williamson, R., Rossor, M., Owen, M., & Hardy, J. (1991). Segregation of a missense mutation in the amyloid precursor protein gene with familial Alzheimer's disease. Nature, 349, 704-706.

Goedert, M. (1987). Neuronal localization of amyloid beta protein precursor mRNA in normal human brain and in Alzheimer's disease. The EMBO Journal, 6, 3627-3632.

Golde, T.E., Estus, S., Younkin, L.H., Selkoe, D.J., & Younkin, S.G. (1992). Processing of the Amyloid Protein Precursor to Potentially Amyloidogenic Derivatives. Science, 255, 728-730.

Goldstein, D.J. & Williams, M.A. (1971). Quantitative autoradiography: an evaluation of visual grain counting, reflectance microscopy, gross absorbance measurements and flying-spot microdensitometry. Journal of Microscopy, 94, 215-239.

Goldstein, G., Scheid, M., Hammerling, U., Boyse, E.A., Schlesinger, D.H., & Niall, H.D. (1975). Isolation of a polypeptide that has lymphocyte-differentiating properties and is probably represented unviersally in living cells. Proc Natl Acad Sci USA, 72, 11-15.

Gonzalez, G.A. & Montminy, M.R. (1989). Cyclic AMP stimulates somatostatin gene transcription by phosphorylation of CREB at serine 133. Cell, 59, 675-680.

Grammeman, J.G. & Bannon, M.J. (1991). Splicing pattern of Gsα mRNA in human and rat brain. Journal of Neurochemistry, 57, 1019-1023.

Gray, A. & Fenn, P. (1993). Alzheimer's disease: the burden of the illness in England. Health Trends, 25, 31-37.

Graziano, M.P., Casey, P.J., & Gilman, A.G. (1987). Expression of cDNAs for G Proteins in Escerichia coli Two Forms of $G_{s\alpha}$ Stimulate Adenylate Cyclase. The Journal of Biological Chemistry, 262, 11375-11381.

Graziano, M.P., Freissmuth, M., & Gilman, A.G. (1989). Expression of $G_{s\alpha}$ in Escherichia coli Purification and Properties of Two Forms of the Protein. The Journal of Biological Chemistry, 264, 409-418.

Gropper, R., Brandt, R.A., Elias, S., Bearer, C.F., Mayer, A., Schwartz, A.L., & Ciechanover, A. (1991). The ubiquitin-activating enzyme, E1, is required for stress-induced lysosomal degradation of cellular proteins. The Journal of Biological Science, 266, 3602-3610.

Haass, C., Koo, E.H., Mellon, A., Hung, A.Y., & Selkoe, D.J. (1992a). Targeting of cell-surface β-amyloid precursor protein to lysosomes: alternative processing into amyloid-bearing fragments. Nature, 357, 500-503.

Haass, C., Schlossmacher, M.G., Hung, A.Y., Vigo-Pelfrey, C., Mellon, A., Ostaszewski, B.L., Lieberburg, I., Koo, E.H., Schenk, D., Teplow, D.B., & Selkoe, D.J. (1992b). Amyloid β-peptide is produced by cultured cells during normal metabolism. Nature, 359, 322-327.

Hamos, J.E., Oblas, B., Pulaski-Salo, D., Welch, W.J., Bole, D.G., & Drachman, D.A. (1991). Expression of heat shock proteins in Alzheimer's disease. Neurology, 41, 345-350.

Han, S.-H., Hulette, C., Saunders, A.M., Einstein, G., Pericak-Vance, M., Strittmatter, W.J., Roses, A.D., & Schmechel, D.E. (1994). Apolipoprotein E is present in hippocampal neurons without neurofibrillary tangles in Alzheimer's disease and in age-matched controls. Exp Neurol, 128, 13-26.

Harris, B.A. (1988). Complete cDNA sequence of a human stimulatory GTP-binding protein alpha subunit. Nucleic Acids Research, 16, 3585

Harrison, P.J. & Pearson, R.C.A. (1989). Gene expression and mental disease. Psychological Medicine, 19, 813-819.

Harrison, P.J., Procter, A.W., Barton, A.J.L., Lowe, S.L., Najlerahim, A., Bertolucci, P.H.F., Bowen, D.M., & Pearson, R.C.A. (1991a). Terminal coma affects messenger RNA detection in post mortem human temporal cortex. Molecular Brain Research, 9, 161-164.

Harrison, P.J., Barton, A.J.L., Najlerahim, A., McDonald, B., & Pearson, R.C.A. (1991b). Regional and neuronal reductions of polyadenylated messenger RNA in Alzheimer's disease. Psychological Medicine, 21, 855-866.

Harrison, P.J., Barton, A.J.L., McDonald, B., & Pearson, R.C.A. (1991c). Alzheimer's disease: specific increases in a G protein subunit ($G_{s}\alpha$) mRNA in hippocampal and cortical neurons. Molecular Brain Research, 10, 71-81.

Harrison, P.J., Barton, A.J.L., & Pearson, R.C.A. (1991d). Expression of amyloid beta-protein precursor mRNAs in familial Alzheimer's disease. Neuroreport, 2, 152-154.

Harrison, P.J., Procter, A.W., Exworthy, T., Roberts, G.W., Najlerahim, A., Barton, A.J.L., & Pearson, R.C.A. (1993). Heat shock protein (Hsx70) mRNA expression in human brain: effects of neurodegenerative disease and agonal state. Neuropathology and Applied Neurobiology, 19, 10-21.

Harrison, P.J., Barton, A.J.L., Procter, A.W., Bowen, D.M., & Pearson, R.C.A. (1994). The Effects of Alzheimer's Disease, Other Dementias, and Premortem Course on β-Amyloid Precursor Protein Messenger RNA in Frontal Cortex. Journal of Neurochemistry, 62, 635-644.

Harrison, P.J., Heath, P.R., Eastwood, S.L., Burnet, P.W.J., McDonald, B., & Pearson, R.C.A. (1995). The relative importance of premortem acidosis and postmortem interval for human brain gene expression studies: selective mRNA vulnerability and comparison with their encoded proteins. Neuroscience Letters, 200, 151-154.

Harrison, P.J., Wighton-Benn, W.H., Heffernan, J.M., Sanders, M.W., & Pearson, R.C.A. (1996). Amyloid precursor protein mRNAs in Alzheimer's disease. Neurodegeneration, 5, 409-415.

Hayashi, K. (1994). Manipulation of DNA by PCR. In K.B. Mullis, F. Ferré & R.A. Gibbs (Eds.). The Polymerase Chain Reaction (pp. 3-13). Cambridge, MA: Birkhäuser Boston

Hayashi, T., Tanaka, J., Kamikubo, T., Takada, K., & Matsuda, M. (1993). Increase in ubiquitin conjugates dependent on ischemic damage. Brain Research, 620, 171-173.

Hayashi, Y., Kashiwagi, K., & Yoshikawa, K. (1992). Protease inhibitors generate cytotoxic fragements from Alzheimer amyloid protein precursor in cDNA-transfected glioma cells. Biochemical and Biophysical Research Communications, 187, 1249-1255.

Heath, P.R., Sanders, M.W. & Pearson, R.C.A. (1996). Oligonucleotide method with ^{35}S: Human brain and paraffin embedded brain. In Z. Henderson (Ed.). In situ hybridisation techniques for the brain. IBRO Handbook Series. Methods in the Neurosciences 17. Chichester: John Wiley and sons.

Hedreen, J.C., Raskin, L.S., & Price, D.L. (1994). A quick silver method for senile plaques and neurofibrillary tangles in paraffin sections. Brain Res Bull, 35, 279-284.

Hefferman, J.M. Amyloid Precursor Protein Gene Expression Studies in Human Brain. M.Phil. thesis submitted 1996 to the University of Sheffield.

Henderson, V.W., Paganini-Hill, A., Emanuel, C.K., Dunn, M.E., & Buckwalter, J.G. (1994). Estrogen replacement therapy in older women. Comparisons between Alzheimer's disease cases and nondemented control subjects. Arch Neurol, 51, 896-900.

Hendriks, L., Van Duijn, C.M., Cras, P., Cruts, M., Van Hul, W., Van Harskamp, F., Warren, A., McInnis, M.G., Antonarakis, S.E., Martin, J.-J., Hofman, A., & Van Broeckhoven, C. (1992). Presenile dementia and cerebral haemorrhage linked to a mutation at codon 692 of the β-amyloid precursor protein gene. Nature Genetics, 1, 219-221.

Hershko, A., Leshinsky, E., Ganoth, D., & Heller, H. (1984). ATP-dependent degradation of ubiquitin-protein conjugates. Proc Natl Acad Sci, 81, 1619-1623.

Hescheler, J., Rosenthal, W., Trautwein, W., & Schultz, G. (1987). The GTP-binding protein, G_o, regulates neuronal calcium channels. Nature, 325, 445-447.

Heydari, A.R., Wu, B., Takahashi, R., Strong, R., & Richardson, A. (1993). Expression of Heat Shock Protein 70 Is Altered by Age and Diet at the Level of Transcription. Molecular and Cellular Biology, 13, 2909-2918.

Higashi, T., Takechi, H., Uemura, Y., Kikuchi, H., & Nagata, K. (1994). Differential induction of mRNA species encoding several classes of stress proteins following focal cerebral ischemia in rats. Brain Res, 650, 239-248.

Ho, G.J., Gregory, E.J., Smirnova, I.V., Zoubine, M., & Festoff, B.W. (1994). Cross-linking of β-amyloid protein precursor catalyzed by tissue transglutaminase. FEBS Letters, 349, 151-154.

Ho, L., Fukuchi, K., & Younkin, S.G. (1996). The alternatively spliced kunitz protease inhibitor domain alters amyloid β protein precusor processing and amyloid β protein production in cultured cells. The Journal of Biological Chemistry, 271, 30929-30934.

Hoof, T., Riordan, J.R., & Tümmler, B. (1991). Quantitation of mRNA by the kinetic polymerase chain reaction assay: A tool for monitoring P-glycoprotein gene expression. Analytical Biochemistry, 196, 161-169.

Hope, R.A. & Keene, J. (1996). Behavioural problems in dementia and biochemistry: Clinical aspects. Neurodegeneration, 5, 399-402.

Hsu, W.H., Rudolph, U., Sanford, J., Bertrand, P., Olate, J., Nelson, C., Moss, L.G., Boyd, A.E., Codina, J., & Birnbaumer, L. (1990). Molecular Cloning of a Novel Splice Variant of the α Subunit of the Mammalian G_o Protein. The Journal of Biological Chemistry, 265, 11220-11226.

Huang, Y., Li, X., & Kandel, E.R. (1994). cAMP contributes to mossy fiber LTP by initiating both a covalently mediated early phase and macromolecular synthesis-dependent late phase. Cell, 79, 69-79.

Ikezu, T., Okamoto, T., Komatsuzaki, K., Matsui, T., Jeevendra Martyn, J.A., & Nishimoto, I. (1996). Negative transactivation of cAMP response element by familial Alzheimer's mutants of APP. EMBO, 15, 2468-2475.

Innis, M.A. & Gelfand, D.H. (1990). Optimization of PCRs. In M.A. Innis, D.H. Gelfand, J.J. Sninsky & T.J. White (Eds.). PCR Protocols: A Guide to Methods and Applications (pp. 3-12). London: Academic Press Inc

Iqbal, K., Grundke-Iqbal, I. & Wisniewski, H.M. (1987). Alterations of the neuronal cytoskeleton in Alzheimer's disease and related conditions. In G. Perry (Ed.). Alterations in the neuronal cytoskeleton in Alzheimer disease (pp. 109-136). Plenum Publishing Corporation

Itagaki, S., Akiyama, H., Saito, H., & McGeer, P.L. (1994). Ultrastructural localization of complement membrane attack complex (MAC)-like immunoreactivity in brains of patients with Alzheimer's disease. Brain Res, 645, 78-84.

Itoh, H., Kozasa, T., Nagata, S., Nakamura, S., Katada, T., Ui, M., Iwai, S., Ohtsuka, E., Kawasaki, H., Suzuki, K., & Kaziro, Y. (1986). Molecular cloning and sequence determination of cDNAs for α subunits of the guanine nucleotide-binding proteins G_S, G_i, and G_O from rat brain. Proc Natl Acad Sci, 83, 3776-3780.

Iwatsubo, T., Odaka, A., Suzuki, N., Mizusawa, H., Nukina, N., & Ihara, Y. (1994). Visualization of Aβ42(43) and Aβ40 in senile plaques with end- specific Aβ monoclonals: Evidence that an initially deposited species is Aβ42(43). Neuron, 13, 45-53.

Jacobsen, J.S., Spruyt, M.A., Brown, A.M., Sahasrabudhe, S.R., Blume, A.J., Vitek, M.P., Muenkel, H.A., & Sonnenberg-Reines, J. (1994). The release of Alzheimer's disease b amyloid peptide is reduced by phorbol treatment. The Journal of Biological Chemistry, 269, 8376-8382.

Jacobsen, J.S., Blume, A.J., & Vitek, M.P. (1991). Quantitative measurement of alternatively spliced amyloid precursor protein mRNA expression in Alzheimer's disease and normal brain by S_1 nuclease protection analysis. Neurobiology of Aging, 12, 585-592.

Jarrett, J.T., Berger, E.P., & Lansbury, P.T. (1993). The carboxy terminus of the β amyloid protein is critical for the seeding of amyloid formation: Implications for the pathogenesis of Alzheimer's disease. Biochemistry, 32, 4693-4697.

Joachim, C.L., Morris, J.H., & Selkoe, D.J. (1988a). Clinically diagnosed Alzheimer's Disease: Autopsy results in 150 cases. Ann Neurol, 24, 50-56.

Joachim, C.L., Duffy, L.K., Morris, J.H., & Selkoe, D.J. (1988b. Protein chemical and immunocytochemical studies of meningovascular β-amyloid protein in Alzheimer's disease and normal aging. Brain Research, 474, 100-111.

Johnson, S.A., McNeill, T., Cordell, B., & Finch, C.E. (1990). Relation of neuronal APP-751/APP-695 mRNA ratio and neuritic plaque density in Alzheimer's disease. Science, 248, 854-857.

Johnson, S.A., Rogers, J., & Finch, C.E. (1989). APP-695 transcript prevalence is selectively reduced during Alzheimer's disease in cortex and hippocampus but not in cerebellum. Neurobiology of Aging, 10, 267-272.

Johnson-Wood, K.L., Henriksson, T., Seubert, P., Oltersdorf, T., Lieberburg, I., & Schenk, D.B. (1994). Identification of secreted β-amyloid precursor protein binding sites on intact human fibroblasts. Biochemical and Biophysical Research Communications, 200, 1685-1692.

Johnston, J.A., Norgren, S., Ravid, R., Wasco, W., Winblad, B., Lannfelt, L., & Cowburn, R.F. (1996a). Quantification of APP and APLP2 mRNA in APOE genotyped Alzheimer's disease brains. Molecular Brain Research, 43, 85-95.

Johnston, J.A., Norgren, S., Annerén, G., Cowburn, R.F., & Lannfelt, L. (1996b). A new quantitative solution hybridisation-RNase protection assay for APP and APLP2 mRNA. Molecular Brain Research, 43, 77-84.

Jorm, A.F., Korten, A.E., & Henderson, A.S. (1987). The prevalence of dementia: a quantitative integration of the literature. Acta Psychiatr Scand, 76, 465-479.

Jouneaux, C., Mallat, A., Serradeil-Le Gal, C., Goldsmith, P., Hanoune, J., & Lotersztajn, S. (1994). Coupling of Endothelin B Receptors to the Calcium Pump and Phospholipase C via Gs and Gq in Rat Liver. The Journal of Biological Chemistry, 269, 1845-1851.

Kalaria, R.N., Cohen, D.L., & Premkumar, D.R.D. (1996a). Cellular aspects of the inflammatory response in Alzheimer's disease. Neurodegeneration, 5, 497-503.

Kalaria, R.N., Premkumar, D.R.D., Pax, A.B., Cohen, D.L., & Lieberburg, I. (1996b). Production and increased detection of amyloid β protein and amyloidogenic fragments in brain microvessels, meningeal vessels and choroid plexus in Alzheimer's disease. Molecular Brain Research, 35, 58-68.

Kametani, F., Tanaka, K., Tokuda, T., & Ikeda, S. (1994). Secretory cleavage site of Alzheimer amyloid precursor protein is heterogeneous in Down's syndrome brain. FEBS Lett, 351, 165-167.

Kang, J., Lemaire, H., Unterbeck, A., Salbaum, J.M., Masters, C.L., Grzeschik, K., Multhaup, G., Beyreuther, K., & Müller-Hill, B. (1987). The precursor of Alzheimer's disease amyloid A4 protein resembles a cell-surface receptor. Nature, 325, 733-736.

Katada, T., Northup, J.K., Bokoch, G.M., Ui, M., & Gilman, A.G. (1984). The Inhibitory Guanine Nucleotide-binding Regulatory Component of Adenylate Cyclase Subunit Dissociation and Guanine Nucleotide-Dependent Hormonal Inhibition. The Journal of Biological Chemistry, 259, 3578-3585.

Kato, H., Liu, X., Nakata, N., & Kogure, K. (1993). Immunohistochemical visualisation of heat shock protein-70 in the gerbil hippocampus following repeated brief cerebral ischemia. Brain Research, 615, 240-244.

Katzman, R. (1993). Education and the prevalence of dementia and Alzheimer's disease. Neurology, 43, 13-20.

Kawamata, J., Tanaka, S., Shimohama, S., Ueda, K., & Kimura, J. (1994). Apolipoprotein E polymorphism in Japanese patients with Alzheimer's disease or vascular dementia. J Neurol Neurosurg Psychiatry, 57, 1414-1416.

Kawarabayashi, T., Shoji, M., Harigaya, Y., Yamaguchi, H., & Hirai, S. (1991). Expression of APP in the early stage of brain damage. Brain Research, 563, 334-338.

Kawasaki, E.S. (1990). Amplification of RNA. In M.A. Innis, D.H. Gelfand, J.J. Sninsky & T.J. White (Eds.). PCR Protocols A Guide to Methods and Applications (pp. 21-27). London: Academic Press Inc. Harcourt Brace Jovanovich, Publishers

Khachaturian, Z.S. (1985). Diagnosis of Alzheimer's disease. Arch Neurol, 42, 1097-1105.

Khatoon, S., Grundke-Iqbal, I., & Iqbal, K. (1994). Levels of normal and abnormally phosphorylated tau in different cellular and regional compartments of Alzheimer disease and control brains. FEBS Lett, 351, 80-84.

Kiang, J.G. & Tsokos, G.C. (1996). Cell signalling and heat shock protein expression. J Biomed Sci, 3, 379-388.

Kingsbury, A.E., Foster, O.J.F., Nisbet, A.P., Cairns, N., Bray, L., Eve, D.J., Lees, A.J., & Marsden, C.D. (1995). Tissue pH as an indicator of mRNA preservation in human post-mortem brain. Molecular Brain Research, 28, 311-318.

Kinouchi, H., Sharp, F.R., Hill, M.P., Koistinaho, J., Sagar, S.M., & Chan, P.H. (1993). Induction of 70-kDa heat shock protein and hsp70 mRNA following transient focal cerebral ischemia in the rat. Journal of Cerebral Blood Flow and Metabolism, 13, 105-115.

Kishimoto, A., Nishiyama, K., Nakanishi, H., Uratsuji, Y., Nomura, H., Takeyama, Y., & Nishizuka, Y. (1985). Studies on the phosphorylation of myelin basic-protein by protein-kinase C and adenosine 3'-5'-monophosphate dependent protein-kinase. Journal of Biological Chemistry, 260, 2492-2499.

Kitaguchi, N., Takahashi, Y., Tokushima, Y., Shiojiri, S., & Ito, H. (1988). Novel precursor of Alzheimer's disease amyloid protein shows protease inhibitory activity. Nature, 331, 530-532.

Kleuss, C., Hescheler, J., Ewel, C., Rosenthal, W., Schultz, G., & Wittig, B. (1991). Assignment of G-protein subtypes to specific receptors inducing inhibition of calcium currents. Nature, 353, 43-48.

Kleuss, C., Scher"bl, H., Hescheler, J., Schultz, G., & Wittig, B. (1993). Selectivity in signal transduction determined by gamma subunits of heterotrimeric G proteins. Science, 259, 832-834.

Koo, E.H., Sisodia, S.S., Cork, L.C., Unterbeck, A., Bayney, R.M., & Price, D.L. (1990). Differential expression of amyloid precursor protein mRNAs in cases of Alzheimer's disease and in aged nonhuman primates. Neuron, 2, 97-104.

Kowall, N.W., Beal, M.F., Busciglio, J., Duffy, L.K., & Yanker, B.A. (1991). An in vivo model for the neurodegenerative effects of β-amyloid and protection by substance P. Proc Natl Acad Sci USA, 88, 7247-7251.

Kowall, N.W. & McKee, A.C. (1993). The histopathology of neuronal degeneration and plasticity in Alzheimer disease. Advances in Neurology, 59, 5-33.

Kozasa, T., Itoh, H., Tsukamoto, T., & Kaziro, Y. (1988). Isolation and characterization of the human $G_{s\alpha}$ gene. Proc Natl Acad Sci, 85, 2081-2085.

König, G., Mönning, U., Czech, C., Prior, R., Banati, R., Schreiter-Gasser, U., Bauer, J., Masters, C.L., & Beyreuther, K. (1992). Identification and differential expression of a novel alternative splice isoform of the βA4 amyloid precursor protein (APP) mRNA in leukocytes and brain microglial cells. The Journal of Biological Chemistry, 267, 10804-10809.

Kurz, A., Haupt, M., Pollmann, S., & Romero, B. (1992). Alzheimer's disease: is there evidence of phenomenological subtypes?. Dementia, 3, 320-327.

LaDu, M.J., Falduto, M.T., Manelli, A.M., Reardon, C.A., Getz, G.S., & Frail, D.E. (1994). Isoform-specific binding of apolipoprotein E to b-amyloid. J Biol Chem, 269, 23403-23406.

LaFerla, F.M., Tinkle, B.T., Bieberich, C.J., Haudenschild, C.C., & Jay, G. (1995). The Alzheimer's Aβ peptide induces neurodegeneration and apoptotic cell death in transgenic mice. Nature Genetics, 9, 21-30.

Larson, J.S., Schuetz, T.J., & Kingston, R.E. (1988). Activation in vitro of a sequence specific DNA binding by a human regulatory factor. Nature, 335, 372-375.

Laskey, R.A. (1993). Review 23 Efficient detection of biomolecules by autoradiography, fluorography or chemiluminescence. Amersham International plc.

Lassmann, H., Bancher, C., Breitschopf, H., Wegiel, J., Bobinski, M., Jellinger, K., & Wisniewski, H.M. (1995). Cell death in Alzheimer's disease evaluated by DNA fragmentation in situ. Acta Neuropathol, 89, 35-41.

Laugwitz, K.L., Offermanns, S., Spicher, K., & Schultz, G. (1993). Mu and delta opioid receptors differentially couple to G-protein subtypes in membanes of human neuroblastoma SH-SY5Y cells. Neuron, 10, 233-242.

Lavu, S., Clark, J., Swarup, R., Matsushima, K., Paturu, K., Moss, J., & Kung, H.F. (1988). Molecular cloning and DNA sequence analysis of the human guanine nucleotide-binding protein $G_o\alpha$. Biochemical and Biophysical Research Communications, 150, 811-815.

Law, S.F., Yasuda, K., Bell, G.I., & Reisine, T. (1993). G(1-alpha-3) and G(o-alpha) selectively associate with the cloned somatostatin receptor subtype-SSTR2. Journal of Biological Chemistry, 268, 10721-10727.

Lee, R.K.K., Wurtman, R.J., Cox, A.J., & Nitsch, R.M. (1995). Amyloid precursor protein processing is stimulated by metabotropic glutamate receptors. Proc Natl Acad Sci USA, 92, 8083-8087.

Lenk, S.E., Dunn, W.A., Trausch, J.S., Ciechanover, A., & Schwartz, A.L. (1992). Ubiquitin-activating enzyme, E1, is associated with maturation of autophagic vacuoles. The Journal of Cell Biology, 118, 301-308.

Leonard, S., Logel, J., Luthman, D., Casanova, M., Kirch, D., & Freedman, R. (1993). Biological stability of mRNA isolated from human postmortem brain collections. Biological Psychiatry, 33, 456-466.

Levy, E., Carman, M.D., Fernandez-Madrid, I.J., Power, M.D., Lieberburg, I., van Duinen, S.G., Bots, G.T.A.M., Luyendijk, W., & Frangione, B. (1990). Mutation of the Alzheimer's disease amyloid gene in Hereditary Cerebral Hemorrhage, Dutch Type. Science, 248, 1124-1126.

Levy-Lahad, E., Wasco, W., Poorkaj, P., Romano, D.M., Oshima, J., Pettingell, W.H., Yu, C., Jondro, P.D., Schmidt, S.D., Wang, K., Crowley, A.C., Fu, Y., Guenette, S.Y., Galas, D., Nemens, E., Wijsman, E.M., Bird, T.D., Schellenberg, G.D., & Tanzi, R.E. (1995). Candidate gene for the chromosome 1 familial Alzheimer's disease locus. Science, 269, 973-977.

Li, X., Greenwood, A.F., Powers, R., & Jope, R.S. (1996). Effects of postmortem interval, age, and Alzheimer's disease on G-proteins in human brain. Neurobiology of Aging, 17, 115-122.

Lindwall, G. & Cole, R.D. (1984). Phosphorylation affects the ability of tau protein to promote microtubule assembly. The Journal of Biological Chemistry, 259, 5301-5305.

Lishman, W.A. (1987). Organic Psychiatry. (2nd ed.) Oxford: Blackwell Scientific Publications.

Liu, R.Y., Kim, D., Yang, S.-H., & Li, G.C. (1993). Dual control of heat shock response: involvement of a constitutive heat shock element-binding factor. Proc Natl Acad Sci, 90, 3078-3082.

Lledo, P.M., Homburger, V., Bockaert, J., & Vincent, J.D. (1992). Differential G-protein mediated coupling of D2 dopamine receptors to K+ and CA2+ currents in rat anterior pituitary cells. Neuron, 8, 455-463.

Löw, P., Doherty, F.J., Sass, M., Kovács, J., Mayer, R.J., & László, L. (1993). Immunogold localisation of ubiquitin-protein conjugates in Sf9 insect cells Implications for the biogenesis of lysosome-related organelles. FEBS Letters, 316, 152-156.

Lue, L. & Rogers, J. (1992). Full complement activation fails in diffuse plaques of the Alzheimer's disease cerebellum. Dementia, 3, 308-313.

Luini, A. & De Matteis, M.A. (1993). Receptor-mediated regulation of constitutive secretion. Trends in Cell Biology, 3, 290-292.

Lund, P.K., Moats-Staats, B.M., Simmons, J.G., Hoyt, E., D'Ercole, A.J., Martin, F., & Van Wyk, J.J. (1985). Nucleotide sequence analysis of a cDNA encoding human ubiquitin reveals that ubiquitin is synthesized as a precursor. The Journal of Biological Chemistry, 260, 7609-7613.

Lyons, J. (1994). Identification of Mutant Forms of G-Protein α Subunits in Human Neoplasia by Polymerase Chain Reaction-Based Techniques. Methods in Enzymology, 237, 295-308.

Maguire, M.E. & Erdos, J.J. (1980). Inhibition of magnesium uptake by β-adrenergic agonists and prostaglandin E_1 is not mediated by cyclic AMP. The Journal of Biological Chemistry, 255, 1030-1035.

Mahley, R.W. (1988). Apolipoprotein E: Cholesterol transport protein with expanding role in cell biology. Science, 240, 622-630.

Mak, K., Yang, F., Vinters, H.V., Frautschy, S.A., & Cole, G.M. (1994). Polyclonals to b-amyloid(1-42) identify most plaque and vascular deposits in Alzheimer cortex, but not striatum. Brain Research, 667, 138-142.

Makridimitri, A. Synaptophysin Messenger RNA in the Human Hippocampus in Neurodegenerative and Neuropsychiatric Disease. M.Med.Sci. dissertation submitted 1991 to the University of Sheffield.

Mandybur, T.I. (1975). The incidence of cerebral amyloid angiopathy in Alzheimer's disease. Neurology, 25, 120-126.

Maness, L.M., Banks, W.A., Podlisny, M.B., Selkoe, D.J., & Kastin, A.J. (1994). Passage of human amyloid β-protein 1-40 across the murine blood-brain barrier. Life Sciences, 55, 1643-1650.

Mann, D.M.A. (1988). The pathological association between Down syndrome and Alzheimer disease. Mechanisms of Ageing and Development, 43, 99-136.

Mann, D.M.A., Brown, A., Prinja, D., Davies, C.A., Landon, M., Masters, C.L., & Beyreuther, K. (1989). An Analysis of the Morphology of Senile Plaques in Down's Syndrome Patients of Different Ages Using Immunocytochemical and Lectin Histochemical Techniques. Neuropathology and Applied Neurobiology, 15, 317-329.

Mann, D.M.A. (1996). Pyramidal nerve cell loss in Alzheimer's disease. Neurodegeneration, 5, 423-427.

Mann, D.M.A., Yates, P.O., Marcyniuk, B., & Ravindra, C.R. (1986). The topography of plaques and tangles in Down's syndrome patients of different ages. Neuropathology and Applied Neurobiology, 12, 447-457.

Markesbery, W.R., Wang, H.Z., Kowall, N.W., Kosik, K.S., & McKee, A.C. (1993). Morphometric image analysis of neuropil threads in Alzheimer's disease. Neurobiology of Aging, 14, 303-307.

Maruyama, K., Kawamura, Y., Asada, H., Ishiura, S., & Obata, K. (1994). Cleavage at the N-Terminal Site of Alzheimer Amyloid β/A4 Protein is Essential for its Secretion. Biochemical and Biophysical Research Communications, 202, 1517-1523.

Masters, C.L., Simms, G., Weinman, N.A., Multhaup, G., McDonald, B.L., & Beyreuther, K. (1985a). Amyloid plaque core protein in Alzheimer disease and Down syndrome. Proc Natl Acad Sci U S A, 82, 4245-4249.

Masters, C.L., Multhaup, G., Simms, G., Pottgiesser, J., Martins, R.N., & Beyreuther, K. (1985b). Neuronal origin of a cerebral amyloid: neurofibrillary tangles of Alzheimer's disease contain the same protein as the amyloid of plaque cores and blood vessels. The EMBO Journal, 4, 2757-2763.

Matesic, D.F., Manning, D.R., & Luthin, G.R. (1991). Tissue-dependent association of muscarinic acetylcholine-receptors with guanine nucleotide-binding regulatory proteins. Molecular Pharmacology, 40, 347-353.

Matsumoto, A. (1994). Altered processing characteristics of β-amyloid-containing peptides in cytosol and in media of familial Alzheimer's disease cells. Biochimica et Biophysica Acta, 1225, 304-310.

Matsumoto, A. & Matsumoto, R. (1994). Familial Alzheimer's disease cells abnormally accumulate b-amyloid-harbouring peptides preferentially in cytosol but not in extracellular fluid. Eur J Biochem, 225, 1055-1062.

Matsuoka, M., Itoh, H., & Kaziro, Y. (1990). Characterization of the Human Gene for $G_{x\alpha}$, a Pertussis Toxin-insensitive Regulatory GTP-binding Protein. The Journal of Biological Chemistry, 265, 13215-13220.

Mattera, R., Graziano, M.P., Yatani, A., Zhou, Z., Graf, R., Codina, J., Birnbaumer, L., Gilman, A.G., & Brown, A.M. (1989). Splice variants of the α subunit of the G protein Gs activate both adenylyl cyclase and calcium channels. Science, 243, 804-807.

May, D.C., Ross, E.M., Gilman, A.G., & Smigel, M.D. (1985). Reconstitution of Catecholamine-stimulated Adenylate Cyclase Activity Using Three Purified Proteins. The Journal of Biological Chemistry, 260, 15829-15833.

Mayer, R.J., Landon, M., Laszlo, L., Lennox, G., & Lowe, J. (1992). Protein processing in lysosomes: the new therapeutic target in neurodegenerative disease. The Lancet, 340, 156-159.

McInosh, K. (1997). Dementia drug cash call. Hospital Doctor, 10 April, 8

McKee, A.C., Kosik, K.S., & Kowall, N.W. (1991). Neuritic pathology and dementia in Alzheimer's disease. Ann Neurol, 30, 156-165.

McKeith, I. (1997). Alzheimer's disease - a suitable case for treatment?. Progress in Neurology and Psychiatry, 1, 7-8.

McKhann, G., Drachman, D., Folstein, M.F., Katzman, R., Price, D., & Stadlan, E.M. (1984). Clinical diagnosis of Alzheimer's disease: Report of the NINCDS-ADRDA work group under the auspices of Department of Health and Human Services task force on Alzheimer's disease. Neurology, 34, 939-944.

McLaughlin, M., Ross, B.M., Milligan, G., McCulloch, J., & Knowler, J.T. (1991). Robustness of G Proteins in Alzheimer's Disease: An Immunoblot Study. Journal of Neurochemistry, 57, 9-14.

McRae, A., Dahlström, A., & Ling, E.A. (1997). Microglial in neurodegenerative disorders: Emphasis on Alzheimer's disease. Gerontology, 43, 95-108.

Mees, C.E.K. (1942). The theory of the photographic process. New York: The Macmillan Company.

Messamore, E., Bogdanovich, N., Schr×der, H., & Winblad, B. (1994). Astrocytes associated with senile plaques possess muscarinic acetylcholine receptors. Neuroreport, 5, 1473-1476.

Migeon, J.C., Thomas, S.L., & Nathanson, N.M. (1994). Regulation of cAMP-mediated gene transcription by wild type and mutated G-protein α subunits. The Journal of Biological Chemistry, 269, 29146-29152.

Miller, J.A. (1991). The calibration of 35S or 32P with 14C-labelled brain paste or 14C-plastic standards for quantitative autoradiography using LKB Ultrofilm or Amersham Hyperfilm.. Neuroscience Letters, 121, 211-214.

Mirra, S.S., Heyman, A., McKeel, D., Sumi, S.M., Crain, B.J., Brownlee, L.M., Vogel, F.S., Hughes, J.P., van Belle, G., Berg, L., & participating CERAD neuropathologists. (1991). The Consortium to Establish a Registry for Alzheimer's Disease (CERAD). Neurology, 41, 479-486.

Moir, R.D., Lynch, T., Bush, A.I., Whyte, S., Henry, A., Portbury, S., Multhaup, G., Small, D.H., Tanzi, R.E., Beyreuther, K., & Masters, C.L. (1998). Relative increase in Alzheimer's disease of soluble forms of cerebral Aβ amyloid protein precursor containing the kunitz protease inhibitory domain. Journal of Biological Chemistry, 273, 5013-5019.

Montminy, M.R. & Bilezikjian, L.M. (1987). Binding of a nuclear protein to the cyclic-AMP response element of the somatostatin gene. Nature, 328, 175-178.

Mori, H., Kondo, J., & Ihara, Y. (1987). Ubiquitin is a component of paired helical filaments in Alzheimer's disease. Science, 235, 1641-1644.

Mori, S., Sternberger, N.H., Herman, M.M., & Sternberger, L.A. (1991). Leakage and neuronal uptake of serum protein in aged and Alzheimer brains A postmortem phenomenon with antemortem etiology. Laboratory Investigation, 64, 345-351.

Moriarty, T.M., Padrell, E., Carty, D.J., Omri, G., Landau, E.M., & Iyengar, R. (1990). G_o protein as signal transducer in the pertussis toxin-sensitive phosphatidylinositol pathway. Nature, 343, 79-82.

Morimoto, S., Komatsu, S., Takahashi, R., Matsuo, M., & Goto, S. (1993). Age-related change in the amount of ubiquinated histones in the mouse brain. Arch Gerontol Geriatr, 16, 217-224.

Mosser, D.D., Kotzbauer, P.T., Sarge, K.D., & Morimototo, R.I. (1990). In vitro activation of heat shock transcription factor DNA-binding by calcium and biochemical conditions that affect protein conformation. Proc Natl Acad Sci, 87, 3748-3752.

Moya, K.L., Contaloni, A., & Allinquant, B. (1994). In vivo neuronal synthesis and axonal transport of Kunitz protease inhibitor (KPI)-containing forms of the amyloid precursor protein. J Neurochem, 63, 1971-1974.

Mullan, M., Crawford, F., Axelman, K., Houlden, H., Lilius, L., Winblad, B., & Lannfelt, L. (1992). A pathogenic mutation for probable Alzheimer's disease in the APP gene at the N-terminus of β-amyloid. Nature Genetics, 1, 345-347.

Mullaney, I., Dodd, M.W., Buckley, N., & Milligan, G. (1993). Agonist activation of transfected human M1 muscarinic acetylcholine receptors in CHO cells results in down-regulation of both the receptor and the α subunit of the G-protein Gq. Biochemical Journal, 289, 125-131.

Mullis, K.B. (1994). PCR and scientific invention: The trial of DuPont vs. Cetus. In K.B. Mullis, F. Ferré & R.A. Gibbs (Eds.). The Polymerase Chain Reaction (pp. 427-441). Cambridge, MA: Birkhäuser Boston

Mumby, S.M., Kleuss, C., & Gilman, A.G. (1994). Receptor regulation of G-protein palmitoylation. Proc Natl Acad Sci U S A, 91, 2800-2804.

Munro, S. & Pelham, H. (1985). What turns on heat shock genes?. Nature, 317, 477-478.

Murrell, J., Farlow, M., Ghetti, B., & Benson, M.D. (1991). A mutation in the amyloid precursor protein associated with hereditary Alzheimer's disease. Science, 254, 97-99.

Müller, F.U., Boheler, K.R., Eschenhagen, T., Schmitz, W., & Scholz, H. (1993). Isoprenaline Stimulates Gene Transcription of the Inhibitory G Protein α-Subunit $G_{i\alpha-2}$ in Rat Heart. Circulation Research, 72, 696-700.

Nagy, Z., Esiri, M.M., Jobst, K.A., Morris, J.H., King, E.M., McDonald, B., Litchfield, S., Smith, A., Barnetson, L., & Smith, A.D. (1995). Relative roles of plaques and tangles in the dementia of Alzheimer's disease: correlations using three sets of neuropathological criteria. Dementia, 6, 21-31.

Namba, Y., Tomonaga, M., Kawasaki, H., Otomo, E., & Ikeda, K. (1991). Apolipoprotein E immunoreactivity in cerebral amyloid deposits and neurofibrillary tangles in Alzheimer's disease and kuru plaque amyloid in Creutzfeldt-Jacob disease. Brain Research, 541, 163-166.

Neary, D., Snowden, J.S., Mann, D.M.A., Bowen, D.M., Sims, N.R., Northen, B., Yates, P.O., & Davison, A.N. (1986). Alzheimer's disease: a correlative study. Journal of Neurology, Neurosurgery and Psychiatry, 49, 229-237.

Neve, R.L., Rogers, J., & Higgins, G.A. (1990). The Alzheimer amyloid precursor-related transcript lacking the β/A4 sequence is specifically increased in Alzheimer's disease brain. Neuron, 5, 329-338.

Newton, C.R. (1997). Setting up a PCR Laboratory. In C.R. Newton (Ed.). PCR Essential Data (pp. 7-11). Chichester: John Wiley and sons in association with BIOS Scientific Publishers Ltd.

Nishimoto, I., Okamoto, T., Matsuura, Y., Takahashi, S., Murayama, Y., & Ogata, E. (1993). Alzheimer amyloid protein precursor complexes with brain GTP-binding protein G_o. Nature, 362, 75-79.

Nitsch, R.M. (1996). From acetylcholine to amyloid: Neurotransmitters and the pathology of Alzheimer's disease. Neurodegeneration, 5, 477-482.

Nitsch, R.M., Slack, B.E., Farber, S.A., Borghesani, P.R., Schulz, J.G., Kim, C., Felder, C.C., Growdon, J.H., & Wurtman, R.J. (1997). Receptor-coupled amyloid precursor protein processing. Annals New York Academy of Sciences, 122-127.

Nitsch, R.M., Deng, M., Growdon, J.H., & Wurtman, R.J. (1996). Serotonin 5-HT2a and 5-HT2c receptors stimulate amyloid precursor protein ectodomain secretion. The Journal of Biological Chemistry, 271, 4188-4194.

Nitsch, R.M., Slack, B.E., Wurtman, R.J., & Growdon, J.H. (1992). Release of Alzheimer amyloid precursor derivatives stimulated by activation of muscarinic acetylcholine receptors. Science, 258, 304-307.

Nixon, R.A., Cataldo, A.M., Paskevich, P.A., Hamilton, D.J., Wheelock, T.R., & Kanaley-Andrews, L. (1992). The lysosomal system in neurons: involvement at multiple stages of Alzheimer's disease pathogenesis. Annals New York Academy of Sciences, 674, 65-88.

Nixon, R.A. & Cataldo, A.M. (1993). The Lysosomal System in Neuronal Cell Death:A Review. Annals of the New York Academy of Sciences, 679, 87-109.

Nixon, R.A. & Cataldo, A.M. (1994). Free radicals, proteolysis, and the degeneration of neurons in Alzheimer disease: How essential is the b-amyloid link. Neurobiol Aging, 15, 463-469.

Noonan, K.E. & Roninson, I.B. (1988). mRNA phenotyping by enzymatic amplification of randomly primed cDNA. Nucleic Acids Research, 16, 10366

Northup, J.K., Sternweis, P.C., Smigel, M.D., Schleifer, L.S., Ross, E.M., & Gilman, A.G. (1980). Purification of the regulatory component of adenylate cyclase. Proc Natl Acad Sci, 77, 6516-6520.

Nowak, T.S., Bond, U., & Schlesinger, M.J. (1990). Heat shock RNA levels in brain and other tissues after hyperthermia and transient ischemia. Journal of Neurochemistry, 54, 451-458.

O'Neill, C., Wiehager, B., Fowler, C.J., Ravid, R., Winblad, B., & Cowburn, R.F. (1994). Regionally selective alterations in G protein subunit levels in the Alzheimer's disease brain. Brain Res, 636, 193-201.

Okamoto, T., Takeda, S., Murayama, Y., Ogata, E., & Nishimoto, I. (1995). Ligand-dependent G protein coupling function of amyloid transmembrane protein. The Journal of Biological Chemistry, 270, 4205-4208.

Oltersdorf, T., Fritz, L.C., Schenk, D.B., Lieberburg, I., Johnson-Wood, K.L., Beattie, E.C., Ward, P.J., Blacher, R.W., Dovey, H.F., & Sinha, S. (1989). The secreted form of the Alzheimer's amyloid precursor protein with the Kunitz domain is protease nexin-II. Nature, 341, 144-147.

Oltersdorf, T., Ward, P.J., Henriksson, T., Beattie, E.C., Neve, R., Lieberburg, I., & Fritz, L.C. (1990). The Alzheimer amyloid precursor protein: Identification of a stable intermediate in the biosynthetic/degradative pathway. The Journal of Biological Chemistry, 265, 4492-4497.

Orrego, C. (1990). Organizing a Laboratory for PCR Work. In M.A. Innis, D.H. Gelfand, J.J. Sninsky & T.J. White (Eds.). PCR Protocols A Guide to Methods and Applications (pp. 447-454). London: Academic Press, Inc. Harcourt Brace Jovanovich, Publishers

Ott, A., Breteler, M.M.B., Van Harskamp, F., Claus, J.J., van der Cammen, T.J.M., Grobbee, D.E., & Hofman, A. (1995). Prevalence of Alzheimer's disease and vascular dementia: Association with education. The Rotterdam study.. BMJ, 310, 970-973.

Oyama, F., Shimada, H., Oyama, R., Titani, K., & Ihara, Y. (1993). β-amyloid protein precursor and τ mRNA levels versus β-amyloid plaque and neurofibrillary tangles in the aged human brain. Journal of Neurochemistry, 60, 1658-1664.

Paganini-Hill, A. & Henderson, V.W. (1994). Estrogen deficiency and risk of Alzheimer's disease in women. Am J Epidemiol, 140, 256-261.

Palmer, A.M., Francis, P.T., Bowen, D.M., Benton, J.S., Neary, D., Mann, D.M.A., & Snowden, J.S. (1987). Catecholaminergic neurones assessed ante-mortem in Alzheimer's disease. Brain Research, 414, 365-375.

Palmer, A.M. (1996). Neurochemical studies of Alzheimer's disease. Neurodegeneration, 5, 381-391.

Palmert, M.R., Golde, T.E., Cohen, M.L., Kovacs, D.M., Tanzi, R.E., Gusella, J.F., Usiak, M.F., Younkin, L.H., & Younkin, S.G. (1988). Amyloid protein precursor messenger RNAs: differential expression in Alzheimer's disease. Science, 241, 1080-1084.

Palmert, M.R., Podlisny, M.B., Witker, D.S., Oltersdorf, T., Younkin, L.H., Selkoe, D.J., & Younkin, S.G. (1989). The β-amyloid protein precursor of Alzheimer disease has soluble derivatives found in human brain and cerebrospinal fluid. Proc Natl Acad Sci U S A, 86, 6338-6342.

Pangalos, M.N., Shioi, J., Efthimiopoulos, S., Wu, A., & Robakis, N.K. (1996). Characterization of Appican, the chondroitin sulfate proteoglycan form of the Alzheimer amyloid precursor protein. Neurodegeneration, 5, 445-451.

Pappolla, M.A., Sambamurti, K., Efthimiopoulos, S., Refolo, L., Omar, R.A., & Robakis, N.K. (1995). Heat-shock induces abnormalities in the cellular distribution of amyloid precursor protein (APP) and APP fusion proteins. Neuroscience Letters, 192, 105-108.

Parolaro, D., Rubino, T., Gori, E., Massi, P., Bendotti, C., Patrini, G., Marcozzi, C., & Parenti, M. (1993). In situ hybridization reveals specific increases in Gas and Gao mRNA in discrete brain regions of morphine-tolerant rats. Eur J Pharmacol Mol Pharmacol, 244, 211-222.

Paulssen, E.J., Paulssen, R.H., Gautvik, K.M., & Gordeladze, J.O. (1992). 'Cross-talk' between phospholipase C and adenylyl cyclase involves regulation of G-protein levels in GH3 rat pituitary cells. Cellular Signalling, 4, 747-755.

Pearson, R.C.A., Barton, A.J.L., Heath, P.R. & Harrison, P.J. (1992). Changes in Messenger RNA in Dementia. In A.J. Hunter & M. Clark (Eds.). Neurodegeneration (pp. 151-165). London: Academic Press Limited

Pearson, R.C.A. & Powell, T.P.S. (1989). The neuroanatomy of Alzheimer's disease. Reviews in the Neurosciences, 2, 101-122.

Perlmutter, L.S., Myers, M.A., & Barr×n, E. (1994). Vascular basement membrane components and the lesions of Alzheimer's disease: Light and electron microscopic analyses. Microsc Res Tech, 28, 204-215.

Perry, E.K., Tomlinson, B.E., Blessed, G., Bergmann, K., Gibson, P.H., & Perry, R.H. (1978). Correlation of cholinergic abnormalities with senile plaques and mental test scores in senile dementia. British Medical Journal, 2, 1457-1459.

Perry, G., Cras, P., Siedlak, S.L., Tabaton, M., & Kawai, M. (1992). β protein immunoreactivity is found in the majority of neurofibrillary tangles of Alzheimer's disease. American Journal of Pathology, 140, 283-290.

Perry, G., Friedman, R., Shaw, G., & Chau, V. (1987). Ubiquitin is detected in neurofibrillary tangles and senile plaque neurites of Alzheimer disease brains. Proc Natl Acad Sci, 84, 3033-3036.

Pike, C.J., Cummings, B.J., & Cotman, C.W. (1992). β-amyloid induces neuritic dystrophy in vitro: similarities with Alzheimer pathology. Neuroreport, 3, 769-772.

Pike, C.J., Walencewicz, A.J., Glabe, C.G., & Cotman, C.W. (1991a). In vitro aging of β-amyloid protein causes peptide aggregation and neurotoxicity. Brain Research, 563, 311-314.

Pike, C.J., Walencewicz, A.J., Glabe, C.G., & Cotman, C.W. (1991b). Aggregation-related toxicity of synthetic β-amyloid protein in hippocampal cultures. European Journal of Pharmacology, 207, 367-368.

Pitas, R.E., Boyles, J.K., Lee, S.H., Foss, D., & Mahley, R.W. (1987). Astrocytes synthesize apolipoprotein E and metabolize apolipoprotein E-containing lipoproteins. Biochimica et Biophysica Acta, 917, 148-161.

Ponte, P., Gonzalez-DeWhitt, P., Schilling, J., Miller, J., Hsu, D., Greenberg, B., Davis, K., Wallace, W., Lieberburg, I., Fuller, F., & Cordell, B. (1988). A new A4 amyloid mRNA contains a domain homologous to serine proteinase inhibitors. Nature, 331, 525-527.

Powers, W.J., Perlmutter, J.S., Videen, T.O., Herscovitch, P., Griffeth, L.K., Royal, H.D., Siegel, B.A., Morris, J.C., & Berg, L. (1992). Blinded clinical evaluation of positron emission tomography for diagnosis of probable Alzheimer's disease. Neurology, 42, 765-770.

Prelli, F., Castano, E., Glenner, G.G., & Frangione, B. (1988). Differences between vascular and plaque core amyloid in Alzheimer's disease. Journal of Neurochemistry, 51, 648-651.

Price, B.H., Gurvit, H., Weintraub, S., Geula, C., Leimkuhler, E., & Mesulam, M. (1993). Neuropsychological patterns and language deficits in 20 consecutive cases of autopsy-confirmed Alzheimer's disease. Arch Neurol, 50, 931-937.

Price, S.R., Tsai, S., Adamik, R., Angus, C.W., Serventi, I.M., Tsuchiya, M., Moss, J., & Vaughan, M. (1989). Expression of $G_{o\alpha}$ mRNA and Protein in Bovine Tissues. Biochemistry, 28, 3803-3807.

Procter, A.W. (1996). Neurochemical correlates of dementia. Neurodegeneration, 5, 403-407.

Querfurth, H.W., Wijsman, E.M., St.George-Hyslop, P.H., & Selkoe, D.J. (1995). βAPP mRNA transcription is increased in cultured fibroblasts from the familial Alzheimer's disease-1 family. Molecular Brain Research, 28, 319-337.

Rabins, P.V. (1996). Developing treatment guidelines for Alzheimer's disease and other dementias. Journal of Clinical Psychiatry, 57, 37-38.

Rabizadeh, S., Bitler, C.M., Butcher, L.L., & Bredesen, D.E. (1994). Expression of the low-affinity nerve growth factor receptor enhances b-amyloid peptide toxicity. Proc Natl Acad Sci USA, 91, 10703-10706.

Raport, C.J., Dere, B., & Hurley, J.B. (1989). Characterization of the Mouse Rod Transducin α Subunit Gene. The Journal of Biological Chemistry, 264, 7122-7128.

Reaume, A.G., Howland, D.S., Trusko, S.P., Savage, M.J., Lang, D.M., Greenberg, B.D., Siman, R., & Scott, R.W. (1996). Enhanced amyloidogenic processing of the β-amyloid precursor protein in gene-targeted mice bearing the Swedish familial Alzheimer's disease mutations and a "humanised" Aβ sequence. The Journal of Biological Chemistry, 271, 23380-23388.

Rebeck, G.W., Reiter, J.S., Strickland, D.K., & Hyman, B.T. (1993). Apolipoprotein E in sporadic Alzheimer's disease: Allelic variation and receptor interactions. Neuron, 11, 575-580.

Ripellino, J.A., Vassilacopoulou, D., & Robakis, N.K. (1994). Solubilization of full-length amyloid precursor proteins from PC12 cell membranes. J Neurosci Res, 39, 211-218.

Ritchie, K. & Touchon, J. (1992). Heterogeneity in senile dementia of the Alzheimer type: individual differences, progressive deterioration or clinical sub-types?. J Clin Epidemiol, 45, 1391-1398.

Roberts, G.W., Allsop, D., & Bruton, C. (1990a). The occult aftermath of boxing. Journal of Neurology, Neurosurgery and Psychiatry, 53, 373-378.

Roberts, G.W., Whitwell, H.L., Acland, P.R., & Bruton, C.J. (1990b). Dementia in a punch-drunk wife. The Lancet, 335, 918-919.

Robinshaw, J.D., Russell, D.W., Harris, B.A., Smigel, M.D., & Gilman, A.G. (1986a). Deduced primary structure of the α subunit of the GTP-binding stimulatory protein of adenylate cyclase. Proc Natl Acad Sci USA, 83, 1251-1255.

Robinshaw, J.D., Smigel, M.D., & Gilman, A.G. (1986b). Molecular basis for two forms of the G protein that stimulates adenylate cyclase. The Journal of Biological Chemistry, 261, 9587-9590.

Robinson, C.A., Clark, A.W., Parhad, I.M., Fung, T.S., & Bou, S.S. (1994). Gene expression in Alzheimer neocortex as a function of age and pathologic severity. Neurobiol Aging, 15, 681-690.

Rocca, W.A., Hofman, A., Brayne, C., Breteler, M.M.B., Clarke, M., Copeland, J.R.M., Dartigues, J.-F., Engedal, K., Hagnell, O., Heeren, T.J., Mann, A.H., Mölsä, P.K., Morgan, K., O'Connor, D.W., da Silva Droux, A., Sulkava, R., Kay, D.W.K., & Amaducci, L. (1991). Frequency and distribution of Alzheimer's disease in Europe: A collaborative study of 1980-1990 prevalence findings. Ann Neurol, 30, 381-390.

Rockenstein, E.M., Mc Conlogue, L., Tan, H., Power, M., Masliah, E., & Mucke, L. (1995). Levels and alternative splicing of amyloid β protein processor (APP) transcripts in brains of APP transgenic mice and humans with Alzheimer's disease. The Journal of Biological Chemistry, 270, 28527-28267.

Roerig, S.C., Loh, H.H., & Law, P.Y. (1992). Identification of three separate guanine nucleotide-binding proteins that interact with the delta-opioid receptor in NG108-15 neuroblastoma x glioma hybrid cells. Molecular Pharmacology, 41, 822-831.

Rogaev, E.I., Sherrington, R., Rogaeva, E.A., Levesque, G., Ikeda, M., Liang, Y., Chi, H., Lin, C., Holman, K., Tsuda, T., Mar, L., Sorbi, S., Nacmias, B., Piacentini, S., Amaducci, L., Chumakov, I., Cohen, D., Lannfelt, L., Fraser, P.E., Rommens, J.M., & St.George-Hyslop, P.H. (1995). Familial Alzheimer's disease in kindreds with missense mutations in a gene on chromosome 1 related to the Alzheimer's disease type 3 gene. Nature, 376, 775-778.

Rogers, A.W. (1979). Techniques of Autoradiography. (3rd ed.) Oxford: Elsevier/North-Holland Biomedical Press.

Rogers, J., Cooper, N.R., Webster, S., Schultz, J., McGeer, P.L., Styren, S.D., Civin, W.H., Brachova, L., Bradt, B., Ward, P., & Lieberburg, I. (1992). Complement activation by β-amyloid in Alzheimer disease. Proc Natl Acad Sci USA, 89, 10016-10020.

Rogers, J., Kirby, L.C., Hempelman, S.R., Berry, D.L., McGeer, P.L., Kaszniak, A.W., Zalinski, J., Cofield, M., Mansukhani, L., Willson, P., & Kogan, F. (1993). Clinical trial of indomethacin in Alzheimer's disease. Neurology, 43, 1609-1611.

Rogers, S.L., Friedhoff, L.T., & Donepezil Study Group. (1996). The efficacy and safety of Donepezil in patients with Alzheimer's disease: Results of a US multicentre, randomized, double-blind, placebo-controlled trial. Dementia, 7, 293-303.

Rogers, S.L., Yamanishi, Y. & Yamatsu, K. (1991). The pharmacology of a piperidine cholinesterase inhibitor. In R. Becker & E. Giacobini (Eds.). Cholinergic Basis for Alzheimer Therapy (pp. 314-320). Boston: Birkhauser

Ross, B.M., Knowler, J.T., & McCulloch, J. (1992). On the stability of messenger RNA and ribosomal RNA in the brains of control human subjects and patients with Alzheimer's disease. Journal of Neurochemistry, 58, 1810-1819.

Rothwell, N.J. & Relton, J.K. (1993). Involvement of cytokines in acute neurodegeneration in the CNS. Neuroscience and Biobehavioural Reviews, 17, 217-227.

Rudelli, R., Strom, J.O., Welch, P.T., & Ambler, M.W. (1982). Posttraumatic premature Alzheimer's disease: Neuropathologic findings and pathogenic considerations. Archives of Neurology, 39, 570-575.

Rumble, B., Retallack, R., Hilbich, C., Simms, G., Multhaup, G., Martins, R., Hockey, A., Montgomery, P., Beyreuther, K., & Masters, C.L. (1989). Amyloid A4 Protein and its Precursor in Down's Syndrome and Alzheimer's disease. The New England Journal of Medicine, 320, 1446-1447.

Saitoh, T., Kang, D., Mallory, M., DeTeresa, R., & Masliah, E. (1997). Glial cells in Alzheimer's disease: Preferential effect of APOE risk on scattered microglia. Gerontology, 43, 109-118.

Salbaum, M., Weidemann, A., Lemaire, H., Masters, C.L., & Beyreuther, K. (1988). The promoter of Alzheimer's disease amyloid A4 precursor gene. The EMBO Journal, 7, 2807-2813.

Salomon, R.N. (1995a). Introduction to Quantitative Reverse Transcription Polymerase Chain Reaction. Diagnostic Molecular Pathology, 4, 82-84.

Salomon, R.N. (1995b). Introduction to Reverse Transcription Polymerase Chain Reaction. Diagnostic Molecular Pathology, 4, 2-3.

Salvesen, G., Lloyd, C., & Farley, D. (1987). cDNA encoding a human homolog of yeast ubiquitin 1. Nucleic Acids Research, 15, 5485

Sambrook, J., Fritsch, E.F. & Maniatis, T. (1989). Molecular Cloning A Laboratory Manual. (2nd ed.) Cold Spring Harbor, New York: Cold Spring Harbor Laboratory Press.

Sandbrink, R. & Beyreuther, K. (1996). State of the Art Unravelling the molecular pathway of Alzheimer's disease: research about presenilins gathers momentum. Molecular Psychiatry, 1, 438-444.

Sandbrink, R., Hartmann, T., Masters, C.L., & Beyreuther, K. (1996). Genes contributing to Alzheimer's disease. Molecular Psychiatry, 1, 27-40.

Sandbrink, R., Masters, C.L., & Beyreuther, K. (1994a). β A4-amyloid protein precursor mRNA isoforms without exon 15 are ubiquitously expressed in rat tissues including brain, but not in neurons. The Journal of Biological Chemistry, 269, 1510-1517.

Sandbrink, R., Masters, C.L., & Beyreuther, K. (1994b). Similar alternative splicing of a non-homologous domain in bA4-amyloid protein precursor-like proteins. The Journal of Biological Chemistry, 269, 14227-14234.

Sandbrink, R., Mömming, U., Masters, C.L., & Beyreuther, K. (1997). Expression of the APP gene family in brain cells, brain development and aging. Gerontology, 43, 119-131.

Sano, M., Ernesto, C., Thomas, R.G., Klauber, M.R., Schafer, K., Grundman, M., Woodbury, P., Growdon, J., Cotman, C.W., Pfeiffer, E., Schneider, L.S., & Thal, L.J. (1997). A controlled trial of selegiline, alpha-tocopherol, or both as treatment for Alzheimer's disease. The New England Journal of Medicine, 336, 1216-1222.

Saunder, A.M., Strittmatter, W.J., Schmechel, D., St.George-Hyslop, P.H., Pericak-Vance, M.A., Joo, S.H., Rosi, B.L., Gusella, J.F., Crapper McLachlan, D.R., Alberts, M.J., Hulette, C., Crain, B., Goldgaber, D., & Roses, A.D. (1993). Association of apolipoprotein E allele of ∈4 with late-onset familial and sporadic Alzheimer's disease. Neurology, 43, 1467-1472.

Schellenberg, G.D., Bird, T.D., Wijsman, E.M., Orr, H.T., Anderson, L., Nemens, E., White, J.A., Bonnycastle, L., Weber, J.L., Alonso, M.E., Potter, H., Heston, L.L., & Martin, G.M. (1992). Genetic Linkage Evidence for a Familial Alzheimer's Disease Locus on Chromosome 14. Science, 258, 668-671.

Schellenberg, G.D. (1995). Genetic dissection of Alzheimer's disease, a heterogeneous disorder. Proc Natl Acad Sci USA, 92, 8552-8559.

Scheuermann, R.H. & Bauer, S.R. (1993). Polymerase chain reaction-based mRNA quantification using an internal standard: Analysis of oncogene expression. Methods in Enzymology, 218, 446-473.

Schlesinger, D.H. & Goldstein, G. (1975). Molecular conservation of 74 amino acid sequence of ubiquitin between cattle and man. Nature, 255, 423-424.

Schlesinger, M.J., Asburner, M. & Tissieres, A. (1982). Heat Shock from Bacteria to Man. Cold Spring Harbor, New York: Cold Spring Harbor Laboratory Press.

Schneider, L.S. (1996). New therapeutic approaches to Alzheimer's disease. Journal of Clinical Psychiatry, 57, 30-36.

Selkoe, D.J., Podlisny, M.B., Joachim, C.L., Vickers, E.A., Lee, G., Fritz, L.C., & Oltersdorf, T. (1988). β-amyloid precursor protein of Alzheimer disease occurs as 110- to 135-kilodalton membrane-associated proteins in neural and nonneural tissues. Proc Natl Acad Sci USA, 85, 7341-7345.

Selkoe, D.J. (1991). The molecular pathology of Alzheimer's disease. Neuron, 6, 487-498.

Seubert, P., Vigo-Pelfrey, C., Esch, F., Lee, M., Dovey, H.F., Davis, D., Sinha, S., Schlossmacher, M.G., Whaley, J., Swindlehurst, C., McCormack, R., Wolfert, R., Selkoe, D.J., Lieberburg, I., & Schenk, D. (1992). Isolation and quantification of soluble Alzheimer's β-peptide from biological fluids. Nature, 359, 325-327.

Seubert, P., Oltersdorf, T., Lee, M.G., Barbour, R., Blomquist, C., Davis, D.L., Bryant, K., Fritz, L.C., Galasko, D., Thal, L.J., Lieberburg, I., & Schenk, D.B. (1993). Secretion of β-amyloid precursor protein cleaved at the amino terminus of the β-amyloid peptide. Nature, 361, 260-263.

Shaw, G. & Kamen, R. (1986). A conserved AU sequence from the 3' untranslated region of GM-CSF mRNA mediates selective mRNA degradation. Cell, 46, 659-667.

Shea, T.B. (1994). Amyloid precursor protein as a glial-derived growth factor. Trends Neurosci, 17, 338-339.

Shercliff, F.E., Bridges, L.R., Gentleman, S.M., Sivaloganathan, S., & Wilson, S. (1994). Markers of axonal injury in post mortem human brain. Acta Neuropathol (Berl), 88, 433-439.

Sherrington, R., Rogaev, E.I., Liang, Y., Rogaeva, E.A., Levesque, G., Ikeda, M., Chi, H., Lin, C., Li, G., Holman, K., Tsuda, T., Mar, L., Foncin, J.F., Bruni, A.C., Montesi, M.P., Sorbi, S., Rainero, I., Pinessi, L., Nee, L., Chumadov, I., Pollen, D., Brookes, A., Sanseau, P., Polinsky, R.J., Wasco, W., Da Silva, H.A.R., Haines, J.L., Pericak-Vance, M.A., Tanzi, R.E., Roses, A.D., Fraser, P.E., Rommens, J.M., & St.George-Hyslop, P.H. (1995). Cloning of a gene bearing missense mutations in early-onset familial Alzheimer's disease. Nature, 375, 754-760.

Shoji, M., Golde, T.E., Ghiso, J., Cheung, T.T., Estus, S., Shaffer, L.M., Cai, X.-D., McKay, D.M., Tintner, R., Frangione, B., & Younkin, S.G. (1992). Production of the Alzheimer amyloid β protein by normal proteolytic processing. Science, 258, 126-129.

Shoji, M., Hirai, S., Yamaguchi, H., Harigaya, Y., & Kawarabayashi, T. (1990). Amyloid β-protein precursor accumulates in dystrophic neurites of senile plaques in Alzheimer-type dementia. Brain Research, 512, 164-168.

Siebert, P.D. (1993). Quantitative RT-PCR. Palo Alto, CA: CLONTECH Laboratories, Inc..

Silverman, W. & Wisniewski, H.M. (1993). Alzheimer's disease: Empirical evaluation of diagnostic methods. Alzheimer Disease and Associated Disorders, 7, 132-135.

Siman, R., Card, J.P., Nelson, R.B., & Davis, L.G. (1989). Expression of β-amyloid precursor protein in reactive astrocytes following neuronal damage. Neuron, 3, 275-285.

Singer-Sam, J. & Riggs, A.D. (1993). Quantitative analysis of messenger RNA levels: Reverse transcription-polymerase chain reaction single nucleotide primer extension assay. Methods in Enzymology, 225, 344-351.

Sisodia, S.S. (1992). β-amyloid precursor protein cleavage by a membrane-bound protease. Proc Natl Acad Sci U S A, 89, 6075-6079.

Sisodia, S.S., Koo, E.H., Beyreuther, K., Unterbeck, A., & Price, D.L. (1990). Evidence that β-amyloid protein in Alzheimer's disease is not derived by normal processing. Science, 248, 492-495.

Shurt, H.H., Thinakaran, G., Von Koch, C., Lo, A.C.Y., Tanzi, R.E., & Sisodia, S.S. (1994). Expression of a ubiquitous, cross-reactive homologue of the mouse β-amyloid precursor protein (APP). The Journal of Biological Chemistry, 269, 2637-2644.

Smith, A.D., Jobst, K.A., Edmonds, Z., Hindley, N.J., & King, E.M.-F. (1996a). Neuroimaging and early Alzheimer's disease. The Lancet, 348, 829-830.

Smith, A.D., Jobst, K.A., Johnston, C., Joachim, C.L., & Nagy, Z. (1996b). Apolipoprotein-E genotyping in diagnosis of Alzheimer's disease. The Lancet, 348, 483-484.

Smith-Swintosky, V.L., Pettigrew, L.C., Craddock, S.D., Culwell, A.R., Rydel, R.E., & Mattson, M.P. (1994). Secreted forms of b-amyloid precursor protein protect against ischemic brain injury. J Neurochem, 63, 781-784.

Sohma, H., Hashimoto, H., Hiraike, N., Ohguro, H., & Akino, T. (1993). Different functional forms of G-protein bgamma-subunits, bgamma-I and bgamma-II, in bovine brain. Biochim Biophys Acta Mol Cell Res, 1178, 111-116.

Spicher, K., Nuernberg, B., Jäger, B., Rosenthal, W., & Schultz, G. (1992). Heterogeneity of three electrophoretically distinct Go α-subunits in mammalian brain. FEBS, 307, 215-218.

Sprecher, C.A., Grant, F.J., Grimm, G., O'Hara, P.J., Norris, F., Norris, K., & Foster, D.C. (1993). Molecular Cloning of the cDNA for a Human Amyloid Precursor Protein Homolog: Evidence for a Multigene Family. Biochemistry, 32, 4481-4486.

St George-Hyslop, P., Haines, J.L., Farrer, L.A., Polinsky, R., Van Broeckhoven, C., Goate, A., Crapper McLachlan, D.R., Orr, H., Bruni, A.C., Sorbi, S., Rainero, I., Foncin, J.F., Pollen, D., Cantu, J.M., Tupler, R., Voskresenskaya, N., Mayeux, R., Growdon, J., Fried, V.A., Myers, R.H., Nee, L., Backhovens, H., Martin, J.J., Rossor, M., Owen, M.J., Mullan, M., Percy, M.E., Karlinsky, H., Rich, S., Heston, L., Montesi, M., Mortilla, M., Nacmias, N., Gusella, J.F., Hardy, J.A., & and other members of the FAD Collaborative Study Group. (1990). Genetic linkage studies suggest that Alzheimer's disease is not a single homogeneous disorder. Nature, 347, 194-197.

St.John, T., Gallatin, W.M., Siegelman, M., Smith, H.T., Fried, V.A., & Weissman, I.L. (1986). Expression cloning of a lymphocyte homing receptor cDNA: Ubiquitin is the reactive species. Science, 231, 845-850.

Sternweis, P.C. (1986). The purified α subunits of Go and Gi from bovine brain require βgamma for association with phospholipid vesicles. Journal of Biological Chemistry, 261, 631-637.

Sternweis, P.C., Northup, J.K., Smigel, M.D., & Gilman, A.G. (1981). The Regulatory Component of Adenylate Cyclase Purification and Properties. The Journal of Biological Chemistry, 256, 11517-11526.

Sternweis, P.C. & Robinshaw, J.D. (1984). Isolation of Two Proteins with High Affinity for Guanine Nucleotides from Membranes of Bovine Brain. The Journal of Biological Chemistry, 259, 13806-13813.

Stewart, P.A., Hayakawa, K., Akers, M.A., & Vinters, H.V. (1992). A morphometric study of the blood-brain barrier in Alzheimer's disease. Laboratory Investigation, 67, 734-742.

Strittmatter, S.M., Valenzuela, D., Kennedy, T.E., Neer, E.J., & Fishman, M.C. (1990). G_o is a major growth cone protein subject to regulation by GAP-43. Nature, 344, 836-841.

Strittmatter, S.M., Valenzuela, D., Sudo, Y., Linder, M.E., & Fishman, M.C. (1991). An Intracellular Guanine Nucleotide Release Protein for G_o GAP-43 Stimulates Isolated α Subunits by a Novel Mechanism. The Journal of Biological Chemistry, 266, 22465-22471.

Strittmatter, W.J., Saunders, A.M., Schmecel, D., Pericak-Vance, M., Enghild, J., Salvesen, G.S., & Roses, A.D. (1993). Apolipoprotein E: High-avidity binding to β-amyloid and increased frequency of type 4 allele in late-onset familial Alzheimer's disease. Proc Natl Acad Sci, 90, 1977-1981.

Strittmatter, W.J., Saunders, A.M., Goedert, M., Weisgraber, K.H., Dong, L.-M., Jakes, R., Huang, D.Y., Pericak-Vance, M., Schmechel, D., & Roses, A.D. (1994). Isoform-specific interactions of apolipoprotein E with microtubule-associated protein tau: Implications for Alzheimer disease. Proc Natl Acad Sci USA, 91, 11183-11186.

Suzuki, K. & Terry, R.D. (1967). Fine Structural Localisation of Acid Phosphatase in Senile Plaques in Alzheimer's Presenile Dementia. Acta Neuropathologica, 8, 276-284.

Suzuki, N., Cheung, T.T., Cai, X.-D., Odaka, A., Otvos, L., Jr., Eckman, C., Golde, T.E., & Younkin, S.G. (1994). An increased percentage of long amyloid β protein secreted by familial amyloid β protein precursor (βAPP717) mutants. Science, 264, 1336-1340.

Tabaton, M., Nunzi, M.G., Xue, R., Usiak, M., Autilio-Gambetti, L., & Gambetti, P. (1994). Soluble amyloid β-protein is a marker of Alzheimer amyloid in brain but not in cerebrospinal fluid. Biochemical and Biophysical Research Communications, 200, 1598-1603.

Tanaka, S., Liu, L., Kimura, J., Shiojiri, S., Takahashi, Y., Kitaguchi, N., Nakamura, S., & Ueda, K. (1992). Age-related changes in the proportion of amyloid precursor protein mRNAs in Alzheimer's disease and other neurological disorders. Molecular Brain Research, 15, 303-310.

Tanaka, S., Nakamura, S., Kimura, J., & Ueda, K. (1993). Age-related change in the proportion of amyloid precursor protein mRNAs in the gray matter of cerebral cortex. Neuroscience Letters, 163, 19-21.

Tang, M.-X., Jacobs, D., Stern, Y., Marder, K., Schofield, P., Gurland, B., Andrews, H., & Mayeux, R. (1996). Effect of oestrogen during menopause on risk and age at onset of Alzheimer's disease. The Lancet, 348, 429-432.

Tanzi, R.E., Gusella, J.F., Watkins, P.C., Bruns, G.A.P., St George-Hyslop, P., Van Keuren, M.L., Patterson, D., Pagan, S., Kurnit, D.M., & Neve, R.L. (1987). Amyloid β Protein Gene: cDNA, mRNA Distribution, and Genetic Linkage Near the Alzheimer Locus. Science, 235, 880-884.

Tanzi, R.E., McClatchey, A.I., Lamperti, E.D., Villa-Komaroff, L., Gusella, J.F., & Neve, R.L. (1988). Protease inhibitor domain encoded by an amyloid protein precursor mRNA associated with Alzheimer's disease. Nature, 331, 528-530.

Tanzi, R.E., Wenniger, J.J., & Hyman, B.T. (1993). Cellular specificity and regional distribution of amyloid β protein precursor alternative transcripts are unaltered in Alzheimer hippocampal formation. Molecular Brain Research, 18, 246-252.

Tariot, P.N. (1996). Treatment strategies for agitation and psychosis in dementia. Journal of Clinical Psychiatry, 57, 21-29.

Terry, R.D. (1993). Regeneration in Alzheimer's disease and aging. Advances in Neurology, 59, 1-4.

Thomas, M. & Isaac, M. (1987). Alois Alzheimer: a memoir. TINS, 10, 306-307.

Tien, R.D., Felsberg, G.J., Ferris, N.J., & Osumi, A.K. (1993). The dementias: Correlation of clinical features, patholphysiology, and neuroradiology. AJR, 161, 245-255.

Tomiyama, T., Asano, S., Suwa, Y., Morita, T., Kataoka, K., Mori, H., & Endo, N. (1994). Rifampicin prevents the aggregation and neurotoxicity of amyloid b protein in vitro. Biochem Biophys Res Commun, 204, 76-83.

Tomlinson, B.E., Blessed, G., & Roth, M. (1970). Observations on the brains of demented old people. Journal of Neurological Sciences, 11, 205-242.

Tsuda, T., Lopez, R., Rogaeva, E.A., Freedman, M., Rogaev, E., Drachman, D., Pollen, D., Haines, J., Liang, Y., Crapper McLachlan, D.R., Duara, R., & St George-Hyslop, P. (1994). Are the Associations Between Alzheimer's Disease and Polymorphisms in the Apolipoprotein E and the Apolipoprotein CII Genes Due to Linkage Disequilibrium?. Ann Neurol, 36, 97-100.

Turner, J. & Raphael, B. (1997). Requesting necropsies. British Medical Journal, 314, 1499-1450.

Tytell, M., Barbe, M.F., & Brown, I.R. (1993). Stress (Heat Shock) Protein Accumulation in the Central Nervous System Its Relationship to Cell Stress and Damage. Advances in Neurology, 59, 293-303.

Valerio, A., Tinti, C., Albertici, A., Belloni, M., Buonamici, M., Spano, P.F., & Memo, M. (1993). Deafferentation induces early and delayed differential changes in the pattern of expression of the various guanine nucleotide binding protein mRNAs in rat striatum. Neuroscience Letters, 164, 109-112.

Van Gool, W.A., Walstra, G.J.M., Teunisse, S., Van der Zant, F.M., Weinstein, H.C., & Van Royen, E.A. (1995). Diagnosing Alzheimer's disease in elderly, mildly demented patients: the impact of routine single photon emission computed tomography. J Neurol, 242, 401-405.

Van Gool, W.A., Schenk, D.B., & Bolhuis, P.A. (1994). Concentrations of amyloid-X(10UβX(8U protein in cerebrospinal fluid increase with age in patients free from neurodegenerative disease. Neurosci Lett, 172, 122-124.

Vandevyver, C. & Raus, J. (1995). Quantitative Analysis of Lymphokine mRNA Expression by an Automated, Non-radioactive method. Cellular and Molecular Biology, 41, 683-694.

VanDongen, A.M.J., Codina, J., Olate, J., Mattera, O.R., Joho, R., Birnbaumer, L., & Brown, A.M. (1988). Newly Identified Brain Potassium Channels Gated by the Guanine Nucleotide Binding Protein G_O. Science, 242, 1433-1437.

Wagner, S.L., Peskind, E.R., Nochlin, D., Provow, S., Farrow, J.S., Pandian, M.R., Cleveland, M., Ito, R.K., & Farlow, M.R. (1994). Decreased levels of soluble amyloid β-protein precursor are associated with Alzheimer's disease in concordant and discordant monozygous twin pairs. Ann Neurol, 36, 215-220.

Waldemar, G., Walovitch, R.C., Andersen, A.R., Hasselbalch, S.G., Begelow, R., Joseph, J.L., Paulson, O.B., & Lassen, N.A. (1994). ^{99m}Tc-Bicisate (Neurolite) SPECT brain imaging and cognitive impairment in dementia of the Alzheimer type: A blinded read of image sets from a multicenter SPECT trial. Journal of Cerebral Blood Flow and Metabolism, 14, S99-S105.

Wasco, W., Bupp, K., Magendantz, M., Gusella, J.F., Tanzi, R.E., & Solomon, F. (1992). Identification of a mouse brain cDNA that encodes a protein related to the Alzheimer disease-associated amyloid β protein precursor. Proc Natl Acad Sci USA, 89, 10758-10762.

Wasco, W., Gurubhagavatula, S., Dparadis, M., Romano, D.M., Sisodia, S.S., Hyman, B.T., Neve, R.L., & Tanzi, R.E. (1993). Isolation and characterization of APLP2 encoding a homolog of the Alzheimers associated amyloid beta-protein precursor. Nature Genetics, 5, 95-100.

Watson, S. & Arkinstall, S. (1994). The G-Protein Linked Receptor Facts Book. London: Academic Press, Harcourt Brace & Company, Publishers.

Webster, M.-T., Groome, N., Francis, P.T., Pearce, B.R., Sherriff, F.E., Thinakaran, G., Felsenstein, K.M., Wasco, W., Tanzi, R.E., & Bowen, D.M. (1995). A novel protein, amyloid precursor-like protein 2, is present in human brain, cerebrospinal fluid and conditioned media. Biochemistry Journal, 310, 95-99.

Wedegaertner, P.B. & Bourne, H.R. (1994). Activation and Depalmitoylation of Gsα. Cell, 77, 1063-1070.

Wegiel, J. & Wisniewski, H.M. (1990). The complex of microglial cells and amyloid star in three-dimensional reconstruction. Acta Neuropathol, 81, 116-124.

Weidemann, A., Konig, G., Bunke, D., Fischer, P., Salbaum, J.M., Masters, C.L., & Beyreuther, K. (1989). Identification, Biogenesis, and Localization of Precursors of Alzheimer's Disease A4 Amyloid Protein. Cell, 57, 115-126.

Weiner, M.F., Tintner, R.J. & Goodkin, K. (1991a). Differential diagnosis. In M.F. Weiner (Ed.). The Dementias: diagnosis and management (pp. 77-106). Washington, D C: American Psychiatric Press, Inc.

Weiner, M.F., Bruhn, M., Svetlik, D., Tintner, R., & Horn, J. (1991b). Experiences with depression in a dementia clinic. Journal of Clinical Psychiatry, 52, 234-238.

Weiner, M.F., Edland, S.D., & Luszczynska, H. (1994). Prevalence and incidence of major depression in Alzheimer's disease. American Journal of Psychiatry, 151, 1006-1009.

Weinstein, L.S. & Shenker, A. (1993). G protein mutations in human disease. Clinical Biochemistry, 26, 333-338.

Westwood, J.T., Clos, J., & Wu, C. (1991). Stress-induced oligomerization and chromosomal relocalization of heat-shock factor. Nature, 353, 822-827.

Wiborg, O., Pederson, M.S., Wind, A., Berglund, L.E., Marcker, K.A., & Vuust, J. (1985). The human ubiquitin multigene family: some genes contain multiple directly repeated ubiquitin coding sequences. The EMBO Journal, 4, 755-759.

Wighton-Benn, W., Vardy, E., Heath, P.R. & Pearson, R.C.A. Poster entitled 'Alterations in Messenger RNA's Encoding Major Isoforms of Amyloid Precursor Protein in Alzheimer's Disease Neocortex.' at the Society for Neuroscience, San Diego, November 11-16, 1995.

Wilcock, G.K. (1996). Current approaches to the treatment of Alzheimer's disease. Neurodegeneration, 5, 505-509.

Will, R.G., Ironside, J.W., Zeidler, M., Cousens, S.N., Estibeiro, K., Alperovitch, A., Poser, S., Pocchiari, M., Hofman, A., & Smith, P.G. (1996). A new variant of Creutzfeldt-Jakob disease in the UK. The Lancet, 347, 921-925.

Wisniewski, H.M. (1993). β-Protein Fibrillogenesis and Its Impact on Neuropil and Microvessels. Neurobiology of Aging, 14, 665-666.

Wisniewski, H.M. & Wegiel, J. (1992). Alzheimer's disease neuropathology Current status of interpretation of lesion development. Annals New York Academy of Sciences, 673, 270-284.

Wisniewski, T., Casta±o, E.M., Golabek, A., Vogel, T., & Frangione, B. (1994). Acceleration of Alzheimer's fibril formation by apolipoprotein E in vitro. Am J Pathol, 145, 1030-1035.

Wisniewski, T. & Frangione, B. (1992). Apolipoprotein E: A pathological chaperone protein in patients with cerebral and systemic amyloid. Neuroscience Letters, 135, 235-238.

Wisniewski, T., Golabek, A., Matsubara, E., Ghiso, J., & Frangione, B. (1993). Apolipoprotein E: Binding to soluble Alzheimer's β-amyloid. Biochemical and Biophysical Research Communications, 192, 359-365.

Wolozin, B., Lesch, P., Lebovics, R., & Sunderland, T. (1993). Olfactory neuroblasts from Alzheimer Donors: Studies on APP processing and cell regulation. Biological Psychiatry, 34, 824-838.

World Health Organisation. (1992). The ICD-10 classification of mental and behavioural disorders. Geneva Switzerland: World Health Organisation.

Worley, P.F., Baraban, J.M., Van Dop, C., Neer, E.J., & Snyder, S.H. (1986). G_o, a guanine nucleotide-binding protein: Immunohistochemical localization in rat brain resembles distribution of second messenger systems. Proc Natl Acad Sci, 83, 4561-4565.

Wu, C., Zimarino, V., Tsai, B., Walker, B. & Wilson, S. (1990). Transcriptional regulation of heat shock genes. In R.I. Morimoto, G. Tissières & C. Georgopoulus (Eds.). Stress Proteins in Biology and Medicine (pp. 429-442). Cold Spring Harbor, New York: Cold Spring Harbor Laboratory Press

Wu, R.S., Kohn, K.W., & Bonner, W.M. (1981). Metabolism of ubiquitinated histones. Journal of Biological Chemistry, 256, 5916-5920.

Yamaguchi, H., Hirai, S., Morimatsu, M., Shoji, M., & Ihara, Y. (1988). A variety of cerebral amyloid deposits in the brains of the Alzheimer-type dementia demonstrated by β protein immunostaining. Acta Neuropathol, 76, 541-549.

Yamatsuji, T., Okamoto, T., Takeda, S., Muryama, Y., Tanaka, N., & Nishimoto, I. (1996a). Expression of V642 APP mutant causes cellular apoptosis as Alzheimer trait-linked phenotype. EMBO, 15, 498-509.

Yamatsuji, T., Matsui, T., Okamoto, T., Komtsuzaki, K., Takeda, S., Fukumoto, H., Iwatsubo, T., Suzuki, N., Asami-Odaka, A., Ireland, S., Kinane, B., Giambarella, U., & Nishimoto, I. (1996b). G protein-mediated neuronal DNA fragmentation induced by familial Alzheimer's disease-associated mutants of APP. Science, 272, 1349-1352.

Yang, F., Mak, K., Vinters, H.V., Frautschy, S.A., & Cole, G.M. (1994). Monoclonal antibody to the C-terminus of β-amyloid. Neuroreport, 5, 2117-2120.

Yanker, B.A., Duffy, L.K., & Kieschner, D.A. (1990). Neurotrophic and neurotoxic effects of amyloid β protein: reversal by tachykinin neuropeptides. Science, 250, 279-282.

Yatani, A., Codina, J., Imoto, Y., Reeves, J.P., Birnbaumer, L., & Brown, A.M. (1987). A G protein directly regulates mammalian cardiac calcium channels. Science, 238, 1288-1292.

Yates, C.M., Butterworth, J., Tennant, M.C., & Gordon, A. (1990). Enzyme activities in relation to pH and lactate in postmortem brain in Alzheimer-type and other dementias. Journal of Neurochemistry, 55, 1624-1630.

Yin, J.C.P., Wallach, J.S., Del Vecchio, M., Wilder, E.L., Zhou, H., Quinn, W.G., & Tully, T. (1994). Induction of a dominant negative CREB transgene specifically blocks long-term memory in drosophila. Cell, 79, 49-58.

Yoshikawa, K., Aizawa, T., & Hayashi, Y. (1992). Degeneration *in vitro* of post-mitotic neurons overexpressing the Alzheimer amyloid protein precursor. Nature, 359, 64-67.

Zaidi, S.H.E., Denman, R., & Malter, J.S. (1994). Multiple proteins interact at a unique cis-element in the 3'-untranslated region of amyloid precursor protein mRNA. J Biol Chem, 269, 24000-24006.

Zaidi, S.H.E. & Malter, J.S. (1994). Amyloid precursor protein mRNA stability is controlled by a 29-base element in the 3'-untranslated region. The Journal of Biological Chemistry, 269, 24007-24013.

Zemlan, F.P., Vogelsang, G.D., McLaughlin, L., & Dean, G.E. (1994). Alzheimer's paired helical filaments: Amyloid precursor protein epitope mapping. Brain Research Bulletin, 33, 387-392.

Zhang, C., Lambert, M.P., Bunch, C., Barber, K., Wade, W.S., Krafft, G.A., & Klein, W.L. (1994). Focal adhesion kinase expressed by nerve cell lines shows increased tyrosine phosphorylation in response to Alzheimer's Ab peptide. J Biol Chem, 269, 25247-25250.

Zubenko, G.S., Stiffler, S., Stabler, S., Kopp, U., Hughes, H.B., Cohen, B.M., & Moossy, J. (1994). Association of the apolipoprotein E ×4 allele with clinical subtypes of autopsy-confirmed Alzheimer's disease. Am J Med Genet, 54, 199-205.

NEURODEGENERATION, *Vol. 5, pp 409–415* (1996)

Amyloid Precursor Protein mRNAs in Alzheimer's Disease

Paul J. Harrison,[1] Wendy H. Wighton-Benn,[2,3] Josephine M. Heffernan,[1] Maurice W. Sanders[2] and R. Carl A. Pearson[2]

[1]*Departments of Psychiatry and Clinical Neurology (Neuropathology), University of Oxford; Departments of* [2]*Biomedical Science and* [3]*Psychiatry, University of Sheffield*

Hybridization studies of mRNA link genetic with neurochemical and neuropathological approaches to Alzheimer's disease (AD). Here we review the distribution and abundance of amyloid precursor protein mRNAs in normal and AD-afflicted brains. The expression of apolipoprotein E and presenilin mRNAs are also discussed.

Key words: β-amyloid, dementia, gene expression, human brain, in situ hybridization, messenger RNA

AS CANDIDATES FOR THREE seminal advances in Alzheimer's disease (AD) research of the past twenty years we would propose: the discovery of the cholinergic deficit (Bowen *et al.*, 1976; Davies & Moloney, 1976; Perry *et al.*, 1977), the sequencing of β-amyloid (Glenner & Wong, 1984; Masters *et al.*, 1985), and the finding of a causative β-amyloid precursor protein (APP) mutation (Goate *et al.*, 1991). These discoveries played critical roles in, respectively, the neurochemical, neuropathological and genetic understanding of AD.

Investigation of gene expression has helped integrate these research fields in several ways. Here we focus upon studies of APP mRNAs and the information they have provided with regard to the involvement of APP in AD. We also review briefly the expression of apolipoprotein E (apoE) and the presenilins. The use of gene expression methodologies to investigate other areas of AD and relevant experimental models is discussed in Harrison (1994, 1995).

β-amyloid precursor protein (APP) mRNAs

Following the cloning of the human APP gene (Tanzi *et al.*, 1987) it became possible to examine the expression of its mRNA. Two obvious questions arose. Which tissues and cells express APP? Is the expression of APP altered in AD? Both have proved surprisingly difficult to answer unequivocally.

Distribution of amyloid precursor protein mRNAs

Initial blot hybridization studies showed that APP mRNA is abundant in the brain (as well as other tissues) at all stages of life (Tanzi *et al.*, 1987; Goedert, 1987), and cellular *in situ* hybridization histochemistry (ISHH) showed that expression occurs primarily (Bahmanyar *et al.*, 1987) but not exclusively (Schmechel *et al.*, 1988) in neurons. Subsequently, matters became more complicated with the identification of multiple APP transcripts and the realization that the mRNAs are expressed differentially in terms of localization and relative abundance (Neve *et al.*, 1988, 1990; Palmert *et al.*, 1988; Tanzi *et al.*, 1988, 1993; Spillantini *et al.*, 1989; Tanaka *et al.*, 1989; Golde *et al.*, 1990; Kang & Muller-Hill, 1990). A simplified summary is shown in Table 1 and illustrated in Figure 1. Some details, however, remain unclear, largely as a result of three methodological issues. (1) Some studies have used probes or conditions which detect more than one isoform or which may cross-hybridize to APP homologues. (2) Interpretation of findings based upon homogenized tissue is hindered by uncertainty as to its composition with regard to the proportions of grey and white matter, meninges, etc. The presence of leukocytes and microglia is relevant, since

Correspondence to: Dr P.J. Harrison, University Department of Psychiatry, Warneford Hospital, Warneford Lane, Oxford OX3 7JX. E-mail: paul.harrison@psychiatry.ox.ac.uk

1055-8330/96/040409 + 7 $25.00/0

Table 1. Localization and relative abundance of APP mRNA isoforms in human brain[a]

Isoform	Missing exons[b]	Abundance in brain relative to other organs	Abundance in brain relative to total APP mRNA	Main cell types expressing the isoform in brain
APP695	7,8	++++	++++	Neurons >> other cells
APP714	7	++	+/−	Meninges, glia, endothelia, ?neurons
APP751	8	+	+++	Neurons > other cells
APP770	None	+	+(+)	Glia, meninges, endothelia > neurons
L-APP[c]	15	−	(+)	Lymphocytes, microglia. Not in neurons
APP365[d]	?9–19	Unknown	+	Unknown
APP563[d]	?8–19	Unknown	+	Unknown

[a]The table is a consensus interpretation of the data.
[b]Derived from Yoshikai *et al.* (1990). β-amyloid is encoded by parts of exons 16 and 17. Thus, all APP isoforms other than APP365 and APP563 are potential sources of β-amyloid.
[c]Several L-APP transcripts exist. They differ in whether they also skip exons 7 (L-APP696), 8 (L-APP733), neither (L-APP752) or both (L-APP677).
[d]These isoforms cannot be described purely in terms of missing APP exons, and both also contain non-APP sequences.

they express significant levels of some APP transcripts (Table 1; Allen *et al.*, 1991; Konig *et al.*, 1992). (3) The techniques differ in their sensitivities. In particular, reverse transcriptase-PCR (Golde *et al.*, 1990) analyses of APP mRNA will detect transcripts present at extremely low levels. In this instance, point (2) becomes especially germane.

Notwithstanding these considerations, two conclusions regarding the distribution of APP expression may be drawn. Firstly, APP mRNA expression is widespread and lifelong in the human brain. As such, APP expression is not *per se* a pathological event, and no extra-cerebral origin of the β-amyloidosis of AD need be postulated. Secondly, within the brain, APP is synthesized primarily in neurons. However, the occurrence of some APP transcripts in non-neuronal cells inside and outside the brain means that β-amyloid could still arise from these alternative sources.

Quantitative alterations of APP mRNAs in Alzheimer's disease?

As well as examining where and in what proportions APP transcripts are expressed in normal subjects, research has attempted to ascertain whether these parameters are altered in AD. In particular, it was a plausible hypothesis that β-amyloid deposition in AD was caused by simple overexpression of APP, as is thought to be the case in Down's syndrome. Although this possibility was soon ruled out, a complete answer to the question posed in the title above has proved elusive. This is due partly to the number and complex distribution of transcripts, and partly to the methodological and interpretational problems which affect quantitative mRNA studies in human brain.

A number of changes have been reported in the abundance of one or more APP mRNAs in one or more regions of the AD brain (reviewed in Harrison (1994) and Rockenstein *et al.* (1995)). However, the findings overall have been inconsistent. An important reason for this is that APP mRNA expression is now known to be highly variable between brains (Koo *et al.*, 1990; Oyama *et al.*, 1991, 1993; Robinson *et al.*, 1994). Oyama *et al.* (1991, 1993) studied 38 individuals and showed a several-fold range in the abundance and proportions of cortical APP mRNAs. The variation did not correlate with age, post mortem interval or β-amyloid deposition. In the light of this variability, the possibility of false positive and false negative results from quantitative APP mRNA studies—which have often been carried out on small ($n < 8$) numbers of cases—is clear.

Clues to the origin of APP expression variability were provided by a study of brains collected by Drs Andy Procter and David Bowen. The subjects, mostly demented, had been prospectively assessed during the days before death. Preservation of APP mRNA was found to be affected by the duration of terminal coma and by pyrexia, and it correlated strongly with the activity of glutamic acid decarboxylase (GAD), an enzyme known to be vulnerable to prolonged modes of death (Harrison *et al.*, 1994; Procter *et al.*, 1994; see also Burke *et al.*, 1991). The finding that APP mRNAs are affected by premortem course (agonal state) probably explains much of the observed variation in brain APP mRNA levels between individuals. Conversely, post mortem interval does not (Harrison *et al.*, 1994). Premortem events are not, however, likely to be the

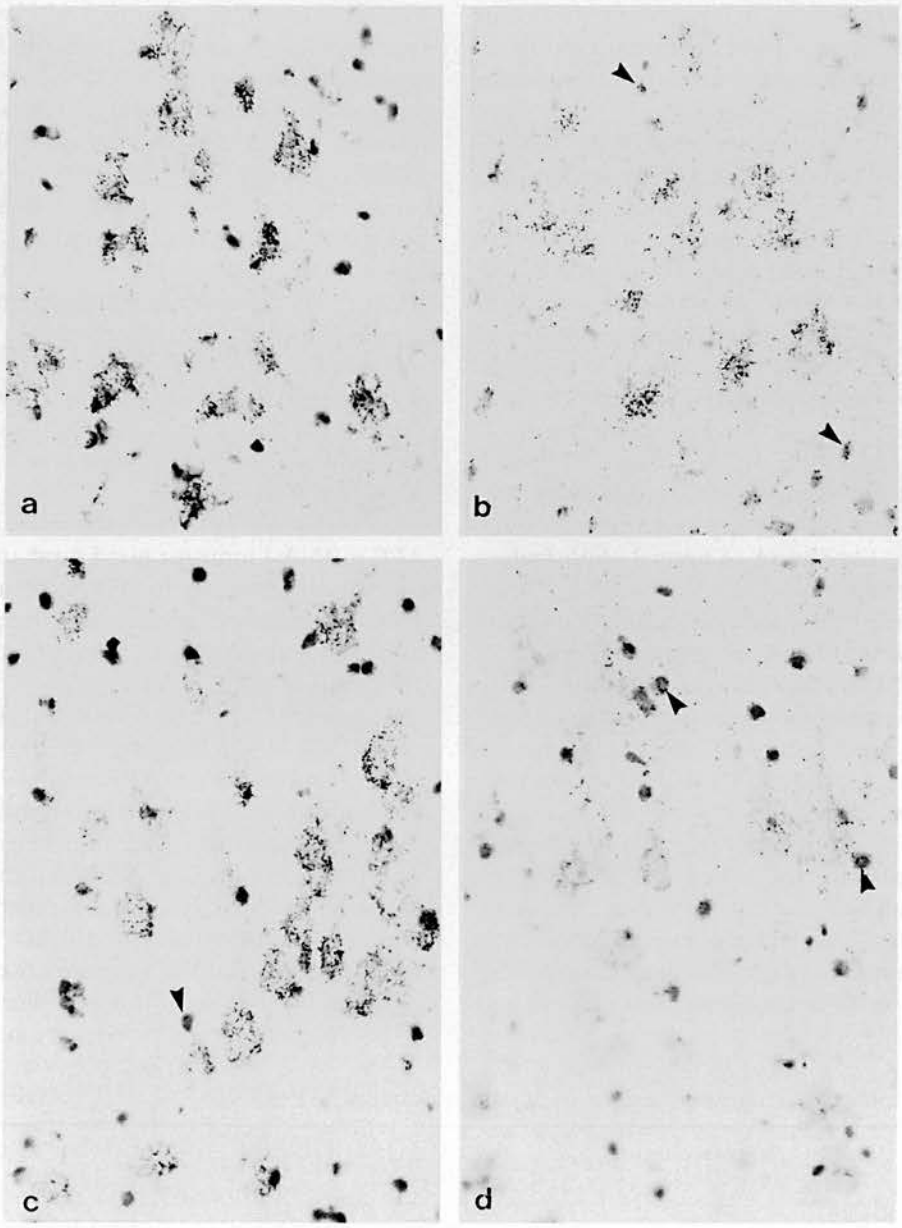

Figure 1. Cellular expression of APP mRNAs in the normal human hippocampus (CA3 field) using isoform-specific ^{35}S-labelled oligonucleotide probes and liquid emulsion autoradiography. (a) APP695 mRNA using an exon 6/9 junction probe. (b) APPins mRNA, using a probe to a region within exon 7. (c) APP751 mRNA, using an exon 7/9 junction probe. (d) APP770 mRNA using a probe to a region within exon 8. Only neurons are seen to express APP695 and APP751 mRNAs, whereas APP770 mRNA is absent from neurons and present at low levels in putative glia. Signal for APP770 mRNA, although weak, is specific, since sense strand hybridization produced no grain clustering, and the APP770 oligonucleotide was validated in a northern blot. The similar images in B and C reflect the fact that most APPins mRNA in brain is APP751 mRNA.

sole cause of variability in APP expression since a similar phenomenon is observed in lymphocytes (Ebstein *et al.*, 1996), and to a lesser extent in brains of monkeys (Koo *et al.*, 1990) whose mode of death was presumably rapid and uniform.

Within the Procter/Bowen series, APP695 mRNA was decreased in AD frontal cortex compared to controls (Harrison *et al.*, 1994), as had been found in several earlier studies (see Rockenstein *et al.*, 1995). We also showed that the decrease was present relative to total poly(A)$^+$mRNA content, and that it distinguished the AD cases from a mixed group of non-AD dementias. APPins mRNAs were reduced to a similar extent as APP695 mRNA; therefore we did not replicate an increase in the ratio of KPI-encoding to KPI-lacking APP transcripts in AD cases reported previously. The three comparison groups were reasonably matched for GAD activity and terminal coma, thus reducing the likelihood of agonal state factors confounding the results.

Recently we have examined APP mRNAs in material from the Oxford Study to Investigate Memory in Ageing (OPTIMA), wherein people with early dementia and age matched controls are assessed and followed up at regular intervals. Clinical, neuropsychological, neuroradiological and ultimately neuropathological measurements are made. Brains from a subgroup of control, AD and non-AD dementia subjects were selected for APP mRNA studies. The groups were matched for demographic and confounding variables. The AD and non-AD dementia groups were matched for degree of dementia (MMSE score), but there were a wide range of clinical and pathological severities within the AD group (Table 2). Initial results of hippocampal APP mRNA expression in the OPTIMA cases are presented in Figure 2. No significant differences in APP695 or APPins mRNAs were seen in the established AD cases compared to normal controls or cases of non-AD dementia. We found no differences in the ratio of the two APP isoforms between the groups or in relation to age (data not shown). These negative findings, in a well characterized and relatively large series, suggest that major changes in APP mRNA expression do not occur in the hippocampus in AD. Moreover, no relationship was seen between the abundance of APP mRNAs and the severity of AD as assessed using the indices listed in Table 2 (data not shown), suggesting that aberrant hippocampal APP expression is not prominent at any stage of the AD process.

Indeed, more generally, the main conclusion of the APP mRNA literature must be that no unequivocal, specific abnormality in AD has been demonstrated. This negative conclusion seems to apply to familial AD too (Harrison *et al.*, 1991a, but see Querfurth *et al.*, 1995) and is supported by the failure to find AD-associated alterations in APP transcriptional regulation (Lukiw *et al.*, 1994). It is in keeping with the view that the critical abnormalities in APP metabolism occur either upstream in the gene itself, in familial AD cases due to a mutation in the gene, or downstream in the proteolytic processing of APP in other forms of AD (Checler, 1995). Even where positive APP mRNA findings have been described in AD (such as decreased APP695 mRNA), their interpretation and pathogenic significance is often unclear. For example, some

Table 2. Demographic details of cases used for study of hippocampal APP mRNAs

	Normal controls (n = 7)	Alzheimer's disease[a] (n = 10)	Non-Alzheimer dementias[b] (n = 6)
Sex (M:F)	3:4	6:4	3:3
Age (y)	79 (8)	76 (9)	80 (8)
CSF pH[c]	6.69 (0.41)	6.66 (0.37)	6.85 (0.29)
PMI (h)	40 (17)	36 (13)	23 (13)
Freezer storage (y)	1.9 (1.1)	2.6 (1.6)	3.6 (1.3)
MMSE (0–30)	27 (3)	8 (11) (n = 9)	9 (5)
Braak stage (0–6)	1.0 (0.9) (n = 5)	4.7 (1.2) (n = 8)	2.4 (0.5)
Neuritic plaques[d]	0 (n = 2)	0.81 (1.40) (n = 4)	0 (n = 4)
NFTs[d]	0 (n = 2)	3.3 (3.5) (n = 4)	0 (n = 4)

Values are mean (SD). PMI = post mortem interval. MMSE = last recorded mini-mental state score (tested within 6 months of death).
[a]Definite (n = 9) or probable (n = 1) AD by CERAD criteria.
[b]Diagnoses: Parkinson's disease, Binswanger's disease, multi-infarct dementia with Parkinson's disease, normal pressure hydrocephalus, corticobasal degeneration, Huntington's disease.
[c]Agonal state marker (Harrison *et al.*, 1995).
[d]Mean density in hippocampus (Nagy *et al.*, 1996).

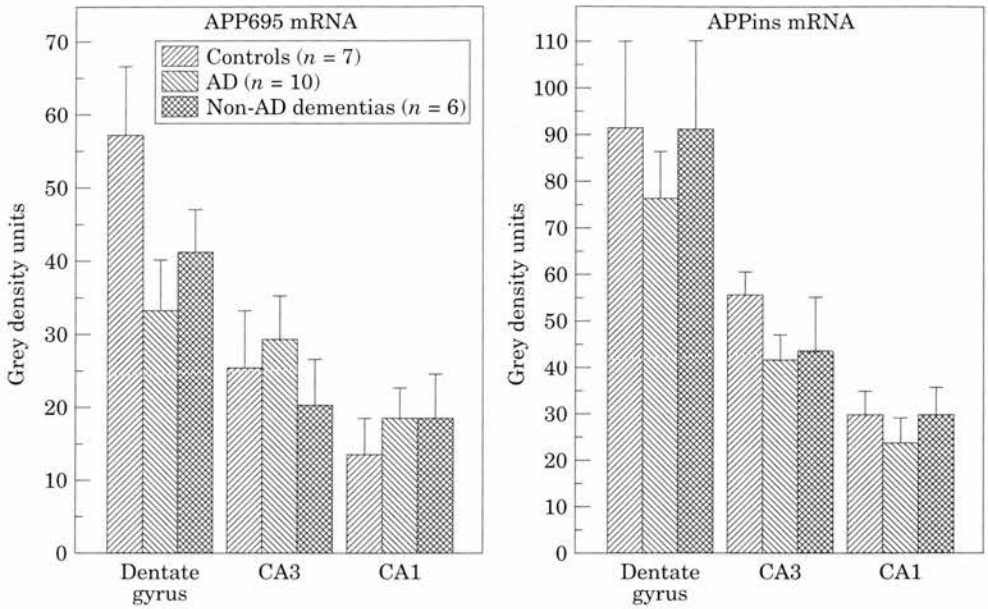

Figure 2. APP mRNAs in hippocampal subfields in Alzheimer's disease and non-Alzheimer dementias compared to controls using ISHH and film autoradiography. See Harrison *et al.* (1994) for experimental methods. Error bars are SEM. There are no significant ($P < 0.05$) differences between groups.

studies have neglected possible differences in overall gene expression levels (Harrison *et al.*, 1991b). Others have not taken into account possible changes in cellular composition of the tissue or have not considered whether a change identified in AD also occurs in other degenerative disorders. Such factors must all be determined before a given change in APP mRNA can be concluded to be gene-, isoform-, cell- or AD-specific. These conceptual issues are in addition to the methodological confounders of agonal state. Equally, however, these uncertainties mean that a significant but currently unrecognized alteration in APP mRNA expression in AD may exist. For example, several studies report that APP770 mRNA, although rare in brain, is increased in AD, probably occurring in glia, meninges and/or other non-neuronal cells (Tanaka *et al.*, 1989; Golde *et al.*, 1990; Jacobsen *et al.*, 1991; Premkumar & Kalaria, 1996).

Overall, therefore, studies of APP expression in AD should continue, but will benefit from greater attention being paid to the factors discussed here. Interpretation of the data will be enhanced by clarification of two other issues: by establishing more clearly the quantitative relationship between each mRNA and the APP isoform which it encodes, and by determining if β-amyloid arises proportionally from all APPs. These data are needed to identify whether the abundance of an APP mRNA predicts that of the encoded protein (an assumption implicit in most gene expression studies) and, if so, whether any particular APP transcript is of special relevance as an amyloidogenic precursor.

Other candidate gene mRNAs in Alzheimer's disease

Following the discovery that the apoE and presenilin (PS) genes contribute to AD, the expression of their transcripts has begun to be investigated.

Distribution of apolipoprotein E mRNA

ApoE mRNA is expressed in astrocytes but not in neurons (Diedrich *et al.*, 1991), an important consideration when developing models to explain the mechanism by which apoE is involved in AD. It indicates that neuronal apoE immunoreactivity (Han *et al.*, 1994) is due to uptake, rather than synthesis, of apoE by neurons. In the same paper, Diedrich *et al.* (1991) reported elevated apoE mRNA in AD. Although this is unsurprising given the gliosis which occurs in the disease, apoE mRNA is increased by a greater degree than is glial fibrillary acidic protein mRNA (Yamada *et al.*,

1995), suggesting that the enhanced apoE expression in AD is not entirely due to gliosis. No association has been found either between apoE genotype and the abundance of apoE mRNA (Yamada *et al.*, 1995), APP or tau mRNAs (Oyama *et al.*, 1995) in the cortex. These negative observations imply that the influence of apoE variants on AD, including their effect upon its neuropathology and neurochemistry, are not exerted via altered apoE, APP or tau expression.

Distribution of presenilin mRNAs

Initial data on the human expression of PS1 and PS2 show that they are synthesized in the brain and in some peripheral tissues (Rogaev *et al.*, 1995; Suzuki *et al.*, 1995; Kovacs *et al.*, 1996; Levy-Lahad *et al.*, 1996). ISHH and immunocytochemical data indicate that, within the brain, PS1 is predominantly neuronal (Suzuki *et al.*, 1995; Elder *et al.*, 1996; Kovacs *et al.*, 1996), but abundant PS1 (and PS2) mRNA is seen in corpus callosum on northern blots (Rogaev *et al.*, 1995), suggesting that some glial populations also express them at high levels. The possibility that aberrant PS expression contributes to the roles of these genes in AD will presumably be investigated in the near future. It is to be hoped that these studies avoid the pitfalls of the equivalent studies of APP mRNAs discussed above.

Acknowledgements

We thank David Bowen and Andy Procter for productive collaborations, and gratefully acknowledge all members of the OPTIMA study, especially Zsuzsa Nagy, Brendan McDonald, Margaret Esiri, Catharine Joachim, James Morris, Lin Barnetson and David Smith. Amanda Barton contributed to the earlier stages of our APP mRNA work. WHW-B is an MRC Training Fellow. PJH is a Wellcome Senior Research Fellow.

References

Allen JS, Murphy GR, Eng L, Stultz K, Davies HD, Pickford L, Tinklenberger JR (1991) Alzheimer's disease: β-amyloid precursor protein mRNA expression in mononuclear blood cells. Neurosci Lett 132:109–112

Bahmanyar S, Higgins GA, Goldgaber D, Lewis DA, Morrison JH, Wilson MC, Shankar SK, Gajdusek DC (1987) Localization of amyloid β protein messenger RNA in brains from patients with Alzheimer's disease. Science 237:77–80

Bowen DM, Smith CB, White P, Davison AN (1976) Neurotransmitter-related enzymes and indices of hypoxia in senile dementia and other abiotrophies. Brain 99:459–496

Burke WL, O'Malley KL, Chung HD, Harmon SK, Miller JP, Berg L (1991) Effect of pre- and post-mortem variables on specific mRNA levels in human brain. Mol Brain Res 11:37–41

Checler F (1995) Processing of the β-amyloid precursor protein and its regulation in Alzheimer's disease. J Neurochem 65:1431–1444

Davies AP, Moloney AJF (1976) Selective loss of cholinergic neurons in Alzheimer's disease. Lancet ii:1403–1404

Diedrich JF, Minnigan H, Carp RI, Whitaker JN, Race R, Frey W II, Haase AT (1991) Neuropathological changes in Alzheimer's disease are associated with increased expression of apolipoprotein E and cathepsin D in astrocytes. J Virol 65:4759–4768

Ebstein RP, Nemanov L, Lubarski G, Dano M, Trevis T, Korczyn AD (1996) Changes in expression of lymphocyte amyloid precursor protein mRNA isoforms in normal aging and Alzheimer's disease. Mol Brain Res 35:260–268

Elder GA, Tezapsidis N, Carter J, Shioi J, Bowas C, Li H-C, Johnston JM, Efthimiopoulos S, Friedrich VL Jr, Robakis NK (1996) Identification and neuron specific expression of the S182/presenilin I protein in human and rodent brains. J Neurosci Res 45:308–320

Glenner GG, Wong D (1984) Alzheimer's disease: initial report of the purification and characterization of a novel cerebrovascular amyloid protein. Biochem Biophys Res Commun 120:885–890

Goate A, Chartier-Harlin M-C, Mullan M, Brown J, Crawford F, Fidani L, Guiffra L, Haynes A, Irving N, James L, Mant R, Newton P, Rooke K, Roques P, Talbot C, Pericak-Vance M, Roses A, Williamson R, Rossor M, Owen M, Hardy J (1991) Segregation of a missense mutation in the amyloid precursor protein gene with familial Alzheimer's disease. Nature 349:704–706

Goedert M (1987) Neuronal localization of amyloid beta protein precursor mRNA in normal human brain and in Alzheimer's disease. EMBO J 6:3627–3632

Golde TE, Estus S, Usiak M, Younkin LH, Younkin SG (1990) Expression of β amyloid protein precursor mRNAs: recognition of a novel alternatively spliced form and quantitation in Alzheimer's disease using PCR. Neuron 4:253–267

Han S-H, Einstein G, Weisgraber KH, Strittmatter WJ, Saunders AM, Pericak-Vance M, Roses AD, Schmechel DE (1994) Apolipoprotein E is localized to the cytoplasm of human cortical neurons: a light and electron microscopic study. J Neuropathol Exp Neurol 53:535–544

Harrison PJ, ed (1994) Regulation of Gene Expression and Brain Function. Basic and Clinical Aspects of Neuroscience, volume 6, Springer-Verlag, Berlin

Harrison PJ (1995) In vitro brain imaging: techniques for studying and localizing the pathogenesis of psychiatric diseases. In Neuroimaging (Neurobiology and Psychiatry volume 3), ed Kerwin RW. Cambridge University Press, Cambridge, pp 157–174

Harrison PJ, Barton AJL, Pearson RCA (1991a) Expression of amyloid beta-protein mRNAs in familial Alzheimer's disease. NeuroReport 2:151–154

Harrison PJ, Barton AJL, Najlerahim A, McDonald B, Pearson RCA (1991b) Regional and neuronal reductions of polyadenylated messenger RNA in Alzheimer's disease. Psychol Med 21:855–866

Harrison PJ, Barton AJL, Procter AW, Bowen DM, Pearson RCA (1994) The effects of Alzheimer's disease, other dementias, and premortem course on β-amyloid precursor protein messenger RNA in frontal cortex. J Neurochem 62:635–644

Harrison PJ, Heath PR, Eastwood SL, Burnet PWJ, McDonald B, Pearson RCA (1995) The relative importance of premortem acidosis and postmortem interval for human brain gene expression studies: selective mRNA vulnerability and a comparison with their encoded proteins. Neurosci Lett 200:151–154

Jacobsen JS, Blume AJ, Vitek MP (1991) Quantitative measurement of alternatively spliced amyloid precursor protein mRNA expression in Alzheimer's disease and normal brain by S1 nuclease protection analysis. Neurobiol Aging 12:585–592

Kang J, Muller-Hill B (1990) Differential splicing of Alzheimer's disease amyloid A4 precursor RNA in rat tissues: PreA4(695) mRNA is predominantly produced in rat and human brain. Biochem Biophys Res Commun 166:1192–1200

Konig G, Monning U, Czech C, Prior R, Banati R, Schreiter-Gasser U, Bauer J, Masters CL, Beyreuther K (1992) Identification and differential expression of another alternative splice isoform of the beta-A4 amyloid precursor protein (APP) mRNA in leukocytes and brain microglial cells. J Biol Chem 267:10804–10809

Koo EH, Sisodia SS, Cork LC, Unterbeck A, Bayney RM, Price DL (1990) Differential expression of amyloid precursor protein mRNAs in cases of Alzheimer's disease and in aged nonhuman primates. Neuron 2:97–104

Kovacs DM, Fausett HJ, Page KJ, Kim T-W, Moir RD, Merriam DE, Hollister RD, Hallmark OG, Mancini R, Felsenstein KM, Hyman BT, Tanzi RE, Wasco W (1996) Alzheimer-associated presenilins 1 and 2: Neuronal expression in brain and localization to intracellular membranes in mammalian cells. Nature Med 2:224–229

Levy-Lahad E, Poorkaj P, Wang K, Fu YH, Oshima J, Mulligan J, Schellenberg GD (1996) Genomic structure and expression of STM2, the chromosome 1 familial Alzheimer disease gene. Genomics 34:198–204

Lukiw WJ, Rogaev EI, Wong L, Vaula G, McLachlan DRC, St George Hyslop P (1994) Protein-DNA interactions in the promoter region of the amyloid precursor protein (APP) gene in human neocortex. Mol Brain Res 22:121–131

Masters CL, Simons G, Weinman NA, Multhaup G, McDonald BL, Beyreuther K (1985) Amyloid plaque core protein in Alzheimer's disease and Down's syndrome. Proc Natl Acad Sci USA 82:4245–4249

Nagy Z, Jobst KA, Esiri MM, Morris JH, King E, MacDonald B, Litchfield S, Barnetson L, Smith AD (1996) Hippocampal pathology reflects memory deficit and brain imaging measurements in Alzheimer's disease: clinicopathologic correlations using three sets of pathologic diagnostic criteria. Dementia 7:76–81

Neve RL, Finch EA, Dawes LR (1988) Expression of the Alzheimer amyloid precursor gene transcripts in the human brain. Neuron 1:669–677

Neve RL, Rogers J, Higgins GA (1990) The Alzheimer amyloid precursor-related transcript lacking the β/A4 sequence is specifically increased in Alzheimer's disease brain. Neuron 5:329–338

Oyama F, Shimada H, Oyama R, Titani K, Ihara Y (1991) Differential expression of β amyloid protein precursor (APP) and tau mRNA in the aged human brain: individual variability and correlation between APP-751 and four-repeat tau. J Neuropathol Exp Neurol 50:560–578

Oyama F, Shimada H, Oyama R, Titani K, Ihara Y (1993) β-amyloid protein precursor and τ mRNA levels versus β-amyloid plaque and neurofibrillary tangles in the aged human brain. J Neurochem 60:1658–1664

Oyama F, Shimada H, Oyama R, Ihara Y (1995) Apolipoprotein E genotype, Alzheimer's pathologies and related gene expression in the aged population. Mol Brain Res 29:92–98

Palmert MR, Golde TE, Cohen DM, Kovacs DM, Tanzi RE, Gusella JF, Usiak MF, Younkin LH, Younkin SG (1988) Amyloid protein precursor messenger RNAs: differential expression in Alzheimer's disease. Science 241:1080–1084

Perry EK, Perry RH, Blessed B, Tomlinson BE (1977) Neurotransmitter enzyme abnormalities in senile dementia: CAT and GAD activities in necropsy tissue. J Neurol Sci 32:247–265

Premkumar DRD, Kalaria RN (1996) Altered expression of amyloid β precursor mRNAs in cerebral vessels, meninges, and choroid plexus in Alzheimer's disease. Ann NY Acad Sci 777:288–292

Procter AW, Francis PT, Holmes C, Webster M-T, Qume M, Stratmann GC, Doshi R, Mann DMA, Harrison PJ, Pearson RCA, Bowen DM (1994) β-amyloid precursor protein isoforms show correlations with neurones but not with glia of demented subjects. Acta Neuropathol (Berl) 88:545–552

Querfurth HW, Wijsman E, St George Hyslop P, Selkoe DJ (1995) βAPP mRNA transcription is increased in cultured fibroblasts from the familial Alzheimer's disease-1 family. Mol Brain Res 28:318–337

Robinson CA, Clark AW, Parhad IM, Fung TS, Bou SS (1994) Gene expression in Alzheimer neocortex as a function of age and severity. Neurobiol Aging 15:681–690

Rockenstein EM, McConologue L, Tan H, Power M, Masliah E, Mucke L (1995) Levels and alternative splicing of amyloid β protein precursor (APP) transcripts in brains of APP transgenic mice and humans with Alzheimer's disease. J Biol Chem 270:28257–28267

Rogaev E, Sherrington R, Rogaeva E, Levesque G, Ikeda M, Liang Y, Chi H, Lin C, Holman K, Tsuda T, Mar L, Sorbi S, Nacmias B, Piacentini S, Amaducci L, Chumakov I, Cohen D, Lannfelt L, Fraser P, Rommens J, St George-Hyslop P (1995) Familial Alzheimer's disease in kindreds with missense mutations in a gene on chromosome 1 related to the Alzheimer's disease type 3 gene. Nature 376:775–778

Schmechel DE, Goldgaber D, Burkhardt DS, Gilbert JR, Gajdusek DC, Roses AD (1988) Cellular localization of messenger RNA encoding amyloid-beta-protein in normal tissue and in Alzheimer disease. Alz Dis Assoc Disord 2: 96-111

Spillantini MG, Hunt SP, Ulrich J, Goedert M (1989) Expression and cellular localization of amyloid β-protein precursor transcripts in normal human brain and Alzheimer's disease. Mol Brain Res 6:143–150

Suzuki T, Nishiyama K, Murayama S, Yamamoto A, Sato S, Kanazawa I, Sakaki Y (1996) Regional and cellular *presenilin 1* gene expression in human and rat tissues. Biochem Biophys Res Commun 219:708–713

Tanaka S, Shiojiri S, Takahashi Y, Kitaguchi N, Ito H, Kameyama M, Kimura J, Nakamura S, Ueda S (1989) Tissue-specific expression of three types of β-protein precursor mRNA: enhancement of protease inhibitor-harboring types in Alzheimer's disease brain. Biochem Biophys Res Commun 165:1404–1414

Tanzi RE, Gusella JF, Watkins PC, Bruns GAP, St George-Hyslop P, van Keuren ML, Patterson D, Pagan S, Kurnit DM, Neve RL (1987) Amyloid β protein gene: cDNA, mRNA distribution, and genetic linkage near the Alzheimer locus. Science 235:880–884

Tanzi RE, McClatchey AI, Lamperti E, Villa-Komaroff L, Gusella JF, Neve RL (1988) Protease inhibitor domain encoded by an amyloid protein precursor mRNA associated with Alzheimer's disease. Nature 331:528–530

Tanzi RE, Wenninger JJ, Hyman BT (1993) Cellular specificity and regional distribution of amyloid β protein precursor alternative transcripts are unaltered in Alzheimer hippocampal formation. Mol Brain Res 18:246–252

Yamada T, Kondo A, Takamatsu J, Tateishi J, Goto I (1995) Apolipoprotein E mRNA in the brains of patients with Alzheimer's disease. J Neurol Sci 129:56–61

Yoshikai S, Sasaki H, Doh-ura K, Furuya H, Sakaki Y (1990) Genomic organization of the human amyloid beta-protein precursor gene. Gene 87:257–263